

N64 18107
Code - 1

DESIGN DATA
FOR
PRESSURIZED GAS SYSTEMS

Prepared for
NATIONAL AERONAUTICS AND SPACE ADMINISTRATION

Contract NAS7-105

NOVEMBER 1963



STANFORD RESEARCH INSTITUTE
MENLO PARK, CALIFORNIA

FOREWORD

This handbook was prepared by Stanford Research Institute for the National Aeronautics and Space Administration, Western Operations Office, under Contract No. NAS7-105, SRI Project PSU-4000, entitled "Investigation of the Space Storability of Pressurizing Gases." The work was administered under the direction of the Jet Propulsion Laboratory, Liquid Propulsion Section, Propulsion Division; Mr. Richard N. Porter of the Jet Propulsion Laboratory served as Technical Manager, and Mr. Frank E. Compitello of NASA/Washington (Liquid Propulsion Systems) was Project Manager.

The technical effort at Stanford Research Institute was directed by Dr. R. F. Muraca, Assistant General Manager, Physical Sciences Research Area; A. P. Brady, J. L. Brenner, F. M. Church, E. C. Follett, and J. S. Whittick assisted in the preparation of various sections.

TABLE OF CONTENTS

Section-Part	Title
I	INTRODUCTION AND CONVERSION TABLES
II	THE SPACE ENVIRONMENT
II-1	Introduction
II-2	Density, Pressure, Temperature
II-3	Meteoroids
II-4	Cosmic Radiation
II-5	Solar Emanations
II-6	Electromagnetic Radiation
II-7	Magnetic Fields
II-8	Effects of Space Environment on Materials
II-9	References
III	ATTITUDE CONTROL THEORY
III-1	Introduction
III-2	Torques Acting on Spacecrafts
III-3	Sensors
III-4	Cold-Gas Systems
III-5	References
IV	NOZZLE PERFORMANCE
IV-1	Introduction
IV-2	Nozzle Design Parameters
IV-3	Computation of Specific Impulse of Noncondensing Gases
IV-4	Performance of Nozzles with Condensing Fluids
IV-A	Appendix: Summary of Equations for Nozzle Performance Calculations
V	STORAGE EFFICIENCY
VI	ZERO GRAVITY CONSIDERATIONS
VII	HEAT BALANCE
VIII	PERMEABILITY THEORY
VIII-1	Introduction
VIII-2	Polymeric Materials
VIII-3	Glasses
VIII-4	Metals
VIII-5	Laminates
VIII-6	Distinction Between Permeation and Mass Flow
VIII-7	References

CONTENTS

Section-Part	Title
IX	PROPERTIES OF GASES
IX-1	Introduction
IX-2	Properties of Nitrogen
IX-3	Properties of Hydrogen
IX-4	Properties of Helium
IX-5	Properties of Oxygen
IX-6	Properties of Carbon Dioxide
IX-7	Properties of Perchloryl Fluoride
IX-8	Properties of Chlorine Trifluoride
IX-9	Properties of Hydrazine
IX-10	Properties of Nitrogen Tetroxide
IX-11	Properties of UDMH (Unsymmetrical Dimethylhydrazine)
IX-12	Properties of Water
IX-13	Properties of Propane
IX-14	Properties of <i>n</i> -Butane
IX-15	Properties of Ammonia
IX-16	Properties of Hydrogen Peroxide
IX-17	Properties of Freon-11 (CCl_3F)
IX-18	Properties of Freon-12 (CCl_2F_2)
IX-19	Properties of Freon-13 (CClF_3)
IX-20	Properties of Freon-14 (CF_4)
X	PRESSURE VESSELS
X-1	Introduction
X-2	Spherical Vessels
X-3	Cylindrical Vessels
X-4	Design Weights of Pressure Vessels
X-5	References
XI	PRESSURIZATION SYSTEMS
XII	MATERIALS
XII-1	Introduction
XII-2	Compatibility of Materials with Pressurizing Gases and Propellants
XII-3	Properties of Materials Used for Pressure Tanks
XII-4	Permeability of Materials to Gases
XIII	RELIABILITY
XIII-1	Introduction
XIII-2	Reliability Models
XIII-3	Probability Distribution
XIII-4	Reliability Sampling
XIII-5	Design of Experiments
XIII-6	Tolerance Limits
XIII-7	References
XIV	VALVES
XV	RINGS AND SEALS

I INTRODUCTION AND CONVERSION TABLES

Table of Contents

<u>Section</u>	<u>Title</u>	<u>Section-Page</u>
I	Introduction	I-1
	Design Data Reference Units	I-3
	Universal Gas Constant	I-3
	Standard Gravity	I-3
	Absolute Zero	I-3
	Pressure Units	I-3
	Volume Units	I-4
	Weight Units	I-4
	Density Units	I-4
	Viscosity Units	I-4
	Thermal Units	I-5
	Work and Energy Units	I-5
	Temperature Conversion Table	I-6
	Pressure Conversion Chart	I-13

I INTRODUCTION

The primary purpose of this book is to present concise summaries of available information on the fundamental parameters governing the design of pressurized-gas systems for spacecrafts. It is intended that the information contained in this book be used in conjunction with the various methodologies currently employed to select component combinations and to establish the design details of suitable pressurized-gas systems. Sufficient room is available in the binder to provide for future expansion of the various sections and to enable the user to incorporate additional pages of information.

The section on "Space Environment" summarizes the available information on the composition of the upper atmosphere, the distribution of meteoroids, and on the various types of radiations encountered by spacecrafts.

The section entitled "Attitude Control Theory" consists of a very brief presentation of the salient principles underlying the design of pressurized-gas attitude-control systems.

The behavior of liquids in essentially gravitationally-free systems (zero-g) is summarized under the heading "Zero-Gravity Considerations." Only those aspects related to pressurized-gas systems are discussed.

A section entitled "Nozzle Performance" summarizes the computation of the performance of fluids expanding through nozzles; it includes condensable as well as noncondensable gases.

A very brief discussion of the aspects of defining the storage efficiency of gases from the viewpoint of weight, performance, reliability, etc. is given in the section "Storage Efficiency."

The section on "Pressure Vessels" indicates some of the newer computational methods for the design of vessels subjected to thermal as well as pressure stresses.

A brief review and summary of the principles of statistical relationships as applied to test programs is presented in the section entitled "Reliability," and is intended to provide guidelines for the engineer.

Brief collections of data on the physical properties of the metals most frequently used to construct pressurized-gas systems are contained in the section entitled "Materials"; synoptic data on the compatibility of these materials with selected gases and liquids are also included.

The fundamental aspects of diffusion and permeability theory are given in the section entitled "Permeability Theory," together with data on the permeability of various polymers and elastomers.

The section on "Rings and Seals" includes data on the effect of the space environment on materials used to effect tight junctures in pressurized-gas systems.

The section "Properties of Gases" consists of an extensive tabular and graphic compilation of the physical and thermodynamic properties of the gases or liquids which may be used in pressurized-gas systems. The data in this section are the most accurate available at this time and may be used freely to compute or estimate pressurized-gas performance.

Sections on "Valves" and "Pressurization Systems" include no information; it is anticipated that material selected for inclusion in these sections will be made available in the future.

DESIGN DATA REFERENCE UNITS

UNIVERSAL GAS CONSTANT	
ergs/°C/mole	8.3170×10^7
cal(15 °C)/ C/mole	1.9869
cc-atm/°C/g-mole	82.0567
liter-atm/°C/g-mole	0.0820544
in ³ -atm/°F/lb-mole	1260.
in ³ -psi/°F/lb-mole	18510.
ft ³ -atm/°F/lb-mole	0.730228
ft-lb/°F/lb-mole	1545.2
btu/°P/lb-mole	1.9869

STANDARD GRAVITY
980.665 cm/sec/sec
32.174 ft/sec/sec

ABSOLUTE ZERO
-273.15°C
-459.67°F

PRESSURE UNITS			
Unit Equivalent	1 Std. Atmos.	1 mm of Hg at 0°C	1 dyne/cm ²
atmosphere	1.	0.0013158	9.8692×10^{-7}
mm of Hg at 0 °C	760	1	7.5006×10^{-4}
in of Hg at 32.0 °F	29.921	0.0393700	2.953×10^{-5}
g/cm ²	1033.2	1.3595	0.00101971
psia	14.696	0.019337	1.4504×10^{-5}
lb/ft ²	2116.224	2.7845	0.0020886
dynes/cm ²	1.01325×10^6	1333.22	1.

DESIGN DATA REFERENCE UNITS (Cont'd)

VOLUME UNITS				
Unit Equivalent	1 ft ³	1 liter	1 cc/g	1 ft ³ /lb
ft ³	1.	0.035316		
liter	28.316	1.		
cc/g			1.	0.016018
ft ³ /lb			62.43	1

WEIGHT UNITS	
1 lb	= 453.5924 g
1 g	= 0.0022046 lb

DENSITY UNITS			
Unit Equivalent	1 g/cc	1 lb/in ³	1 lb/ft ³
g/cc	1.	27.680	0.016018
lb/in ³	0.03613	1.	5.787×10^{-4}
lb/ft ³	62.43	1728.0	1.

VISCOSITY UNITS			
Unit Equivalent	1 poise	1 lb/ft-sec	1 lb/ft-hr
poise	1.	14.91	0.00413
lb/ft-sec	0.0672	1.	2.77×10^{-6}
lb/ft-hr	242.	3608.22	1.

DESIGN DATA REFERENCE UNITS (Cont'd)

THERMAL UNITS	
Heat capacity:	cal/g = Btu/lb
Heat of Vaporization:	cal/g \times 1.79882 = Btu/lb
Heat of fusion:	cal/g \times 1.79882 = Btu/lb
Thermal conductivity:	(cal/sec-cm-°C) \times 242 = Btu/hr-ft°F

WORK AND ENERGY UNITS					
Unit Equivalent	1 Btu (mean)	1 ft-lb	1 g-cal (mean)	1 ft ³ -atm	1 liter-atm
kwh	2.930×10^{-4}	3.7662×10^{-7}	1.1628×10^{-6}	7.9705×10^{-4}	2.815×10^{-5}
cal (mean)	251.98	3.2389×10^{-4}	1.	680.74	24.2052
cal (15°C)	252.04	3.2381×10^{-4}	1.000238	680.58	24.1994
Btu (mean)	1.	0.0012854	0.0039685	2.7203	0.09607
ft ³ -atm	0.3676	4.7253×10^{-4}	0.001459	1.	0.035319
liter-atm	10.409	0.013381	0.041311	28.313	1.
ft-lb	777.97	1.	3.0874	2116.3	74.735
joules (abs)	1054.8	1.35582	4.186	2869.4	101.328
ergs	1.0548×10^{10}	1.35582×10^7	4.186×10^7	2.8496×10^{10}	1.0132×10^9

TEMPERATURE CONVERSION

READING IN ° F OR ° C TO BE CONVERTED	° C	° K	° F	° R
-459.67	-273.15	0	+122.67	0
-458	-272.22	0.93		1.67
-456	-271.11	2.04		3.67
-454	-270.00	3.15		5.67
-452	-268.89	4.26		7.67
-450	-267.78	5.37		9.67
-448	-266.67	6.48		11.67
-446	-265.56	7.59		13.67
-444	-264.44	8.71		15.67
-442	-263.33	9.82		17.67
-440	-262.22	10.93		19.67
-438	-261.11	12.04		21.67
-436	-260.00	13.15		23.67
-434	-258.89	14.26		25.67
-432	-257.78	15.37		27.67
-430	-256.67	16.48		29.67
-428	-255.56	17.59		31.67
-426	-254.44	18.71		33.67
-424	-253.33	19.82		35.67
-422	-252.22	20.93		37.67
-420	-251.11	22.04		39.67
-418	-250.00	23.15		41.67
-416	-248.89	24.26		43.67
-414	-247.78	25.37		45.67
-412	-246.67	26.48		47.67
-410	-245.56	27.59		49.67
-408	-244.44	28.71		51.67
-406	-243.33	29.82		53.67
-404	-242.22	30.93		55.67
-402	-241.11	32.04		57.67
-400	-240.00	33.15		59.67
-398	-238.89	34.26		61.67
-396	-237.78	35.37		63.67
-394	-236.67	36.48		65.67
-392	-235.56	37.59		67.67
-390	-234.44	38.71		69.67
-388	-233.33	39.82		71.67
-386	-232.22	40.93		73.67
-384	-231.11	42.04		75.67
-382	-230.00	43.15		77.67
-380	-228.89	44.26		79.67
-378	-227.78	45.37		81.67
-376	-226.67	46.48		83.67
-374	-225.56	47.59		85.67
-372	-224.44	48.71		87.67
-370	-223.33	49.82		89.67
-368	-222.22	50.93		91.67
-366	-221.11	52.04		93.67
-364	-220.00	53.15		95.67
-362	-218.89	54.26		97.67
-360	-217.78	55.37		99.67
-358	-216.67	56.48		101.67
-356	-215.56	57.59		103.67
-354	-214.44	58.71		105.67
-352	-213.33	59.82		107.67
-350	-212.22	60.93		109.67

TEMPERATURE CONVERSION (Cont'd)

READING IN °F OR °C TO BE CONVERTED	°C	°K	°F	°R
-348	-211.11	62.04		111.67
-346	-210.00	63.15		113.67
-344	-208.89	64.26		115.67
-342	-207.78	65.37		117.67
-340	-206.67	66.48		119.67
-338	-205.56	67.59		121.67
-336	-204.44	68.71		123.67
-334	-203.33	69.82		125.67
-332	-202.22	70.93		127.67
-330	-201.11	72.04		129.67
-328	-200.00	73.15		131.67
-326	-198.89	74.26		133.67
-324	-197.78	75.37		135.67
-322	-196.67	76.48		137.67
-320	-195.56	77.59		139.67
-318	-194.44	78.71		141.67
-316	-193.33	79.82		143.67
-314	-192.22	80.93		145.67
-312	-191.11	82.04		147.67
-310	-190.00	83.15		149.67
-308	-188.89	84.26		151.67
-306	-187.78	85.37		153.67
-304	-186.67	86.48		155.67
-302	-185.56	87.59		157.67
-300	-184.44	88.71		159.67
-298	-183.33	89.82		161.67
-296	-182.22	90.93		163.67
-294	-181.11	92.04		165.67
-292	-180.00	93.15		167.67
-290	-178.89	94.26		169.67
-288	-177.78	95.37		171.67
-286	-176.67	96.48		173.67
-284	-175.56	97.59		175.67
-282	-174.44	98.71		177.67
-280	-173.33	99.82		179.67
-278	-172.22	100.93		181.67
-276	-171.11	102.04		183.67
-274	-170.00	103.15		185.67
-273.15	-169.53	103.62		186.52
-273.15		0	-459.67	0
-272	-168.89	104.26	-457.6	2.07
-270	-167.78	105.37	-454.0	5.67
-268	-166.67	106.48	-450.4	9.27
-266	-165.56	107.59	-446.8	12.87
-264	-164.44	108.71	-443.2	16.47
-262	-163.33	109.82	-439.6	20.07
-260	-162.22	110.93	-436.0	23.67
-258	-161.11	112.04	-432.4	27.27
-256	-160.00	113.15	-428.8	30.87
-254	-158.89	114.26	-425.2	34.47
-252	-157.78	115.37	-421.6	38.07
-250	-156.67	116.48	-418.0	41.67

TEMPERATURE CONVERSION (Cont'd)

READING [°] F OR [°] C IN TO BE CONVERTED	[°] C	[°] K	[°] F	[°] R
-248	-155.56	117.59	-414.4	45.27
-246	-154.44	118.71	-410.8	48.87
-244	-153.33	119.62	-407.2	52.47
-242	-152.22	120.93	-403.6	56.07
-240	-151.11	122.04	-400.0	59.67
-238	-150.00	123.15	-396.4	63.27
-236	-148.89	124.26	-392.8	66.87
-234	-147.78	125.37	-389.2	70.47
-232	-146.67	126.48	-385.6	74.07
-230	-145.56	127.59	-382.0	77.67
-228	-144.44	128.71	-378.4	81.27
-226	-143.33	129.82	-374.8	84.87
-224	-142.22	130.93	-371.2	88.47
-222	-141.11	131.94	-367.6	92.07
-220	-140.00	133.15	-364.0	95.67
-218	-138.89	134.26	-360.4	99.27
-216	-137.78	135.37	-356.8	102.87
-214	-136.67	136.48	-353.2	106.47
-212	-135.56	137.59	-349.6	110.07
-210	-134.44	138.71	-346.0	113.67
-208	-133.33	139.82	-342.4	117.27
-206	-132.22	140.93	-338.8	120.87
-204	-131.11	142.04	-335.2	124.47
-202	-130.00	143.15	-331.6	128.07
-200	-128.89	144.26	-328.0	131.67
-198	-127.78	145.37	-324.4	135.27
-196	-126.67	146.48	-320.8	138.87
-194	-125.56	147.59	-317.2	142.47
-192	-124.44	148.71	-313.6	146.07
-190	-123.33	149.82	-310.0	149.67
-188	-122.22	150.93	-306.4	153.27
-186	-121.11	152.04	-302.8	156.87
-184	-120.00	153.15	-299.2	160.47
-182	-118.89	154.26	-295.6	164.07
-180	-117.78	155.37	-292.0	167.67
-178	-116.67	156.48	-288.4	171.27
-176	-115.56	157.59	-284.8	174.87
-174	-114.44	158.71	-281.2	178.47
-172	-113.33	159.82	-277.6	182.07
-170	-112.22	160.93	-274.0	185.67
-168	-111.11	162.04	-270.4	189.27
-166	-110.00	163.15	-266.8	192.87
-164	-108.89	164.26	-263.2	196.47
-162	-107.78	165.37	-259.6	200.07
-160	-106.67	166.48	-256.0	203.67
-158	-105.56	167.59	-252.4	207.27
-156	-104.44	168.71	-248.8	210.87
-154	-103.33	169.84	-245.2	214.47
-152	-102.22	170.93	-241.6	218.07
-150	-101.11	172.04	-238.0	221.67
-148	-100.00	173.15	-234.4	225.27
-146	-98.89	174.26	-230.8	228.87
-144	-97.78	175.37	-227.2	232.47
-142	-96.67	176.48	-223.6	236.07
-140	-95.56	177.59	-220.0	239.67

TEMPERATURE CONVERSION (Cont'd)

READING IN °F OR °C TO BE CONVERTED	°C	°K	°F	°R
-138	-94.44	178.71	-216.4	243.27
-136	-93.33	179.82	-212.8	246.87
-134	-92.22	180.93	-209.2	250.38
-132	-91.11	182.04	-205.6	254.07
-130	-90.00	183.15	-202.0	257.67
-128	-88.89	184.26	-198.4	261.27
-126	-87.78	185.37	-194.8	264.87
-124	-86.67	186.43	-191.2	268.47
-122	-85.56	187.59	-187.6	272.07
-120	-84.44	188.61	-184.0	275.67
-118	-83.33	189.82	-180.4	279.27
-116	-82.22	190.93	-176.8	282.87
-114	-81.11	192.04	-173.2	286.47
-112	-80.00	193.15	-169.6	290.07
-110	-78.89	194.26	-166.0	293.67
-108	-77.78	195.37	-162.4	297.27
-106	-76.67	196.48	-158.8	300.87
-104	-75.56	197.59	-155.2	304.47
-102	-74.44	198.71	-151.6	308.07
-100	-73.33	199.82	-148.0	311.67
-98	-72.22	200.93	-144.4	315.27
-96	-71.11	202.04	-140.8	318.87
-94	-70.00	203.15	-137.2	322.47
-92	-68.89	204.26	-133.6	326.07
-90	-67.78	205.37	-130.00	329.67
-88	-66.67	206.48	-126.4	333.27
-86	-65.56	207.59	-122.8	336.87
-84	-64.44	208.71	-119.2	340.47
-82	-63.33	209.82	-115.6	344.07
-80	-62.22	210.93	-112.0	347.67
-78	-61.11	212.04	-108.4	351.27
-76	-60.00	213.15	-104.8	354.87
-74	-58.89	214.26	-101.2	358.47
-72	-57.78	215.37	-97.6	362.07
-70	-56.67	216.48	-94.0	365.67
-68	-55.56	217.59	-90.4	369.27
-66	-54.44	218.71	-86.8	372.87
-64	-53.33	219.82	-83.2	376.47
-62	-52.22	220.93	-79.6	380.07
-60	-51.11	222.04	-76.0	383.67
-58	-50.00	223.15	-72.4	387.27
-56	-48.89	224.26	-68.88	390.87
-54	-47.78	225.37	-65.2	394.47
-52	-46.67	226.48	-61.6	398.07
-50	-45.56	227.59	-58.0	401.67
-48	-44.44	228.71	-54.4	405.27
-46	-43.33	229.82	-50.8	408.87
-44	-42.22	230.93	-47.20	412.47
-42	-41.11	232.04	-43.6	416.07
-40	-40.00	233.15	-40.0	419.67
-38	-38.89	234.26	-36.4	423.27
-36	-37.78	235.37	-32.8	426.87
-34	-36.67	236.48	-29.2	430.47
-32	-35.56	237.59	-25.6	434.07
-30	-34.44	238.71	-22.0	437.67

TEMPERATURE CONVERSION (Cont'd)

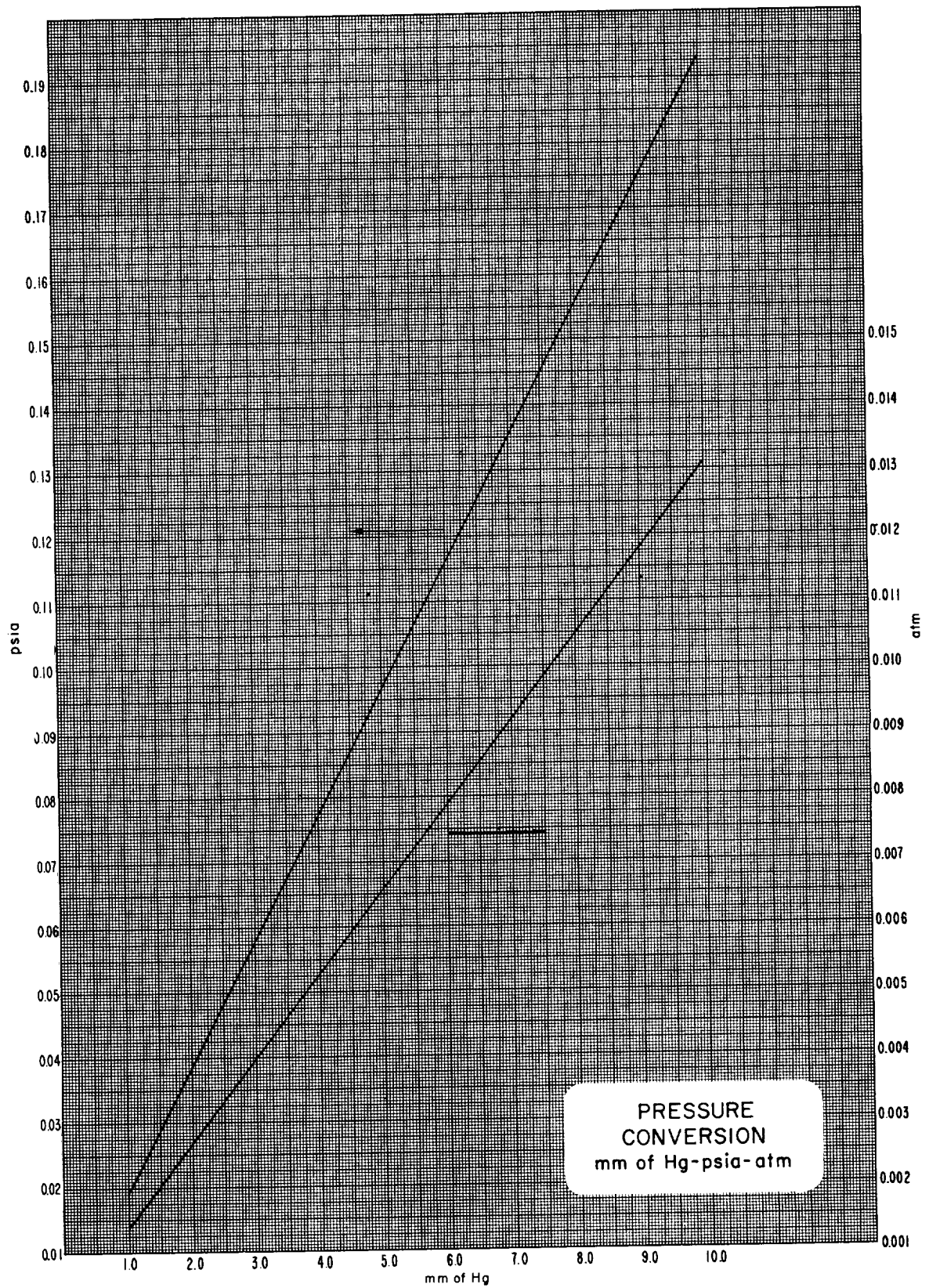
READING IN °F OR °C TO BE CONVERTED	°C	°K	°F	°R
-28	-33.33	239.82	-18.4	441.27
-26	-32.22	240.93	-14.8	444.87
-24	-31.11	242.04	-11.2	448.47
-22	-30.00	243.15	-7.6	452.07
-20	-28.89	244.26	-4.0	455.67
-18	-27.78	245.37	-0.4	459.27
-16	-26.67	246.48	+3.2	462.87
-14	-25.56	247.59	+6.8	466.07
-12	-24.44	248.71	+10.4	470.07
-10	-23.33	249.82	+14.0	473.67
-8	-22.22	250.93	+17.6	477.27
-6	-21.11	252.04	+21.2	480.87
-4	-20.00	253.15	+24.8	484.47
-2	-18.89	254.16	+28.4	488.07
0.00	-17.78	255.37	+32.0	491.67
+2	-16.67	256.48	+35.6	495.27
+4	-15.56	257.59	+39.2	498.87
+6	-14.44	258.71	+42.8	502.47
+8	-13.33	259.82	+46.4	506.07
+10	-12.22	260.93	+50.0	509.67
+12	-11.11	262.04	+53.6	513.27
+14	-10.00	263.15	+57.2	516.87
+16	-8.89	264.26	+60.8	520.47
+18	-7.78	265.37	+64.4	524.07
+20	-6.67	266.48	+68.0	527.67
+22	-5.56	267.59	+71.6	531.27
+24	-4.44	268.71	+75.2	534.87
+26	-3.33	269.82	+78.8	538.47
+28	-2.22	270.93	+82.4	542.07
+30	-1.11	272.04	+86.0	545.67
+32	0.00	273.15	+89.6	549.27
+34	+1.11	274.26	+93.2	552.87
+36	+2.22	275.37	+96.8	556.47
+38	+3.33	276.48	+100.4	560.07
+40	+4.44	277.59	+104.0	563.67
42	5.56	278.71	107.6	567.27
44	6.67	279.82	111.2	570.87
46	7.78	280.93	114.8	574.47
48	8.89	282.04	118.4	578.07
50	10.00	283.15	122.0	581.67
52	11.11	284.26	125.6	585.27
54	12.22	285.37	129.2	588.87
56	13.33	286.48	132.8	592.47
58	14.44	287.59	136.4	596.07
60	15.56	288.71	140.0	599.67
62	16.67	289.82	143.6	603.27
64	17.78	290.93	147.2	606.87
66	18.89	292.04	150.8	610.47
68	20.00	293.15	154.4	614.07
70	21.11	294.26	158.0	617.67
72	22.22	295.37	161.6	621.27
74	23.33	296.48	165.2	624.87
76	24.44	297.59	168.8	628.47
78	25.56	298.71	172.4	632.07
80	26.67	299.82	176.0	635.67

TEMPERATURE CONVERSION (Cont'd)

READING IN °F OR °C TO BE CONVERTED	°C	°K	°F	°R
82	27.78	300.93	179.6	639.27
84	28.89	302.04	183.2	642.87
86	30.00	303.15	186.8	646.47
88	31.11	304.26	190.4	650.07
90	32.22	305.37	194.0	653.67
92	33.33	306.48	197.6	657.27
94	34.44	307.59	201.2	660.87
96	35.56	308.71	204.8	664.47
98	36.67	309.82	208.4	668.07
100	37.78	310.93	212.0	671.67
102	38.89	312.04	215.6	675.27
104	40.00	313.15	219.2	678.87
106	41.11	314.26	222.8	682.47
108	42.22	315.37	226.4	686.07
110	43.33	316.48	230.0	689.67
112	44.44	317.59	233.6	693.27
114	45.56	318.71	237.2	696.87
116	46.67	319.82	240.8	700.47
118	47.78	320.93	244.4	704.07
120	48.89	322.04	248.0	707.67
122	50.00	323.15	251.6	711.27
124	51.11	324.26	255.2	714.87
126	52.22	325.37	258.8	718.47
128	53.33	326.48	262.4	722.07
130	54.44	327.59	266.0	725.67
132	55.56	328.66	269.6	729.27
134	56.67	329.82	273.2	732.87
136	57.78	330.93	276.8	736.47
138	58.89	332.04	280.4	740.07
140	60.00	333.15	284.0	743.67
142	61.11	334.26	287.6	747.27
144	62.22	335.37	291.2	750.87
146	63.33	336.48	294.8	754.47
148	64.44	337.59	298.4	758.07
150	65.56	338.71	302.0	761.67
152	66.67	339.82	305.6	765.27
154	67.78	340.93	309.2	768.87
156	68.89	341.64	312.8	772.47
158	70.00	343.15	316.4	776.07
160	71.11	344.26	320.0	779.67
162	72.22	345.37	323.6	783.27
164	73.33	346.48	327.2	786.87
166	74.44	347.59	330.8	790.47
168	75.56	348.71	334.4	794.07
170	76.67	349.82	338.0	797.67
172	77.78	350.93	341.6	801.27
174	78.89	352.04	345.2	804.87
176	80.00	353.15	348.8	808.47
178	81.11	354.26	352.4	812.07
180	82.22	355.37	356.0	815.67
182	83.33	356.48	359.6	819.27
184	84.44	357.59	363.2	822.87
186	85.56	358.71	366.8	826.47
188	86.67	359.82	370.4	830.07
190	87.78	360.93	374.0	833.67

TEMPERATURE CONVERSION (Concluded)

READING IN °F OR °C TO BE CONVERTED	°C	°K	°F	°R
192	88.89	362.04	377.6	837.27
194	90.00	363.15	381.2	840.87
196	91.11	364.26	384.8	844.47
198	92.22	365.37	388.4	848.07
200	93.33	366.48	392.0	851.67
202	94.44	367.59	395.6	855.27
204	95.56	368.71	399.2	858.87
206	96.67	369.82	402.8	862.47
208	97.78	370.93	406.4	866.07
210	98.89	372.04	410.0	869.67
212	100.00	373.15	413.6	873.27
214	101.11	374.26	417.2	876.87
216	102.22	375.37	420.8	880.47
218	103.33	376.48	424.4	884.07
220	104.44	377.59	428.0	887.67



1

2

3

4

5

II THE SPACE ENVIRONMENT

Table of Contents

<u>Section-Part</u>	<u>Title</u>	<u>Section-Part. Page</u>
II-0	List of Tables ,	II-0.2
II-0	List of Figures	II-0.3
II-1	Introduction	II-1.1
II-2	Density, Pressure, Temperature	II-2.1
II-3	Meteoroids	II-3.1
II-4	Cosmic Radiation	II-4.1
II-5	Solar Emanations	II-5.1
II-6	Electromagnetic Radiation	II-6.1
II-7	Magnetic Fields	II-7.1
II-8	Effects of Space Environment on Materials	II-8.1
II-9	References	II-9.1

II LIST OF TABLES

<u>Section-Part-Table</u>	<u>Title</u>	<u>Section-Part-Page</u>
II-2-1	Atmospheric Parameters <i>versus</i> Altitude	II-2.5
II-2-2	Properties of the Atmosphere (English Units)	II-2.6
II-2-3	Properties of the Atmosphere (Metric Units)	II-2.7
II-2-4	Variation of Gaseous Composition with Altitude	II-2.8
II-3-1	Meteoroid Bumper Materials for Equivalent Protection . .	II-3.3
II-8-1	Estimated Sublimation Losses of Metals in Space at 150°C	II-8.9
II-8-2	Typical Outgassing Rate for Materials	II-8.9
II-8-3	Estimated Maximum Radiation Dosages for Various Orbits	II-8.7

II-0 LIST OF FIGURES

<u>Section-Part-Figure</u>	<u>Title</u>	<u>Section-Part.Page</u>
II-2-1	Density of the Atmosphere vs. Altitude	II-2.9
II-2-2	Pressure of the Atmosphere vs. Altitude	II-2.10
II-2-3	Mean Free Path vs. Altitude	II-2.11
II-2-4	U.S. Standard Atmosphere, 1962 (1)	II-2.12
II-2-5	U.S. Standard Atmosphere, 1962 (2)	II-2.13
II-3-1	Probability of No Meteoroid Penetration in 100 Square Feet of Surface Area	II-3.5
II-3-2	Estimates of Meteoroid Flux in the Vicinity of the Earth	II-3.6
II-3-3	Distribution of Meteor Flux about the Plane of the Ecliptic at the Earth's Distance from the Sun.	II-3.7
II-4-1	Integral Number-Energy Spectrum of Primary Cosmic Rays	II-4.3
II-4-2	Vertical Flux of Particles Near the Top of the Earth's Atmosphere as a Function of Geomagnetic Latitude	II-4.4
II-5-1	Normal Daytime Ion Distribution During Sunspot Maximum	II-5.5
II-5-2	Idealized Distribution of Radiation	II-5.6
II-5-3	Distribution of Protons	II-5.7
II-6-1	Spectral Energy Curves Related to the Sun	II-6.3
II-6-2	A Typical Spectral Emissive Power Curve for the Thermal Radiation Leaving the Earth	II-6.4
II-8-1	Atmospheric Pressure vs. Altitude	II-8.11

1

2

3

4

5

II-1 INTRODUCTION

The purpose of this section is to provide a summary of the physical properties of the upper atmosphere and the space environment. Environmental parameters, such as pressure and density, the acceleration of gravity, temperature, ionization, radiation, magnetism, etc., must be considered in the design of storage systems for pressurizing gases. The discussion in this section is based upon a survey of unclassified literature and in many instances the data, particularly at high altitudes, may be altered significantly as more satellite and space-probe data are accumulated.

The most common method of deriving the atmospheric properties of pressure, density, gravity, etc. is based upon the perfect gas law and the hydrostatic equation, but results obtained for altitudes above 300 miles are questionable largely because these relationships do not take into account differences in the molecular composition of the atmosphere in the upper regions. Kallman and Juncosa⁵ derived the variation of pressure with height from the variation of density with height by numerical integration of data obtained from rocket and satellite observations without assuming a scale height or temperature gradient. The Satellite Environment Handbook⁷ contains a comprehensive review of the data available through 1960 regarding the physical properties of the upper atmosphere, radiation, micrometeorites, etc.

Since the atmosphere is not heated uniformly by the sun, its physical properties at a given altitude at any time can vary greatly from a particular value derived from a "model atmosphere" based on the gas law and the hydrostatic equation. It has been estimated from satellite data that the density can vary by a factor of 10 at an altitude of 700 km, within a 24-hour period.

II-1.1

1

2

3

4

5

II-2 DENSITY, PRESSURE, TEMPERATURE

The density of the atmosphere versus altitude is shown in Figure II-2-1, and Figure II-2-2 illustrates the pressure of the atmosphere versus altitude. Table II-2-1, which summarizes atmospheric parameters as a function of altitude, is derived from the models of Kallman and Juncosa⁵ and those of the Satellite Environment Handbook.⁷ The data in columns titled "Solar Max." and "Solar Min." are from the Satellite Environment Handbook; the columns titled "K & J Model A" are from Kallman and Juncosa. The drop in mean molecular weight at 1600 and 800 km at solar maximum and minimum, respectively, is attributed to the presence of atomic hydrogen in the atmosphere, but the particle-concentration data are tentative. The variation of gaseous compositions from the earth's atmosphere to outer space is indicated in Table II-2-4 (Jaffe and Rittenhouse⁶).

By definition, free molecular flow occurs whenever the mean free path of the molecules is larger than the linear dimension of the body under consideration. The ratio of the length of the mean free path to the linear dimension of the body is known as the Knudsen number (K) and free molecular flow is assumed for large values of K. Because of the low density and long mean free path in outer space, atmospheric drag and heat transfer to a spacecraft are to be computed from the theory of free molecular flow.

Figure II-2-3 shows the mean free path in feet versus the altitude in km, assuming that the mean molecular weight of the atmosphere is 15. At 90 km, the mean free path is about 6.5×10^{-2} ft; at 240 km, about 1000 ft. Thus above 240 km, the heating effect of drag is negligible, and solar radiation is the main influence in determining the shell temperature of a spacecraft as it moves into and out of the earth's shadow. The temperature of the spacecraft in this region depends upon the absorptivity and the emissivity of its surface and the heat capacity of the outer shell. If the absorptivity is high, the temperature may vary by 100°C or more per revolution; for example, the shell temperature of Explorer I ranged from -25°C to 75°C, although most observations indicated a temperature of $0 \pm 25^\circ\text{C}$ at a perigee distance of 270 km, and an apogee distance of 1800-2250 km.

II-2.1

Recently, three new model atmospheres have been established, by ARDC, COSPAR, AND COESA respectively. The COSPAR atmosphere is published in [14], and the (COESA) U.S. Standard Atmosphere 1962, Figure II-2-4 and Figure II-2-5, is discussed in [15]. In the latter reference, seasonal and latitudinal variations are explained, and basic temperature profiles are given.

A few derived densities are plotted by Sissenwine *et al.*¹⁵, for altitudes 80-700 km. They seem to be higher than those of the curves in Figure II-2-1 by a factor of 10. The ranges indicated in Figure II-2-1 at 400 km are the data quoted in Kallman-Bijl, *et al.*,¹⁴ and also lie mostly above the curves. Densities at great altitudes are inferred from satellite observations. It is known that there is a strong correlation between density and 10-cm (or 20-cm) solar electromagnetic radiation; semi-annual and diurnal variations are well-documented. It is now customary to normalize density measurements against these effects; for example, it is assumed that density is proportional to the energy of 10-cm solar radiation, and the normalized value of the latter is taken to be 220×10^{-22} watts m^{-2} cycle $^{-1}$ sec $^{-1}$ by H. K. Paetzold [14, p. 81].

Experimental Methods

The temperature of a satellite in space is not determined by the kinetic temperature of the environment, but by the radiative heat gains and losses. (See p. II-6.2.)

Atmospheric parameters are based on the following measurements.

- (a) The drag of the atmosphere on a satellite has been measured at great altitudes. The drag is not uniform in time (even at a fixed altitude), and its nature is uncertain; some workers claim that at very great altitudes a metallic satellite becomes electrically charged and attracts a cloud of ions around itself. This cloud increases the effective area the satellite presents to the braking effect of the atmosphere through which it passes.

There is fairly uniform agreement among physicists as to the drag mechanism and the importance of the ion-cloud effect. It is fair to note that this agreement amounts to a (probably correct) physical assumption, which has not been confirmed experimentally. Existence of charged particles (ions) at great altitudes has been confirmed in satellite experiments, which have also measured the proportion of some molecular species.

II-2.2

- (b) At very low altitudes (less than 30 miles), sensors in balloons have established molecular composition, pressure, density, and temperature by direct measurement.
- (c) At intermediate altitudes (20-200 miles), rocket-borne equipment has taken soundings of pressure, and sampled the environment in bottles. In general, it has been rather difficult to correlate these soundings with the perturbations of satellite orbits at the same altitude. A satellite must fly above about 100 km to remain in orbit for any length of time.
- (d) Direct measurement of temperature at altitudes above 30-50 miles with a temperature sensor is difficult because of the long response time and weight of most sensors.

Finally, it should be remarked that values of density derived from drag measurements are most useful for estimating expected drag, and probably somewhat less useful for estimating totally unrelated phenomena, such as rate of diffusion. The reason for this is that a certain amount of analysis involving physical assumptions necessarily intervenes in any data reduction process. (In using observed drag to compute density, the assumption is made that density in the neighborhood of perigee is orders of magnitude greater than density at apogee. Moreover, the density gradient is assumed to be exponential. On the other hand, rate of diffusion is governed by number of particles, i.e. by degree of dissociation of the molecules, which is difficult to estimate from drag observations.)

Besides pressure, density, molecular weight, acceleration of gravity, and temperature, certain other properties of the space environment must be considered in designing pressurized gas systems.

Table II-2-1
ATMOSPHERIC PARAMETERS VERSUS ALTITUDE

Height Km	Density-gm., cm. ⁻³			Pressure-dyns. cm. ⁻²			Molecular Wgt.		Log ₁₀ Particles per cm.		Accel. of Gravity -g	Temperature °K	
	Solar Max.	Solar Min.	K. & J. Model A	Solar Max.	Solar Min.	K. & J. Model A	Solar Max.	Solar Min.	Solar Max.	Solar Min.	K. & J. Model A	Solar Max.	Solar Min.
100	2.82x10 ⁻¹⁰	2.82x10 ⁻¹⁰	6.93x10 ⁻¹⁰	1.74x10 ⁻¹	1.74x10 ⁻¹	5.34x10 ⁻¹	27.8	27.8	12.78	12.78	950.5	206	206
120	2.88x10 ⁻¹¹	1.95x10 ⁻¹¹	6.34x10 ⁻¹¹	3.39x10 ⁻²	2.09x10 ⁻²	7.67x10 ⁻²	28.1	28.1	11.80	11.65	944.7	390	340
140	4.68x10 ⁻¹²	2.88x10 ⁻¹²	1.24x10 ⁻¹¹	1.05x10 ⁻²	4.57x10 ⁻³	1.98x10 ⁻²	24.5	24.3	11.06	10.82	938.9	662	500
160	1.51x10 ⁻¹²	7.76x10 ⁻¹³	3.24x10 ⁻¹²	5.13x10 ⁻³	1.86x10 ⁻³	7.38x10 ⁻³	23.7	22.9	10.60	10.33	933.1	926	628
180	7.76x10 ⁻¹³	3.02x10 ⁻¹³	1.21x10 ⁻¹²	3.09x10 ⁻³	9.12x10 ⁻⁴	3.64x10 ⁻³	22.8	21.5	10.30	9.96	927.4	1115	722
200	4.17x10 ⁻¹³	1.48x10 ⁻¹³	5.91x10 ⁻¹³	1.85x10 ⁻³	5.01x10 ⁻⁴	2.06x10 ⁻³	22.0	20.8	10.06	9.65	921.8	1230	807
220	2.69x10 ⁻¹³	7.76x10 ⁻¹⁴	3.22x10 ⁻¹³	1.20x10 ⁻³	2.82x10 ⁻⁴	1.25x10 ⁻³	21.2	19.5	9.82	9.37	916.2	1303	865
240	1.70x10 ⁻¹³	4.27x10 ⁻¹⁴	1.89x10 ⁻¹³	8.51x10 ⁻⁴	1.78x10 ⁻⁴	7.98x10 ⁻⁴	20.8	18.9	9.66	9.15	910.6	1356	906
260	1.12x10 ⁻¹³	2.63x10 ⁻¹⁴	1.16x10 ⁻¹³	6.46x10 ⁻⁴	1.15x10 ⁻⁴	5.27x10 ⁻⁴	20.0	18.3	9.52	8.95	905.1	1400	937
280	7.94x10 ⁻¹⁴	1.62x10 ⁻¹⁴	7.38x10 ⁻¹⁴	4.68x10 ⁻⁴	7.59x10 ⁻⁵	3.59x10 ⁻⁴	19.5	17.9	9.37	8.76	899.7	1430	959
300	5.75x10 ⁻¹⁴	1.05x10 ⁻¹⁴	4.84x10 ⁻¹⁴	3.83x10 ⁻⁴	5.13x10 ⁻⁵	2.51x10 ⁻⁴	19.1	17.5	9.26	8.58	894.3	1455	973
320	4.27x10 ⁻¹⁴	6.92x10 ⁻¹⁵	3.27x10 ⁻¹⁴	2.69x10 ⁻⁴	3.47x10 ⁻⁵	1.80x10 ⁻⁴	18.7	17.2	9.12	8.41	888.9	1472	984
340	3.09x10 ⁻¹⁴	4.79x10 ⁻¹⁵	2.28x10 ⁻¹⁴	2.04x10 ⁻⁴	2.35x10 ⁻⁵	1.32x10 ⁻⁴	18.4	16.9	9.00	8.23	883.6	1485	991
360	2.29x10 ⁻¹⁴	3.31x10 ⁻¹⁵	1.61x10 ⁻¹⁴	1.55x10 ⁻⁴	1.66x10 ⁻⁵	9.82x10 ⁻⁵	18.0	16.7	8.88	8.08	878.4	1491	996
380	1.78x10 ⁻¹⁴	2.24x10 ⁻¹⁵	1.17x10 ⁻¹⁴	1.23x10 ⁻⁴	1.15x10 ⁻⁵	7.40x10 ⁻⁵	17.8	16.5	8.77	7.92	873.2	1496	998
400	1.38x10 ⁻¹⁴	1.58x10 ⁻¹⁵	8.74x10 ⁻¹⁵	9.77x10 ⁻⁵	8.32x10 ⁻⁶	5.63x10 ⁻⁵	17.5	16.3	8.67	7.78	868.0	1500	1000
450	7.25x10 ⁻¹⁵	6.76x10 ⁻¹⁶	4.35x10 ⁻¹⁵	5.25x10 ⁻⁵	3.83x10 ⁻⁶	2.94x10 ⁻⁵	17.0	16.0	8.40	7.42	855.3	1500	1000
500	4.07x10 ⁻¹⁵	3.09x10 ⁻¹⁶	2.28x10 ⁻¹⁵	2.88x10 ⁻⁵	1.86x10 ⁻⁶	1.58x10 ⁻⁵	16.6	15.9	8.16	7.08	842.9	1500	1000
600	1.32x10 ⁻¹⁵	6.31x10 ⁻¹⁷	6.68x10 ⁻¹⁶	9.99x10 ⁻⁶	3.39x10 ⁻⁷	4.97x10 ⁻⁶	16.3	15.6	7.88	6.99	818.8	1500	1000
700	4.57x10 ⁻¹⁶	1.29x10 ⁻¹⁷	2.04x10 ⁻¹⁶	3.55x10 ⁻⁶	7.94x10 ⁻⁸	1.79x10 ⁻⁶	16.1	14.7	7.23	5.76	795.8	1500	1000
800	1.66x10 ⁻¹⁶	2.88x10 ⁻¹⁸	<u>8.63x10⁻¹⁷</u>	1.32x10 ⁻⁶	2.40x10 ⁻⁸	<u>8.63x10⁻⁷</u>	16.0	10.3	6.80	5.24	<u>773.7</u>	1500	1000
900	6.03x10 ⁻¹⁷	7.25x10 ⁻¹⁹		4.90x10 ⁻⁷	1.26x10 ⁻⁸		15.8	8.1	6.37	4.96		1500	1000
1000	2.40x10 ⁻¹⁷	2.69x10 ⁻¹⁹		1.91x10 ⁻⁷	9.77x10 ⁻⁹		15.7	2.3	5.96	4.85		1500	1000
1200	3.80x10 ⁻¹⁸	1.07x10 ⁻¹⁹		3.16x10 ⁻⁸	7.24x10 ⁻⁹		15.2	1.3	5.18	4.72		1500	1000
1400	6.81x10 ⁻¹⁹	7.59x10 ⁻²⁰		6.76x10 ⁻⁹	6.17x10 ⁻⁹		13.0	1.0	4.51	4.65		1500	1000
1600	1.35x10 ⁻¹⁹	6.31x10 ⁻²⁰		2.09x10 ⁻⁹	5.13x10 ⁻⁹		8.3	1.0	4.00	4.57		1500	1000
1800	3.55x10 ⁻²⁰	5.62x10 ⁻²⁰		1.15x10 ⁻⁹	4.27x10 ⁻⁹		3.5	1.0	3.76	4.49		1500	1000
2000	1.45x10 ⁻²⁰	4.79x10 ⁻¹²		6.55x10 ⁻¹⁰	3.80x10 ⁻⁹		1.8	1.0	3.88	4.44		1500	1000
2500	6.03x10 ⁻²¹	3.39x10 ⁻²⁰		7.24x10 ⁻¹⁰	2.82x10 ⁻⁹		1.0	1.0	3.54	4.31		1500	1000

Table II-2-2
 PROPERTIES OF THE ATMOSPHERE (ENGLISH UNITS)
 (Ref. 16)

ALTITUDE		TEMPERATURE °R	PRESSURE lb/ft ²	SPEED OF SOUND, ft/sec
Ft x 10 ³	Miles			
0	0	518.69	2.1162×10^3	1116.4
5	0.95	500.86	1.7609×10^3	1097.1
25	4.73	429.64	7.8633×10^2	1016.1
50	9.47	390.00	2.4361×10^2	968.08
100	18.94	418.79	2.3085×10	1003.2
150	28.41	500.11	3.0597×10	1096.3
200	37.88	449.00	4.715×10^{-1}	1038.7
250	47.30	328.20	4.364×10^{-2}	888.1
300	56.82	299.2	2.118×10^{-3}	846.5
400	75.76	923.9	3.762×10^{-5}	
500	94.70	1933.	1.036×10^{-5}	
600	113.64	2478.	4.908×10^{-6}	
700	132.58	2545.	2.592×10^{-6}	
800	151.52	2547.	1.438×10^{-6}	
900	170.45	2551.	8.294×10^{-7}	
1000	189	2564.	4.949×10^{-7}	
1200	227	2619	1.923×10^{-7}	
1400	267	2706	8.246×10^{-8}	
1500	284	2758	5.571×10^{-8}	
1700	322	2873	2.684×10^{-8}	
1900	341	2999	1.376×10^{-9}	
2100	397	3130	7.442×10^{-9}	
2300	435	3265	4.215×10^{-9}	

Table 11-2-3
 PROPERTIES OF THE ATMOSPHERE (METRIC UNITS)
 (Ref. 16)

ALTITUDE, Km	TEMP., °K	PRESSURE, mm Hg	SOUND SPEED, m·sec ⁻¹
0	288.16	7.6000×10^2	340.29
1	281.66	6.7413×10^2	336.43
5	255.69	4.0539×10^2	320.54
10	223.26	1.9876×10^2	299.53
20	216.66	4.1473×10	295.07
50	282.66	6.5899×10^{-1}	337.03
70	209.59	4.5160×10^{-2}	290.22
90	165.7	1.015×10^{-3}	258.00
100	199.0	1.604×10^{-4}	
110	286.7	3.680×10^{-5}	
120	477.0	1.533×10^{-5}	
130	664.9	8.632×10^{-6}	
140	849.9	5.627×10^{-6}	
150	1031.	4.001×10^{-6}	
175	1359	2.102×10^{-6}	
200	1404.	1.222×10^{-6}	
250	1415.	4.608×10^{-7}	
300	1423.	1.924×10^{-7}	
350	1445.	8.729×10^{-8}	
400	1480.	4.246×10^{-8}	
450	1525.	2.191×10^{-8}	
500	1576.	1.190×10^{-8}	
550	1632.	6.751×10^{-9}	
600	1691.	3.981×10^{-9}	
650	1751.	2.429×10^{-9}	
700	1812	1.528×10^{-9}	

Table II-2-4
 VARIATION OF GASEOUS COMPOSITION WITH ALTITUDE
 (Ref. 6)

ALTITUDE	GASEOUS COMPOSITION
Sea level	78% N ₂ , 21% O ₂ , 0.94% A
30 km	N ₂ , O ₂ , A
200 km	N ₂ , O, O ₂ , O ⁺
800 km	O, O ⁺ , H
6500 km	H ⁺ , H
Above 22,000 km	85% H ⁺ , 15% He ⁺⁺

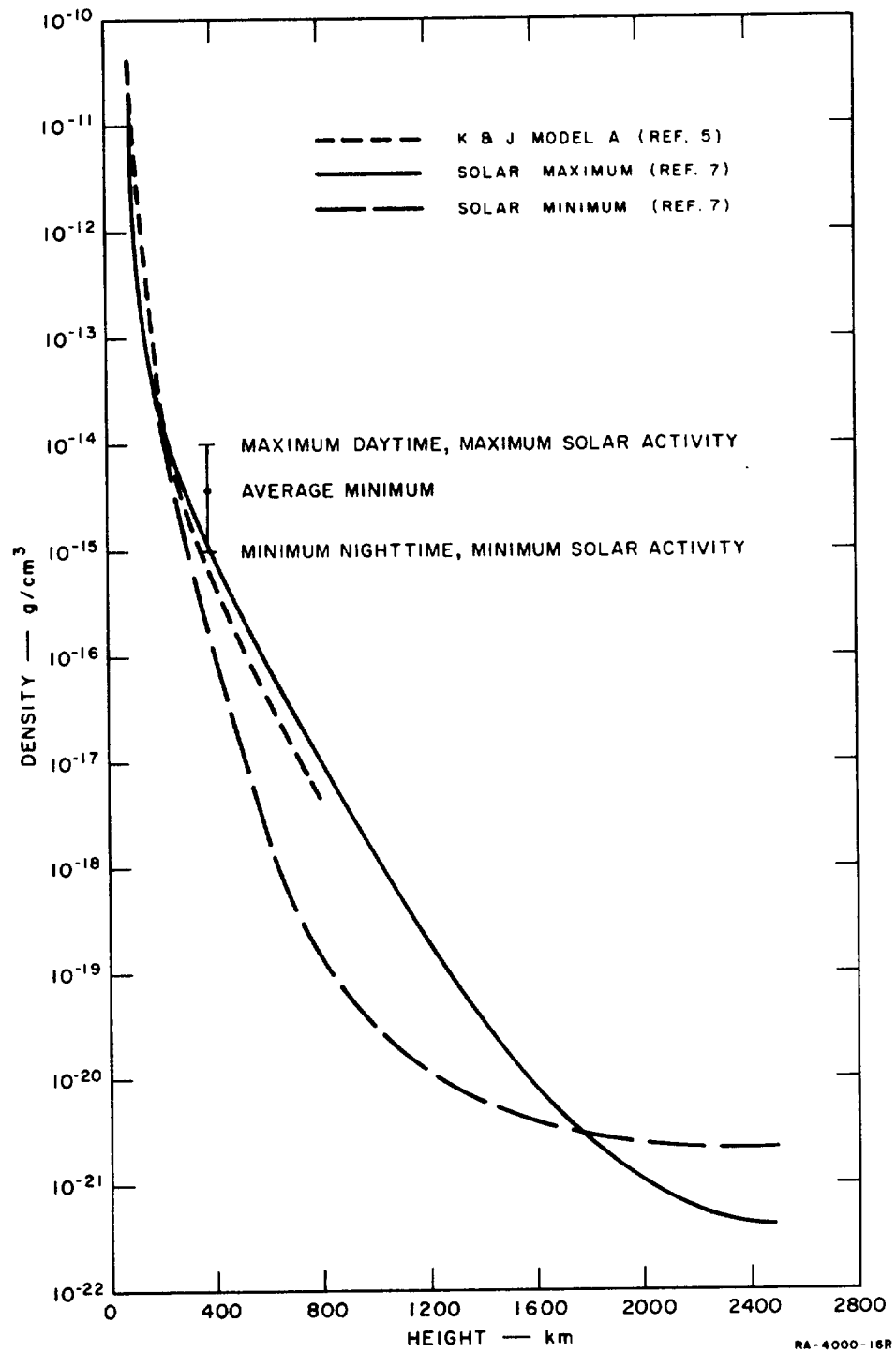


FIG. II-2-1 DENSITY OF THE ATMOSPHERE vs. ALTITUDE

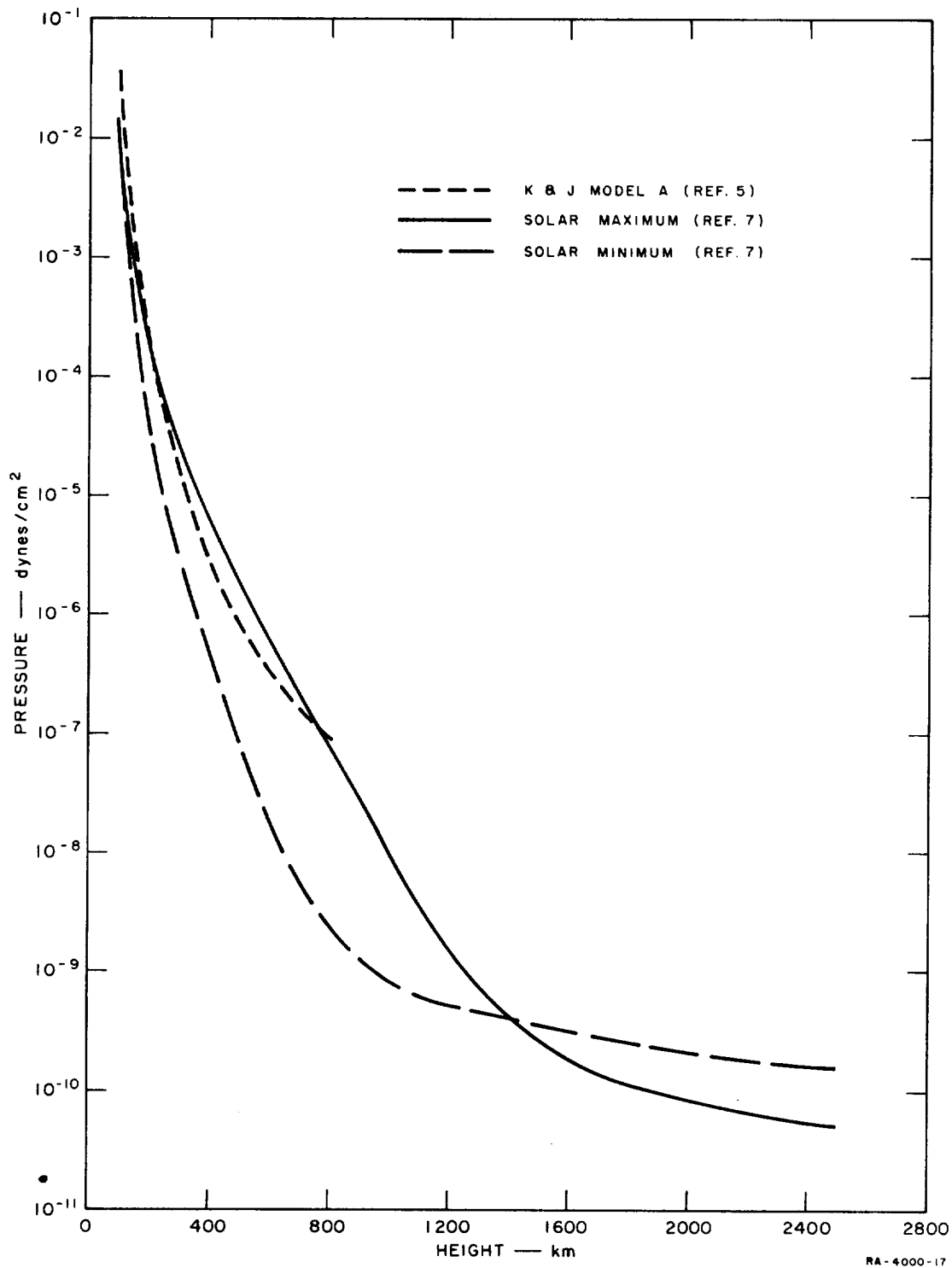


FIG. II-2-2 PRESSURE OF THE ATMOSPHERE vs. ALTITUDE

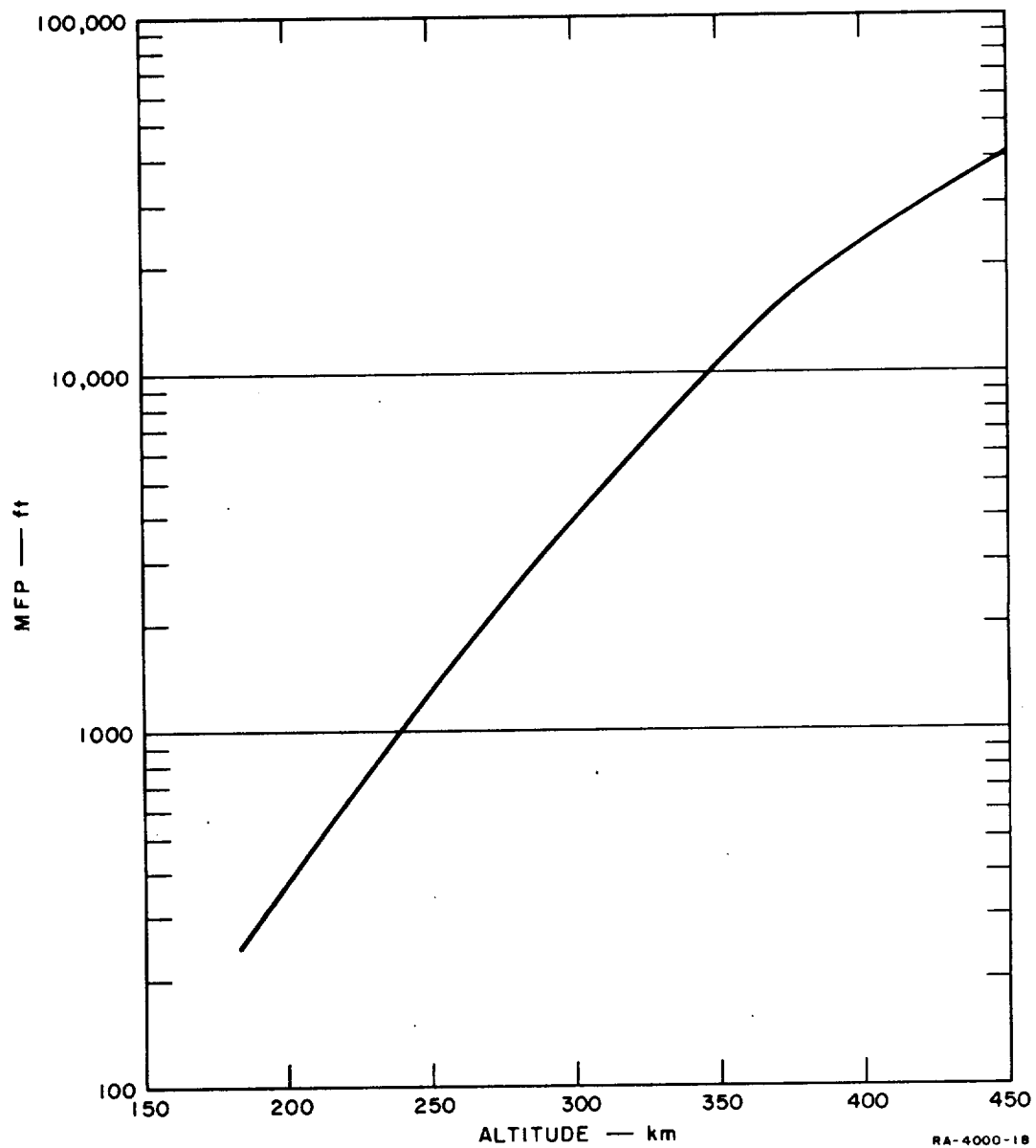


FIG. II-2-3 MEAN FREE PATH vs. ALTITUDE

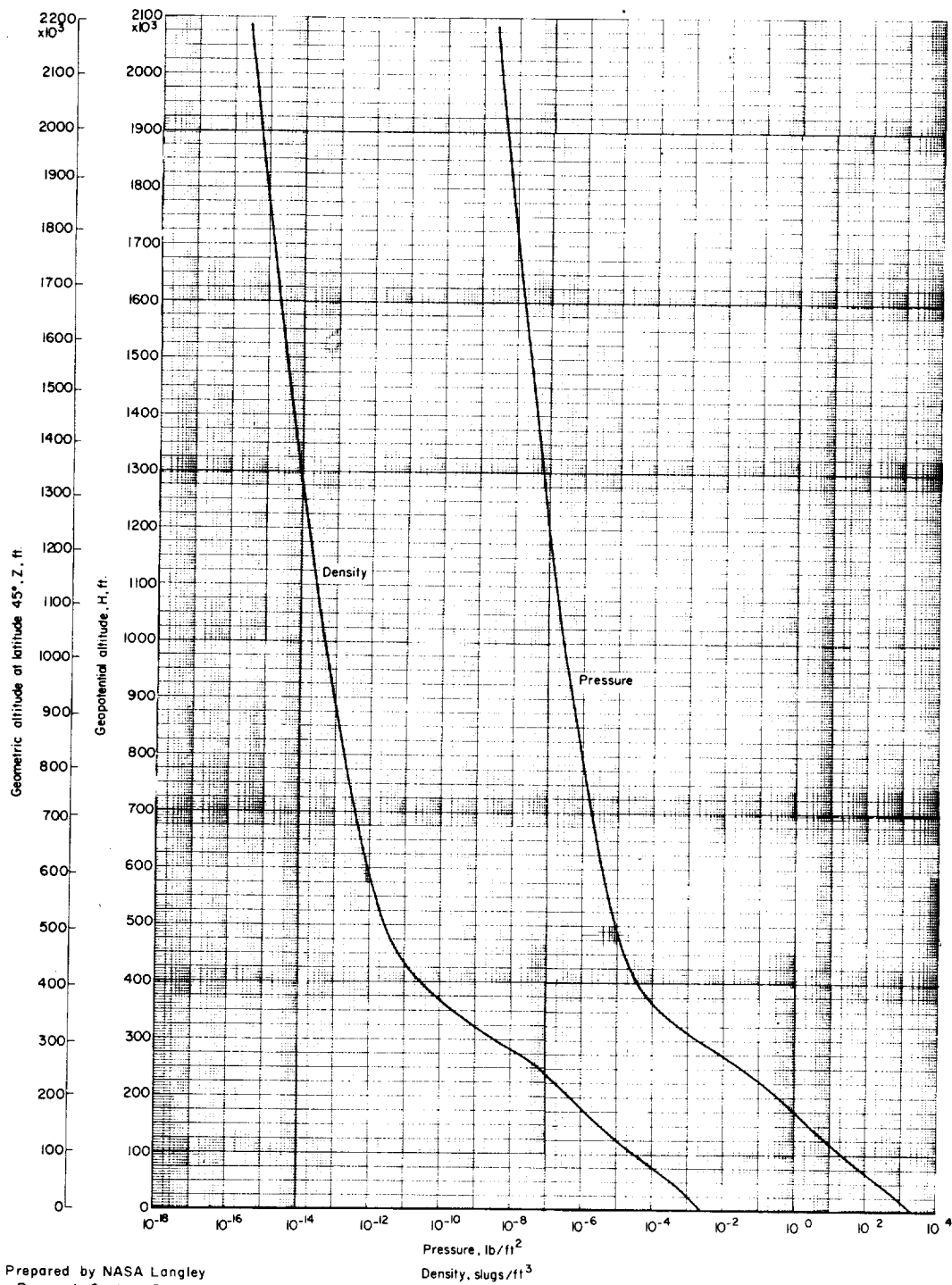


FIG. II-2-4 U.S. STANDARD ATMOSPHERE, 1962 (1)

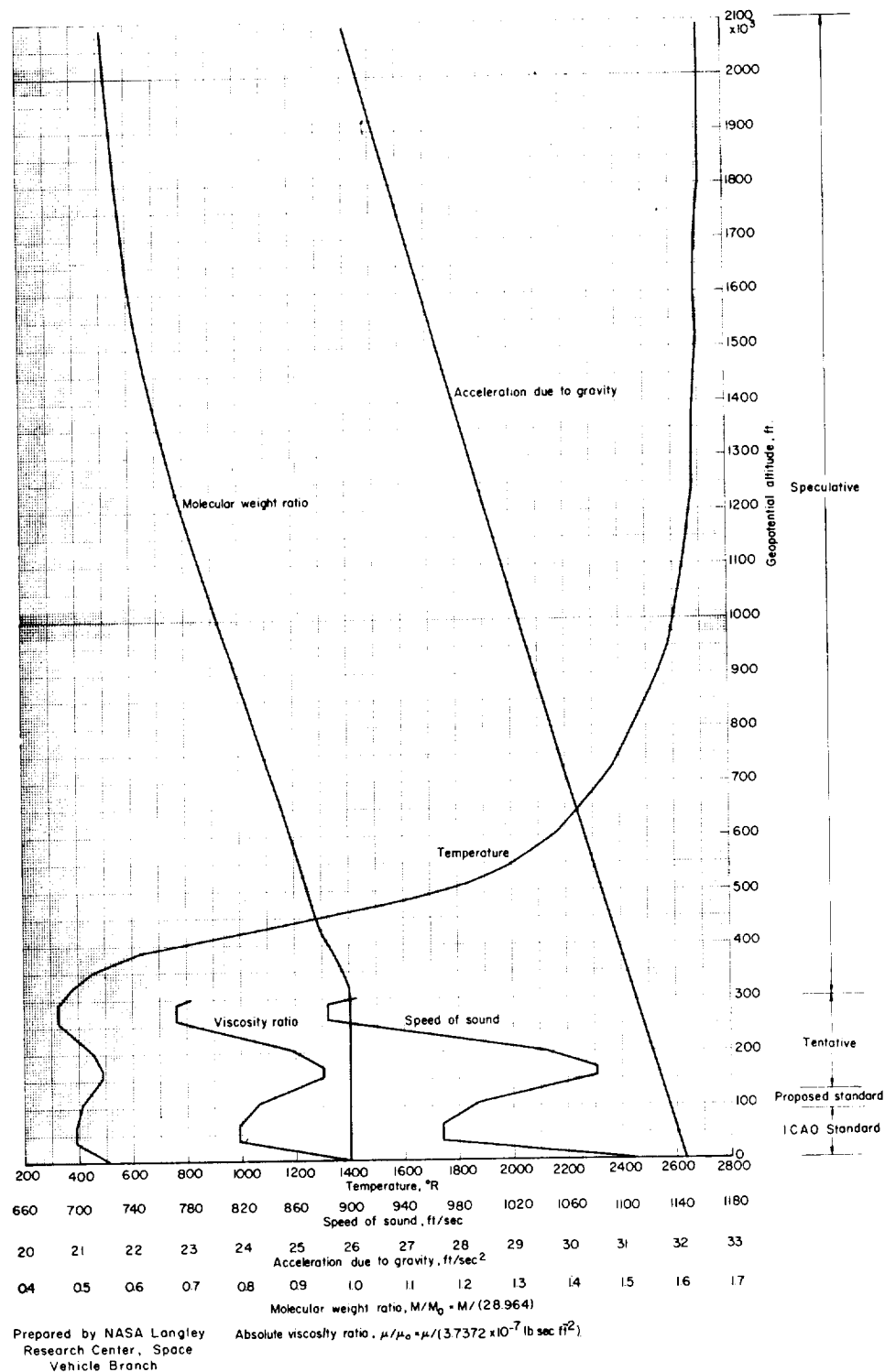


FIG. II-2-5 U.S. STANDARD ATMOSPHERE, 1962 (2)

(

(

(

(

(

II-3 METEORIODS

Meteoroids are solid particles in the solar system which range in size from 0.1 micron to several feet in diameter, and in weight from 10^{-15} grams to many tons with the small meteoroids being more prevalent than the larger ones. It is believed that the total meteoric accretion by earth is 1000 metric tons per day. The velocity of meteoroids is 28×10^3 m/sec (Whipple); for magnitudes 7 to 20, the average velocity decreases linearly from 28×10^3 to 15×10^3 m/sec. Meteoritic particles smaller than magnitude 30 are presumed to be swept out of the solar system by radiation pressure. The mass of individual meteoroids decreases by a factor of $10^{-0.4}$ for each apparent visual magnitude step and the number increases at the rate of $10^{+0.4}$ for each magnitude step. Thus, the mass of a meteoroid of magnitude $M + 1$ is $1/2.512$ times the mass of magnitude M and the number of magnitude $M + 1$ is 2.512 times the number of magnitude M .^{*} Although considerable information regarding meteoroids near or within the earth's atmosphere has been gathered, little information is currently available regarding size-density distributions in outer space. It is believed, however, that meteoroids are not randomly distributed in space (results of Mariner-II Venus flight) but that they are concentrated in orbits around the sun that intersect the earth's orbit.

The observed velocities of meteoroids on collision with the earth's atmosphere range from 10 to 80 km/sec. Space vehicles are also subjected to meteoroid bombardment; from 4 to 11×10^{-4} impacts/sec/cm² to less than 10^{-8} impacts/sec/cm² have been registered by meteoroid sensors on satellites. A meteoroid with a diameter as large or larger than the thickness of a space vehicle's shell, or with a mass equal to or greater than the mass of the shell, will penetrate with a clean hole, and the greater part of the initial momentum will be retained by the meteoroid as it passes through the shell. Meteoroids with diameters of from 10 to 20 percent of the shell thickness will just penetrate, or nearly penetrate; a crater will be formed on the impact site and the opposite side of the shell will show spalling.

^{*} A zero magnitude meteoroid is approximately 25 grams (Whipple).

The impact of micrometeoroids on the shell of a space craft will cause surface craters of microscopic size which gradually erode the surface. It is estimated that about one percent of the total surface area of a satellite reasonably close to the earth will be cratered at the end of one year,^{12,13} thus gradually affecting the vehicle's equilibrium temperature by changing the absorptivity (or emissivity) of the outer surface.

Calculation of the frequency of penetration of a space vehicle by meteoroids is, at best, uncertain. Wiederhorn,¹³ on the basis of Bjork's penetration theory, Whipple's frequency estimates, and an average meteoroid velocity of 70,000 ft/sec, constructed the graph shown in Figure II-3-1 which indicates the probability of no penetrations per 100 square feet of surface area versus time and wall thickness. The graph shows that for a propellant storage tank of reasonable volume, mounted outside a space vehicle, the required wall thickness for a high probability of no penetration over a relatively long time period would be too great to be practical. Hence, various systems of "meteor bumpers" are being considered as an approach to a light-weight protection system.

When a "bumper" or a double skin is used to afford protection from meteoroid penetration, incident particles are shattered as they penetrate the outer skin and then stopped completely by the inner skin. Tests have shown that a bumper skin at least $\frac{3}{4}$ -in. away from the inner skin is effective; either skin may be the load-carrying structure of the spacecraft. The two skins may be proportioned:

$$T_1 = \frac{T_0}{12} \qquad T_2 = \frac{T_0}{4}$$

where T_1 and T_2 are the thicknesses of the outer and inner skins, respectively, and T_0 is the total thickness required to give the desired degree of protection (Figure II-3-1). Although aluminum is generally considered adequate for protective skins, other materials may be substituted; data given in Table II-3-1 indicates thickness and weight trade-offs which result from use of materials other than aluminum.

II-3.2

Table II-3-1

METEOROID BUMPER MATERIALS FOR EQUIVALENT PROTECTION

MATERIAL	DENSITY	RELATIVE THICKNESS	RELATIVE WEIGHT
Aluminum	0.098	1.00	1.00
Magnesium	0.065	1.32	0.88
Beryllium	0.066	0.72	0.48
Filament wound plastic	0.077	1.61	1.24
Fused silica	0.079	1.05	0.85
6Al-4V titanium	0.160	0.72	1.18
17-7PH steel	0.276	0.49	1.38

—

—

—

—

—

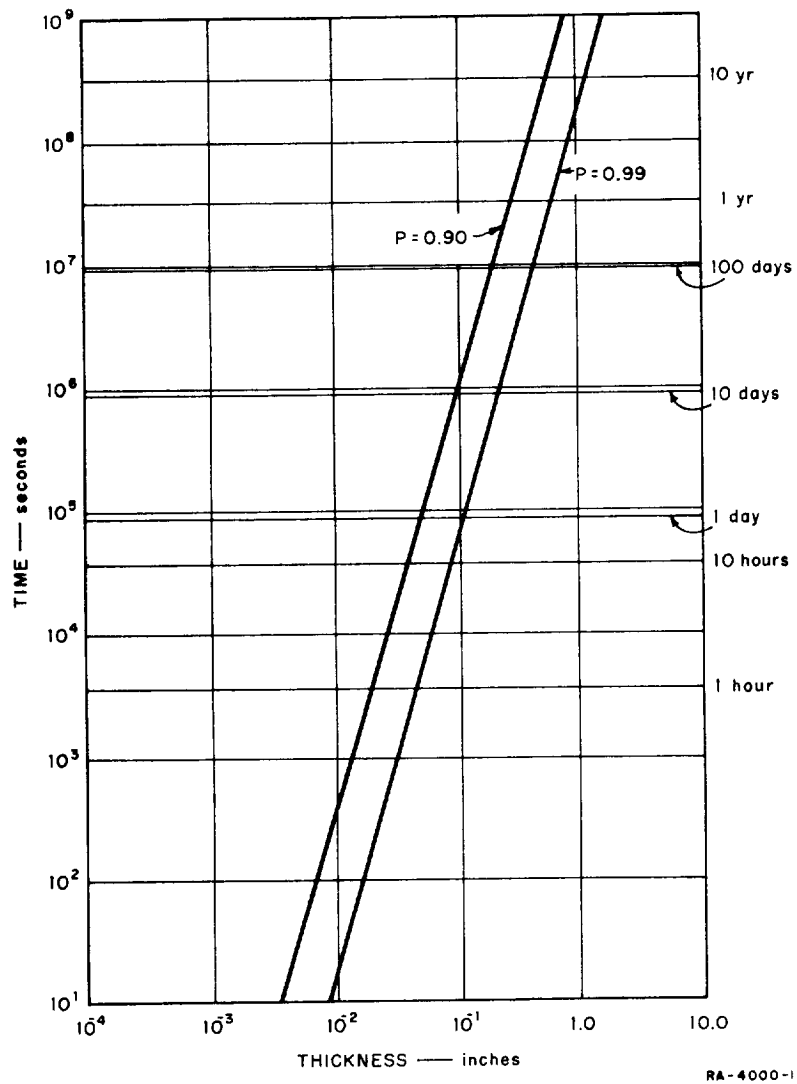


FIG. II-3-1 PROBABILITY OF NO METEOROID PENETRATION
IN 100 SQUARE FEET OF SURFACE AREA

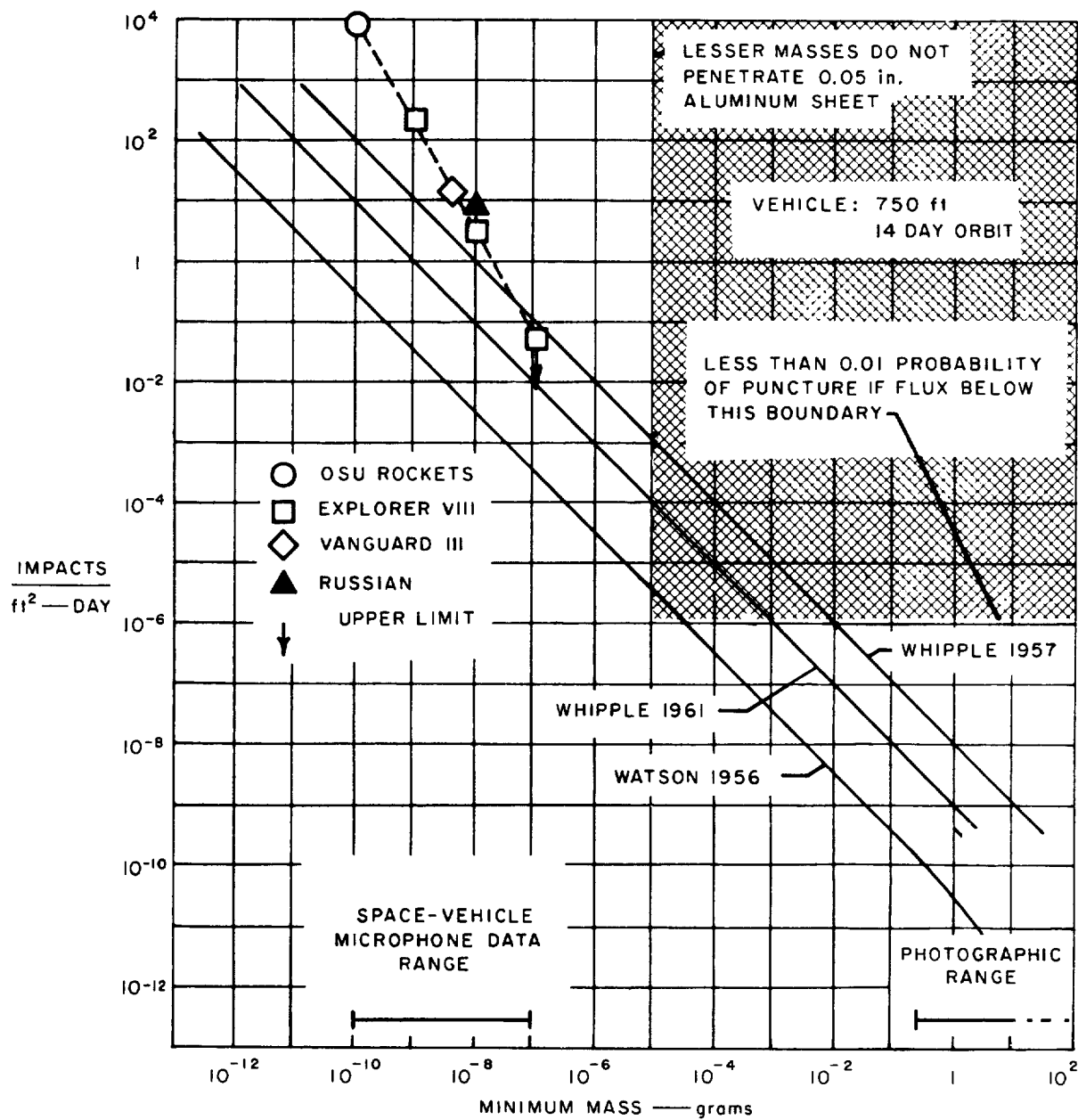


FIG. II-3-2 ESTIMATES OF METEOROID FLUX IN THE VICINITY OF THE EARTH (Ref. 21)

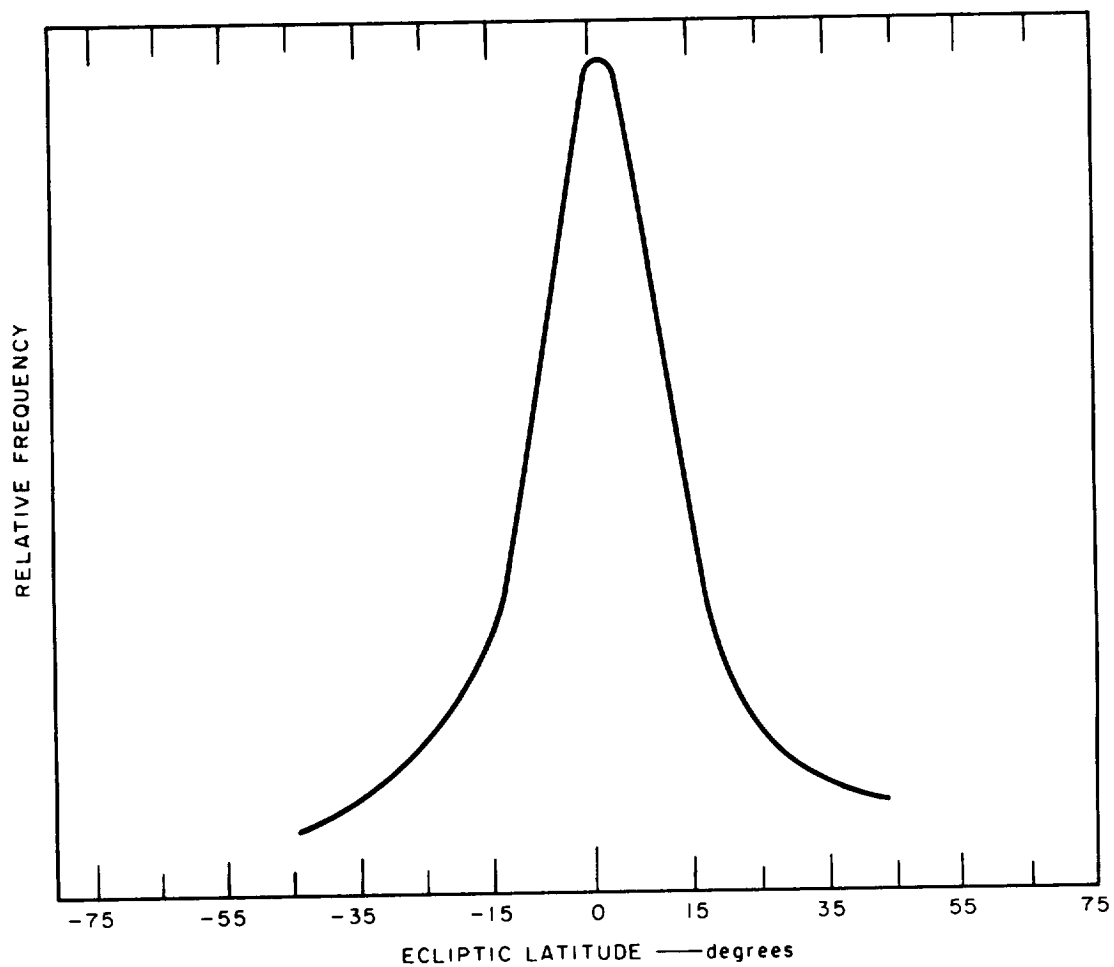


FIG. II-3-3 DISTRIBUTION OF THE METEOR FLUX ABOUT THE PLANE OF THE ECLIPTIC AT THE EARTH'S DISTANCE FROM THE SUN (Ref. 21)

II-4 COSMIC RADIATION

Cosmic radiation is the flux of highly energetic particles existing outside the earth's atmosphere and assumed to permeate interplanetary and intergalactic space. The nature of the cosmic radiation immediately outside the earth's atmosphere depends appreciably upon the geographical location and direction of observation relative to a vertical on the earth's surface. The geographical and directional dependence of the cosmic radiation has been shown to be governed by the interaction of the earth's magnetic field and the charged particles of the cosmic radiation. The primary cosmic radiation is extraterrestrial in origin.

Upon arrival of the primary radiation in the vicinity of the earth, but well outside of its atmosphere, the primary particles follow curved paths in the terrestrial magnetic field without interacting in any way with their surroundings. Primary particles which fall closer to the earth follow practically rectilinear paths and generally interact with the atoms or ions of the outer fringes of the earth's atmosphere to produce less energetic secondary cosmic radiation. Thus, the outer atmosphere of the earth contains a mixture of primary and secondary radiation of a composition governed chiefly by ambient pressure.

Secondary cosmic radiation is composed of diverse elementary particles and some nuclei which are heavier than protons. The most common elementary particles found in secondary cosmic radiation are: electrons, positrons, photons, mu-mesons, pi-mesons, protons, neutrons, and neutrinos.

Showers of cosmic radiations are readily observed on the earth's surface whenever surges of primary cosmic radiations interact with the upper atmosphere at altitudes between 15 and 35 km, and the resulting highly energetic secondary cosmic rays react further to yield extraordinary amounts of additional secondary radiation.

Galactic cosmic radiation consists primarily of protons and alpha particles with smaller quantities of heavier elements; the composition of galactic cosmic radiation reflects heavily the distribution of atoms in the universe as indicated in the following table:

II-4.1

APPROXIMATE COMPOSITION OF THE UNIVERSE
AND OF COSMIC RADIATION

ELEMENT	% OF ATOMS IN UNIVERSE	% OF ATOMS IN COSMIC RAYS
H	90	90
He	9.0	9.0
C, N, O	0.9	0.5
Other	0.1	0.1

The energy spectrum of cosmic rays is indicated in Figure II-4-1; it can be seen that the free-space flux of cosmic ray particles is quite small and of concern only for very long missions in space. Shielding for particles of these very high energies is impractical and there is likelihood that secondary x-rays and particles produced by shielding may actually increase damage.

The vertical flux of cosmic particles is a function of the geomagnetic latitude (see Figure II-4-2).

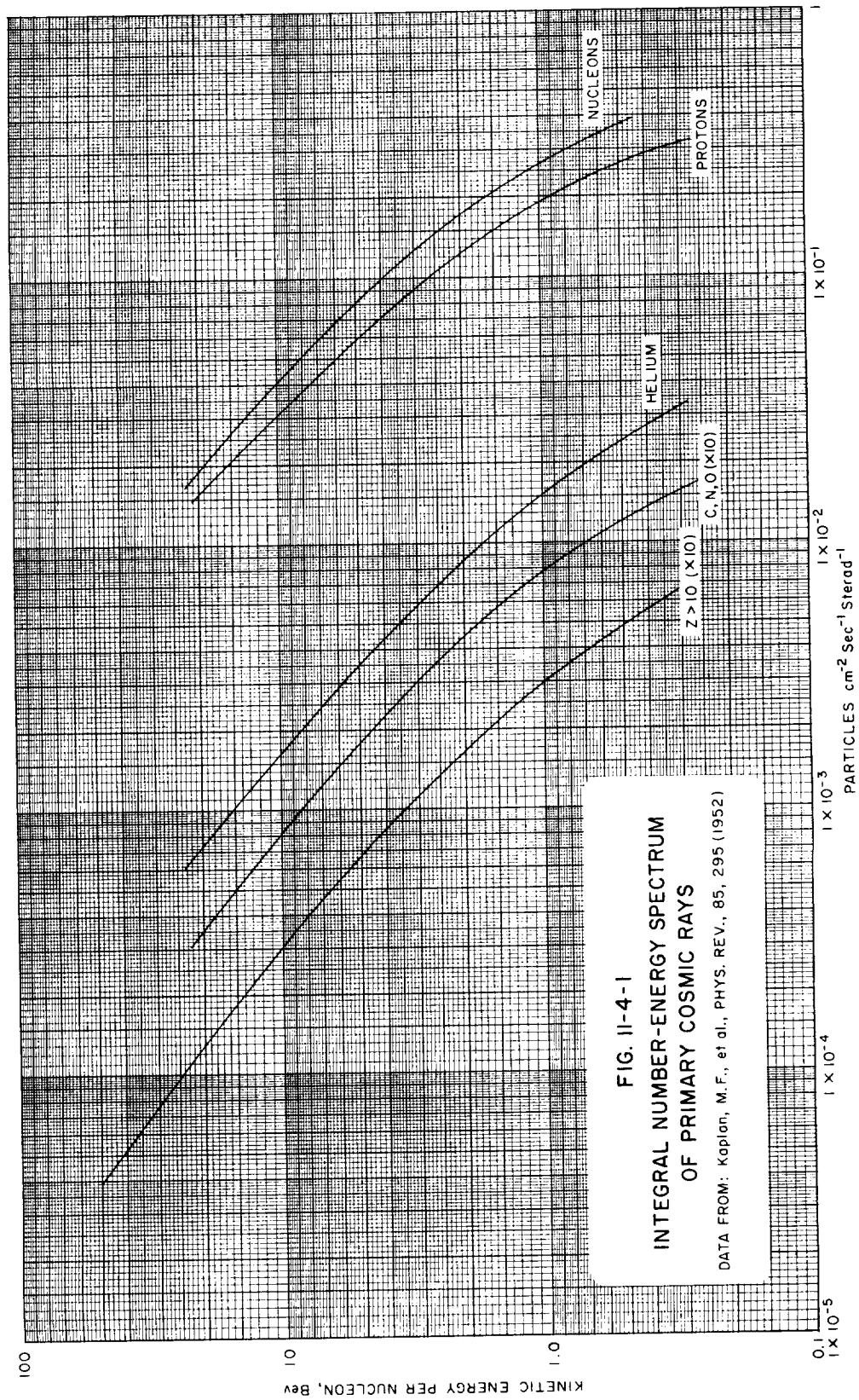
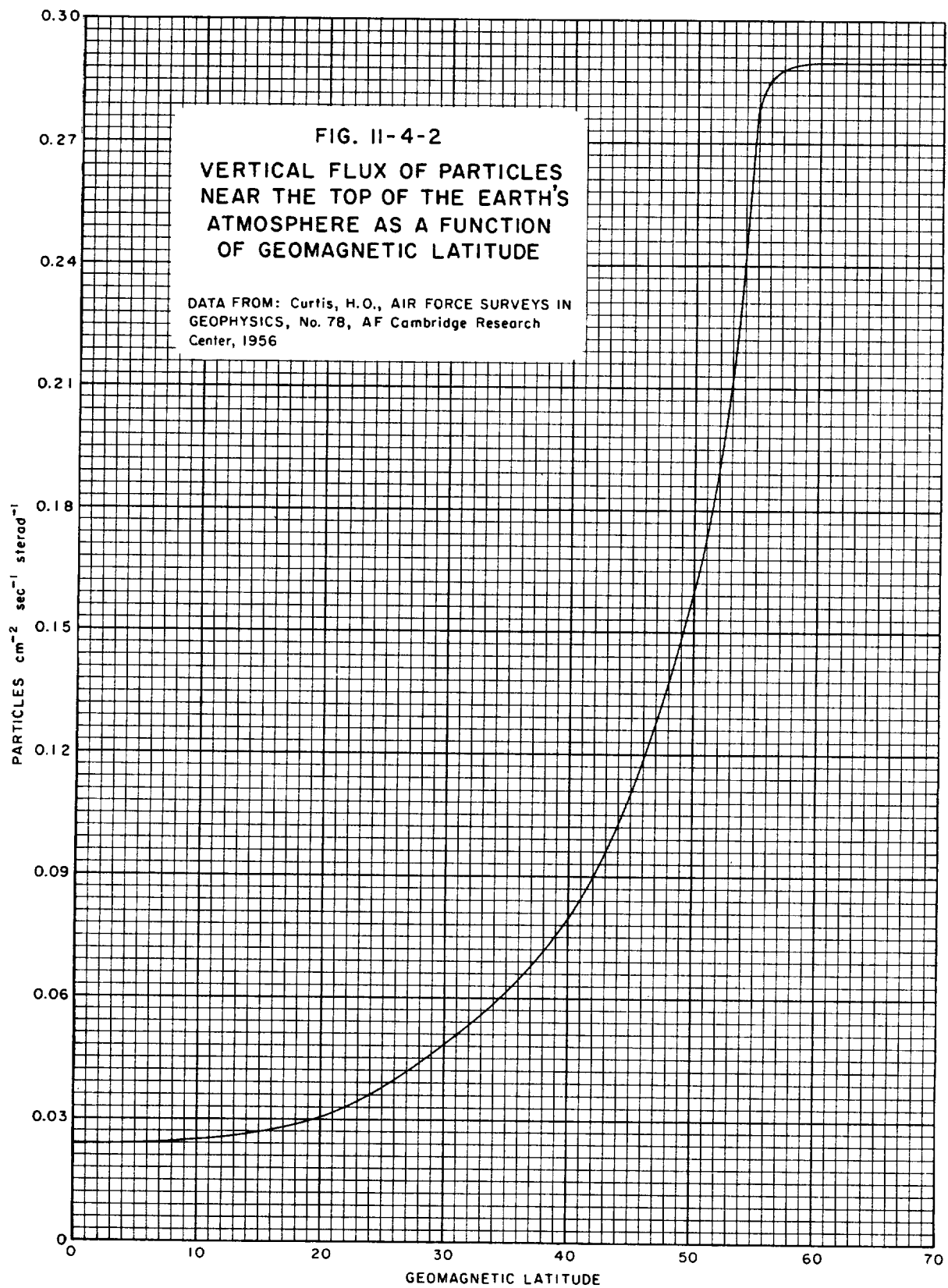


FIG. II-4-1
 INTEGRAL NUMBER-ENERGY SPECTRUM
 OF PRIMARY COSMIC RAYS
 DATA FROM: Kaplan, M. F., et al., PHYS. REV., 85, 295 (1952)



II-4.4

II-5 SOLAR EMANATIONS

Solar Winds

The sun issues a continuous stream of particles from its surface which extends far beyond the earth. These particles have an average velocity of 500 km/sec and an equivalent kinetic temperature of the order of 2×10^6 °K. The concentration of particles at 1 earth distance from the sun varies widely as a function of solar activity; generally, however, the concentration is of the order of 10-100 particles/cc.

Solar Flares

When great storms erupt on the surface of the sun, solar winds increase dramatically. A solar flare can create an average energy and particle density many times greater than the normal, continuous radiation from the sun's corona and photosphere. The highest energy particles released by a flare (greater than 10^4 Mev) begin to arrive at the earth almost instantaneously, followed by particles of lower energy; the particles continue to arrive at the earth for many hours, and, in extreme cases, for days after the disappearance of the flare. During large flares, average fluxes are as high as 10^4 - 10^5 particles/cm²/sec and, in general, the energy spectrum ranges from 30 to 300 Mev. The frequency of solar flares tends to follow sun-spot activity, and during periods of high activity, 10-12 flares may occur each year.

Interplanetary Zone

Radiation in the interplanetary zone consists of primary cosmic radiation from outside our solar system and the primary cosmic radiation indigenous to solar winds and solar flares. The primary cosmic radiation originating outside of our solar system is extremely stable and of exceptionally high energy; the cosmic radiation with solar phenomena is temporally erratic and of relatively smaller energy. On the other hand, very large solar flares have occurred in which enormous quantities of energy are released in the form of highly relativistic protons; energetic flares such as these are relatively rare, and only nine have occurred in the last 20 years. Smaller solar flares may occur as often as 8 times a day.

Effect of Solar Emanations

Radiation from the sun causes appreciable ionization of the earth's atmosphere at high altitudes. Because of the low atmospheric density which exists at high altitudes, recombination of ions and electrons proceeds so slowly that concentrations of electrons persist even throughout the night. The electron density varies with the eleven-year solar cycle, and is generally higher during sunspot maximum.

During the day, five distinct layers are recognized, the *D*, *E*, *F*, *F*₂, and protonosphere. The graph shown in Figure II-5-1 (from Johnson⁷) identifies the regions and shows a typical daytime distribution of electrons as a function of altitude.

The shape and strength of the earth's magnetic field determines the extent to which charged particles from solar eminences (or from interaction of cosmic rays with the very outer fringes of the earth's atmosphere) are trapped and maintained in the earth's vicinity. The earth's geomagnetic axis is tilted about 11.5 degrees with respect to the axis of rotation of the earth, and it is therefore necessary to make allowances for this difference when making estimations of the radiation encountered in a trajectory or orbit. The general shape of the envelope of trapped particles around the earth is indicated in Figure II-5-2, where it can be seen that the particles are concentrated in an inner and an outer belt (Van Allen belts). The inner belt has a maximum intensity about 2000 miles above the ground at low latitudes; the maximum for the outer belt is at about 10,000 miles and extends to much lower heights at high altitudes.

The Inner Belt

Prior to the high altitude nuclear test bomb blast of July 9, 1962 above Johnston Island (Pacific Ocean), the inner belt was characterized as being composed essentially of protons; at present, there exist a large number of fission electrons of a peak omnidirectional intensity of the order of $10^9 \text{ cm}^{-2}\text{sec}^{-1}$ at an altitude of 1300 to 5500 km. The electrons have energies of the order of 5 to 7 Mev and approximately half have energies below one Mev. Measurements of the temporal decay of the fission electrons indicate a surprisingly low decay rate and it is expected that the artificial belt may last as long as 10 years.

Isointensity contours of the artificial electron belt are shown in Figure II-5-3.

Proton isointensity contours for particles of energy greater than 40 Mev are also shown in Figure II-5-3. The intensity contours in the inner radiation zone show small variations, generally less than about 3%, owing to arrivals of particles from solar storms. On the other hand, the earth's geomagnetic field acts as an excellent shield, for it excludes protons of energies less than about 6.8 Bev from the equatorial plane at altitudes below about 1.25 earth radii. A typical distribution in the heart of the inner belt may be:

10^4 protons/cm ² /sec	$E > 40$ Mev
10^{10} electrons/cm ² /sec	$E > 20$ Kev
10^8 electrons/cm ² /sec	$E > 200$ Kev
10^7 electrons/cm ² /sec	$E > 600$ Kev

The Outer Belt

The trapped particles in this belt consist principally (i.e., greater than 100 particles cm⁻²sec⁻¹) of electrons and protons of energy less than 10 Mev. The outer zone begins at about 2.25 earth radii and extends to about 10 R_e , with the heart located at about 3.6 R_e . The particle fluxes in the outer belt is influenced by solar storms, it not being uncommon to being increased by 10- to 20-fold or more. Magnetic storms and variations also may cause diurnal variations of two- or three-fold. Average values for particle fluxes in the heart of the belt are:

protons	more than 140 Kev	about 1×10^8 cm ⁻² sec ⁻¹
protons	more than 100 Mev	about 10 cm ⁻² sec ⁻¹
electrons	more than 500 Kev	about 2×10^7 cm ⁻² sec ⁻¹

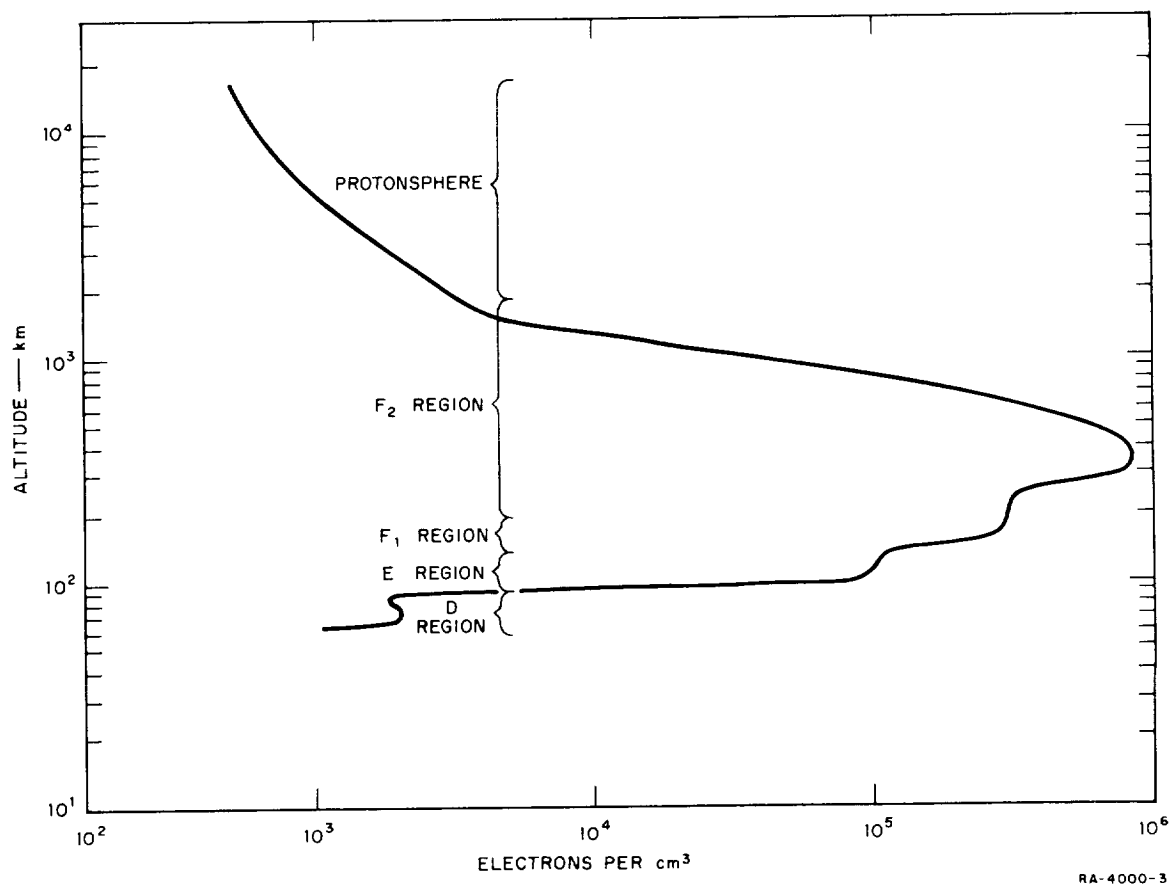


FIG. II-5-1 NORMAL DAYTIME ION DISTRIBUTION DURING SUNSPOT MAXIMUM

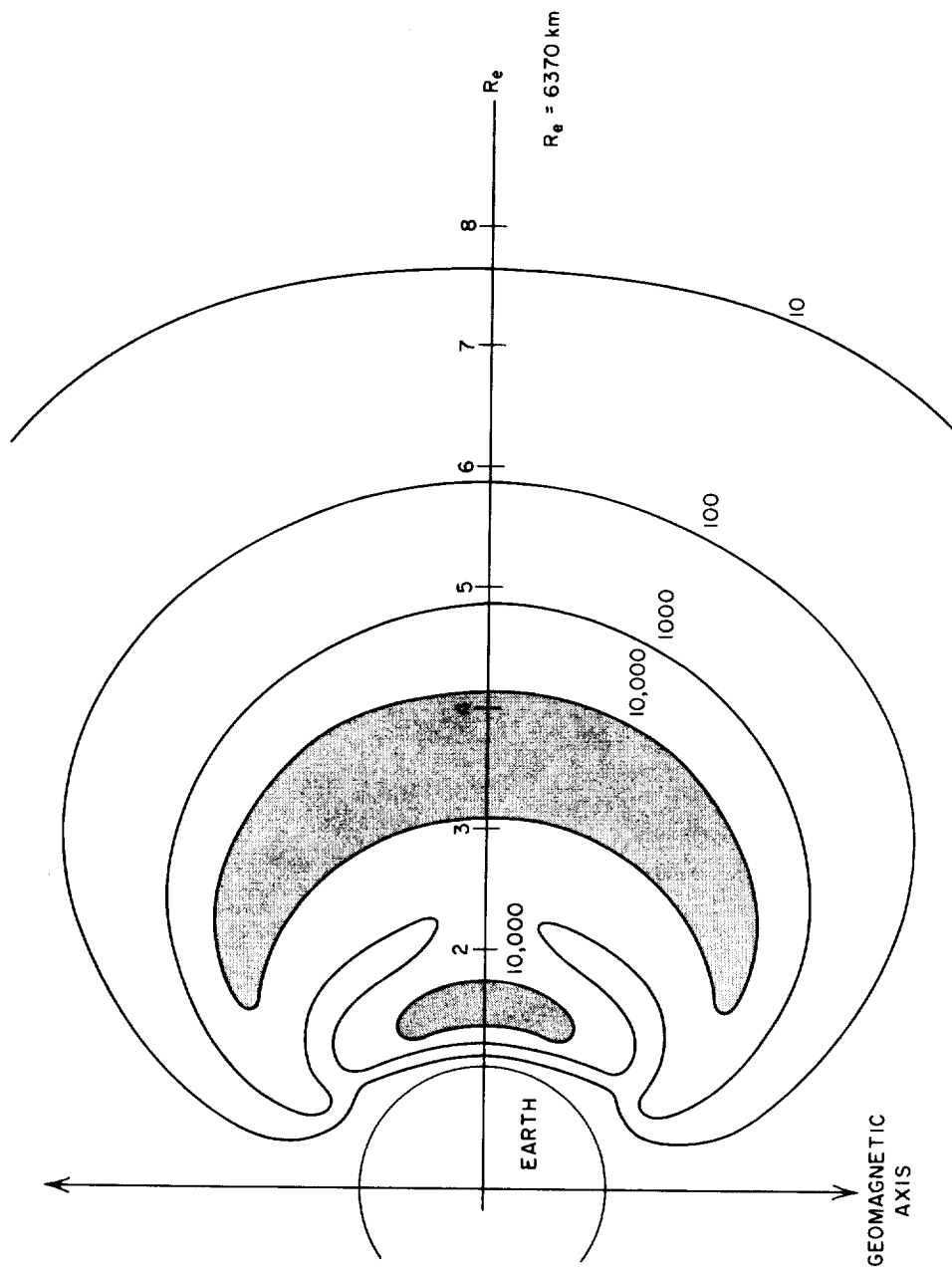


FIG. II-5-2 IDEALIZED DISTRIBUTION OF RADIATION

The contour lines indicate the counting rates of Geiger counters carried in Explorer IV and Pioneer III, and the shaded areas define the position of the two belts of intense radiation.

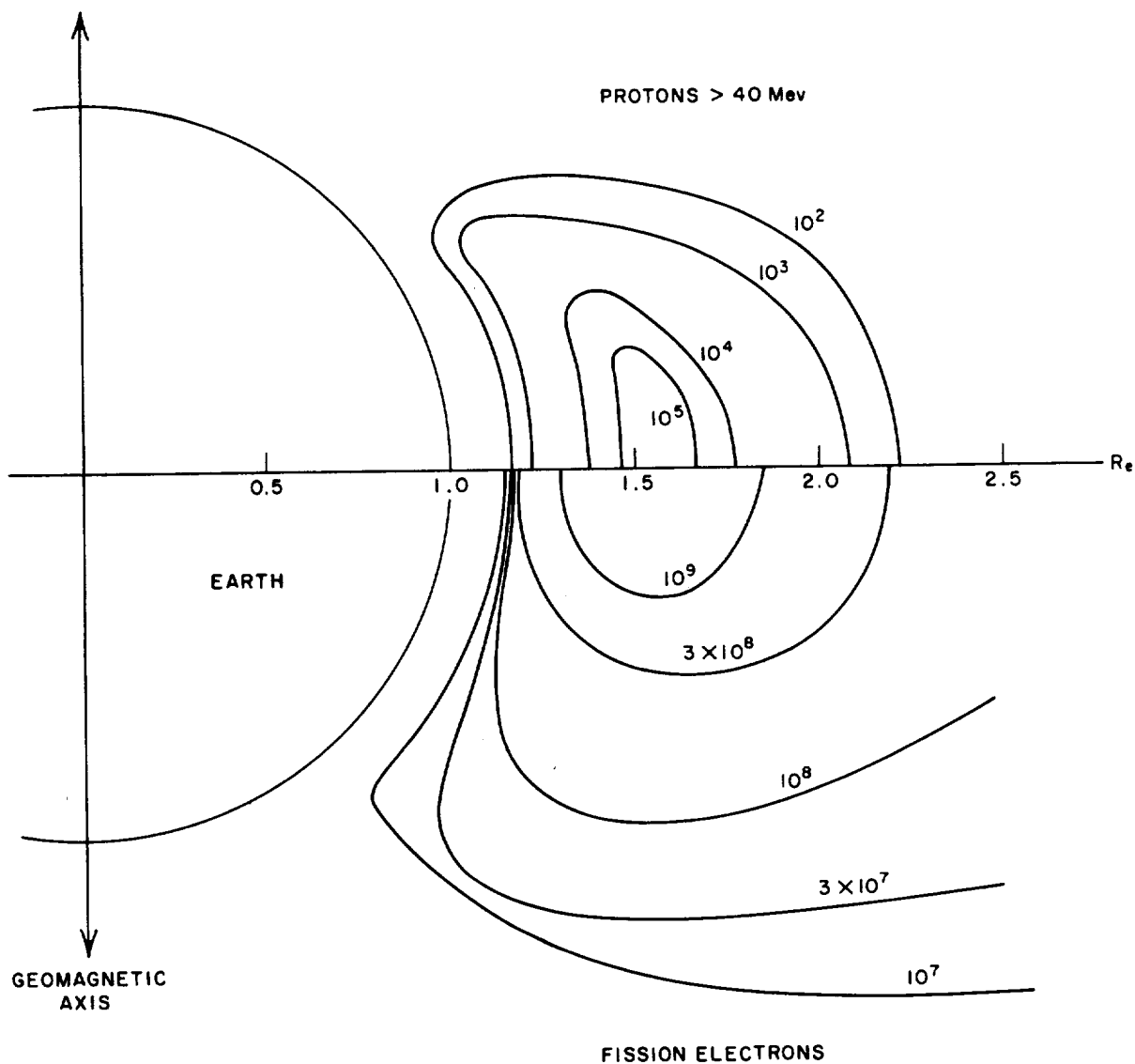


FIG. II-5-3 DISTRIBUTION OF PROTONS

The distribution of protons in the inner radiation belt is given in the upper part; the isocontour lines indicate protons $\text{cm}^{-2} \text{sec}^{-1}$. The approximate distribution of electrons in the artificial belt created by the high altitude nuclear blast of July 9, 1962 is indicated in the lower part of the diagram; the isocontour lines are electrons $\text{cm}^{-2} \text{sec}^{-1}$.

II-6 ELECTROMAGNETIC RADIATION

The spectrum of radiation emanating from the sun ranges from long radio waves (>1 cm), through infrared, visible and ultraviolet light, to x-rays (<100 Angstroms). Approximately 99% of the total energy flux lies within the wavelength region of 0.3 to 4 microns, but only the energy in the range of about 0.3 to 3 microns can penetrate the earth's atmosphere. The solar constant (irradiation per unit area normal to the direction of the sun) above the earth's atmosphere is generally accepted as being about $0.14 \text{ watts-cm}^{-2}\text{-min}^{-1}$; Figure II-6-1 illustrates the difference in the solar constant at sea level and outside the atmosphere, and also illustrates the attenuation of radiation by the earth's atmosphere. The unit of radiation, measured in g-calories per square centimeter is the langley (ly). Hence, $1 \text{ g-cal/cm}^2/\text{unit time}$ equals 1 ly/unit time ; in engineering units, $1 \text{ ly/min} = 1 \text{ cal/cm}^2/\text{min} = 221.2 \text{ Btu/ft}^2/\text{hr} = 698 \text{ watts/m}^2$. The solar constant is 1.95 ly/min .

The amount of solar radiation reflected from a planet's surface and atmosphere (albedo) must be considered in computations of radiation incident on spacecraft. The albedo figures can only be considered as average figures, and estimates have ranged from 0.30 to 0.40 for the earth; for most heat balance computations, the figure of 0.34 has been used. The most recent average albedo figures for some other planets and the moon are as follows: Moon, 0.07; Mars, 0.26; Venus, 0.73; Jupiter, 0.44.

The amount of thermal radiation emitted from the earth (wavelengths longer than 4 microns) also enters into computations for heat balance of a spacecraft in near-earth orbit. Figure II-6-2 illustrates a typical spectral-radiance curve for thermal radiation leaving the earth (from Johnson, Ref. 8); it is emphasized that this curve is only illustrative, since many variables enter into the problem.

The major effect of the electromagnetic radiation upon a propellant and its storage system is produced by the absorption of radiation which is transmitted as a heat input to the propellant. In the case of cryogenic propellants, heavy insulation and a venting system are required to minimize evaporation of the propellant and tank rupture.

In the case of storable propellants in unvented tanks, an equilibrium temperature will be reached where the rate of heat absorption will equal the rate of energy emitted from the surface of the storage tank.

For a tank that is tumbling in space and exposed to direct radiation, this temperature is equal to:

$$T = 3.3 \times 10^2 [A_r \cdot \alpha \cdot S/e]^{1/4}$$

where

A_r = ratio of average cross-sectional area to total surface area.

α = the average absorptivity of the surface of solar radiation.

S = solar constant in calories/cm²/min

e = emissivity of the surface corresponding to the temperature of the surface.

For a tank that is oriented in space, a complex temperature gradient would be established throughout the tank's surface and its content. However, it has been pointed out¹³ that in either case the equilibrium temperature is sensibly determined by the ratio of d/e , and this ratio can be controlled within reasonable limits, i.e., within the range of α/e from 0.15 to 20, through selection of the surface coatings.

Since α/e is determined solely by the properties of the surface, the stability of the surface to space environment is of importance. For example, radiation in the ultraviolet region will degrade organic paints and discolor inorganic material thus changing the ratio of α/e with time. It has also been observed that for materials with low values of α/e , the ratio tends to increase with time when exposed to an ultraviolet source. Thus one could expect the average temperature of a tank and its propellant to increase with time.

Additional information on the equilibrium temperatures of spacecrafts is given in Section VII, Heat Balance.

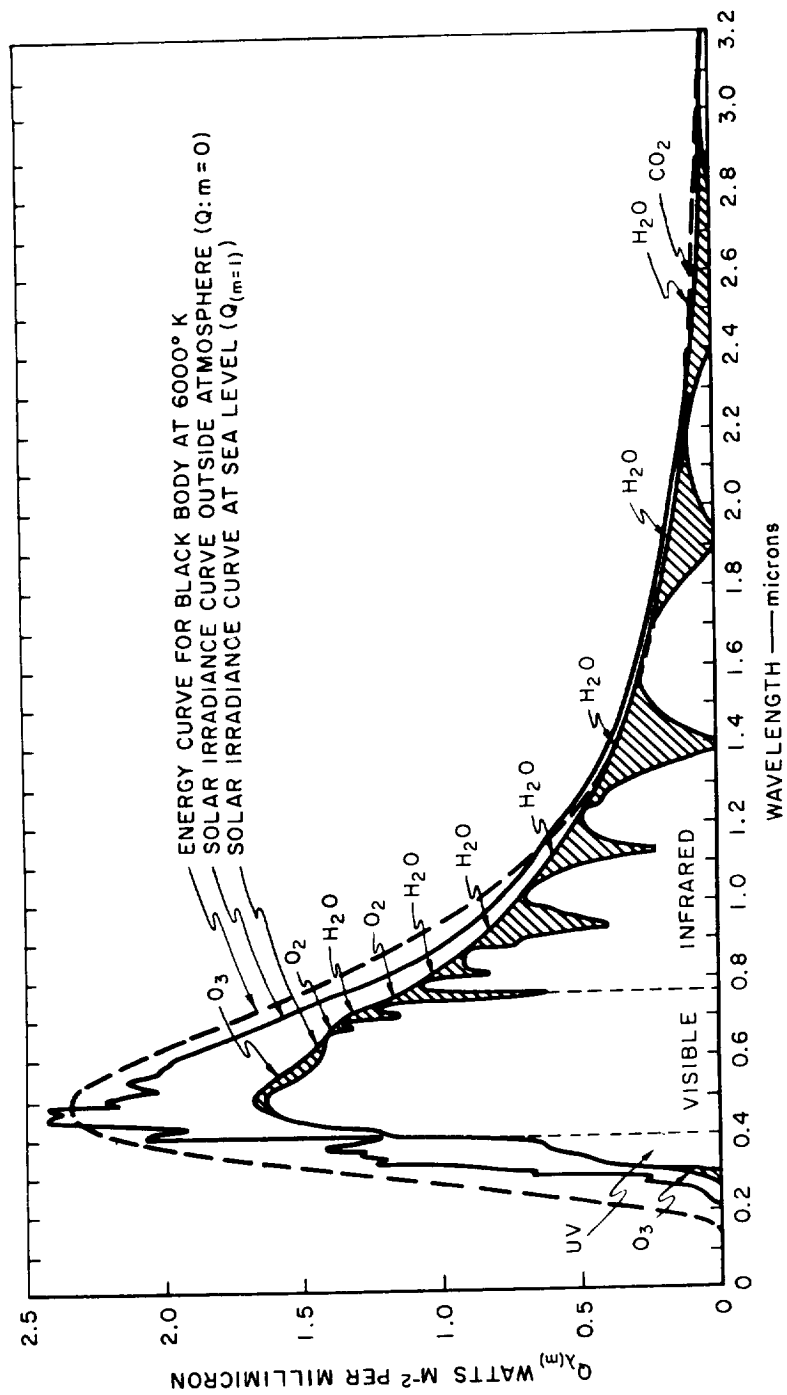


FIG. II-6-1 SPECTRAL ENERGY CURVES RELATED TO THE SUN

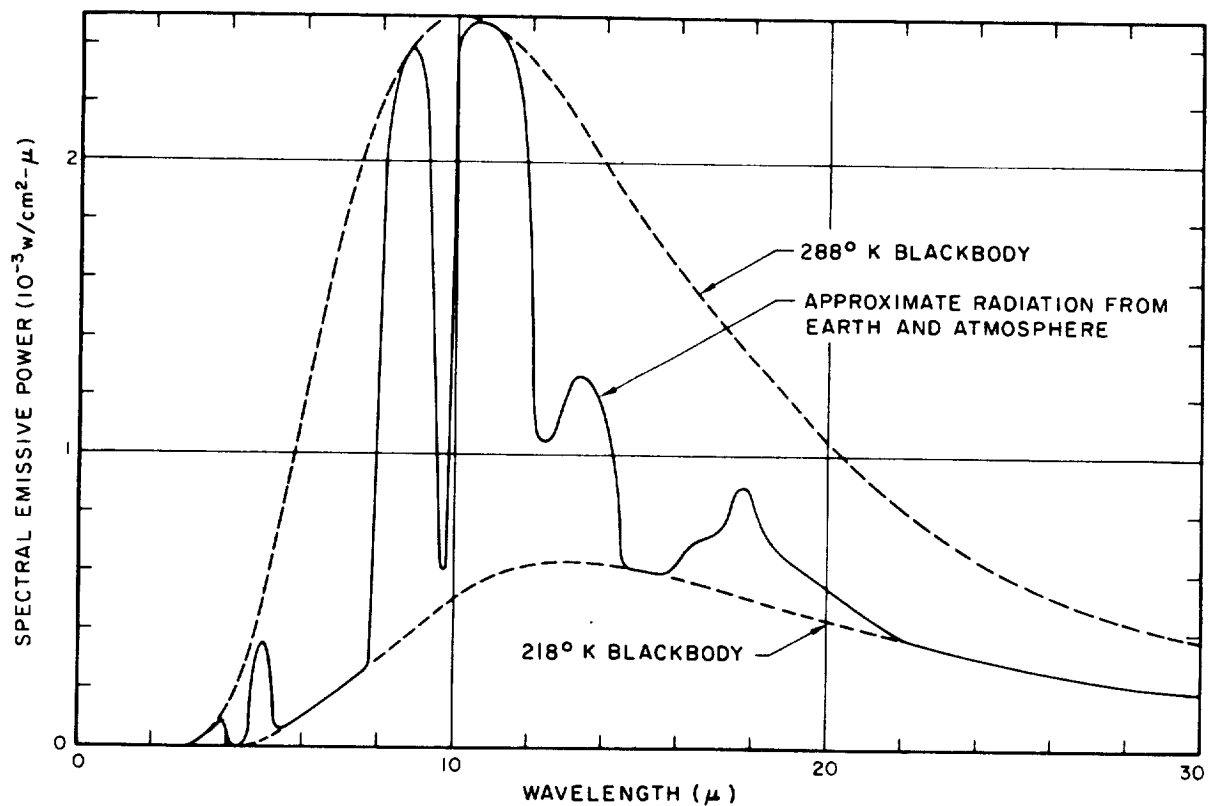


FIG. II-6-2 A TYPICAL SPECTRAL EMISSIVE POWER CURVE FOR THE THERMAL RADIATION LEAVING THE EARTH
 (The 288° K blackbody curve approximates the radiation from the earth's surface, and the 218° K blackbody curve approximates the radiation from the atmosphere in those spectral regions where the atmosphere is opaque.)
 (Ref. 8)

II-7 MAGNETIC FIELDS

Like the earth, the sun is known to have a magnetic field, and it is speculated that the sun's magnetic field is dipolar similar to the earth's. The origin of these magnetic fields is unknown although it is commonly thought that the earth's field is the result of the dynamic action of its molten metallic core. The fact that Venus apparently has no magnetic field and is probably not rotating lends support to this hypothesis; Venus should have an appreciable core. With the exception of Jupiter, nothing is known concerning the existence of magnetic fields around the other planets. Recent observations of radio emissions from Jupiter suggest that it has an ionosphere and a field with an intensity of about 2 gauss; the intensity of the earth's field ranges from 0.5 to 0.7 gauss at its surface. The best judgment at the present time is that the superior planets have magnetic fields of intermediate intensity.

Magnetic fields do not directly affect the storage of propellants in space. However, they do affect the collection and motion of charged particles; a planet without a magnetic field can not have a Van Allen radiation belt, since cosmic particles would not be bound in quasi-periodic orbits. Also, a metallic satellite orbiting a planet that possesses a magnetic field would be subject to attitude perturbing torques, and thus might need an elaborate attitude control system.

1

2

3

4

5

II-8 EFFECTS OF SPACE ENVIRONMENT ON MATERIALS

One of the major problems in the design of spacecraft systems is the requirement that the materials of construction withstand and perform in the space environment, *i.e.*, at zero gravity in a high vacuum simultaneously with ultraviolet and penetrating charged-particle radiations. Much experimental and theoretical work has been performed in an effort to determine the effects of the space environment because it is impossible, at this time, to simulate accurately the combination of conditions known to exist in space.

It is particularly difficult to simulate the charged-particle radiation of the space environment first because the particle distribution is not accurately known, and second because the energy spectrum (ranging from a few electron volts to as much as 10 billion electron volts) is not easily accessible. Thus, all laboratory values relating to the behavior of materials in a space environment can only be regarded as approximate at this time; it is anticipated that future space stations will provide facilities for testing of materials in the true environment.

Vacuum

The low pressure encountered in space is conducive to the loss of materials of construction by sublimation (or evaporation) because molecules which leave the surface of materials are not returned by collisions with ambient gas molecules. Thus, above altitudes of about 100 miles, the mean free path of a molecule at ambient temperatures is so long in comparison with the size of the spacecraft that any molecule which leaves the surface will not return. Loss of material by sublimation in the vacuum of space is intuitively obvious, but the effect of very high vacuum on the rupture and fatigue properties of materials is unexpected; however, experiments have indicated^{17,18} that the density of the gas surrounding a material is an important parameter defining its behavior under stress. Apparently, the character of the gas layer adsorbed on materials influences certain mechanical properties. Thus, prolonged exposure of materials to a space environment will alter or remove adsorbed

gas layers and some of the physical properties of the materials in space will be different than on earth.

The removal of material from a spacecraft structure will obviously lead to an over-all weakening of members. The weakening of a member can be simply computed by knowledge of the mass-strength relationship. Where gross sublimation of a material is involved, tests made before and after exposure of specimens to a vacuum will furnish experimental values. Ideally, the tests should be performed in an atmosphere closely resembling the space environment; however, for practical evaluation of the effects of sublimation, the most important condition to be met is that a molecule leaving the surface of the test piece has a negligible chance of returning.

The test chamber for evaluating the effects of sublimations on a material must provide the following:

- (1) A residual pressure low enough so that the mean free path of molecules is long with respect to chamber dimensions. For the residual-gas molecules in the chamber, the mean free path at 1×10^{-5} mm of Hg is of the order of several meters and thus, by maintaining a vacuum of at least this order of magnitude, the motion of molecules leaving the surface of the test piece is governed essentially by their collisions with the walls of the chamber and not by collisions with residual-gas molecules.

A high probability that molecules leaving the test piece will be removed from the chamber rather than returned to the surface of the test piece. This can be accomplished when the cross-sectional area of the pumping duct is large in comparison with the exposed area of the test piece and when both the test piece and the pumping duct can be freely exposed to the chamber. For testing materials, such as metal, which condense readily at ambient temperature, this condition is easily met because molecules leaving the test piece will condense on the chamber walls; however, when polymeric materials are to be tested, elaborate precautions must be taken to ensure removal of released substances. Baffles maintained at liquid nitrogen temperatures are often employed to condense organic matter and cooled baffles must always be employed in pump throats to prevent back-streaming of pump-fluid vapors.

The rate of evaporation of an ideal, pure substance is given by Langmuir's equation¹⁹:

$$E = \frac{P}{17.14} \sqrt{\frac{M}{T}}$$

where

E is rate in $\text{g}\cdot\text{sec}^{-1}\cdot\text{cm}^{-2}$ of exposed surface,

M is the molecular weight of the material,

P is the equilibrium vapor pressure in mm of Hg,

and

T is the absolute temperature, $^{\circ}\text{K}$.

Comparison of predictions from the above equation with experimental data indicate that the Langmuir equation is conservative; thus, the equation must be employed cautiously. Further, it is necessary to recognize that its use to predict vacuum volatility is limited by the following:

- (1) The vapor pressure, P , in the equation is the equilibrium pressure. In the space environment, molecules which leave the surface of the liquid or solid phase do not return, and thus equilibrium is not established.
- (2) The molecular weight of the evaporating molecules must be known; for most materials, this molecular weight is frequently different than assumed (association).
- (3) Oxide films or thin coatings may act as barriers to the escape of molecules.
- (4) In practice, most materials are complex mixtures (alloys or polymers) which defy simple treatment. The average, assumed molecular weight of a system can not be used in the equation.
- (5) The process of evaporation for systems of practical interest is very different from the purely random process assigned to ideal systems. For example, evaporation from localized planes of high surface energy is much greater than from planes of low energy; this leads to uneven evaporation, and etching of the surface becomes evident.

As is evident from the above discussion, the Langmuir equation is limited to approximations of evaporation rates in a space environment; it is useful in that it assists in the selection of appropriate materials of construction for spacecraft. For example, the equation indicates that every substance has a rate of evaporation in free space as long as the absolute temperature is not zero. Thus, at a given temperature, say 25°C , one should select materials which exhibit very low vapor pressures;

obviously, the usual metals of construction (iron, copper, etc.) can qualify, but there is some question about the lighter metals such as cadmium, magnesium, aluminum, etc. Table II-8-1 illustrates the estimated sublimation losses suffered by metals in a space environment at a temperature of 150°C; it is evident that cadmium and zinc do not appear to be useful metals for the construction of spacecrafts or components which are exposed to the high vacuum of space. Pure magnesium metal barely qualifies for the construction of spacecrafts; however, the alloys of magnesium which are currently used show considerably lower losses because the surface presented to the space environment acts as a barrier for sublimation (oxide-chromate conversion coatings, etc.). It is of interest to note that thin films of lead (as in soldered joints) may be weakened by prolonged exposure to the space environment. On the other hand, a thin coating of pure tin will act as an efficient barrier for sublimation of other materials.

The sublimation of materials from polymers or resinous matter is a complex phenomenon not expressible in the ideal case by a simple formula such as the Langmuir equation. This comes about because these materials contain a variety of ingredients; the basic polymer structure is usually composed of a distribution of nonvolatile molecules composed of a range of numbers of repetitive units but there are generally present various substances of relatively low vapor pressure which are added deliberately to modify properties (e.g., plasticizers).

Since the composition of plastic or polymeric materials of the type used in the construction of spacecrafts are not divulged in detail by commercial suppliers, and since it is impractical to approximate sublimation rates from theoretical considerations, experiments are necessary to determine the effect of exposure to the simulated vacuum of space. As a consequence there appear interspersed throughout the available literature results of various tests performed largely to determine the sublimation losses of typical polymeric material and, in some instances, the effect of these losses on physical properties.

For the most part, the sublimation loss suffered by polymeric materials is found by determining the loss in weight incurred over a period of time after exposure at a given temperature to a vacuum of at least 1×10^{-6} mm of Hg. The results obtained are thus largely determined by factors such as the geometry of the test specimen, the temperature,

the mobility of the easily volatile components within the specimen, the pressure of residual gas in the test system, etc. Furthermore, since the generic structure of most polymeric materials has a very low vapor pressure, only low-molecular weight material is removed by sublimation (especially if the polymer is cross-linked). Thus, it is meaningless to extrapolate the observed weight loss to make estimates of the "life" of a polymeric substance in space (as can be done for pure metals). On the other hand, if a material suffers a loss of 5-10% after exposure for 100 hours at a temperature of not more than 125°C, it may be assumed that the physical properties are so altered by this loss that the material should not be used for construction of spacecrafts. But even in these instances, an actual check on the physical properties is necessary before the material is summarily rejected. The irregular behavior of polymers and the necessity for long exposure time indicates that published results must be examined carefully for validity.

Numerous tables of values for the outgassing rates of various polymeric substances are available and are useful for determining the type of materials to be used for construction of vacuum systems. It is to be emphasized, however, that a high outgassing rate should not be used as a criterion for rejecting materials for use in spacecrafts (see Table II-8-2).

The physical properties of most polymeric materials suitable for space use seldom change more than 10% on exposure to vacuum at temperatures less than 125°C. For the most part, physical property tests have been performed on samples "before" and "after" exposure; it is only recently that a limited number of results have been obtained for tests performed *in vacuo*. The results obtained *in situ* supposedly reveal the effect of an adsorbed gas layer on the mechanical properties of the material. It is not possible at this time to predict what kind of gas film will form on a material in space, and it is probably even more difficult to provide a synthetic environment on earth that will deposit the required gas film. As a consequence, and largely because all of the test equipment employed thus far for *in situ* polymer testing are notoriously poor in design (from the viewpoint of control of adherent gas films) it is recommended that published results be regarded with skepticism.

Radiation

Intense nuclear radiations alter properties of solid materials so profoundly that extensive studies have been required to establish the behavior of engineering materials in piles or in the vicinity of reactors. The interaction of radiation with matter leads to the production of ionization effects, vacancies and interstitial atoms, thermal spikes, displacement spikes, impurity atoms, etc. Depending on the type of material subjected to radiation, any or several of these interactions will define the response of the material. Metals are very sensitive to vacancies, interstitial atoms, etc., while the behavior of organic materials can best be explained as the results of ionization effects.

The ionization and electronic excitation produced by passage of charged particles through organic matter generally results in the rupture of bonds, formation of free radical, luminescence, and even coloration. The greater part of the energy of the incident radiation is discharged in organic material by ionization mechanisms; thus, as a general rule, the gross radiation damage produced in an organic substance is proportional to the energy absorbed. The semiconductor properties of organic substances are extremely sensitive to radiation-induced displaced atoms, and it is incorrect in these (or similar) instances to assess damage by total energy absorption.

When radiation damage can be assessed by energy absorption, the radiation tolerance is expressed in energy units, typically as ergs per gram, although it is also common to indicate the radiation environment in r units (Roentgens). The relationship is, approximately, $1 r = 87 \text{ ergs/g}$ in air. Most tests of the radiation resistance of polymers have been performed in air; consequently, the values imply that the degradation mechanisms include the reaction of ionized air molecules with the basic organic structure. Some tests have been performed in vacuum; in these instances, it is necessary to examine the experimental technique in order to ascertain that the specimens were thoroughly outgassed (very difficult to achieve in thick sections).

Various estimates have been made of the radiation dose rates encountered by spacecrafts in various types of near-earth orbits established in the hearts of the inner or outer zones of radiation²⁰. The following table summarizes the typical dosages:

Table II-8-3
ESTIMATED MAXIMUM RADIATION DOSAGES FOR VARIOUS ORBITS

ORBIT	APPROX. PERIOD	MAX. PARTICLES/cm ² /DAY		MAX. DOSAGE, rad/day		
		Electrons	Protons	Electrons	Protons	Total
Polar	3 hr	10 ¹³	10 ⁹	10 ⁵	10 ²	10 ⁵
Polar	12 hr	10 ¹³	--	10 ⁵	--	10 ⁵
Equatorial	3 hr	10 ¹⁴	10 ¹⁰	10 ⁶	10 ³	10 ⁶
Equatorial	12 hr	10 ¹³	--	10 ⁵	--	10 ⁵

The values given in Table II-8-3 can easily be converted to more realistic values for orbits outside the radiation belts by comparisons with expected particle densities as indicated in Figures II-5-2 and II-5-3. However, since most of the polymers used in spacecrafts begin to degrade at total radiation dosages of the order of 10⁸, the data given in Table II-8-3 indicate that spacecraft performance may be affected in 4 to 12 months if orbits are established in the radiation belts (provided the polymers are exposed). Fortunately, the mere interposition of a thin metal shield significantly decreases the deleterious effects of the particles of the radiation belts. For example, the total dosage of a maximum of 10⁶ rad per day indicated in Table II-8-3 can be reduced about a thousand-fold with 50-mil aluminum shielding.

The various elements of the ionizing radiation environment can have a number of reactions with a propellant and its storage system. Liquid propellant losses during space flights may occur because of the following possible effects:¹³

A change in absorptivity and emissivity of outer metallic or metal oxide surfaces due to sputtering.

Radiation embrittlement of metals due to dislocations.

Embrittlement of structural materials due to radiation-induced dissociation of hydrogen and diffusion of the hydrogen atoms into metals with the formation of hydrides.

Desorption of gases absorbed in multi-layer radiation shielding thereby changing the gas pressure within the shielding.

Formation of ozone in liquid oxygen, or oxides on the inside tank walls.

Decomposition of hydrazine and UDMH.

On the basis of the best estimates available regarding the flux and energy spectrum of radiation in space, including an average input of solar flares, Wiederhorn¹³ states that the total dosage received by a propellant in a stainless steel tank with a wall thickness of 50 mils would be of the order of a few rads per hour in the center of the inner Van Allen belt; it is stated that this dosage rate is so low that the effects listed above are all negligible.

Table II-8-1
ESTIMATED SUBLIMATION LOSSES OF METALS IN SPACE AT 150°C

METAL	RATE OF EVAPORATION (g/cm ² -sec-1)	PERCENT LOSS IN ONE YEAR FOR INITIAL THICKNESS OF METAL IN INCHES			
		0.2	0.1	0.05	0.01
Aluminum	1 x 10 ⁻¹⁴	2 x 10 ⁻⁵	5 x 10 ⁻⁵	1 x 10 ⁻⁴	5 x 10 ⁻⁴
Cadmium	1 x 10 ⁻⁶	←	100%	→	→
Copper	1 x 10 ⁻¹⁹	←	negligible	→	→
Iron	1 x 10 ⁻²⁰	←	negligible	→	→
Lead	1 x 10 ⁻¹⁰	0.055	0.10	0.20	1.0
Magnesium	5 x 10 ⁻¹⁰	1.8	3.5	7.0	35
Tin	5 x 10 ⁻¹³	4.3 x 10 ⁻⁴	8.5 x 10 ⁻⁴	1.7 x 10 ⁻³	8.5 x 10 ⁻³
Zinc	1 x 10 ⁻⁷	←	100%	→	→

Table II-8-2
TYPICAL OUTGASSING RATES FOR MATERIALS

MATERIAL	OUTGASSING RATE, -2 liter-mm-sec-1-cm ² AFTER INITIAL EVACUATION	
	1 Hour	8 Hours
Aluminum	10 ⁻⁶	10 ⁻⁸
Stainless steel	10 ⁻⁶	10 ⁻⁸
Silver	10 ⁻⁶	10 ⁻⁸
Steatite	10 ⁻⁷	10 ⁻⁸
High vacuum waxes	10 ⁻⁷	10 ⁻⁸
Polyethylene	10 ⁻⁶	10 ⁻⁷
Nylon	10 ⁻⁵	10 ⁻⁶
Methacrylates	10 ⁻⁵	10 ⁻⁶
Teflon	10 ⁻⁶	10 ⁻⁸

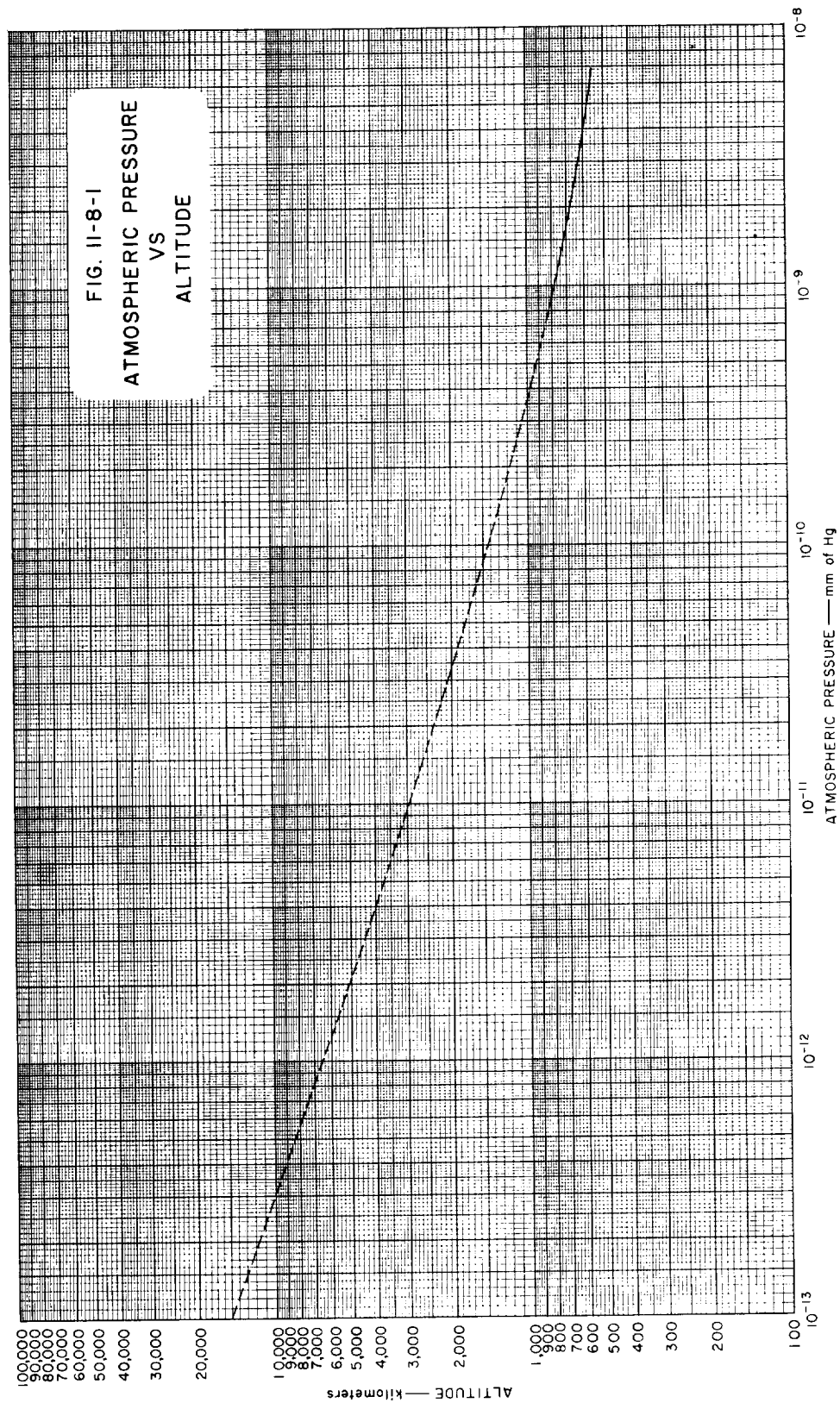
—

—

—

—

—



(

(

(

(

(

II-9 SPACE ENVIRONMENT REFERENCES

1. Anon., *NACA TN-1235*, 1955.
2. Batrakov, Yu., B., and Proskurin, V. F., *NASA TT F-46*, November 1960.
3. Cook, G. E., Roy. Aircraft Establ., *TN-GW531*, September 1959.
4. Gazley, C., Jr., Kellogg, W. W., and Vestine, E. H., *J. Aerospace Sci.*, **26**, No. 12, 770 (1959).
5. Kallman, H. K., and Juncosa, M. L., RAND, *Rept. No. RM-2286*, October 1958.
6. Jaffe, L. D., and Rittenhouse, J. B., Jet Propulsion Laboratory, *Tech Rept. No. 32-150*, November 1, 1961.
7. Johnson, F. S., *LMSD-895006*, December 1960.
8. Johnson, F. S., "Satellite Environment Handbook," Stanford University Press, 1961, p. 115.
9. McCoy, T. M., "R&D Handbook 1960-1961," *Space/Aeronautics*, p. 8-5.
10. Mooney, D. A., "Mechanical Engineering Thermodynamics," Prentice-Hall, New York, 1953.
11. Sears, F. W., "Mechanics, Heat, and Sound," Addison-Wesley Publishing Co., Reading, Mass., 1950.
12. Shaw, J. H., Ohio State Univ. Research Foundation, *RF Project 847*, January 1960.
13. Wiederhorn, N., A. D. Little, Inc., *Rept. No. 63270-02-1*, September 1961.
14. Kallman-Bijl, H., *et al.*, *CIRA 1961*, North Holland Publishing Co., Amsterdam, 1961.
15. Sissenwine, N., Wexler, H., and Dubin, M., "The U.S. Standard Atmosphere, 1962," *ARS Preprint No. 2678-62*, November 13-18, 1962.
16. United States Air Force, "Handbook of Geophysics," Revised Edition, The Macmillan Company, New York, 1961, p. 16-15.
17. Shahinian, P., and Achter, M. R., *Trans. Met. Soc. of AIME*, **215**, 37 (1959).
18. Wadsworth, N. J., and Hutchings, J., *Phil. Mag.*, **3**, 1154 (1958).
19. Dushman, S., *Vacuum Technique*, John Wiley & Sons, Inc., New York, 1949.
20. Brady, B. P., and Salvinski, R. J., Space Technology Laboratories, Inc., *Report 8651-6016-RU-000*, March 1963.
21. Davidson, J. R., and Sandorff, P. E. *NASA TN D-1493*, January 1963.

1

2

3

4

5

III ATTITUDE CONTROL THEORY

Table of Contents

<u>Section-Part</u>	<u>Title</u>	<u>Section-Part. Page</u>
III-0	List of Tables	III-0.2
III-0	List of Figures	III-0.2
III-1	Introduction	III-1.1
III-2	Torques Acting on Spacecrafts	III-2.1
III-3	Sensors	III-3.1
III-4	Hardware Design	III-4.1
III-5	References	III-5.1

III-0 LIST OF TABLES

<u>Section-Part-Table</u>	<u>Title</u>	<u>Section-Part.Page</u>
III-3-1	Typical Attitude Sensors	III-3.3
III-4-1	Time Delays in Gas Attitude-Control Systems	III-4.3

III-0 LIST OF FIGURES

<u>Section Part-Figure</u>	<u>Title</u>	<u>Section-Part.Page</u>
III-4-1	Cold Gas System Hardware Implementation	III-4.5

III-1 INTRODUCTION

Attitude control is used to stabilize a space vehicle or portions of the vehicle about a tracking line from a reference on the vehicle to an external reference. An external reference may be a vertical to a planet, the sun or a star, a gravitational or magnetic field, or an imaginary line between any two bodies in space.

The accuracy of attitude control depends on the mission of the vehicle, and for most purposes a limit of ± 1 degree is sufficient. On the other hand, special experiments may require accuracies of 10-20 seconds, and in the case of vehicles bearing telescopes (OAO), about ± 0.1 sec of arc is the minimum acceptable. In general, the over-all system performance is the result of compromises in design limitations, available accuracy within weight allowances, average power available on board, the vehicle's moment of inertia, and the nature and magnitude of disturbing torques. The last two factors greatly influence the performance of an attitude control system, but, unfortunately, they are outside the responsibility of the control system's designer and depend upon factors such as the vehicle's configuration and materials of construction.

There are seven primary sources of torque which must be counteracted by the attitude-control system; these are: atmospheric drag; gravitational gradient; solar radiation pressure; magnetic fields; micrometeoroid impact; movements internal to the vehicle; apparent torques arising from rotation of reference axes.

The methodology utilized in the design of a space-vehicle attitude-control system generally involves the following:

- (a) The operational requirements of the attitude-control system are determined by the operational specifications of the mission the vehicle is to perform. These specifications will determine system characteristics such as how accurate a control is required, whether the whole vehicle or only a part must be stabilized, the portion of the trajectory or orbit over which control must be exercised, the lifetime of the control system, and even whether any control at all is required. The operational

requirements will also determine some of the restrictions to be imposed on the control system, such as size, weight, and consumption of power.

- (b) The co-ordinate reference system and the vehicle reference axes are then selected; suitable deviation angles between the two are then established, and these determine the differential equations of motion for the control system.
- (c) The actual design and constructional features are tentatively determined after solution of the differential equations of motion. At this point, factors to be taken into consideration include: limitations of size, weight, and power consumption; internal and external torques which need to be counteracted by the control system; magnitude of the control torques available within size and weight limitations, etc. Whenever possible, the system is designed or programmed to utilize ambient field torques (such as the earth's magnetic field or solar radiation) to accomplish or aid in the control function. At this stage of the design, the control-torque mechanisms and the sensors and control-system computer scheme are determined.
- (d) Once the general design and constructional features of the control system are determined, analytical studies of the performance of the system are made. However, the analysis tends to be complicated because of the non-linear characteristics of the control system and because there is generally three-axis coupling. Often, simplifying assumptions are made in order to avoid intractable mathematics; techniques developed for nonlinear control theory are often applied.

III-2 TORQUES ACTING ON SPACECRAFTS

The sources of torque which act on spacecrafts act as disturbances, but they may be used as sources of energy for control. The determination of the magnitude of torques acting on a spacecraft and the anticipated time over which they will act establishes the total impulse required to maintain attitude control. For example, if a 1000-lb satellite in a synchronous orbit is subjected to a continuous force of 10^{-5} lb over two years because of gravitational gradient (*vide infra*), about 630 lb-sec of impulse will be required to maintain a geographically-fixed position; thus the minimum total impulse of the attitude control system (one axis) is established. For the other axes, assuming that nearly static positioning is required (no spin), the natural frequency of oscillation about an axis must be computed and the on-off time for each attitude-control thrust generator must be determined as a function of the sensitivity of the attitude sensors, thrust levels, etc., in order to obtain the total impulse required for the mission. The following sections summarize the nature and magnitude of the torques which affect spacecrafts.

Atmospheric Drag

Aerodynamic drag predominates below 500 miles and is often used for control by moving surfaces in the slip stream. At 500 miles, typical drag corresponds to a dynamic pressure of about 6×10^{-5} dyne/cm² (1.25×10^{-9} lb-ft⁻²); at 80 miles, it is about 5 dynes/cm² (10^{-2} lb-ft⁻²). The drag can be calculated on the basis of free molecular flow, but the computations are quite complex. If the molecular speed ratio is at least 10, good approximations ($\pm 10\%$ for altitudes below 375 miles) can be made by assuming Newtonian flow with a drag coefficient of 2. When aerodynamic drag is used for control, some form of damping must also be employed.

Internal Motions

These torques are unpredictable; they can, however, be held to low values by system design. Typical torques result from moving vanes, extensible booms, mechanisms for winding film, scanning devices, etc.

Gravity Gradient

In general, a spacecraft is accelerated in the direction of the mass-attraction vertical at its center, but the attraction is essentially in equilibrium with the centrifugal force resulting from the orbital velocity of the vehicle. However, since the earth is not a body of revolution about its poles, it does not have a truly radial and uniform gravitational vector ; moreover, for vehicles not in an equatorial plane, a gradient exists which is attributable to a slight dipole distribution of the earth's mass relative to the equatorial plane. As a consequence, a space vehicle tends to be rotated about its center of mass by the gravity gradient across it, and the tendency is to cause an alignment of the long axis of an unsymmetrical vehicle with the gradient. The earth's oblateness also causes rotation of the vehicle's orbit plane about the earth's polar axis and oscillation about the line of nodes; it also leads to an aperiodic rotation of the orbit's major axis and a periodic variation of its semi-major axis.

The horizontal component of gravitational acceleration that is attributable to the slight dipole distribution of the earth's mass relative to the equatorial plane may be expressed¹ as follows:

$$g = - \frac{3G(I_2 - I_1)}{2r^4} \sin 2\theta$$

where

g = horizontal component, ft/sec²

G = universal gravitational constant,
 1.068×10^{-9} ft³/lb-sec²

$I_2 - I_1$ = difference of principal moments of inertia in the
equatorial plane, lb-ft²

r = orbital radius, ft

θ = angular position relative to the earth's major
axis in the equatorial plane.

As an example of the magnitude of this disturbance, a 1000-lb satellite in a 24-hour orbit ($r = 1.38 \times 10^8$ ft) at an angular position $\theta = 70^\circ$ and for which $I_2 - I_1 = 1.22 \times 10^{35}$ lb-ft² is influenced by a component g of about 3.4×10^{-7} ft/sec²; the force on the satellite is eastward and about 10^{-5} lb (5 dynes). Hence, the satellite will drift 20° longitudinally

III.2.2

to the west in about 200 days; since this drift represents the limit of the western boundary of a typical communication satellite system, this example gives an idea of the minimum frequency with which adjustments must be made.

Gravitational accelerations of the sun and moon are much larger (several magnitudes) than the horizontal component of the earth's field but they tend to average out (except for a small residual). However, solar and lunar gravitational perturbations eventually tilt the orbital plane of a synchronous-orbit satellite relative to the equatorial plane; the average tilt rate corresponds to about 1 degree per year.

Magnetic Fields

A magnetic field generates a torque which is perpendicular to the field; thus, if one of a vehicle's control axes is parallel to the field, torques are produced about only two of the axes. The earth's magnetic field sensibly extends beyond 10,000 miles; it is cyclic in position and time, and is affected by solar storms. The earth's field is warped and, thus, the effect on a spacecraft is difficult to predict with any degree of accuracy. The sun's magnetic field predominates at distances beyond 10,000 miles from the earth; it is extremely random in strength and orientation. Fortunately, disturbing effects from magnetic fields can be reduced by using nonmagnetic materials for construction of spacecrafts, avoiding closed conductive loops as much as possible, and eliminating spin. Magnetic torques as little as 10 dyne-cm can be realized by appropriate vehicle design.

Solar Radiation

The photon stream from the sun can also produce torques on the axes of a spacecraft, and these torques are particularly significant on asymmetrical vehicles, or vehicles with surface materials of different reflectivities, because the center of pressure will not be aligned with the center of mass at all angles of incidence. For example, if the center of pressure is six inches away from the center of mass of a medium reflectivity surface 100 ft² in area, a solar pressure of 1.4×10^{-7} lb-ft⁻² will exert a torque of about 7×10^{-6} lb-ft. The solar radiation pressure in the vicinity of earth is at most 2×10^{-7} lb-ft⁻² at normal incidence on a specularly reflecting surface; it should be possible to design a space vehicle so that the torque attributable to solar radiation is below about 10^{-5} lb-ft.

Meteoroids

Impacts from meteoroids produce the largest impulsive forces on space vehicles. There is available very little tangible information on the density of meteoroids in space, but estimates may be used to provide an idea of the demands on an attitude control system. Mariner II data obtained in the region between earth and Venus seems to indicate that the concentration of tiny cosmic particles in deep space is about a ten-thousandth of the concentration near earth. For example, only one dust particle impact occurred during a 129-day period of the Mariner II mission in deep space, while as many as 3700 impacts are registered in periods of 500 hours by satellites in the vicinity of earth.

The impact of meteoroids (especially as a shower or as exceptionally heavy particles) may produce torque which can not be offset by the attitude control system (saturation). A meteoroid may be large enough to penetrate the vehicle's skin and damage internal equipment as well as produce an overturning moment.

If it is assumed that the total meteoric accretion by earth is 10^6 kg per day and that the mass accretion in each magnitude is equal² for each of 30 magnitudes (see Section II-3), the total accretion may be expressed by

$$\sum_{m=0}^{m=30} M_m^E N_m^E = 31 M_0^E N_0^E = 10^6 \text{ kg} \quad (1)$$

Since the mass M_0^E of a zero magnitude meteoroid is assumed to be 25×10^{-3} kg, the number, N_0^E , meteorites falling on earth per day is found by solving the above equation:

$$N_0^E = 1.3 \times 10^6 \quad (2)$$

Now, the number of meteorites of magnitude $M + 1$ is 2.512 times the number of magnitude M (see Section II-3); thus, the average number of meteorites falling on the earth in t hours is

$$N_m^* = \frac{N_0 10^{0.4m} t}{24} \quad (3)$$

The number, N_m , of meteoroids of magnitude m impinging on a vehicle in the time interval t hours is:

$$N_m = \frac{N_0^E 10^{0.4m} t}{24} \left(\frac{A_S}{A_E} \right) \quad (4)$$

where

A_S = effective surface area of the vehicle,

A_E = surface area of the earth,

and

$N_0^E = 1.3 \times 10^6$ impacts per day (zero magnitude).

The effective area of the vehicle can be expressed as

$$A_S = A \left[1 - \left(\frac{R_0}{2R} \right)^2 \right] \quad (5)$$

where A is the actual area of the vehicle, R_0 is the radius of the earth, and R is the altitude of the vehicle from the center of the earth. Thus, the number of meteoroids striking a vehicle is a function of the altitude; at low altitudes, the earth shields the underside of a vehicle from meteoroid impacts.

The angular velocity change in degrees per second, θ , imparted to a vehicle by a meteoroid impact of magnitude and mass M_m is:

$$\theta = \frac{57.3 M_m V L}{I} \quad (6)$$

where V is the average velocity of a meteoroid (28×10^3 m/sec), L is the moment arm to the center of mass (m), and I is the vehicle's inertia, kg/m^2 . This equation may be written as

$$\theta = \frac{57.3 M_0 V 10^{-0.4m} L}{I} \quad (7)$$

by substitution of $M_m = M_0 10^{-0.4m}$ and then transformed to:

$$N_m = \frac{KA_S t L}{\theta I} \quad (8)$$

by solving it for $10^{0.4m}$, substituting into Equation (4), and recognizing the constant term $(57.3 M_0 N_0 V)/(24 A_E) = K$.

In order to express the angular disturbance as a function of probability, the meteoroid distribution is assumed to be a Poisson function; thus, taking N_m as the mean, the probability of h hits on a vehicle in t time is

$$P = N_m^h \exp(-N_m)/h! \quad (9)$$

and the probability of no hits is

$$P_d = \exp(-N_m) \quad (10)$$

while the probability of the vehicle being hit one or more times, P_{1+} , plus the probability of no hit is obviously:

$$P_{1+} + P_0 = 1 \quad (11)$$

Hence,

$$P_{1+} = 1 - \exp(-N_m) \quad (12)$$

represents the probability of one or more hits in an interval of time t . Substituting Equation (8) into (12), yields the probability for one or more hits on the vehicle:

$$P_{1+} = 1 - \exp(KA_S t L / \theta I) \quad (13)$$

or,

$$\theta = - \frac{KA_S t L}{I \ln(1 - P_{1+})} = - \frac{KA_S t L}{I \ln P_0} \quad (14)$$

Equation (14) permits computation of the angular disturbance of any vehicle configuration from one impact of each visual magnitude, but nothing has been said about disturbances resulting from multiple hits of combinations of meteoroids of the same or various magnitudes. The most probable disturbance is, however, the result of a single impact, as shown below.

The disturbance resulting from h impacts of magnitude m is found from Equation (7):

$$\theta = h \frac{57.3 M_0 V 10^{-0.4m} L}{I} \quad (15)$$

Substituting Equation (4) into (15) and recognizing the constant K :

$$N_m = \frac{KA_S t L h}{\theta I} \quad (16)$$

On the other hand, the probability of h hits on the vehicle is given by Equation (9); hence,

$$P = (Zh)^h \exp (-Zh)/h! \quad (17)$$

where

$$Z = KA_S t L / \theta I.$$

Since P is a maximum when $Z = 1$ for any value of h , the maximum probability occurs when

$$\theta = KA_S t L / I \quad (18)$$

Further, since P is a maximum for $Z = 1$ when $h = 1$, it follows that the most probable disturbance occurs from only one impact.

The number of impacts of magnitude m per second per square meter is

$$N_{m,s} = \frac{N_0 10^{0.4m}}{(24)(3600)A_E}$$

and the total number of impacts per second per square meter is

$$N_T = \frac{N_0 10^{12}}{(24)(3600)A_E} \sum_{n=0}^{n=30} \left(\frac{1}{2.512} \right)^n$$

III-3 SENSORS

The two basic operational functions of an attitude-control system are sensing and actuation; in some instances, these functions can be combined in a single device. Additionally, the system must provide some form of damping, usually a feed-back loop. Thus, for each control axis, a control system is composed of a sensor, electronics for processing the sensor's signals and issuing control signals, an actuator, and a damping device. The electronic system requirements for attitude control are well within the state of the art, although some improvement is desirable in reliability and life of components. The greatest room for improvement is in the field of sensors and actuators. Specifically, actuators (valves) and sensors are needed which will provide greater accuracy and reliability than currently available.

Table III-3-1 indicates the types of sensors currently used, the accuracies they provide, and the accuracies which it is hoped future developments may provide. However, some of the accuracies hoped for may not be achievable; indeed, a study of the Ranger vehicle indicates that it is highly unlikely that control accuracies of the order of 0.005 degree will be possible in any spacecraft because of flexing of one part of the vehicle with respect to another. On the other hand, the flimsy vehicles currently launched into space may be replaced with sturdy craft when larger boosters are available.

The major problem encountered in the design and use of sensors is that the phenomena they utilize to derive information are either poorly defined or swamped by spurious signals. Thus far, practical sensors have relied on only a few phenomena: direction of the sun; gravity fields; magnetic fields; stellar radiation; horizons or infrared interfaces.

Earth and planet horizon sensors detect infrared differences which are easily obscured by clouds or large temperature gradients on the planet surface. Thus, to increase sensor accuracy, considerable improvement in signal-to-noise ratio must be realized. Similarly, solar trackers lose accuracy when they are required to track within magnitudes approaching the sun's subtended angle. The sun itself presents a disc which subtends an

III-3.1

arc of about $\frac{1}{2}$ degree as viewed from earth, but the sun is surrounded by concentric rings of ionized gases (which also radiate infrared energy) and subtend as much as several degrees of arc. During solar eruptions the rings may have temperatures approaching the central core.

When a star is used to activate a sensor, a bright star against a black background obviously gives an optimum signal-to-noise ratio. However, this ideal case can seldom be realized, for the portion of the sky to be used for reference is determined by the mission of the vehicle and, as is often the case, the selected star is but one in the midst of others of nearly equal magnitude. Hence, discrimination is based on spectral radiation and brightness, and since the sensor must have high selectivity to track dimmer images, its signal-to-noise ratio will tend to be low.

Gyroscopes perform well in spacecraft (e.g., Mariner II) and are often used to sense deviations from orbit planes. However, the limited life of bearings and the inevitable accumulation of drift errors appears to dampen enthusiasm for their continued employ. The drift rate of free gyroscopes is far too great for long missions (0.1 to 0.5 deg/min), but single-degree-of-freedom, rate-integrating gyroscopes of high quality offer drift rates of the order of 0.001 deg/hr and may even sense angular velocities of the order of small fractions of the earth's rate. Life expectancies can be improved by turning off the gyroscopes during coast periods (Mariner II).

The most widely used sensor is the horizon scanner. In principle, the scanner uses a thermistor bolometer to detect the high temperature gradient which exists between the earth and empty space at the horizon. However, accuracies are limited to 0.2 to 0.5 degree because, at altitudes below 1000 miles, uneven distribution of water vapor and the earth's oblateness limit the sensing of the horizon to no better than ± 0.1 degree.

Table III-3-1
TYPICAL ATTITUDE SENSORS

TYPE	SENSED	ACCURACY (RMS deg)	
		Present	Future
Solar	any plane	0.1	0.01
Planet	any plane	0.2	0.01
Stellar	any plane	1	0.01
Horizon	local vertical	0.2-0.5	0.1
Rate Gyro	rate of deviation from any plane	0.2/hr	0.001/hr

III-4 HARDWARE DESIGN

Hardware implementation of the block diagram of Figure III-4-1 illustrates the essentials of a cold gas system. The operation of this idealized control system is as follows: There are three sets of controls, one for each axis (pitch, yaw, roll). In each of the three controls, the desired attitude is either set in a gyro before flight, acquired by a sensing device, or telemetered from an outboard master control. This desired attitude may be constant, or may vary according to a preset program. In the latter case, the desired attitude may require a combination of a memory device and a timed cam-operated read-off mechanism.

The current attitude signal is fed back to a synthesizer which computes attitude error θ . Usually the attitude error is differentiated to give rate of change of attitude $\dot{\theta}$. Finally, the signal $\theta + K\dot{\theta}$ is relayed to a switch. (K is a positive number, typically 0.1 sec). If this signal exceeds a threshold value $\pm\epsilon$, it activates a switch for right (if positive) or left (if negative) rudder.

In this case a "rudder" is a pair of reaction jets which produces a torque. Activation of the right rudder switch automatically inactivates the left rudder switch, and vice versa. However, complications can occur because of delayed response on the one hand, and difference between the pull-in- and release-voltage (both nominally $\pm\epsilon$) on the other hand (see Table III-4-1). These complications can even cause the switch to chatter. On-off periods, levels of thrust, and the natural oscillation period about an axis must be closely matched in order to minimize nutations.

The number of on-off cycles contemplated has some influence on the choice of the fuel. Because of its high reliability, a cold gas system has been preferred when the expected number of on-off cycles is large (>1000).

III-4.1

1

2

3

4

5

Table III-4-1
TIME DELAYS IN GAS ATTITUDE-CONTROL SYSTEMS
(Ref. 3)

SYSTEM TYPE	THRUST PER JET	TIME DELAY
Cold gas-high thrust jet	20 lb	5-10 milliseconds
Cold gas-low thrust jet	5 lb	<5-10 milliseconds
Hot gas-hydrogen peroxide (high thrust)	44 lb	no thrust for 48 msec; then decreasing substan- tially, and returning to full thrust 108 msec after valves are activated.

1

2

3

4

5

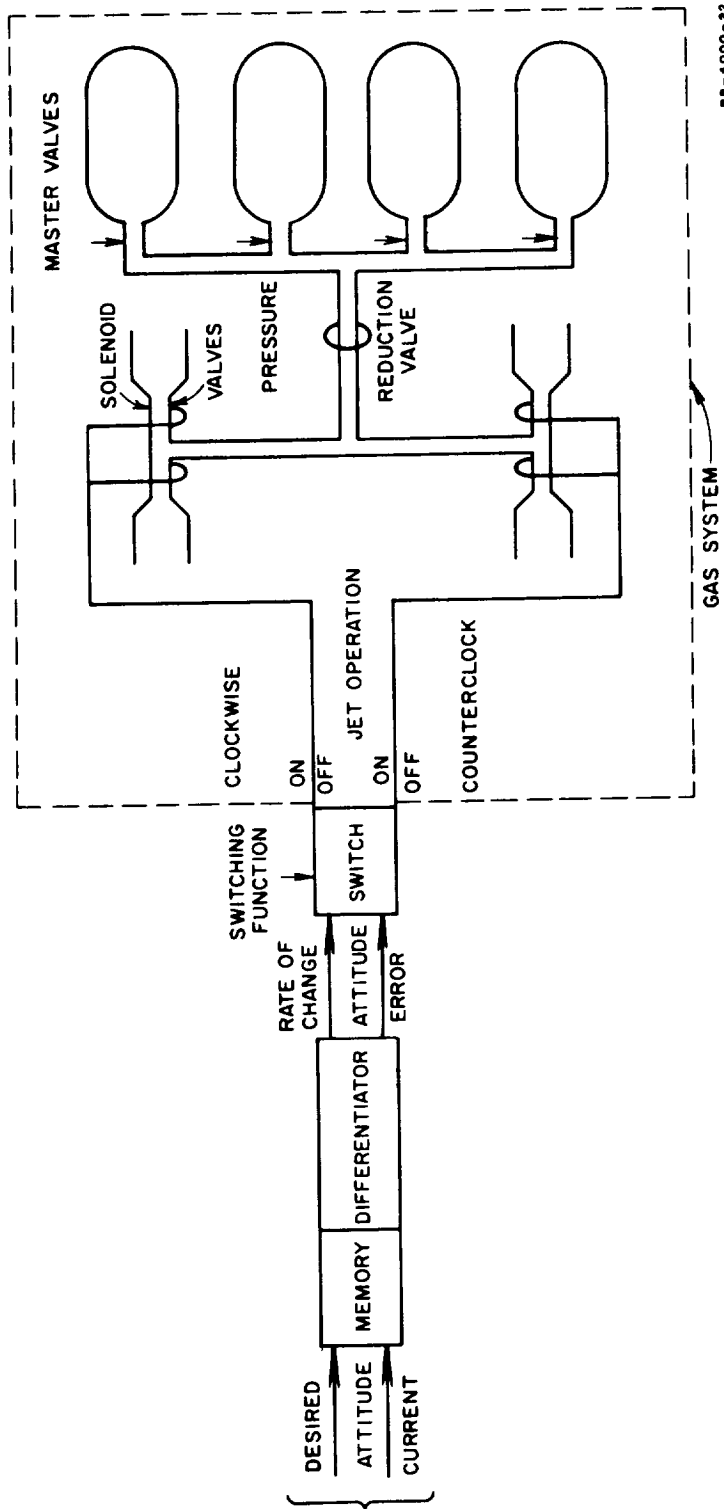


FIG. III-4-1 COLD GAS SYSTEM HARDWARE IMPLEMENTATION

1

2

3

4

5

III-5 ATTITUDE CONTROL THEORY REFERENCES

1. Olds, R. H., *AIAA J.*, **1**, 852 (1963).
2. White, J. B., *ARS J.*, **31**, 75 (1961).
3. Traynelis, K. A., and Ryan, D. L., *Control Eng.*, **8**, 109 (1961).

1

2

3

4

5

IV NOZZLE PERFORMANCE

Table of Contents

Section-Part	Title	Section-Part. Page
IV-0	List of Tables	IV-0.2
IV-0	List of Figures	IV-0.3
IV-1	Introduction	IV-1.1
IV-2	Nozzle Design Parameters	IV-2.1
IV-3	Computation of Specific Impulse of Noncondensing Gases . . .	IV-3.1
IV-4	Performance of Nozzles with Condensing Fluids	IV-4.1
IV-A	APPENDIX—Summary of Equations for Nozzle Performance Calculations	IV-A.1

IV-0 LIST OF TABLES

Section-Table	Title	Section-Part-Page
IV-1	Values of Functions of the Specific Heat Ratio, K	IV-4.5
IV-2	Values of the Function $\left[1 - \left(\frac{P_e}{P_i} \right)^{\frac{K-1}{K}} \right]$	IV-4.6
IV-3	Values of the Function $\sqrt{1 - \left(\frac{P_e}{P_i} \right)^{\frac{K-1}{K}}}$	IV-4.7
IV-4	Summary of Computations for Performance of Nozzles with Water Vapor	IV-4.8

IV-0 LIST OF FIGURES

Section-Figure	Title
IV-1	Values of Functions of Specific Heat Ratio, K $\left(\frac{K-1}{K} \quad \text{and} \quad \sqrt{\frac{2RK}{g(K-1)}} \right)$
IV-2	Values of the Functions of Specific Heat Ratio, K $\left(\frac{K}{K-1} \quad \text{and} \quad \sqrt{\frac{K}{K-1}} \right)$
IV-3 (a,b)	Values of the Function $\eta = \left[1 - \left(\frac{P_e}{P_i} \right)^{\frac{K-1}{K}} \right]$
IV-4 (a,b)	Values of the Function $\sqrt{\eta} = \sqrt{1 - \left(\frac{P_e}{P_i} \right)^{\frac{K-1}{K}}}$
IV-5	Value of $\left(\frac{P_{\text{exit}}}{P_{\text{inlet}}} \right)^{\frac{K-1}{K}}$; Pressure Ratio = 1-100.
IV-6	Value of $\left(\frac{P_{\text{exit}}}{P_{\text{inlet}}} \right)^{\frac{K-1}{K}}$; Pressure Ratio = 10-10 ⁶ .
IV-7	Calculated Performance of Saturated Water Vapor

)

)

)

)

)

IV-1 INTRODUCTION

The optimization of a pressurized gas system which is to be used in conjunction with attitude-control systems may involve calculation of the efficiency of performance of working fluids and an evaluation of nozzle design parameters.

The gases which are generally used as working fluids for pressurization or in attitude-control systems are employed at temperatures greatly in excess of their saturation or critical temperatures, and are seldom expanded to the point where they are cooled sufficiently to cause condensation; these gases will be referred to as "noncondensing" gases in this section of the Handbook. On the other hand, certain working fluids may be used which are expanded in operating cycles to the point where condensation occurs; these gases will be referred to as "condensing" gases.

Computation of nozzle performances with noncondensing working fluids is outlined in this section and details of the computations of nozzle performance with a condensing gas (water vapor) are presented.

)

)

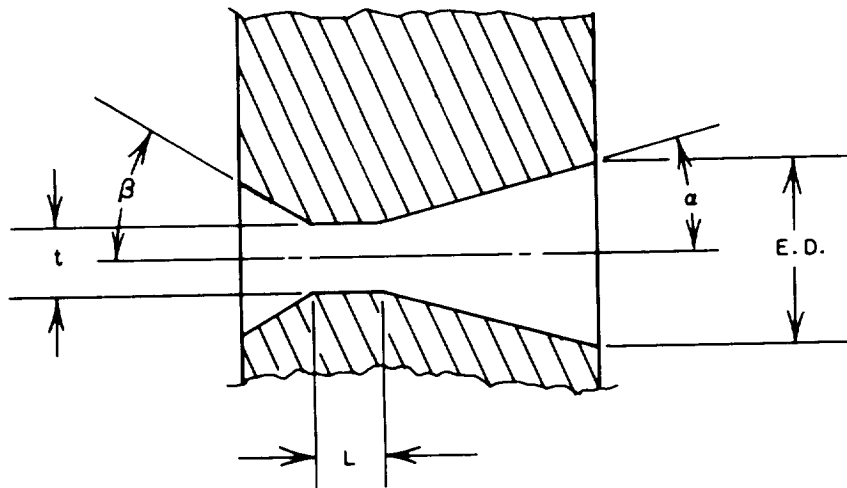
)

)

)

IV-2 NOZZLE DESIGN PARAMETERS

The designs of cold-gas attitude-control nozzles is based on the general principles of design of nozzles for use in rockets. The major difference is, of course, that the cold-gas attitude-control nozzles are very small and, consequently, little effort is made to control the exact shape of the exit bell or the throat. A characteristic design for cold-gas attitude-control nozzles is given in the sketch below:



α = nozzle cone divergence half-angle

β = nozzle cone convergence half-angle

t = throat diameter

E.D. = exit diameter

L = throat length.

The throat diameter of a cold-gas nozzle may be as small as 0.006 inch, but generally is of the order of 0.025 inch for vernier controls. The length of the throat section, L , generally is 1 to 4 throat diameters; the longer throats are relatively difficult to produce with smooth bores. Discontinuities in the contour of the throat wall may cause shock waves and thus reduce nozzle performance.

The convergence half-angle, β , is not very critical and is usually 15 to 30 degrees. On the other hand, the divergence half-angle, of the nozzle is important in that it affects the energy recovery from the exhaust. Highly divergent exhausts have large radial velocity components which are not useful in producing thrust. Correction for the nonaxial component of the gas velocity factor can be made with the aid of the following table:

NOZZLE ANGLE CORRECTION FACTOR

Thus, for a rocket nozzle with a divergence half-angle of 20° , the exhaust velocity would be 96.98% of the theoretical exit velocity. It is of interest to note that the theoretical computation of nozzle performance is based on the spherical area obtained from the assumption of radial flow in the expansion cone and not on the plane area in the exit cone normal to the axis; however, this error is quite small.*

HALF-ANGLE, DEGREES	CORRECTION FACTOR
0	1.0000
2	0.9997
4	0.9988
6	0.9972
8	0.9951
10	0.9924
12	0.9890
14	0.9851
16	0.9806
18	0.9755
20	0.9698
22	0.9636
24	0.9567

Most nozzles for cold-gas attitude-control systems are relatively short in length and seldom offer expansion ratios of more than 100, that is, the area of the throat is seldom less than 1% of the area of the exit plane. As a result, because of their operation in space, the nozzles are always *underexpanding* and they discharge working fluid at a pressure greater than the external or ambient pressure.

Nozzles for cold-gas attitude-control systems are usually constructed of metals and very little attention is given to selection of material because there is no need to provide great strength or resistance to high temperatures as for rocket nozzles. Little effort is made to fabricate nozzles of minimum weight.

* Landsbaum, Ellis M., ARS J., **29**, 212 (1959).

IV-3 COMPUTATION OF SPECIFIC IMPULSE OF NONCONDENSING GASES

The method for the computation of the specific impulse of "non-condensing" gases is based on the consideration of the working fluid as an ideal gas and is patterned after the usual methods for computing the performance of rocket nozzles.

Theoretical Specific Impulse

The computation of the theoretical specific impulse of a working fluid gas flowing through a properly-shaped and constructed nozzle is based on the following assumptions:

- (a) The working fluid is a perfect gas and obeys the ideal gas laws; condensation does not occur in the nozzle.
- (b) The working fluid is a singular substance undergoing no decomposition or dissociation.
- (c) Flow through the nozzle is adiabatic; there is no heat transfer to the nozzle wall.
- (d) The flow of the working fluid through the nozzle is constant.
- (e) The velocity of the working fluid is uniform across any section normal to the axis of the nozzle.
- (f) The flow of the exhaust fluid has an axially-directed velocity.
- (g) There is no resistance to the flow of fluid at any point within the nozzle.

The noncondensing gases generally used for working fluids for pressurization or in attitude-control systems are operating at relatively low pressures and at temperatures well above saturation and thus follow the perfect gas laws close enough to permit evaluation of their performance in nozzles by the classical treatment of adiabatic ideal gases. A summary of the important relationships between nozzle performance and the thermodynamics of ideal gases is presented as an Appendix to this section. The specific impulse obtainable from a working fluid is given by the relation:

IV-3.1

$$I_s = \sqrt{\frac{2R'k}{g(k-1)} \frac{T_i}{M} \left[1 - \left(\frac{P_e}{P_i} \right)^{(k-1)/k} \right]} + \left(\frac{P_e - P_a}{\dot{W}} \right) A_e \quad (13^*)$$

where

- R' = universal gas constant (1545.2 ft-lb/R°/lb-mole)
- k = specific heat ratio
- T_i = temperature of the working fluid at the inlet, R°
- M = molecular weight of the working fluid,
- P_e = pressure of the working fluid at the nozzle exit plane
- P_i = pressure of the working fluid at the inlet
- P_a = ambient pressure into which the nozzle exhausts
- A_e = area of the exhaust jet
- \dot{W} = flow rate of the working fluid.

When the pressure in the exit plane of the nozzle is equal to the ambient pressure, the second term in the above equation becomes 0 and the expression for the specific impulse is independent of flow rate; therefore, the expression permits computation of the optimum impulse:

$$\text{optimum } I_s = \sqrt{\frac{2R'k}{g(k-1)} \frac{T_i}{M} \left[1 - \left(\frac{P_e}{P_i} \right)^{(k-1)/k} \right]} = \sqrt{\frac{2R'k}{g(k-1)}} \sqrt{\eta} \sqrt{\frac{T_i}{M}} \quad (12)$$

where η is the *ideal cycle* efficiency of an engine operating between the pressure P_e and P_i . As the exit pressure approaches 0, the cycle efficiency approaches 1, and the maximum specific impulse obtainable from a working fluid is given by the expression:

$$\text{max. } I_s = \sqrt{\frac{2R'k}{g(k-1)}} \sqrt{\frac{T_i}{M}}$$

Computation of the theoretical optimum impulse and the maximum theoretical impulse for a noncondensing working fluid is a simple matter with the aid of tables and graphs for the square root of the ideal cycle efficiency and other functions of the specific heat ratio (see Tables IV-1

* The equation numbers refer to the numerical sequence in the Appendix.

to IV-3 and Figures IV-1 to IV-6). The temperature of the exhaust working fluid is computed from the relation for isentropic flow:

$$T_e = T_i \left(\frac{P_e}{P_i} \right)^{(k-1)/k} \quad (21)$$

As was indicated before, most working fluids do not condense during expansion through nozzles; however, the above equation should be used to compute the exit temperature and assist in selection of an expansion ratio which will prevent occurrence of condensation. If condensation occurs, the computation of impulse by any of the above equations is invalid.

Actual Specific Impulse

The estimation of the actual specific impulse provided by a working fluid in small attitude-control nozzles is severely influenced by the design and construction of the nozzle and gas supply system and only relatively minorly influenced by deviation of the working fluid from an ideal gas. The following factors largely determine the actual specific impulse obtainable from attitude-control nozzles:

- (a) The smoothness of the nozzle throat and bell. Resistance to flow and the formation of shock waves from discontinuities may lead to losses in performance.
- (b) Underexpanding nozzles. Loss due to underexpansion can be computed from the thrust coefficient [Equation (17) in the Appendix]. Losses computed in this way generally are in accurate agreement with observed results.
- (c) Nozzle exit angle. In order to achieve large expansion ratios in short distances, nozzle exit angles generally are greater than 20° (half-angle). Correction of the theoretical exit velocity by use of nozzle angle correction factors permits estimation of loss in performance with a fairly high degree of accuracy.
- (d) Specific heat ratios. The values for the specific heat ratios of many of the gases used as working fluids in cold-gas attitude-control systems are quite constant at high temperatures and pressures. However, at the temperatures and pressures commonly encountered in attitude-control systems, specific heat ratios of fluids may change considerably during flow through a nozzle.

The effect of shifting specific heat ratios may be estimated by computing performances with an iterative process in which a preliminary estimation of the exit temperature and pressure is used to approximate the final specific heat ratio and then using an average of the initial and final specific heat ratios in successive computations.* Graphs showing the value of specific heat ratios as a function of temperature and pressure are given for various working fluids in Section IX.

- (e) Heat transfer. The working fluid may gain or lose heat in the inlet section between the control valve and the nozzle throat; additional heat transfer may occur in the bell of the nozzle itself. This exchange of heat may lead to deviation from computed performances, especially when the inlet section is much colder than the entering working fluid. It is exceedingly difficult, if at all possible, to estimate changes in expected performance when heat exchange is possible, and especially for the occasional pulses of short duration characteristic of attitude-control systems. It should be recognized that evaluations of nozzle performances in the laboratory are generally performed under the steady-state conditions obtained when all working parts have achieved equilibrium temperatures; thus, the results of these tests are not indicative of the actual performance obtained during occasional short-duration operation periods.

* Iberall, A. S., *J. Appl. Phys.*, **19**, 997 (1948).

IV-4 PERFORMANCE OF NOZZLES WITH CONDENSING FLUIDS

The performance of nozzles with condensing fluids cannot be calculated with the same formulas that are used for "noncondensing" fluids. Condensation releases the latent heat of vaporization (or sublimation) and thus tends to relieve adiabatic cooling effects; the additional heat also provides more energy for thrust than is available from the expansion of "noncondensing" working fluids.

The theoretical maximum impulse obtained from condensing working fluids may be computed by the following formula:

$$I_{sp} = 6.954 \sqrt{\Delta H}$$

where ΔH is the enthalpy change in Btu per lb undergone by the fluid in its reversible expansion through the nozzle. When the working fluid is a saturated vapor in equilibrium with its condensed phase, condensation occurs immediately as the vapor expands; the thrust obtained from expansion through a nozzle will be a maximum if equilibrium between the phases can be maintained at all times.

At any instance during an expansion, conservation of mass requires

$$M_c + M_v = M_i$$

where the subscript c refers to the mass of the condensed phase, v the mass of the vapor phase, and i the mass of the original volume of vapor undergoing expansion. Similarly, conservation of energy requires

$$M_c \Delta H_c + M_v \Delta H_v = M_i \Delta H_i - \Delta(pv)$$

where ΔH is the total enthalpy (over absolute zero) per unit mass of the respective phases and $\Delta(pv)$ is the work done by the system.

Consider one pound of saturated vapor entering the throat section of a nozzle at P_i = initial pressure in atmospheres, T_i = initial saturation temperature in Rankine degrees, V_i = initial volume in ft³/lb (specific

volume), and ΔH_i = initial total enthalpy in Btu/lb. After expansion to a new volume in the nozzle, the remaining vapor will occupy the new volume at equilibrium with the condensed phase; the following equation relates the temperature, the total enthalpy of the system, and the specific volume of the vapor:

$$\frac{V_f}{V_{spv}^{T_f}} \Delta H_v^{T_f} + \left(1 - \frac{V_f}{V_{spv}^{T_f}}\right) \Delta H_c^{T_f} = \Delta H_i - \Delta(PV)$$

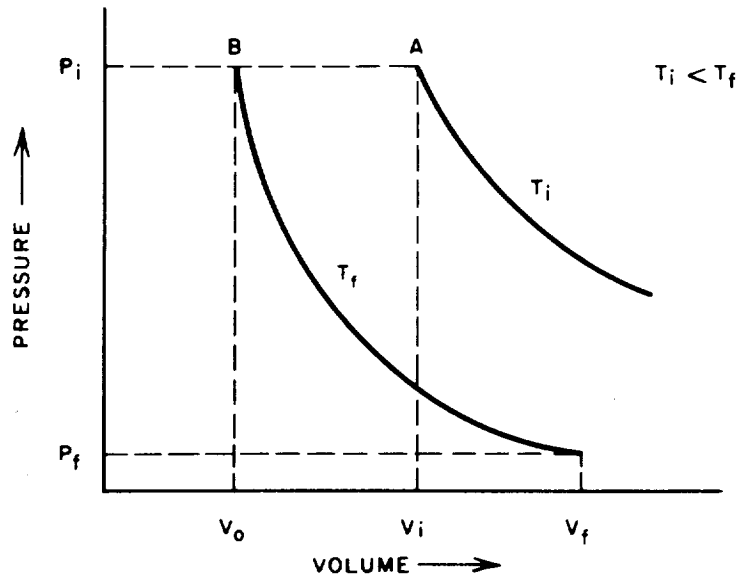
where V_f = final volume, and $V_{spv}^{T_f}$ = specific volume of the vapor at the final temperature. (It is assumed that the volume of the condensed phase is negligible in comparison to the volume of the vapor phase.)

The specific volume of the vapor at large expansions may be computed from ideal gas relationships (actual values of specific volumes seldom are available at low temperatures and low pressures); consequently,

$$V_{spv} = \frac{0.7302}{M} \frac{T_f}{P_f}$$

where T_f is the final temperature, P_f is the final pressure in atmospheres, and M is the molecular weight of the gas.

The work expended by an expanding *undersaturated* working fluid is obtained by consideration of the cycle in the following figure:



Starting at point A with the fluid at temperature T_i and pressure P_i at the initial volume V_i , reduce the temperature to T_f at constant P_i . The work done on the fluid is the area ABV_oV_i and is equal to $P_i(V_i - V_o)$ for an ideal gas. The work expended during isothermal expansion of the fluid from point B(P_i, T_f, V_o) to the final conditions, P_f, V_f, T_f is the area under the T_f curve between V_o and V_f ; for an ideal gas the work for one mole is: $RT_f \ln V_f/V_o$. Hence, the net work is

$$\Delta(PV) = RT_f \ln \frac{V_f}{V_o} - P_i V_i + P_i V_o$$

For an ideal gas at constant pressure, $V_o = V_i T_f / T_i$, and the net work is given by the expression,

$$\Delta(PV) = P_i V_i \left(\frac{T_f}{T_i} - 1 \right) + RT \ln \frac{V_f T_i}{V_i T_f}$$

Thus, the maximum work available from an initial mass of one pound of working fluid at T_i and P_i (equal to saturation temperature and pressure, respectively) which has a volume V_i and a total enthalpy of ΔH_i , and is expanded reversibly to V_f final volume is:

$$\max \Delta(PV) = 2.7203 P_i V_i \left(\frac{T_f}{T_i} - 1 \right) + \frac{X}{M} (2.303)(1.9869) T_f \log \frac{V_f T_i}{V_i T_f}$$

where X is the weight (pounds) of vapor in the final volume (ft^3), P_i is the initial pressure in atmospheres, T_f is the final temperature ($^{\circ}R$), and $\Delta(PV)$ is in Btu's. Introducing the above expression for maximum work in the earlier expression relating the distribution of total enthalpy, and recognizing that the weight of the vapor (X) in the final volume is $V_f/V_{spv}^{T_f}$, the conditions at any point downstream of the throat must fulfill the equation:

$$\begin{aligned} X \Delta H_v^{T_f} + (1 - X) \Delta H_c^{T_f} &= \Delta H_i - \left[2.7203 P_i V_i \left(\frac{T_f}{T_i} - 1 \right) \right. \\ &\quad \left. + 4.5758 \frac{X}{M} T_f \log \frac{V_f T_i}{V_i T_f} \right] \end{aligned}$$

Solution of this equation is simplified by use of tables or graphs of total enthalpies and specific volumes versus temperature. An estimate of the final temperature is made, and then the left-hand and right-hand members of the above equation are computed for two temperatures in the vicinity of the estimated final temperature. The values for each member of the equation are straight-line functions over narrow temperature ranges (several degrees); hence, the intersection of the plotted line of the left-hand member with the plotted line of the right-hand member closely represents the actual final temperature, and the corresponding work term of the right-hand member is used to compute the maximum specific impulse $[I_{sp} = 6.954 \sqrt{\Delta(PV)}]$.

Specific impulse values computed in this way are based on the following assumptions:

- (a) The unsaturated working fluid performs as an ideal gas at low pressures and temperatures.
- (b) The condensed and uncondensed phases are at all times in reversible equilibrium.
- (c) The condensed phase is of such a small particle size that its axial velocity in the nozzle is at all times equal to the velocity of the uncondensed phase.
- (d) The enthalpy difference between the total enthalpy available in the throat section and the vapor at the nozzle exit plane is completely available for production of thrust.
- (e) The condensed phase is a negligible fraction of the uncondensed phase.
- (f) There is no heat transfer to the nozzle.

A summary of computations for the performance of water vapor is given in Table IV-4 and Figure IV-5. It is interesting to note that there is very little difference in specific impulse when supercooled water is formed as the condensed phase rather than ice. Moreover, variations in the initial temperature and pressure do not influence performance significantly, especially at the relatively low expansion ratios usually available in attitude-control nozzles. This is due to the fact that L_e , the latent heat of vaporization of water is so large that dL_e/dT is a relatively small number.

Table IV-1

VALUES OF FUNCTIONS OF THE SPECIFIC HEAT RATIO, K
 ($g = 32.1740 \text{ ft/sec}^2$; $R = 1545.0 \text{ ft-lb/}^\circ\text{R/mole}$)

K	$\frac{K-1}{K}$	$\frac{K}{K-1}$	$\sqrt{\frac{K}{K-1}}$	$\sqrt{\frac{2gK}{K-1}}$	$\sqrt{\frac{2gK}{g(K-1)}}$	$\left(\frac{2}{K+1}\right)^{K/(K-1)}$	$K_2 \sqrt{\frac{2}{K+1}}$	K	$\frac{K-1}{K}$	$\frac{K}{K-1}$	$\sqrt{\frac{K}{K-1}}$	$\sqrt{\frac{2gK}{K-1}}$	$\sqrt{\frac{2gK}{g(K-1)}}$	$\left(\frac{2}{K+1}\right)^{K/(K-1)}$	$K \sqrt{\frac{2}{K+1}}$
1.10	0.0909	11.000	3.317	26.608	32.51	0.5846	0.6590	1.40	0.2857	3.500	1.871	15.009	18.36	0.5282	0.8102
1.11	0.0991	10.991	3.177	25.485	31.14	0.5826	0.6642	1.41	0.2908	3.439	1.855	14.880	18.18	0.5266	0.8151
1.12	0.1071	9.333	3.055	24.506	29.94	0.5806	0.6694	1.42	0.2958	3.381	1.839	14.752	18.02	0.5250	0.8199
1.13	0.1150	8.692	2.948	23.648	28.89	0.5787	0.6748	1.43	0.3007	3.326	1.824	14.632	17.88	0.5232	0.8248
1.14	0.1228	8.143	2.854	22.894	28.80	0.5763	0.6798	1.44	0.3056	3.273	1.809	14.511	17.73	0.5216	0.8297
1.15	0.1304	7.667	2.769	22.212	27.14	0.5744	0.6848	1.45	0.3103	3.222	1.795	14.399	17.59	0.5202	0.8348
1.16	0.1379	7.250	2.699	21.651	26.45	0.5723	0.6900	1.46	0.3151	3.174	1.782	14.295	17.46	0.5184	0.8394
1.17	0.1452	6.882	2.623	21.041	25.71	0.5704	0.6951	1.47	0.3197	3.128	1.769	14.190	17.34	0.5167	0.8442
1.18	0.1525	6.556	2.560	20.536	25.09	0.5683	0.7002	1.48	0.3243	3.083	1.756	14.086	17.21	0.5152	0.8491
1.19	0.1597	6.263	2.506	20.102	24.56	0.5665	0.7054	1.49	0.3289	3.041	1.744	13.990	17.09	0.5135	0.8538
1.20	0.1667	6.000	2.450	19.653	24.01	0.5645	0.7104	1.50	0.3333	3.000	1.732	13.894	16.97	0.5120	0.8586
1.21	0.1736	5.762	2.400	19.252	23.52	0.5626	0.7155	1.51	0.3377	2.961	1.721	13.805	16.87	0.5104	0.8634
1.22	0.1803	5.545	2.355	18.891	23.08	0.5606	0.7207	1.52	0.3421	2.923	1.710	13.717	16.76	0.5089	0.8682
1.23	0.1870	5.348	2.312	18.546	22.66	0.5587	0.7256	1.53	0.3464	2.887	1.699	13.629	16.65	0.5073	0.8729
1.24	0.1936	5.167	2.273	18.233	22.28	0.5567	0.7306	1.54	0.3506	2.852	1.689	13.549	16.55	0.5057	0.8778
1.25	0.2000	5.000	2.236	17.937	21.91	0.5549	0.7356	1.55	0.3548	2.818	1.679	13.468	16.45	0.5042	0.8826
1.26	0.2064	4.846	2.201	17.656	21.57	0.5530	0.7408	1.56	0.3590	2.786	1.669	13.388	16.36	0.5026	0.8873
1.27	0.2126	4.704	2.169	17.399	21.26	0.5512	0.7457	1.57	0.3630	2.754	1.660	13.316	16.27	0.5013	0.8919
1.28	0.2188	4.571	2.138	17.150	20.95	0.5494	0.7507	1.58	0.3670	2.724	1.651	13.244	16.18	0.4997	0.8968
1.29	0.2248	4.448	2.109	16.918	20.67	0.5475	0.7558	1.59	0.3710	2.695	1.642	13.172	16.09	0.4982	0.9015
1.30	0.2308	4.333	2.082	16.701	20.40	0.5457	0.7608	1.60	0.3750	2.667	1.633	13.099	16.00	0.4973	0.9062
1.31	0.2366	4.226	2.055	16.485	20.14	0.5439	0.7658	1.61	0.3789	2.639	1.625	13.035	15.92	0.4953	0.9109
1.32	0.2424	4.125	2.031	16.292	19.90	0.5422	0.7707	1.62	0.3826	2.613	1.616	12.963	15.84	0.4939	0.9156
1.33	0.2481	4.030	2.008	16.108	19.68	0.5404	0.7758	1.63	0.3865	2.587	1.608	12.899	15.76	0.4924	0.9203
1.34	0.2537	3.941	1.985	15.923	19.45	0.5386	0.7807	1.64	0.3903	2.562	1.600	12.835	15.68	0.4910	0.9250
1.35	0.2593	3.857	1.964	15.755	19.25	0.5368	0.7856	1.65	0.3940	2.538	1.593	12.786	15.61	0.4894	0.9294
1.36	0.2647	3.778	1.944	15.594	19.05	0.5351	0.7906	1.66	0.3976	2.515	1.586	12.722	15.54	0.4881	0.9344
1.37	0.2701	3.703	1.924	15.434	18.85	0.5334	0.7954	1.67	0.4013	2.492	1.579	12.666	15.47	0.4867	0.9390
1.38	0.2754	3.632	1.906	15.289	18.68	0.5316	0.8004	1.68	0.4048	2.470	1.572	12.610	15.40	0.4853	0.9437
1.39	0.2806	3.564	1.888	15.145	18.50	0.5300	0.8054	1.69	0.4083	2.449	1.565	12.554	15.34	0.4839	0.9483
								1.70	0.4119	2.428	1.558	12.498	15.27	0.4825	0.9530

Table IV-2

$$\text{VALUE OF THE FUNCTION } \left[1 - \left(\frac{P_e}{P_i} \right)^{\frac{K-1}{K}} \right]$$

$\frac{P_i}{P_e}$	K												
	1.10	1.15	1.20	1.25	1.30	1.35	1.40	1.45	1.50	1.55	1.60	1.65	1.70
1													
5	0.136	0.189	0.235	0.275	0.310	0.341	0.369	0.393	0.415	0.435	0.453	0.470	0.485
10	0.189	0.260	0.319	0.369	0.412	0.450	0.482	0.511	0.536	0.558	0.578	0.596	0.612
50	0.299	0.400	0.479	0.542	0.595	0.637	0.673	0.703	0.729	0.750	0.769	0.785	0.800
100	0.342	0.452	0.536	0.602	0.655	0.697	0.732	0.760	0.785	0.805	0.822	0.836	0.850
500	0.432	0.555	0.645	0.711	0.762	0.801	0.830	0.854	0.874	0.890	0.903	0.914	0.923
1 000	0.466	0.594	0.684	0.749	0.787	0.833	0.861	0.883	0.900	0.914	0.925	0.934	0.942
5 000	0.539	0.671	0.785	0.818	0.860	0.890	0.912	0.929	0.942	0.951	0.959	0.965	0.970
10 000	0.567	0.699	0.785	0.842	0.880	0.908	0.928	0.943	0.954	0.962	0.968	0.973	0.978
50 000	0.626	0.756	0.835	0.885	0.918	0.939	0.955	0.965	0.973	0.979	0.983	0.987	0.988
100 000	0.649	0.777	0.853	0.900	0.930	0.950	0.963	0.972	0.979	0.983	0.987	0.989	0.991
500 000	0.697	0.819	0.888	0.928	0.951	0.967	0.977	0.983	0.987	0.990	0.992	0.994	0.996
1 000 000	0.715	0.835	0.900	0.937	0.959	0.972	0.981	0.986	0.990	0.993	0.994	0.996	0.997

Table IV-3

$$\text{VALUE OF THE FUNCTION } \sqrt{1 - \left(\frac{P_e}{P_i}\right)^{\frac{K-1}{K}}}$$

$\frac{P_i}{P_e}$	K													
	1.10	1.15	1.20	1.25	1.30	1.35	1.40	1.45	1.50	1.55	1.60	1.65	1.70	
1														
5	0.369	0.435	0.485	0.524	0.557	0.584	0.607	0.627	0.644	0.660	0.673	0.686	0.696	
10	0.435	0.510	0.565	0.607	0.642	0.671	0.694	0.715	0.732	0.747	0.760	0.772	0.782	
50	0.547	0.632	0.692	0.736	0.771	0.798	0.820	0.838	0.854	0.866	0.877	0.886	0.894	
100	0.585	0.672	0.732	0.776	0.809	0.835	0.856	0.872	0.886	0.897	0.907	0.914	0.922	
500	0.657	0.745	0.803	0.843	0.873	0.895	0.911	0.924	0.935	0.943	0.950	0.956	0.961	
1 000	0.683	0.771	0.827	0.866	0.893	0.913	0.928	0.940	0.949	0.956	0.962	0.966	0.971	
5 000	0.734	0.819	0.871	0.904	0.928	0.943	0.955	0.964	0.971	0.975	0.979	0.982	0.985	
10 000	0.753	0.836	0.886	0.918	0.938	0.953	0.963	0.971	0.977	0.981	0.984	0.987	0.989	
50 000	0.791	0.870	0.914	0.941	0.958	0.969	0.977	0.982	0.987	0.989	0.991	0.994	0.994	
100 000	0.806	0.881	0.924	0.949	0.965	0.975	0.981	0.986	0.989	0.991	0.993	0.995	0.996	
500 000	0.835	0.905	0.942	0.963	0.975	0.983	0.989	0.991	0.994	0.995	0.996	0.997	0.998	
1 000 000	0.846	0.914	0.949	0.968	0.979	0.986	0.990	0.993	0.995	0.996	0.997	0.998	0.998	

Table IV-4
SUMMARY OF COMPUTATIONS FOR PERFORMANCE
OF NOZZLES WITH WATER VAPOR

Saturated water vapor at 585°R (about 52°C) $P_{sat} = 0.13329 \text{ atm.}$ Specific volume = $V_i = 177.78 \text{ ft}^3/\text{lb}$ $\Delta H_i = 1389.7 \text{ btu/lb}$						
EXPANSION RATIO	$o_{R_{exit}}$	% CONDENSED	CONDENSED PHASE	P_{exit} , atm	ENTHALPY DIFFERENCE	SPECIFIC IMPULSE
2	558.3	2.8	water	0.062	41.4	44.7
5	527.2	6.1	water	0.0227	87.2	65.0
10	506.4	7.8	water	0.0111	117.3	75.0
20	487.9	9.4	water	0.00507	144.3	83.5
20	488.2	8.3	ice	0.00513	146.1	84.1
40	472.4	11.0	water	0.00241	168.7	90.3
40	472.6	10.2	ice	0.00242	170.6	90.8
100	453.5	12.4	water	0.00091	198.4	98.0
100	453.8	11.2	ice	0.00092	201.5	98.7
1 000	412.3	16.2	water	0.00008	256.9	111.5
1 000	412.4	15.3	ice	0.00008	260.1	112.2
10 000	378.4	14.1	ice	0.000007	307.2	121.8
Saturated water vapor at 530°R (about 21°C) $P_{sat} = 0.02497$ Specific volume = $V_i = 859.69 \text{ ft}^3/\text{lb}$ $\Delta H_i = 1365.7 \text{ btu/lb}$						
2	508.8	2.6	water	0.0117	37.3	42.5
5	484.4	5.6	water	0.00431	80.7	62.5
5	484.7	4.3	ice	0.00436	81.9	62.9
40	441.4	11.4	water	0.00046	158.4	87.5
40	441.7	10.0	ice	0.00047	160.0	88.0
100	424.9	12.7	water	0.00018	186.0	94.8
100	425.0	11.8	ice	0.00018	188.0	95.4
1 000	391.9	12.3	ice	0.00002	256.6	109.6
10 000	358.4	18.3	ice	0.000001	291.1	118.7

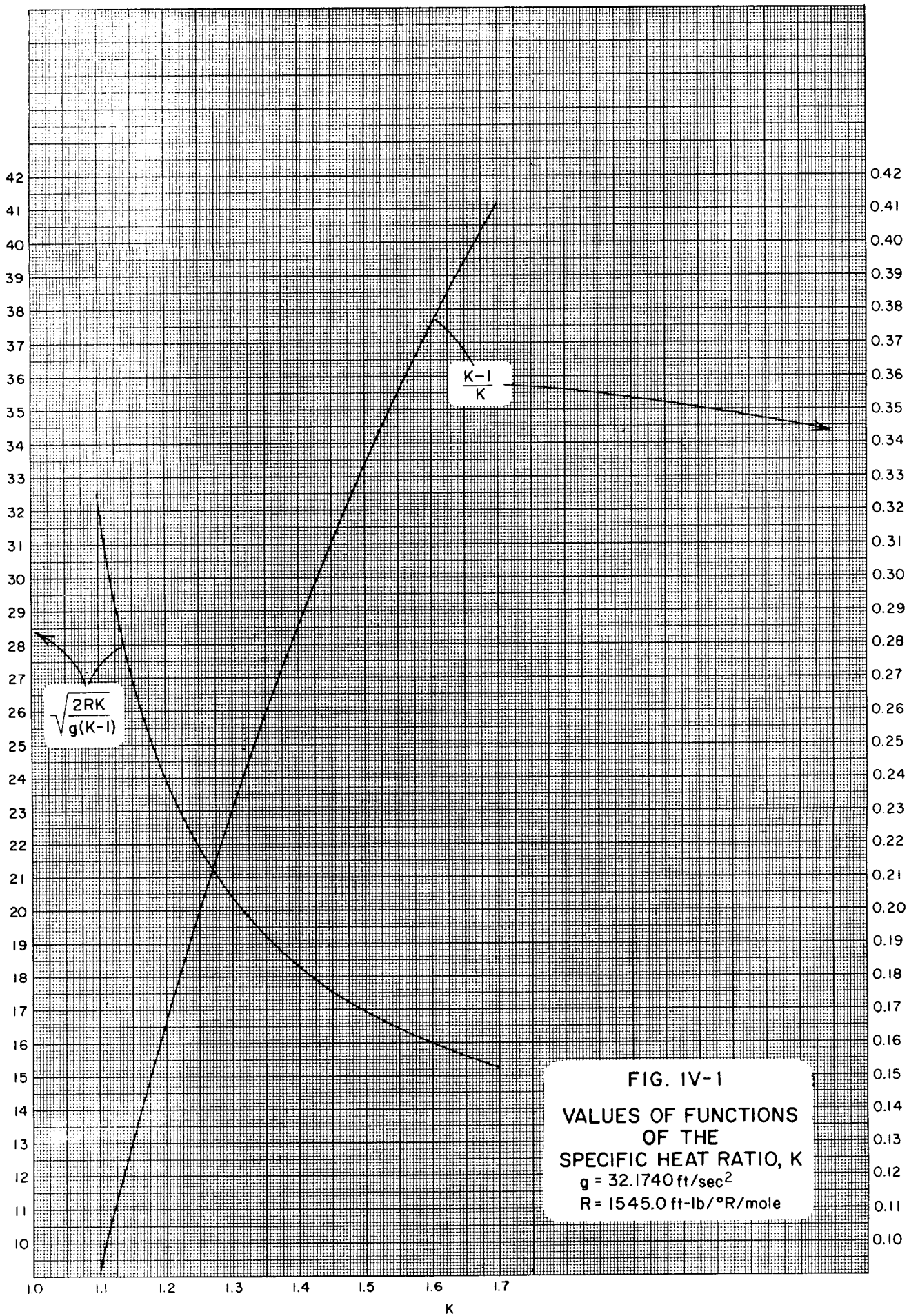
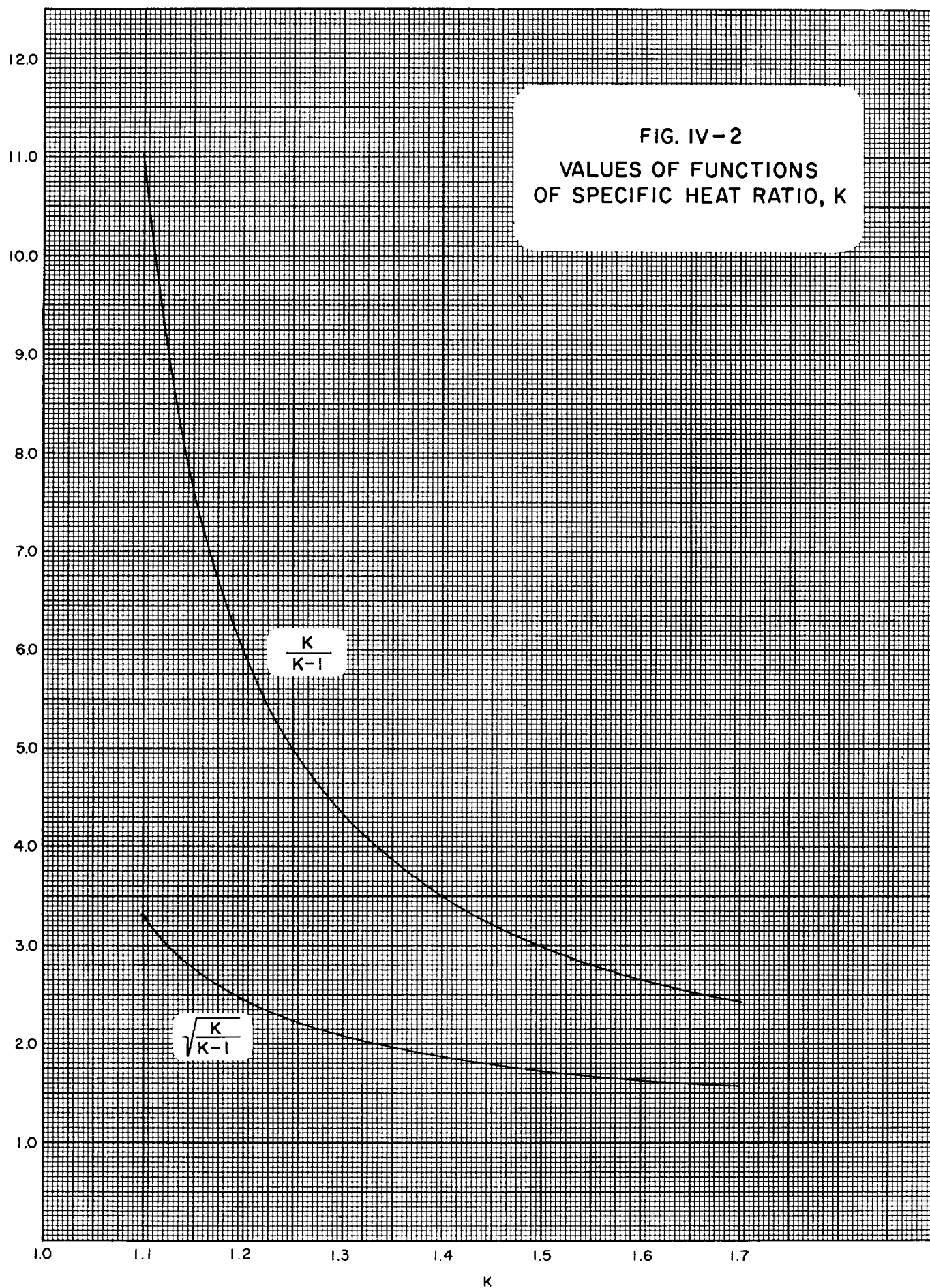
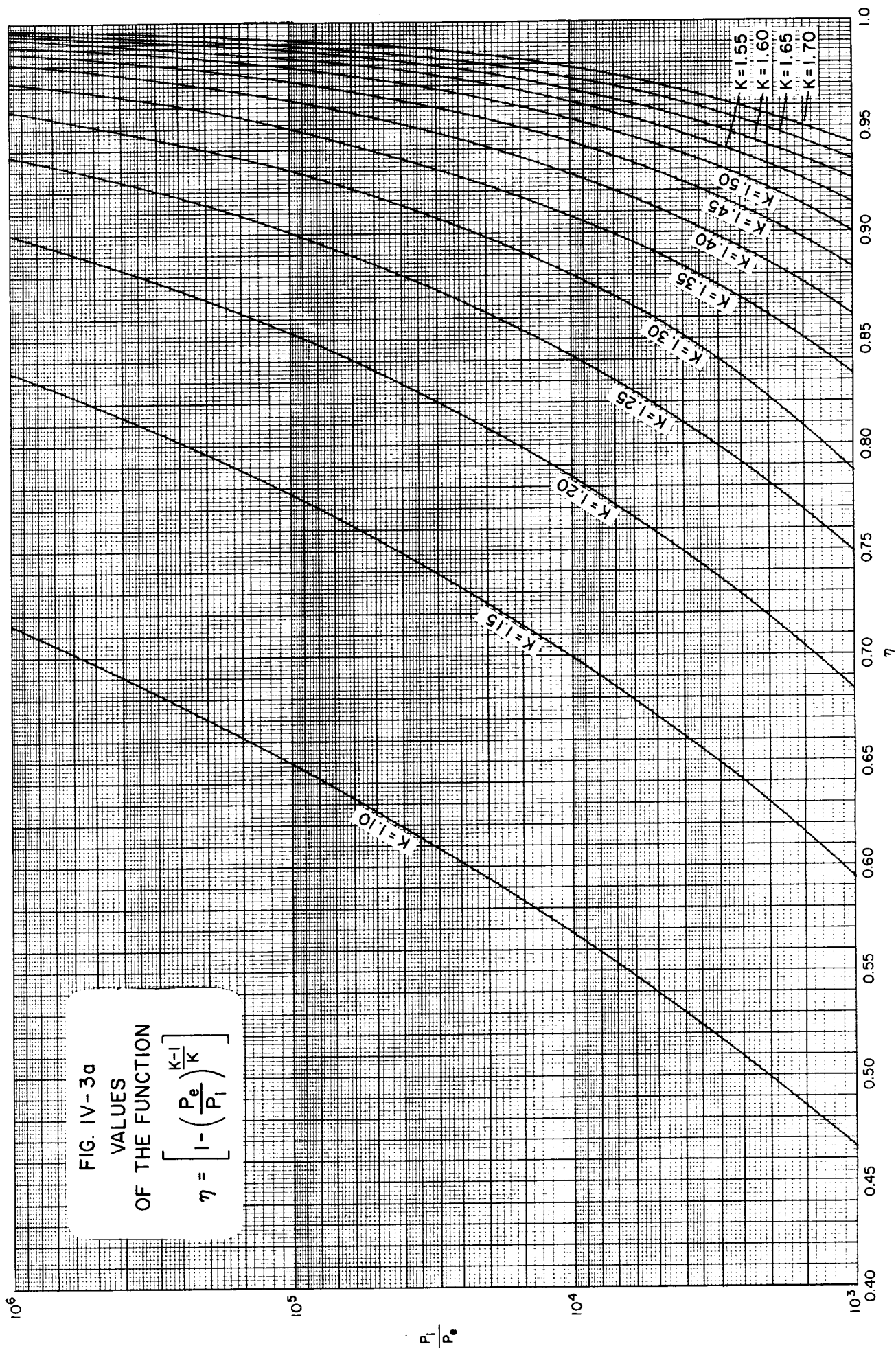


FIG. IV-2
VALUES OF FUNCTIONS
OF SPECIFIC HEAT RATIO, K





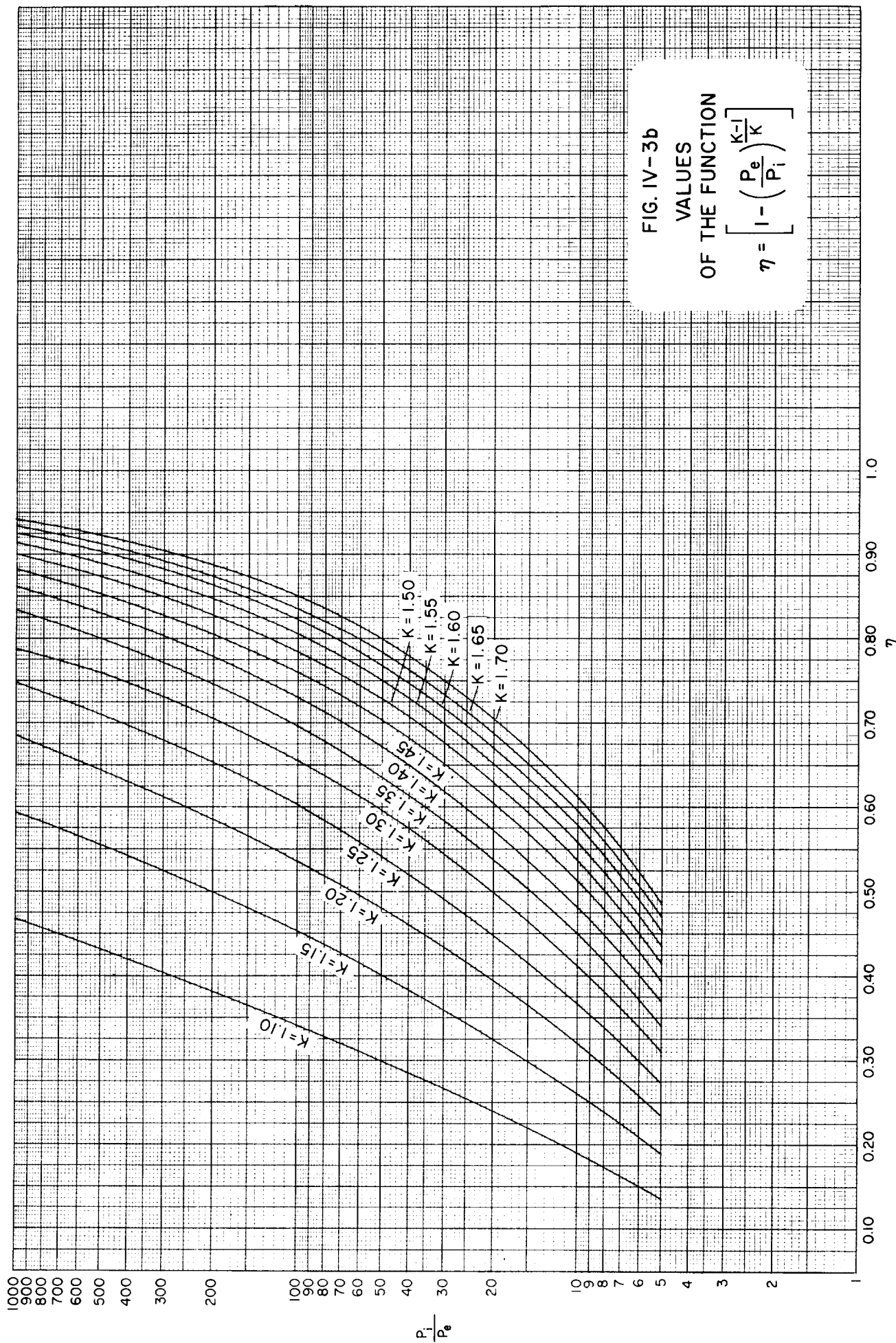


FIG. IV-3b
VALUES
OF THE FUNCTION
 $\eta = \left[1 - \left(\frac{P_e}{P_i} \right)^{\frac{K-1}{K}} \right]$

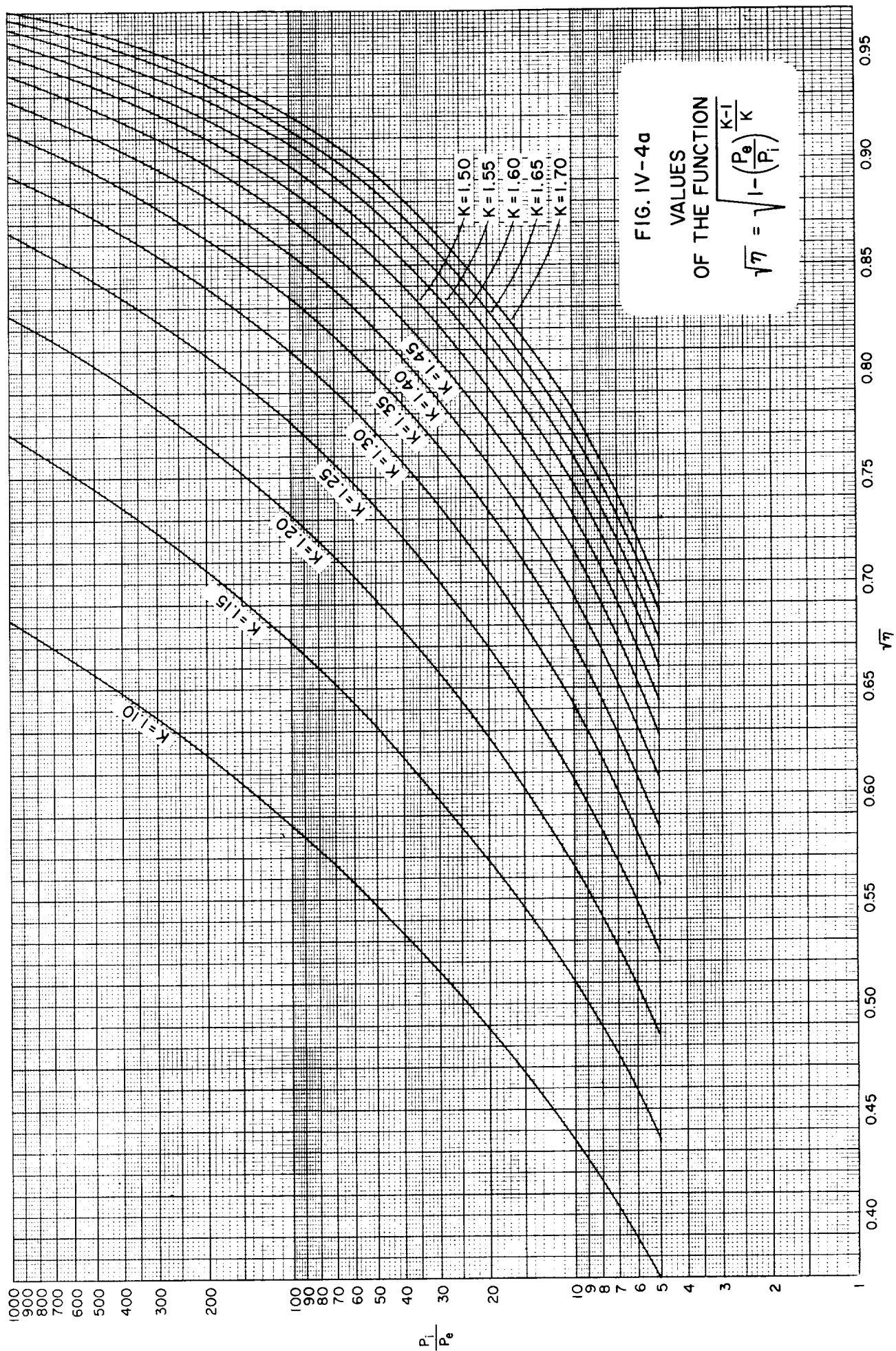
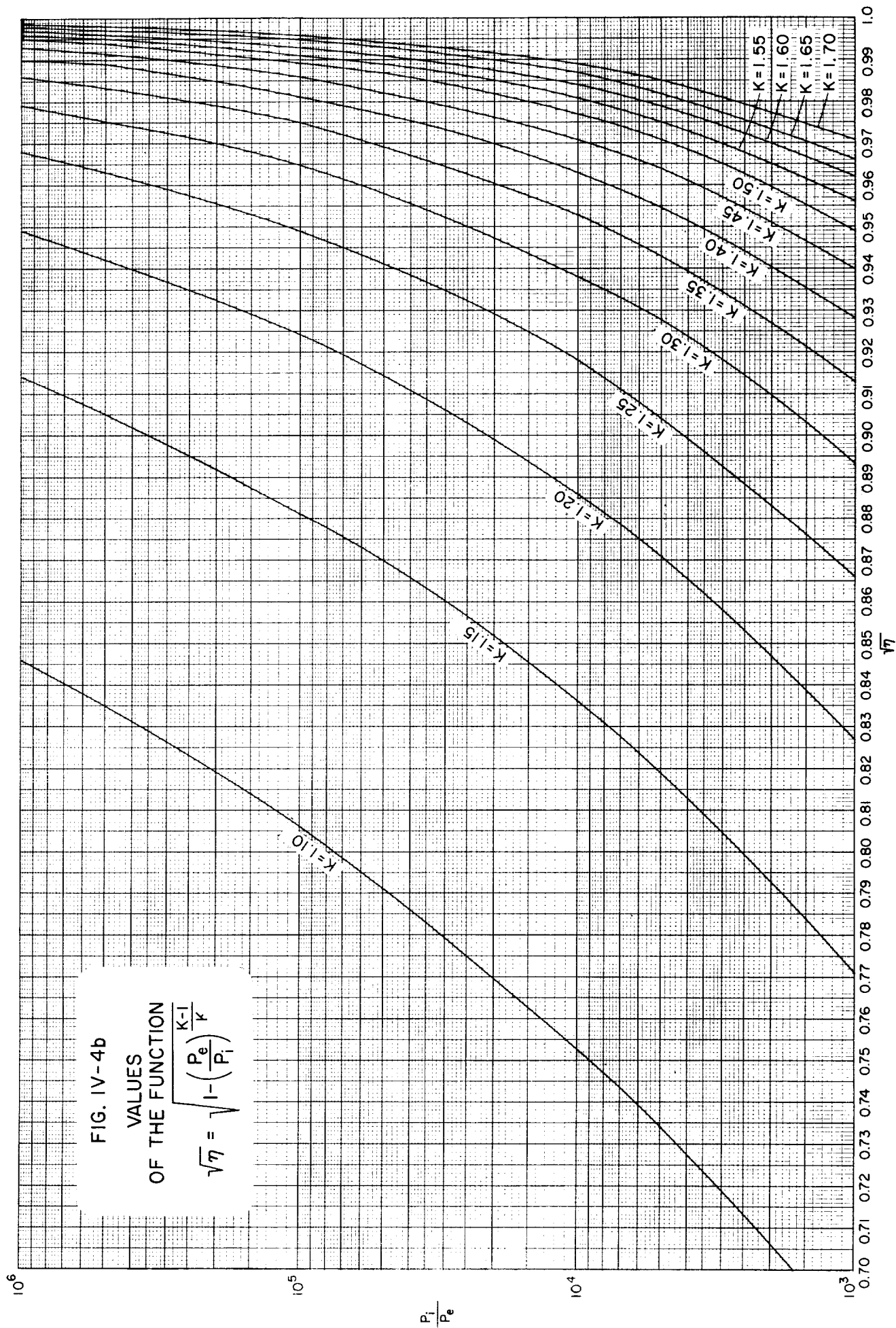


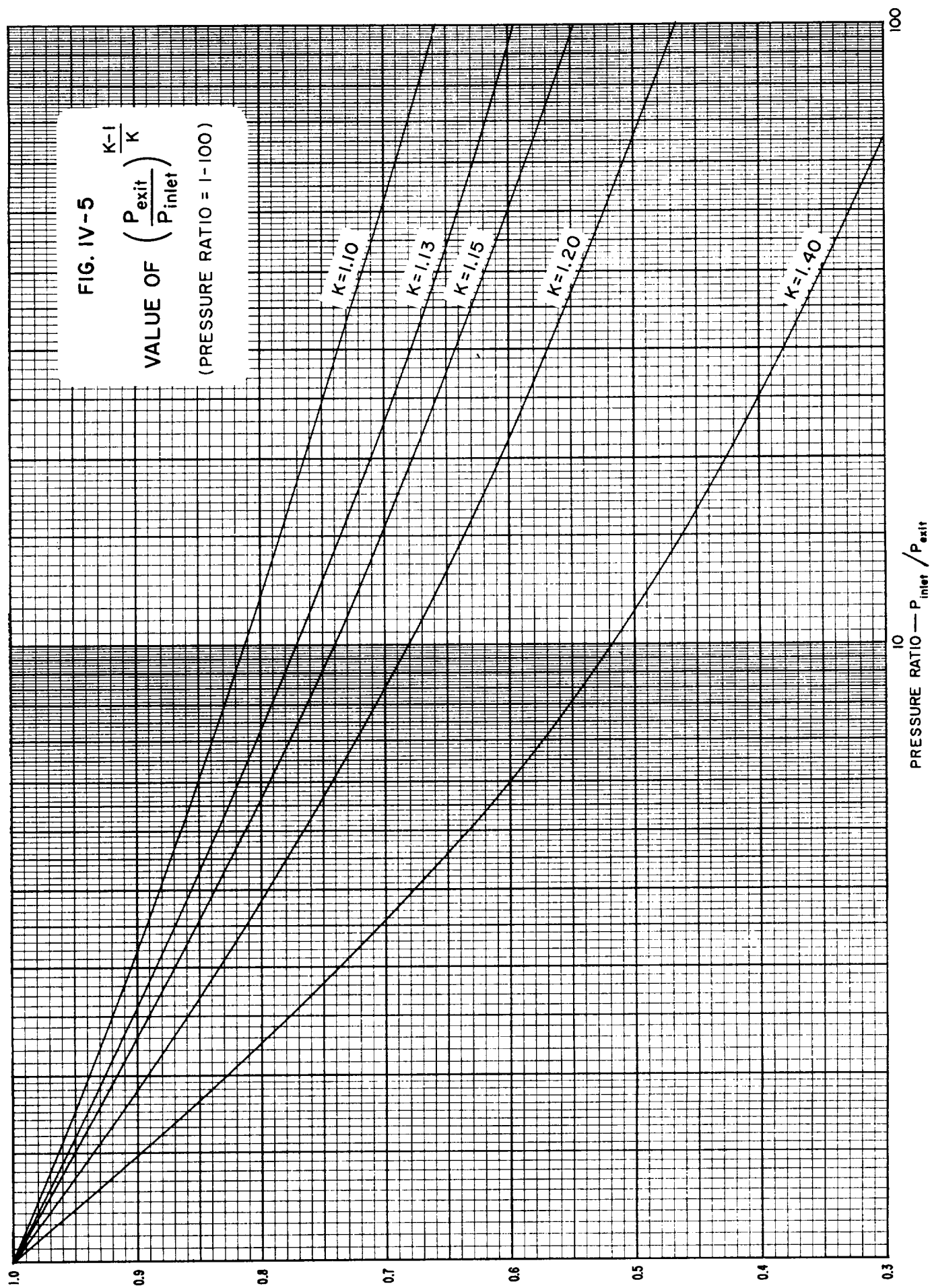
FIG. IV-4a

VALUES

OF THE FUNCTION

$$\sqrt{\eta} = \sqrt{1 - \left(\frac{P_e}{P_i}\right)^{\frac{K-1}{K}}}$$





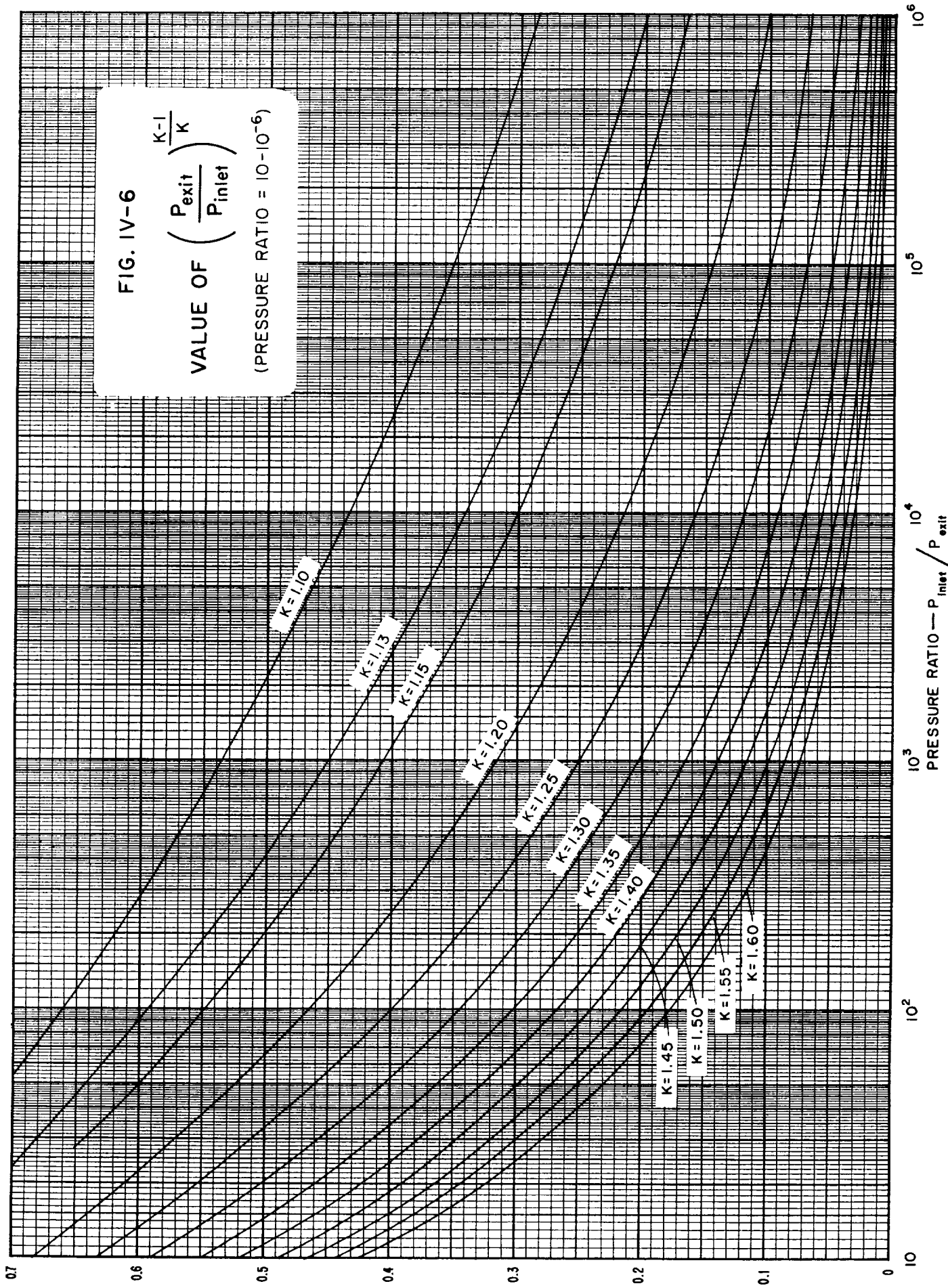
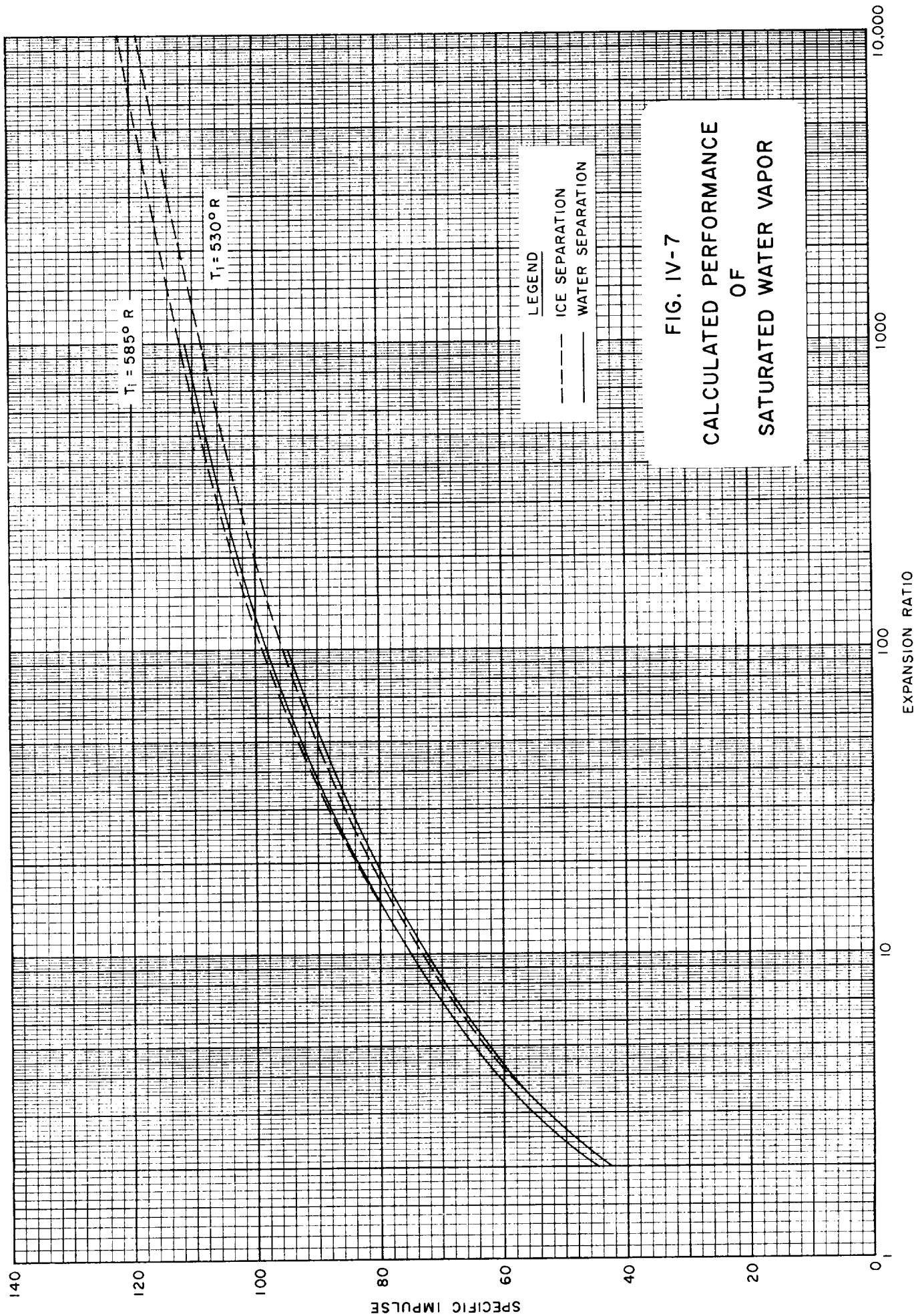


FIG. IV-6

$$\text{VALUE OF } \left(\frac{P_{\text{exit}}}{P_{\text{inlet}}} \right)^{\frac{K-1}{K}}$$

(PRESSURE RATIO = $10^{-10^{-6}}$)

PRESSURE RATIO $\rightarrow \frac{P_{\text{inlet}}}{P_{\text{exit}}}$



)

)

)

)

)

IV-A APPENDIX

SUMMARY OF EQUATIONS FOR NOZZLE PERFORMANCE CALCULATIONS

Specific Impulse is defined as the thrust obtained from unity flow rate of propellant, i.e.,

$$I_s = \frac{F}{\dot{W}} = \frac{C}{g} \quad (1)$$

where C is the effective exhaust velocity, g is the gravitational constant, \dot{W} is the weight flow rate of the propellants, and F is the thrust.

Total Impulse is the integral of the thrust, F , over the duration of operation, t :

$$I_t = \int_0^t F dt = I_s \dot{W} dt \quad (2)$$

Effective Exhaust Velocity

$$C = \frac{Fg}{\dot{W}} = V_2 + \frac{(P_2 - P_3)A_e g}{\dot{W}} \quad (3)$$

where

- A_e = exhaust jet area
- P_2 = exhaust jet pressure
- P_3 = pressure behind exhaust jet
- V_2 = exhaust velocity

Nozzle Exhaust Velocity

$$V_2 = \sqrt{\frac{2gk}{k-1} \frac{R'T_1}{M} \left[1 - \left(\frac{P_2}{P_1} \right)^{\frac{k-1}{k}} \right]} + V_1^2 \quad (4)$$

where

subscripts 1 are inlet conditions,

subscripts 2 are outlet conditions,

$k = C_p/C_v$,

M = molecular weight,

R' = universal gas constant = 1545.2 ft-lb per °R-lb-mole

Generally $V_2 \gg V_1$, and hence V_1 can be neglected. T_1 is the nozzle inlet temperature, and for isentropic flow is also equal to the stagnation temperature. At infinite pressure ratio, i.e., when the nozzle exhausts into a vacuum,

$$V_2 = \sqrt{\frac{2gk}{k-1} \frac{R'T_0}{M}} \quad (5)$$

where

T_0 is the stagnation temperature.

From equations (1) and (3), the external force or thrust exerted by a nozzle is given by

$$F = \frac{\dot{W}}{g} V_2 + (P_e - P_a)A_e \quad (6)$$

where

P_a is the ambient pressure.

P_e is the exit pressure

A_e is the exhaust jet area.

But, the nozzle exhaust velocity is:

$$V = \sqrt{\frac{2gk}{k-1} \frac{R'T_i}{M} \left[1 - \left(\frac{P_e}{P_i} \right)^{\frac{k-1}{k}} \right]} + V_i^2 \quad (7)$$

where the i subscripts refer to inlet conditions.

Hence,

$$F = \frac{\dot{W}}{g} \sqrt{\frac{2gk}{k-1} \frac{R'T_i}{M} \left[1 - \left(\frac{P_e}{P_i} \right)^{\frac{k-1}{k}} \right]} + V_i^2 + (P_e - P_a)A_e \quad (8)$$

where V_i can be ignored because it is much less than the exhaust velocity.

Now, in order to carry a minimum of fuel weight, the thrust must be maximized. Thus, since P_i can easily be fixed (as also T_i), only A_e and P_e need be considered. We need find conditions for which

$$\left(\frac{\partial F}{\partial A_e} \right)_{P_e} = P_e - P_a = 0$$

and

$$\left(\frac{\partial F}{\partial P_e} \right)_{A_e} = 0$$

From the first, the equation is maximized when $P_e = P_a$ and $P_e \neq 0$; from the second,

$$\begin{aligned} \left(\frac{\partial F}{\partial P_e} \right)_{A_e} &= - \frac{\dot{W}}{2g} \frac{\frac{k-1}{k} \left(\frac{2gk}{k-1} \frac{R'T_i}{M} \right) P_e^{\frac{k-1}{k}} - 1}{\sqrt{\frac{2gk}{k-1} \frac{R'T_i}{M} \left[1 - \left(\frac{P_e}{P_i} \right)^{\frac{k-1}{k}} \right]} P_i^{\frac{k-1}{k}}} + A_e \\ &= A_e - \dot{W} \frac{\frac{R'T_i}{M \sqrt{\frac{2gk}{k-1} \frac{R'T_i}{M} \left[1 - \left(\frac{P_e}{P_i} \right)^{\frac{k-1}{k}} \right]}}}{\frac{P_e^{-\frac{1}{k}}}{P_i^{\frac{k-1}{k}}}} \\ &= A_e - \frac{\dot{W} R'T_i}{M \sqrt{\frac{2gk}{k-1} \frac{R'T_i}{M} \left[1 - \left(\frac{P_e}{P_i} \right)^{\frac{k-1}{k}} \right]}} \frac{P_e^{-\frac{1}{k}}}{P_i^{\frac{k-1}{k}}} \quad (9) \end{aligned}$$

In other words, for $(\partial F / \partial P_e)_{A_e} = 0$, it is necessary for A_e to be equal to the right term; alternatively, there exists for each A_e an unique P_e for which the thrust is maximum. Since calculations with random selections of P_e are unwieldy, it is preferable to select the first condition, i.e.,

$$\left(\frac{\partial F}{\partial A_e} \right)_{P_e} = 0$$

and the equation is:

$$F_{\text{optimum}} = \frac{\dot{W}}{g} \sqrt{\frac{2gk}{k-1} \frac{R' T_i}{M}} \sqrt{1 - \left(\frac{P_e}{P_i} \right)^{\frac{k-1}{k}}} \quad (10)$$

This equation can be rewritten as:

$$F_{\text{optimum}} = \sqrt{\frac{2gk}{k-1} \frac{R' T_i}{M}} \left[\left(\frac{\dot{W}}{g} \right) \eta^{1/2} \right] \quad (11)$$

where η is the *ideal cycle* efficiency of an engine operating between the pressures P_e and P_i .

In view of equations (1) and (11), the optimum impulse is

$$\text{optimum } I_s = \sqrt{\frac{2R'k}{g(k-1)} \frac{T_i}{M}} (\eta^{1/2}) \quad (12)$$

where $\eta^{1/2} \rightarrow 1$ when $P_e \rightarrow 0$.

The equation for the actual impulse, however, is found by combining equation (1) with equation (8):

$$\begin{aligned} I_s &= \sqrt{\frac{2gk}{k-1} \frac{R' T_i}{gM}} \left[1 - \left(\frac{P_e}{P_i} \right)^{\frac{k-1}{k}} \right] + \left(\frac{P_e - P_a}{\dot{W}} \right) A_e \\ &= \sqrt{\frac{2R'k}{g(k-1)} \frac{T_i}{M}} (\eta^{1/2}) + \left(\frac{P_e - P_a}{\dot{W}} \right) A_e \end{aligned} \quad (13)$$

Returning to equation (8) and introducing the expressions for critical velocity or throat velocity [equation (27)]

$$V_{tc} = \sqrt{\frac{gkR'T_t}{M}} \quad (14)$$

and the expression for the value of the specific volume and temperature [equation (25)],

$$V_{tc} = V_1 \left(\frac{k+1}{2} \right)^{\frac{1}{k-1}} \quad (15)$$

there results a new equation for the thrust:

$$F = A_t P_i \sqrt{\frac{2k^2}{k-1} \left(\frac{2}{k+1} \right)^{\frac{k+1}{k-1}} \left[1 - \left(\frac{P_e}{P_i} \right)^{\frac{k-1}{k}} \right]} + (P_e - P_a) A_e \quad (16)$$

where A_t = throat area.

Now, we define a thrust coefficient by:

$$C_F = \sqrt{\frac{2k^2}{k-1} \left(\frac{2}{k+1} \right)^{\frac{k+1}{k-1}} \left[1 - \left(\frac{P_e}{P_i} \right)^{\frac{k-1}{k}} \right]} + \frac{P_e - P_a}{P_i} \frac{A_e}{A_t} \quad (17)$$

For optimum expansion, $P_e = P_a$, and the last term becomes zero. Then, the *ideal thrust equation* becomes:

$$F = C_F A_t P_i \quad (18)$$

Hence, in view of equation (1),

$$I_s = \frac{C_F A_t P_i}{\dot{W}} \quad (19)$$

$$I_s = \frac{A_t P_i}{\dot{W}} \sqrt{\frac{2k^2}{k-1} \frac{2}{k+1} \frac{k+1}{k-1} \eta + \frac{P_e - P_a}{P_i} \epsilon} \quad (20)$$

where $\epsilon = A_e/A_t$ = area ratio.

Equation (19) is the more useful because there are available tabulated values of C_F where P_a = vacuum.

When $P_e = P_a$, the optimum area ration ϵ and the pressure ratio P_e/P_i are related by the equation:

$$\epsilon = \frac{\left(\frac{2}{k+1}\right)^{\frac{k+1}{2(k-1)}}}{\left(\frac{P_e}{P_i}\right)^{\frac{1}{k}} \sqrt{\frac{2}{k-1} \left[1 - \left(\frac{P_e}{P_i}\right)^{\frac{k-1}{k}}\right]}} \quad (21)$$

An additional useful relation for isentropic flow of ideal gases through a nozzle is:

$$\left(\frac{V_i}{V_e}\right)^{k-1} = \frac{T_e}{T_i} = \left(\frac{P_e}{P_i}\right)^{\frac{k-1}{k}} \quad (22)$$

Weight Flow. For an isentropic, steady flow process, the general equation for the weight flow in a nozzle between any section x and the nozzle inlet section is given by:

$$\dot{W} = \frac{A_x P_1 M}{R'} \sqrt{2gJ} \sqrt{\frac{C_p}{T_1} \left[\left(\frac{P_x}{P_1}\right)^{\frac{2}{k}} - \left(\frac{P_x}{P_1}\right)^{\frac{k+1}{k}} \right]} \quad (23)$$

where J = mechanical equivalent of heat. (777.97 ft-lb per btu.)

Throat Conditions. The throat pressure for which the isentropic weight flow is a maximum is called the *critical pressure* and is obtained from (23):

$$P_{tc} = P_1 \left(\frac{2}{k+1} \right)^{\frac{k}{k-1}} \quad (24)$$

The specific volume in the throat at critical pressure is:

$$V_{tc} = V_1 \left(\frac{k+1}{2} \right)^{\frac{1}{k-1}} \quad (25)$$

The temperature in the throat at critical pressure is:

$$T_{tc} = T_1 \left(\frac{2}{k+1} \right) \quad (26)$$

The critical velocity is:

$$v_{tc} = \sqrt{\frac{2gk}{k+1} \frac{R'T_1}{M}} = \sqrt{\frac{gkR'T_t}{M}} \quad (27)$$

The weight flow in the critical section is:

$$\dot{W} = \frac{A_t v_{tc}}{V_{tc}} = A_t P_1 g \frac{k \sqrt{\frac{2}{k+1} \frac{k+1}{k-1}}}{\sqrt{\frac{gkR'T_1}{M}}} \quad (28)$$

Specific Impulse from Enthalpy Change

When the enthalpy change which a fluid undergoes in an isentropic expansion through a nozzle is known, the exhaust velocity is given by the equation:

$$v = \sqrt{2gJ\Delta H} \quad (29)$$

where

J = mechanical equivalent of heat (777.97 ft-lb/btu),

g = 32.174 ft-sec²

ΔH = enthalpy change, btu per lb.

Since $I_s = v/g$, equation (29) may be converted to:

$$I_s = 6.954\sqrt{\Delta H} \quad . \quad (30)$$

V STORAGE EFFICIENCY

Table of Contents

	<u>Title</u>	<u>Section-Page</u>
Section V	Storage Efficiency	V-1
Table V-1	Weight Storage Efficiencies	V-1
Table V-2	Use of Alcohols to Increase Weight Storage Efficiency . . .	V-2
Figure V-1	Storage Efficiency of Nitrogen and Propane When Used in Cold Gas Jets at 20°C (No Condensation in Nozzle)	V-5

1

2

3

4

5

V STORAGE EFFICIENCY

The definition of the storage efficiency of a pressurized gas in a spacecraft system is determined largely by the particular use to which it is put, but for any given hardware system, the following equation will give the efficiency of storage on a basis of weight:

$$\text{W.S.E.} = \text{weight storage efficiency} = \frac{\text{wt of gas}}{\text{wt of gas plus wt of system}} \quad (1)$$

In general, the hardware system weight is merely the weight of the vessel confining the pressurized gas; hence, the above equation becomes:

$$\text{W.S.E.} = \frac{\text{wt of gas}}{\text{wt of gas plus wt of vessel}} \quad (2)$$

Equation (2) is useful for comparing various gases initially at the same pressure and temperature in similar confining vessels; however, the equation is meaningful only for comparing "noncondensable" gases like helium, hydrogen, etc. When condensable gases are taken into consideration, Equation (2) is also employed but comparison is best restricted to the condensable gases. Table V-1 shows some weight storage efficiencies computed with the aid of Figure V-1 and indicates the great efficiency of storage of liquefied gases.

Table V-1
WEIGHT STORAGE EFFICIENCIES

"NON-CONDENSABLE" GASES 1500 psia, 12" Ti TANK, 4.0 lb		"CONDENSABLE" GASES 500 psia max, 12" Ti TANK, 2.0 lb	
GAS	W. S. E.	GAS	W. S. E.
Hydrogen	0.06	Propane	0.89
Helium	0.13	Ammonia	0.91
Nitrogen	0.49	Water	0.94

Equation (2) also permits comparison of various schemes for enhancing the storage efficiencies of pressurized "noncondensable" gases by assessing the effect of decreases in the weight of the confining vessels which can be brought about by various expedients. For example, introduction of a solid or liquid which can dissolve or trap large volumes of gas may make it possible to increase the weight storage efficiency of the gas.

Hydrogen and nitrogen under high pressure are much more soluble in water or solvents like ethanol and methanol. The solubility of hydrogen and nitrogen in alcohols at 25°C are:

Hydrogen: 86.95 cc STP per 100 gm methanol at 100 atm.

Nitrogen: 1180 cc STP per 100 gm ethanol at 100 atm.

At higher temperatures (and constant pressure), the solubilities of these gases are greater. Converted to a weight basis, the solubilities at 25°C are:

Hydrogen: 0.00782 gm/gm methanol at 100 atm.

Nitrogen: 0.0148 gm/gm ethanol at 100 atm.

It is not possible to use methanol or ethanol in pressure vessels in an effort to increase the storage capacity of hydrogen and nitrogen, as indicated in Table V-2.

Table V-2
USE OF ALCOHOLS TO INCREASE WEIGHT STORAGE EFFICIENCY

TANK = 12" TITANIUM SPHERE - Wt = 4 lb - PRESSURE = 1500 psia				
Gas	Solvent	Solvent, % of Tank Volume	Gas Volume ft ³	W.S.E.
Hydrogen	Methanol	0	0.520	0.0608
Hydrogen	Methanol	3.85	0.520	0.0605
Hydrogen	Methanol	19.2	0.519	0.0593
Nitrogen	Ethanol	0	0.520	0.485
Nitrogen	Ethanol	3.85	0.519	0.484
Nitrogen	Ethanol	19.2	0.518	0.478

When a pressurized gas is to be used as a working fluid for cold-gas reaction jets, a more appropriate definition of the storage efficiency is:

$$\text{Impulse Storage Efficiency} = \text{I.S.E.} = \frac{\text{total impulse of gas wt}}{\text{gas wt plus system wt}} \quad (3)$$

and even more definitive:

$$(\text{I.S.E.})_{\%R} = \frac{\text{total impulse of gas wt}}{\text{gas wt plus wt of confining system}} \quad (4)$$

in which the term $(\text{I.S.E.})_{\%R}$ means the impulse storage efficiency at a given percent level of reliability, and the term in the denominator "... confining system" means the storage vessel, meteoroid bumpers, brackets, and all appurtenances required to conduct the gas to the point in the spacecraft where it is to perform its useful function (i.e., the inlet to the on-off valves just ahead of the nozzles).

Equations (3) or (4) can be modified readily for pressurizing gases used as working fluids for propellant tank pressurization, actuators, etc. by replacing the numerators with appropriate terms.

Returning to Equation (4), the numerator is $I_{sp}^* \cdot W$, and hence:

$$(\text{I.S.E.})_{\%R}^M = I_{sp}^* \left[\frac{\text{wt of gas for the mission}}{\text{wt of gas plus confining system}} \right] \quad (5)$$

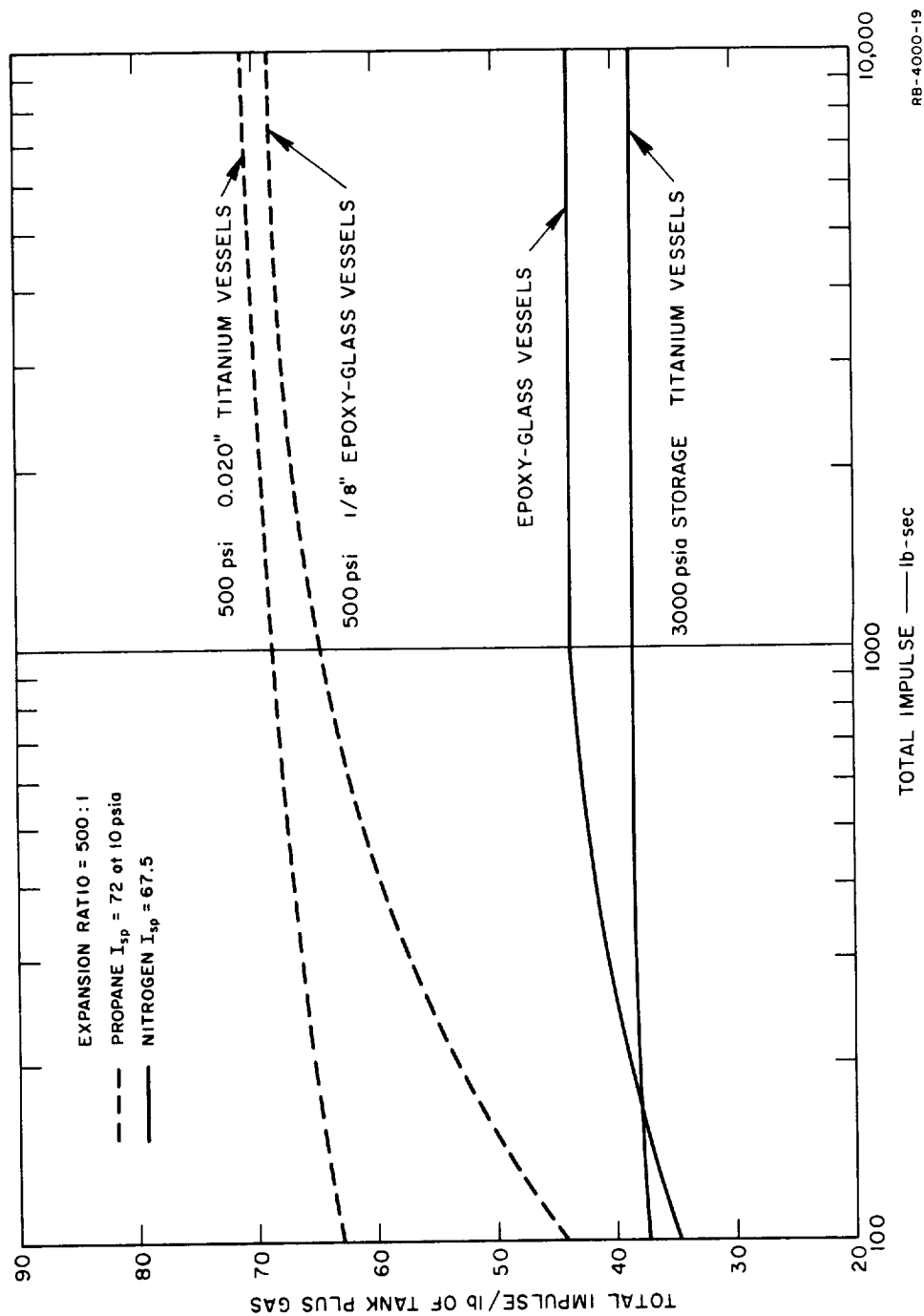
where I_{sp}^* is the specific impulse under the operating conditions in the spacecraft and the term $(\text{I.S.E.})_{\%R}^M$ means the impulse storage efficiency for accomplishing the mission M with $\%R$ reliability.

The optimum weight of gas required for a mission (for Figure V-1 it is to supply a given total impulse) obviously is largely determined by (a) the molecular weight of the gas, (b) its specific heat ratio, (c) the temperature of the gas let into the nozzle, and (d) the expansion ratio afforded by the nozzle; the computation for determining the gas weight is quite straightforward. The factors determining the weight of a confining system must be analyzed carefully for each suggested modification of current gas-storage systems in order to assess the relative merits of each contemplated modification.

The weight of a confining system is largely a function of the following parameters:

- (a) *Storage Pressure.* The pressure required to confine a gas determines the weight of the storage vessel, fittings, reducing valves, etc.; the strength of available materials of construction is a major factor.
- (b) *Permissible Permeability.* The rate of loss of a pressurized gas from leaks and permeability will determine the excess gas which must be stored in the confining system in order to accomplish a given mission successfully.
- (c) *Rupture Reliability.* The weight of a pressurized storage vessel is determined by the level of reliability (with respect to rupture) required by the mission.
- (d) *Valve Performance Reliability.* Leakless valves or pressure reducers, and on-off valves with high reliability of action for prolonged periods generally tend to be heavier than the less reliable counterparts.
- (e) *Meteoroid Protection.* Shields and other methods of minimizing meteoroid penetration obviously influence system weights. In particular, certain systems are more vulnerable than others and require added protection.
- (f) *Other Factors.*
 - (1) For gases which require temperature control to provide high performance, increased system weights may easily result.
 - (2) The efficiency of the confined gas as a working fluid and its specific gravity determine the over-all size of the storage system.
 - (3) The required weight of auxiliary systems, e.g., batteries, also influence the over-all weight of the system.

Most of the parameters which determine the weight of the confining system can be reduced to weight penalties which, when introduced into the denominator of Equation (3), permit accurate assessment of storage efficiency.



RB-4000-19

FIG. V-1 STORAGE EFFICIENCY OF NITROGEN AND PROPANE
 When Used in Cold Gas Jets at 20°C (No Condensation in Nozzle)

)

)

)

)

)

VI ZERO GRAVITY CONSIDERATIONS

Table of Contents

Section	Title	Section-Page
VI-0	List of Figures	VI-0.1
VI	Zero Gravity Considerations	VI-1
	Introduction	VI-1
	Forces on Liquids at Zero- G	VI-2
	The Central Vapor Bubble	VI-5
	Vapor Pressure Relationships	VI-6
	Film Thickness	VI-8
	Equilibrium Configuration	VI-9
	Separation of Liquid and Vapor Phases	VI-10
	References.	VI-15

VI-0 LIST OF FIGURES

Table of Contents

<u>Section-Figure</u>	<u>Title</u>	<u>Section-Page</u>
VI-1	Diagram of Change of Liquid from a Central Drop to a Wall-Wetting Configuration	VI-13
VI-2	Pressures Across Capillary Membranes	VI-13
VI-3	Equilibrium Conditions at Zero-G for a Vapor Bubble	VI-13

VI ZERO GRAVITY CONSIDERATIONS

Introduction

The state of apparent weightlessness, called zero-gravity, is experienced by matter within space vehicles when moving solely under action of gravitation as in "free fall" or in orbit around Earth. Actually, the term "zero gravity" is a misnomer because the effects attributed to weightlessness are due to the vehicle and its contents experiencing the same gravitational acceleration, which varies widely but is never zero; it is the acceleration of the contents that is zero with respect to the confining vehicle. Hence, it is more appropriate to use the term "zero-g" to describe the state of weightlessness commonly associated with space flight.

In zero-g state, the vehicle and its contents both "fall" at the same rate. Thus, there is no "up" or "down" even though every body within the spacecraft and the craft itself has mass but does not exert any weight forces on its environment. As a consequence, fluids exert no hydrostatic head; buoyancy, convection, and other "natural" phenomena depending on weight or density differences are not observable.

Of the many engineering problems associated with the handling of fluids in zero-g, the only ones of major interest to the engineer concerned with pressurized gas systems are:

- (1) The location of the bulk of the liquid contained in a tank.
- (2) Methods for separating liquid and gaseous phases.
- (3) Effects of temperature gradients.
- (4) Liquid behavior in capillary or permeable-membrane systems.

The spatial configuration of loosely-contained liquids at a given time in zero-g is a function of many things, among which are: the shape of the container, liquid-to-volume ratio, interfacial energies, mechanical disturbances, heat transfer, and minor residual forces such as atmospheric drag or even thrusts from the attitude-control system.

Forces on Liquids at Zero-G

The orienting forces on a liquid in an orbiting tank include the following:

- (a) Gravitational force between liquid and tank-vehicle system
- (b) Aerodynamic drag forces
- (c) Centrifugal forces due to vehicle spin
- (d) Electric field forces
- (e) Magnetic field forces
- (f) Inertial forces due to mass and motion of the liquid
- (g) Viscous forces within the liquid
- (h) Cohesive forces; wetting at liquid-solid interfaces
- (i) Magnetic field forces.

Most of these forces can be combined as ratios to express recognizable, nondimensional parameters:¹

$$\frac{\text{inertial force}}{\text{viscous force}} = \frac{\rho V L}{\mu} \quad (\text{Reynolds number, } R_e) \quad (1)$$

$$\frac{\text{inertial force}}{\text{compressibility force}} = \frac{\rho V^2}{E} \quad (\text{Cauchy number, } C_a = M_a^2) \quad (2)$$

$(M_a = \text{mach number})$

$$\frac{\text{inertial force}}{\text{cohesive force}} = \frac{\rho V^2 L}{\sigma} \quad (\text{Weber number, } W_e) \quad (3)$$

$$\frac{\text{inertial force}}{\text{gravitational force}} = \frac{V^2}{gL} \quad (\text{Froude number, } F_r) \quad (4)$$

$$\frac{\text{gravitational force}}{\text{cohesive force}} = \frac{\rho L^2 g}{\sigma} \quad (\text{Bond number, } B_0) \quad (5)$$

$$\frac{\text{viscous force}}{\text{cohesive force}} = \frac{V\mu}{\sigma} = \frac{W_e}{R_e} \quad (6)$$

$$\frac{\text{viscous force}}{\text{gravitational force}} = \frac{V\mu}{g\rho L^2} = \frac{F_r}{W_e} \quad (7)$$

$$\frac{\text{centrifugal force}}{\text{gravitational force}} = \frac{V^2}{Rg} \quad (8)$$

where

- L = characteristic dimension
- R = radius of curvature
- V = velocity of flow
- g = gravitational acceleration
- ρ = density
- μ = viscosity
- E = bulk elasticity
- σ = liquid-gas interfacial tension.

It is of interest to ascertain the value of these nondimensional ratios as gravity is reduced to zero; obviously the Froude number increases to infinity and the Bond number to zero. Fluid motion is defined by the Reynolds number, Weber number, Mach number, and cohesive forces at all values of g . Wetting at all values of g is determined by the interaction of cohesive and adhesive forces, and since they do not act in the same direction, their net effect is the result of their vectorial combination. Under zero- g , cohesion and adhesion vectors are to be combined with inertial, viscous, and compressibility vectors. When a liquid is at rest or moving at very low velocities, the adhesive and cohesive forces predominate; inertial forces predominate at reasonably high values of Reynolds and Weber numbers.

The predominant external force acting on a liquid in zero- g is the vector force resulting from aerodynamic drag. Even at altitudes as high as 300 miles, the force is sufficient to insure that the liquid (at equilibrium) will gather at the forward end of the tank; the gas-liquid interfaces will, in general, be highly curved as demanded by surface tension forces.² At higher altitudes, centripetal acceleration forces the liquid to opposite ends of the confining vessel.

Although not a force, heat input, such as may arise from the absorption of solar energy, leads to thermal gradients within a liquid bulk at zero-g and inevitably causes transfer of liquid from warmer to colder sections of the container by successive vaporization and condensation. The net effect is thus a mass and heat transfer which upsets equilibrium tendencies that are established by balancing of the forces described above.

Convection is absent in zero-g; hence, a significant heat transfer mechanism is not active. As a result, and because vapor bubbles tend to cling to heated surfaces at zero-g, burnout of heating elements is possible. Furthermore, there is a finite possibility that cohesive forces which normally tend to make wetting liquids at zero-g gather in some symmetrical shape about the walls of their containers (*vide infra*) are prevented from coming into play by an interceding vapor barrier generated by a heated container wall.

The equilibrium spatial configuration of liquids loosely confined in tanks at zero-g is essentially the result of the interplay of adhesive and cohesive forces, and requires time for establishment. When a fluid is displaced from equilibrium, the surface tension forces tend to restore the equilibrium spatial configuration, but an overshooting usually occurs and the configuration cannot be restored until the surface free energy in excess of that energy existing at equilibrium is dissipated (generally by conversion to heat). The time required for attainment of equilibrium is not only a function of fluid parameters (like viscosity) and the magnitude of the disturbance but also the size of the container and the mass of the fluid. The mass of the fluid to be placed in the equilibrium position increases as the cube of the tank radius while the surface free energy increases only as the square of the radius.

The spreading coefficient governs the wetting of a solid by a liquid:

$$S = \gamma_{sv} - \gamma_{sl} - \gamma_{lv} = -\Delta F \quad (9)$$

The above equation also indicates that the spreading coefficient is actually the negative value of the free energy change for the process of spreading liquid over the solid, and that it is positive for liquid-solid systems in which spreading is spontaneous. When S is negative,

Young's equation defines the contact angle:

$$\gamma_{SV} = \gamma_{SL} + \gamma_{LV} \cos \theta \quad (10)$$

Liquids in contact with solids which have relatively high surface free energies generally exhibit small or zero contact angles; i.e., for these systems Young's equation becomes:

$$\gamma_{SV} \geq \gamma_{SL} + \gamma_{LV} \quad (11)$$

and it follows that spreading occurs readily. Most liquid propellants used in rocketry exhibit zero contact angles on all metals³ and ceramic or inorganic glassy solids, and it follows that propellants will wet tank walls in zero-g and that adhesive forces will take part in the establishment of an equilibrium spatial configuration.

The Central Vapor Bubble⁴

Consider a tank containing a mass of liquid located at its center and not in contact with the sides. The liquid will have a convex surface; actually, the liquid mass will be contained in the form of a sphere, its shape entirely independent of the shape of the tank. Under these conditions, the inside area of the tank will be greater than the area of the surface of the centrally-located mass of liquid (see Figure VI-1):

$$A_t > A_d \quad (12)$$

Now, consider a tank in which the same mass of liquid is distributed uniformly over its internal surface area and that the layer of liquid is thick enough so that the liquid-vapor interface is not influenced by the wall material. The change in the interfacial free energy in going from the free-floating mass of liquid surrounded by vapor to a volume of vapor surrounded by liquid is:

$$\Delta F = -\gamma_{SV}A_t + \gamma_{LS}A_t + \gamma_{LV}(A_b - A_d) \quad (13)$$

If ΔF is negative, then the configuration in which the liquid in contact with the tank walls is favored. Rearranging the above equation to give:

$$\Delta F + \gamma_{SV}A_t - \gamma_{LS}A_t = \gamma_{LV}(A_b - A_d) \quad (14)$$

and recognizing (Figure VI-1) that

$$A_t > A_b - A_d \quad (15)$$

it follows that

$$\Delta F + \gamma_{SV}A_t - \gamma_{LS}A_t < \gamma_{LV}A_t \quad (16)$$

or that

$$\Delta F < A_t(-\gamma_{SV} + \gamma_{LS} + \gamma_{LV}) \quad (17)$$

Now, referring to Young's equation [Equation (11)], if the equal sign is assumed, then the quantity in parentheses in Equation (17) is zero and the free energy is less than zero or negative. If the inequality is assumed in Young's equation, then the free energy is again less than the negative quantity in the parentheses. Thus, the wet-wall configuration is preferred over the centrally-located liquid mass.

Vapor Pressure Relationships

The pressure of vapor in equilibrium with a liquid which has a flat surface (ordinary definition of vapor pressure) is different from that in equilibrium with a curved surface. For curvatures of radius of the order of millimeters or larger, the differences in pressure are very small but significant. The equilibrium pressure of a curved liquid surface in comparison with a flat surface is given by the relationship:

$$RT \ln P/P_0 = V(r_1^{-1} + r_2^{-1}) \quad (18)$$

where V is the molar volume of the liquid and P_0 is the vapor pressure over the flat surface. The pressures on the two sides of a curved surface are related by the equation of capillarity:

$$P_1 - P_2 = \gamma(r_1^{-1} + r_2^{-1}) \quad (19)$$

where P_1 is the pressure of the liquid and P_2 is the pressure in the vapor. As a consequence, a drop of liquid will have a higher internal hydrostatic pressure than the gas surrounding it and a vapor bubble will have a higher pressure than the liquid surrounding it.

Figure VI-2 depicts capillary action in a gravitational field for liquids which wet (contact angle = 0°) and for liquids which do not wet (contact angle $\rightarrow 180^\circ$) the material from which the capillary tube is constructed; only the liquid and its vapor are present. According to Equation (19) the qualitative relationships of the pressures across the menisci are:

$$P_6 > P_5 \quad (20)$$

$$P_3 = P_4 \quad (21)$$

$$P_2 > P_1 \quad (22)$$

and according to Equation (18) the relative vapor pressures are:

$$P_5 > P_3 > P_2 \quad (23)$$

Since only the liquid and its vapor are present, P_3 is the ordinary vapor pressure of the liquid. Hence, the pressures may be arranged in decreasing order:

$$P_6 > P_5 > P_4 (= P_3) > P_2 > P_1 \quad (24)$$

If the vapor phase is interspersed with other gases (such as air or pressurizing gases), the pressures in the system depicted in Figure VI-2 would be increased in an almost uniform increment and the relative order of the pressures indicated above would remain unchanged. Also, the system shown in this figure is in equilibrium even though the pressure (P_5) is greater over the left meniscus than over the right; the pressure exists because of meniscus curvature and is consistent with the gravity pressure gradient.

In zero-g, the conditions depicted in Figure VI-2 are the same and the pressure relationships given by Equation (24) also hold. Capillarity

and effects due to adhesive or cohesive forces will occur in zero-g and can be used to advantage in spacecraft design.

Film Thickness

Physical adsorption on flat surfaces when more than three or four monolayers are involved is defined by the Frenkel-Halsey-Hill equation⁵

$$\ln P/P_0 = -k/n^S \quad (25)$$

where n is the thickness in monolayers, k is theoretically of the order of magnitude of unity,⁶ and S is a constant (approximately 3).

For a system in which a flat surface covered by an adsorbed film of liquid is in equilibrium with a concave surface of bulk liquid of equal radii of curvature, Equation (25) can be combined with Equation (18) to give:

$$-\frac{k}{n^S} = \gamma(V/RT)(r_1^{-1} + r_2^{-1}) \quad (26)$$

and since $r_1 = r_2$,

$$n = (-kRT/2\gamma V)^{1/S} \quad (27)$$

When adsorption takes place on a strongly concave surface, the adsorbed film will be much thicker than given by Equation (27) because, by derivation of Equation (25), on a concave surface there will be more of the solid close enough to a given molecule in the film to exert an appreciable attractive force. However, the radii of curvature in propellant tanks of the kinds used in pressurized systems generally are large enough to be considered as flat surfaces, but some error may be incurred for smaller radii. Nevertheless, the wet film thickness is small, as indicated by the following examples:

For water at 273°K in a tank of 2 cm radius, the number of molecule layers in the wet film is found by Equation (27):

$$n = \left(\frac{-4(8.317 \times 10^7)(273)(-2)}{2(75.6)(18.02)} \right)^{1/3} = 406$$

using $k = 4$, $S = 3$, $\gamma = 75.6$ dyne-cm, $V = 18.02$ cc/mole, and $R = 8.317 \times 10^7$ erg/°K/mole.

The thickness of the wet film is computed from the molecular diameter, 4.68 \AA , and is, thus,

$$n \cdot d = 406 \cdot 4.68 = 1900 \text{ \AA} \quad \text{or} \quad 190 \text{ m}\mu.$$

If the water were contained in a tank of about 10 feet in diameter, then the tank radius is essentially 150 cm, and the thickness of the wet film would be about $800 \text{ m}\mu$. Hence, the wet film thickness is very small and the bulk of the liquid (see Figure VI-3) is for all practical purposes contained on both sides of the hemispherical boundaries.

Equilibrium Configuration

In a previous section, it was established that the wet-wall configuration for the equilibrium figure of a mass of liquid within a tank is preferred over a centrally-located mass. The following considerations indicate some additional details about the nature of the configuration.

The equilibrium configuration of the centrally-located vapor pocket is of such shape that the interfacial free energy will be a minimum, i.e., there will be no ripples or bumps on the liquid surface and the surface area will be a minimum. If the tank is spherical or if its configuration and size will accommodate a sphere, the vapor pocket will be a sphere.⁷

Returning to Equation (18), since V , P_0 , and γ are constant, the curvature represented by $r_1^{-1} + r_2^{-1}$ determines the vapor pressure over the surface (radii are positive in the liquid and negative in the vapor). Thus, for equilibrium to be established, the pressure must be uniform throughout the vapor volume and the curvature must be constant for all surfaces at equilibrium.

The first three diagrams of Figure IV-3 are consistent with the above statements, but as the amount of liquid in the tank of Figure IV-3 is reduced, the vapor pocket increases in size and its volume becomes such that a sphere of the minimum tank diameter cannot suffice. Hence, the configuration must become a cylinder with hemispherical ends. If

the ends have a radius r' , then the curvature will impose a particular vapor pressure on the system:

$$RT \ln P/P_0 = \gamma V [(-r')^{-1} + (-r')^{-1}] = -2/r' \gamma V . \quad (28)$$

If the cylindrical section were backed by bulk liquid, the vapor pressure over this surface would be greater than that over the hemispherical ends

$$-\frac{1}{r'} > -\frac{2}{r'}$$

but this can not exist at equilibrium. Thus, it is necessary to assume that the cylindrical section is not backed by bulk liquid but by a film of such thinness that the attractive force of the tank material on the surface molecules of the liquid film reduces the vapor pressure to the same level as in equilibrium with the hemispherical surfaces. The thickness of the film may be computed with the aid of Equation (27).

In a tank of the configuration indicated in Figure VI-3, as more liquid is removed, the hemispherical confining surfaces will recede toward the ends of the tank. At any time, however, the central cylindrical section will have a very thin film-wet surface, and bulk liquid must define the hemispherical ends of the vapor envelope; this means that if the envelope migrates towards one end of the tank, the liquid thickness between the tank wall and the envelope will adjust itself to any irregularities in the tank wall in such a way as to maintain an hemispherical surface.

For most liquids, $d\gamma/dT$ is negative. Thus, if there were a higher rate of heat flow through one wall of a tank, the surface tension would be lower on the warm side. The reduced surface tension would allow the warm surface to be drawn toward the colder areas. The over-all effect is a movement of the envelope.

Separation of Liquid and Vapor Phases

Maintaining a discrete liquid phase in a tank at zero-g is a difficult task. For tanks containing propellants used in high-level thrust units (such as rocket engines), the problem is of little concern because the moment the thrust units are activated by the propellants remaining in feed lines, sufficient accelerative forces are brought into

play to position the liquid masses in their tanks. Alternatively, small thrust units may be employed to provide forces for positioning propellants before the large thrust units are activated. For specialized applications, such as dumping propellant, special systems have been devised and successfully applied.²

The use of bladders, diaphragms, pistons, and other artifacts for maintaining intact a mass of liquid in zero-g while permitting pressurization has been employed extensively. The most common of these systems involve use of diaphragms or bags, but the biggest problems encountered are the permeability of materials and the extremely corrosive nature of most rocket propellants. For short-time missions, diaphragms can be made which are flexible and quite impermeable; however, for extended missions, permeability must be taken into consideration.

The problem of withdrawing gas or reducing the vapor or gas pressure in a pressurized system containing a liquid phase at zero-g is exceedingly complex and has been solved only in limited instances, for example the rapid-dump system for blowdown or venting of the Agena vehicle.² This problem is particularly vexing in the case of systems for supplying pressure from liquefied gas; in instances where the systems are to perform effectively for extremely long periods of time (such as satellite attitude control systems), it is especially important to insure clean separation of the phases. Since most pressurizing systems utilizing a liquefied gas include diaphragm-type pressure regulators, separation of phases can be conveniently effected by use of bags or diaphragms to contain the liquefied gas, and the liquid phase is bled through the regulator into an expansion chamber; however, for long missions, the permeability of the bag to both the pressurizing gas and the contained liquid will eventually lead to diffusion of the pressurizing gas into the bag. If piston-and-seal-type systems can be utilized, the greatly reduced area for permeability (e.g., an O-ring) will insure a longer period of performance.

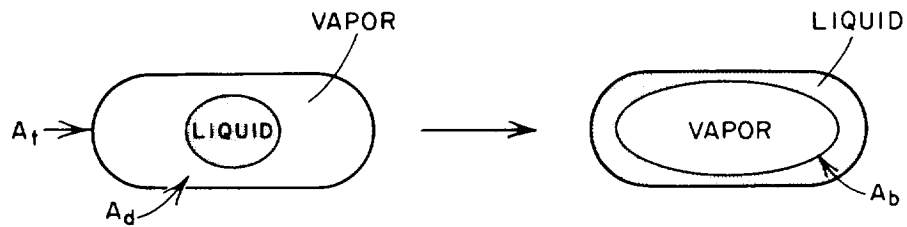
)

)

)

)

)



A_t = AREA OF INNER TANK SURFACE

A_d = AREA OF SURFACE OF DROP

A_b = AREA OF INNER BUBBLE SURFACE

FIG. VI-1 DIAGRAM OF CHANGE OF LIQUID FROM A CENTRAL DROP TO A WALL-WETTING CONFIGURATION

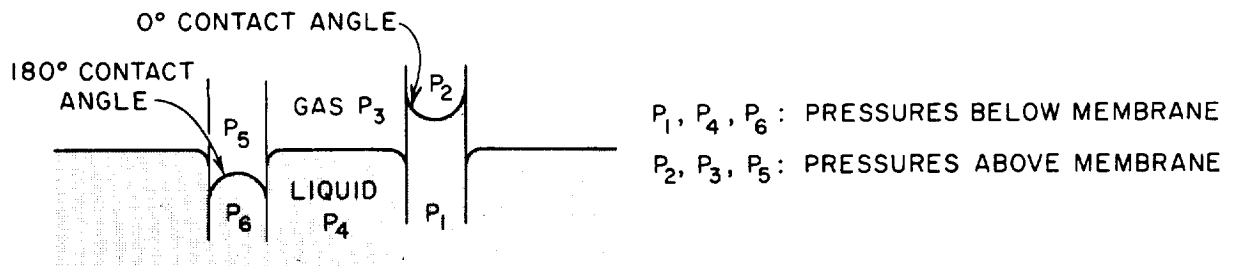


FIG. VI-2 PRESSURES ACROSS CAPILLARY MEMBRANES

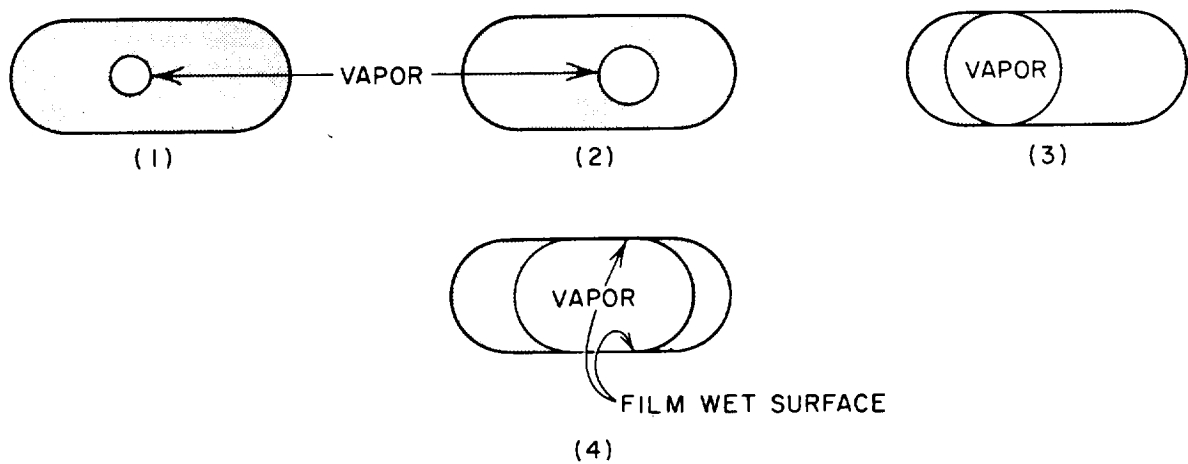


FIG. VI-3 EQUILIBRIUM CONDITIONS AT ZERO-G FOR A VAPOR BUBBLE

)

)

)

)

)

VI ZERO GRAVITY CONSIDERATIONS REFERENCES

1. Unterberg, W., and Congelliere, J., *ARS J.*, **32**, 862 (1962).
2. Satterlee, H. M., *Space/Aeronautics*, **38**, July 1962, p. 72.
3. "Studies of the Contact Angles of Storable Liquid Propellants," Stanford Research Institute, Final Report, Project PD-3462, 1961; Muraca, R. F., Longwell, A. P., and Burns, E. A., *Rev. Sci. Inst.*, **34**, 479 (1963).
4. Neu, J. T., and Good, R. G., *AIAA J.*, **1**, 814 (1963).
5. Hill, T. L., "Theory of Physical Adsorption" in *Advances in Catalysis*, edited by Frankenburg, Komarensky, and Rideal, Academic Press, New York, 1952, Vol. IV, Ch. 5.
6. MacMillan, W. G., and Teller, E., *J. Chem. Phys.*, **19**, 25 (1951).
7. Li, T. C. H., *J. Chem. Phys.*, **36**, 2369 (1962).

)

)

)

)

)

VII HEAT BALANCE

Table of Contents

	Title	Section-Page
Table VII-1	Equilibrium Temperatures of Spherical Space Probes with Various Coatings	VII-1
Table VII-2	Representative Materials for Passive Thermal Control of Space Vehicles	VII-2
Figure VII-1	Variations with Temperature of Emissivity and Absorptivity and of their Ratio for Two Metals	VII-3
Figure VII-2	Variation of Equilibrium Temperature with Distance from Sun in Case of Aluminum or Silver Sphere having Uniform Temperature	VII-4
Figure VII-3	Variation of Equilibrium Temperature with Distance from Sun in Case of a Sphere having Uniform Temperature	VII-5
Figure VII-4	Power Input per Unit Cross-Sectional Area of a Satellite Plotted as a Function of Altitude for the Range 200-3200 Miles	VII-6
Figure VII-5	Power Input per Unit Cross-Sectional Area of a Satellite Plotted as a Function of Altitude for the Range 200-32,000 Miles	VII-7
	References	VII-9

1

2

3

4

5

Table VII-1
EQUILIBRIUM TEMPERATURES OF SPHERICAL SPACE PROBES
WITH VARIOUS COATINGS (Ref. 1)

COATING	SOLAR				TEMPERATURE, °F	
	ρ	α	ϵ	α/ϵ	SPHERE	STRIPED SPHERE
White	0.82	0.18	0.95	0.2	-135	-20
White plus carbon black	0.47	0.53	0.95	0.6	-30	32
Aluminum plus clear lacquer				1.0	40	
Flat black	0.03	0.97	0.95	1.0	45	85
Aluminized silicone				1.3	60	
Flat black plus aluminum	0.05	0.95	0.80	1.2	65	120
Stainless steel				2.5	170	
Aluminum				4.0	250	

Table VII-2
 REPRESENTATIVE MATERIALS FOR PASSIVE THERMAL CONTROL OF SPACE VEHICLES
 (Ref. 2, 3, 4, 5, 6, 7)

MATERIAL	SUBSTRATE AND/OR TREATMENT	ABSORPTANCE, EMISSIVITY			EXAMPLES OF USE
		α_s	ϵ_H	α_s/ϵ_H	
Metals					
Stainless Steel	Sand-blasted	0.81	0.42	1.92	Explorers I, III, IV
Aluminum Foil, (sandblasted)	Fiberglass	0.42	0.21	2.0	Explorer VII
6061 Aluminum Alloy Sheet	Chemically cleaned	0.26	0.06	4.34	
Forging		0.29	0.09	3.22	
Weld Area		0.26	0.10	2.6	
6061 Aluminum Alloy	Degreased, cleaned, acid rinsed	0.39	0.03	13.0	
2024 Aluminum Alloy	Degreased, cleaned, acid rinsed	0.34	0.06	5.67	
QMV Beryllium	Sintered, machined, chemically polished	0.50	0.10	5.00	
Hanovia Gold 6518	René 42	0.53	0.09	6.00	
Oxides					
Rokide A (AlO)	Sand-blasted stainless and/or fiberglass	0.15	0.77	0.20	Explorers I, III, VII
Rokide C	René 14	0.90	0.85	1.06	
Silicon Oxide	Vacuum deposited on aluminum			1.2	Vanguard
Titanium Oxide	From oxidation of Ti vacuum-deposited on Al	0.77	0.14	5.5	Atlas-Able-IV
Titanium Oxide	Adhesive-backed vinyl film	0.25	0.84	0.3	Atlas-Able-IV
Paints					
Silicone Alkyd Enamel + TiO ₂		0.18	0.95	0.19	Journeyman
Grey Alkyd Enamel + Aluminum Flakes		0.95	0.80	1.18	Journeyman
Epoxy Paint + Black Iron Oxide	Plastic	0.97	0.95	1.02	Transit I-B
Polyurethane Lacquer + TiO ₂	Plastic	0.18	0.95	0.19	Transit I-B

* 70°F

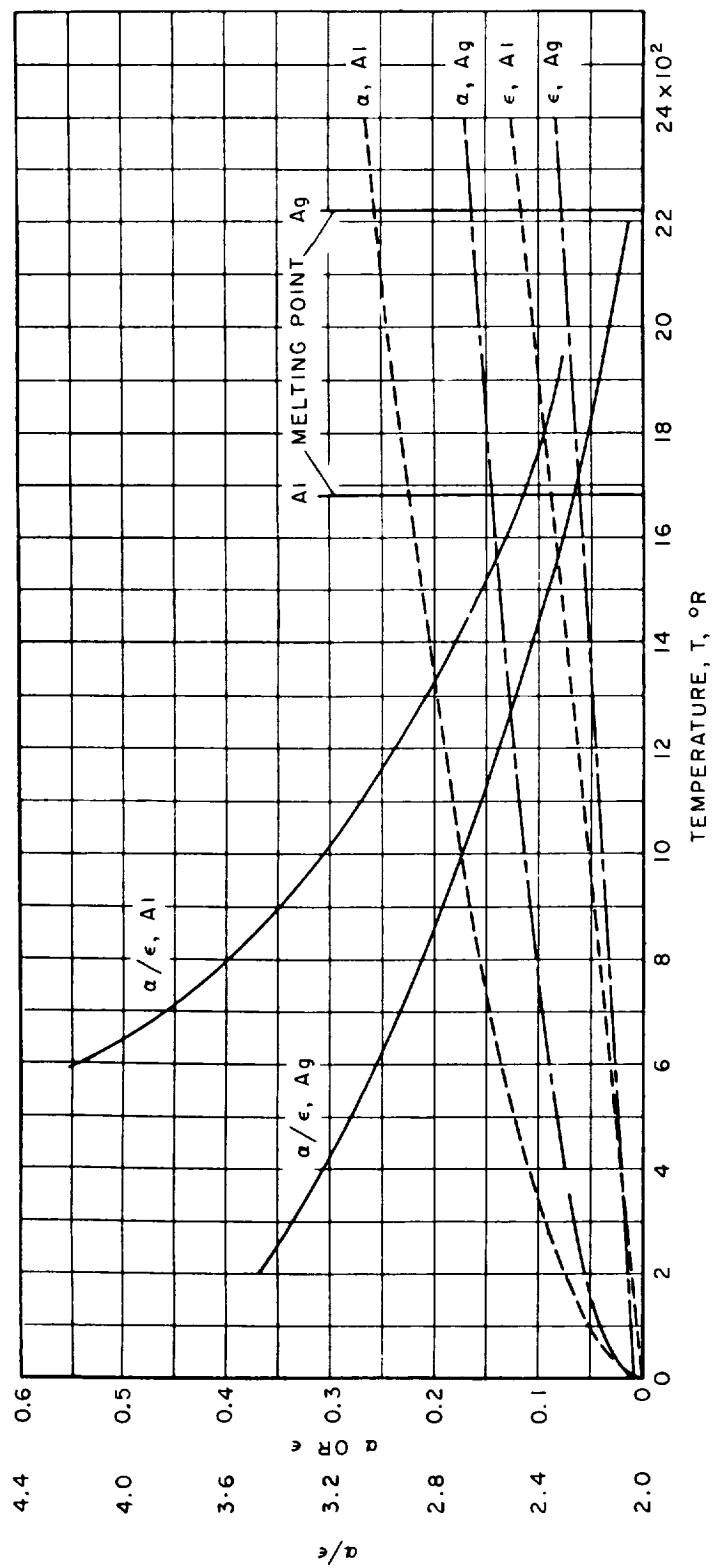


FIG. VII-1 VARIATIONS WITH TEMPERATURE OF EMISSIVITY AND ABSORPTIVITY AND OF THEIR RATIO FOR TWO METALS (Ref. 8, p. 33)

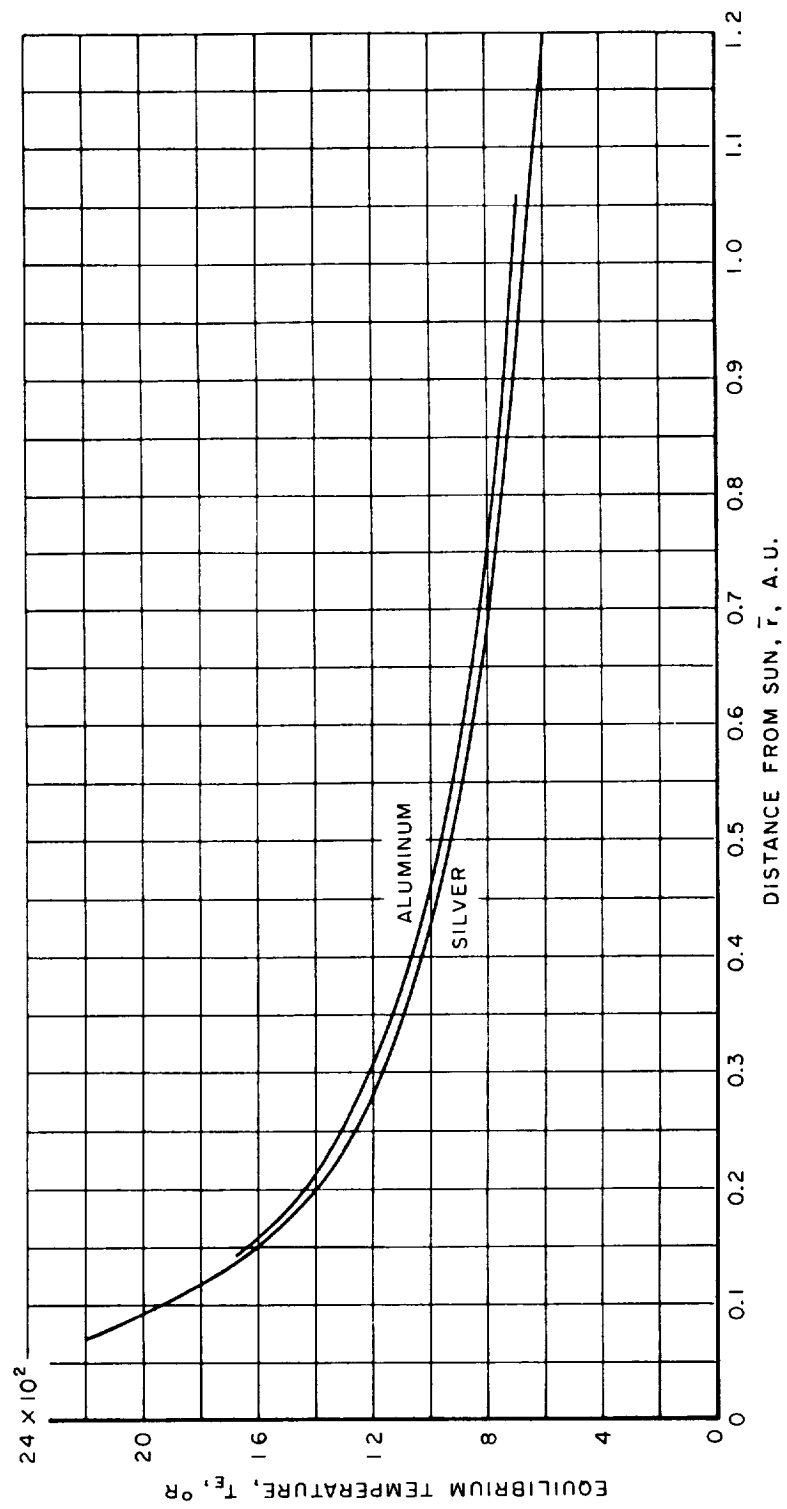


FIG. VII-2 VARIATION OF EQUILIBRIUM TEMPERATURE WITH DISTANCE FROM SUN IN CASE OF ALUMINUM OR SILVER SPHERE HAVING UNIFORM TEMPERATURE (Ref. 9, p. 35)

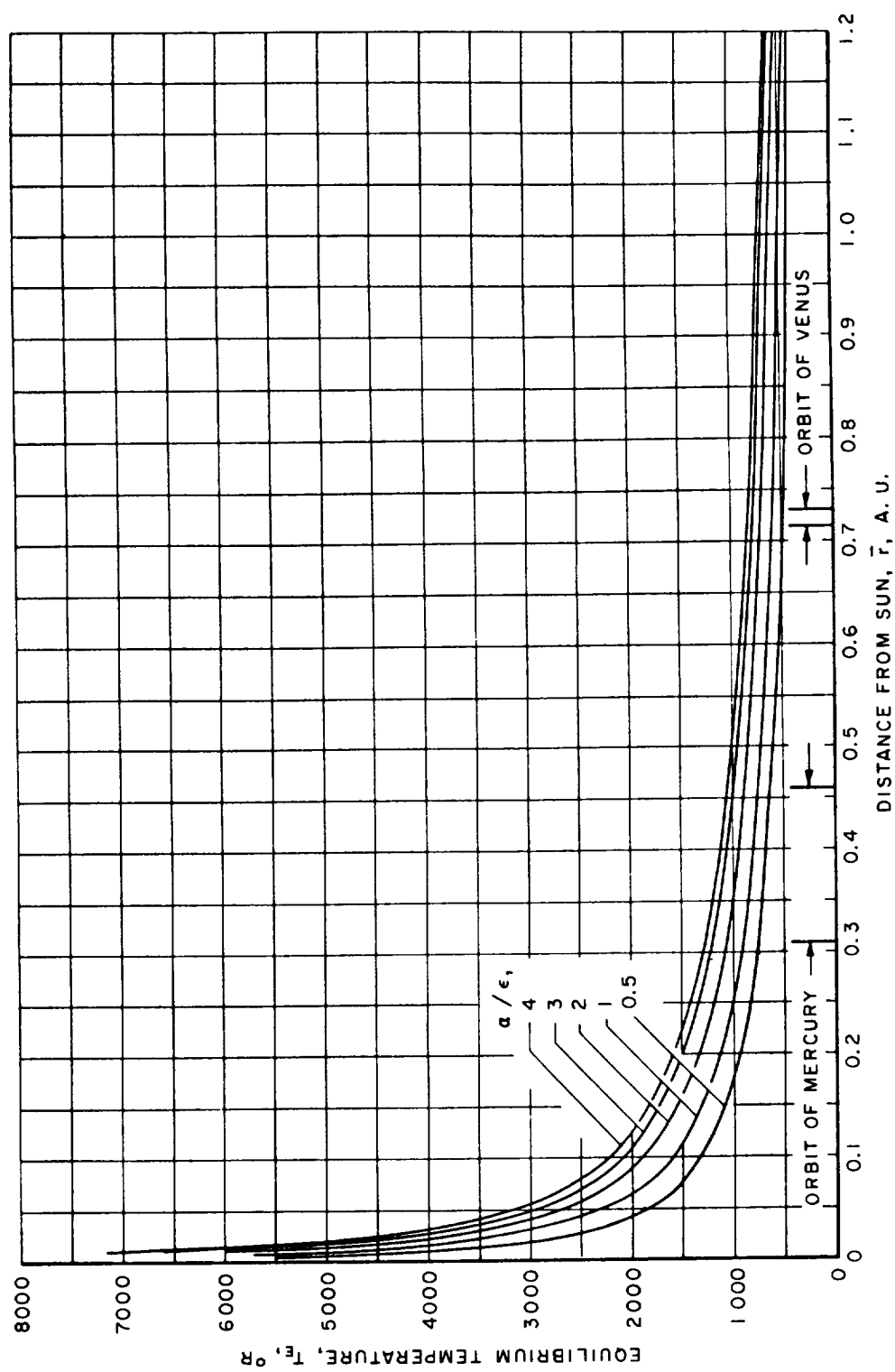


FIG. VII-3 VARIATION OF EQUILIBRIUM TEMPERATURE WITH DISTANCE FROM THE SUN
IN CASE OF A SPHERE HAVING UNIFORM TEMPERATURE (Ref. 8, p. 34)

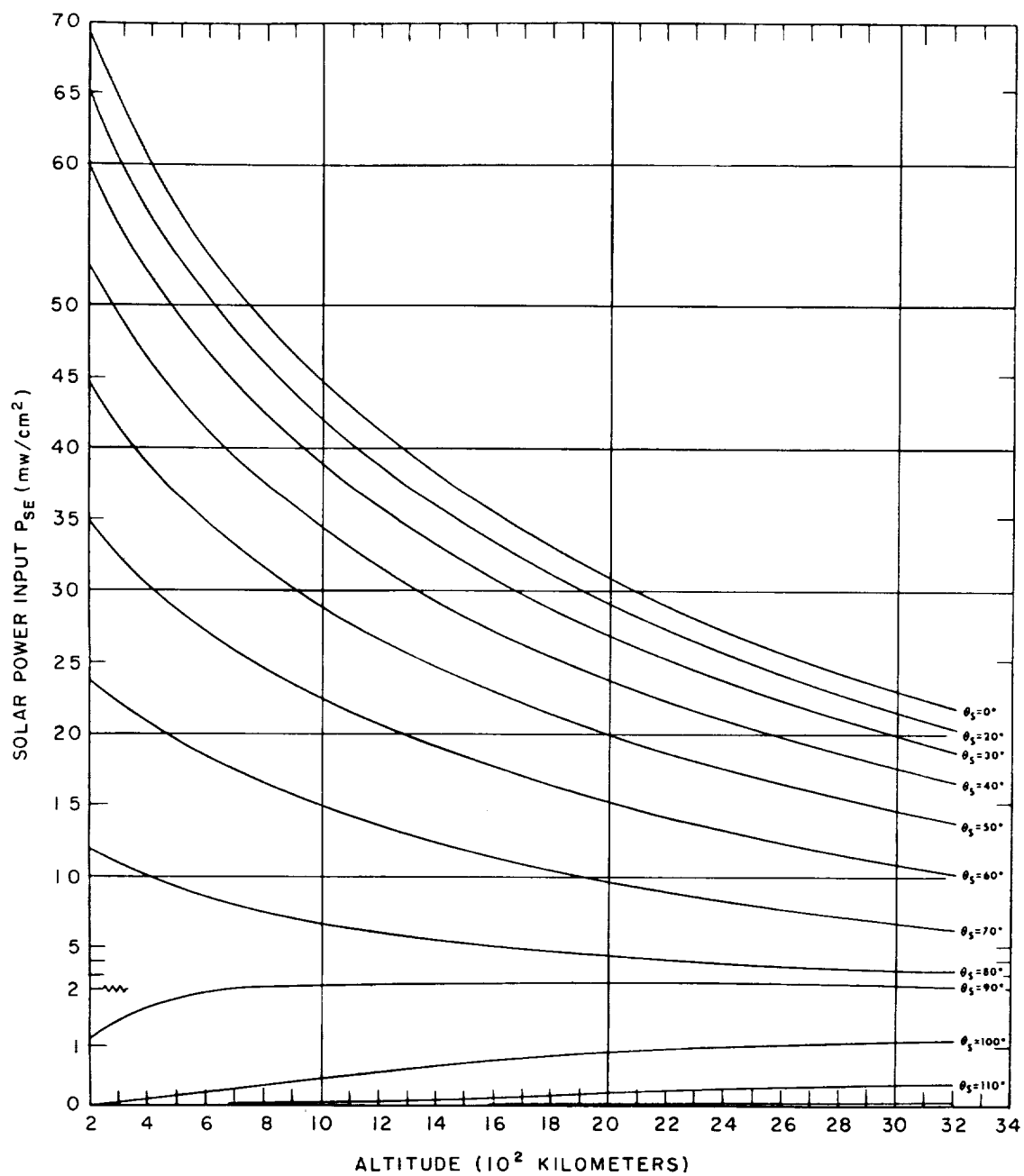


FIG. VII-4 POWER INPUT PER UNIT CROSS-SECTIONAL AREA OF A SATELLITE PLOTTED AS A FUNCTION OF ALTITUDE FOR THE RANGE 200-3200 MILES (Ref. 9, p. 7)

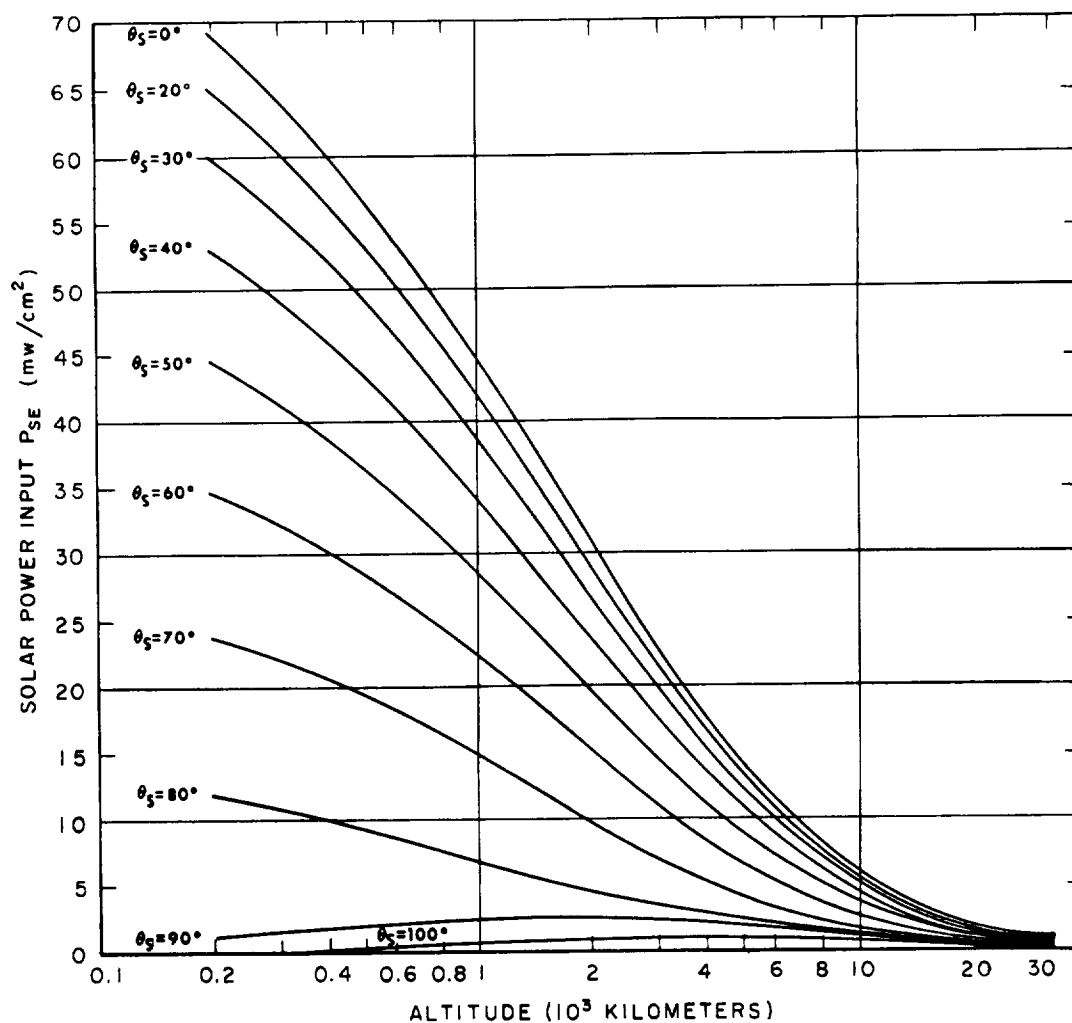


FIG. VII-5 POWER INPUT PER UNIT CROSS-SECTIONAL AREA OF A SATELLITE PLOTTED AS A FUNCTION OF ALTITUDE FOR THE RANGE 200-32,000 MILES (Ref. 9, p. 8)

)

)

)

)

)

VII HEAT BALANCE REFERENCES

1. Weaver, J. H., and Jacobs, C., "Materials Symposium, Phoenix, Arizona, September 1961," ASD TR 61-322, p. 456-469.
2. Gaumer, R. E., *et al.*, "Space Materials Handbook," Lockheed Missiles & Space Company, January 1962, p. 476.
3. Acker, R. M., Lipkins, R. P., and Vehrencamp, J. E., Space Technology Laboratories, Inc., AFBMD Doc. No. 61-04-6963.
4. VanVliet, R. M., Mattice, J. J., and Cross, R. A., WADD TR 60-386, October 1960.
5. Eckard, L. D., Jr., Johns Hopkins University Applied Physics Lab., Report No. CM-1001, September 1961. (AD273 555).
6. Heller, G., and Jones, B. P., NASA TN D-608, July 1961.
7. Heller, G., ARS J., 30, 344 (1960).
8. Dugan, Duane, W., NASA TN D-783, April 1961.
9. Cunningham, F. G., NASA TN D-1099, October 1961.

)

)

)

)

)

VIII PERMEABILITY THEORY

Table of Contents

Section-Part	Title	Section-Part. Page
VIII-0	List of Tables	VIII-0.2
VIII-1	Introduction	VIII-1.1
VIII-2	Polymeric Materials	VIII-2.1
VIII-3	Glasses	VIII-3.1
VIII-4	Metals	VIII-4.1
VIII-5	Laminates	VIII-5.1
VIII-6	Distinction Between Permeation and Mass Flow	VIII-6.1
VIII-7	References	VIII-7.1

VIII-0 LIST OF TABLES

<u>Section-Part-Table</u>	<u>Title</u>	<u>Section-Part-Page</u>
VIII-2-1	Permeability of Three Polyethylenes at 25°C	VIII-2.7
VIII-2-2	Permeability of Plasticized and Unplasticized Polychlorotrifluoroethylene	VIII-2.7

VIII-1 INTRODUCTION

The transmission of a gas or a vapor through a polymeric or metallic film is, in the absence of flaws such as cracks, pinholes and the like, a process of activated diffusion. The gas must first adsorb on the surface of the film, then dissolve in the material, diffuse through the bulk, and desorb on the low pressure side. These steps always occur when gases or vapors diffuse through any material, but the relative importance of the various steps and the rate-controlling processes are sufficiently different to make it convenient to discuss each type of material separately. Accordingly, permeation through organic polymers, through inorganic glasses, and through metals are discussed in this order. This is followed by a brief discussion of laminates (including a metal foil, which may have pinholes, deposited on a polymer) and finally, consideration of simultaneous permeation and mass flow.

Specific permeation data are given for a number of materials in the Materials Section (XII-4) of this Handbook.

)

)

)

)

)

VIII-2 POLYMERIC MATERIALS

With permanent gases, such as He, H₂, O₂, N₂, CO₂, the solubility in the polymer is sufficiently low so that the gases are diffusing through essentially unchanged polymer. Under these circumstances, in the steady state the amount transmitted per unit time per unit area, J , is given by

$$J = -D \frac{dc}{dx} \quad (1)$$

where D is the diffusion constant and dc/dx is the concentration gradient within the polymer film. Because of the small solubility, Henry's law holds and thus $c = Sp$, where S is the solubility coefficient and p is the pressure of the gas. Substituting in Equation (1),

$$J = -DS \frac{dp}{dx} \quad (2)$$

The product DS is the permeability constant, P . Since in the steady state J is independent of x , Equation (2) can be integrated to give

$$P = \frac{-Jd}{\Delta p} \quad (3)$$

where d is the thickness of the film.

The usual method of measuring the permeability of a polymeric film is to establish a known pressure of the gas or vapor on one side of the film and to observe the transmission of the gas or vapor by the pressure increase on the other side. The low pressure side is generally at high vacuum, so that the pressure drop across the film is substantially constant during the course of the experiment. The method has the advantage of simple mathematical analysis but can be very slow under some circumstances. The method used by Stanford Research Institute measures the rate of permeation (as opposed to the total amount permeated) by means of a mass spectrometer, and allows the simultaneous determination of two or more species in a mixture.

VIII-2.1

Both methods are amenable to the analysis of the transient state to separate the diffusion and solubility coefficient parts of the permeability coefficient. One means of analysis of the transient state can be termed the "late" approximation and the other the "early" approximation. The mass spectrometer method is particularly suitable for the latter, and in certain circumstances this can, in addition to separating diffusion and solubility, considerably shorten the time of the experiment.

Both means of analyzing the transient state start with Fick's second law and the assumption that the diffusion constant is independent of concentration which, in the one dimensional case, gives

$$\frac{dc}{dt} = D \frac{d^2c}{dx^2} \quad (4)$$

where t is the time. The late approximation was introduced by Daynes⁷ and developed by Barrer.³ Solution of Equation (4) by a Fourier series in the coordinates and an exponential in the time with the boundary conditions $c = c_0$ at $x = 0$ for all t , $c = 0$ for $0 < x < d$ for $t = 0$, and $c = 0$ at $x = 1$ for all t , leads to

$$Q = \frac{AD}{d} c_0 \left[t - \frac{d^2}{6D} - \frac{2d^2}{\pi^2 D} \sum_{n=1}^{\infty} (-1)^n \frac{\exp(-n^2 \pi^2 D t / d^2)}{n^2} \right] \quad (5)$$

where A is the area of the film and Q is the quantity transported across the film in time t . At sufficiently long times Equation (5) reduces to

$$Q = \frac{ADc_0}{d} (t - \tau) \quad (6)$$

Thus Q becomes linear in t with a slope $(APp_0)/d$ (since $c_0 = Sp_0$, where p_0 is the upstream pressure) and an intercept on the time axis τ and

$$D = \frac{d^2}{6\tau} \quad (7)$$

Hence, by this method, one can obtain both P and D and, consequently, S . An independent check is to measure the solubility directly. Excellent

agreement has been reported for a number of elastomer-gas systems by van Amerongen.³³

The "early" approximation was used by Rogers, Buritz and Alport.²⁴ By a transformation a solution of Equation (4) is

$$J = 2Sp_1(D/\pi t)^{1/2} \sum_{m=1}^{\infty} \exp [-(d^2/4Dt)(2m+1)^2] \quad (8)$$

At times sufficiently short only the leading term in the series is important. Multiplying both sides of Equation (8) by $t^{1/2}$ and taking natural logarithms leads to

$$\ln (Jt^{1/2}) = \ln [(2Sp_1)(D/\pi)^{1/2}] - d^2/4Dt \quad (9)$$

Thus plotting the left hand number against t^{-1} should give a straight line of slope $-d^2/4Dt$. Having determined D , the value of S is given by

$$S = \left(\frac{\pi}{D}\right)^{1/2} \left(\frac{Jt^{1/2}}{2p_1}\right) \exp (d^2/4Dt) \quad (10)$$

and, since $P = DS$, this quantity is also determined.

From the early approximation all the quantities of interest can be derived. It is especially useful in the mass spectrometer method because rates are required, which are determined directly. The late approximation requires an integration. Rogers *et al.* actually used the pressure rise method in their application of the early approximation which, of course, required a differentiation and its accompanying errors.

At $t = 2.7\tau$ both the early and the late approximation are in error by 1.2%, so this can be considered a rough dividing line for the region of validity of the two methods.

Both D and S obey the Arrhenius relations:

$$S = S_0 e^{-\Delta H/RT}$$

$$D = D_0 e^{-E_P/RT}$$

VIII. 2. 3

where ΔH is the heat of solution of the gas in the polymer and E_d is the activation energy of diffusion within the polymer. Consequently,

$$P = P_0 e^{-E_p/RT}$$

where $E_p = \Delta H + E_d$. In all cases E_d is positive (rate of diffusion increases with increasing temperature). The quantity ΔH is small and positive for the permanent gases, but may be negative and large in the case of easily condensable gases owing to the contribution of the heat of condensation.²⁵ As a result, a plot of the logarithm of the permeability vs. the reciprocal of the absolute temperature gives very nearly a straight line in the case of the permanent gases (increase in permeability with increasing temperature), but with easily condensable gases (e.g., water through Nylon 6-6 or polyvinyl alcohol,¹⁹ methyl bromide through polyethylene²⁶) when the temperature is decreased the permeability may first decrease, pass through a minimum, and actually increase at still lower temperatures.

A knowledge of the chemical nature of the polymeric film is not sufficient to define its permeability—one important factor is crystallinity. In Table VIII-2-1 are given the permeability of some polyethylene films of different crystallinities (as determined by density) for selected gases. Fairly good correlation can be obtained by assuming that the gases are soluble only in the amorphous portion of the polyethylene; similar results have been reported for permeation of water vapor through polyethyleneterephthalate.¹⁴ Table VIII-2-2 illustrates another effect, that caused by plasticizer. Chemical analysis of the two polymers would be nearly identical, but it can be seen that the presence of low molecular weight material enormously increases the permeability. This effect, in contrast to the effect of crystallinity, is largely due to an increase in the diffusion constant. Polyethyleneterephthalate shows in addition crystallinity effects such as those illustrated for polyethylene.

It would be desirable to be able to predict the permeability of an arbitrary gas-polymer system through basic principles or an empirical correlation requiring very few measurements. Unfortunately, no method of general applicability has been found. The solubility portion can, in a given polymer, be correlated fairly well with the normal boiling point of the gas,²⁵ its critical temperature,³³ or its Lennard-Jones force constant.¹⁶ Correlations of diffusion constants have not been nearly so successful.

VIII-2.4

Michaels and Brixter¹⁷ have had some success in correlating diffusion in polyethylene with a geometric impedance factor, a chain immobilization factor, and a "reduced diameter" (involving the mean unoccupied distance between two chain segments). However, use of this correlation requires a great deal of knowledge about the polymer and its extension to other polymers has not yet been made. Salame²⁹ has published a correlation of the permeability of various organic materials through polyethylene by use of a "permachore." Although useful for related polymers such as polypropylene, he specifically states that the method cannot be applied to polymers such as nylon, Delrin, and other nitrogen- or oxygen-containing polymers.

The simplest correlation suggested is that of Rogers *et al.*,²⁵ who noted that the ratio of the permeabilities of some of the fixed gases is roughly independent of the nature of the polymer. Hence they suggested a "G value" for the following gases (at 30°C): $N_2 = 1.0$ (arbitrary), $O_2 = 3.8$, $H_2S = 21.9$, $CO_2 = 24.2$. This may serve as a guide in many cases, but it fails badly in other cases. Thus from Table VIII-2-1 it can be seen that the ratio of the permeability of O_2 to that of N_2 is indeed approximately 3, but CO_2 is only about twice as permeable as N_2 . In the case of polytrichloroethylene (Table VIII-2-2), on the other hand, the CO_2/N_2 ratio is 13-19.

The above discussion has been confined to the permeability of permanent gases, except for brief mention of temperature effects with easily condensable vapors. If the vapor is appreciably soluble in the polymer, the situation can become quite complicated, since in general Henry's Law will not be obeyed; this plus the plasticizing effect of the permeant will cause a strong dependence of the permeability constant on the vapor pressure of the permeant and the more or less unpredictable temperature effects already mentioned. Under these circumstances, the polymeric material is generally not suitable for space applications. In some cases, however, the possibility of such behavior must be expected, as in the following example.

According to a Bell Aerosystems report¹³ MON (and hence presumably N_2O_4) comes to equilibrium across a 7-mil Teflon sheet in a few days. For a long mission with a re-start, it might be desirable to know the permeability with a relatively low pressure differential and near saturation on both sides.

In the mass spectrometric method for measuring permeabilities, the pressure on one side is set at p_0 and on the other at essentially zero. By definition, the over-all permeability \bar{P} , the thickness t , the flux J , and p_0 are related by:

$$J = \bar{P}p_0/t \quad . \quad (11)$$

One can equally well define a differential permeability by ($0 < x < t$):

$$J = Pdp/dx \quad . \quad (12)$$

Equating (11) and (12) and integrating from $x = 0$, $p = 0$ to $x = t$, $p = p_0$ gives a relation analogous to a well-known case for integral and differential diffusion coefficients:

$$\bar{P} = \frac{1}{p_0} \int_0^{p_0} p dp \quad (13)$$

Differentiating (13) with respect to p_0 gives the relation sought:

$$P = \bar{P} + d\bar{P}/d \ln p_0 \quad . \quad (14)$$

For most "permanent" gases through most films, \bar{P} is independent of p_0 and Equation (14) is trivial. Where swelling occurs, however, P and \bar{P} may differ appreciably. For water through Nylon 6-6 at 25°C, $P(\text{sat.}) = 7.5\bar{P}(\text{sat.})$, calculated from data of Myers *et al.*,¹⁸ and for methyl bromide through polyethylene at -15°C, $P(\text{sat.}) \approx 7.8\bar{P}(\text{sat.})$, calculated from the data of Myer *et al.*¹⁵

Table VIII-2-1
PERMEABILITY OF THREE POLYETHYLENES AT 25°C
(Ref. 17)

α = vol. fraction amorphous

GAS	PERMEABILITY [cc(STP)/cm-sec-atm] $\times 10^7$		
	Grex ($\alpha = 0.23$)	Alathon 14 ($\alpha = 0.57$)	Hydropol ($\alpha = 0.71$)
He	0.087	0.375	1.20
O ₂	0.0308	0.220	0.86
A	0.129	0.208	0.84
CO ₂	0.0275	0.113	0.47
N ₂	0.0109	0.074	0.304

Table VIII-2-2
PERMEABILITY OF PLASTICIZED AND UNPLASTICIZED
POLYCHLOROTRIFLUOROETHYLENE
(Ref. 20)

GAS	TEMP., °C	PERMEABILITY [cc(STP)/ cm-sec-atm] $\times 10^8$	
		Unplasticized	Plasticized ^a
N ₂	50	0.014	0.42
	75	0.065	1.95
O ₂	0	0.003	0.083
	30	0.040	0.42
	60	0.22	2.13
CO ₂	50	0.27	5.70

^a Plasticized with low molecular weight
polychlorotrifluoroethylene.

1

2

3

4

5

VIII-3 GLASSES

The permeability of fused silica and certain glasses to helium is well known and can be troublesome under certain circumstances. Vacuum Dewars of some types of glass, for example, can be used to store liquid helium only for a day or two since they will lose their vacuum through helium permeation. Hydrogen, deuterium, and neon will also permeate fused silica, but the permeabilities of molecules larger than these (a dividing line of about 2.5 Å diameter) are enormously less.²¹

The permeabilities of the small gas molecules through glass follow an Arrhenius law as in the case of polymeric films just discussed, $P = P_0 e^{-E_p/RT}$. The glass composition plays a dominant role. The rate of permeation decreases as the content of glass formers, $\text{SiO}_2 + \text{B}_2\text{O}_3 + \text{P}_2\text{O}_5$ decreases; when this sum drops to 20-30%, the helium permeation rate is cut down, compared to silica glass, by a factor of a million.²¹ This effect is attributed to alkali and alkaline earth oxides blocking the passages in the relatively open network of the glass-forming oxides. A similar picture of channels closing explains the fact that the permeability of quartz to helium is less than that of vitreous silica by a factor of 10^7 or more.

In summary, glass could involve a permeability problem, particularly with helium, but one that can easily be circumvented by proper choice of composition.

)

)

)

)

)

VIII-4 METALS

The permeation of metals by gases is considered separately from polymers and glasses because of three outstanding characteristics: impermeability to noble gases, dissociation of diatomic gases in the process, and influence of surface films on the permeability.

All attempts to measure the permeability of noble gases have been unsuccessful. As examples, Ryder²⁸ found negative results on the permeability of iron to argon, as did Baukloh and Kayser⁵ on that of nickel to helium, neon, argon, and krypton. The rare gas ions can be forced into metals under a potential gradient, but penetration is relatively shallow and upon heating the metal the gas is released.²¹

The processes of adsorption, dissociation, solution, and diffusion of a diatomic gas can lead to quite complicated rate laws under certain circumstances. Various limiting equations are given by Ash and Barrer.¹ However, for most metals at pressures over one atmosphere a square root law is followed as is the exponential relation, already mentioned in the case of polymers and glasses, so the permeability may be expressed by

$$P = \frac{K(p_0^{1/2} - p_1^{1/2})e^{-E_p/RT}}{d}$$

where K is a constant and p_0 and p_1 are the upstream and downstream pressures. This law is not followed when there is an appreciable coherent film (usually oxide) on the metal, when there is radiative or chemical interaction, or when the solubility of the gas is very high. An example of the latter is H_2 -Pd above about one atmosphere, where the permeation rate is proportional to the 0.8 power of the pressure.⁸ Examples of chemical interaction are the diffusion of nitrogen and oxygen through titanium³⁴ and hydrogen through zirconium.¹¹ In these cases a new phase is formed above a limiting pressure (rather low unless the temperature is high) and the reaction becomes essentially a corrosion reaction, with the effective gas pressure in equilibrium with the upper limits of the new phase at the temperature in question. Under these circumstances the above equation becomes quite meaningless.

VIII-4.1

In most studies on the permeation of gases through metals, precautions are taken to eliminate surface films as far as possible in order to simplify interpretation. From a practical standpoint, the effect of surface films must be taken into account. As Flint⁹ points out, surface films may be expected to become important barriers to diffusion when the oxide coating has a specific volume equal to or greater than that of the base metal. Metals falling in this category are Al, Si, Cr, Mn, Fe, Co, Ni, Cu, Zn, Pd, Ce, and Pb. Very few systematic studies have been made in this field. Flint⁹ prepared oxide films on Type 347 stainless steel by treatment in wet hydrogen and observed reduction in permeation rate of as much as 400 fold. However, these might be termed transient tests as the permeability increases with time, presumably as the oxide coating was reduced. Experiments with hydrogen and Inconel have given permeation rates independent of the thickness of the metal, thus indicating an over-riding effect of a surface film.² Several authors^{32,12,30,27} have noted the effect of oxide films on aluminum or aluminum alloys; drops in permeability as much as 1000-fold have been found.

An effect that may become important for hydrogen (and possibly other gases) in space environment is production of atoms by radiation, although recent calculations³⁵ have tended to minimize this factor. Production of atomic hydrogen at iron surfaces by corrosion reactions with water and its subsequent diffusion into the metal is well known to corrosion engineers. The chemically produced atoms are equivalent to those at very high pressures and temperatures for normal hydrogen and, as previously mentioned, it is the atomic hydrogen that affords the mechanism for diffusion. One industrially important consequence of this effect was in the early days of metal vacuum tube manufacture, when it was found that water contained in sodium silicate paint was reacting with the iron, and hydrogen diffusing through the tubes made them gassy and inoperable.²¹ Similarly, it has been found that a glow discharge increased the permeability of aluminum to hydrogen five-fold; conditions were not well enough defined in this case to attach quantitative significance to the result.²⁷

VIII-5 LAMINATES

The discussion up to this point has been concerned with homogeneous materials. There are, however, important practical cases where laminates are used. It is convenient for present purposes to distinguish two cases: one is where two or more plastics or elastomers are laminated and the permeabilities of the materials to the gas in question, while different, are not so far apart that any one of them can be neglected (an example is the use of styrene-butadiene rubber liners in continuous-filament glass fiber-reinforced epoxy pressure vessels); the second is where a metal foil is laminated onto a polymer film as a permeation barrier, in which case the foil may be considered (for noble gases at least) to have zero permeability but the possibility of pinholes and their influence must be considered.

In the plastic laminate case one can, as before, define an over-all permeability, P by

$$P = \frac{Jd}{\Delta p} \quad (15)$$

In the steady state J is the same for all elements i of the laminate, so in addition

$$P_i = \frac{Jd_i}{\Delta p_i}$$

and also

$$\begin{aligned} \Delta p &= \sum_i \Delta p_i \\ &= J \sum_i \frac{d_i}{P_i} \end{aligned} \quad (16)$$

Substitution of (16) into (15) and rearranging gives

$$\frac{d}{P} = \sum_i \frac{d_i}{P_i} \quad (17)$$

VIII-5.1

Equation (17) has been experimentally verified by Bhargava *et al.*,⁶ for polyethylene-glassine laminates.

The case of a foil with pin-hole has been treated by Prins and Hermans.²³ For a foil, impermeable in bulk but with n circular holes/cm² of radius r , laminated onto a polymer of thickness d and permeability P , and for $d/r > 0.3$ (the only case of practical interest) they found (in the present notation)

$$J = \frac{P\Delta p}{d} \theta (1 + 1.18d/r) \quad ; \quad \theta \ll 1 \quad (18)$$

where $\theta = n\pi r^2$, the fraction of free surface. The first two terms on the right of Equation (18) simply express the reduction of permeation because of the reduction in free surface. The third term, however, can be a large multiplying factor, reflecting the spread of the diffusing gas in the polymer film. For very large value of d/r , Equation (18) reduces to

$$J = 3.7nrP\Delta p \quad (19)$$

and the flux becomes proportional to the perimeter of the holes rather than to their area.

VIII-6 DISTINCTION BETWEEN PERMEATION AND MASS FLOW

The question often arises in permeability measurements whether the gas flux observed is all due to true permeation or whether part of it is due to flow through fine capillaries, whether they exist in the very nature of the film being studied (as is postulated by one group³¹ for polystyrene below the glass transition temperature) or because of flaws such as cracks and pinholes. One pragmatic approach, and often a successful one, is to determine apparent permeabilities on a number of samples, with the presumption that they won't all have the same number of flaws, and with different sample thicknesses, with the presumption that a flaw is less likely to penetrate through in the case of the thicker samples. If substantially the same value for P is obtained in all cases it is fairly good evidence either that true permeability is being measured or that other means of passing gas are inherent and uniform in the film being studied.

Sometimes the above method is not practical, possibly because of a limited choice of samples or because individual experiments take too long. Further, if inherent capillaries are suspected, it may be desirable to confirm or disprove the hypothesis. In either case a great deal can be learned from the behavior of the apparent permeability with temperature. The development below will be confined to a slightly soluble gas. As already pointed out, this is the only case where the theoretical temperature behavior of the permeability is simple. For simplicity it will also be confined to the case where the film has uniform capillaries and the gas in the capillaries is in equilibrium with that dissolved in the film, although these simplifications do not appreciably affect the conclusions to be drawn.

In the steady state the over-all flux is simply the sum of that due to diffusion and that due to mass flow:

$$-J = D \frac{dc_f}{dx} + \bar{v} c_g \quad (20)$$

where c_f denotes the concentration of gas dissolved in the film, c_g that in the gas phase in the capillaries, θ the fraction of the cross section that consists of capillaries, and v the velocity of the gas in the capillaries. Substituting $c_f = Sp$ and $c_g = p/RT$, Equation (20) becomes

$$-J = DS \frac{dp}{dx} + \frac{\theta v}{RT} p \quad (21)$$

It is convenient to distinguish two cases: (1) the pressure is low enough, or the capillaries small enough, that Knudsen flow obtains, and (2) the capillaries are large enough that Poiseuille's law is followed.

In the Knudsen case, the velocity is given¹⁰ by

$$v = - \frac{k_K}{\sqrt{\rho p}} \frac{dp}{dx} ; \quad k_K = r/6 \quad (22)$$

where ρ is the density of the gas. If small gas imperfections are neglected, $\sqrt{\rho p} = p\sqrt{M/RT}$. With this relation and Equation (22), Equation (21) becomes

$$-J = DS \frac{dp}{dx} + k_K (RTM)^{-1/2} \frac{dp}{dx} \quad (23)$$

Equation (23) can be integrated directly, in x from 0 to d and in p from 0 to p_0 (for simplicity; a finite pressure on the low pressure side offers no difficulty) to give

$$-Jd = DSP_0 + \theta k_K (RTM)^{-1/2} p_0 \quad .$$

Recalling that the permeability is defined by $-Jd/p_0$, it is evidently given by

$$P = DS + \theta k_K (RTM)^{-1/2} \quad (24)$$

In the Poiseuille case the velocity is given by

$$v = \frac{k_p}{\eta} \frac{dp}{dx} ; \quad k_p = r^2/8 \quad (25)$$

where η is the viscosity of the gas. Again neglecting gas imperfections, η can be expressed by $\eta = \eta_0(MT)^{1/2}$, where η_0 contains constants and the collision diameter. With this relation and Equation (25) substituted in (21), and proceeding exactly as before, the permeability is given by

$$P = DS + \frac{\theta k_p p_0}{2\eta_0 R M^{1/2} T^{3/2}} \quad (26)$$

Frisch¹⁰ using a somewhat different approach arrives at an equation formally identical with Equation (20) [his Equation (8)] and derives a relation identical with Equation (24) [his Equation (10)]. His Equation (12), however, is not the same as Equation (26) above, in that his implicitly contains $T^{-5/2}$ in the second term on the right. This appears to be an algebraic error [not typographical since it is carried on to his Equation (33)]. Intuitively one would expect that if the velocity is proportional to $T^{-1/2}$ the flux, which at a given velocity is proportional to $(RT)^{-1}$, would be proportional to $T^{-3/2}$.

The important point is that the product DS , which might be termed "true" permeability, depends exponentially on the temperature and almost invariably (in the case of permanent gases) strongly increases with increasing temperature. Any component of Knudsen flow, and even more strongly any component of Poiseuille flow, would *decrease* with increasing temperature. Thus the usual Arrhenius type plot of $\log P$ as ordinant vs. $1/T$ as abscissa should show strong curvature convex toward the origin as either of these types of mass transfer become important as the temperature is lowered. Indeed, as Frisch points out, a careful analysis of the temperature dependence of the apparent permeability should allow not only an estimate of how important mass flow is but what type of flow is important (molecular or viscous).

The above development has been based on mass transfer through a polymer film, where p is regarded as the driving force. There is no difficulty in extending it to metals, by simply substituting $c_f = Sp^{1/2}$ in Equation (20) and defining P as $Jd/p^{1/2}$. This would alter the pressure dependence of the second terms to the right in Equations (24) and (26), but the temperature behavior outlined in the previous paragraph would still obtain.

)

)

)

)

)

VIII-7 PERMEABILITY REFERENCES

1. Ash, R., and Barrer, R. M., *Phil. Mag.*, **48**, 1197 (1959).
2. Barrer, R. M., *Trans. Far. Soc.*, **35**, 628 (1939).
3. Barrer, R. M., "Diffusion in and Through Solids," Cambridge Press, London, 1951.
4. Barrer, R. M., and Skirrow, G., *J. Polymer Sci.*, **3**, 549 (1948).
5. Baukloh, W., and Kayser, Z. *Metallik.*, **26**, 156 (1934).
6. Bhargava, R., Rogers, C. E., Stannett, V., and Szwarc, M., *TAPPI*, **40**, 564 (1957).
7. Daynes, H., *Proc. Roy. Soc. (London)*, **A97**, 286 (1920).
8. DeRosset, A. J., *Ind. Eng. Chem.*, **52**, 525 (1960).
9. Flint, P. S., *KAPL-659*, 1951.
10. Frisch, H. L., *J. Phys. Chem.*, **60**, 1177 (1956).
11. Gulbransen, E. A., and Andrew, K. F., *J. Electrochem. Soc.*, **101**, 560 (1954).
12. Huffine, C. L., and Williams, J. M., *Corrosion*, **16**, 430t (1960).
13. Krivetsky, A., et al., Bell Aerosystems Company, Report No. 7129-933003, March 1962.
14. Lasowski, S. W., and Cobbs, W. H., *J. Polymer Sci.*, **36**, 21 (1959).
15. Meyer, J. A., Stannett, V., and Szwarc, M., *Ind. Eng. Chem.*, **49**, 441 (1957).
16. Michaels, A. S., and Bixler, H. J., *J. Polymer Sci.*, **50**, 393 (1961).
17. Michaels, A. S., and Bixler, H. J., *J. Polymer Sci.*, **50**, 413 (1961).
18. Myers, A. W., Meyer, J. A., Rogers, C. E., Stannett, V., and Szwarc, M., *TAPPI*, **44**, 53 (1961).
19. Myers, A. W., Meyer, J. A., Rogers, C. E., Stannett, V., and Szwarc, M., *TAPPI*, **44**, 58 (1961).
20. Myers, A. W., Tammela, V., Stannett, V., and Szwarc, M., *Modern Plastics*, **37**, 139 (1960).
21. Norton, F. J., *J. Appl. Phys.*, **38**, 34 (1956).
22. Norton, F. J., quoted by Flint, Ref. 9.
23. Prins, W., and Hermans, J. J., *J. Phys. Chem.*, **63**, 716 (1959).
24. Rogers, W. A., Buritz, R. S., and Alport, D., *J. Appl. Phys.*, **25**, 868 (1954).
25. Rogers, C., Meyer, J. A., Stannett, V., and Szwarc, M., *TAPPI*, **39**, 741 (1956).
26. Rogers, C. E., Stannett, V., and Szwarc, M., *TAPPI*, **44**, 715 (1961).
27. Russell, A. S., *Metal Progress*, **55**, 827 (1959).
28. Ryder, H. M., *Elect. J.*, **17**, 161 (1920).
29. Salame, M., *SPE Transactions*, October 1961, p. 153.
30. Sawatzky, A., and Rees, M. J., Atomic Energy of Canada, Ltd., *AECL-1252*, 1960.

31. Schulz, G. V., and Gerrens, H., *Z. phys. Chem., N. Folge*, **7**, 182 (1956).
32. Smithells, C. J., and Ransley, C. E., *Proc. Roy. Soc. (London)*, **A150**, 172 (1935).
33. VanAmerongen, G. J., *J. Appl. Phys.*, **17**, 972 (1946).
34. Wasilewski, R. J., and Kehl, G. L., *J. Inst. Metals*, **83**, 94 (1954-55).
35. Wiederhorn, N. M., 2nd Quart. Prog. Report, NASA Contract No. NAS5-664, 1961.

IX PROPERTIES OF GASES

Table of Contents

Section-Part	Title
IX-0	List of Tables
IX-0	List of Figures
IX-1	Introduction
IX-2	Properties of Nitrogen
IX-3	Properties of Hydrogen
IX-4	Properties of Helium
IX-5	Properties of Oxygen
IX-6	Properties of Carbon Dioxide
IX-7	Properties of Perchloryl Fluoride
IX-8	Properties of Chlorine Trifluoride
IX-9	Properties of Hydrazine
IX-10	Properties of Nitrogen (IV) Oxide
IX-11	Properties of UDMH (Unsymmetrical Dimethylhydrazine)
IX-12	Properties of Water
IX-13	Properties of Propane
IX-14	Properties of n-Butane
IX-15	Properties of Ammonia
IX-16	Properties of Hydrogen Peroxide
IX-17	Properties of Freon-11 (CCl_3F)
IX-18	Properties of Freon-12 (CCl_2F_2)
IX-19	Properties of Freon-13 (CClF_3)
IX-20	Properties of Freon-14 (CF_4)

IX-0 LIST OF TABLES

Section-Part-Table	Title
IX-2-1	<i>General Properties of Nitrogen</i>
IX-2-1.1	Some Values of the Gas Constant, R , for Molecular Nitrogen
IX-2-2	Vapor Pressure of Solid Nitrogen
IX-2-3	Vapor pressure of Liquid Nitrogen
IX-2-4	Density of Liquid Nitrogen
IX-2-5	Density of Saturated Liquid Nitrogen
IX-2-6	Density of Saturated Nitrogen Gas
IX-2-7	Density of Gaseous Nitrogen
IX-2-8	Surface Tension of Liquid Nitrogen Against Its Own Vapor
IX-2-9	Viscosity of Liquid Nitrogen
IX-2-10	Viscosity of Gaseous Nitrogen
IX-2-11	Heat of Vaporization of Liquid Nitrogen
IX-2-12	Heat Capacity of Solid and Liquid Nitrogen
IX-2-13	Heat Capacity of Gaseous Nitrogen
IX-2-14	Thermal Conductivity of Liquid Nitrogen
IX-2-15	Total Enthalpy of Nitrogen
IX-2-16	Low Frequency Velocity of Sound in Nitrogen
IX-3-1	<i>General Properties of Normal Hydrogen</i>
IX-3-1.1	Some Values of the Gas Constant, R , for Molecular Hydrogen
IX-3-2	Vapor Pressure of Liquefied Normal Hydrogen
IX-3-3	Density of Liquefied Normal Hydrogen
IX-3-4	Density of Saturated Vapor of Liquefied Normal Hydrogen
IX-3-5	Density of Gaseous Normal Hydrogen
IX-3-6	Surface Tension of Liquefied Normal Hydrogen
IX-3-7	Viscosity of Liquefied Normal Hydrogen
IX-3-8	Viscosity of Saturated Gaseous Normal Hydrogen
IX-3-9	Heat of Vaporization of Liquefied Normal Hydrogen
IX-3-10	Heat Capacity of Liquefied Normal Hydrogen at Saturation Pressure
IX-3-11	Heat Capacity of Hydrogen Gas
IX-3-12	Thermal Conductivity of Gaseous Normal Hydrogen
IX-3-13	Thermal Conductivity of Liquefied Normal and Para Hydrogen

TABLES

Section-Part-Table	Title
IX-3-14	Total Enthalpy of Hydrogen
IX-3-15	Low Frequency Velocity of Sound in Hydrogen
IX-4-1	<i>General Properties of Helium</i>
IX-4-1.1	Some Values of the Gas Constant, R , for Helium
IX-4-2	Melting Point of Helium
IX-4-3	Vapor Pressure of Liquefied Helium
IX-4-4	Density of Saturated Helium Liquid and Vapor
IX-4-5	Density of Gaseous Helium
IX-4-6	Surface Tension of Saturated Liquid Helium Against Its Own Vapor
IX-4-7	Viscosity of Liquid Helium
IX-4-8	Viscosity of Helium Gas at One Atmosphere
IX-4-9	Heat of Vaporization of Helium
IX-4-10	Heat Capacity of Liquid Helium at Saturation Pressure
IX-4-11	Heat Capacity of Gaseous Helium
IX-4-12	Thermal Conductivity of Liquid Helium
IX-4-13	Thermal Conductivity of Helium Gas at One Atmosphere
IX-5-1	<i>General Properties of Oxygen</i>
IX-5-1.1	Some Values of the Gas Constant, R , for Molecular Oxygen
IX-5-2	Vapor Pressure of Liquid Oxygen
IX-5-3	Density of Liquid Oxygen
IX-5-4	Density of Gaseous Oxygen
IX-5-5	Viscosity of Liquid Oxygen
IX-5-6	Viscosity of Gaseous Oxygen
IX-5-7	Heat Capacities of Oxygen
IX-5-8	Thermal Conductivity of Gaseous Oxygen
IX-5-9	Heat of Vaporization of Liquid Oxygen
IX-5-10	Total Enthalpy of Oxygen
IX-5-11	Low Frequency Velocity of Sound in Oxygen
IX-6-1	<i>General Properties of Carbon Dioxide</i>
IX-6-1.1	Some Values of the Gas Constant, R , for Carbon Dioxide
IX-6-2	Vapor Pressure of Solid Carbon Dioxide
IX-6-3	Vapor Pressure of Liquid Carbon Dioxide
IX-6-4	Density of Carbon Dioxide (Saturated Liquid and Vapor)

TABLES

Section-Part-Table	Title
IX-6-5	Density of Gaseous Carbon Dioxide
IX-6-6	Surface Tension of Liquid Carbon Dioxide
IX-6-7	Heat of Vaporization of Carbon Dioxide
IX-6-8	Heat Capacities of Gaseous Carbon Dioxide
IX-6-9	Thermal Conductivity of Gaseous Carbon Dioxide
IX-6-10	Total Enthalpy of Carbon Dioxide
IX-6-11	Low Frequency Velocity of Sound in Carbon Dioxide
IX-7-1	<i>General Properties of Perchloryl Fluoride</i>
IX-7-1.1	Some Values of the Gas Constant, R , for Perchloryl Fluoride
IX-7-2	Vapor Pressure of Liquid Perchloryl Fluoride
IX-7-3	Density of Liquid Perchloryl Fluoride
IX-7-4	Density of Saturated Vapor of Perchloryl Fluoride
IX-7-5	Viscosity of Liquid Perchloryl Fluoride
IX-7-6	Heat Capacity of Saturated Liquid Perchloryl Fluoride
IX-8-1	<i>General Properties of Chlorine Trifluoride</i>
IX-8-1.1	Some Values of the Gas Constant, R , for Chlorine Trifluoride
IX-8-2	Vapor Pressure of Chlorine Trifluoride
IX-8-3	Density of Liquid Chlorine Trifluoride
IX-8-4	Surface Tension of Liquid Chlorine Trifluoride in Contact with its Vapor
IX-8-5	Viscosity of Liquid Chlorine Trifluoride
IX-8-6	Thermal Conductivity of Gaseous Chlorine Trifluoride
IX-8-7	Heat Capacities of Solid and Liquid Chlorine Trifluoride
IX-9-1	<i>General Properties of Hydrazine</i>
IX-9-1.1	Some Values of the Gas Constant, R , for Hydrazine
IX-9-2	Vapor Pressure of Anhydrous Hydrazine
IX-9-3	Density of Liquid Hydrazine
IX-9-4	Viscosity of Hydrazine
IX-9-5	Heat Capacity of Liquid Hydrazine
IX-9-6	Heat Capacity of Gaseous Hydrazine
IX-9-7	Heat Capacity of Hydrazine at Constant Pressure
IX-9-8	Thermal Conductivity of Hydrazine

TABLES

Section-Part-Table	Title
IX-13-7	Surface Tension of Liquid Propane
IX-13-8	Viscosity of Liquid Propane
IX-13-9	Heat of Vaporization of Liquid Propane
IX-13-10	Total Enthalpy Values and Specific Volumes for the Propane System
IX-14-1	<i>General Properties of n-Butane</i>
IX-14-1.1	Some Values of the Gas Constant, R , for n -Butane
IX-14-2	Vapor Pressure of n -Butane
IX-14-3	Density of Liquid n -Butane
IX-14-4	Density of Saturated n -Butane Vapor
IX-14-5	Specific Heat of Liquid n -Butane
IX-14-6	Specific Heat of n -Butane Gas
IX-14-7	Heat of Vaporization of n -Butane
IX-14-8	Viscosity of n -Butane
IX-14-9	Total Enthalpy and Specific Volume of the n -Butane System
IX-15-1	<i>General Properties of Ammonia</i>
IX-15-1.1	Some Values of the Gas Constant, R , for Ammonia
IX-15-2	Vapor Pressure of Liquid Ammonia
IX-15-3	Density of Saturated Ammonia Vapor
IX-15-4	Density of Liquid Ammonia
IX-15-5	Density of Gaseous Ammonia
IX-15-6	Heat Capacities of Solid and Liquid Ammonia
IX-15-7	Heat Capacities of Ammonia Gas
IX-15-8	Heat of Vaporization of Ammonia
IX-15-9	Total Enthalpy and Specific Volume of the Ammonia System
IX-16-1	<i>General Properties of Hydrogen Peroxide</i>
IX-16-1.1	Some Values of the Gas Constant, R , for Hydrogen Peroxide
IX-16-2	Total Vapor Pressure of 98-100% Hydrogen Peroxide Solutions
IX-16-3	Density of Hydrogen Peroxide
IX-16-4	Surface Tension of Hydrogen Peroxide
IX-16-5	Viscosity of Hydrogen Peroxide
IX-16-6	Heat Capacity of Solid Hydrogen Peroxide
IX-16-7	Specific Heat of 98% Hydrogen Peroxide Solution
IX-16-8	Heat Capacity of Hydrogen Peroxide Vapor

IX-0 LIST OF FIGURES

Section-Part-Figure	Title
IX-2-1	<i>Vapor Pressure of Solid Nitrogen</i>
IX-2-2	Vapor Pressure of Liquid Nitrogen
IX-2-3	Density of Liquid Nitrogen
IX-2-4	Density of Saturated Liquid Nitrogen
IX-2-5	Density of Saturated Nitrogen Gas
IX-2-6	Density of Gaseous Nitrogen at One Atmosphere
IX-2-7	Density of Gaseous Nitrogen at 10, 40, and 100 Atmospheres
IX-2-8	Surface Tension of Liquid Nitrogen Against its Own Vapor
IX-2-9	Viscosity of Liquid Nitrogen
IX-2-10	Viscosity of Gaseous Nitrogen
IX-2-11	Heat of Vaporization of Liquid Nitrogen
IX-2-12	Heat Capacity of Solid and Liquid Nitrogen
IX-2-13	Heat Capacity of Gaseous Nitrogen
IX-2-14	Specific Heat Ratios of Nitrogen
IX-2-15	Thermal Conductivity of Liquid Nitrogen
IX-2-16	Thermal Conductivity of Gaseous Nitrogen
IX-2-17	Total Enthalpy of Nitrogen
IX-2-18	Low Frequency Velocity of Sound in Nitrogen
IX-3-1	<i>Vapor Pressure of Liquefied Normal Hydrogen</i>
IX-3-2	Density of Liquefied Normal Hydrogen
IX-3-3	Density of Saturated Vapor of Liquefied Normal Hydrogen
IX-3-4	Density of Gaseous Normal Hydrogen at 1 Atm and 10 Atm
IX-3-5	Density of Gaseous Normal Hydrogen at 10 Atm and 100 Atm
IX-3-6	Surface Tension of Liquefied Normal Hydrogen
IX-3-7	Viscosity of Liquefied Normal Hydrogen
IX-3-8	Viscosity of Saturated Gaseous Normal Hydrogen
IX-3-9	Heat of Vaporization of Liquefied Normal Hydrogen
IX-3-10	Heat Capacity of Liquefied Normal Hydrogen at Saturation Pressure
IX-3-11	Heat Capacity of Hydrogen Gas
IX-3-12	Specific Heat Ratios of Hydrogen
IX-3-13	Thermal Conductivity of Gaseous Normal Hydrogen
IX-3-14	Thermal Conductivity of Liquefied Normal and Para Hydrogen

FIGURES

Section-Part-Figure	Title
IX-6-4	Density of Saturated Vapor of Carbon Dioxide
IX-6-5	Density of Gaseous Carbon Dioxide at One Atmosphere
IX-6-6	Density of Gaseous Carbon Dioxide at 10 and 100 Atmospheres
IX-6-7	Surface Tension of Liquid Carbon Dioxide
IX-6-8	Heat of Vaporization of Carbon Dioxide
IX-6-9	Heat Capacities of Gaseous Carbon Dioxide
IX-6-10	Specific Heat Ratios of Carbon Dioxide (0-40 Atm)
IX-6-11	Specific Heat Ratios of Carbon Dioxide (0-2 Atm)
IX-6-12	Thermal Conductivity of Gaseous Carbon Dioxide
IX-6-13	Total Enthalpy of Carbon Dioxide
IX-6-14	Low Frequency Velocity of Sound in Carbon Dioxide
IX-7-1	<i>Vapor Pressure of Perchloryl Fluoride</i>
IX-7-2	Density of Liquid Perchloryl Fluoride
IX-7-3	Density of Saturated Vapor of Perchloryl Fluoride
IX-7-4	Viscosity of Liquid Perchloryl Fluoride
IX-7-5	Heat Capacity of Saturated Liquid Perchloryl Fluoride
IX-7-6	Heat Capacity of Gaseous Perchloryl Fluoride
IX-8-1	<i>Vapor Pressure of Chlorine Trifluoride</i>
IX-8-2	Density of Liquid Chlorine Trifluoride
IX-8-3	Surface Tension of Liquid Chlorine Trifluoride in Contact with its Vapor
IX-8-4	Viscosity of Liquid Chlorine Trifluoride
IX-8-5	Thermal Conductivity of Gaseous Chlorine Trifluoride
IX-8-6	Heat Capacities of Solid and Liquid Chlorine Trifluoride
IX-9-1	<i>Vapor Pressure of Liquid Hydrazine</i>
IX-9-2	Density of Liquid Hydrazine
IX-9-3	Viscosity of Hydrazine
IX-9-4	Heat Capacity of Liquid Hydrazine
IX-9-5	Heat Capacity of Gaseous Hydrazine
IX-9-6	Heat Capacity of Hydrazine at Constant Pressure
IX-9-7	Thermal Conductivity of Hydrazine

FIGURES

Section-Part-Figure	Title
IX-13-7	Specific Heat Ratios of Propane (0-20 Atm)
IX-13-8	Surface Tension of Liquid Propane
IX-13-9	Viscosity of Liquid Propane
IX-13-10	Heat of Vaporization of Liquid Propane
IX-13-11	Thermal Conductivity of Liquid Propane
IX-13-12	Total Enthalpy of the Propane System
IX-13-13	Specific Volume of Propane Vapor
IX-14-1	<i>Vapor Pressure of n-Butane (330-390°R)</i>
IX-14-2	<i>Vapor Pressure of n-Butane (390-600°R)</i>
IX-14-3	Density of Liquid <i>n</i> -Butane
IX-14-4	Density of Saturated <i>n</i> -Butane Vapor
IX-14-5	Specific Heat of Liquid <i>n</i> -Butane
IX-14-6	Specific Heat of <i>n</i> -Butane Gas
IX-14-7	Heat of Vaporization of <i>n</i> -Butane
IX-14-8	Viscosity of <i>n</i> -Butane
IX-14-9	Specific Heat Ratios of <i>n</i> -Butane (0-2 Atm)
IX-14-10	Specific Heat Ratios of <i>n</i> -Butane (0-20 Atm)
IX-14-11	Thermal Conductivity of Liquid <i>n</i> -Butane
IX-14-12	Total Enthalpy of the <i>n</i> -Butane System
IX-14-13	Specific Volume of <i>n</i> -Butane Vapor
IX-15-1	<i>Vapor Pressure of Liquid Ammonia</i>
IX-15-2	Density of Saturated Ammonia Vapor
IX-15-3	Density of Liquid Ammonia
IX-15-4	Density of Gaseous Ammonia
IX-15-5	Heat Capacities of Solid and Liquid Ammonia
IX-15-6	Heat Capacity of Ammonia Gas
IX-15-7	Specific Heat Ratios of Ammonia (0-20 Atm)
IX-15-8	Specific Heat Ratios of Ammonia (0-3 Atm)
IX-15-9	Heat of Vaporization of Ammonia
IX-15-10	Viscosity of Gaseous and Liquid Ammonia
IX-15-11	Thermal Conductivity of Gaseous and Liquid Ammonia
IX-15-12	Total Enthalpy of the Ammonia System
IX-15-13	Specific Volume of Ammonia Vapor

FIGURES

Section-Part-Figure	Title
IX-20-5	Heat Capacity of Freon-14
IX-20-6	Thermal Conductivity of Gaseous Freon-14

1

2

3

4

5

Table IX-2-2
VAPOR PRESSURE OF SOLID NITROGEN (Ref. 5)

TEMPERATURE		VAPOR PRESSURE		
$^{\circ}\text{K}$	$^{\circ}\text{R}$	mm Hg	psia	atm
52	93.6	5.666	0.1096	0.0075
54	97.2	10.21	0.1974	0.0134
56	100.8	17.64	0.3411	0.0232
58	104.4	29.35	0.5675	0.0386
60	108.0	47.21	0.9129	0.0621
62	111.6	73.64	1.424	0.0969
63.15	113.67	93.88	1.815	0.1235
$\log P_{\text{mm}} = 7.65894 - 359.093/T$				

(See Figure IX-2-1)

Table IX-2-5
DENSITY OF SATURATED LIQUID NITROGEN (Ref. 2)

TEMPERATURE		DENSITY	TEMPERATURE		DENSITY
$^{\circ}\text{K}$	$^{\circ}\text{R}$	lb/ft^3	$^{\circ}\text{K}$	$^{\circ}\text{R}$	lb/ft^3
77.4	139.35	50.38	105.5	190	40.92
80.5	145	49.55	108.2	195	39.68
83.3	150	48.71	111.1	200	38.40
86.1	155	47.85	113.9	205	37.04
88.8	160	47.17	116.7	210	35.46
91.7	165	46.06	119.3	215	33.37
94.4	170	45.15	122.1	220	30.88
97.2	175	44.19	125.0	225	27.60
100.0	180	43.18	126.1	227.0	19.64
102.8	185	42.09			

(See Figure IX-2-4)

Table IX-2-6
DENSITY OF SATURATED NITROGEN GAS (Ref 2)

TEMPERATURE		DENSITY	TEMPERATURE		DENSITY
$^{\circ}\text{K}$	$^{\circ}\text{R}$	lb/ft^3	$^{\circ}\text{K}$	$^{\circ}\text{R}$	lb/ft^3
77.5	139.5	0.2879	105.56	190	2.8818
80.56	145	0.3978	108.33	195	3.3795
83.33	150	0.5179	111.11	200	4.1701
86.11	155	0.6658	113.89	205	5.0000
88.89	160	0.8418	116.67	210	6.0533
91.67	165	1.0617	119.44	215	7.4184
94.44	170	1.3228	122.22	220	9.2593
97.22	175	1.6170	125.00	225	11.990
100.00	180	1.9697	126.11	227	19.640
102.78	185	2.3929			

(See Figure IX-2-5)

Table IX-2-9
VISCOSITY OF LIQUID NITROGEN (Ref. 4)

TEMPERATURE		ABSOLUTE VISCOSITY
$^{\circ}\text{K}$	$^{\circ}\text{R}$	centipoises
111.7	201.06	0.074
77.3	139.14	0.158
76.1	136.98	0.165
71.4	128.52	0.209
69.25	124.65	0.228
69.1	124.38	0.231
64.8	116.64	0.284
64.3	115.74	0.290
63.9	115.02	0.292

(See Figure IX-2-9)

Table IX-2-10
VISCOSITY OF GASEOUS NITROGEN (Ref. 5)

TEMPERATURE		ABSOLUTE VISCOSITY— centipoises		
$^{\circ}\text{K}$	$^{\circ}\text{R}$	1 atm	10 atm	100 atm
100	180	0.00687		
150	270	0.0101		
200	360	0.0129		
250	450	0.0155		
300	540	0.0179	0.0179	0.0197
350	630	0.0200	0.0201	0.0215
400	720	0.0220	0.0221	0.0233
450	810	0.0239	0.0240	0.0250
500	900	0.0257	0.0258	0.0267

(See Figure IX-2-10)

Table IX-2-13
HEAT CAPACITY OF GASEOUS NITROGEN (Ref. 5)

TEMPERATURE		HEAT CAPACITY, C_p --Btu/lb-°R				
°K	°R	1 atm	10 atm	40 atm	70 atm	100 atm
100	180	0.2561				
110	198	0.2530				
120	216	0.2518				
130	234	0.2511				
140	252	0.2505	0.2806			
150	270	0.2501	0.2725			
160	288	0.2498	0.2677			
170	306	0.2496	0.2644			
180	324	0.2494	0.2619	0.3205		
190	342	0.2493	0.2600	0.3065	0.3699	
200	360	0.2491	0.2585	0.2968	0.3445	0.3998
210	378	0.2490	0.2573	0.2895	0.3273	0.3679
220	396	0.2489	0.2562	0.2839	0.3149	0.3466
230	414	0.2489	0.2554	0.2795	0.3055	0.3310
240	432	0.2488	0.2547	0.2759	0.2982	0.3197
250	450	0.2488	0.2541	0.2729	0.2923	0.315
260	468	0.2487	0.2535	0.2705	0.2875	0.3034
270	486	0.2487	0.2531	0.2683	0.2835	0.2977
280	504	0.2487	0.2527	0.2665	0.2802	0.2926
290	522	0.2487	0.2524	0.2650	0.2774	0.2885
300	540	0.2487	0.2521	0.2636	0.2749	0.2850
310	558	0.2487	0.2519	0.2625	0.2728	0.2820
320	576	0.2487	0.2517	0.2615	0.2709	0.2795
330	594	0.2483	0.2515	0.2606	0.2693	0.2772
340	612	0.2488	0.2514	0.2598	0.2679	0.2752
350	630	0.2489	0.2513	0.2592	0.2667	0.2735
360	648	0.2490	0.2512	0.2586	0.2656	0.2720
370	666	0.2491	0.2512	0.2581	0.2646	0.2706
380	684	0.2492	0.2512	0.2577	0.2638	0.2694
390	702	0.2494	0.2512	0.2573	0.2631	0.2684
400	720	0.2496	0.2513	0.2570	0.2624	0.2674
410	738	0.2497	0.2514	0.2568	0.2619	0.2666
420	756	0.2500	0.2515	0.2566	0.2614	0.2659
430	774	0.2502	0.2517	0.2565	0.2611	0.2653
440	792	0.2504	0.2518	0.2564	0.2607	0.2647
450	810	0.2507	0.2520	0.2564	0.2605	0.2643
460	828	0.2510	0.2523	0.2564	0.2603	0.2639
470	846	0.2513	0.2525	0.2564	0.2601	0.2636
480	864	0.2516	0.2528	0.2565	0.2600	0.2633
490	882	0.2519	0.2531	0.2566	0.2600	0.2632
500	900	0.2523	0.2534	0.2568	0.2600	0.2630

(See Figure IX-2-13)

Table IX-2-16

LOW FREQUENCY VELOCITY OF SOUND IN NITROGEN (Ref. 5)

TEMPERATURE		VELOCITY— ft/sec			
°K	°R	0.01 atm	1 atm	10 atm	100 atm
100	180	669.	661.		
120	216	733.	729.		
140	252	792.	788.		
160	288	846.	843.	829.	
180	324	898.	896.	888.	
200	360	945.	945.	941.	1040.
220	396	992.	992.	991.	1083.
240	432	1036.	1036.	1037.	1128.
260	468	1078.	1078.	1081.	1161.
280	504	1119.	1120.	1123.	1207.
300	540	1159.	11.59	1163.	1248.
320	576	1196.	1196.	1202.	1289.
340	612	1233.	1233.	1239.	1327.
360	648	1268.	1269.	1276.	1364.
380	684	1302.	1303.	1310.	1400.
400	720	1335.	1337.	1344.	1435.
420	756	1369.	1370.	1377.	1467.
440	792	1401.	1401.	1408.	1499.
460	828	1432.	1433.	1439.	1530.
480	864	1461.	1461.	1470.	1560.
500	900	1490.	1491.	1499.	1589.

(See Figure IX-2-18)

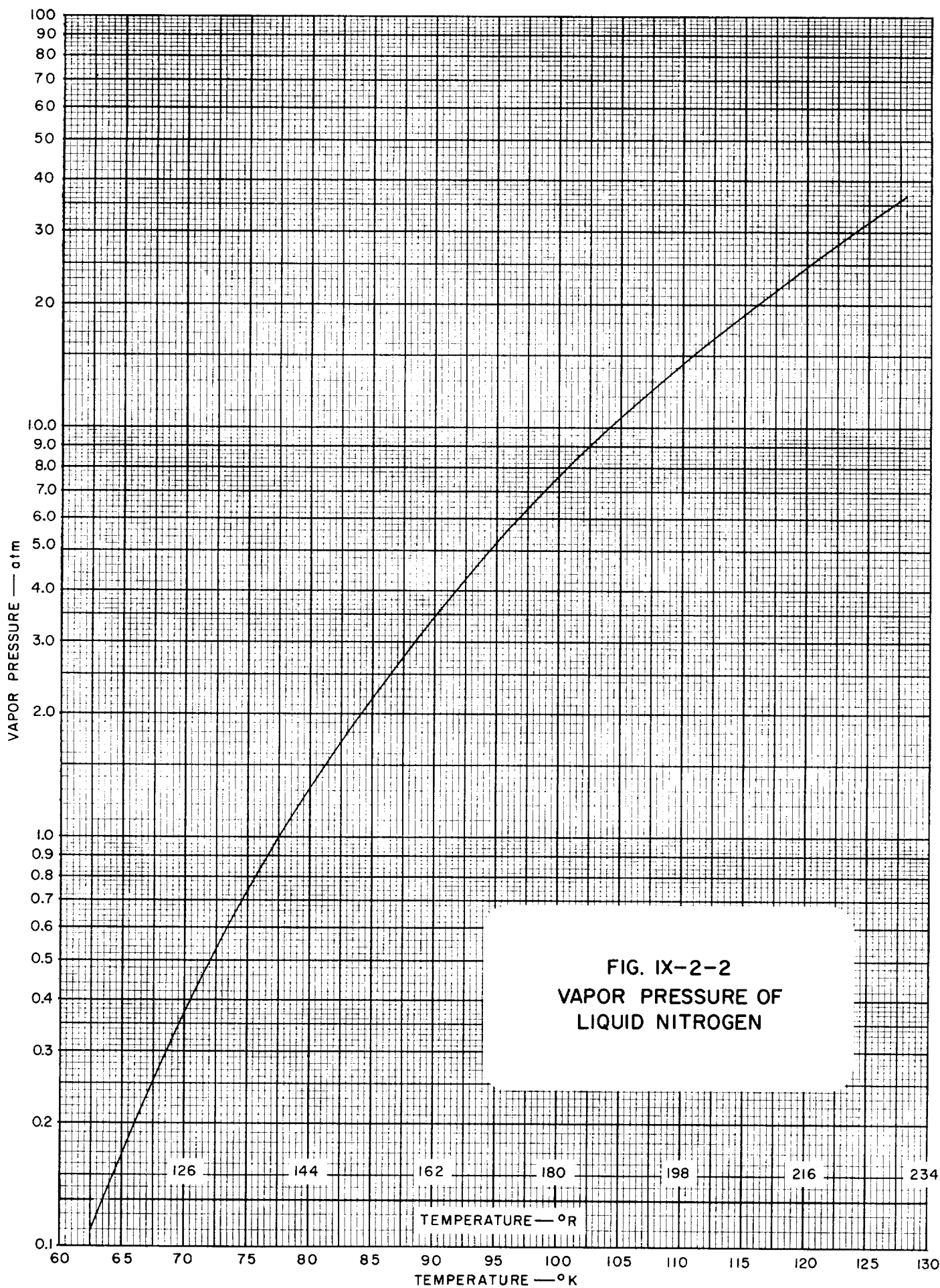


FIG. IX-2-4
DENSITY OF SATURATED
LIQUID NITROGEN

DENSITY — lb/ft³

50.0

45.0

40.0

35.0

30.0

25.0

20.0

80

90

100

110

120

TEMPERATURE — °K

130

140

150

160

170

180

190

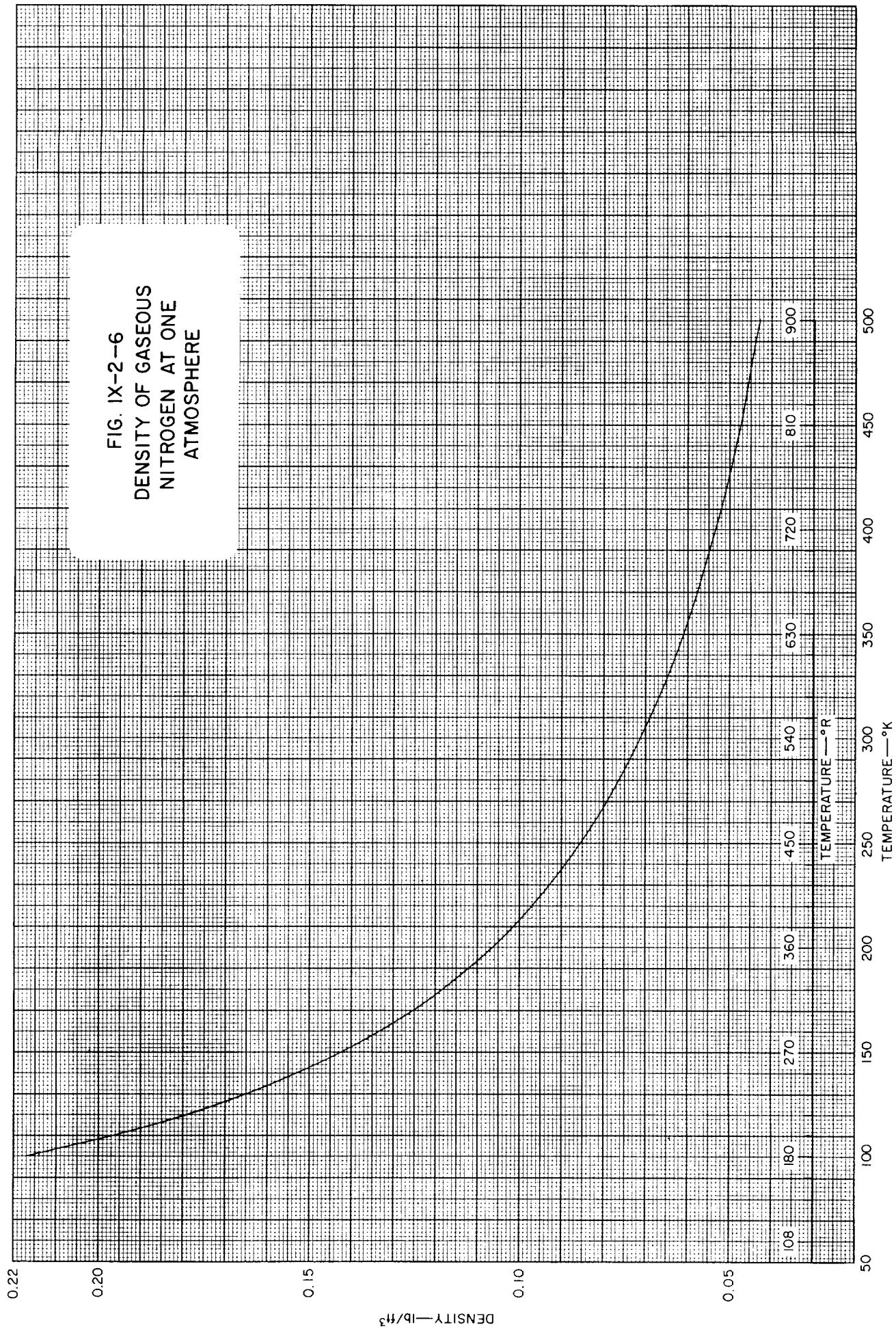
200

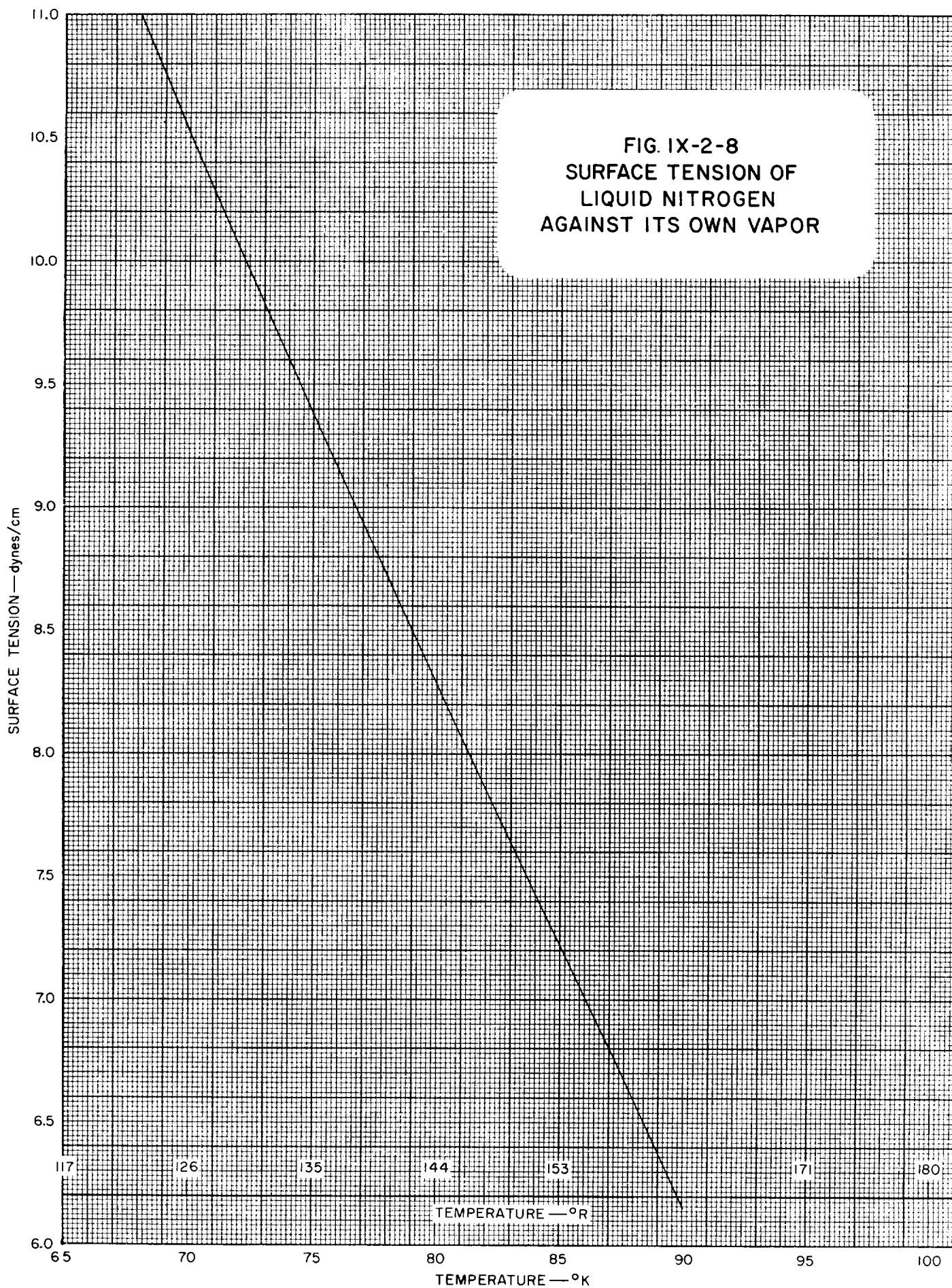
210

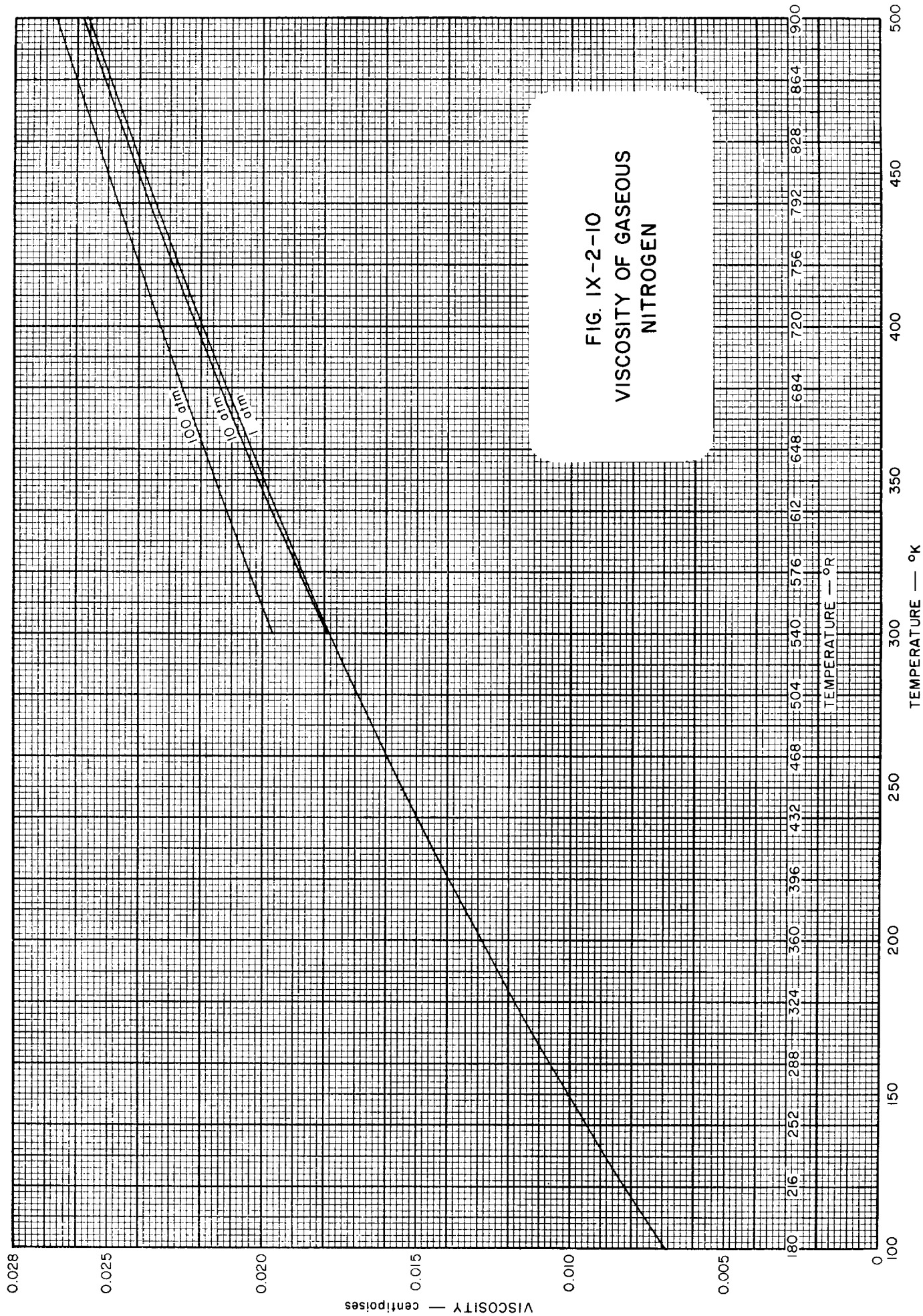
220

230

TEMPERATURE — °R







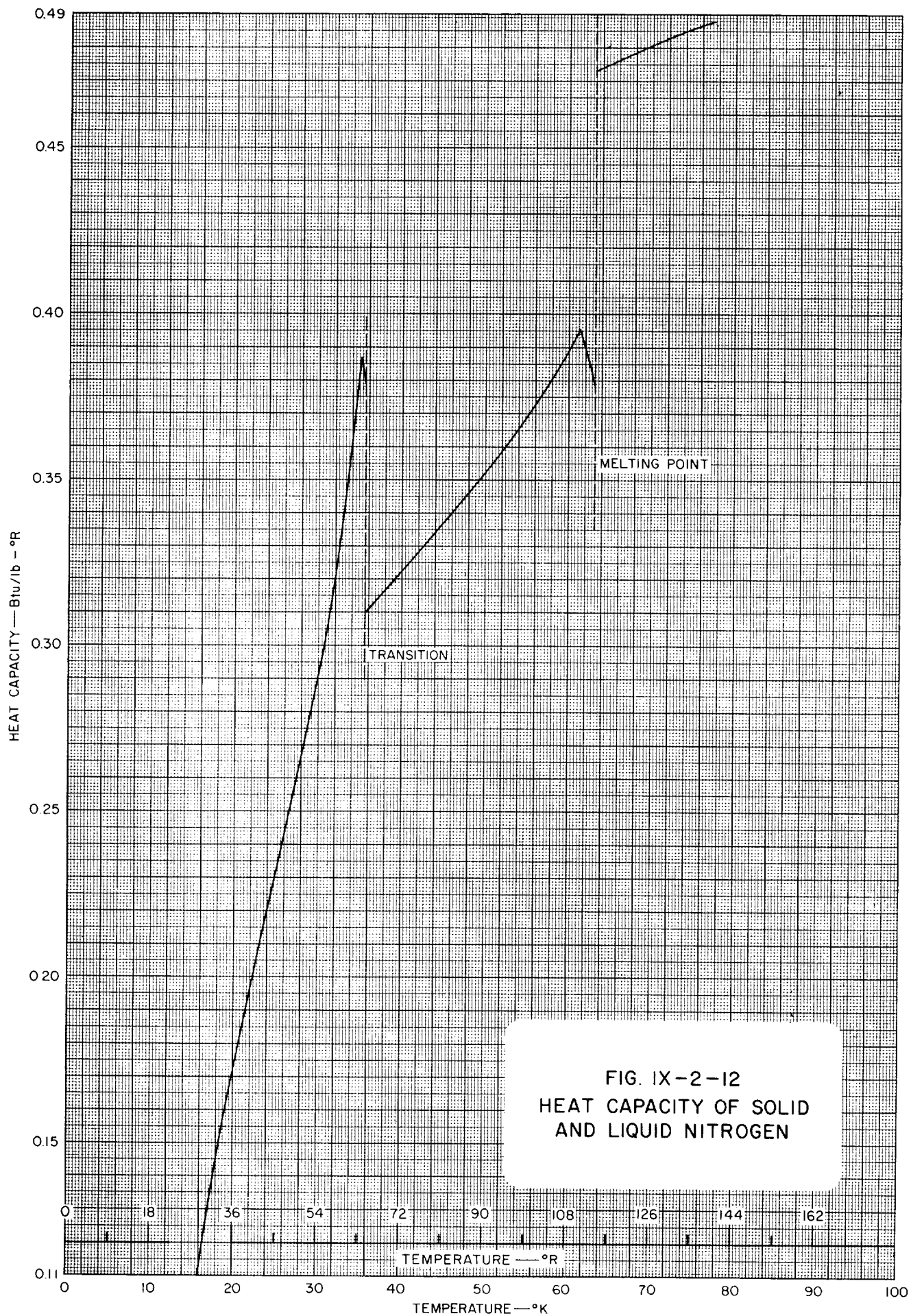
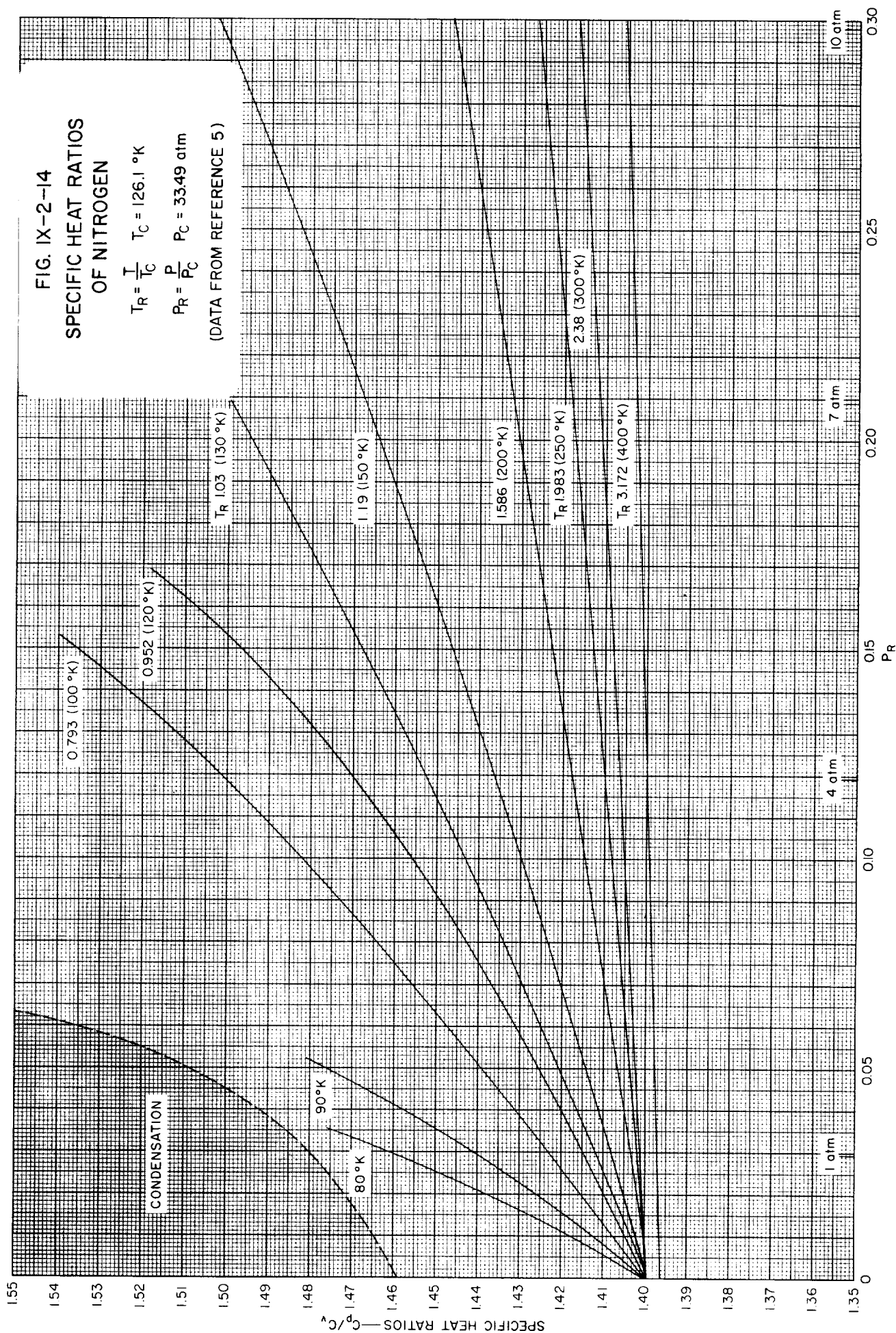


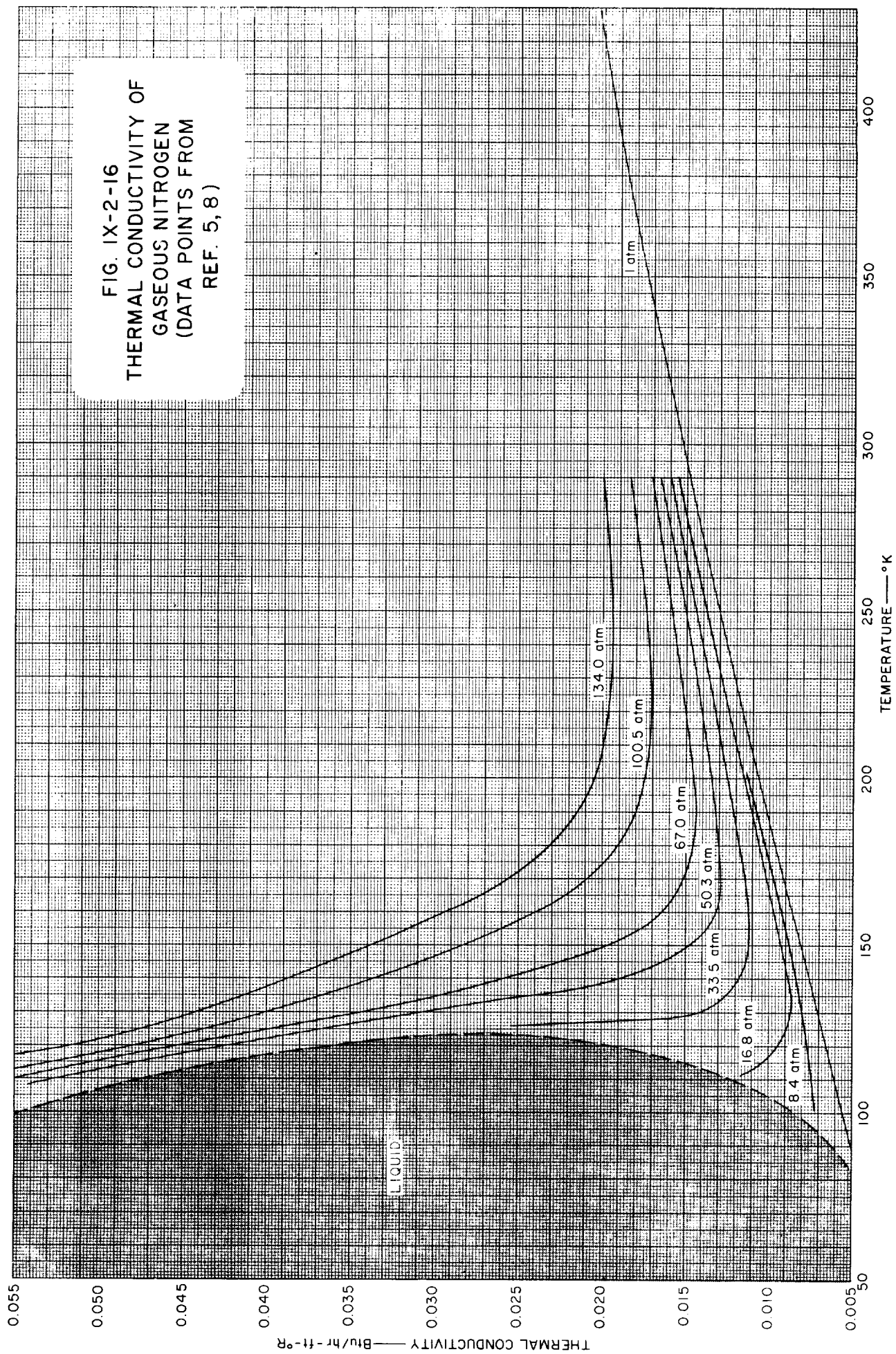
FIG. IX-2-14
SPECIFIC HEAT RATIOS
OF NITROGEN

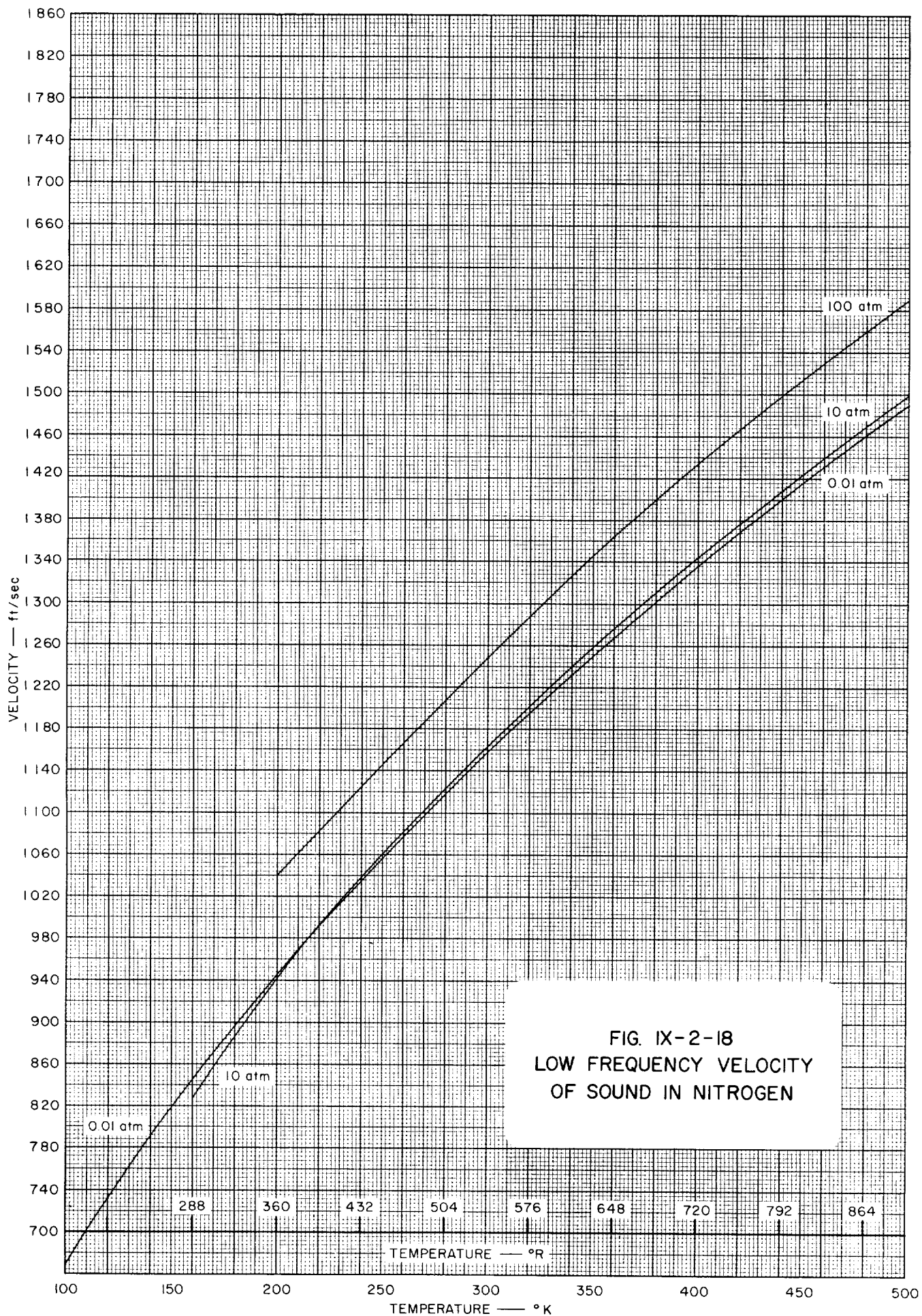
$$T_R = \frac{T}{T_C} \quad T_C = 126.1 \text{ } ^\circ\text{K}$$

$$P_R = \frac{P}{P_C} \quad P_C = 33.49 \text{ atm}$$

(DATA FROM REFERENCE 5)







1

2

3

4

5

Table IX-3-2
VAPOR PRESSURE OF LIQUEFIED
NORMAL HYDROGEN (Ref. 6)

TEMPERATURE		VAPOR PRESSURE	
$^{\circ}\text{K}$	$^{\circ}\text{R}$	psia	atm
14.00	25.20	1.070	0.0728
16.00	28.80	2.965	0.2018
18.00	32.40	6.688	0.4551
20.00	36.00	13.07	0.8891
22.00	39.60	22.99	1.564
24.00	43.20	37.41	2.545
26.00	46.80	57.29	3.899
28.00	50.40	83.69	5.695
30.00	54.00	117.7	8.010
32.00	57.60	160.5	10.923
33.00	59.40	185.6	12.632

(See Figure IX-3-1)

Table IX-3-5

DENSITY OF GASEOUS NORMAL HYDROGEN (Ref. 3)

TEMPERATURE		DENSITY—lb/ft ³		
°K	°R	1 atm	10 atm	100 atm
30	54	0.0529		
40	72	0.0389	0.461	
60	108	0.0257	0.267	2.721
80	144	0.0192	0.194	1.884
100	180	0.0153	0.154	1.452
120	216	0.0128	0.127	1.192
140	252	0.0110	0.109	1.016
160	288	0.00958	0.0953	0.888
180	324	0.00851	0.0846	0.790
200	360	0.00766	0.0762	0.713
220	396	0.00697	0.0693	0.650
240	432	0.00639	0.0635	0.597
260	468	0.00589	0.0586	0.553
280	504	0.00547	0.0544	0.515
300	540	0.00511	0.0508	0.482
320	576	0.00479	0.0477	0.453
340	612	0.00451	0.0449	0.428
360	648	0.00426	0.0424	0.405
380	684	0.00403	0.0402	0.384
400	720	0.00383	0.0382	0.366
420	756	0.00365	0.0364	0.349
440	792	0.00348	0.0347	0.336
460	828	0.00333	0.0332	0.320
480	864	0.00319	0.0318	0.307
500	900	0.00307	0.0306	0.295

(See Figure IX-3-4
Figure IX-3-5)Table IX-3-6
SURFACE TENSION OF
LIQUEFIED NORMAL
HYDROGEN (Ref. 1)

TEMPERATURE		SURFACE TENSION
°K	°R	dynes/cm
13.0	23.5	3.49
15.0	27.0	3.13
20.0	36.0	2.23
25.0	45.0	1.33

(See Figure IX-3-6)

Table IX-3-9
HEAT OF VAPORIZATION OF LIQUEFIED
NORMAL HYDROGEN (Ref. 4)

TEMPERATURE		LATENT HEAT	TEMPERATURE		LATENT HEAT
$^{\circ}\text{K}$	$^{\circ}\text{R}$	Btu/lb	$^{\circ}\text{K}$	$^{\circ}\text{R}$	Btu/lb
15.0	27.0	195.5	26.2	47.16	169.73
17.8	32.04	192.05	27.3	49.14	160.20
19.7	35.46	190.79	28.3	50.94	151.20
20.5	36.90	189.89	30.0	54.00	128.09
22.0	39.60	185.93	31.3	56.34	102.77
23.0	41.40	183.59	32.6	58.68	59.40
24.75	44.55	176.39	33.18	59.72	0.0

(See Figure IX-3-9)

Table IX-3-10
HEAT CAPACITY OF LIQUEFIED
NORMAL HYDROGEN AT
SATURATION PRESSURE
(Ref. 6)

TEMPERATURE		HEAT CAPACITY, C_p
$^{\circ}\text{K}$	$^{\circ}\text{R}$	Btu/lb- $^{\circ}\text{R}$
13.95	25.11	1.642
14.0	25.2	1.642
15.0	27.0	1.716
16.0	28.8	1.801
17.0	30.6	1.900
18.0	32.4	2.004
19.0	34.2	2.118
20.0	36.0	2.232

(See Figure IX-3-10)

Table IX-3-12

THERMAL CONDUCTIVITY OF GASEOUS NORMAL HYDROGEN (Ref. 3, 5)

TEMPERATURE			REDUCED THERMAL CONDUCTIVITY, K_R													
$^{\circ}\text{K}$	$^{\circ}\text{R}$	T_R	Atm	1	1.30	2.60	5.19	7.79	10.40	12.98	25.96	64.9	130	260	650	1298
			P_R	0.077	0.1	0.2	0.4	0.6	0.8	1.0	2.0	5.0	10.0	20.0	50.0	100
20.00	36.00	0.60		0.245							1.80		2.00			
26.54	47.77	0.70		0.270							1.76		2.00			
30.00	54.00	0.80		0.310							1.70		1.98	2.10		
33.18	59.72	0.90		0.345							1.60	1.80	1.97	2.10		
		1.00		0.375							1.50	1.78	1.95	2.09	2.45	2.71
49.70	89.46	1.50		0.545							0.881	1.45	1.77	2.05	2.50	2.92
66.36	119.4	2.00		0.690							0.95	1.35	1.62	2.00	2.53	3.03
99.54	179.2	3.00		1.000								1.43	1.66	1.93	2.55	3.11
132.7	238.9	4.00		1.31								1.60	1.80	2.07	2.61	3.15
165.9	298.6	5.00		1.60									2.00	2.25	2.76	3.27
199.1	358.3	6.00		1.90									2.24	2.45	2.93	3.42
232.3	418.1	7.00		2.18									2.50	2.70	3.10	3.62
265.4	477.8	8.00		2.45									2.75	2.95	3.30	3.81
298.6	537.5	9.00		2.73									3.03	3.20	3.50	4.01
331.8	597.2	10.00		3.00									3.30	3.50	3.71	

$$T_R = \frac{T}{T_c}$$

$$T_c = 33.18 \text{ }^{\circ}\text{K}$$

$$P_R = \frac{P}{P_c}$$

$$P_c = 12.98 \text{ atm}$$

$$K_R = \frac{K}{K_c}$$

$$K_c = 15.9 \times 10^{-5} \text{ cal/sec-cm-}^{\circ}\text{K}$$

(See Figure IX-3-13)

Table IX-3-14
TOTAL ENTHALPY OF HYDROGEN (Ref. 3)

TEMPERATURE		TOTAL ENTHALPY—Btu/lb			
^o K	^o R	0.01 atm	1.0 atm	10 atm	100 atm
60	108	492.82	491.22	476.3	378.7
80	144	583.25	582.23	573.32	512.29
100	180	677.16	676.53	670.91	632.50
120	216	775.92	775.53	771.85	748.26
140	252	879.71	879.47	877.05	863.34
160	288	987.96	987.77	986.37	980.02
180	324	1099.9	1099.8	1099.2	1099.0
200	360	1215.2	1214.9	1214.9	1219.5
220	396	1332.4	1332.4	1332.9	1341.2
240	432	1451.7	1451.8	1452.7	1464.5
260	468	1572.5	1572.7	1573.9	1588.3
280	504	1694.4	1694.5	1696.0	1712.8
300	540	1817.1	1817.3	1819.0	1837.6
320	576	1940.4	1940.6	1942.5	1962.8
340	612	2064.1	2064.4	2066.4	2088.2
360	648	2188.2	2188.4	2190.6	2213.7
380	684	2312.4	2312.6	2315.0	2339.2
400	720	2436.8	2437.1	2439.5	2464.7
420	756	2561.4	2561.6	2564.2	2590.2
440	792	2685.9	2686.2	2688.9	2715.6
460	828	2810.6	2810.9	2813.6	2840.7
480	864	2935.3	2935.6	2938.5	2966.6
500	900	3060.1	3060.4	3063.3	3092.0

(See Figure IX-3-15)

)

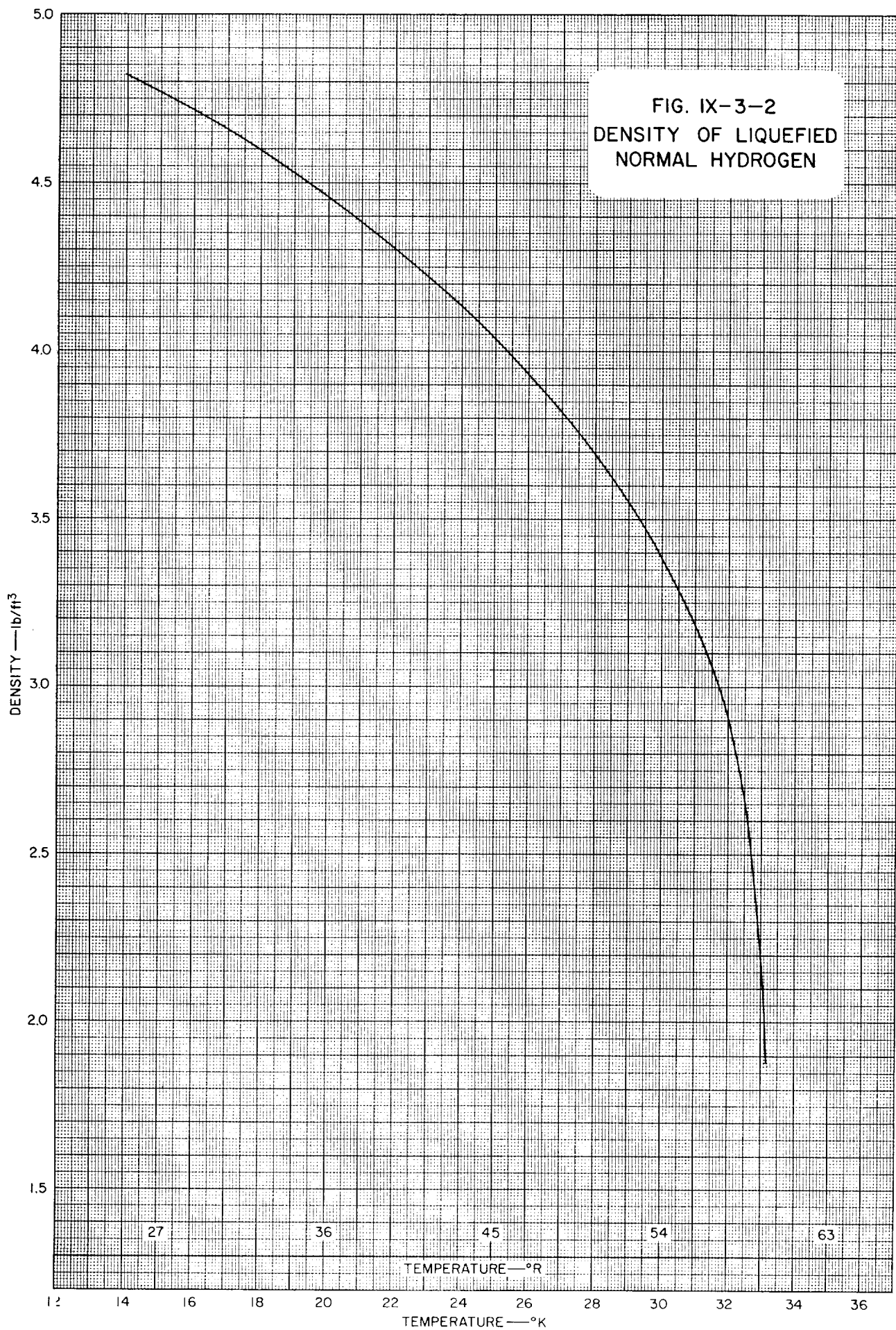
)

)

)

)

FIG. IX-3-2
DENSITY OF LIQUEFIED
NORMAL HYDROGEN



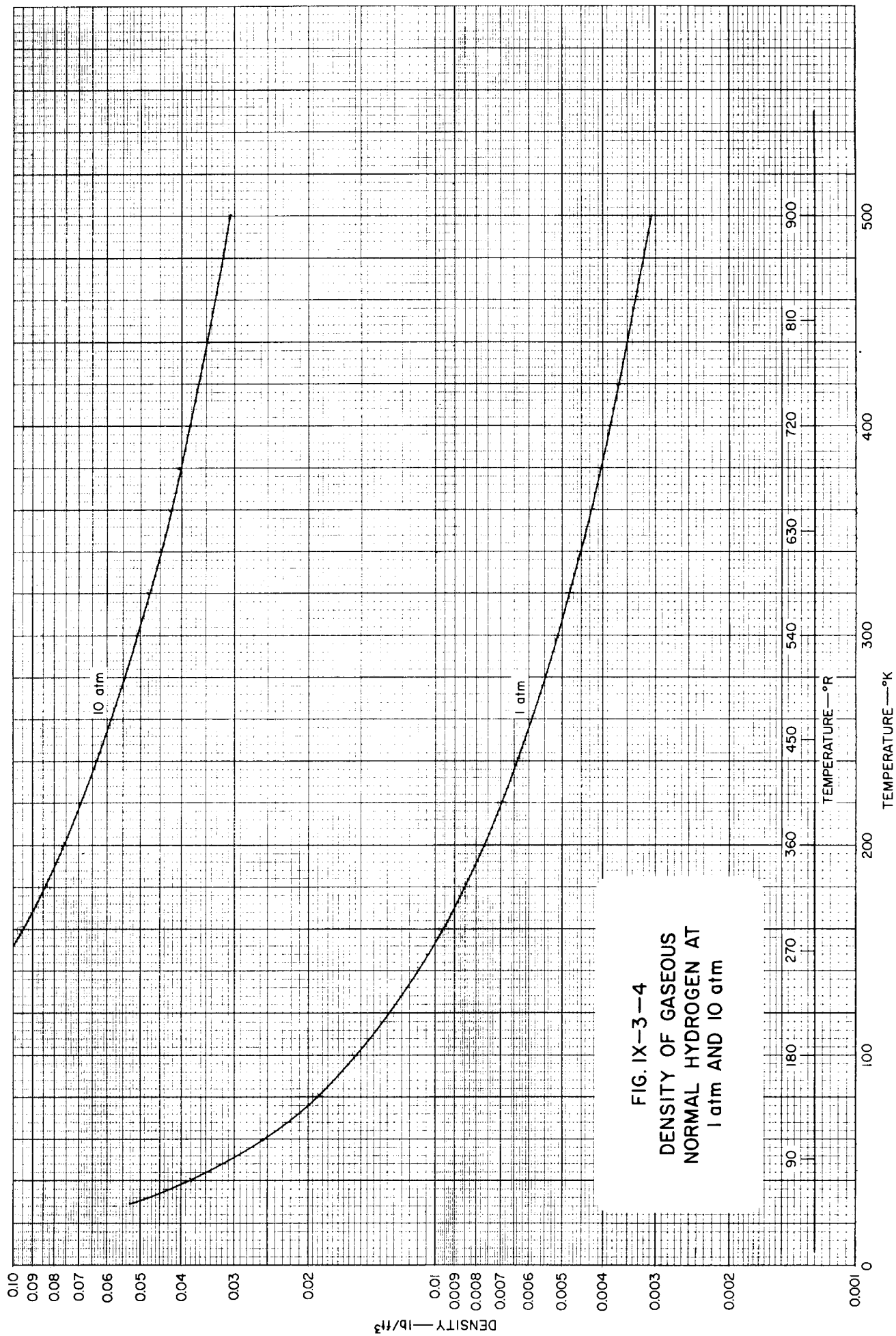
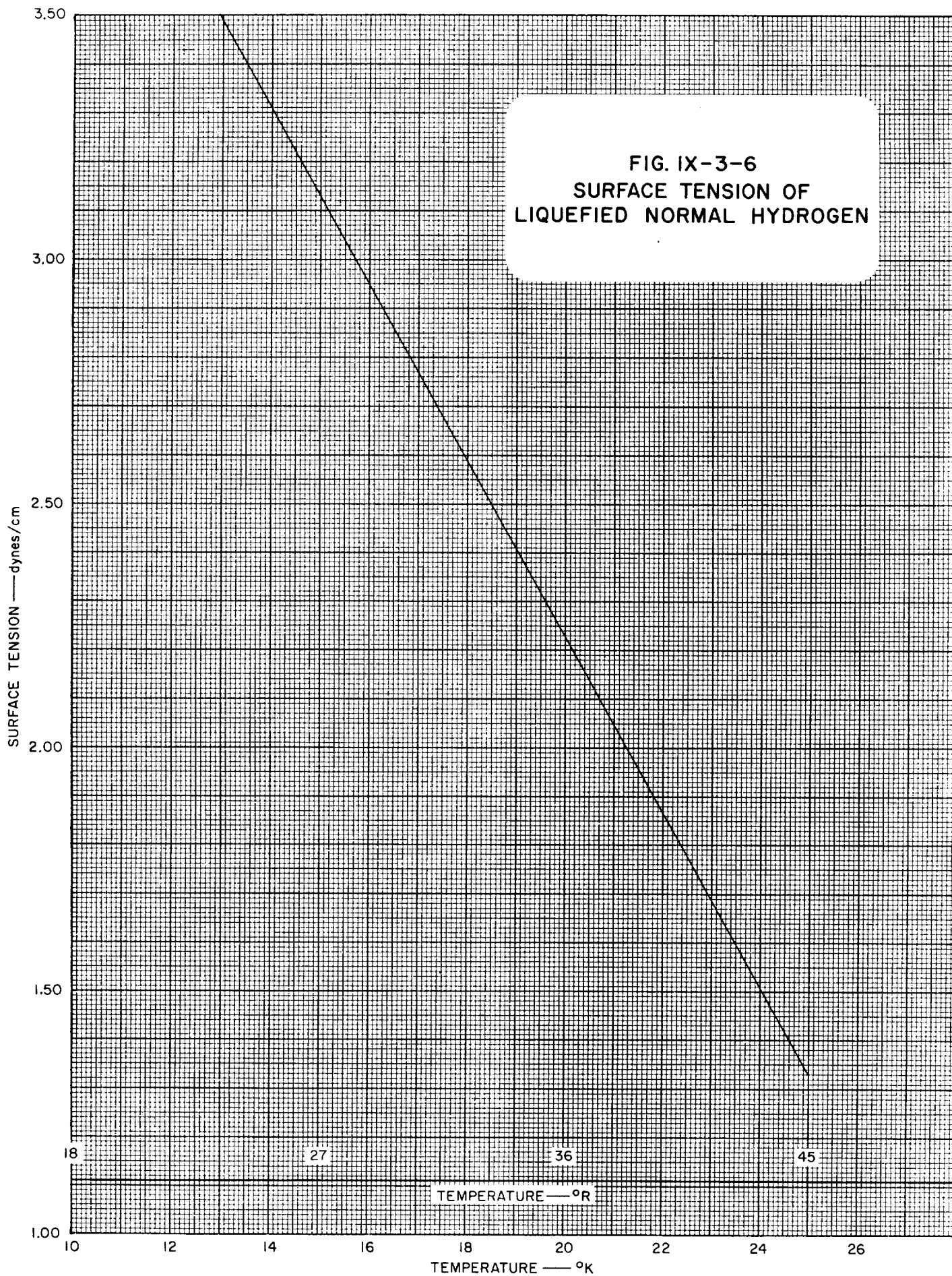


FIG. IX-3-6
SURFACE TENSION OF
LIQUEFIED NORMAL HYDROGEN



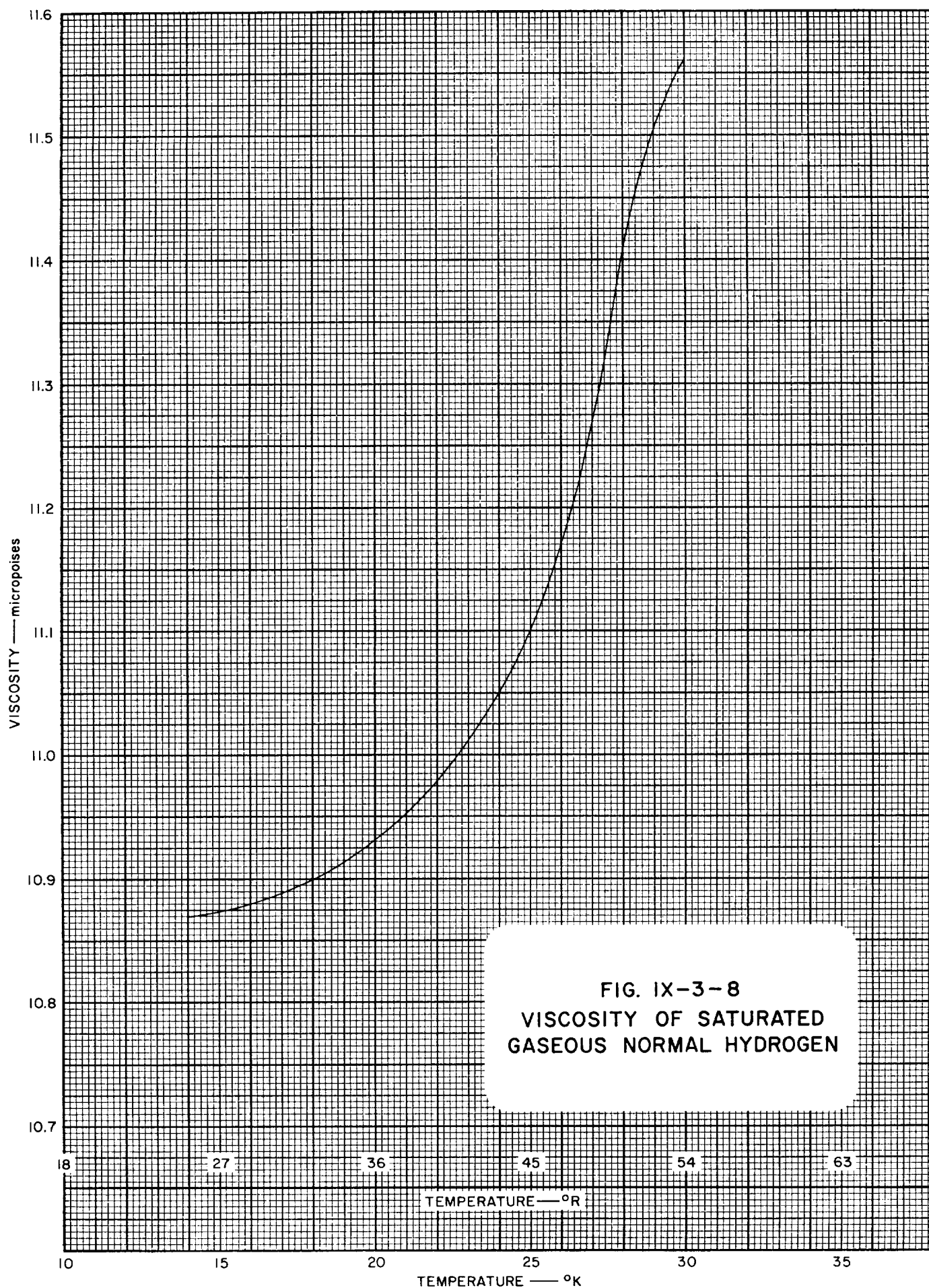
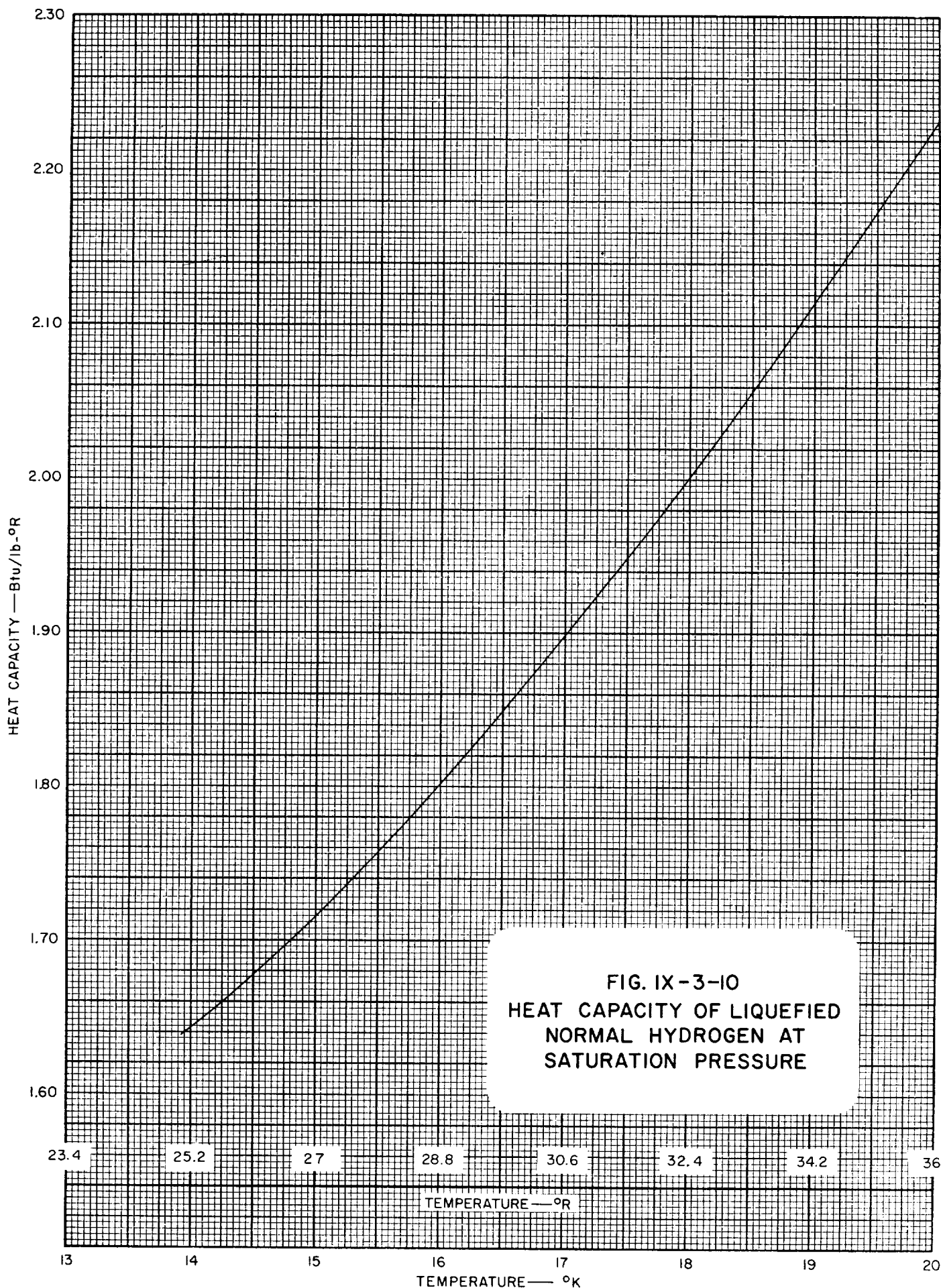
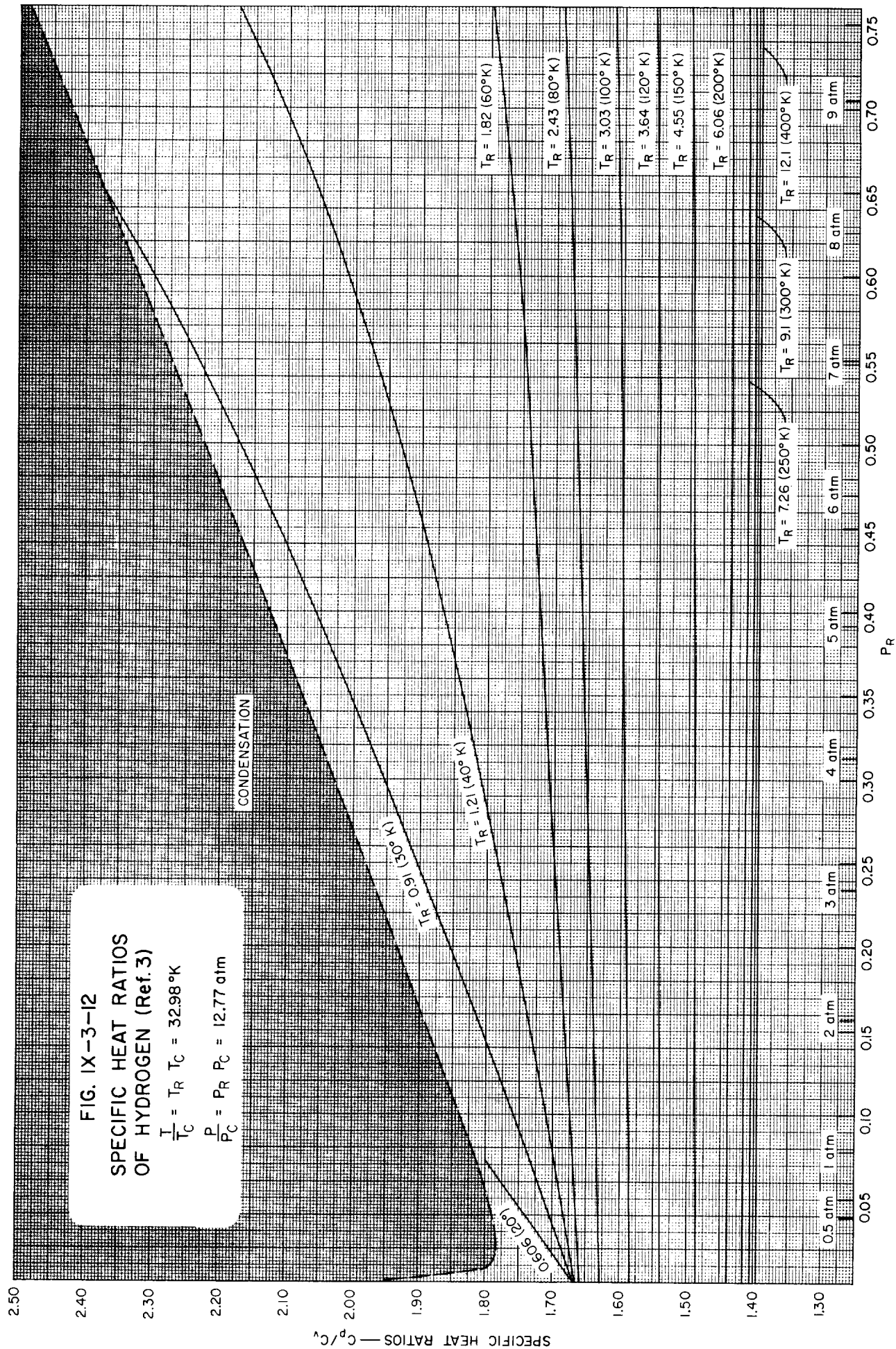


FIG. IX-3-8
VISCOSITY OF SATURATED
GASEOUS NORMAL HYDROGEN





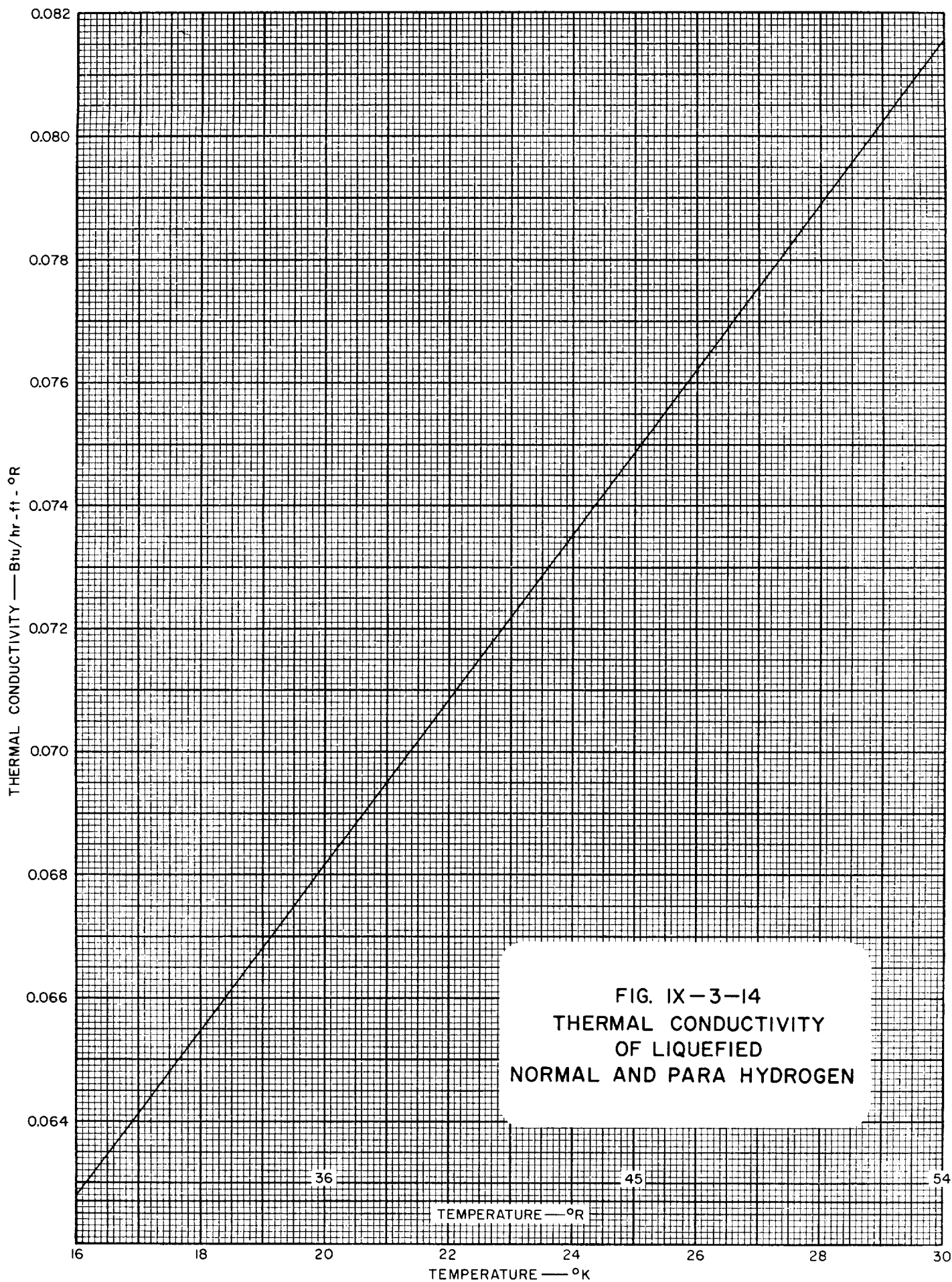


FIG. IX-3-14
THERMAL CONDUCTIVITY
OF LIQUEFIED
NORMAL AND PARA HYDROGEN

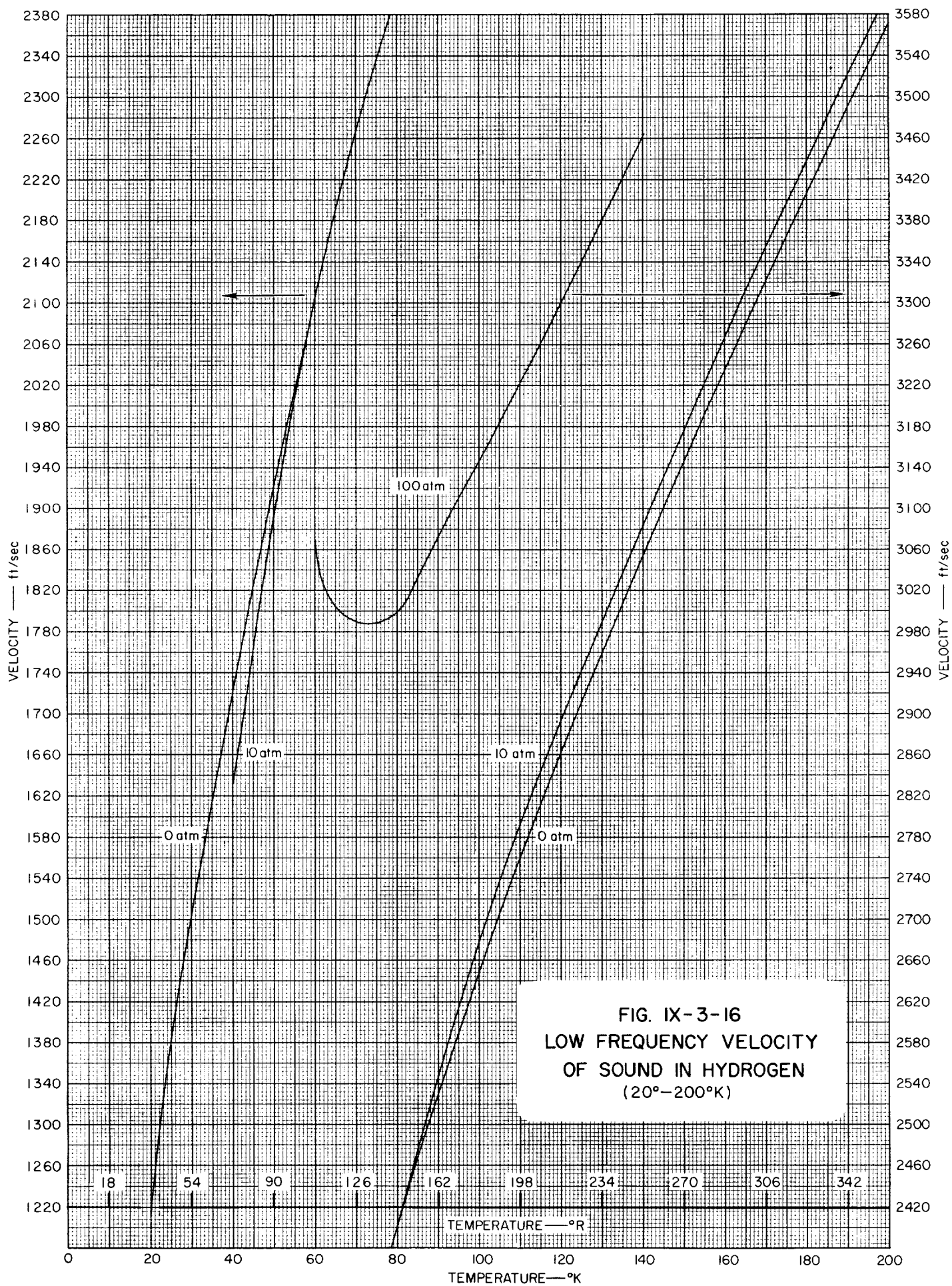


FIG. IX-3-16
LOW FREQUENCY VELOCITY
OF SOUND IN HYDROGEN
(20°-200°K)

)

)

)

)

)

)

)

)

)

)

Table IX-4-2
MELTING POINT OF HELIUM (Ref. 4)

TEMPERATURE		PRESSURE	TEMPERATURE		PRESSURE
$^{\circ}\text{K}$	$^{\circ}\text{R}$	atm	$^{\circ}\text{K}$	$^{\circ}\text{R}$	atm
50.0	90.0	7273.	4.23	7.61	140.5
45.0	81.0	6171.	3.59	6.46	108.8
40.0	72.0	5137.	3.065	5.517	81.5
35.0	63.0	4171.	2.63	4.73	62.8
30.0	54.0	3375.	2.295	4.131	48.6
25.0	45.0	2465.	1.94	3.49	35.7
20.0	36.0	1738.	1.76	3.17	29.8
15.0	27.0	1105.	1.605	2.889	27.4
10.0	18.0	581.	1.42	2.56	26.5
5.0	9.0	196.6	1.22	2.20	25.3
4.5	8.1	156.0			

(See Figure IX-4-1)

Table IX-4-5
DENSITY OF GASEOUS HELIUM (Ref. 3)

TEMPERATURE		DENSITY—lb/ft ³					
°K	°R	1 atm	3.4 atm	10.2 atm	61.2 atm	170.1 atm	408.2 atm
10.94	19.69	0.2873	1.130	4.88			
19.27	34.69	0.1467	0.5414	1.62	6.87	11.10	16.7
33.15	59.67	0.09158	0.3101	0.911	4.52	9.084	14.3
61.00	109.80	0.04982	0.1688	0.50	2.70	6.10	11.10
88.70	159.66	0.03427	0.1161	0.348	1.92	4.62	8.80
116.50	209.70	0.02610	0.08853	0.263	1.49	3.69	7.30
144.20	259.56	0.02110	0.07148	0.213	1.24	3.15	6.24
172.00	309.60	0.01767	0.0600	0.182	1.03	2.63	5.46
199.70	359.46	0.01523	0.0517	0.154	0.893	2.30	4.88
255.30	459.54	0.01199	0.0405	0.121	0.705	1.84	3.98
311.00	559.80	0.009739	0.0332	0.0993	0.581	1.57	3.37

(See Figure IX-4-5
Figure IX-4-6)

Table IX-4-6
SURFACE TENSION OF SATURATED
LIQUID HELIUM AGAINST ITS
OWN VAPOR (Ref. 3)

TEMPERATURE		SURFACE TENSION
°K	°R	dynes/cm
1.00	1.80	0.346
1.50	2.70	0.333
2.00	3.60	0.307
2.179	3.922	0.295
2.50	4.50	0.264
3.00	5.40	0.214
3.50	6.30	0.164
4.00	7.20	0.112
4.50	8.10	0.062
5.00	9.0	0.011
5.12	9.22	0.00

(See Figure IX-4-7)

Table IX-4-9

HEAT OF VAPORIZATION OF HELIUM (Ref. 2)

TEMPERATURE		LATENT HEAT	TEMPERATURE		LATENT HEAT
°K	°R	Btu/lb	°K	°R	Btu/lb
2.2	3.96	9.816	4.2	7.56	9.000
2.4	4.32	9.935	4.4	7.92	8.463
2.6	4.68	10.03	4.6	8.28	7.733
2.8	5.04	10.12	4.8	8.64	6.713
3.0	5.40	10.17	5.0	9.00	5.166
3.2	5.76	10.16	5.1	9.18	3.866
3.4	6.12	10.08	5.15	9.27	2.878
3.6	6.48	9.956	5.18	9.32	1.718
3.8	6.84	9.741			
4.0	7.20	9.419			

(See Figure IX-4-10)

Table IX-4-10

HEAT CAPACITY OF LIQUID HELIUM AT
SATURATION PRESSURE (Ref. 3)

TEMPERATURE		HEAT CAPACITY, C_p	TEMPERATURE		HEAT CAPACITY, C_p
°K	°R	Btu/lb-°R	°K	°R	Btu/lb-°R
1.79	3.22	0.672	3.39	6.10	0.710
1.84	3.31	0.779	3.59	6.46	0.779
1.89	3.40	0.906	3.79	6.82	0.860
1.99	3.58	1.24	3.99	7.18	0.953
2.04	3.67	1.47	4.19	7.54	1.07
2.09	3.76	1.80	4.39	7.90	1.22
2.14	3.85	2.23	4.59	8.26	1.42
2.1635	3.8943	3.01	4.79	8.62	1.80
2.19	3.94	0.951	4.99	8.98	2.75
2.29	4.12	0.631	5.04	9.07	3.23
2.39	4.30	0.569			
2.59	4.66	0.542			
2.79	5.02	0.559			
2.99	5.38	0.595			
3.19	5.74	0.643			

(See Figure IX-4-11)

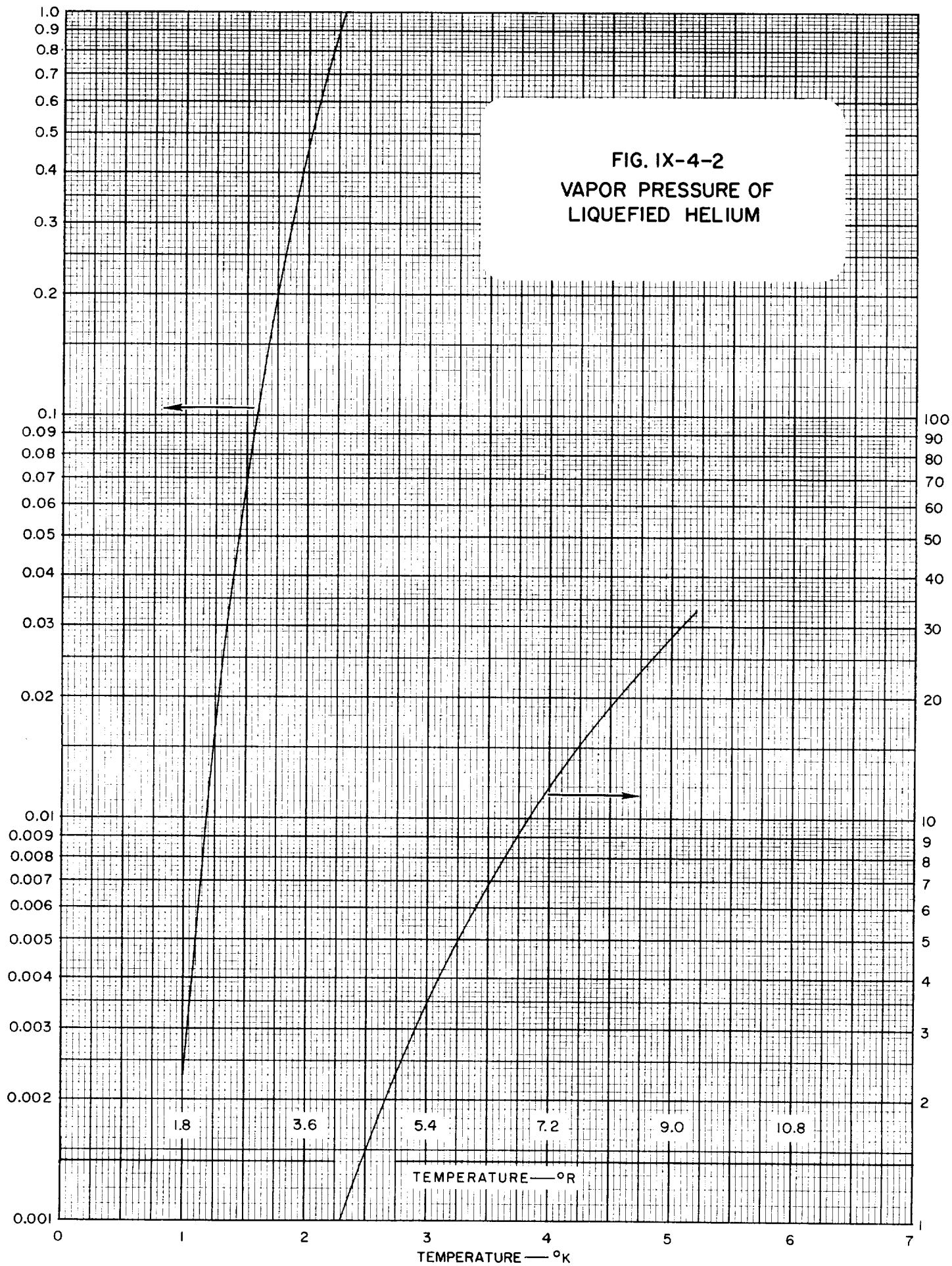
Table IX-4-13
THERMAL CONDUCTIVITY OF HELIUM GAS
AT ONE ATMOSPHERE (Ref. 1)

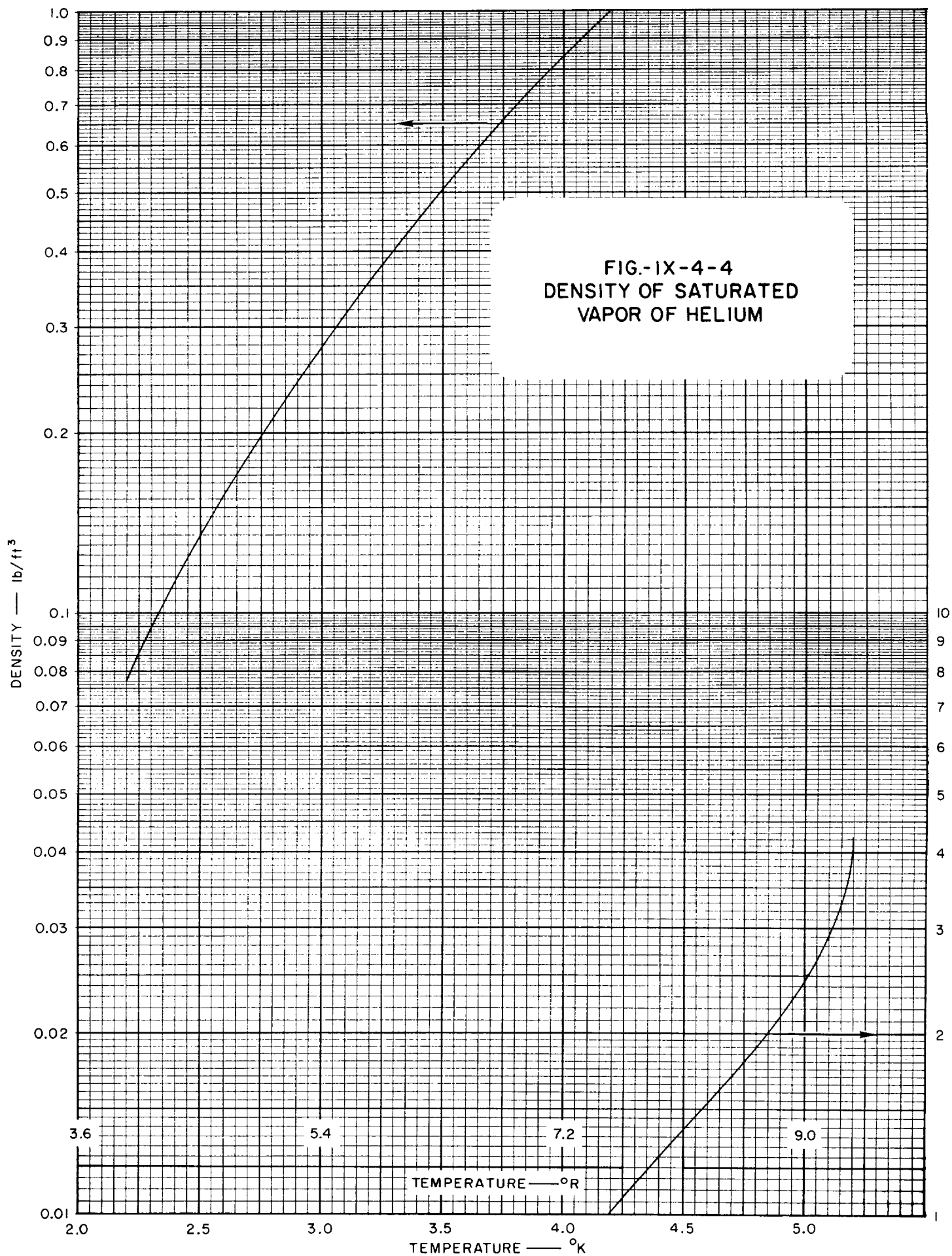
TEMPERATURE		THERMAL CONDUCTIVITY
$^{\circ}\text{K}$	$^{\circ}\text{R}$	Btu/hr-ft- $^{\circ}\text{R}$
2.04	3.67	0.0022
5.37	9.67	0.0063
10.93	19.67	0.0106
16.48	29.67	0.0133
22.04	39.67	0.0160
27.59	49.67	0.0186
33.15	59.67	0.0210
88.71	159.67	0.0400
144.26	259.67	0.0550
199.82	359.67	0.0673
255.37	459.67	0.0792
366.48	659.67	0.1000
477.59	859.67	0.1191

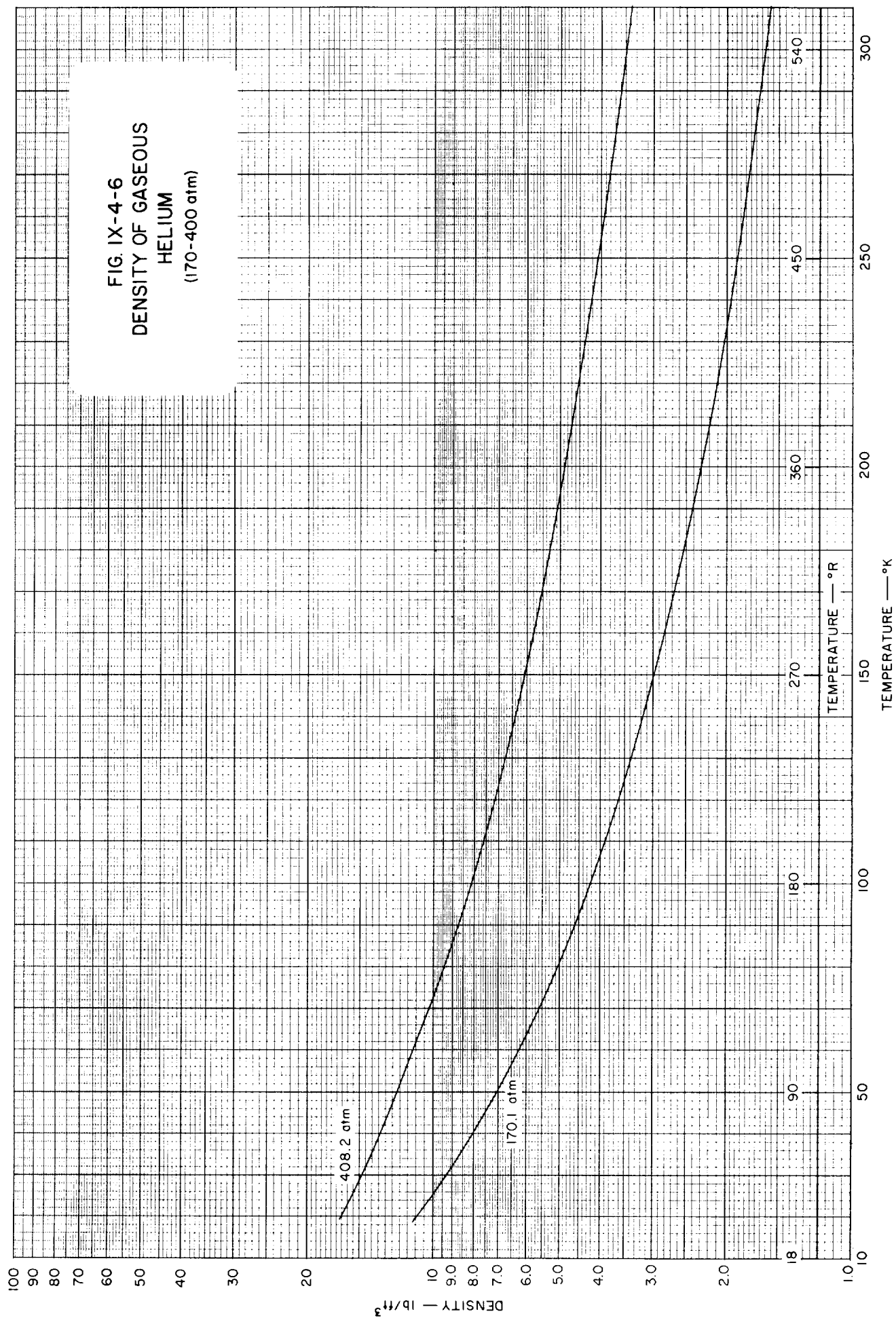
(See Figure IX-4-14)

FIG. IX-4-2
VAPOR PRESSURE OF
LIQUEFIED HELIUM

VAPOR PRESSURE — psia







VISCOSITY—micropoises

35.0
30.0
25.0
20.0
15.0
10.0
5.0
0

FIG. IX-4-8
VISCOSITY OF
LIQUID HELIUM

1.8 3.6 5.4 7.2 9.0

TEMPERATURE—°R

0 1.0 2.0 3.0 4.0 5.0
TEMPERATURE —°K

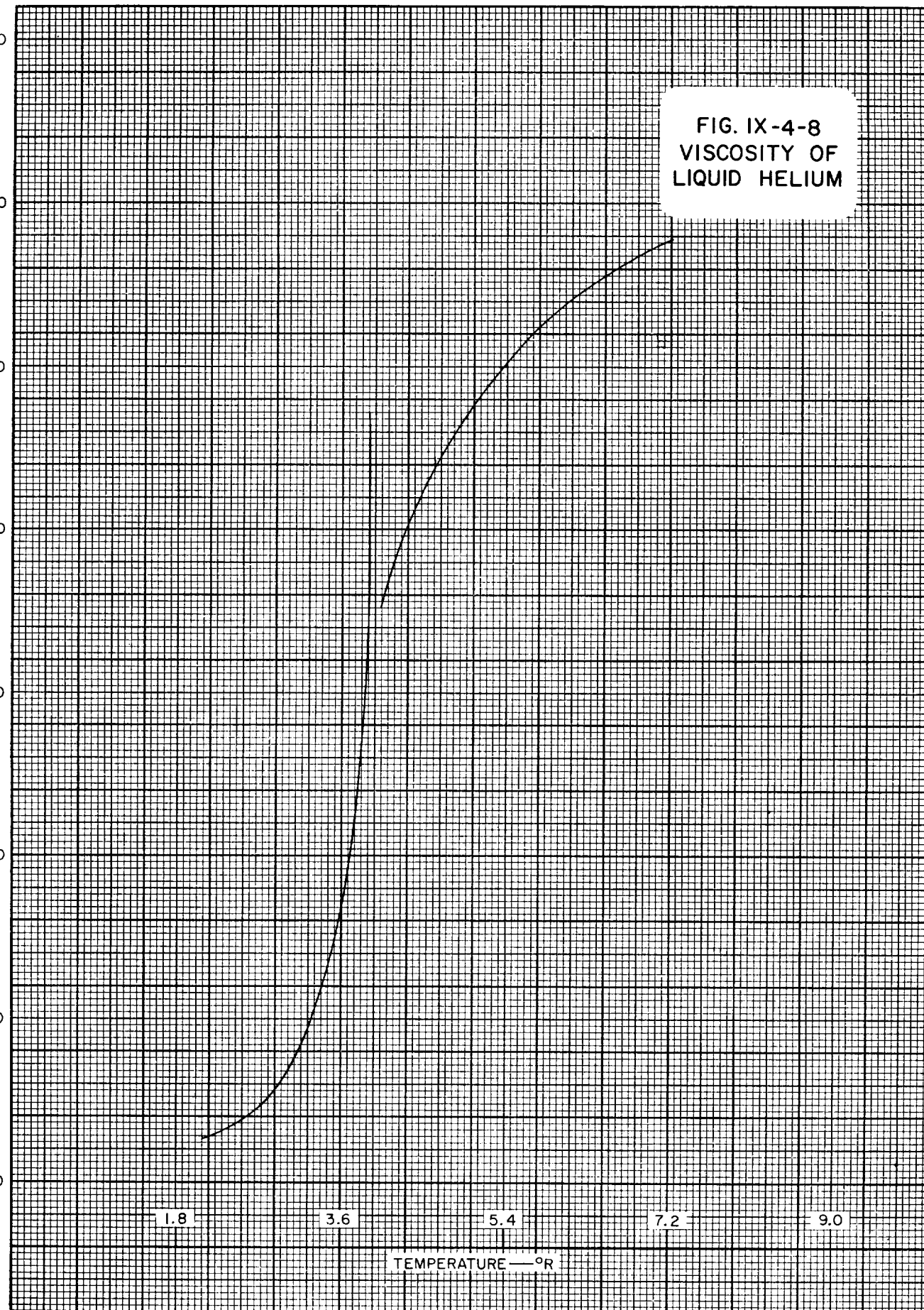
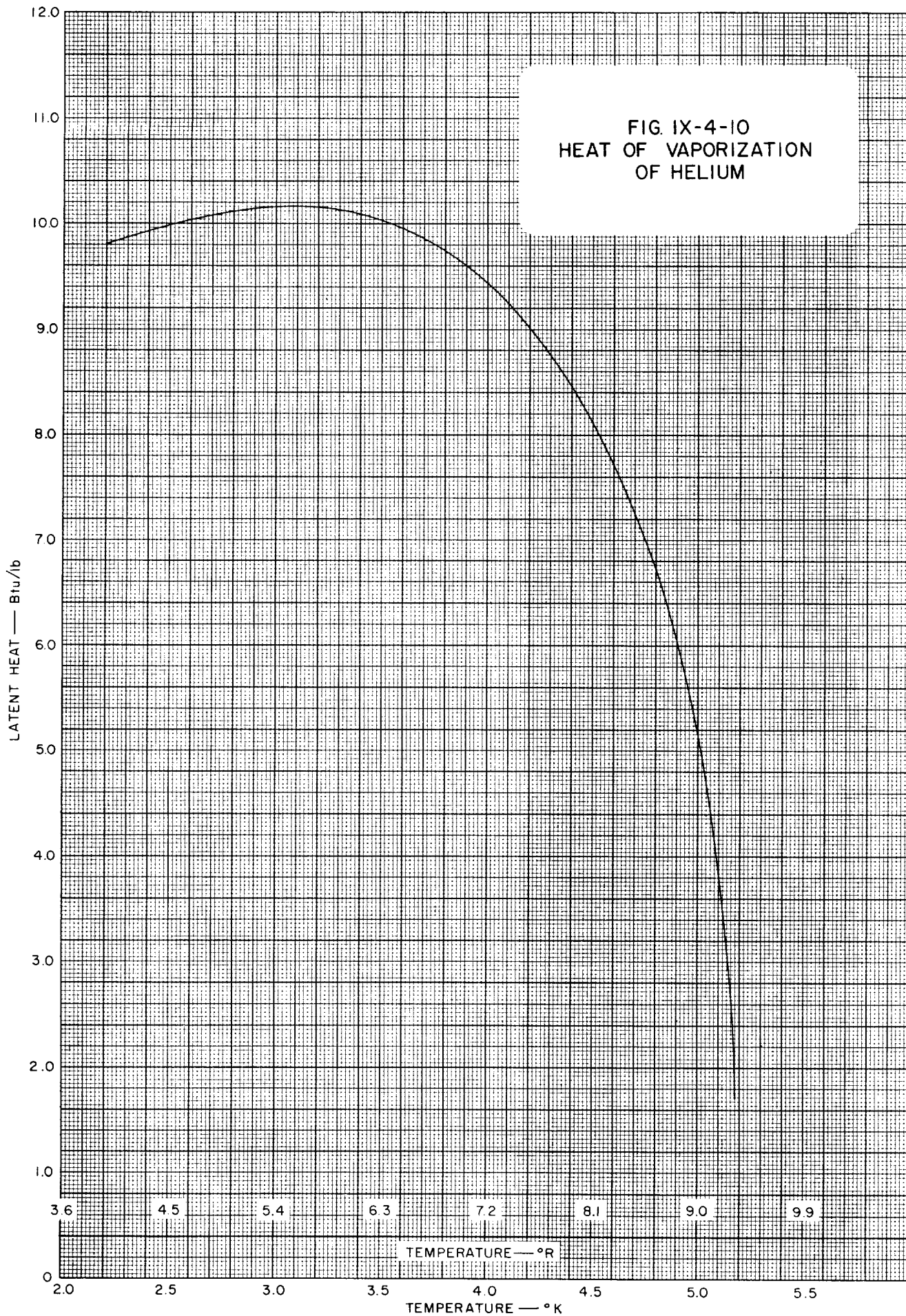
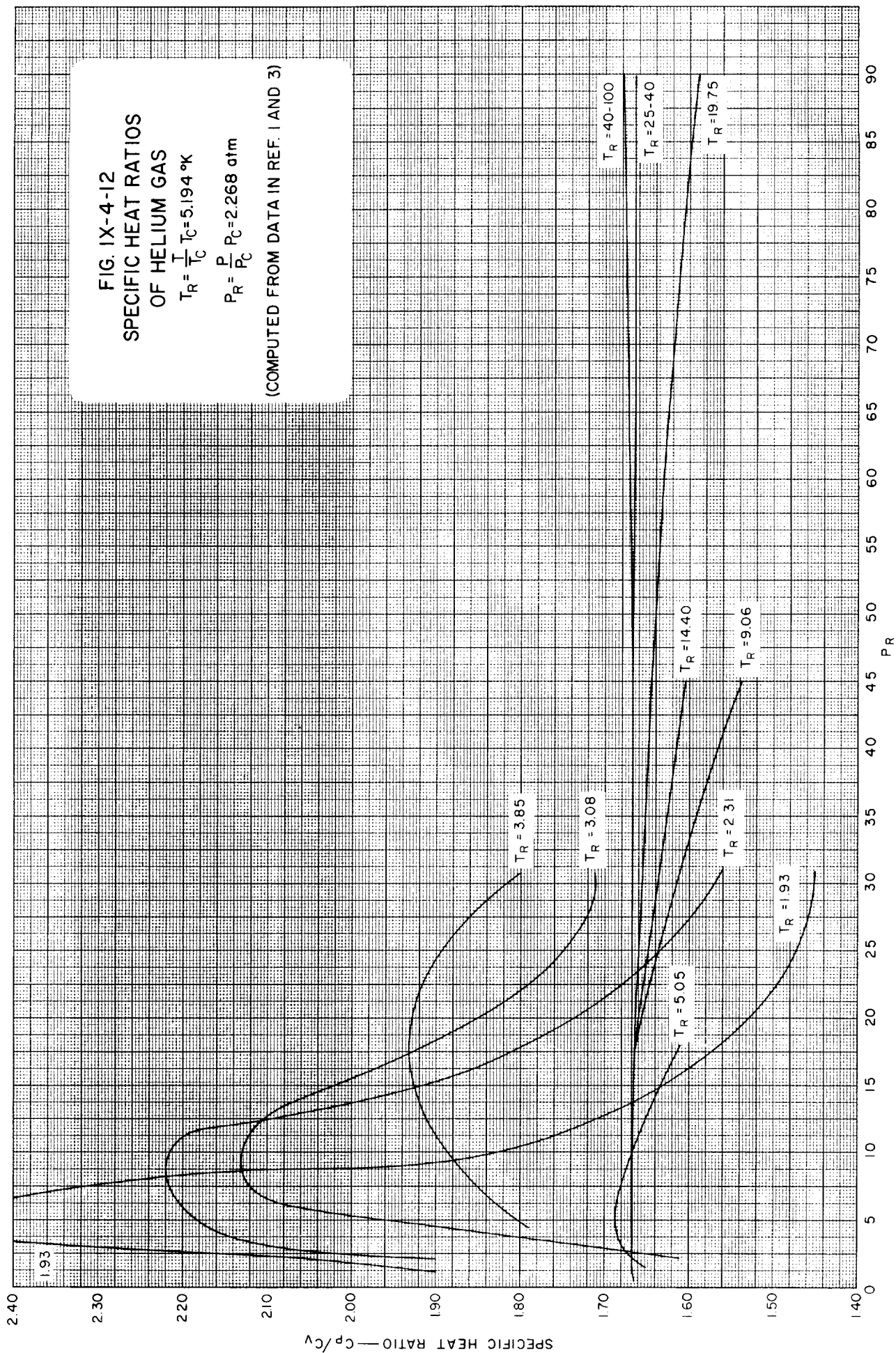
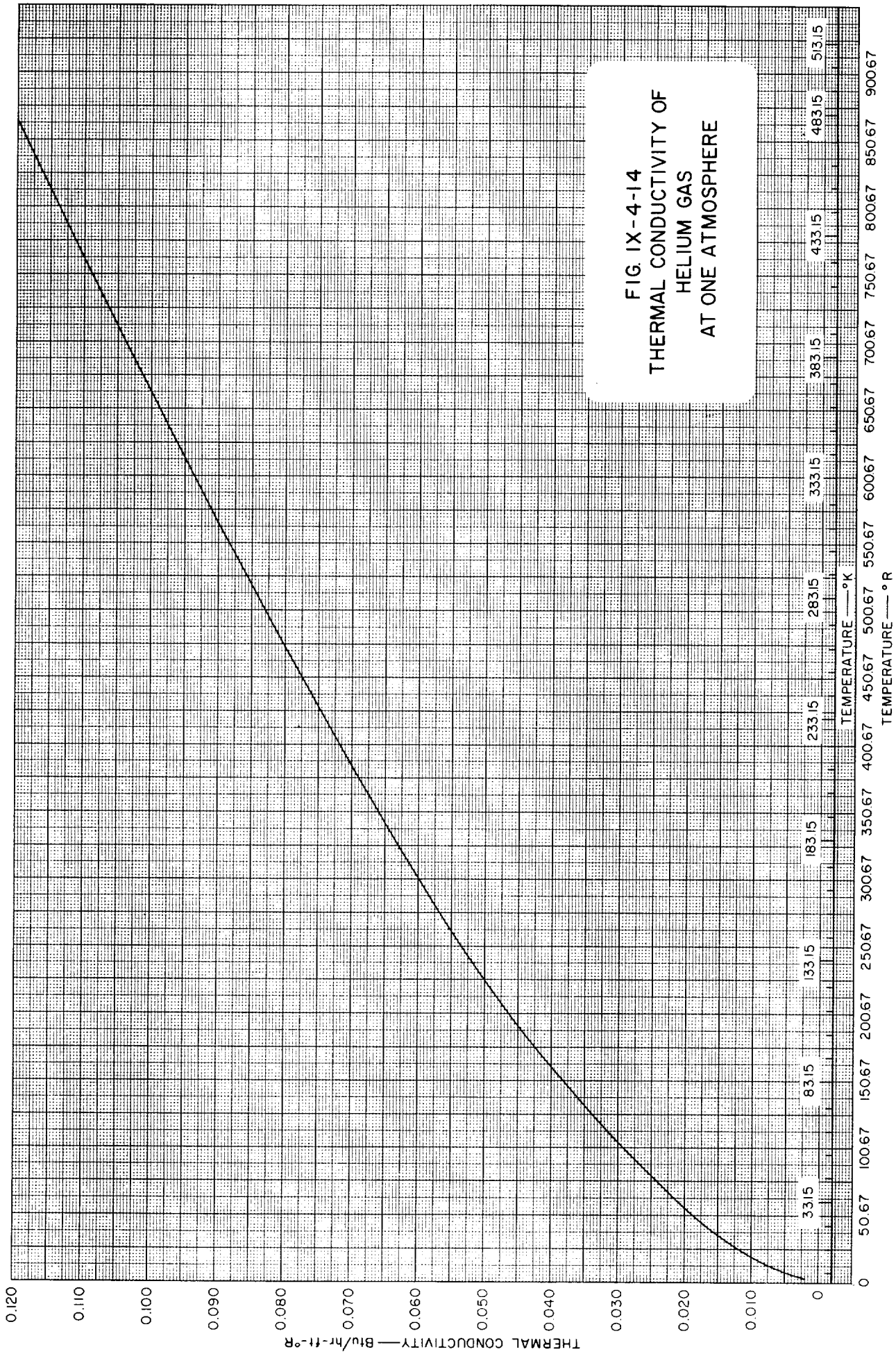


FIG. IX-4-10
HEAT OF VAPORIZATION
OF HELIUM







)

)

)

)

)

Table IX-5-2
VAPOR PRESSURE OF LIQUID OXYGEN
(Ref. 2)

TEMPERATURE		VAPOR PRESSURE	
^o K	^o R	atm	psia
55	99	0.00182	0.027
60	108	0.00716	0.105
65	117	0.0229	0.34
70	126	0.0616	0.90
75	135	0.1430	2.10
80	144	0.2964	4.36
85	153	0.5597	8.23
90	162	0.9803	14.41
95	171	1.6096	23.65
100	180	2.5066	36.84
105	189	3.7345	54.88
110	198	5.3591	78.76
115	207	7.4495	109.48
120	216	10.077	148.09
125	225	13.316	195.70
130	234	17.239	253.40
135	243	21.934	322.30
140	252	27.489	404.00
145	261	34.004	499.70
150	270	41.620	611.60

(See Figure IX-5-1)

Table IX-5-3
DENSITY OF LIQUID OXYGEN
(Ref. 3)

TEMPERATURE		DENSITY
$^{\circ}\text{K}$	$^{\circ}\text{R}$	lb/ft^3
61	109.8	80.035
65	117.0	78.85
70	126.0	77.35
80	144.0	74.35
85	153.0	72.86
90	162.0	71.30
118.6	213.48	60.92
132.9	239.22	54.58
143.2	257.76	48.58
149.8	269.64	42.32
152.7	274.86	37.66

(See Figure IX-5-2)

Table IX-5-4
DENSITY OF GASEOUS OXYGEN (Ref. 2)

TEMPERATURE		DENSITY— lb/ft^3		
$^{\circ}\text{K}$	$^{\circ}\text{R}$	1 atm	10 atm	100 atm
100	180	0.24913		
120	216	0.20565		
140	252	0.17542		
160	288	0.15307	1.6218	
180	324	0.13582	1.4131	
200	360	0.12209	1.2555	17.708
220	396	0.11074	1.1314	13.863
240	432	0.10160	1.0308	11.767
260	468	0.09375	0.9474	10.365
280	504	0.08694	0.8769	9.322
300	540	0.08120	0.8164	8.505
320	576	0.07611	0.7639	7.839
340	612	0.07162	0.7179	7.281
360	648	0.06764	0.6772	6.808
380	684	0.06407	0.6410	6.398
400	720	0.06086	0.6085	6.039
420	756	0.05796	0.5792	5.722
440	792	0.05532	0.5526	5.440
460	828	0.05291	0.5284	5.186
480	864	0.05017	0.5062	4.956
500	900	0.04868	0.4858	4.748

(See Figure IX-5-3
Figure IX-5-4)

Table IX-5-5
VISCOSITY OF LIQUID OXYGEN (Ref. 3)

TEMPERATURE		ABSOLUTE VISCOSITY	TEMPERATURE		ABSOLUTE VISCOSITY
$^{\circ}\text{K}$	$^{\circ}\text{R}$	centipoises	$^{\circ}\text{K}$	$^{\circ}\text{R}$	centipoises
54.4	97.92	0.873	68.9	124.02	0.377
54.5	98.10	0.863	72.3	130.14	0.323
54.6	98.28	0.821	77.4	139.32	0.273
54.9	98.82	0.772	80.0	144.0	0.250
56.4	101.52	0.717	90.0	162.0	0.190
57.4	103.32	0.648	111.0	199.80	0.123
59.7	107.46	0.631	125.8	226.44	0.110
61.7	111.06	0.521	138.2	248.76	0.100
63.5	114.30	0.476	145.5	261.90	0.098
65.4	117.72	0.435	154.1	277.38	0.090

(See Figure IX-5-5)

Table IX-5-6
VISCOSITY OF GASEOUS OXYGEN (Ref. 2)

TEMPERATURE		ABSOLUTE VISCOSITY	TEMPERATURE		ABSOLUTE VISCOSITY
$^{\circ}\text{K}$	$^{\circ}\text{R}$	micropoises	$^{\circ}\text{K}$	$^{\circ}\text{R}$	micropoises
100	180	77.73	320	576	216.75
120	216	93.06	340	612	226.81
140	252	107.86	360	648	236.66
160	288	122.04	380	684	246.23
180	324	135.67	400	720	255.56
200	360	148.60	420	756	264.68
220	396	161.06	440	792	273.58
240	432	173.04	460	828	282.31
260	468	184.57	480	864	290.89
280	504	195.64	500	900	299.30
300	540	206.33			

(See Figure IX-5-6)

Table IX-5-7

HEAT CAPACITIES OF OXYGEN (Ref. 2)

TEMPERATURE		HEAT CAPACITY, C_p --Btu/lb-°R		
°K	°R	1 atm	10 atm	100 atm
120	216	0.2213		
140	252	0.2198		
160	288	0.2190	0.2387	
180	324	0.2186	0.2317	
200	360	0.2184	0.2280	0.471
220	396	0.2183	0.2257	0.357
240	432	0.2184	0.2243	0.307
260	468	0.2187	0.2235	0.2816
280	504	0.2191	0.2231	0.2673
300	540	0.2197	0.2231	0.2585
320	576	0.2205	0.2234	0.2527
340	612	0.2214	0.2239	0.2488
360	648	0.2225	0.2247	0.2462
380	684	0.2236	0.2256	0.2444
400	720	0.2249	0.2266	0.2433
420	756	0.2263	0.2278	0.2427
440	792	0.2277	0.2291	0.2425
460	828	0.2292	0.2301	0.2425
480	864	0.2307	0.2318	0.2428
500	900	0.2322	0.2332	0.2433

(See Figure IX-5-7)

Table IX-5-8

THERMAL CONDUCTIVITY OF GASEOUS OXYGEN (Ref. 1)

TEMPERATURE		THERMAL CONDUCTIVITY--Btu/hr-ft-°R				
°K	°R	1 atm	10 atm	50 atm	100 atm	140 atm
80	144				0.0968	0.0996
100	180	0.0050			0.0838	0.0870
120	216	0.0060	0.0076	0.0644	0.0692	0.0724
140	252	0.0072	0.0084	0.0508	0.0542	0.0582
160	288	0.0082	0.0092	0.0168	0.0392	0.0450
180	324	0.0092	0.0102	0.0128	0.0271	0.0346
200	360	0.0104	0.0112	0.0126	0.0193	0.0268
220	396	0.0114	0.0120	0.0130	0.0159	
240	432	0.0126	0.0130	0.0136	0.0148	
260	468	0.0136	0.0140	0.0144	0.0150	
280	504	0.0147	0.0150	0.0152	0.0154	
300	540	0.0159	0.0159	0.0159	0.0159	

(See Figure IX-5-9)

Table IX-5-9
HEAT OF VAPORIZATION OF
LIQUID OXYGEN (Ref. 3)

TEMPERATURE		LATENT HEAT
°K	°R	Btu/lb
69	124.2	99.58
70	126.0	99.25
72	129.6	98.60
74	133.2	97.92
76	136.8	97.25
78	140.4	96.57
80	144.0	95.85
82	147.6	95.10
84	151.2	94.31
86	154.8	93.45
88	158.4	92.50
90	162.0	91.44

(See Figure IX-5-10)

Table IX-5-10
TOTAL ENTHALPY OF OXYGEN (Ref. 2)

TEMPERATURE		TOTAL ENTHALPY—Btu/lb			
°K	°R	0.01 atm	1.0 atm	10 atm	100 atm
100	180	77.944	76.530		
120	216	93.586	92.609		
140	252	109.24	108.48		
160	288	124.88	124.26	118.33	
180	324	140.53	140.02	135.24	
200	360	156.18	155.76	151.78	101.24
220	396	171.83	171.47	168.10	130.48
240	432	187.51	187.20	184.30	154.16
260	468	203.21	202.93	200.42	175.27
280	504	218.94	218.69	216.49	194.98
300	540	234.71	234.49	232.56	213.90
320	576	250.52	250.33	248.63	232.27
340	612	266.41	266.24	264.73	250.27
360	648	282.37	282.22	280.87	268.15
380	684	298.41	298.28	297.08	285.79
400	720	314.55	314.43	313.37	303.37
420	756	330.77	330.67	329.72	320.82
440	792	347.11	347.01	346.17	338.27
460	828	363.55	363.46	362.72	355.79
480	864	380.09	380.02	379.36	373.24
500	900	396.75	396.68	396.10	390.76

(See Figure IX-5-11)

Table IX-5-11

LOW FREQUENCY VELOCITY OF SOUND IN OXYGEN (Ref. 2)

TEMPERATURE		VELOCITY—Ft/sec			
$^{\circ}\text{K}$	$^{\circ}\text{R}$	0.01 atm	1 atm	10 atm	100 atm
100	180	626.			
120	216	686.	681.		
140	252	741.	736.		
160	288	791.	789.	767.	
180	324	840.	838.	823.	
200	360	885.	884.	874.	
220	396	928.	928.	921.	941.
240	432	969.	969.	965.	987.
260	468	1008.	1008.	1006.	1033.
280	504	1045.	1045.	1046.	1076.
300	540	1082.	1081.	1082.	1119.
320	576	1117.	1117.	1119.	1159.
340	612	1150.	1151.	1153.	1197.
360	648	1183.	1183.	1186.	1233.
380	684	1214.	1214.	1218.	1267.
400	720	1244.	1244.	1248.	1300.
420	756	1273.	1273.	1278.	1332.
440	792	1301.	1301.	1307.	1362.
460	828	1328.	1329.	1333.	1391.
480	864	1355.	1356.	1361.	1419.
500	900	1382.	1383.	1388.	1447.

(See Figure IX-5-12)

)

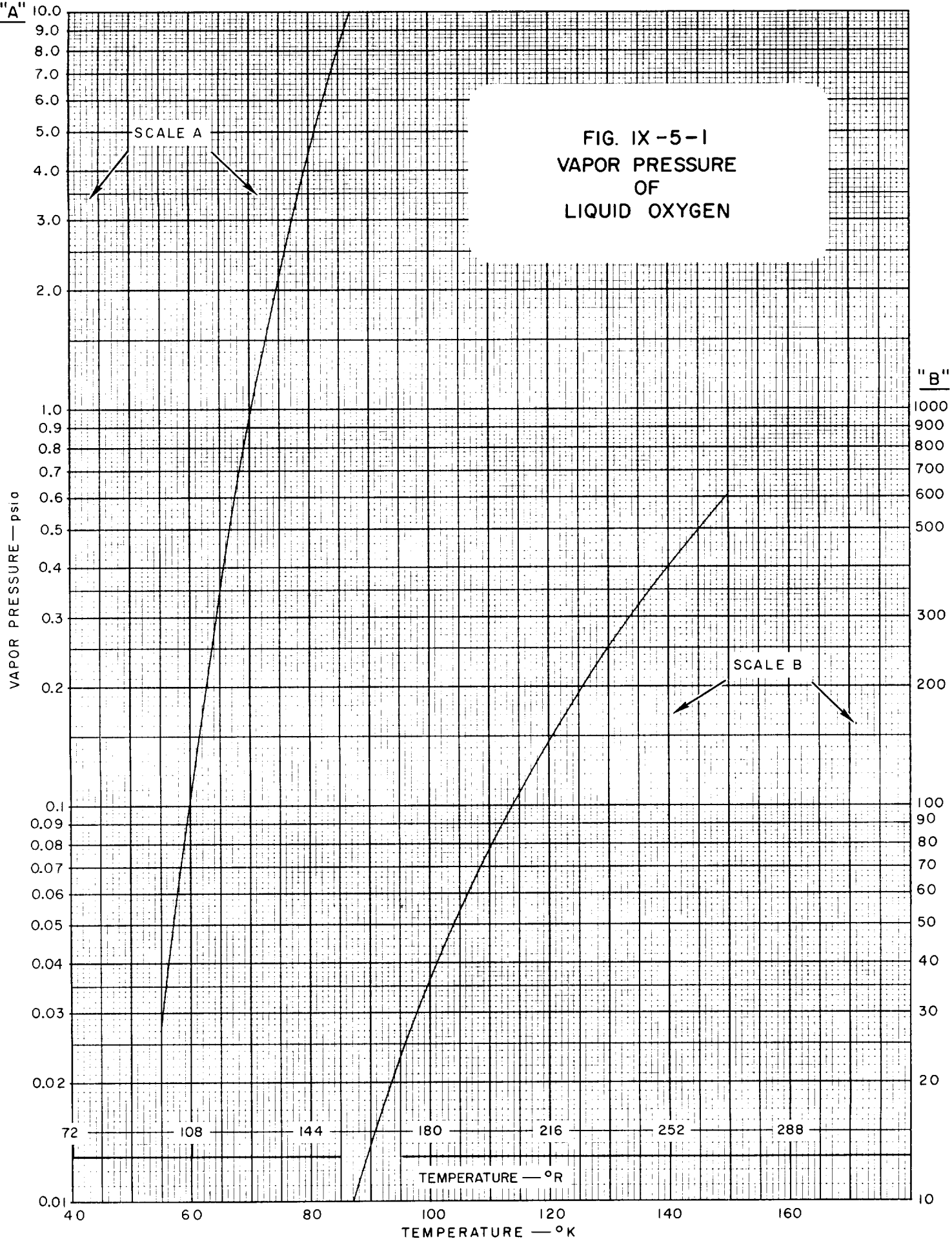
)

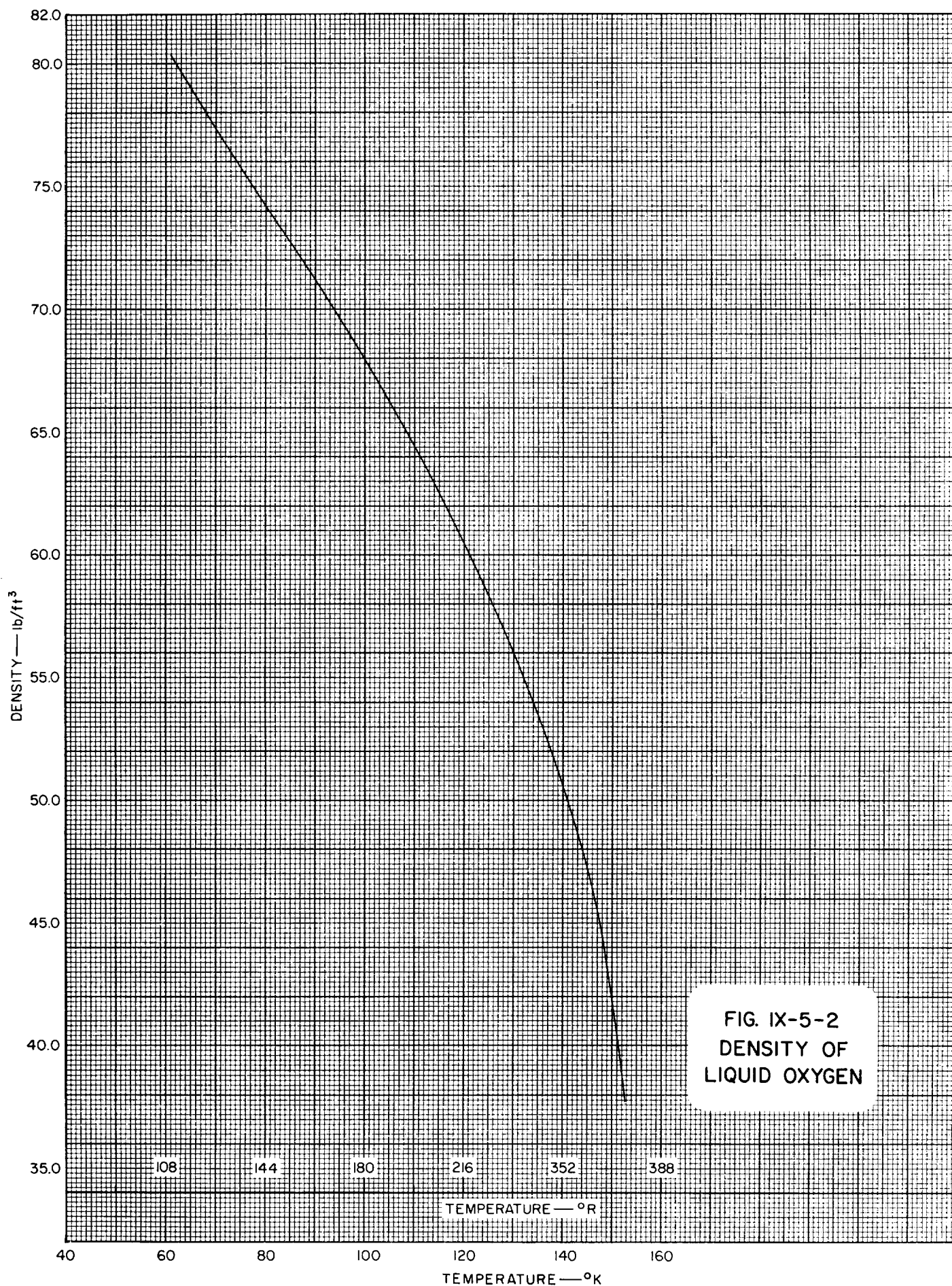
)

)

)

"A"





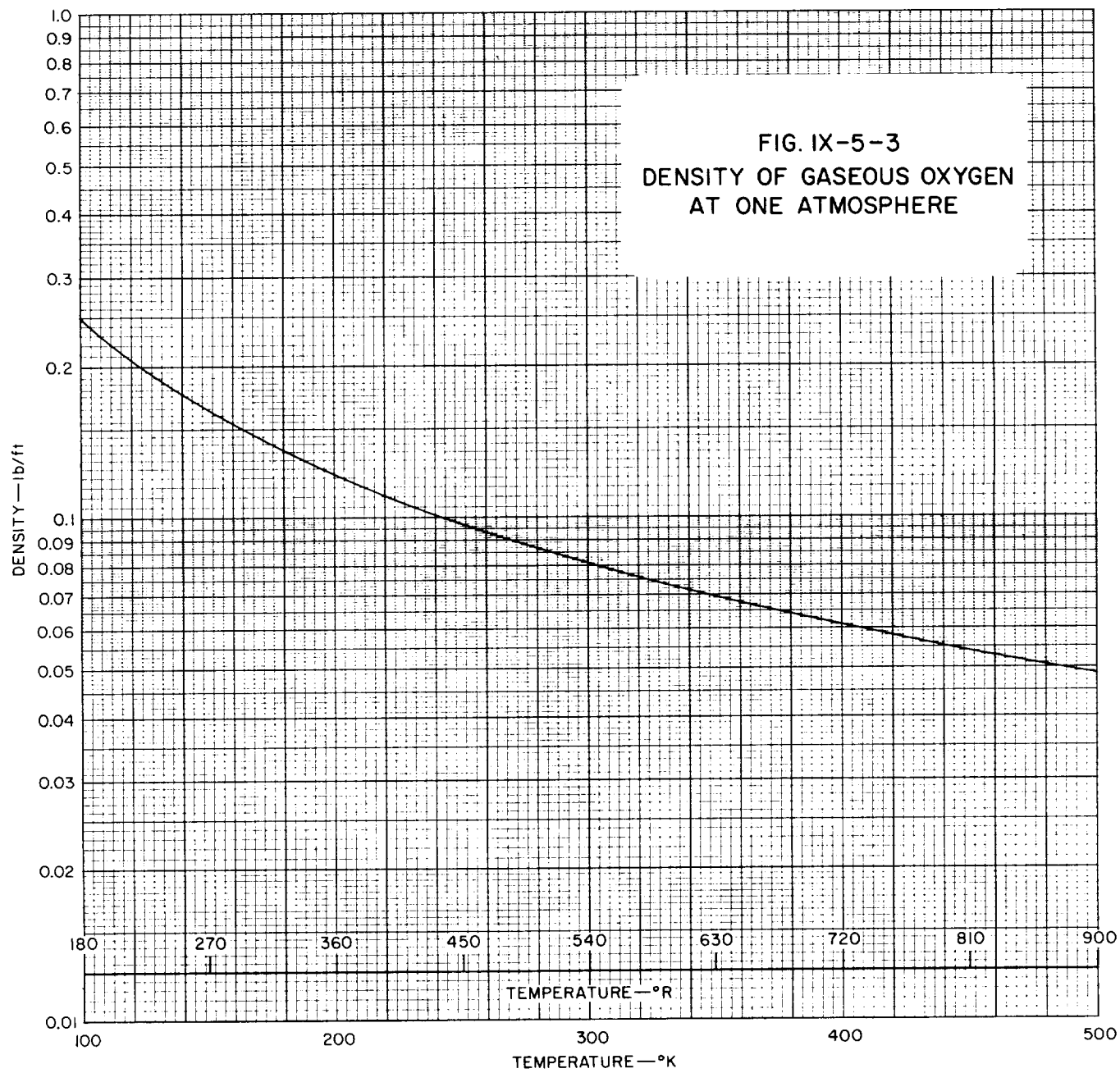


FIG. IX-5-4
DENSITY OF GASEOUS
OXYGEN AT 10
AND 100 atmospheres

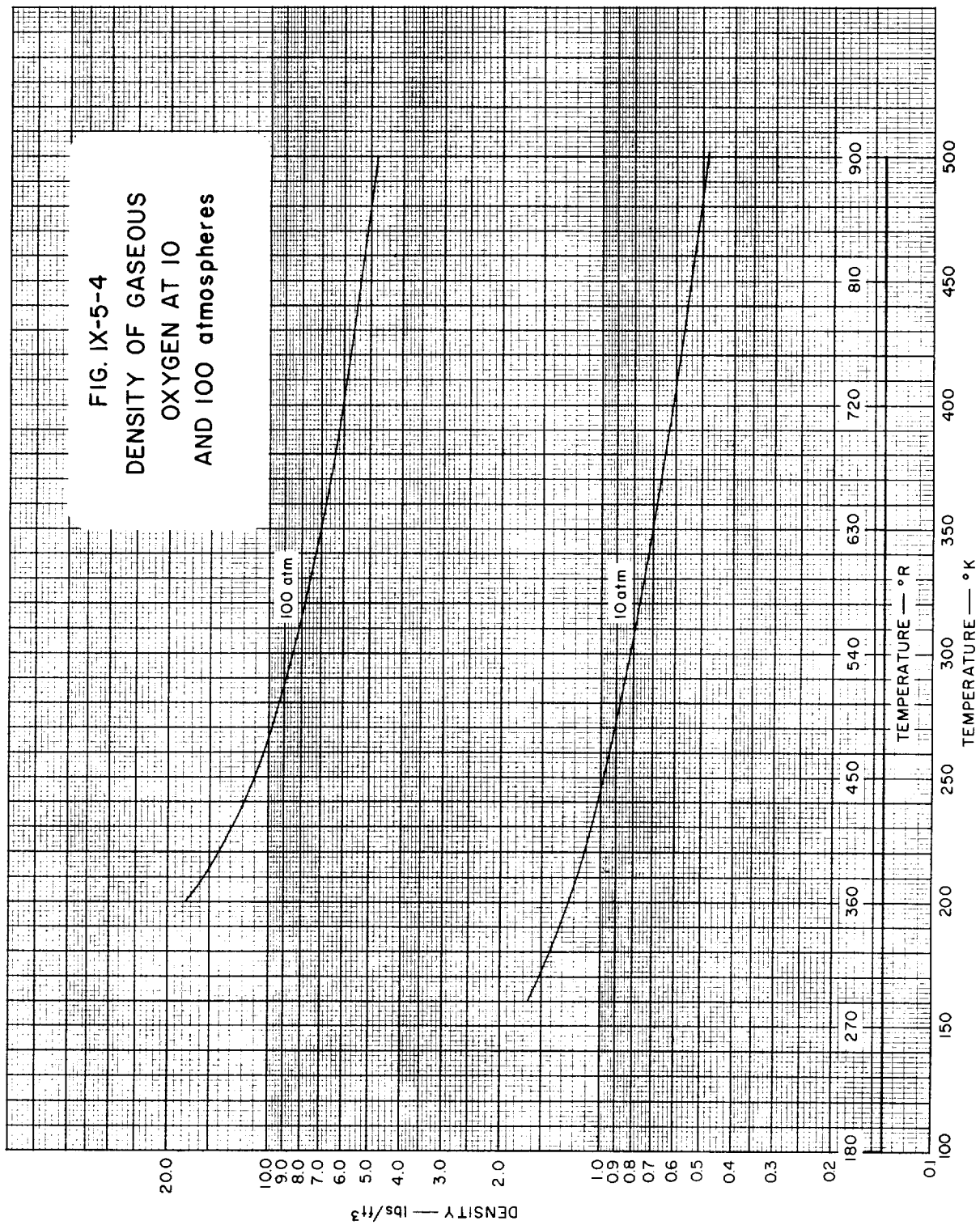
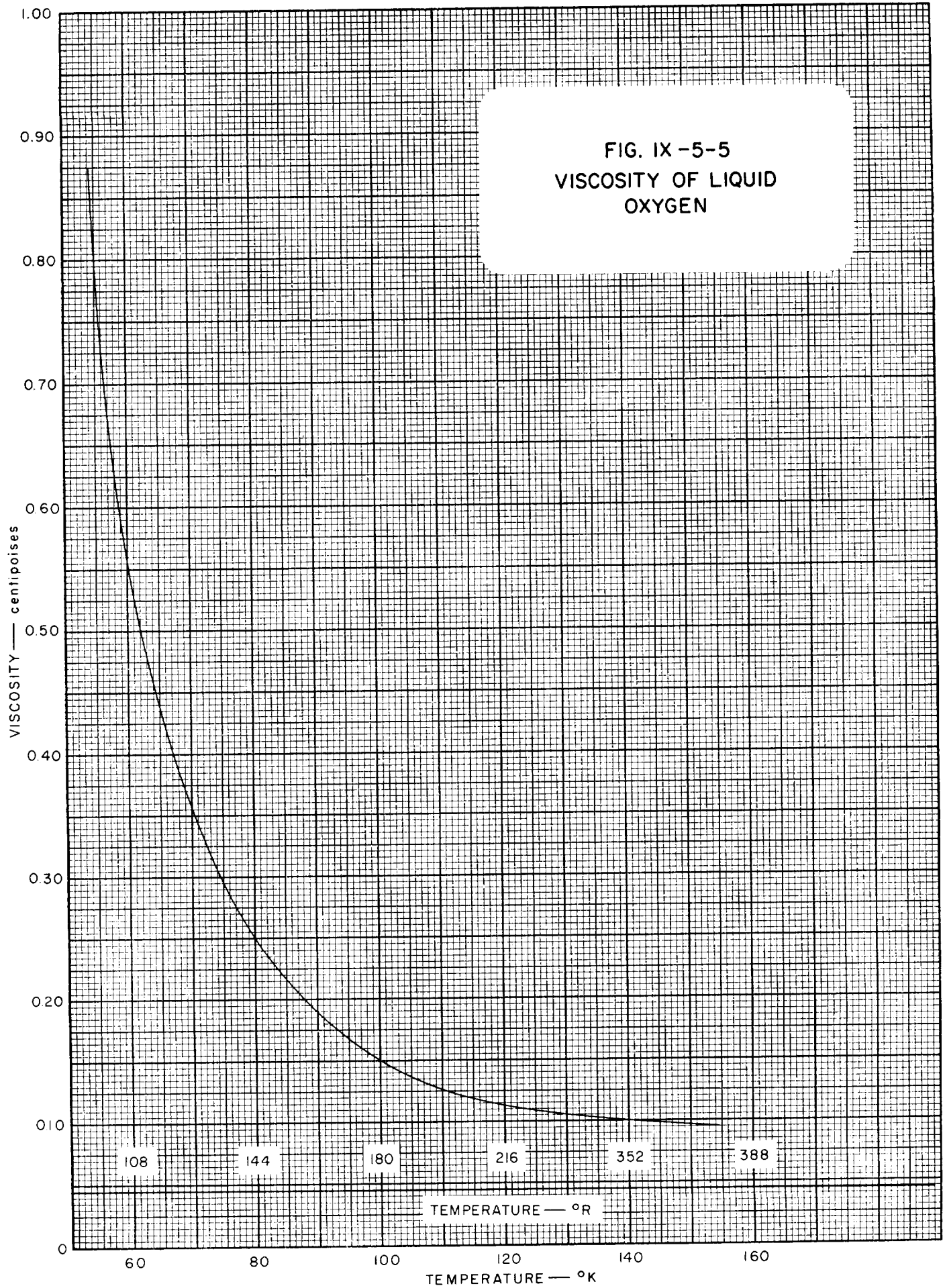


FIG. IX-5-5
VISCOSITY OF LIQUID
OXYGEN



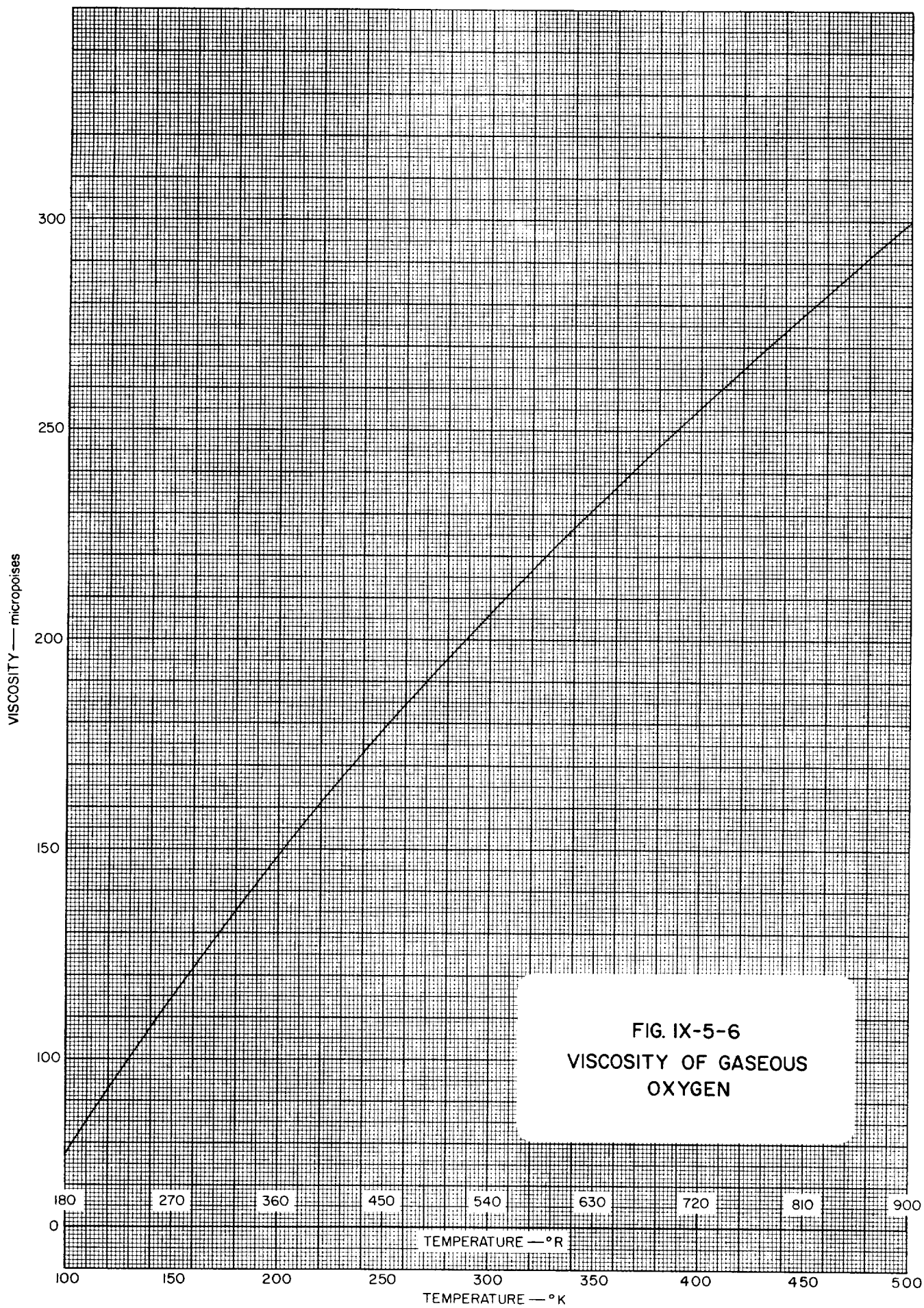
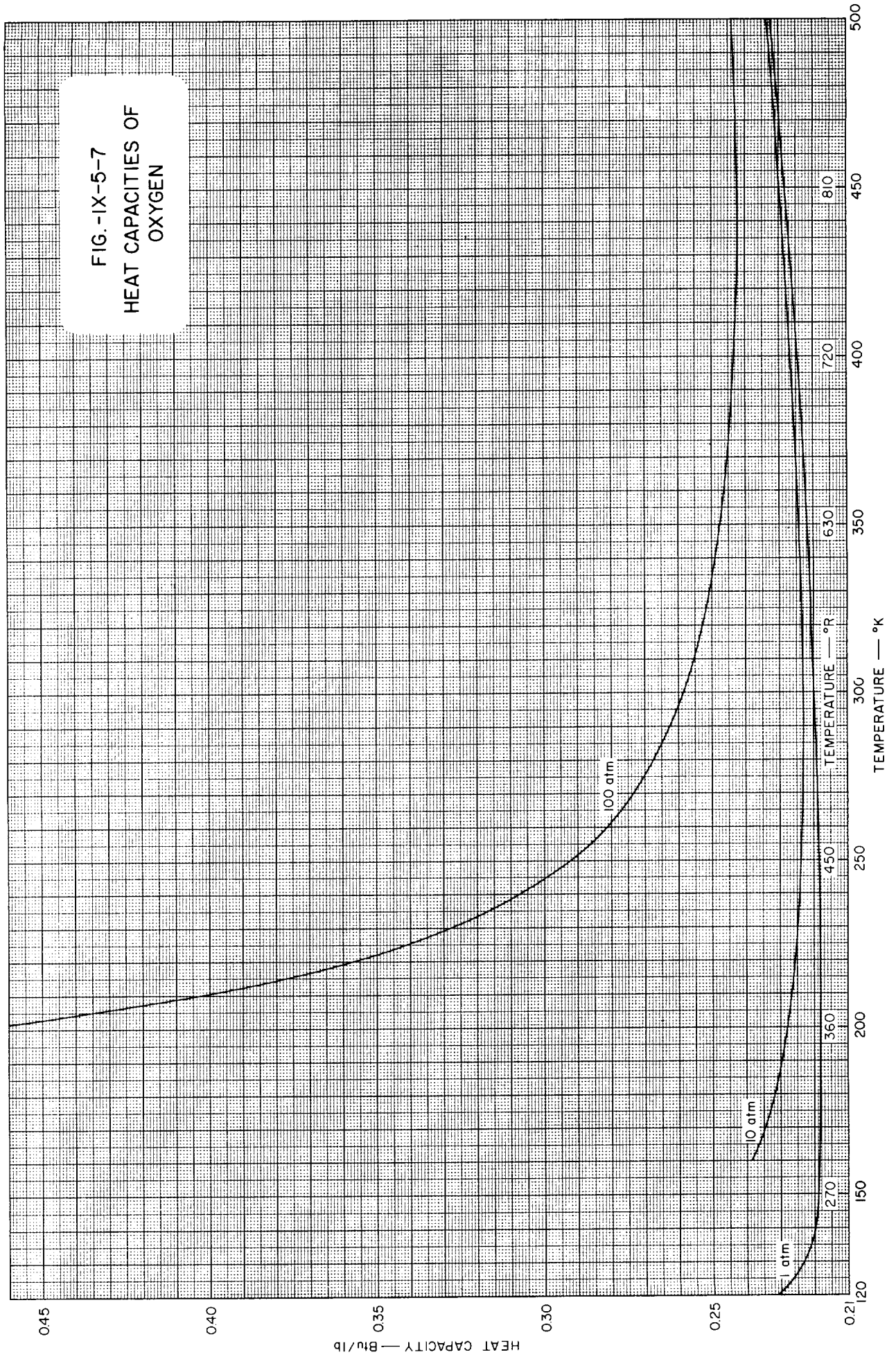


FIG. -IX-5-7
HEAT CAPACITIES OF
OXYGEN



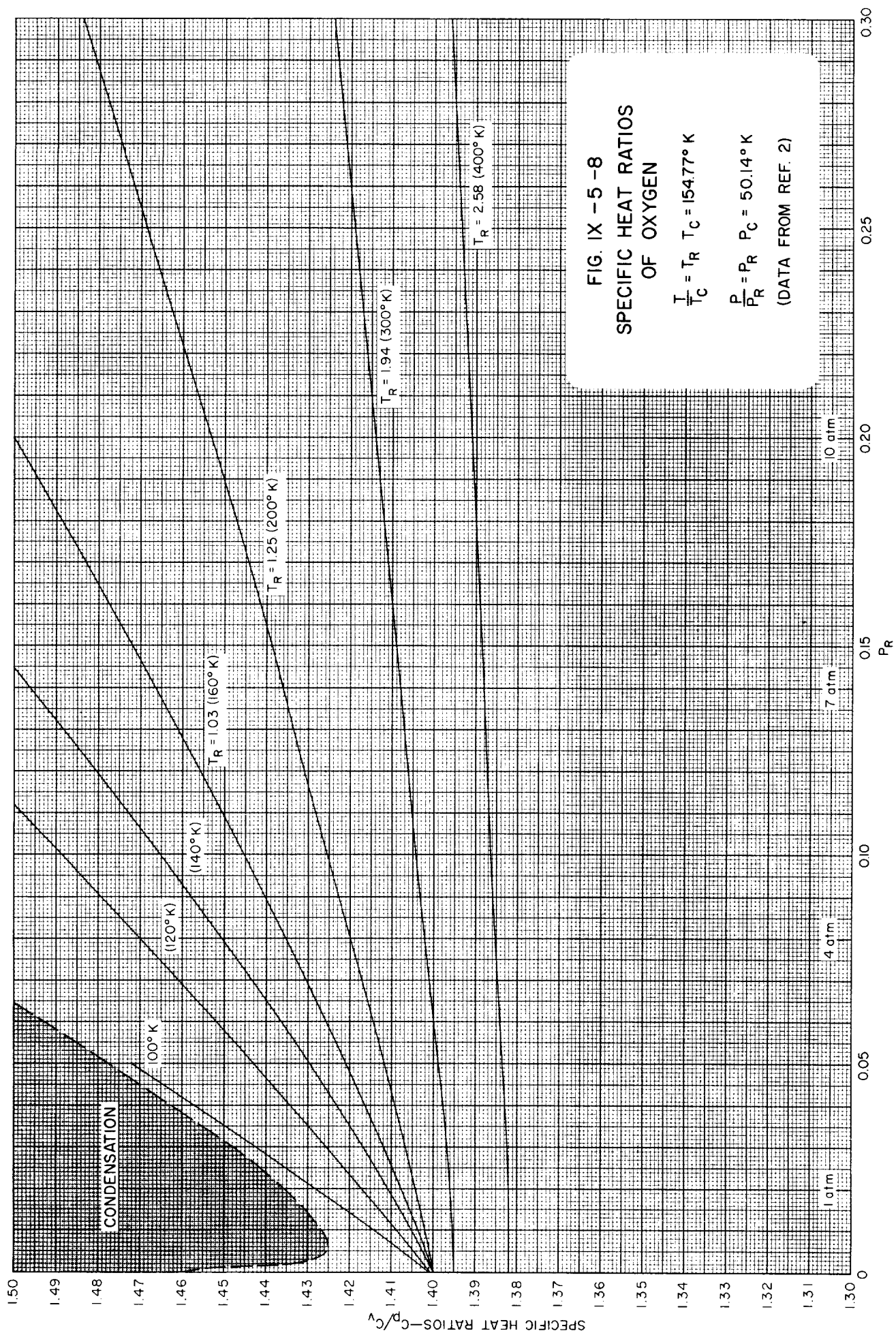


FIG. IX -5-9
THERMAL CONDUCTIVITY
OF GASEOUS OXYGEN

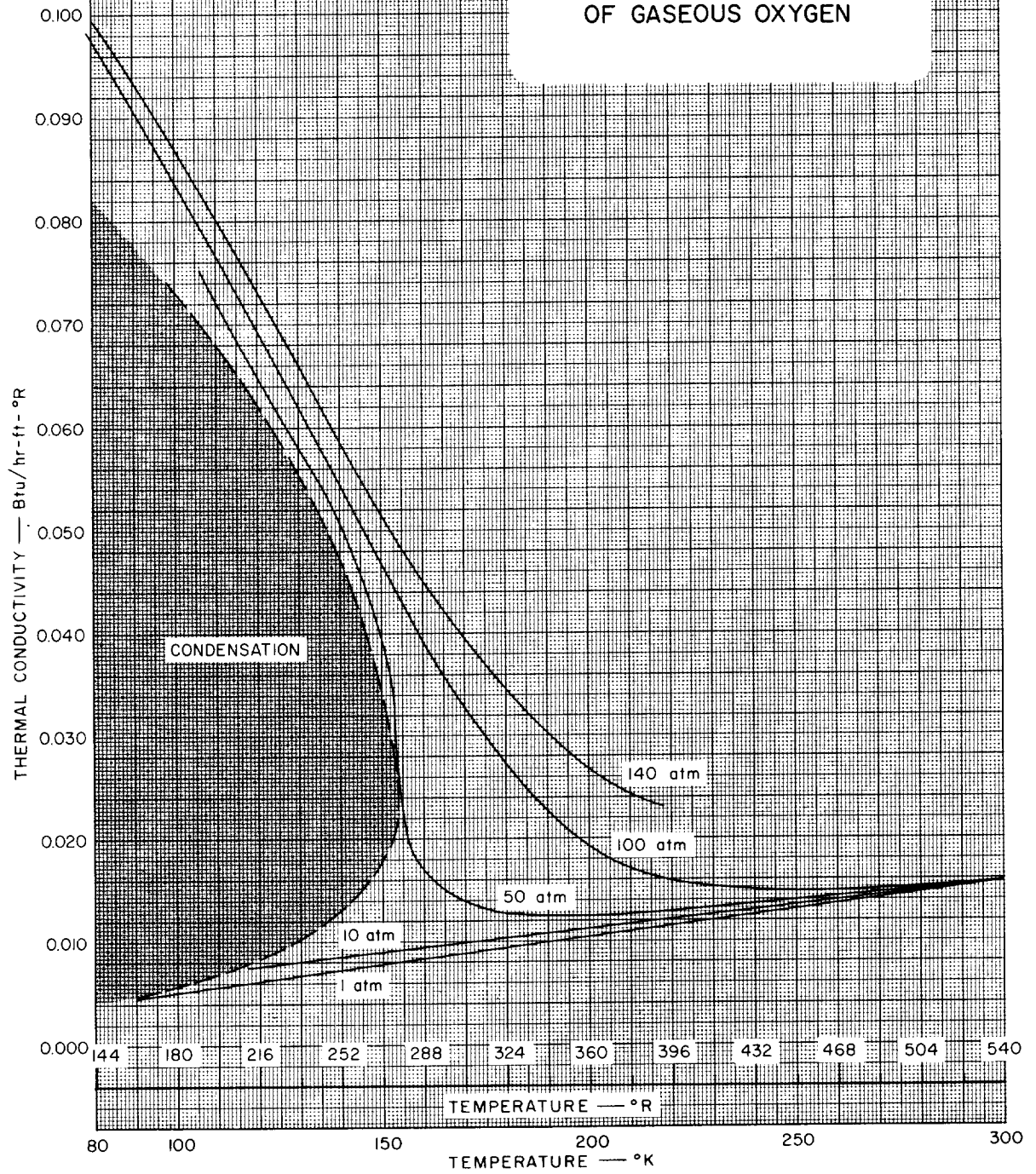
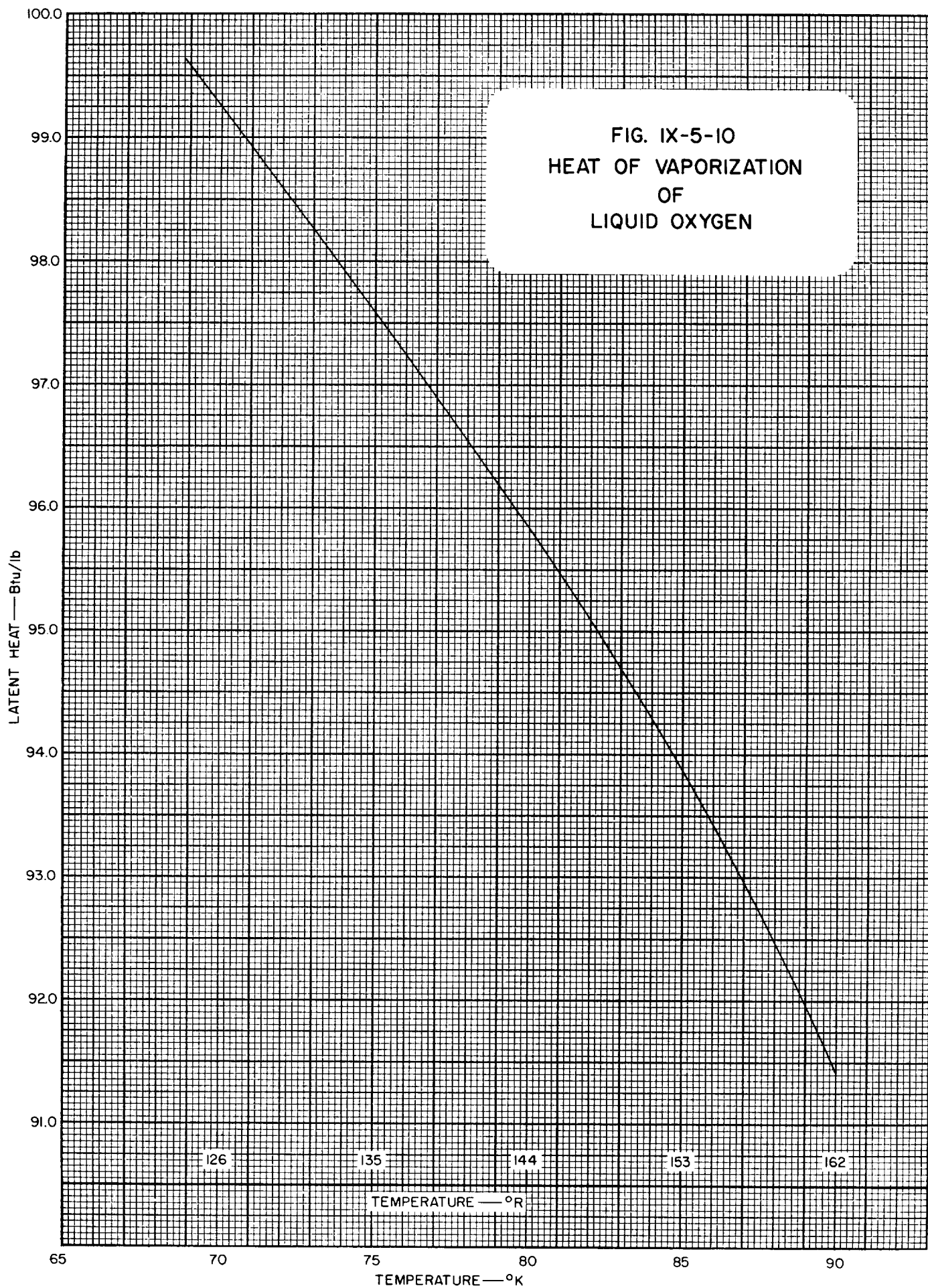
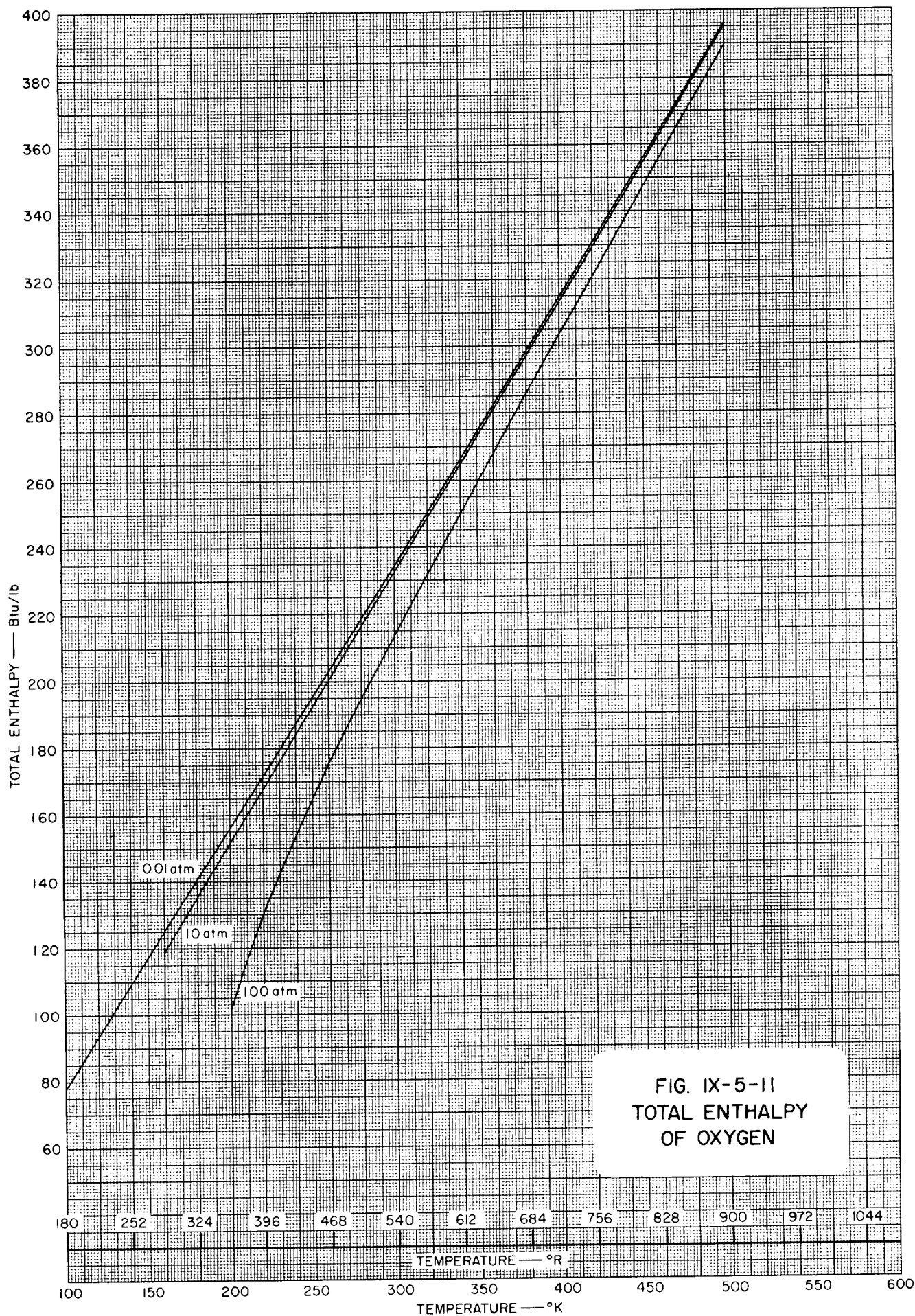
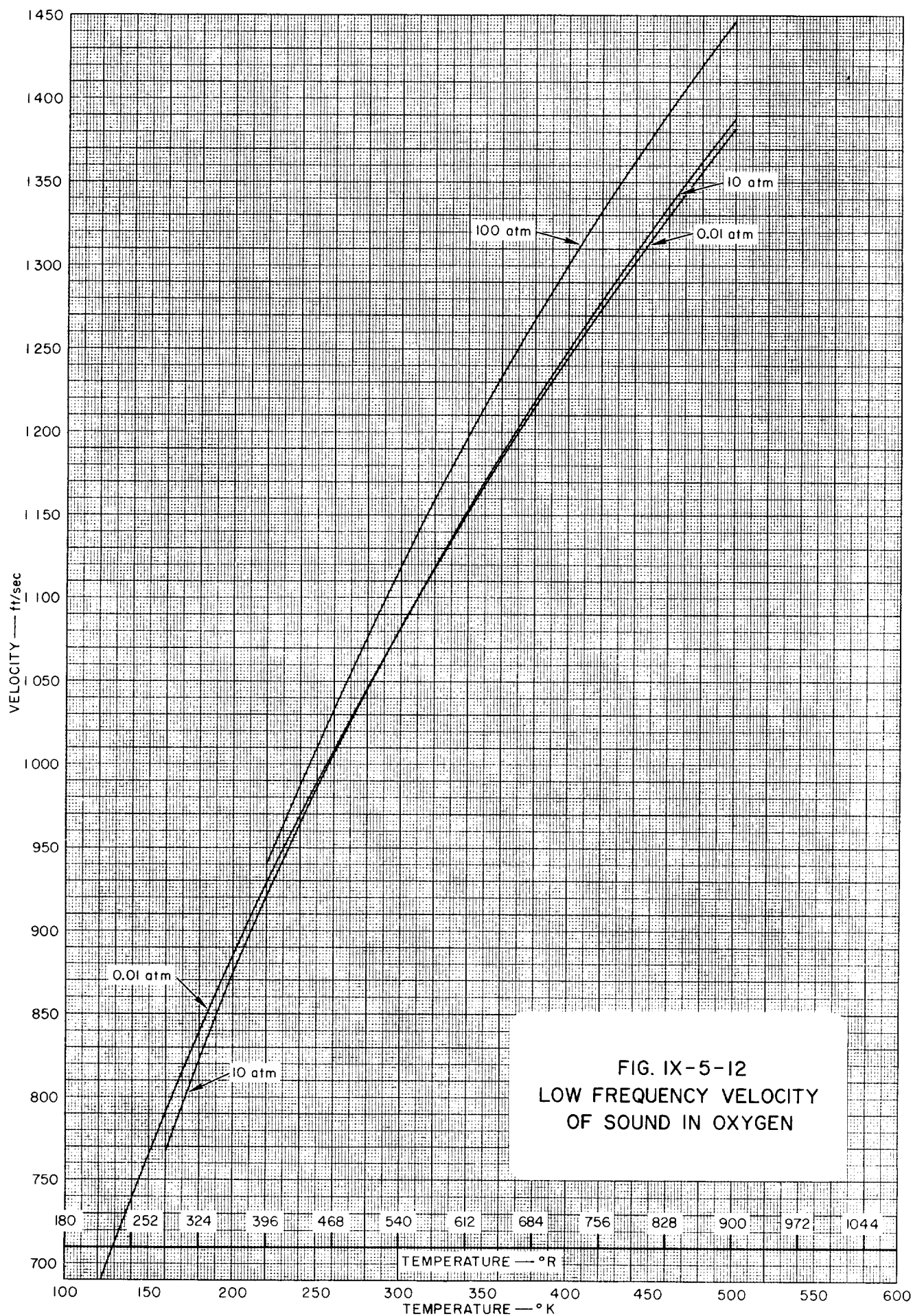


FIG. IX-5-10
HEAT OF VAPORIZATION
OF
LIQUID OXYGEN







IX-5 OXYGEN REFERENCES

1. Chelton, D. B., and Mann, D. B., *UCRL-3421*, May 15, 1956.
2. Hilsenrath, Joseph, *et al.*, *Tables of Thermodynamic and Transport Properties of Gases*, Pergamon Press, New York, 1960.
3. Johnson, V. A., (Ed.), *Properties of Materials at Low Temperatures, Phase I*, Pergamon Press, New York, 1961.

)

)

)

)

)

Table IX-6-1
GENERAL PROPERTIES OF CARBON DIOXIDE

PROPERTY	TEMPERATURE				PRESSURE			REF
	°C	°K	°F	°R	psia	atm	mm of Hg	
Melting Point	-56.6	216.6	- 69.9	389.9	1070.60	72.85		3
Sublimation Point	-78.50	194.65	-109.30	350.37				2
Triple Point	-56.6	216.5	- 69.9	389.8				2
Critical Temp.	31.05	304.20	87.89	547.56				2
Critical Press.								2
Mol. Wt. 44.01								3
Heat of Vaporization. See Table IX-6-7								
Heat of Fusion 45.3 cal/g or 81.54 Btu/lb								

Table IX-6-1.1
SOME VALUES OF THE GAS CONSTANT, R , FOR CARBON DIOXIDE
(See also Conversion Tables, Section I)

TEMPERATURE IN $^{\circ}\text{K}$				
Pressure Density	atm	kg/cm^2	mm of Hg	lb/in^2
g/cm^3	1.86450	1.92645	1417.02	27.4007
mole/cm^3	82.0567	84.7832	62363.1	1205.91
mole/liter	0.0820544	0.0847809	62.3613	1.20587
lb/ft^3	0.0298662	0.0308586	22.6983	0.438914
$\text{lb}/\text{mole}/\text{ft}^3$	1.31441	1.35808	998.952	19.3166
TEMPERATURE IN $^{\circ}\text{R}$				
Pressure Density	atm	kg/cm^2	mm of Hg	lb/in^2
g/cm^3	1.03583	1.07025	787.233	115.2226
mole/cm^3	45.5871	47.1018	34646.2	669.950
mole/liter	0.0455858	0.0471005	34.6452	0.669928
lb/ft^3	0.0165923	0.0171437	12.6102	0.243841
$\text{lb}/\text{mole}/\text{ft}^3$	0.730228	0.754489	554.973	10.7314

Table IX-6-2
VAPOR PRESSURE OF SOLID CARBON DIOXIDE (Ref. 1.2)

TEMPERATURE		VAPOR PRESSURE
$^{\circ}\text{K}$	$^{\circ}\text{R}$	atm
93	167.4	0.000000017
103	185.4	0.000000524
113	203.4	0.00000776
123	221.4	0.0000796
133	239.4	0.000567
140	252.0	0.00183
150	270.0	0.00834
160	288.0	0.03114
170	306.0	0.09863
180	324.0	0.27314
190	342.0	0.6770
200	360.0	1.5339
210	378.0	3.2341
216	388.8	4.9207

(See Figure IX-6-1)

Table IX-6-3
VAPOR PRESSURE OF LIQUID CARBON DIOXIDE (Ref. 2)

TEMPERATURE		VAPOR PRESSURE
°K	°R	atm
216	388.8	4.988
220	396.0	5.922
230	414.0	8.822
240	432.0	12.664
250	450.0	17.622
260	468.0	23.872
270	486.0	31.609
280	504.0	41.047
290	522.0	52.454
300	540.0	66.222
304	547.2	72.534

(See Figure IX-6-2)

Table IX-6-4
DENSITY OF CARBON DIOXIDE (Ref. 5)

TEMPERATURE		SATURATED LIQUID	SATURATED VAPOR
°K	°R	lb/ft ³	lb/ft ³
216.54	389.67	73.53 (tr. pt.)	0.861
222.04	399.67	72.27	1.085
227.59	409.67	70.96	1.335
233.15	419.67	69.61	1.636
238.71	429.67	68.21	1.985
244.26	439.67	66.76	2.395
249.82	449.67	65.25	2.880
255.37	459.67	63.65	3.450
260.93	469.67	61.96	4.115
266.48	479.67	60.13	4.890
272.04	489.67	58.16	5.800
277.59	499.67	55.98	6.935
283.15	509.67	53.56	8.303
288.71	519.67	50.80	10.07
294.26	529.67	47.35	12.44
299.82	539.67	42.36	16.44
304.15	547.47	28.96 (cryst.)	28.96 (c.p.)

(See Figure IX-6-3,
Figure IX-6-4)

Table IX-6-5
DENSITY OF GASEOUS CARBON DIOXIDE (Ref. 2)

TEMPERATURE		DENSITY—lb/ft ³		
°K	°R	1 atm	10 atm	100 atm
220	396	0.15437		
230	414	0.14736		
240	432	0.14100	1.58311	
250	450	0.13517	1.48450	
260	468	0.12983	1.40625	
270	486	0.12490	1.33886	
280	504	0.12034	1.27912	
290	522	0.11610	1.22531	
300	540	0.11216	1.17644	
310	558	0.10849	1.13201	
320	576	0.10506	1.09116	28.0766
330	594	0.10182	1.05351	20.4593
340	612	0.09880	1.01871	16.6777
350	630	0.09595	0.98625	14.7018
360	648	0.09326	0.95601	13.3479
370	666	0.09071	0.92775	12.3186
380	684	0.08831	0.90121	11.5003
390	702	0.08602	0.87628	10.8684
400	720	0.08385	0.85271	10.2648
410	738	0.08180	0.83049	9.7786
420	756	0.07984	0.80951	9.3528
430	774	0.07796	0.78964	8.9739
440	792	0.07619	0.77063	8.6345
450	810	0.07448	0.75274	8.3255
460	828	0.07285	0.73560	8.0437
470	846	0.07130	0.71927	7.7945
480	864	0.06980	0.70362	7.5666
490	882	0.06839	0.68868	7.3522
500	900	0.06700	0.67449	7.1506

(See Figure IX-6-5,
Figure IX-6-6)

Table IX-6-6
SURFACE TENSION OF LIQUID CARBON
DIOXIDE (Ref. 4)

TEMPERATURE		SURFACE TENSION
$^{\circ}\text{K}$	$^{\circ}\text{R}$	lb/ft
223	401	0.0319
228	410	0.0291
233	419	0.0263
238	428	0.0239
243	437	0.0218
248	446	0.0194
253	455	0.0173
258	464	0.0151
263	473	0.0131
268	482	0.0119
273	491	0.0093
278	500	0.0075
283	509	0.0058
288	518	0.0042
293	527	0.0029
298	536	0.0013
303	545	0.0002
308	555	0.0000 (Crit. Point)

(See Figure IX-6-7)

Table IX-6-7
HEAT OF VAPORIZATION OF CARBON DIOXIDE (Ref. 5)

TEMPERATURE		LATENT HEAT	TEMPERATURE		LATENT HEAT
$^{\circ}\text{K}$	$^{\circ}\text{R}$	Btu/lb	$^{\circ}\text{K}$	$^{\circ}\text{R}$	Btu/lb
216.54	389.77	149.6	272.04	489.67	102.4
222.04	399.67	145.8	277.59	499.67	95.04
227.59	409.67	141.9	283.15	509.67	86.56
233.15	419.67	137.8	288.71	519.67	76.45
238.71	429.67	133.7	294.26	529.67	63.90
244.26	439.67	129.5	299.82	539.67	45.30
249.82	449.67	124.9	304.15	547.47	0.00
255.37	459.67	120.0			
260.93	469.67	114.9			
266.48	479.67	109.0			

(See Figure IX-6-8)

Table IX-6-8
HEAT CAPACITIES OF GASEOUS CARBON DIOXIDE (Ref. 2)

TEMPERATURE		HEAT CAPACITY, C_p —Btu/lb-°R		
°K	°R	1 atm	10 atm	100 atm
220	396	0.1870		
230	414	0.1884		
240	432	0.1903	0.331019	
250	450	0.1923	0.2603	
260	468	0.1945	0.2314	
270	486	0.1968	0.21845	
280	504	0.1990	0.21856	
290	522	0.2013	0.2189	
300	540	0.2036	0.2194	
310	558	0.2059	0.2199	
320	576	0.2081	0.2206	0.9331
330	594	0.2104	0.2213	0.5166
340	612	0.2126	0.2225	0.4138
350	630	0.21467	0.2238	0.3912
360	648	0.2168	0.2251	0.3722
370	666	0.2189	0.2265	0.3528
380	684	0.2209	0.2279	0.3366
390	702	0.2230	0.2293	0.3240
400	720	0.2249	0.2308	0.31401
410	738	0.2268	0.2323	0.3058
420	756	0.2287	0.2337	0.29745
430	774	0.2305	0.2352	0.2933
440	792	0.2323	0.2367	0.2885
450	810	0.2341	0.2382	0.2832
460	828	0.2359	0.2397	0.2765
470	846	0.2376	0.2411	0.2725
480	864	0.2392	0.2426	0.2695
490	882	0.2409	0.2441	0.2693
500	900	0.2425	0.2455	0.2714

(See Figure IX-6-9)

Table IX-6-9

THERMAL CONDUCTIVITY OF GASEOUS CARBON DIOXIDE (Ref. 2)

TEMPERATURE		THERMAL CONDUCTIVITY	TEMPERATURE		THERMAL CONDUCTIVITY
$^{\circ}\text{K}$	$^{\circ}\text{R}$	Btu/hr-ft- $^{\circ}\text{R}$	$^{\circ}\text{K}$	$^{\circ}\text{R}$	Btu/hr-ft- $^{\circ}\text{R}$
180	324	0.00477	350	630	0.01182
190	342	0.00513	360	648	0.01231
200	360	0.00554	370	666	0.01276
210	378	0.00588	380	684	0.01325
220	396	0.00625	390	702	0.01374
230	414	0.00665	400	720	0.01422
240	432	0.00704	410	738	0.01473
250	450	0.00745	420	756	0.01523
260	468	0.00786	430	774	0.01571
270	486	0.00827	440	792	0.01623
280	504	0.00870	450	810	0.01673
290	522	0.00914	460	828	0.01726
300	540	0.00958	470	846	0.01777
310	558	0.01001	480	864	0.01830
320	576	0.01044	490	882	0.01883
330	594	0.01090	500	900	0.01937
340	612	0.01137			

(See Figure IX-6-12)

Table IX-6-10
TOTAL ENTHALPY OF CARBON DIOXIDE (Ref. 2)

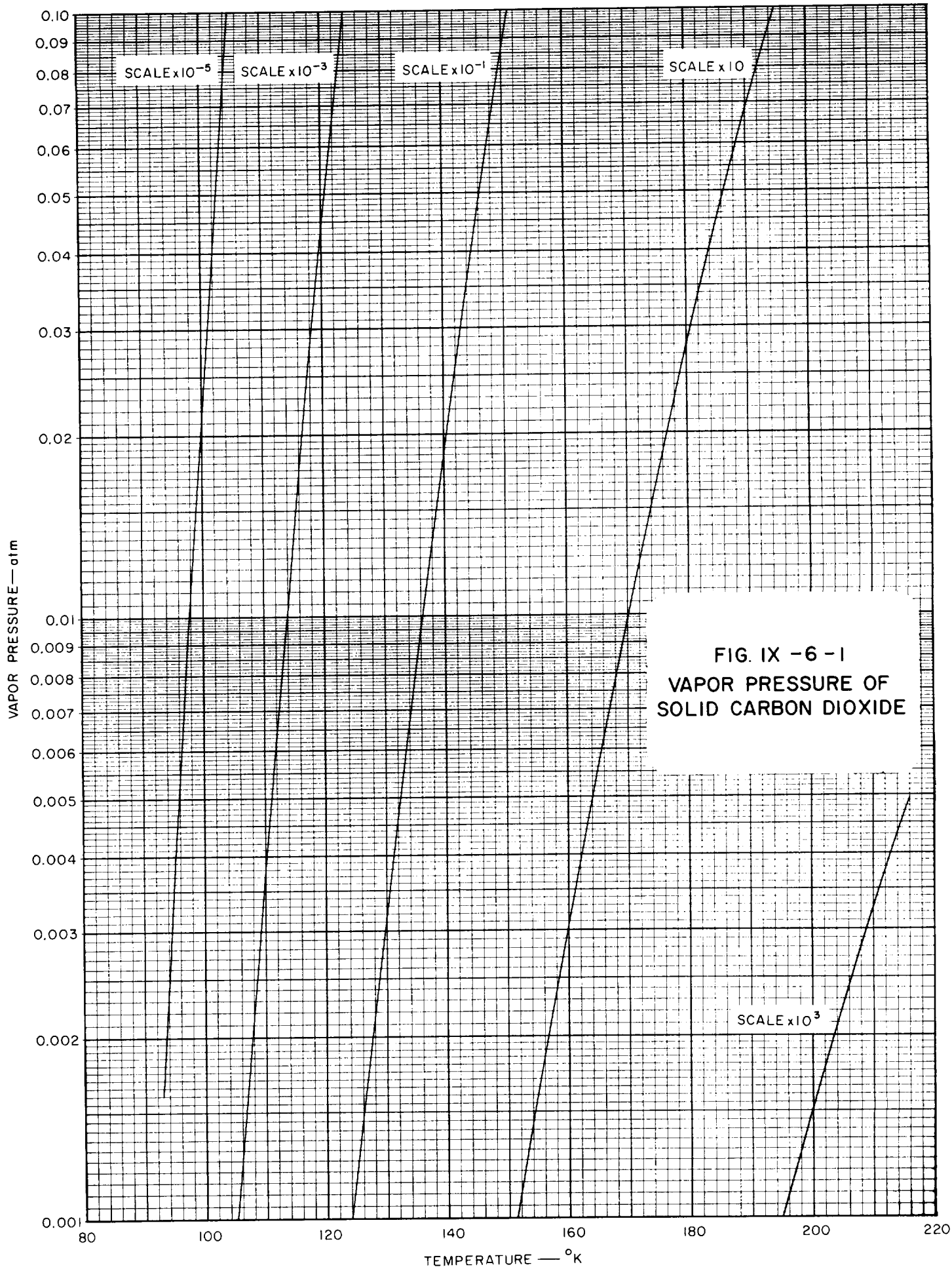
TEMPERATURE		TOTAL ENTHALPY—Btu/lb				
°K	°R	0.01 atm	1.0 atm	10 atm	70 atm	100 atm
200	360	58.136				
220	396	64.557	63.70			
240	432	71.168	70.49	62.52		
260	468	77.975	77.41	72.15		
280	504	84.971	84.49	80.09		
300	540	92.155	91.74	87.97		
320	576	99.514	99.15	95.89	67.7	46.4
340	612	107.04	106.7	103.9	81.4	67.2
360	648	114.74	114.5	112.0	92.7	81.2
380	684	122.59	122.3	120.1	103.4	94.1
400	720	130.59	130.4	128.4	113.8	105.9
420	756	138.74	138.5	137.3	123.8	116.9
440	792	147.02	146.8	145.7	133.6	127.4
460	828	155.43	155.3	154.3	143.2	137.6
480	864	163.97	163.8	162.9	152.8	147.4
500	900	172.63	172.5	171.7	162.3	157.1

(See Figure IX-6-13)

Table IX-6-11
LOW FREQUENCY VELOCITY OF SOUND IN CARBON DIOXIDE (Ref. 2)

TEMPERATURE		VELOCITY—Ft/sec				
°K	°R	0.01 atm	1.0 atm	10 atm	70 atm	100 atm
200	360	736.6				
220	396	768.7	762.			
240	432	799.0	794.	728.		
260	468	828.0	824.	782.		
280	504	855.76	852.5	825.		
300	540	882.58	880.3	856.7		
320	576	908.46	906.4	887.0	719.	554.
340	612	933.51	931.7	916.6	827.	782.
360	648	957.88	956.2	944.4	886.2	828.
380	684	981.65	980.6	970.5	925.0	891.3
400	720	1004.8	1004.	995.8	952.8	936.8
420	756	1027.4	1027.	1020.	987.4	982.3
440	792	1049.5	1049.	1044.	1019.	1022.
460	828	1071.1	1071.	1067.	1050.	1054.
480	864	1092.4	1092.	1089.	1078.	1084.
500	900	1113.1	1113.	1110.	1106.	1115.

(See Figure IX-6-14)



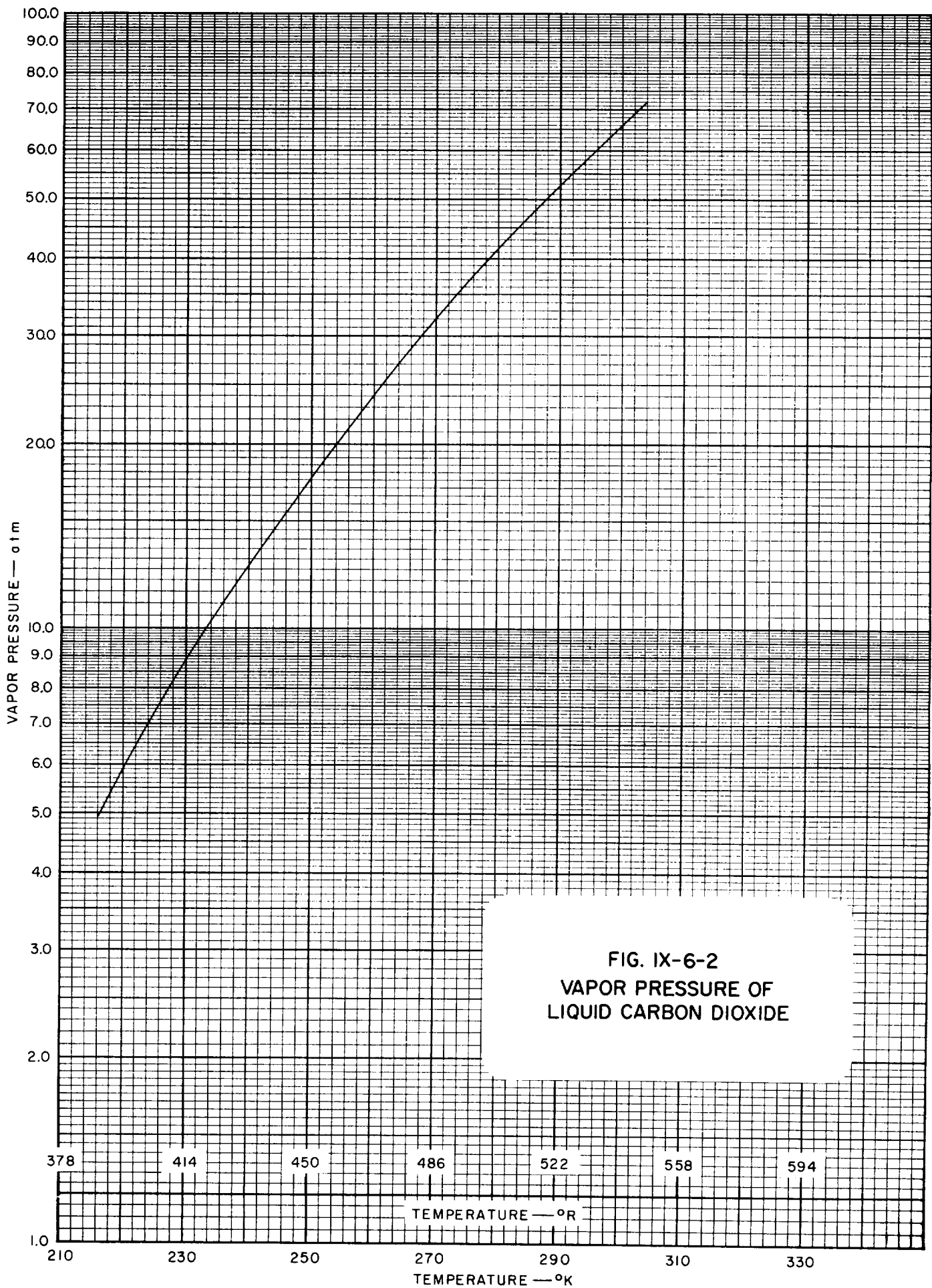


FIG. IX-6-3
DENSITY OF SATURATED LIQUID
CARBON DIOXIDE

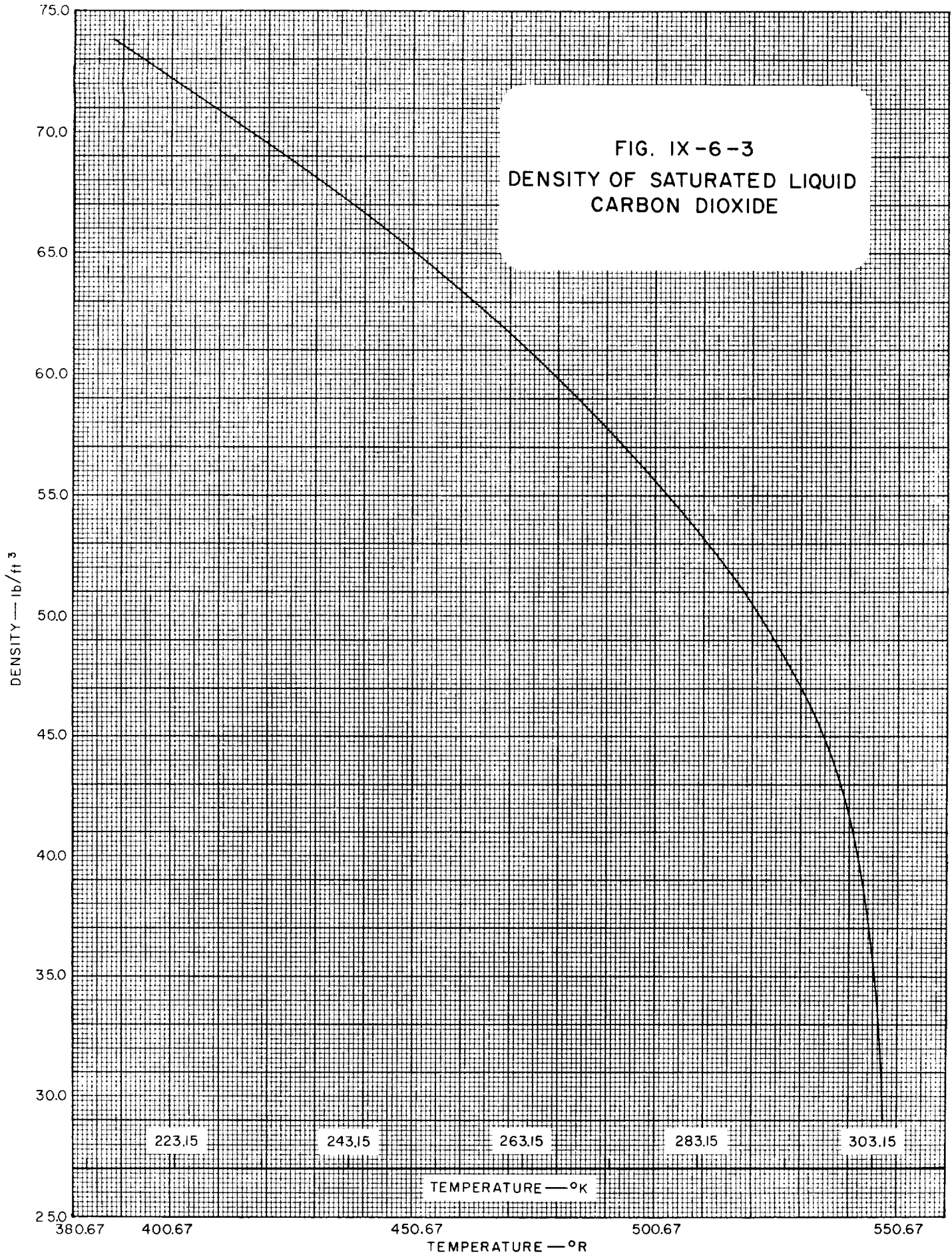


FIG. IX-6-4
DENSITY OF SATURATED VAPOR
OF CARBON DIOXIDE

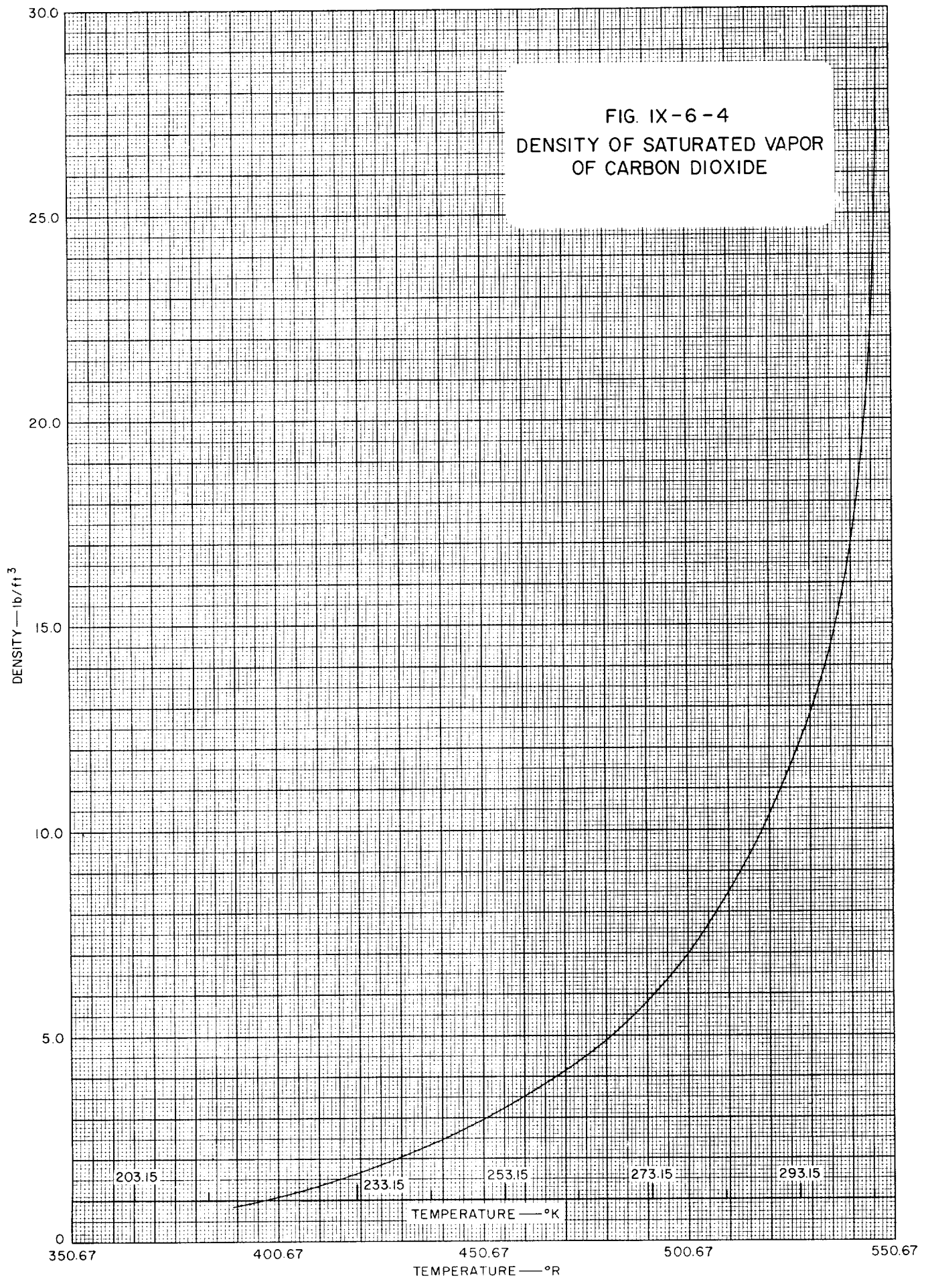
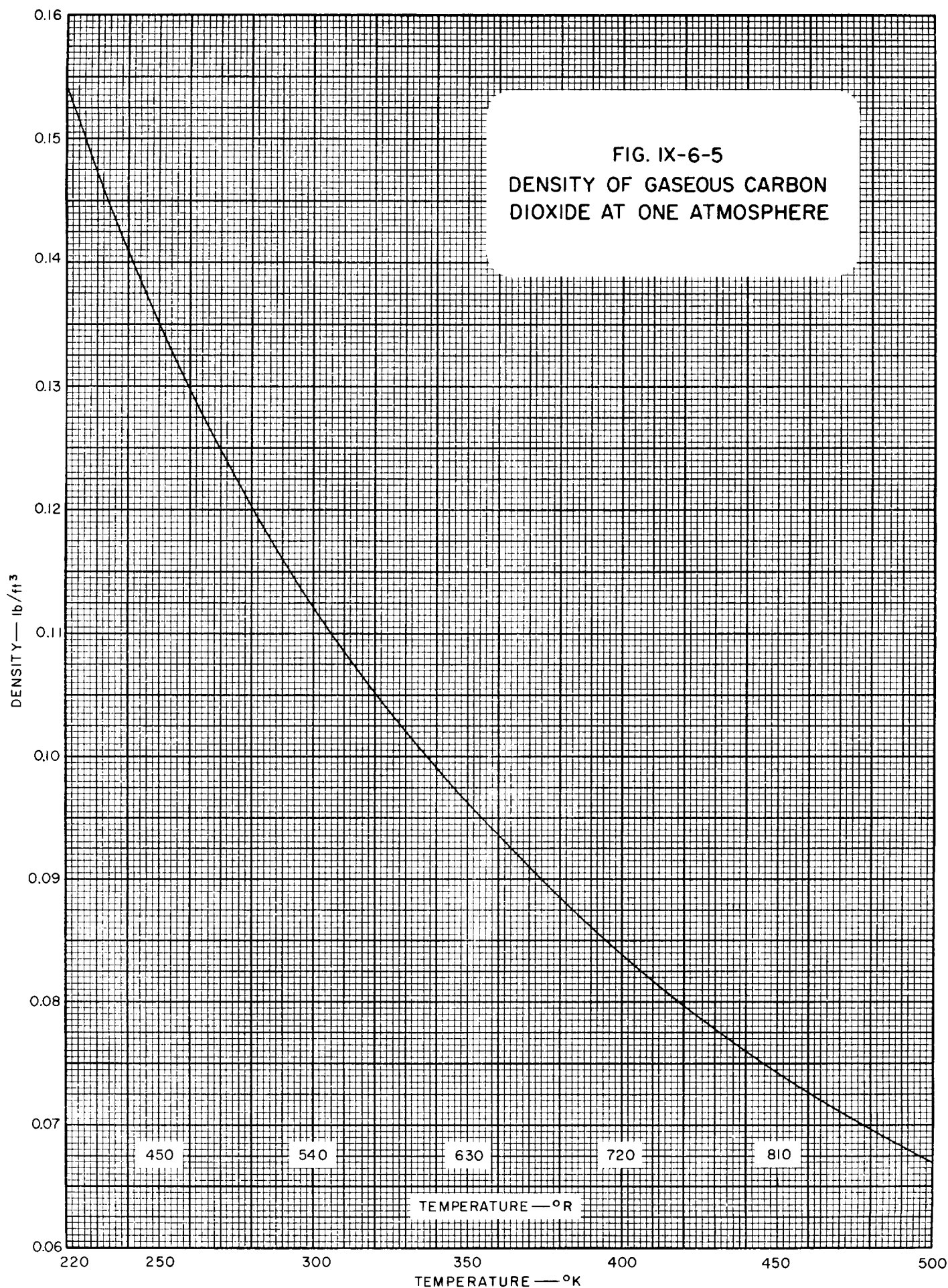


FIG. IX-6-5
DENSITY OF GASEOUS CARBON
DIOXIDE AT ONE ATMOSPHERE



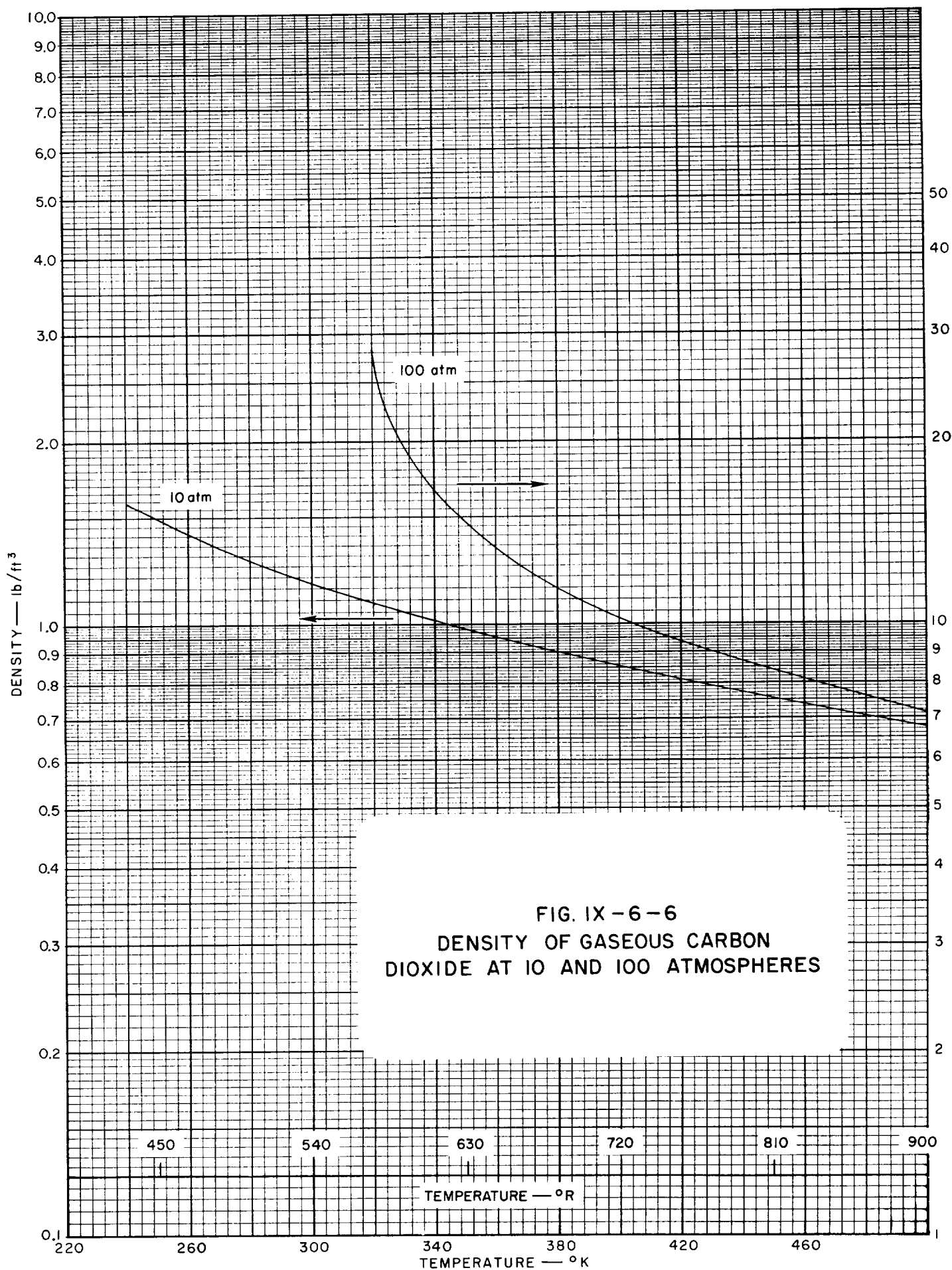


FIG. IX-6-7
SURFACE TENSION OF
LIQUID CARBON DIOXIDE

SURFACE TENSION—lb/ft²

TEMPERATURE—°R

TEMPERATURE—°K

378

450

540

630

210

250

300

350

0

0.005

0.010

0.015

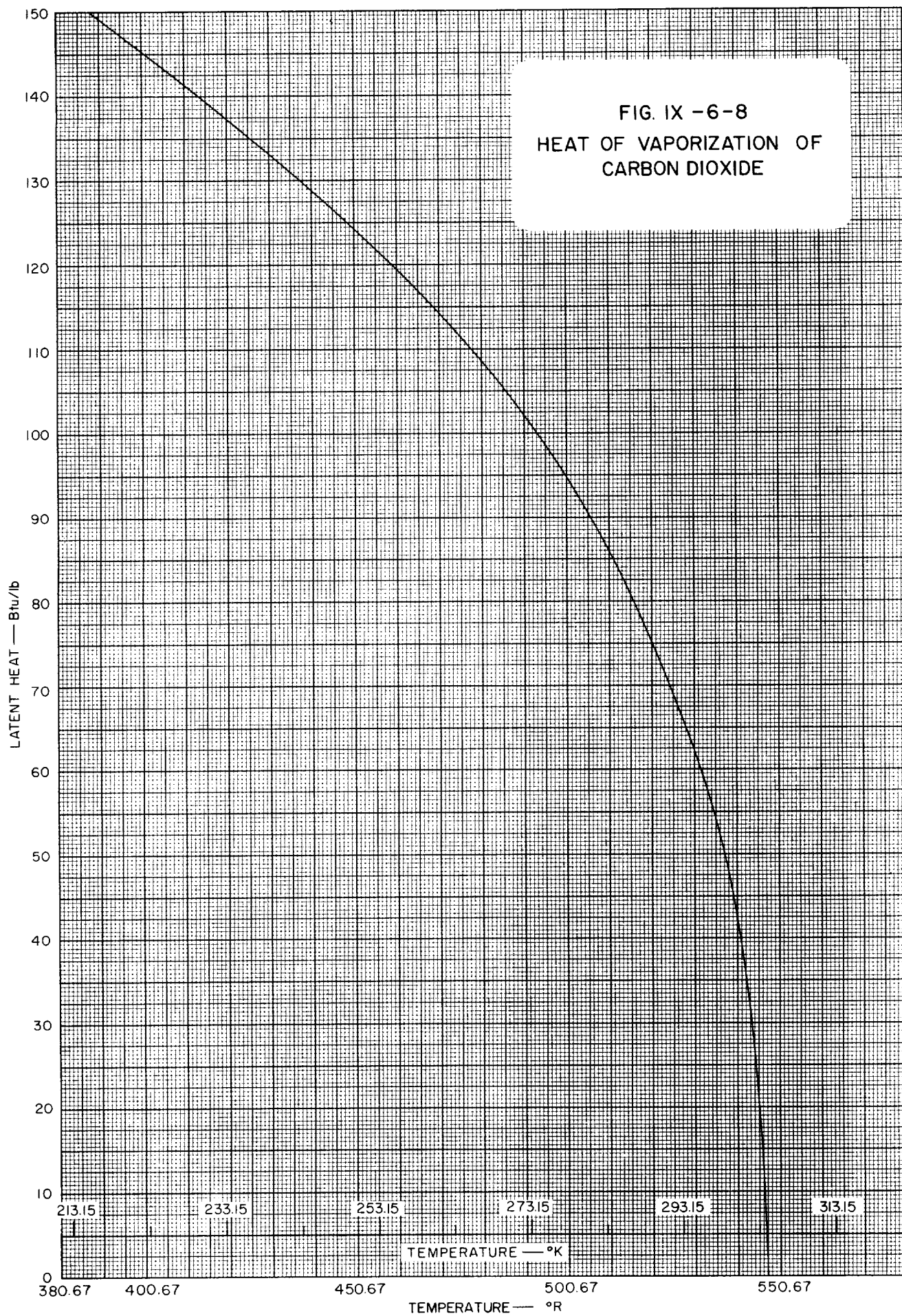
0.020

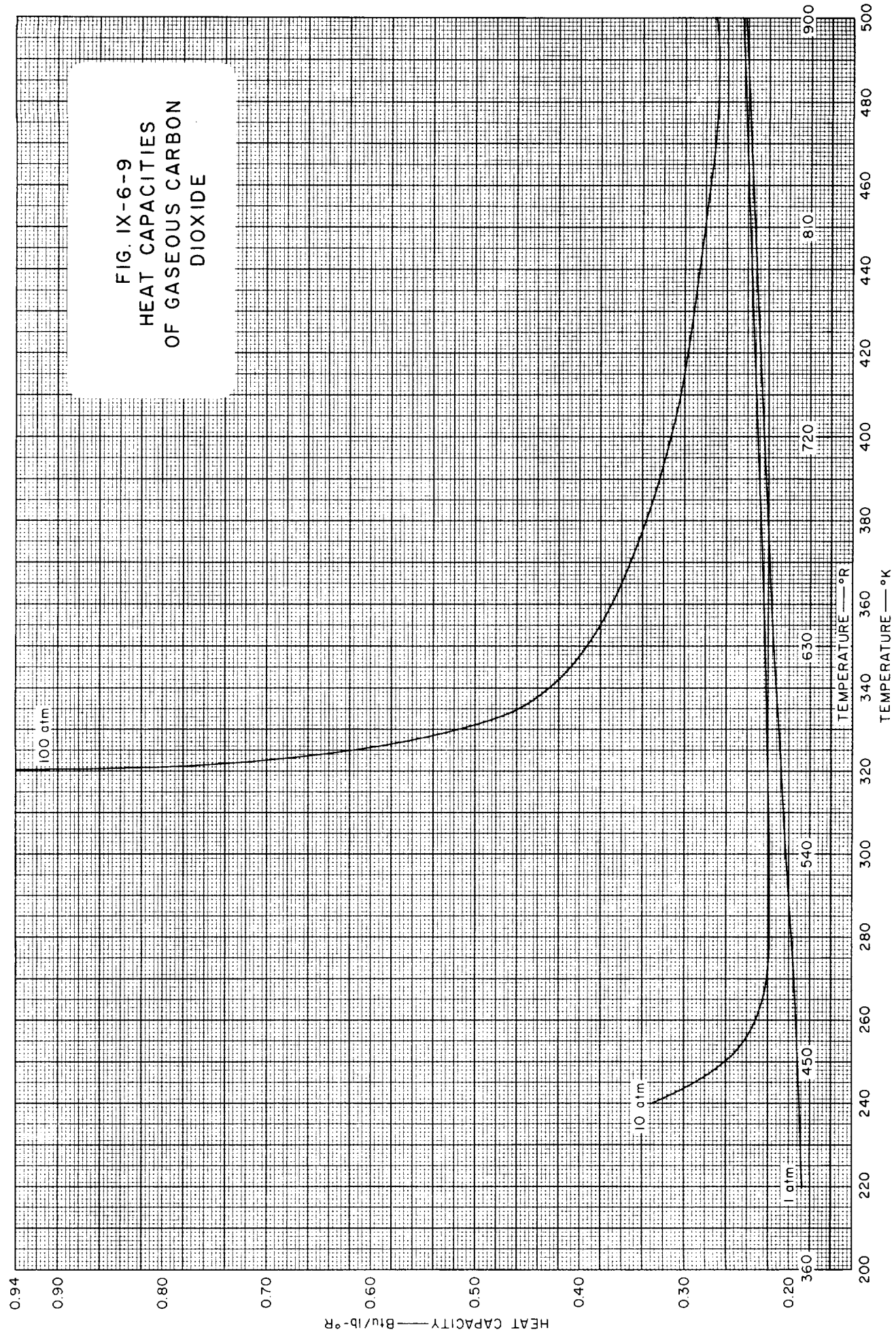
0.025

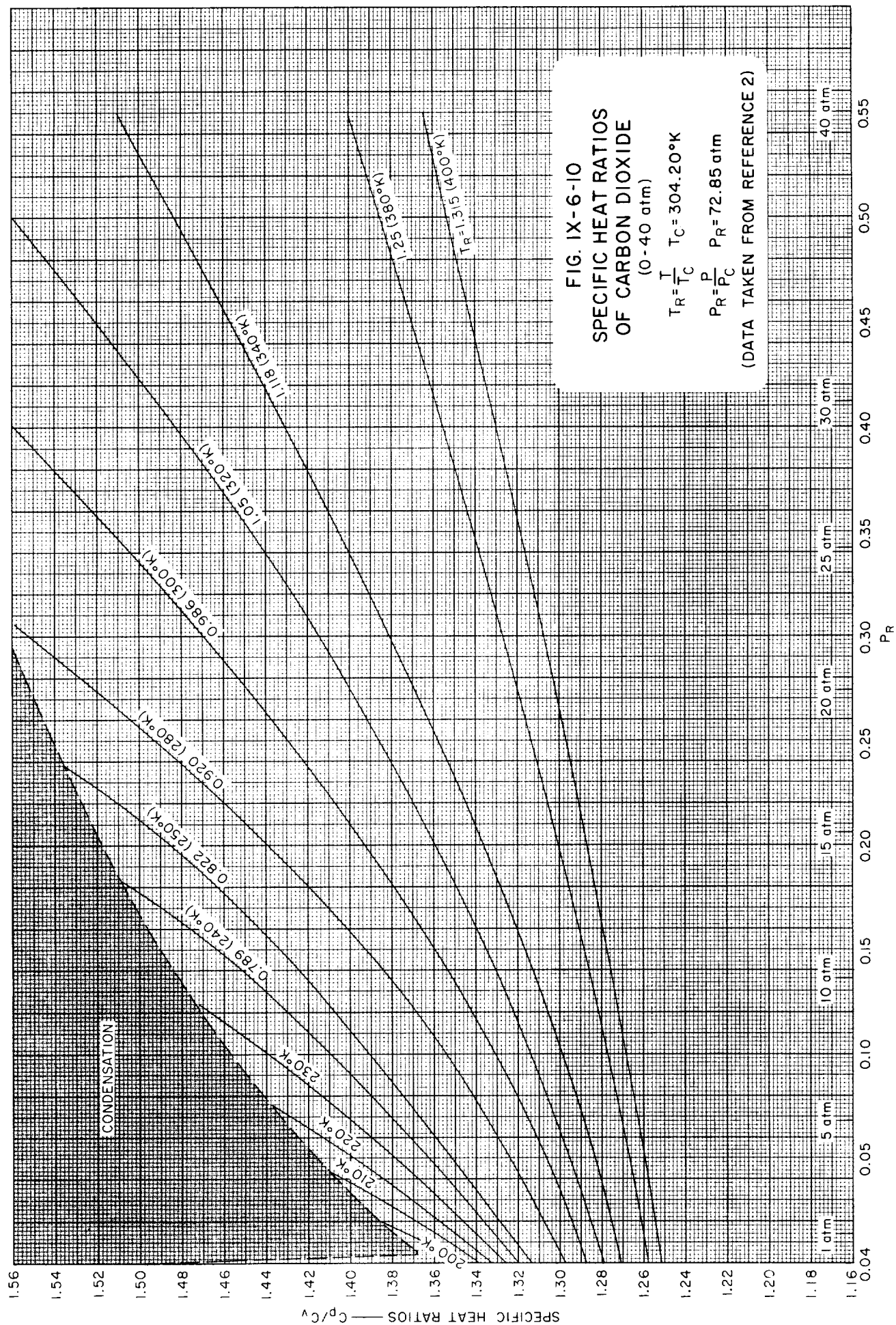
0.030

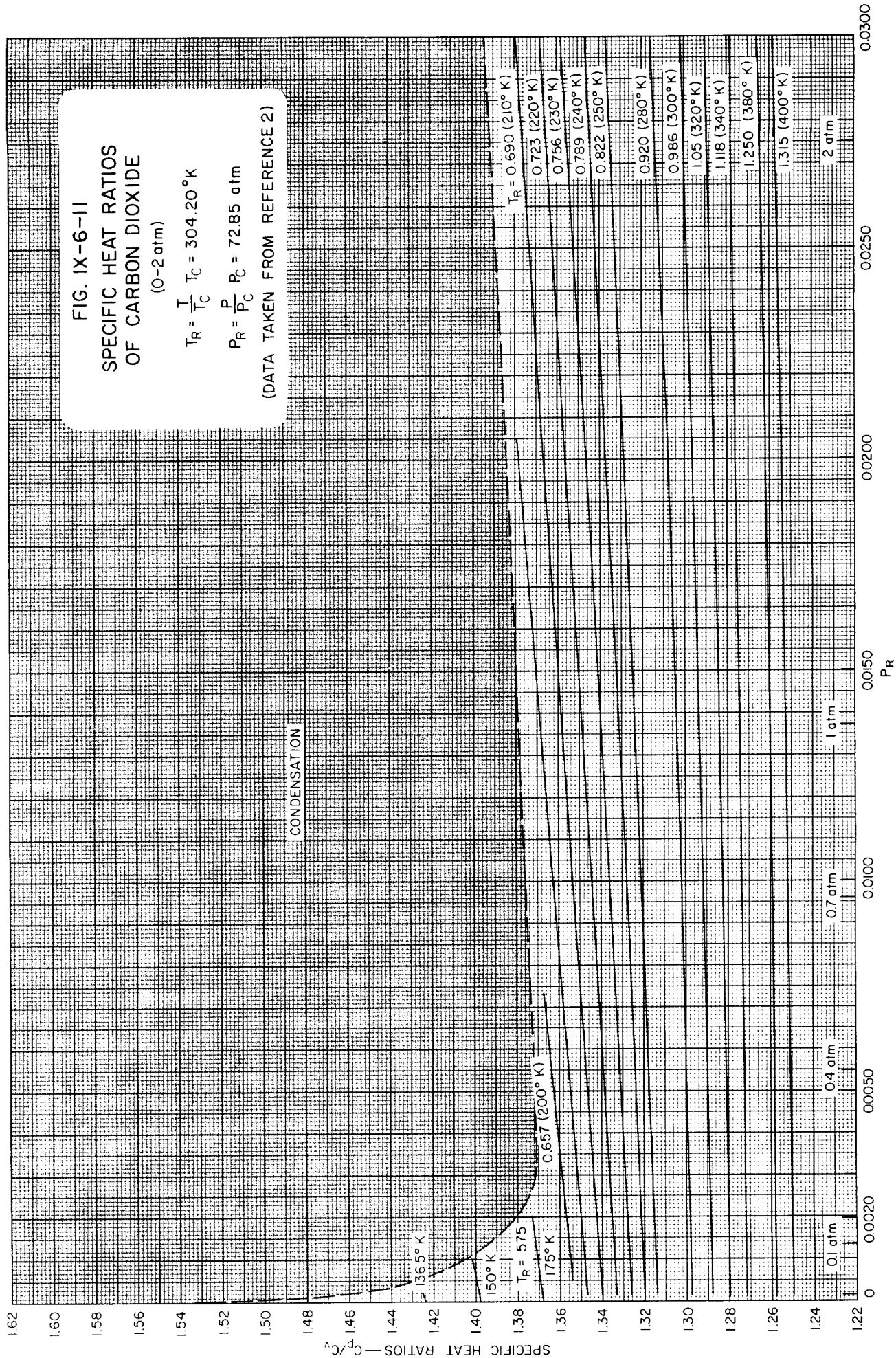
0.035

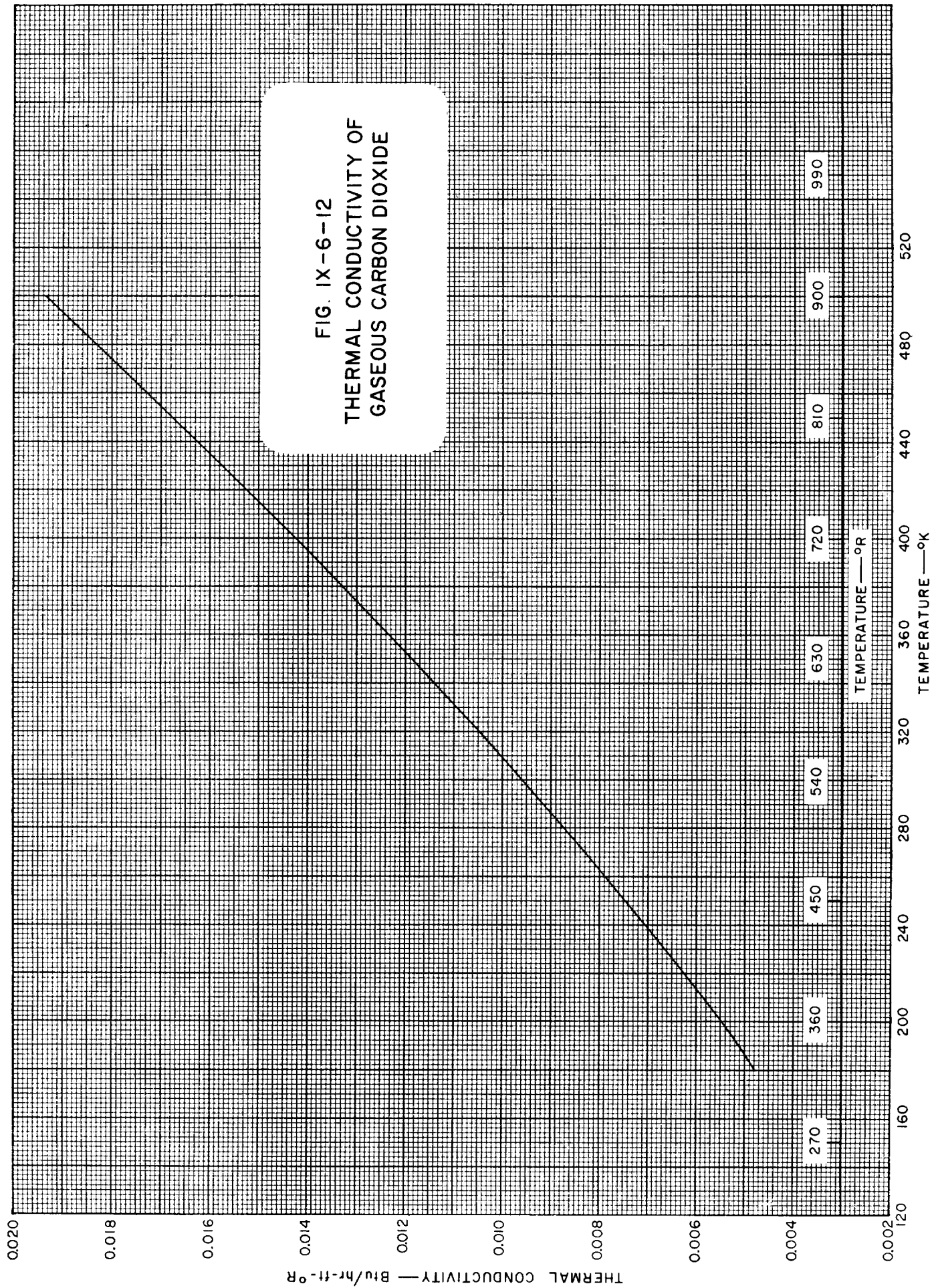
FIG. IX -6-8
HEAT OF VAPORIZATION OF
CARBON DIOXIDE











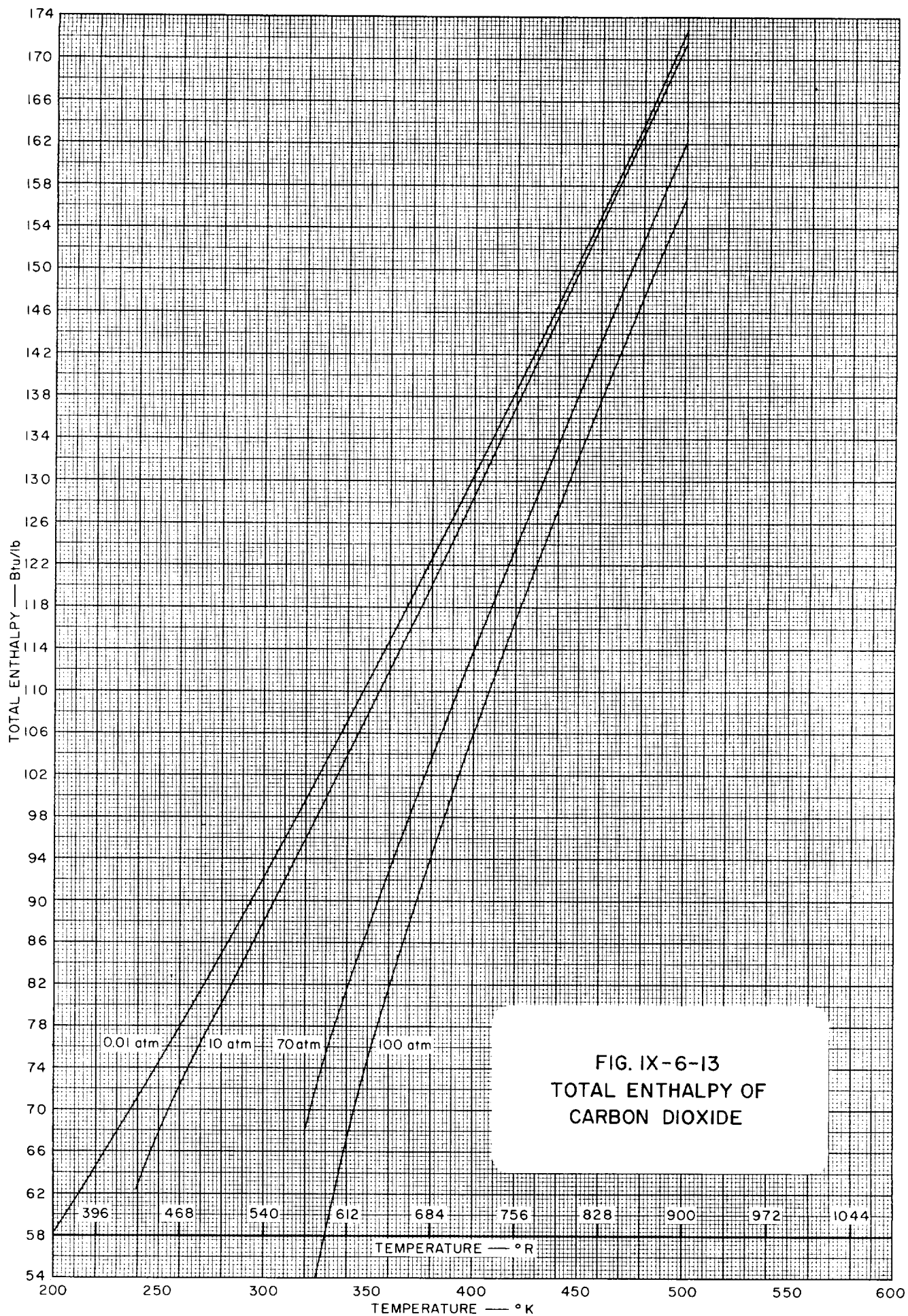
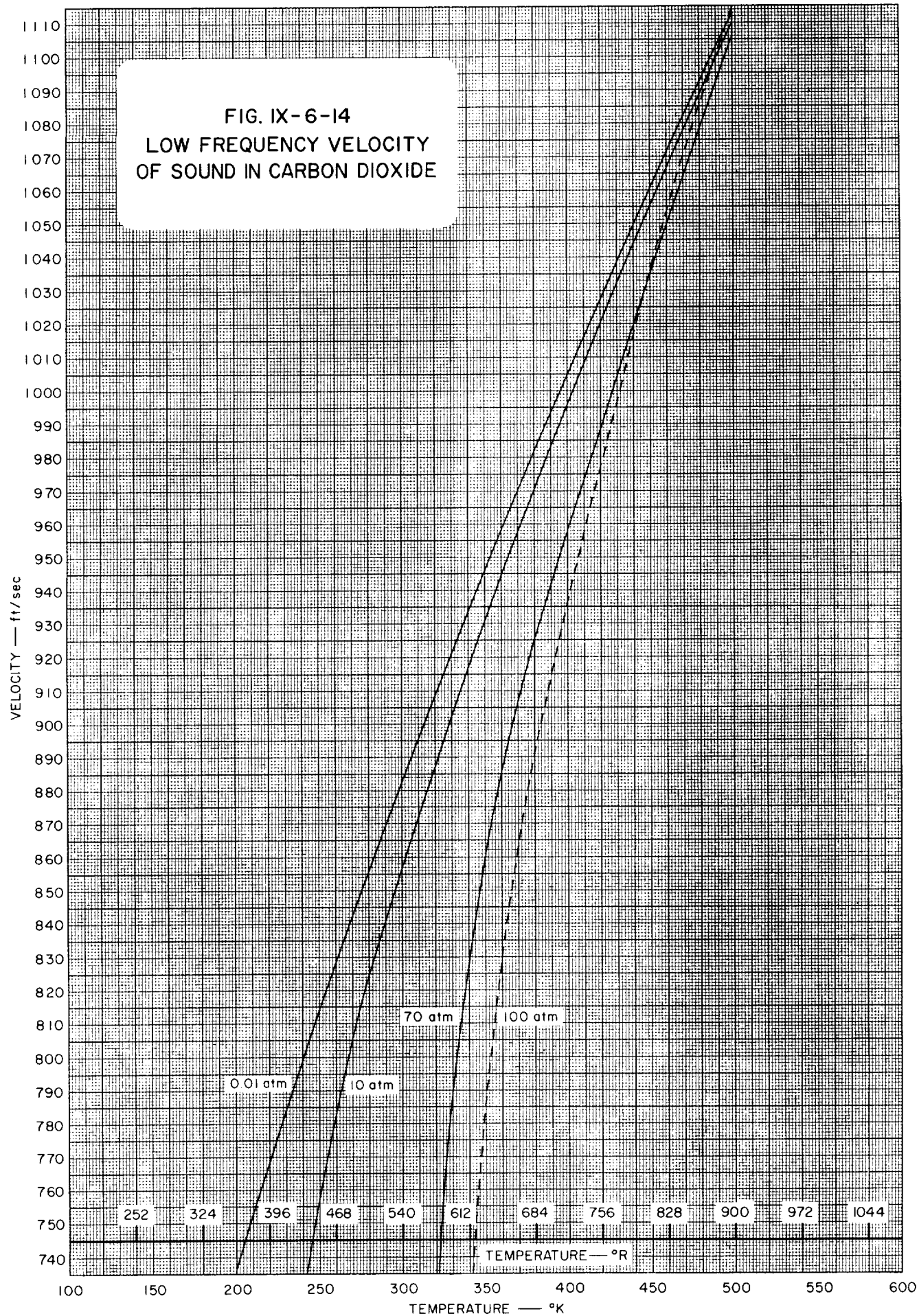


FIG. IX-6-14
LOW FREQUENCY VELOCITY
OF SOUND IN CARBON DIOXIDE



IX-6 CARBON DIOXIDE REFERENCES

1. *Handbook of Chemistry and Physics*, 42nd Edition, Chemical Rubber Publishing Company, Cleveland, Ohio, 1962-63.
2. Hilsenrath, Joseph, *et al.*, *Tables of Thermodynamic and Transport Properties of Gases*, Pergamon Press, New York, 1960.
3. Lange, N. A., *Handbook of Chemistry*, 10th Edition, Handbook Publishers, Inc., Sandusky, Ohio, 1961.
4. Quinn, E. L., *J. Am. Chem. Soc.*, **49**, 2704 (1927).
5. Quinn, E. L., and Jones, C. L., *Carbon Dioxide*, Reinhold Publishing Corp., New York, 1936.

)

)

)

)

)

Table IX-7-1
GENERAL PROPERTIES OF PERCHLORYL FLUORIDE

PROPERTY	TEMPERATURE				PRESSURE			REF
	°C	°K	°F	°R	psia	atm	mm of Hg	
Melting Point		127.						4
Boiling Point	- 46.67	226.48	- 52.87	406.80				5
Triple Point		125.41						5
Critical Temp.	95.2	368.3	203.3	662.9				3
Critical Press.					778.9	53.0		3
Mol. Wt. 102.457								
Heat of Vaporization 45.08 cal/g or 81.14 Btu/lb @ 226.48°K								5
Heat of Fusion 8.943 cal/g or 16.10 Btu/lb								5
Surface Tension 24.05 dynes/cm at 198°K								4

Table IX-7-1.1
SOME VALUES OF THE GAS CONSTANT, *R*, FOR PERCHLORYLFLUORIDE
(See also Conversion Tables, Section I)

TEMPERATURE IN °K				
Pressure Density	atm	kg/cm ²	mm of Hg	lb/in ²
g/cm ³	0.800889	0.827500	608.676	11.7699
mole/cm ³	82.0567	84.7832	62363.1	1205.91
mole/liter	0.0820544	0.0847809	62.3613	1.20587
lb/ft ³	0.0128289	0.0132551	9.74996	0.188534
lb/mole/ft ³	1.31441	1.35808	998.952	19.3166
TEMPERATURE IN °R				
Pressure Density	atm	kg/cm ²	mm of Hg	lb/in ²
g/cm ³	0.444938	0.459722	338.153	6.53884
mole/cm ³	45.5871	47.1018	34646.2	669.950
mole/liter	0.0455858	0.0471005	34.6452	0.669928
lb/ft ³	0.00712717	0.00736396	5.41664	0.104562
lb/mole/ft ³	0.730228	0.754489	554.973	10.7314

Table IX-7-2

VAPOR PRESSURE OF LIQUID PERCHLORYL FLUORIDE (Ref. 3)

TEMPERATURE		VAPOR PRESSURE		TEMPERATURE		VAPOR PRESSURE	
$^{\circ}\text{K}$	$^{\circ}\text{R}$	mm Hg	psia	$^{\circ}\text{K}$	$^{\circ}\text{R}$	atm	psia
152.81	273.78	3.08	0.0596	227.09	408.76	1.033	15.18
157.67	283.81	5.53	0.1069	232.04	417.67	1.290	18.96
162.58	292.64	9.31	0.1801	237.14	426.85	1.606	23.60
167.50	301.50	14.97	0.2895	242.09	435.76	1.969	28.94
172.33	310.19	23.19	0.4484	251.99	453.58	2.891	42.49
177.40	319.32	35.73	0.6909	262.07	471.73	4.048	59.49
182.33	328.19	53.05	1.026	272.04	489.67	5.748	84.47
187.31	337.16	77.13	1.491	282.10	507.78	7.789	114.47
192.25	346.05	109.48	2.226	292.13	525.83	10.170	149.46
197.19	354.94	151.77	2.935	292.24	526.03	10.177	149.56
202.11	363.80	207.50	4.0182	302.17	543.91	13.361	196.35
207.19	372.94	279.66	5.408	312.21	561.98	17.034	250.33
212.20	381.96	370.73	7.169	322.33	580.19	21.388	314.32
217.73	391.91	481.49	9.311	332.41	598.34	26.490	389.30
222.13	399.83	619.33	11.976	342.50	616.50	32.782	481.76
				352.66	634.79	39.959	587.24
				362.92	653.26	48.259	709.21

(See Figure IX-7-1)

Table IX-7-3
DENSITY OF LIQUID PERCHLORYL FLUORIDE (Ref. 1, 3)

TEMPERATURE		DENSITY	TEMPERATURE		DENSITY
°K	°R	lb/ft ³	°K	°R	lb/ft ³
131.31	236.36	124.2	273.15	491.67	95.52
144.46	260.03	121.7	299.55	539.19	88.65
149.58	269.24	120.8	314.45	566.01	84.28
154.79	278.62	119.9	321.35	578.43	81.78
159.84	287.71	118.9	327.15	588.87	79.29
164.66	296.39	118.1	333.75	600.75	76.79
169.62	305.32	117.2	343.45	618.21	72.42
174.50	314.10	116.2	348.15	626.67	70.23
179.52	323.14	115.2	354.55	638.19	66.18
184.54	332.17	114.3	358.15	644.67	63.68
189.50	341.10	113.4	362.95	653.31	59.06
194.44	349.99	112.4	366.05	658.89	54.50
199.38	358.88	111.5			
204.34	367.81	110.5			
209.21	376.58	109.3			
214.21	385.58	108.2			
219.15	394.47	107.3			
224.11	403.40	106.2			
229.23	412.61	105.1			
234.22	421.60	104.1			

(See Figure IX-7-2)

Table IX-7-4
DENSITY OF SATURATED VAPOR
OF PERCHLORYL FLUORIDE
(Ref. 1)

TEMPERATURE		DENSITY
°K	°R	lb/ft ³
273.15	491.67	2.04
299.55	539.19	3.91
314.45	566.01	6.45
321.35	578.43	6.92
327.15	588.87	7.99
333.75	600.75	9.35
343.45	618.21	12.05
348.15	626.67	13.58
354.55	638.19	16.36
358.15	644.67	18.23
362.95	653.31	21.76
366.05	658.89	25.57

(See Figure IX-7-3)

Table IX-7-5
VISCOSITY OF LIQUID PERCHLORYL FLUORIDE (Ref. 6)

TEMPERATURE		ABSOLUTE VISCOSITY	TEMPERATURE		ABSOLUTE VISCOSITY
^o K	^o R	centipoises	^o K	^o R	centipoises
190.15	342.27	0.630	270.15	486.27	0.240
200.15	360.27	0.549	280.15	504.27	0.217
210.15	378.27	0.482	290.15	522.27	0.197
220.15	396.27	0.425	300.15	540.27	0.178
230.15	414.27	0.377	310.15	558.27	0.163
240.15	432.27	0.335	320.15	576.27	0.150
250.15	450.27	0.299	330.15	594.27	0.138
260.15	468.27	0.273			

(See Figure IX-7-4)

Table IX-7-6
HEAT CAPACITY OF SATURATED LIQUID PERCHLORYL FLUORIDE (Ref. 4)

TEMPERATURE		HEAT CAPACITY, C _p	TEMPERATURE		HEAT CAPACITY, C _p
^o K	^o R	Btu/lb- ^o R	^o K	^o R	Btu/lb- ^o R
226.09	406.96	0.2245	278.68	501.64	0.2537
227.58	409.64	0.2267	285.11	513.20	0.2547
233.84	420.91	0.2306	292.01	525.62	0.2602
238.72	429.70	0.2323	298.86	537.95	0.2653
240.25	432.45	0.2346	306.00	550.80	0.2696
243.86	438.95	0.2339	311.41	560.54	0.2769
249.42	448.96	0.2367	318.16	572.69	0.2835
253.74	456.73	0.2406	325.40	585.72	0.2925
255.12	459.22	0.2401	332.88	599.18	0.3023
260.19	468.34	0.2421	340.87	613.57	0.3287
260.76	469.37	0.2424	344.99	619.37	0.3491
261.23	470.21	0.2432	347.99	626.38	0.3614
265.09	477.16	0.2447	356.49	641.68	0.4391
272.31	490.16	0.2492	357.94	644.29	0.4597
277.33	499.19	0.2526	360.18	648.32	0.6106
278.69	501.64	0.2532			

(See Figure IX-7-5)

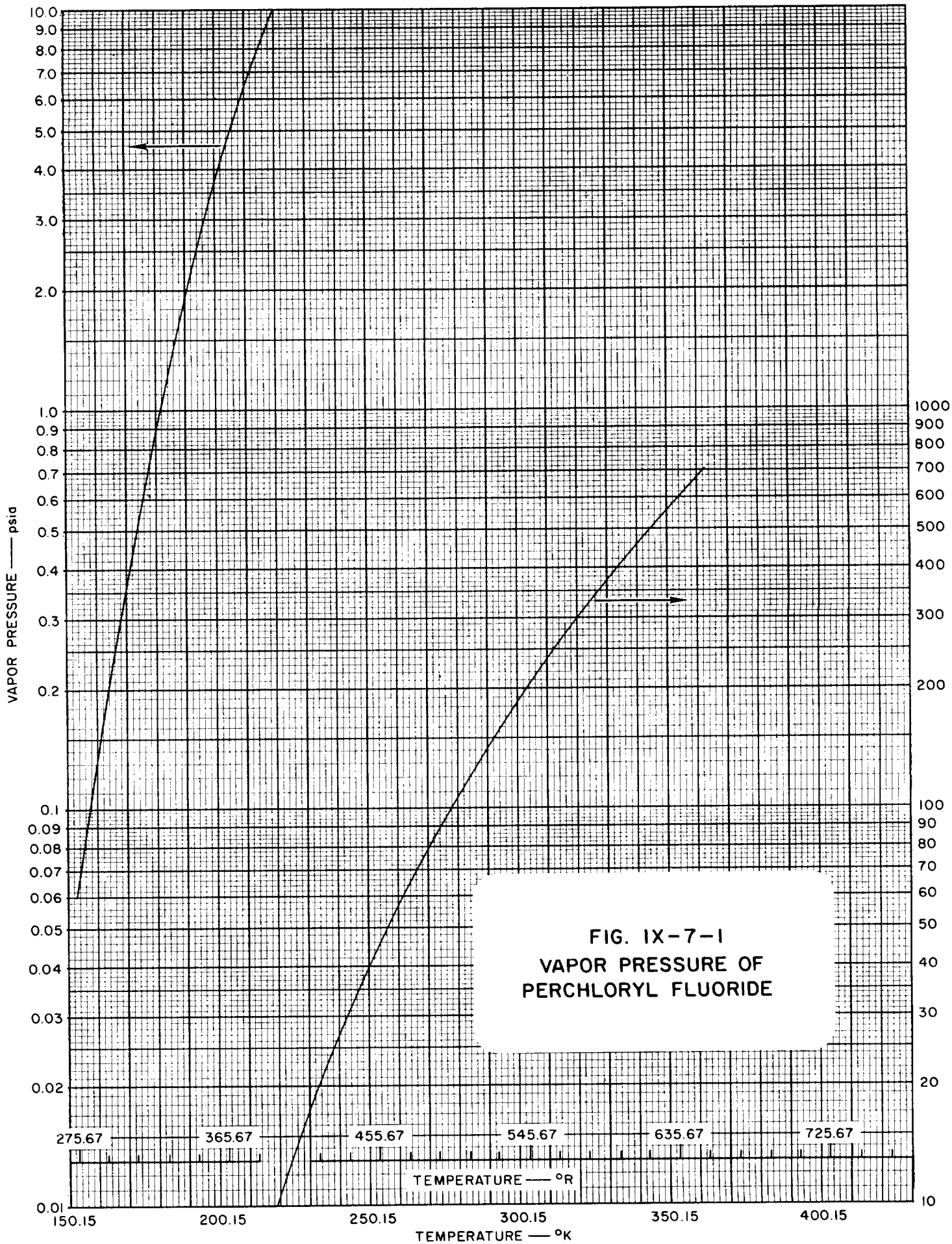
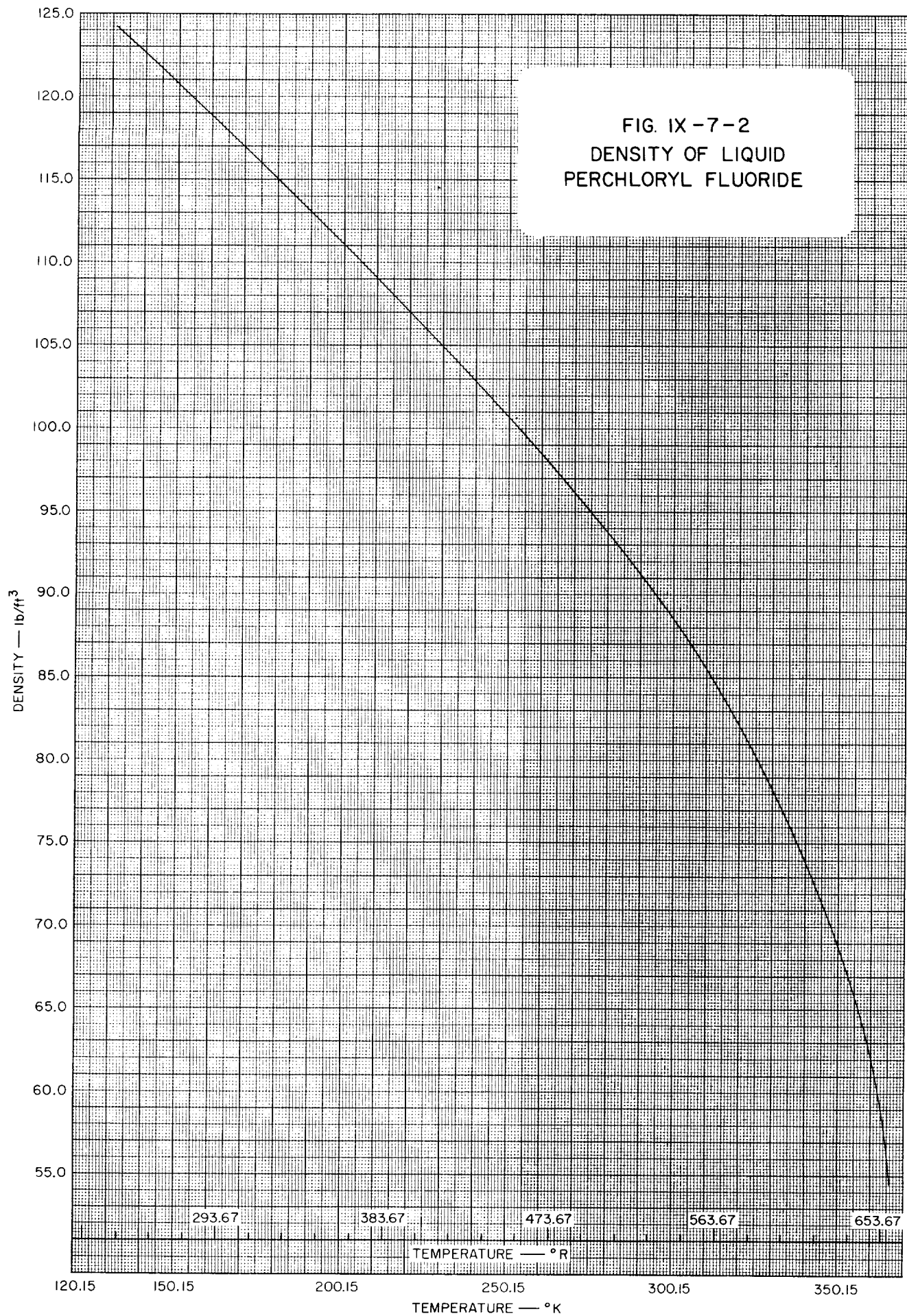


FIG. IX-7-2
DENSITY OF LIQUID
PERCHLORYL FLUORIDE



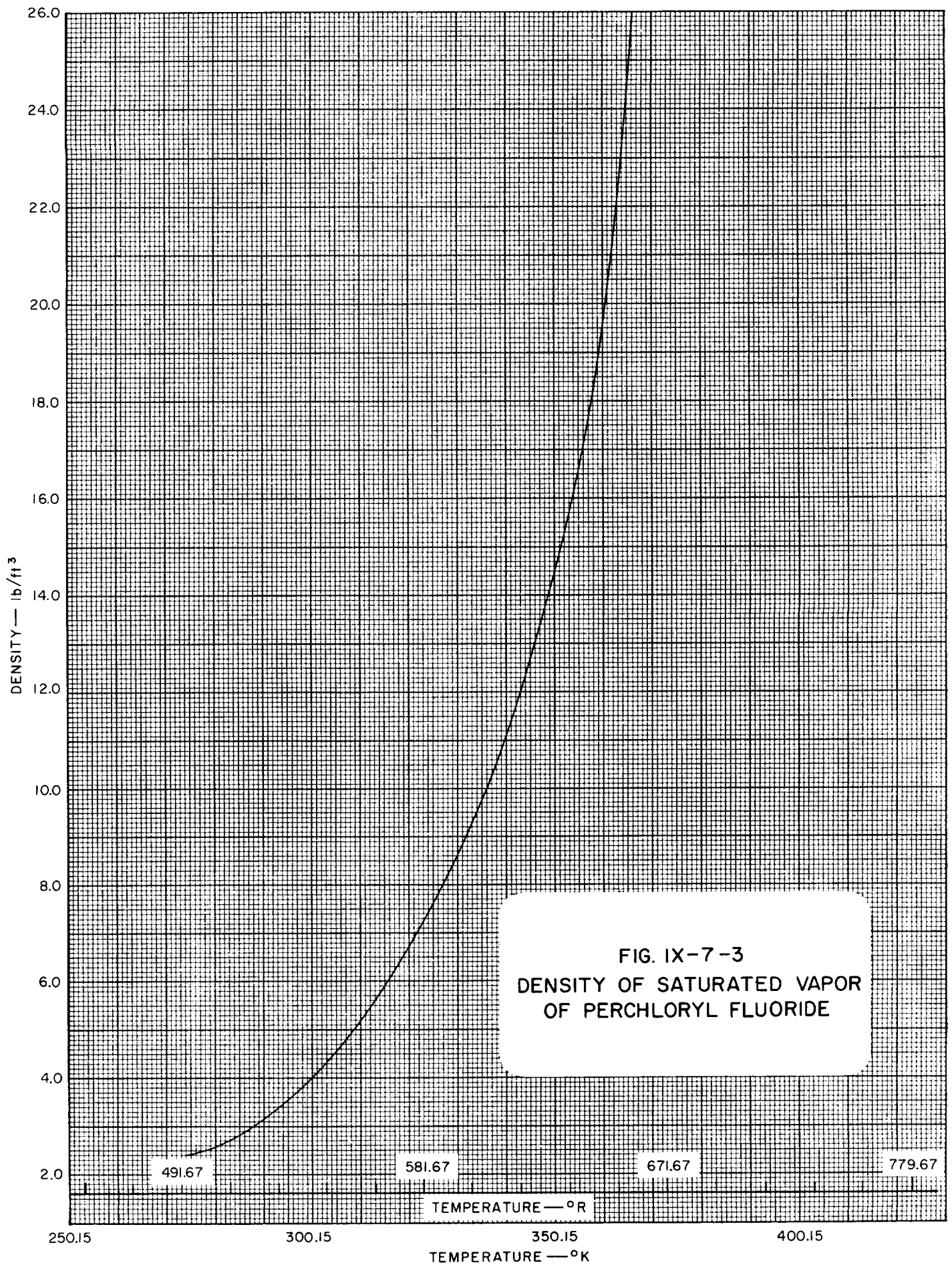


FIG. IX-7-4
VISCOSITY OF LIQUID
PERCHLORYL FLUORIDE

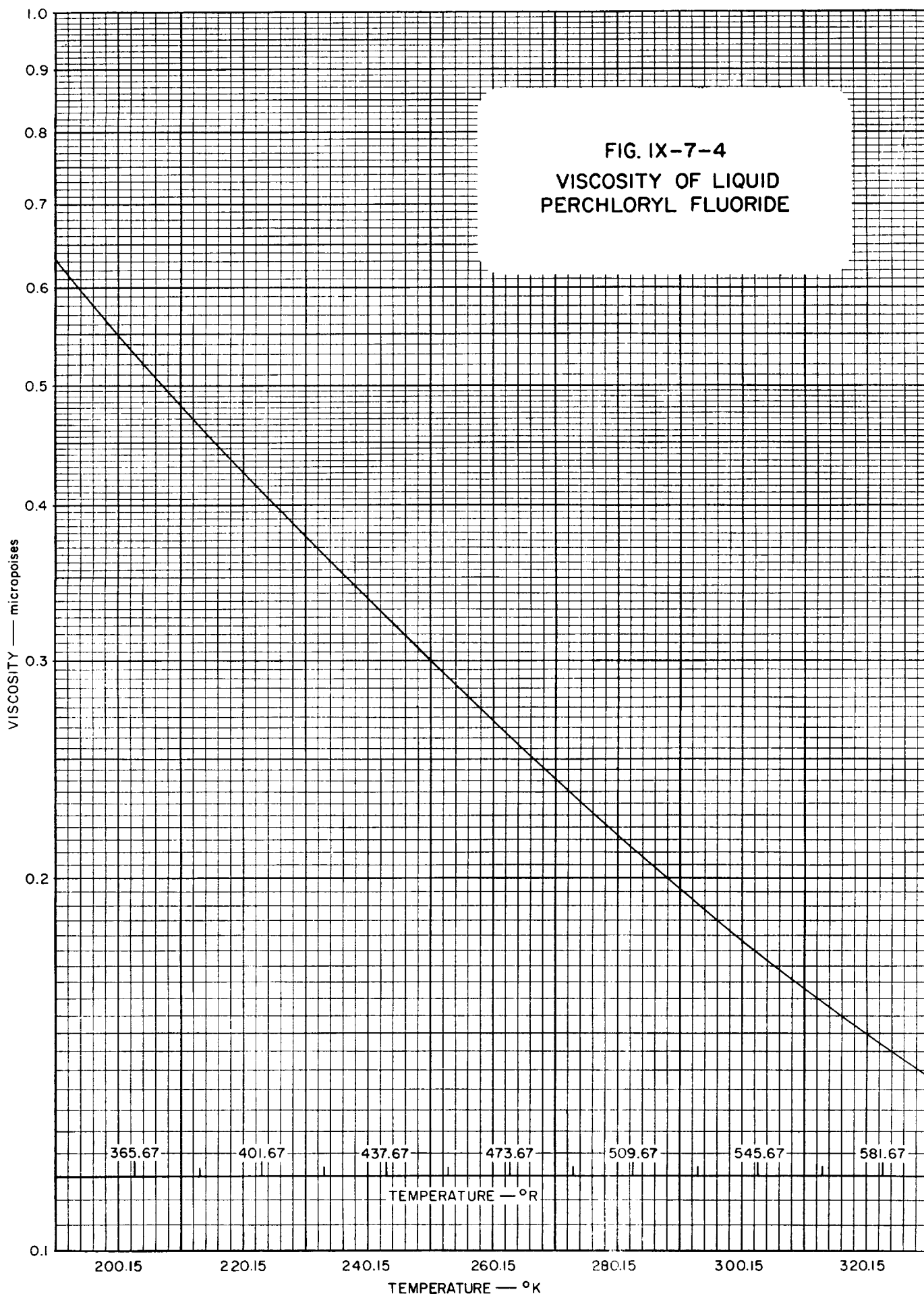
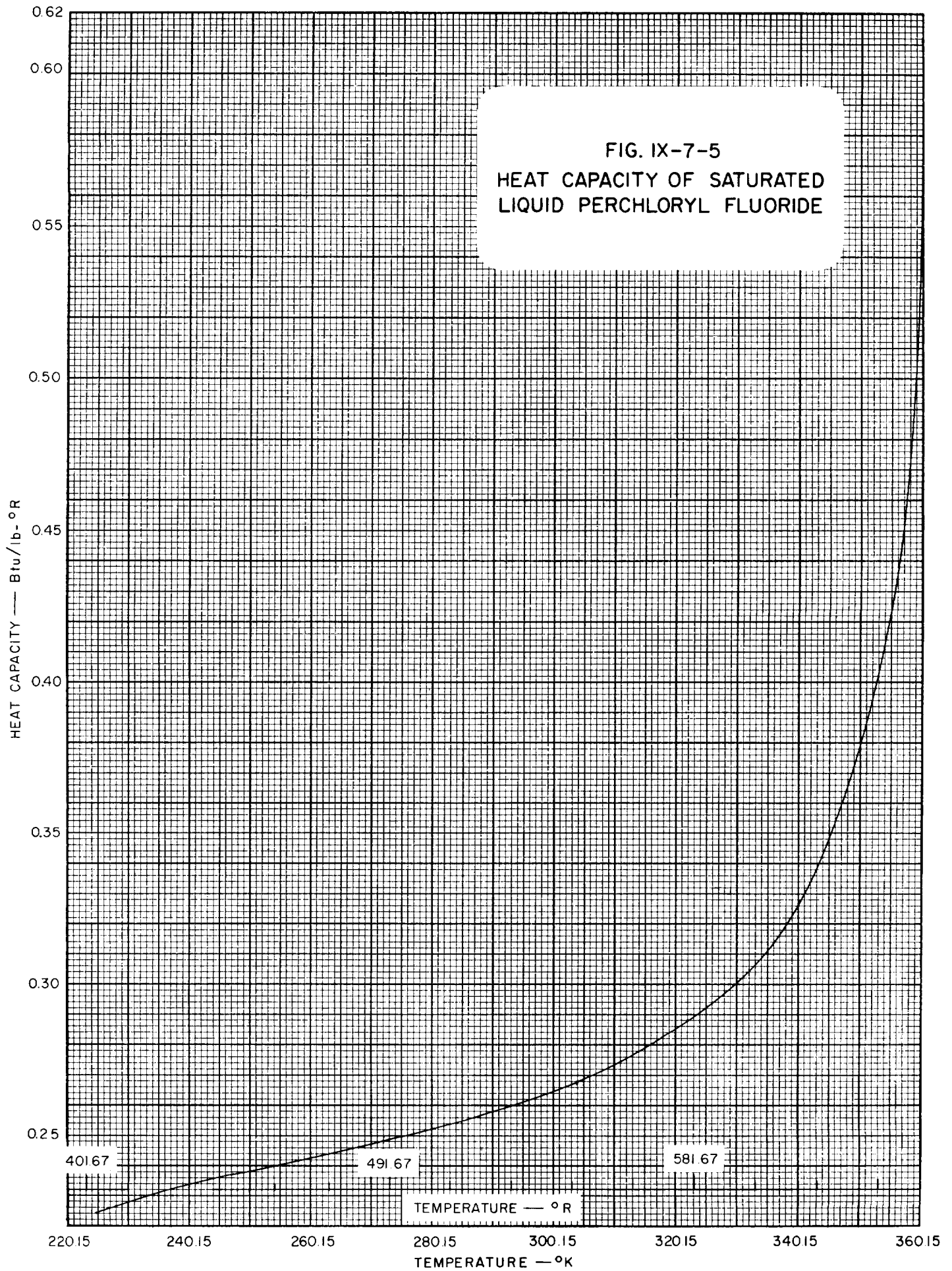
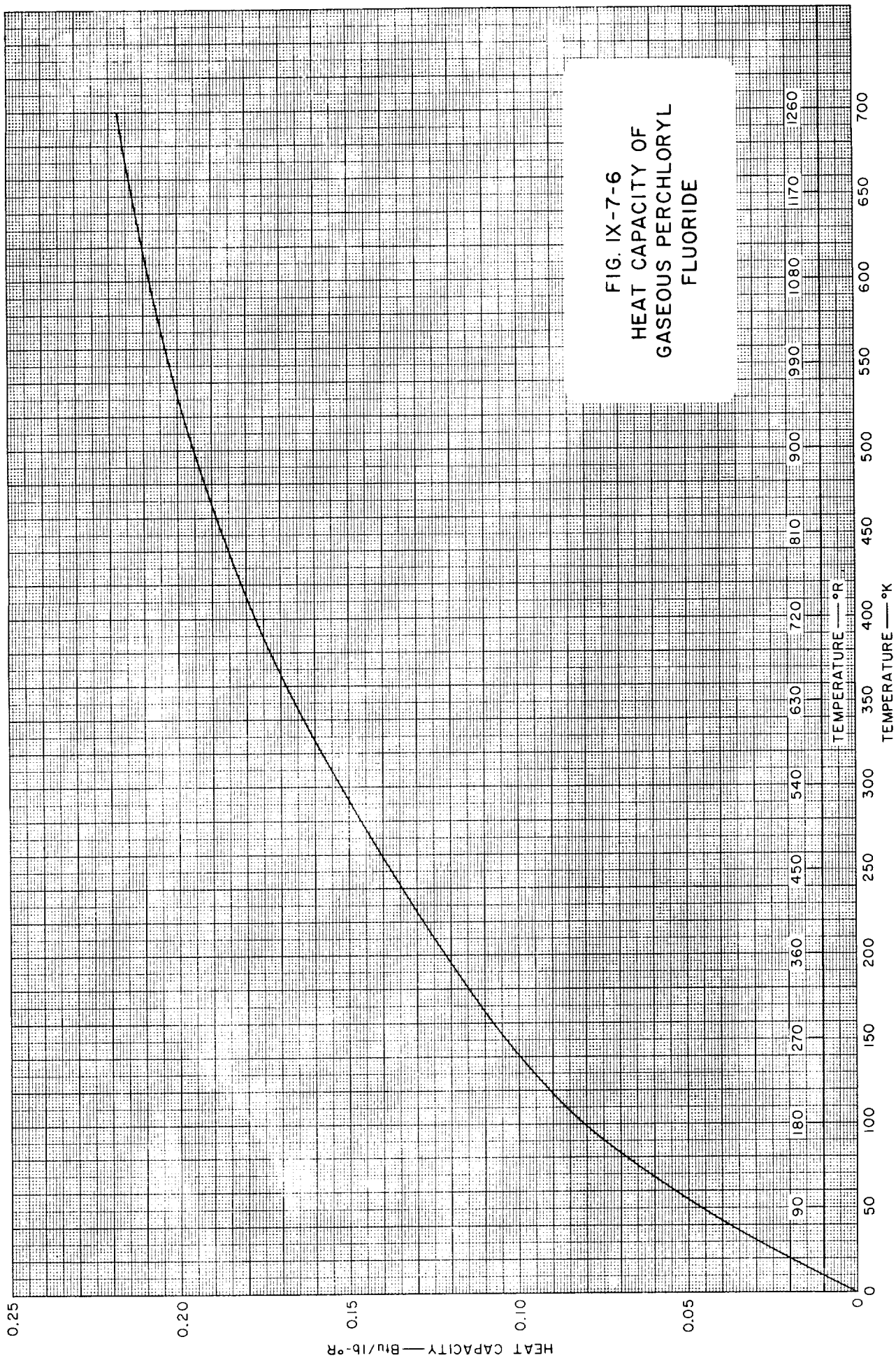


FIG. IX-7-5
HEAT CAPACITY OF SATURATED
LIQUID PERCHLORYL FLUORIDE





IX-7 PERCHLORYL FLUORIDE REFERENCES

1. Engelbrecht, A., and Atzwanger, H., *J. Inorg. Nucl. Chem.*, **2**, 348 (1956).
2. *JANAF Thermochemical Data*, Dow Chemical Company, Midland, Michigan, 1961.
3. Jarry, R. L., *J. Phys. Chem.*, **61**, 498 (1957).
4. Jarry, R. L., and Fritz, J. J., *Ind. Eng. Chem., Chem. Eng. Data Series*, **3**, 34 (1958).
5. Koehler, J. K., and Giaque, W. F., *J. Am. Chem. Soc.*, **80**, 2659 (1958).
6. Simkin, J., and Jarry, Roger L., *J. Phys. Chem.*, **61**, 503 (1957).

)

)

)

)

)

Table IX-8-1
GENERAL PROPERTIES OF CHLORINE TRIFLUORIDE

PROPERTY	TEMPERATURE				PRESSURE			REF
	°C	°K	°F	°R	psia	atm	mm of Hg	
Melting Point								
Boiling Point	11.75	284.90	53.15	512.82				3
Triple Point	- 76.32	196.83	-105.38	354.29				3
Critical Temp.	174	447	345	804				3
Critical Press.					838	57		
Mol. Wt. 92.457								
Heat of Vaporization 71.17 cal/g or 128.1 Btu/lb at B.P.								3
Heat of Fusion 19.68 cal/g or 35.42 Btu/lb at triple point								3

Table IX-8-1.1
SOME VALUES OF THE GAS CONSTANT, *R*, FOR CHLORINE TRIFLUORIDE
(See also Conversion Tables, Section I)

TEMPERATURE IN °K				
Pressure Density	atm	kg/cm ²	mm of Hg	lb/in ²
g/cm ³	0.893031	0.917001	674.509	13.0429
mole/cm ³	82.0567	84.7832	62363.1	1205.91
mole/liter	0.0820544	0.0847809	62.3613	1.20587
lb/ft ³	0.0142164	0.0146888	10.8045	0.208925
lb/mole/ft ³	1.31441	1.35808	998.952	19.3166
TEMPERATURE IN °R				
Pressure Density	atm	kg/cm ²	mm of Hg	lb/in ²
g/cm ³	0.493062	0.509445	374.727	7.24607
mole/cm ³	45.5871	47.1018	34646.2	669.950
mole/liter	0.0455858	0.0471005	34.6452	0.669928
lb/ft ³	0.00789803	0.00816043	6.00250	0.116069
lb/mole/ft ³	0.730228	0.754489	554.973	10.7314

Table IX-8-2
VAPOR PRESSURE OF CHLORINE TRIFLUORIDE (Ref. 3)

TEMPERATURE		VAPOR PRESSURE	TEMPERATURE		VAPOR PRESSURE
°K	°R	psia	°K	°R	psia
226.18	407.12	0.5619	283.00	509.40	13.56
231.64	416.95	0.8278	284.90	512.82	14.70
237.56	427.61	1.230	285.39	513.70	15.00
240.01	432.02	1.437	286.93	516.47	16.01
242.40	436.32	1.671	290.61	523.10	18.60
245.98	442.76	2.081	290.91	523.64	18.83
249.00	448.20	2.477	294.17	529.51	21.417
253.90	457.02	3.278	298.12	536.62	24.935
255.52	459.94	3.578	298.82	537.88	25.616
259.22	466.60	4.376	302.70	544.86	29.597
263.43	474.17	5.441	313.15	563.67	42.837
267.52	481.54	6.672	323.15	581.67	59.436
271.57	488.83	8.111	333.15	599.67	80.641
275.52	495.94	9.739			
279.55	503.19	11.67			

(See Figure IX-8-1)

Table IX-8-3
DENSITY OF LIQUID CHLORINE
TRIFLUORIDE (Ref. 2)

TEMPERATURE		DENSITY
°K	°R	lb/ft ³
273.15	491.67	117.70
283.15	509.67	115.84
285.15	513.67	115.50
288.15	518.67	114.89
293.15	527.67	113.93
298.15	536.67	112.96
303.15	545.67	111.97
308.15	554.67	110.98
313.15	563.67	109.98
318.15	572.67	108.95
323.15	581.67	107.92
333.15	599.67	105.83

(See Figure IX-8-2)

Table IX-8-4
SURFACE TENSION OF LIQUID CHLORINE TRIFLUORIDE
IN CONTACT WITH ITS VAPOR (Ref. 1)

TEMPERATURE		SURFACE TENSION	TEMPERATURE		SURFACE TENSION
°K	°R	dynes/cm	°K	°R	dynes/cm
273.15	491.67	26.6	298.65	537.57	22.7
275.65	496.17	26.3	298.75	537.75	22.8
277.15	498.87	26.0	304.15	547.47	22.2
282.05	507.69	25.35	310.75	559.35	20.4
282.15	507.87	25.15	311.15	560.07	20.3
287.75	517.95	24.3	313.55	564.39	20.5
291.55	524.79	24.05	315.15	567.27	20.0
293.75	528.75	23.1	320.15	576.27	19.1
294.35	529.83	23.3	323.05	581.49	18.7
298.25	536.85	22.8			

(See Figure IX-8-3)

Table IX-8-5

VISCOSITY OF LIQUID CHLORINE
TRIFLUORIDE (Ref. 1)

TEMPERATURE		ABSOLUTE VISCOSITY
$^{\circ}\text{K}$	$^{\circ}\text{R}$	millipoises
284.90	513.02	4.78
288.15	520.67	4.60
290.85	523.53	4.47
292.55	526.59	4.38
293.15	527.67	4.35
298.15	536.67	4.12
303.15	545.67	3.90
308.15	554.67	3.70
313.15	563.67	3.51
318.15	572.67	3.33
323.15	581.67	3.16

(See Figure IX-8-4)

Table IX-8-6

THERMAL CONDUCTIVITY OF GASEOUS
CHLORINE TRIFLUORIDE (Ref. 4)

TEMPERATURE		THERMAL CONDUCTIVITY
$^{\circ}\text{K}$	$^{\circ}\text{R}$	Btu/hr-ft- $^{\circ}\text{R}$
100	180	0.00165
200	360	0.00436
300	540	0.00794
400	720	0.0116
500	900	0.0151
600	1080	0.0184

(See Figure IX-8-5)

Table IX-8-7
HEAT CAPACITIES OF SOLID AND LIQUID
CHLORINE TRIFLUORIDE (Ref. 3)

TEMPERATURE		HEAT CAPACITY, C_p	TEMPERATURE		HEAT CAPACITY, C_p
$^{\circ}\text{K}$	$^{\circ}\text{R}$	Btu/lb- $^{\circ}\text{R}$	$^{\circ}\text{K}$	$^{\circ}\text{R}$	Btu/lb- $^{\circ}\text{R}$
14.04	25.27	0.0111	108.47	195.25	0.1390
15.28	27.50	0.0133	111.35	200.43	0.1409
16.60	29.88	0.0162	119.00	214.20	0.1471
18.03	32.45	0.0188	126.54	227.77	0.1532
20.10	36.18	0.0230	134.34	241.81	0.1592
22.74	40.93	0.0289	141.87	255.37	0.1653
25.88	46.58	0.0363	149.15	268.47	0.1707
29.11	52.46	0.0438	156.22	281.20	0.1761
32.59	58.66	0.0514	160.61	289.10	0.1794
36.42	65.56	0.0593	163.57	294.43	0.1820
40.67	73.21	0.0673	167.80	302.04	0.1847
45.88	82.58	0.0763	171.20	308.16	0.1878
51.29	92.32	0.0842	175.20	315.36	0.1907
51.89	93.40	0.0849	178.62	321.52	0.1934
56.27	101.29	0.0907	180.60	325.08	0.1951
56.30	101.34	0.0911	182.33	328.19	0.1970
62.07	111.73	0.0981	184.96	332.93	0.1997
67.82	122.08	0.1038	187.56	337.61	0.2031
73.16	131.69	0.1092	196.84	354.31	0.2074
78.96	142.13	0.1149	Liquid		
82.94	149.29	0.1185	196.84	354.31	0.2886
88.44	159.19	0.1243	202.76	364.97	0.2894
90.94	163.69	0.1261	204.83	368.69	0.2896
95.62	172.12	0.1301	207.69	373.84	0.2900
97.01	174.62	0.1308	216.53	389.75	0.2914
102.84	185.11	0.1344	219.84	395.71	0.2916
103.44	186.19	0.1349	226.95	408.51	0.2926
			237.83	428.09	0.2944
			248.61	447.50	0.2961
			259.30	466.74	0.2986
			269.86	485.75	0.3011
			278.25	500.85	0.3031

(See Figure IX-8-6)

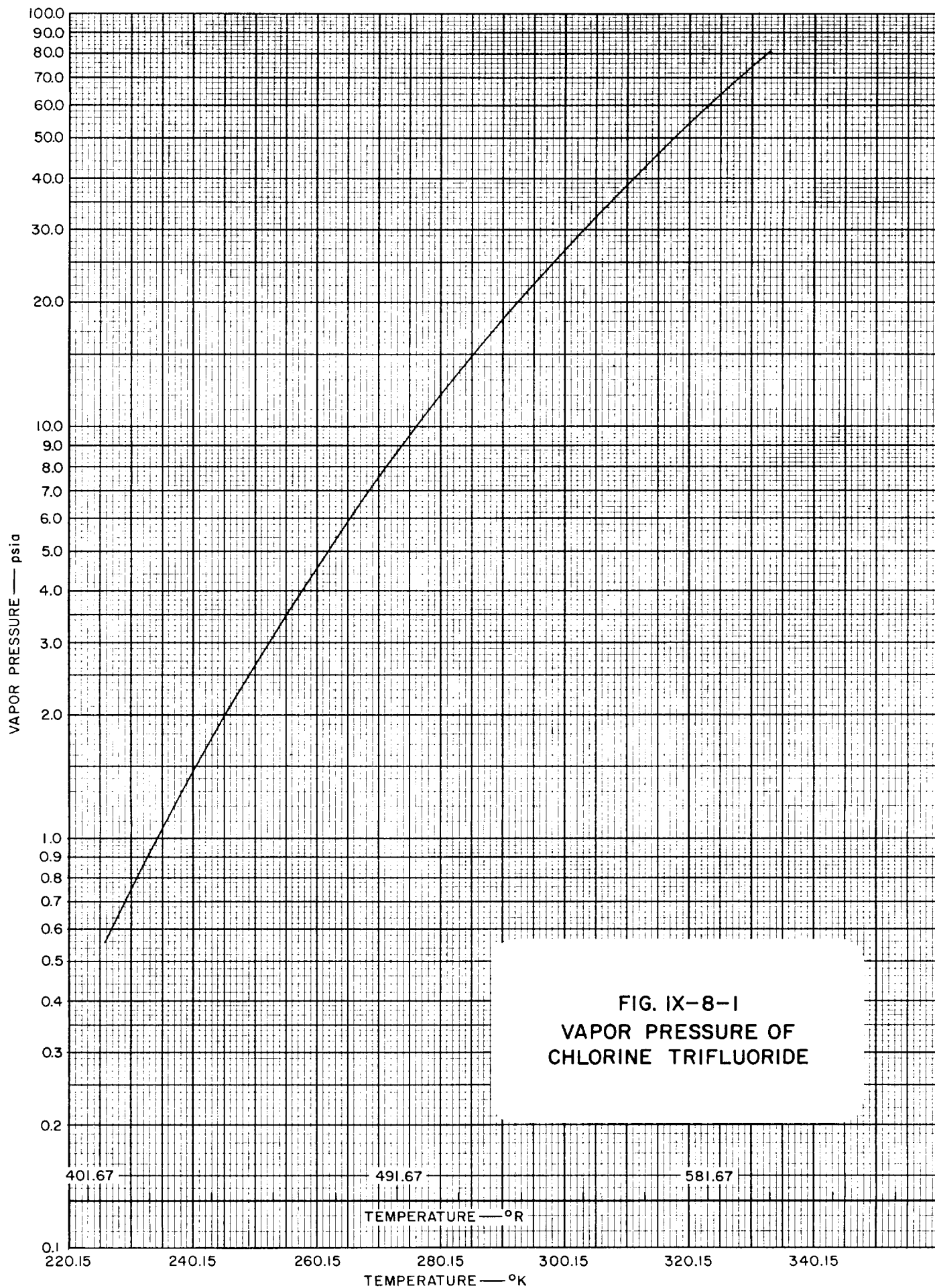
)

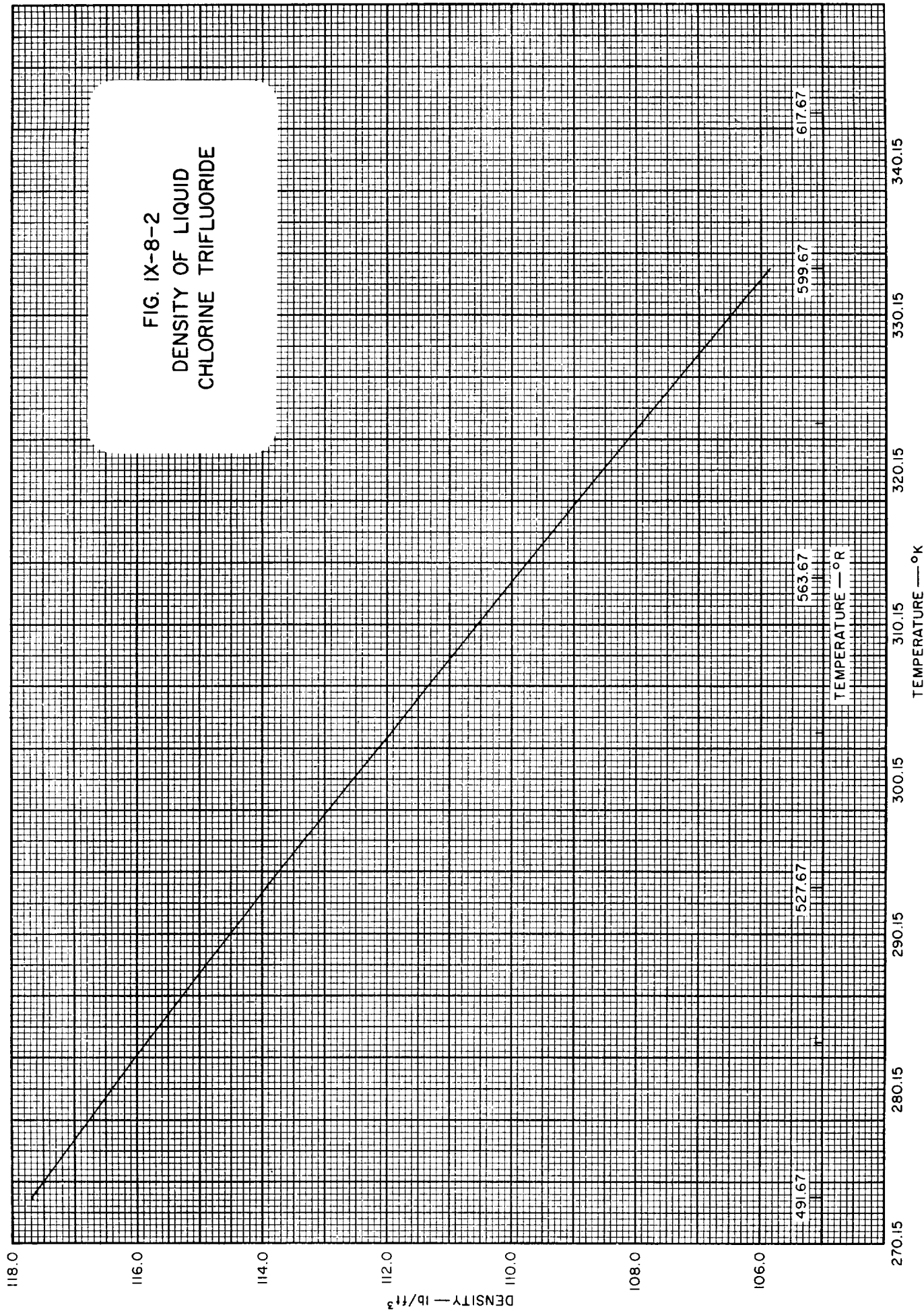
)

)

)

)





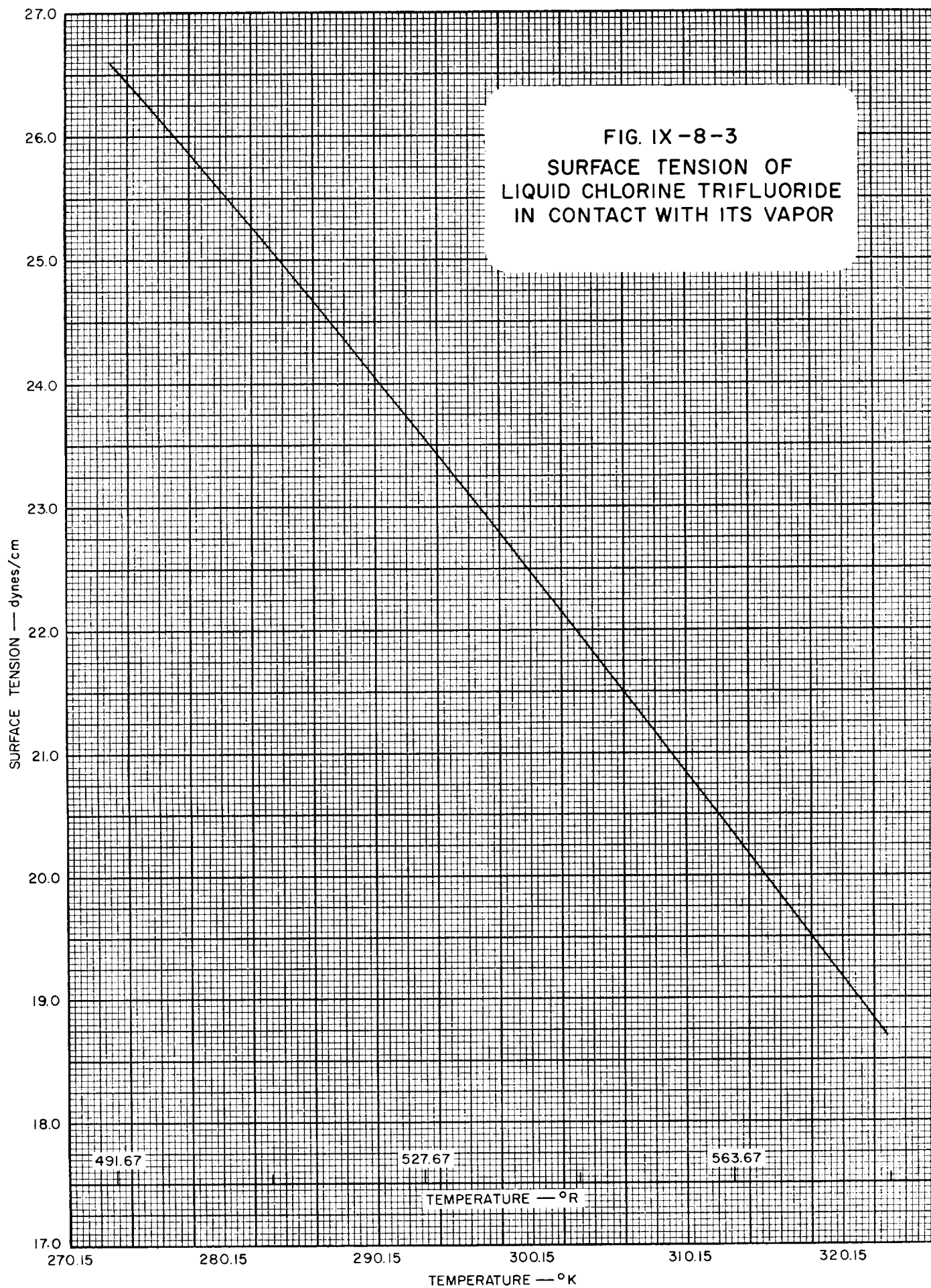
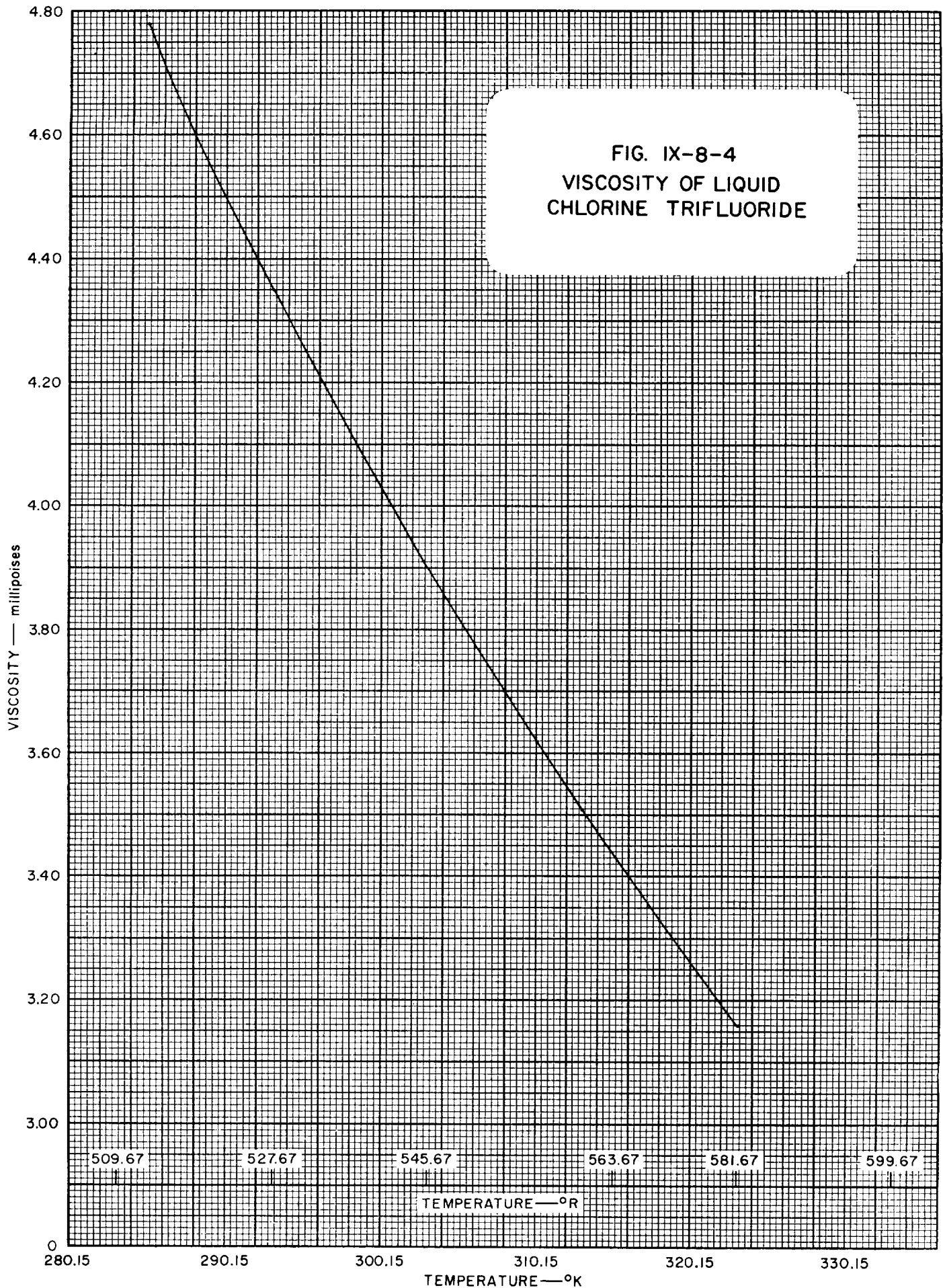
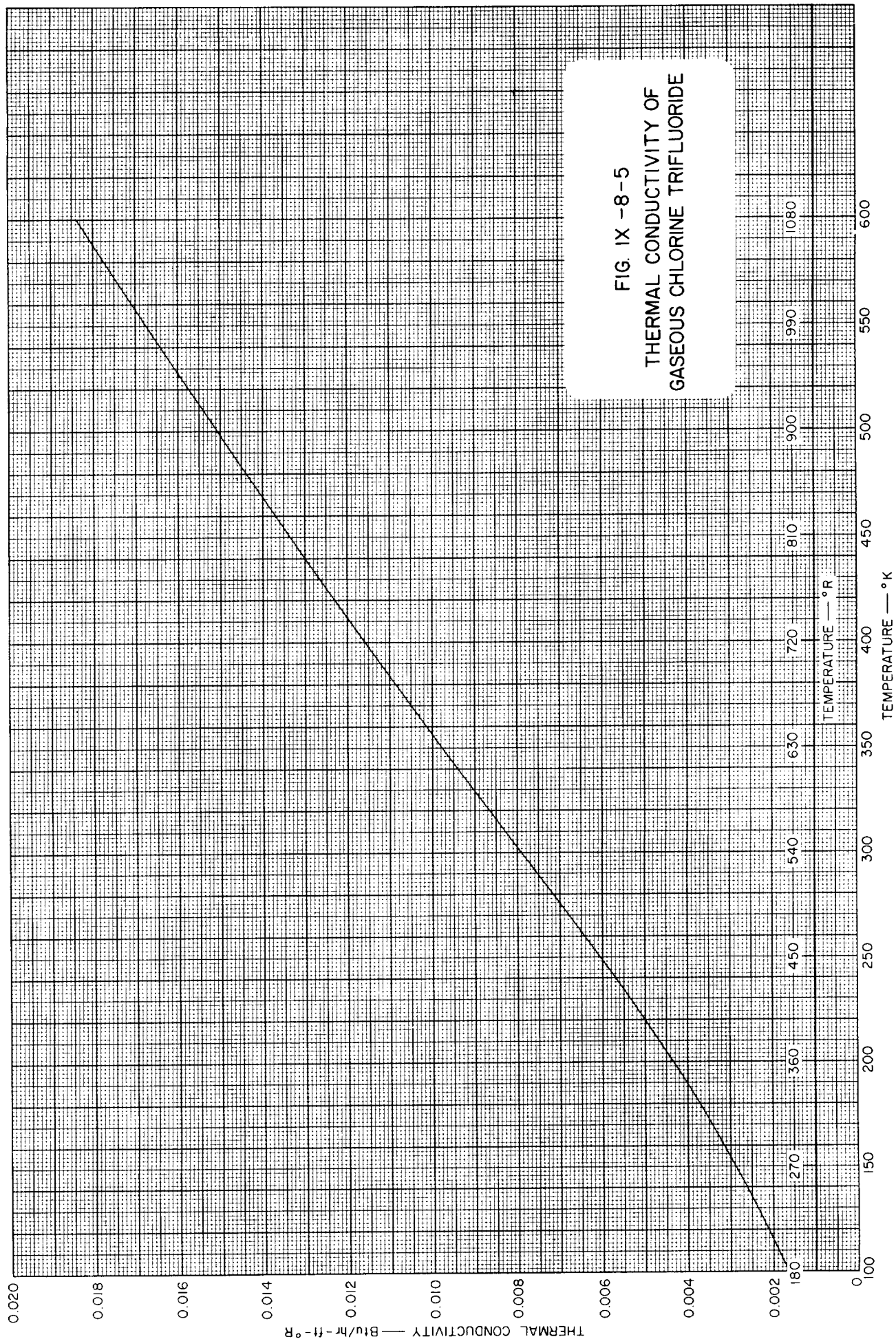


FIG. IX-8-4
VISCOSITY OF LIQUID
CHLORINE TRIFLUORIDE





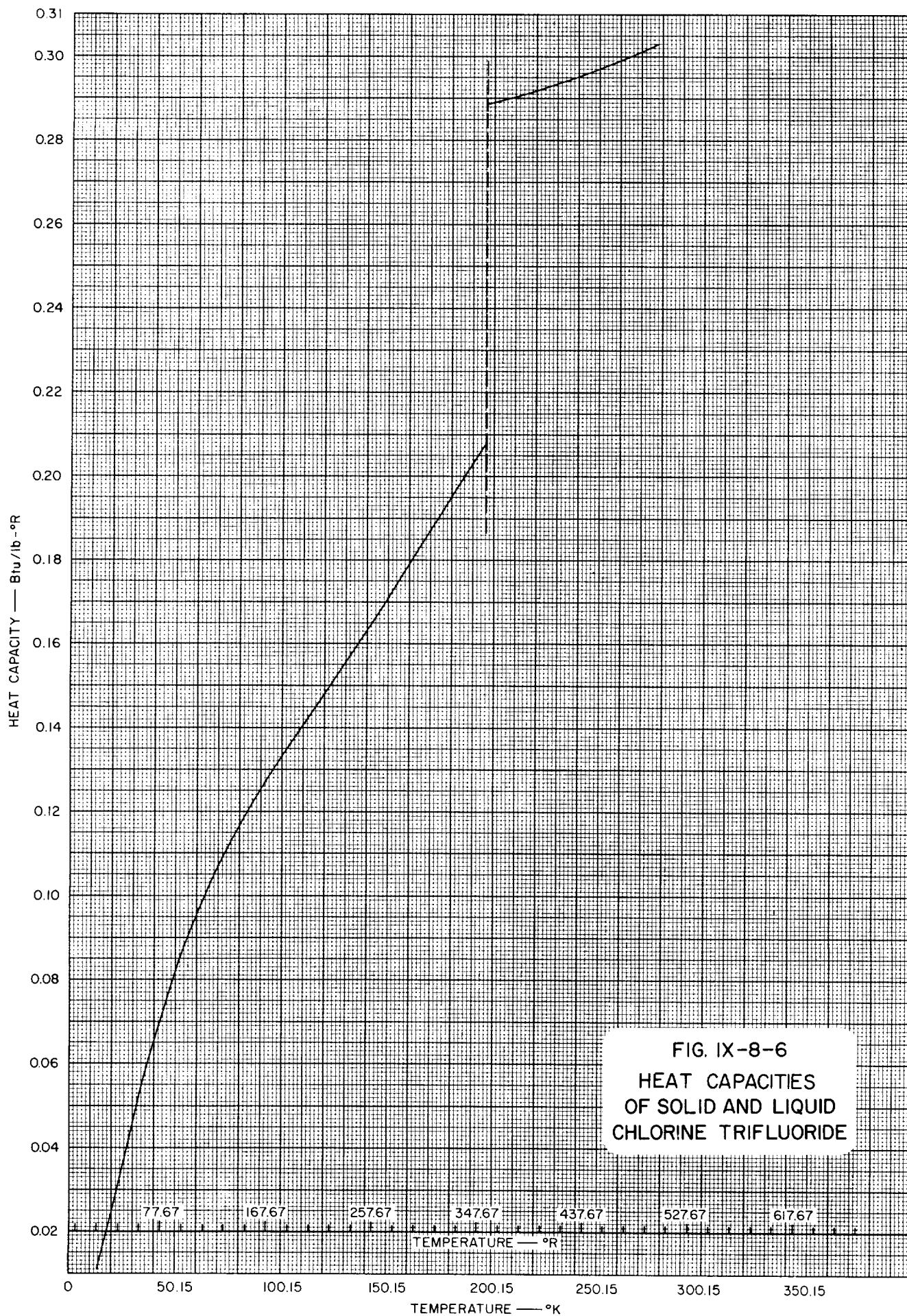


FIG. IX-8-6
HEAT CAPACITIES
OF SOLID AND LIQUID
CHLORINE TRIFLUORIDE

IX-8 CHLORINE TRIFLUORIDE REFERENCES

1. Bank, A. A., Davies, A., and Rudge, A. J., *J. Chem. Soc.*, **1953**, 153.
2. Bank, A. A., and Rudge, A. J., *J. Chem. Soc.*, **1950**, 43.
3. Grisard, J. W., Bernhardt, H. A., and Oliver, G. D., *J. Am. Chem. Soc.*, **73**, 5725 (1951).
4. Svehla, R. A., *Estimated Viscosities and Thermal Conductivities of Gases at High Temperatures*, NASA TR R-132, 1962.

)

)

)

)

)

Table IX-9-1
GENERAL PROPERTIES OF HYDRAZINE

PROPERTY	TEMPERATURE				PRESSURE			REF
	°C	°K	°F	°R	psia	atm	mm of Hg	
Melting Point*	1.6	274.75	33.91	493.58				4
Boiling Point	114.15	387.3	237.47	697.14				2
Triple Point								
Critical Temp.	380	653	716	1176				3
Critical Press.					2131	145	110,200	3
Mol Wt. 32.05								5 5
Heat of Vaporization 333.85 cal/g or 600.9 Btu/lb at 25°C								
Heat of Fusion 94.38 cal/g or 169.9 Btu/lb								

* 99.6%

Table IX-9-1.1
SOME VALUES OF THE GAS CONSTANT, R, FOR HYDRAZINE
(See also Conversion Tables, Section I)

TEMPERATURE IN °K				
Pressure	atm	kg/cm ²	mm of Hg	lb/in ²
Density				
g/cm ³	2.56027	2.64534	1945.80	37.6259
mole/cm ³	82.0567	84.7832	62363.1	1205.91
mole/liter	0.0820544	0.0847809	62.3613	1.20587
lb/ft ³	0.0410112	0.0423738	31.1685	0.602702
lb/mole/ft ³	1.31441	1.35808	998.952	19.3166
TEMPERATURE IN °R				
Pressure	atm	kg/cm ²	mm of Hg	lb/in ²
Density				
g/cm ³	1.42237	1.46963	1081.00	20.9033
mole/cm ³	45.5871	47.1018	34646.2	669.950
mole/liter	0.0455858	0.0471005	34.6452	0.669928
lb/ft ³	0.0227840	0.0235410	17.3159	0.334833
lb/mole/ft ³	0.730228	0.754489	554.973	10.7314

Table IX-9-2
VAPOR PRESSURE OF ANHYDROUS HYDRAZINE
(Ref. 5)

TEMPERATURE		PRESSURE	
$^{\circ}\text{K}$	$^{\circ}\text{R}$	psia	mm Hg
273.2	491.7	0.0516	2.67
288.2	518.7	0.148	7.64
293.2	527.7	0.204	10.53
298.2	536.7	0.277	14.35
303.2	545.7	0.373	19.31
308.2	554.7	0.497	25.70
313.2	563.7	0.654	33.83
318.2	572.7	0.853	44.10
323.2	581.7	1.101	56.93
328.2	590.67	1.408	72.84
333.2	599.67	1.787	92.40
338.2	608.7	2.248	116.26
343.2	617.7	2.807	145.16

(See Figure IX-9-1)

Table IX-9-3
DENSITY OF LIQUID HYDRAZINE (Ref. 1)

TEMPERATURE		DENSITY	TEMPERATURE		DENSITY
°K	°R	lb/ft ³	°K	°R	lb/ft ³
273.2	491.8	64.047	333.2	599.8	60.613
283.2	509.8	63.485	343.2	617.8	60.123
293.2	527.8	62.917	353.2	635.8	59.440
303.2	545.8	62.349	368.2	662.8	58.541
313.2	563.8	61.774			
323.2	581.8	61.200			

(See Figure IX-9-2)

Table IX-9-4
VISCOSITY OF HYDRAZINE (Ref. 1)

TEMPERATURE		KINEMATIC VISCOSITY,	ABSOLUTE VISCOSITY,
°K	°R	centi- stokes	centi- poises
288.15	518.67	1.015	1.0276
298.15	536.67	0.8705	0.8733
308.15	554.67	0.7568	0.7523
318.15	572.67	0.6719	0.6618
328.15	590.67	0.6003	0.5856
338.15	608.67	0.5434	0.5250
348.15	626.67	0.4969	0.4754
358.15	644.67	0.4557	0.4313
368.15	662.67	0.4236	0.3972

(See Figure IX-9-3)

Table IX-9-5
HEAT CAPACITY OF LIQUID
HYDRAZINE (Ref. 5)

TEMPERATURE		HEAT CA- PACITY, C_p
$^{\circ}\text{K}$	$^{\circ}\text{R}$	Btu/lb- $^{\circ}\text{R}$
274.69	494.4	0.727
280	504.0	0.729
290	522.0	0.734
298	536.4	0.737
300	540.0	0.738
310	558.0	0.743
320	576.0	0.748
330	594.0	0.753
340	612.0	0.759

(See Figure IX-9-4)

Table IX-9-6
HEAT CAPACITY OF GASEOUS
HYDRAZINE (Ref. 5)

TEMPERATURE		HEAT CA- PACITY, C_p
$^{\circ}\text{K}$	$^{\circ}\text{R}$	Btu/lb- $^{\circ}\text{R}$
298.2	536.8	0.393
300.0	540.0	0.393
400.0	720.0	0.471
500.0	900.0	0.527
600.0	1080.0	0.571

(See Figure IX-9-5)

Table IX-9-7

HEAT CAPACITY OF HYDRAZINE AT CONSTANT PRESSURE (Ref. 5)

TEMPERATURE		HEAT CA- PACITY, C_p	TEMPERATURE		HEAT CA- PACITY, C_p
$^{\circ}\text{K}$	$^{\circ}\text{R}$	Btu/lb- $^{\circ}\text{R}$	$^{\circ}\text{K}$	$^{\circ}\text{R}$	Btu/lb- $^{\circ}\text{R}$
12	21.6	0.00218	90	162	0.20966
13	23.4	0.00296	95	171	0.22027
14	25.2	0.00359	100	180	0.23010
15	27.0	0.00437	110	198	0.24898
16	28.8	0.00515	120	216	0.26645
17	30.6	0.00640	130	234	0.28298
18	32.4	0.00780	140	252	0.29858
19	34.2	0.00936	150	270	0.31340
20	36.0	0.01092	160	288	0.33072
25	45	0.02122	170	306	0.34117
30	54	0.03448	180	324	0.35443
35	63	0.05008	190	342	0.36738
40	72	0.06646	200	360	0.38048
45	81	0.08346	210	378	0.39343
50	90	0.10031	220	396	0.40654
55	99	0.11669	230	414	0.41948
60	108	0.13198	240	432	0.43259
65	117	0.14664	250	450	0.44554
70	126	0.16052	260	468	0.45864
75	135	0.17348	270	486	0.47174
80	144	0.18611	274.69	494.44	0.47767
85	153	0.19828			

(See Figure IX-9-6)

Table IX-9-8

THERMAL CONDUCTIVITY OF HYDRAZINE (Ref. 6)

(Smoothed Data)

TEMPERATURE		THERMAL CON- DUCTIVITY
$^{\circ}\text{K}$	$^{\circ}\text{R}$	Btu/hr-ft- $^{\circ}\text{R}$
280	504.0	0.2090
350	630.0	0.1972
400	720.0	0.1885
422	760.0	0.1855
477	858.6	0.1770
533	959.4	0.1690

(See Figure IX-9-7)

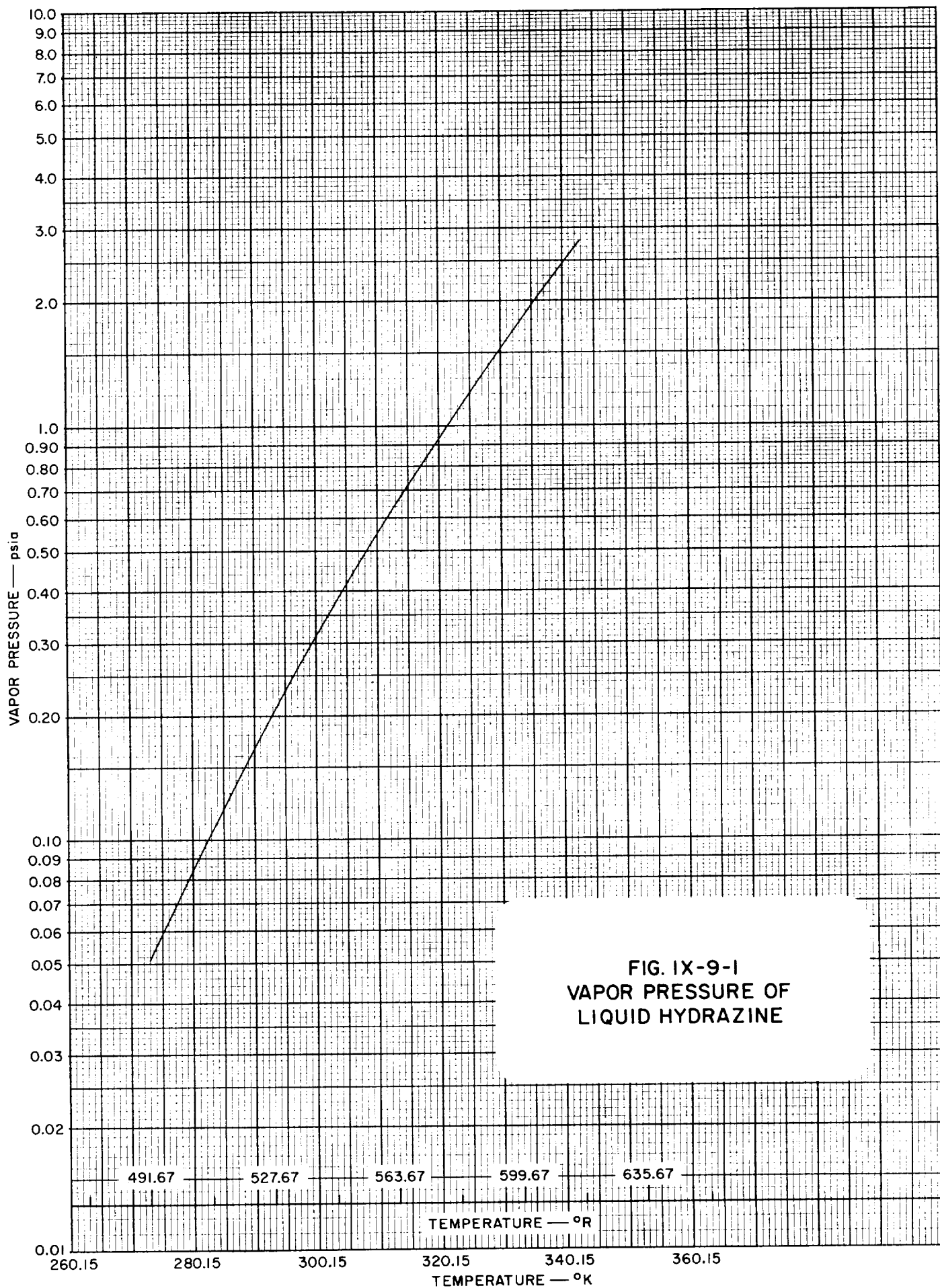
1

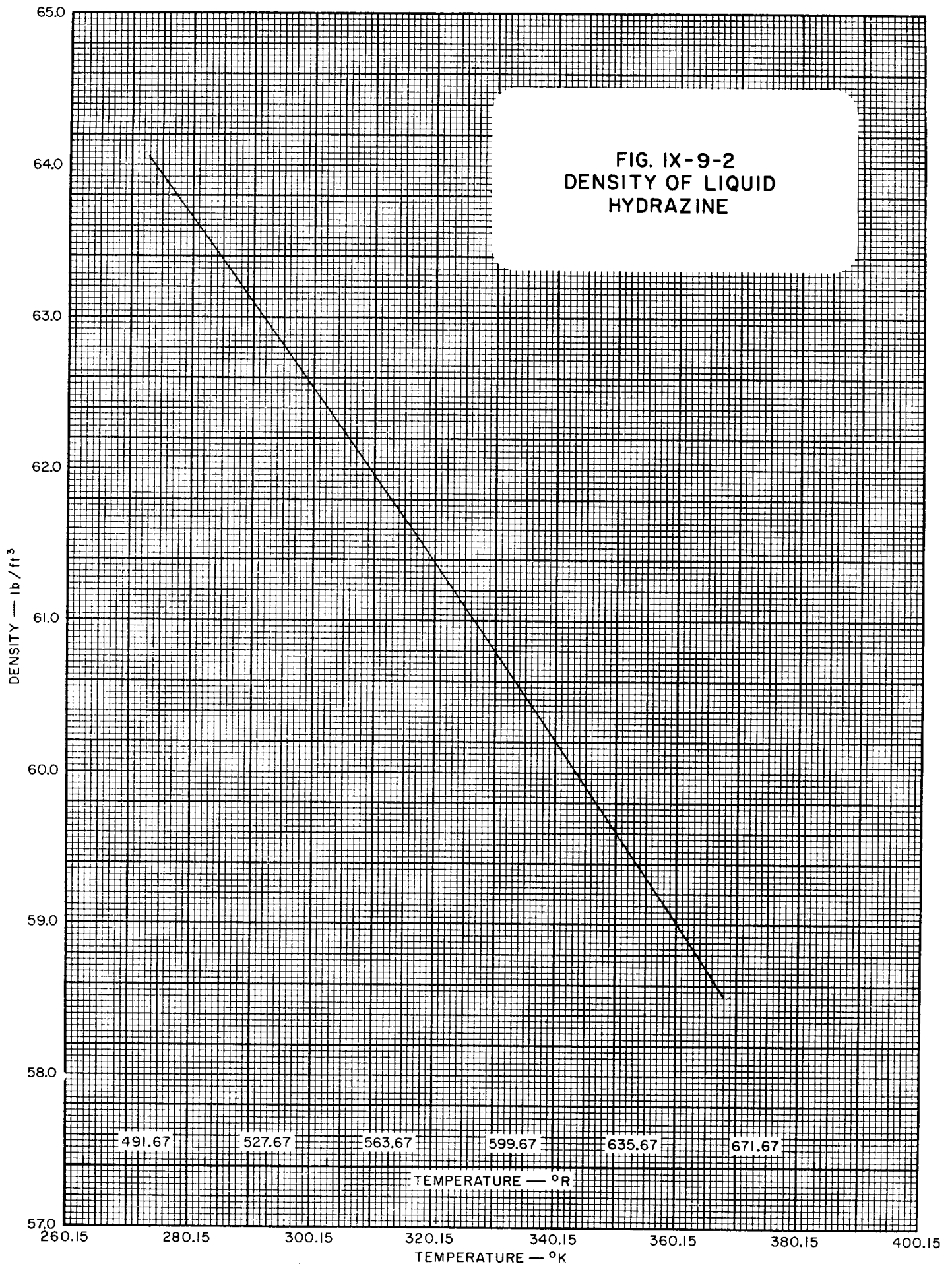
2

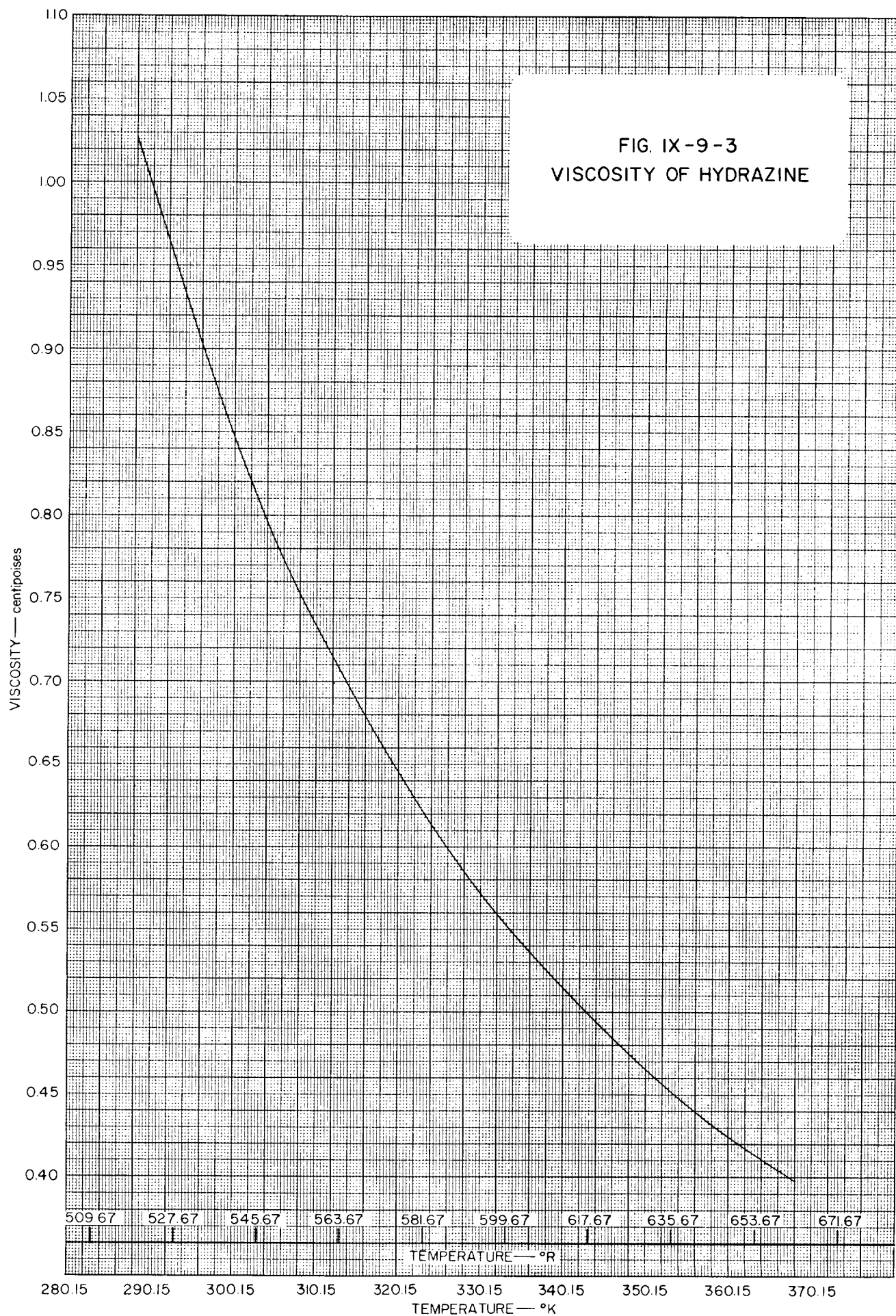
3

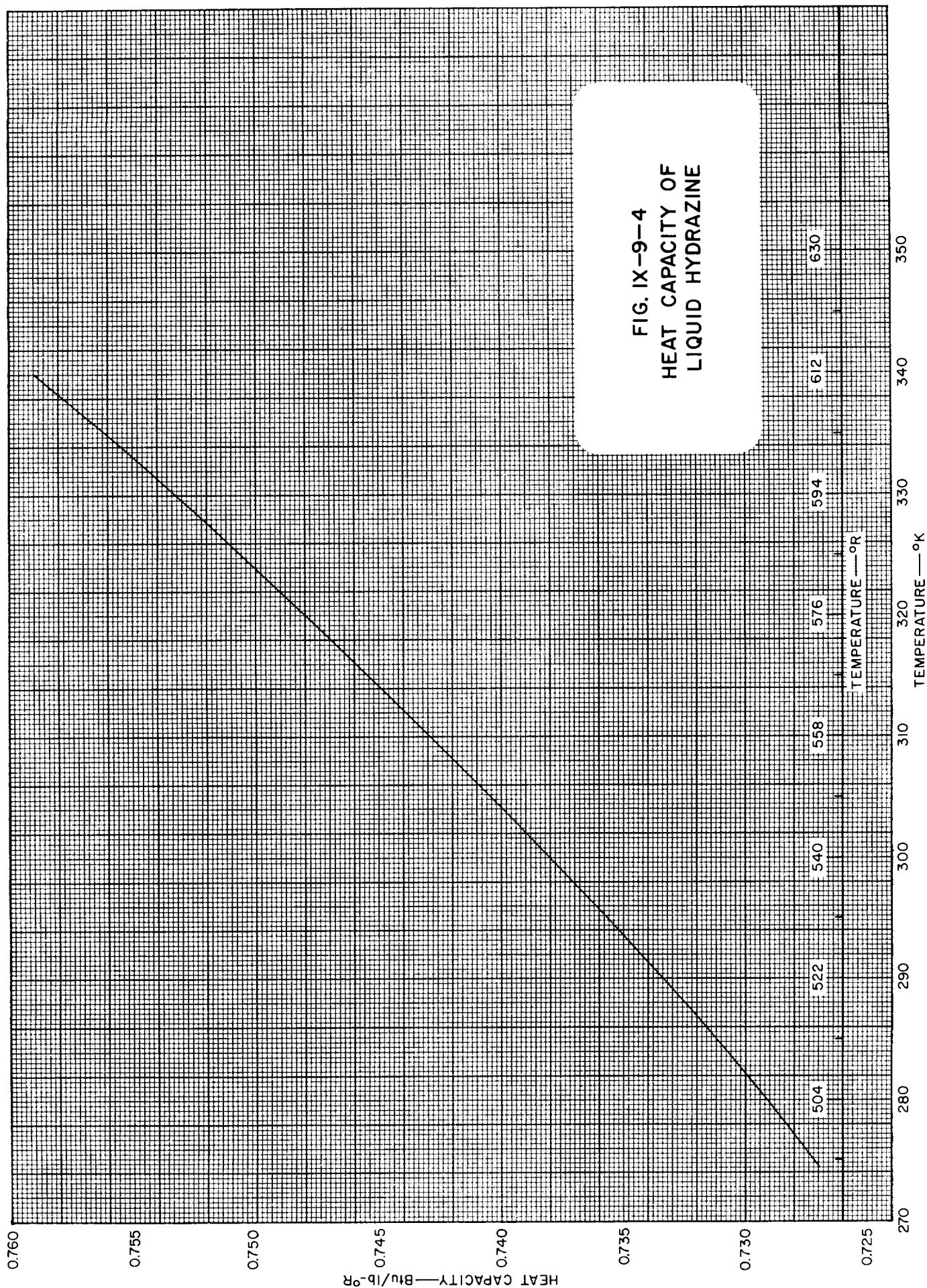
4

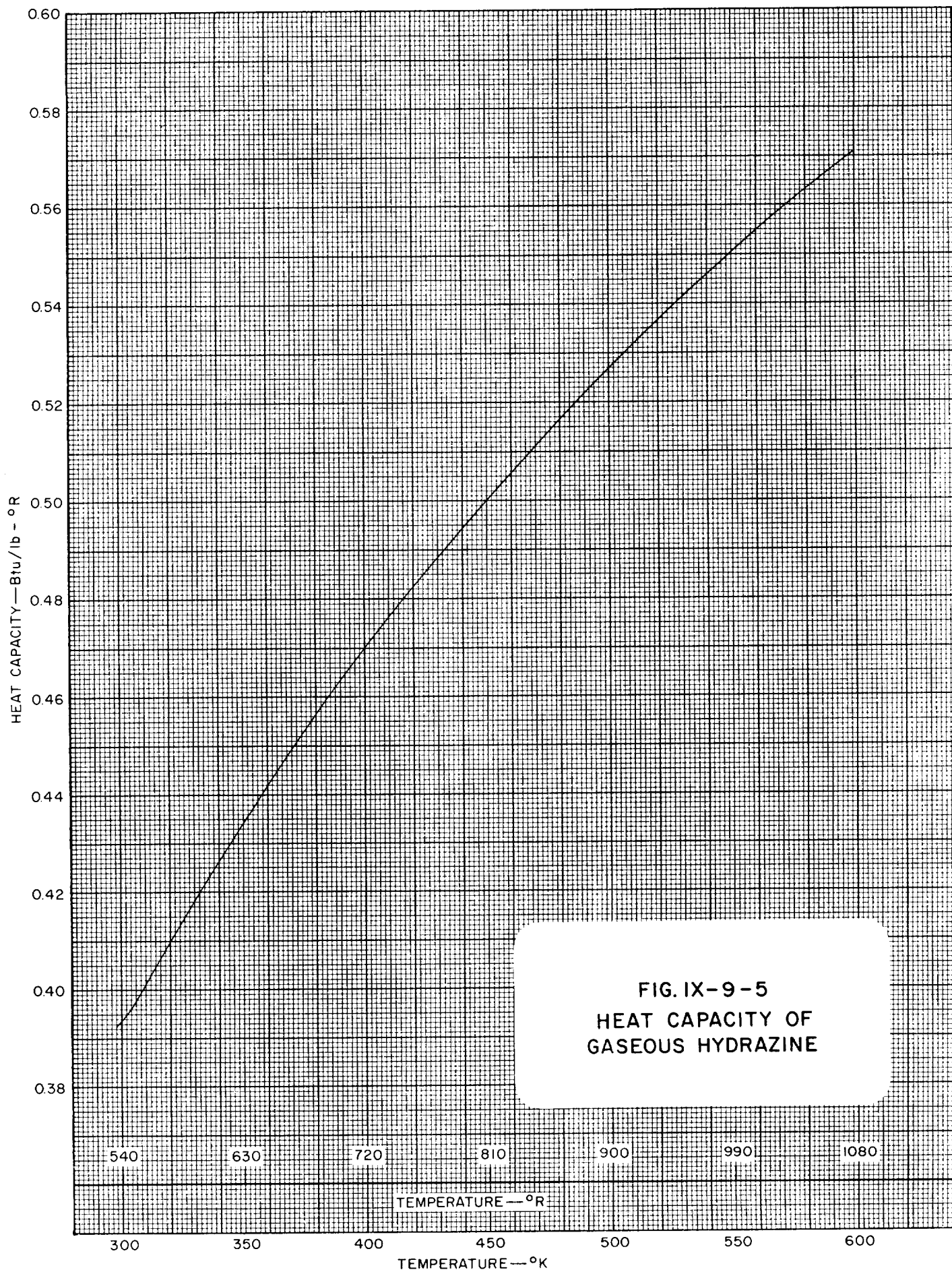
5











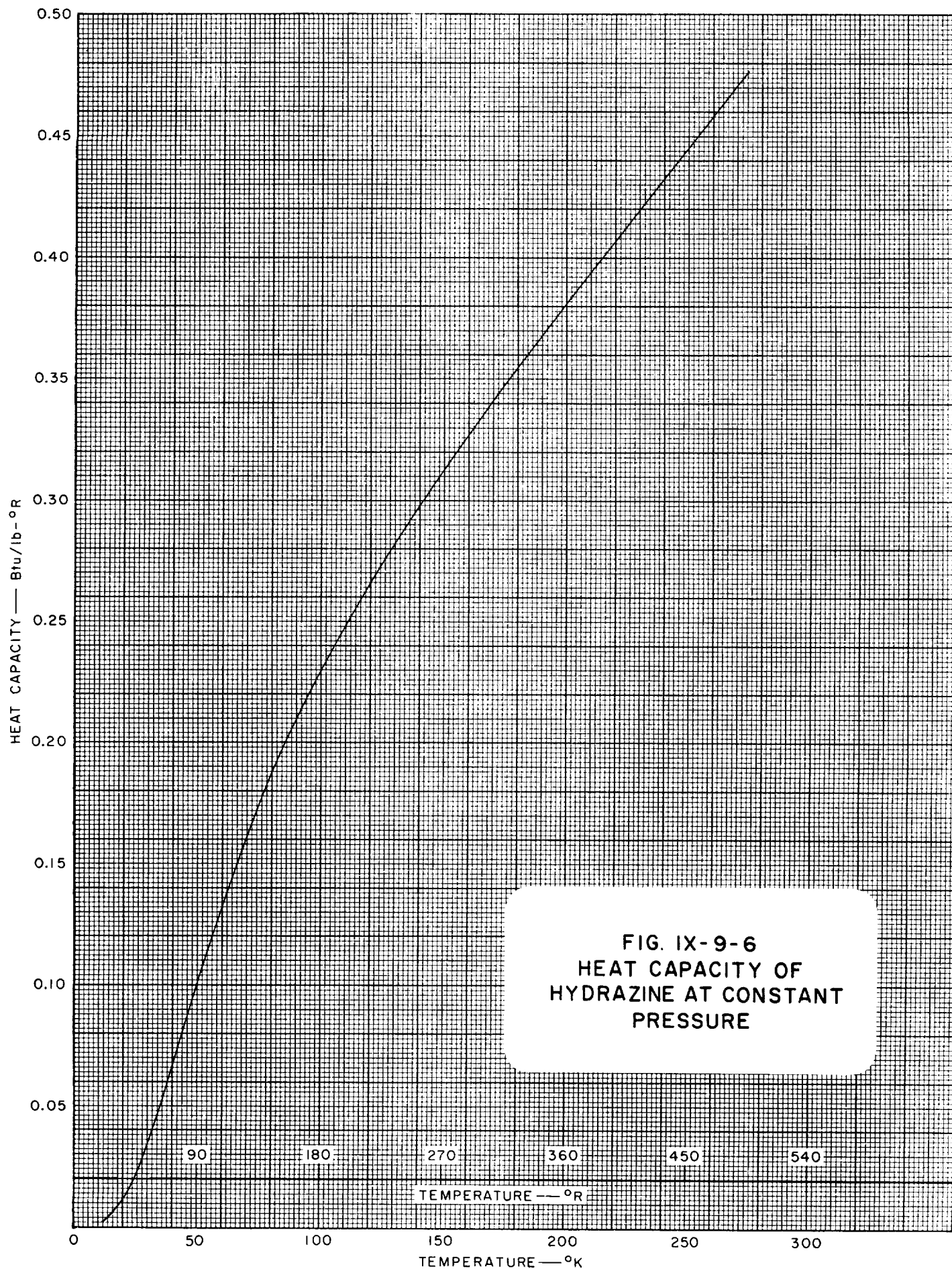
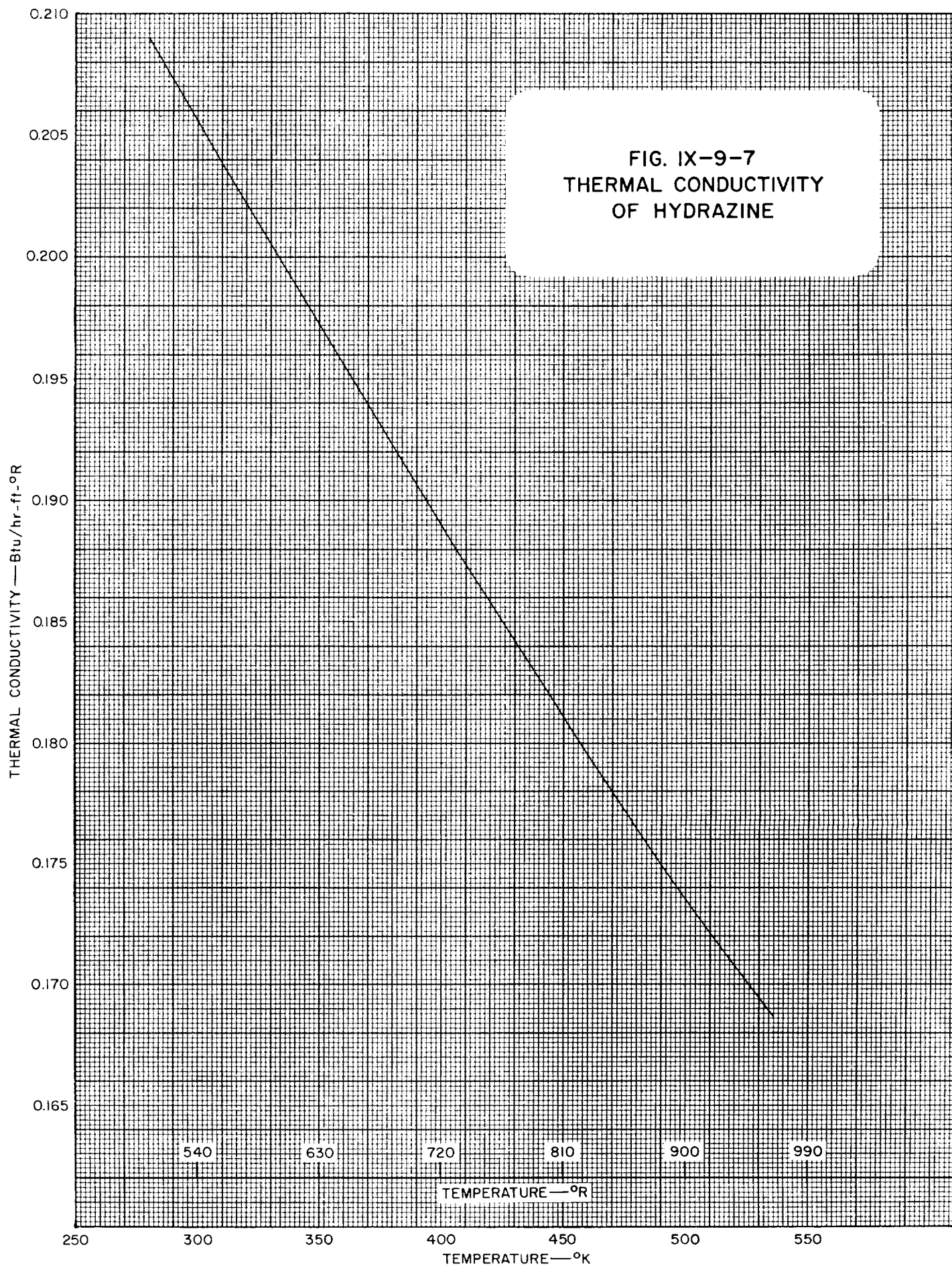


FIG. IX-9-7
THERMAL CONDUCTIVITY
OF HYDRAZINE



1

2

3

4

5

IX-9 HYDRAZINE REFERENCES

1. Ahlert, R. C., Bauerle, G. L., and Lecce, J. V., *J. Chem. Eng. Data*, **37**, No. 1, 158 (1962).
2. Hieber, W., and Woerner, A., *Z. Elektrochem.*, **40**, 252 (1934).
3. Lobrydebruyn, *Rec. trav. Chim.*, **15**, 174 (1896).
4. Mohr, P. H., and Audrieth, L. F., *J. Phys. & Colloid Chem.*, **53**, 901 (1949).
5. Scott, D. W., Oliver, G. D., Gross, M. E., Hubbard, W. N., and Huffman, H. M., *J. Am. Chem. Soc.*, **71**, 2293 (1949).
6. Weber, H. F., *Wiedeman's Ann.*, **10**, 103 (1880).

1

2

3

4

5

Table IX-10-1
GENERAL PROPERTIES OF NITROGEN (IV) OXIDE

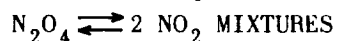
PROPERTY	TEMPERATURE				PRESSURE			REF
	°C	°K	°F	°R	psia	atm	mm of Hg	
Melting Point	- 11.2	261.95	11.84	471.51				1
Boiling Point	21.15	294.30	70.13	529.74				1
Triple Point	- 11.20	261.95	11.84	471.51				1
Critical Temp.	158.2	431.35	316.76	776.43				2
Critical Press.					1469.0	99.96		2
Mol. Wt.	46.01 (NO ₂)							
Heat of Vaporization.	99.00 cal/g at b.p. or 178.20 Btu/lb							1
Heat of Fusion	38.06 cal/g or 68.51 Btu/lb at triple point							1

Table IX-10-2
VAPOR PRESSURE OF N₂O₄ ⇌ 2 NO₂ SYSTEM (Ref. 1,3)

TEMPERATURE		VAPOR PRESSURE	TEMPERATURE		VAPOR PRESSURE
°K	°R	psia	°K	°R	psia
243.15	437.67	0.508	333.15	599.67	74.12
253.15	455.67	1.279	338.70	609.67	91.06
261.95	471.51	2.703 (m.p.)	344.26	619.67	111.24
263.15	473.67	2.893	349.82	629.67	135.14
273.15	491.67	5.078	355.37	639.67	163.29
283.15	509.67	8.555	360.93	649.67	196.35
293.15	527.67	13.925	366.48	659.67	235.01
294.30	529.74	14.696 (b.p.)	372.04	669.67	281.56
294.26	529.67	14.78	377.59	679.67	332.8
299.82	539.67	18.98	383.15	689.67	393.2
305.37	549.67	24.21	388.70	699.67	463.3
310.93	559.67	30.69	394.26	709.67	543.9
316.48	569.67	38.62	399.82	719.67	636.3
322.04	579.67	48.24	(See Figure IX-10-1)		
327.59	589.67	59.98			

Table IX-10-3

DENSITY OF EQUILIBRIUM



(Ref. 2)

TEMPERATURE		DENSITY--lb/ft ³	
^o K	^o R	Saturated Liquid	Saturated Gas
294.30	529.67	89.85	0.212
299.82	539.67	89.13	0.269
305.37	549.67	88.34	0.322
310.93	559.67	87.41	0.397
316.48	569.67	86.58	0.488
322.04	579.67	85.69	0.597
327.59	589.67	84.82	0.731
333.15	599.67	83.89	0.888
338.70	609.67	83.13	1.075
344.26	619.67	82.03	1.293
349.82	629.67	81.17	1.554
355.37	639.67	80.06	1.855
360.93	649.67	78.99	2.197
366.48	659.67	77.82	2.618
372.04	660.67	76.45	3.094
377.59	679.67	75.02	3.646
383.15	689.67	73.42	4.310
388.70	699.67	71.79	5.089
394.26	709.67	69.88	6.013
399.82	719.67	67.84	7.148

(See Figure IX-10-2
Figure IX-10-3)

Table IX-10-4

SPECIFIC HEAT OF THE $\text{N}_2\text{O}_4 \rightleftharpoons 2 \text{NO}_2$ SYSTEM

AT CONSTANT PRESSURE (Ref. 1)

TEMPERATURE		HEAT CAPACITY, C_p	TEMPERATURE		HEAT CAPACITY, C_p
^o K	^o R	Btu/lb-- ^o R	^o K	^o R	Btu/lb-- ^o R
20	36	0.02206	170	306	0.2147
30	54	0.04890	180	324	0.2224
40	72	0.07455	190	342	0.2302
50	90	0.09455	200	360	0.2382
60	108	0.1109	210	378	0.2463
70	126	0.1245	220	396	0.2544
80	144	0.1365	230	414	0.2625
90	162	0.1476	240	432	0.2705
100	180	0.1577	250	450	0.2785
110	198	0.1667	260	468 (solid)	0.2865
120	216	0.1755	270	486 (liquid)	0.3579
130	234	0.1837	280	504	0.3617
140	252	0.1916	290	522	0.3664
150	270	0.1995			
160	288	0.2072			

(See Figure IX-10-4)

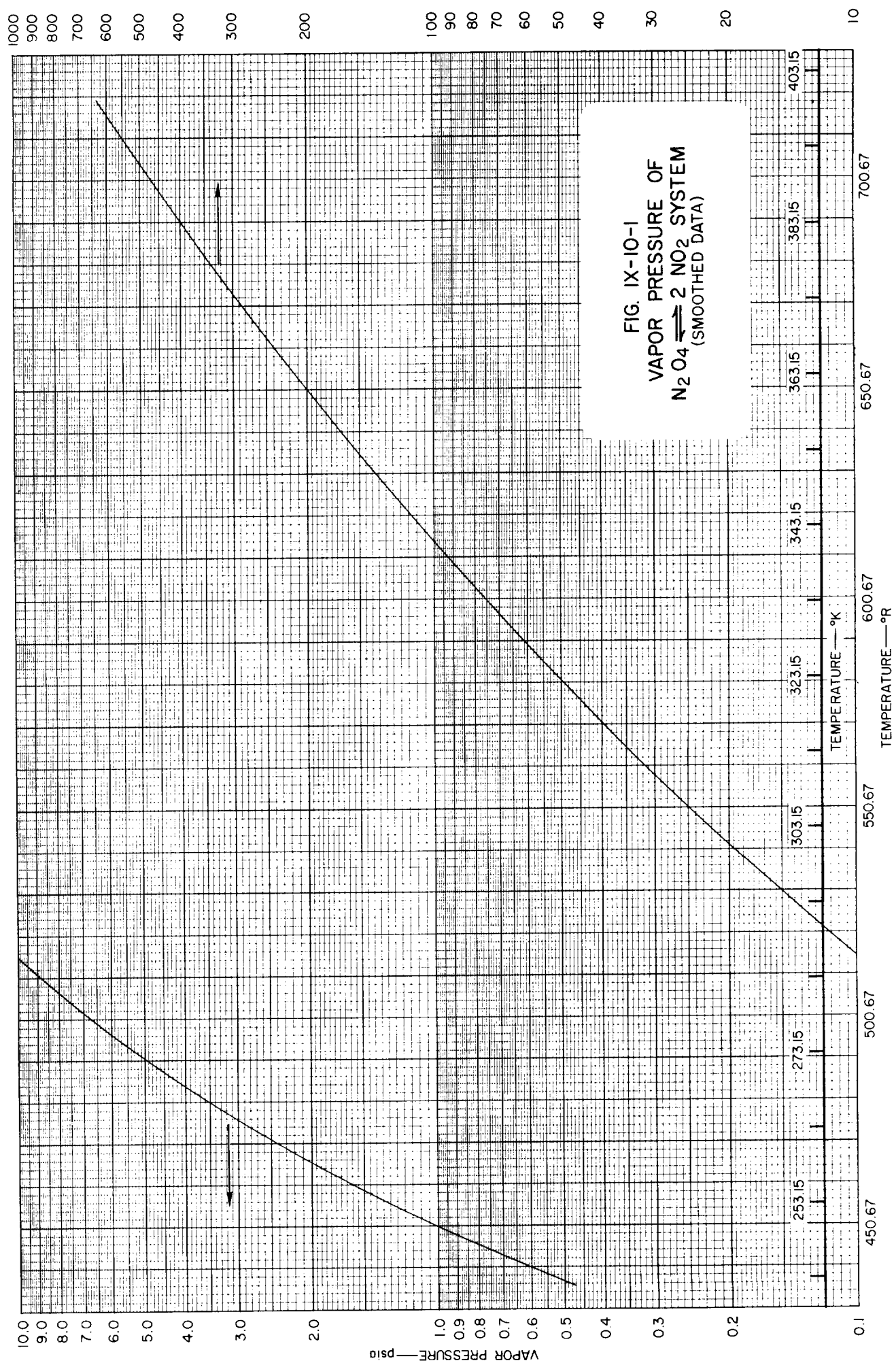
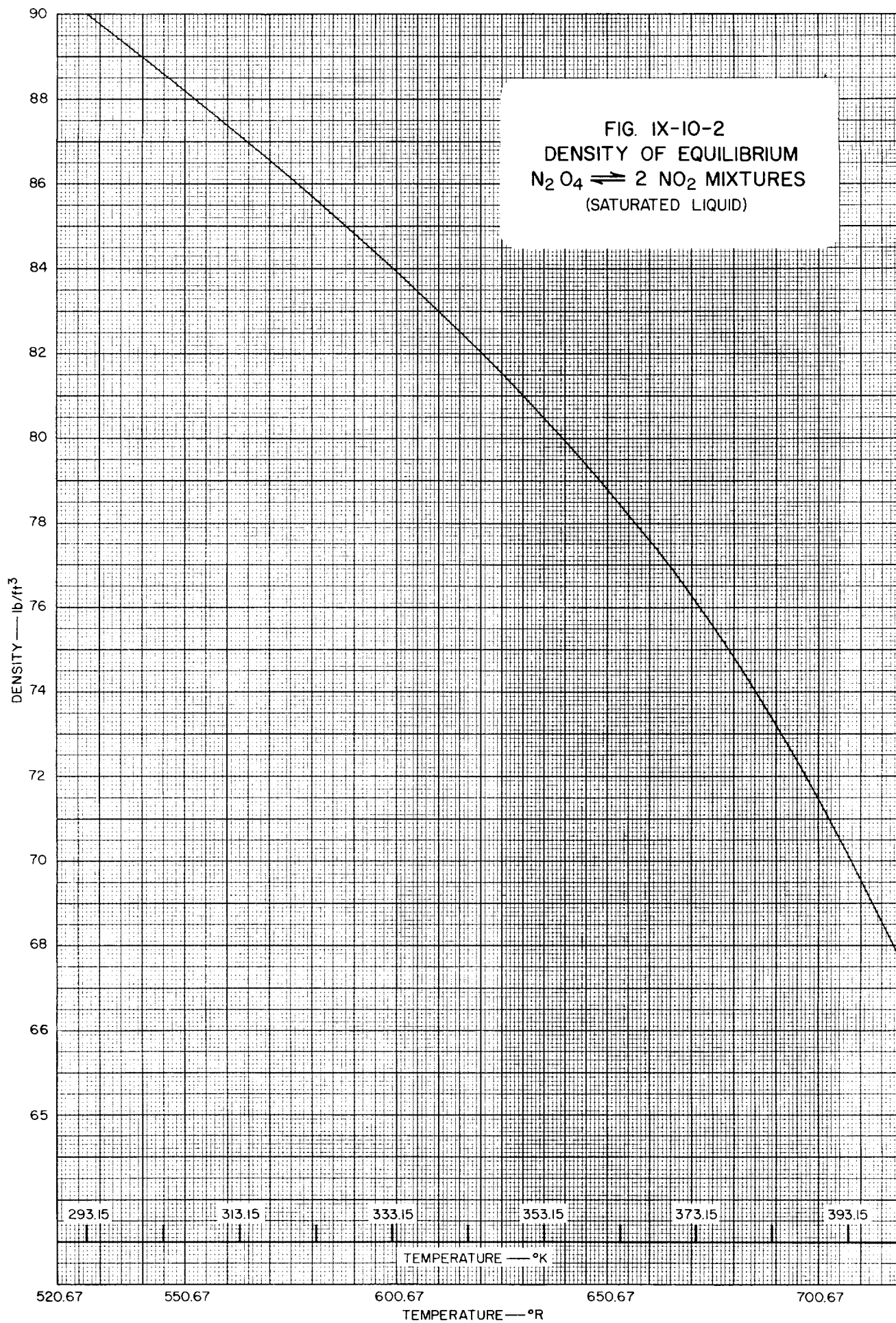
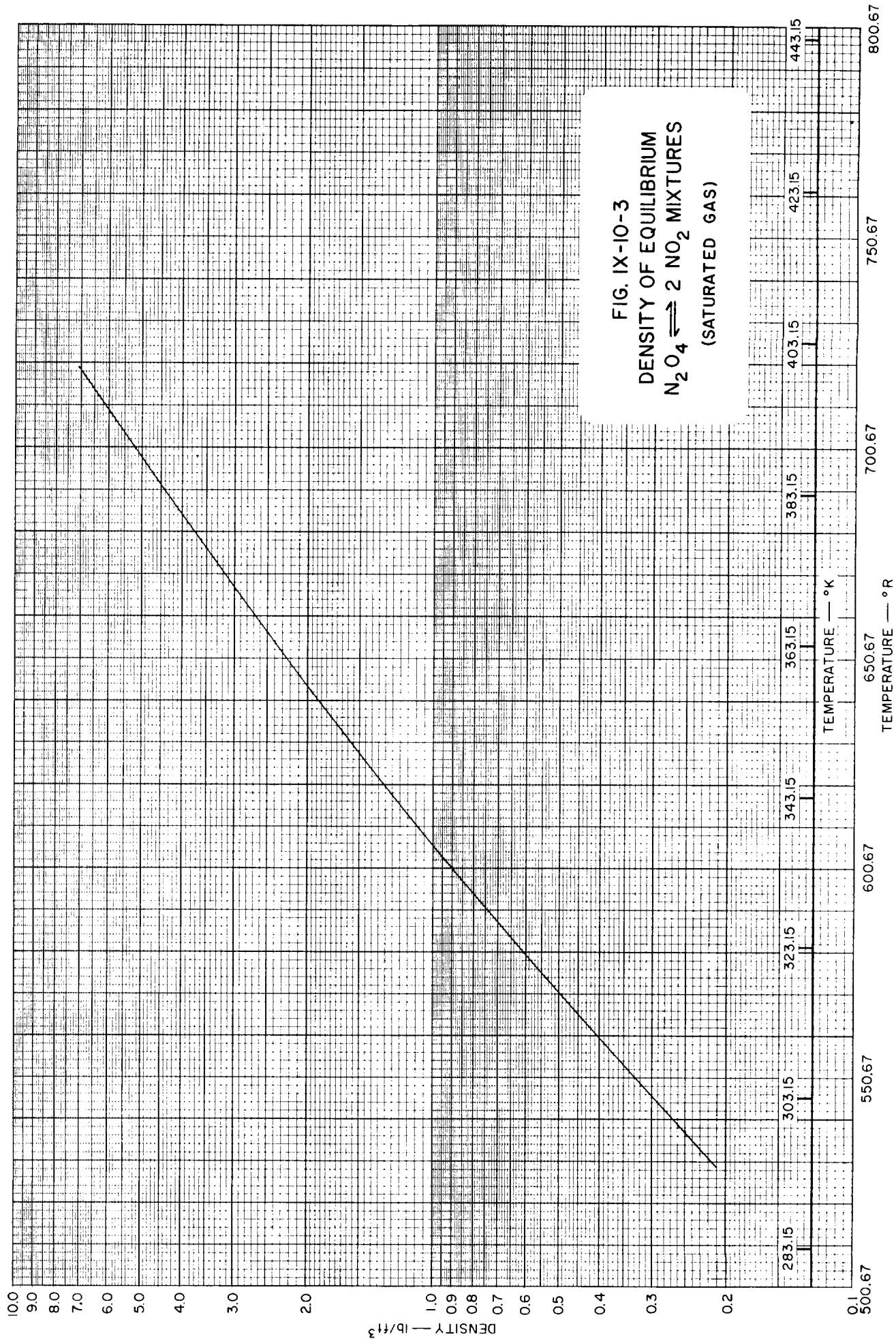
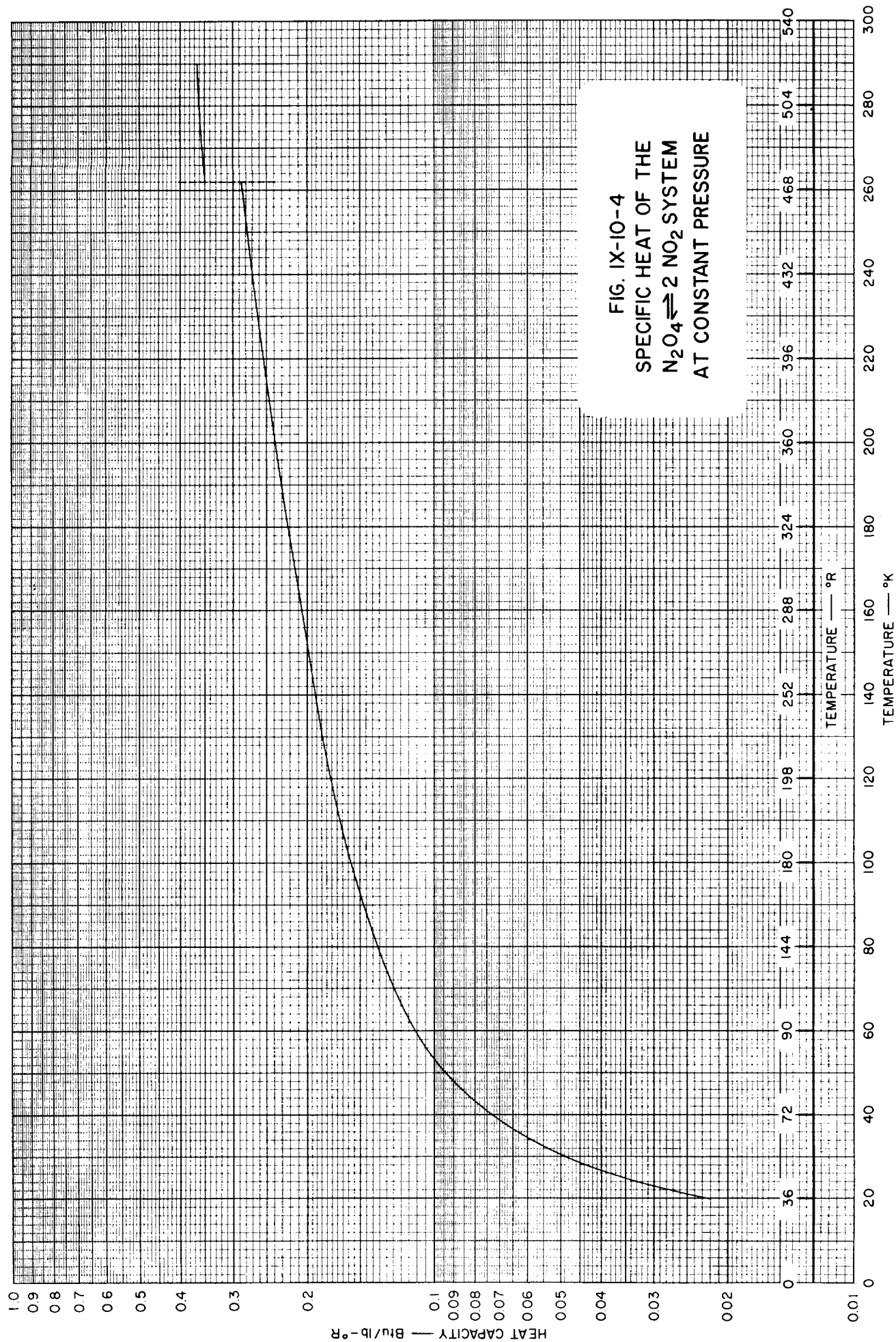


FIG. IX-10-2
DENSITY OF EQUILIBRIUM
 $\text{N}_2\text{O}_4 \rightleftharpoons 2 \text{NO}_2$ MIXTURES
(SATURATED LIQUID)







IX-10 NITROGEN (IV) OXIDE REFERENCES

1. Giauque, W. F., and Kemp, J. D., *J. Chem. Phys.*, **6**, 40 (1938).
2. Reamer, H. H., and Sage, B. H., *Ind. Eng. Chem.*, **44**, 185 (1952).
3. Schlinger, W. G., and Sage, B. H., *Ind. Eng. Chem.*, **42**, 2168 (1950).

Table IX-11-1
GENERAL PROPERTIES OF UDMH
(Unsymmetrical Dimethyl Hydrazine)

PROPERTY	TEMPERATURE				PRESSURE			REF
	°C	°K	°F	°R	psia	atm	mm of Hg	
Melting Point	- 57.21	215.94	- 70.98	388.69				1
Boiling Point	63.4	336.6	146.2	605.9				1
Triple Point	- 57.21	215.94	- 70.98	388.69				1
Critical Temp.	249	522	480	940	882	60	45,600	1
Critical Press.								
Mol. Wt.	60.10							
Heat of Vaporization	139.3 cal/g or 250.6 Btu/lb at 25°C							1
Heat of Fusion	40.06 cal/g or 72.11 Btu/lb							1

Table IX-11-1.1
SOME VALUES OF THE GAS CONSTANT, *R*, FOR UDMH
(See also Conversion Tables, Section I)

TEMPERATURE IN °K				
Pressure	atm	kg/cm ²	mm of Hg	lb/in ²
Density				
g/cm ³	1.36534	1.41070	1037.66	20.0651
mole/cm ³	82.0567	84.7832	62363.1	1205.91
mole/liter	0.0820544	0.0847809	62.3613	1.20587
lb/ft ³	0.0218704	0.0225970	16.6215	0.321408
lb/mole/ft ³	1.31441	1.35808	998.952	19.3166
TEMPERATURE IN °R				
Pressure	atm	kg/cm ²	mm of Hg	lb/in ²
Density				
g/cm ³	0.758520	0.783723	576.475	11.1473
mole/cm ³	45.5871	47.1018	34646.2	669.950
mole/liter	0.0455858	0.0471005	34.6452	0.669928
lb/ft ³	0.0121502	0.0125539	9.23416	0.178559
lb/mole/ft ³	0.730228	0.754489	554.973	10.7314

Table IX-11-2
VAPOR PRESSURE OF UDMH
(Ref. 1)

TEMPERATURE		PRESSURE	
$^{\circ}\text{K}$	$^{\circ}\text{R}$	psia	atm
220	396	0.0136	0.0009
230	414	0.0348	0.0024
240	432	0.081	0.0055
250	450	0.175	0.0119
260	468	0.351	0.0239
270	486	0.663	0.0451
280	504	1.19	0.0808
290	522	2.02	0.138
300	540	3.31	0.225
310	558	5.19	0.353
320	576	7.88	0.536
330	594	11.58	0.788
340	612	16.53	1.125
350	630	23.01	1.566
360	648	31.25	2.126
370	666	41.56	2.828
380	684	54.16	3.686

(See Figure IX-11-1)

Table IX-11-3
DENSITY OF LIQUID UDMH (Ref. 2)

TEMPERATURE		DENSITY	TEMPERATURE		DENSITY
°K	°R	lb/ft ³	°K	°R	lb/ft ³
212.5	382.5	54.64	271.4	488.5	50.95
218.2	392.8	54.22	273.2	491.8	50.89
222.9	401.2	53.96	273.2	491.8	50.72
228.2	410.8	53.56	282.0	507.6	50.26
233.9	421.0	53.32	283.2	509.8	50.06
238.2	428.8	52.97	287.0	516.6	49.75
242.5	436.5	52.76	287.3	517.1	49.89
248.2	446.8	52.30	298.2	536.8	49.08
249.4	448.9	52.45	323.2	581.8	48.39
252.7	454.9	52.08	328.2	590.8	47.58
258.2	464.8	51.69	333.2	599.8	46.96
262.1	471.8	51.51			
268.2	482.8	51.05			

(See Figure IX-11-2)

Table IX-11-4
VISCOSITY OF UDMH (Ref. 2)

TEMPERATURE		ABSOLUTE VISCOSITY
°K	°R	centipoises
218	393	5.114
228	411	3.078
238	429	2.026
248	447	1.462
258	465	1.108
268	483	0.878
273	492	0.783
283	510	0.645
287	517	0.601
298	537	0.509
311	560	0.413
317	571	0.382
322	580	0.356
327	589	0.336
333	600	0.316

(See Figure IX-11-3)

Table IX-11-5
HEAT CAPACITY OF UDMH (Ref. 1)

TEMPERATURE		C _p Btu/lb-°R	TEMPERATURE		C _p Btu/lb-°R
°K	°R		°K	°R	
13	23.4	0.0108	145	261	0.2706
14	25.2	0.0134	150	270	0.2775
15	27.0	0.0158	155	279	0.2846
16	28.9	0.0184	160	288	0.2915
17	30.6	0.0213	165	297	0.2984
18	32.4	0.0243	170	306	0.3052
19	34.2	0.0273	175	315	0.3118
20	36.0	0.0303	180	324	0.3182
21	37.8	0.0333	185	333	0.3254
22	39.6	0.0363	190	342	0.3324
23	41.4	0.0393	195	351	0.3399
24	43.2	0.0423	200	360	0.3475
25	45.0	0.0453	205	369	0.3555
30	54.0	0.0623	210	378	0.3640
35	63.0	0.0784	215	387	0.3722
40	72.0	0.0925	215.95	388.7	0.3738 crystal
45	81.0	0.1056			fusion
50	90.0	0.1180	215.95	388.7	0.6034 liquid
55	99.0	0.1292	220	396	0.6059
60	108.0	0.1385			
65	117.0	0.1483	225	405	0.6100
70	126.0	0.1578	230	414	0.6135
75	135.0	0.1666	235	423	0.6172
80	144.0	0.1754	240	432	0.6202
85	153.0	0.1840	245	441	0.6232
90	162.0	0.1915	250	450	0.6258
95	171.0	0.1987	255	459	0.6285
100	180.0	0.2061	260	468	0.6325
105	189.0	0.2133	265	477	0.6337
110	198.0	0.2206	270	486	0.6363
115	207.0	0.2277	275	495	0.6391
120	216.0	0.2350	280	504	0.6423
125	225.0	0.2423	285	513	0.6455
130	234.0	0.2495	290	522	0.6483
135	243.0	0.2566	295	531	0.6510
140	252.0	0.2636	298.16	536.6	0.6526

(See Figure IX-11-4)

Table IX-11-6
THERMAL CONDUCTIVITY OF UDMH
(Ref. 2,3)

TEMPERATURE		THERMAL CONDUCTIVITY
$^{\circ}\text{K}$	$^{\circ}\text{R}$	Btu/hr-ft- $^{\circ}\text{R}$
227.8	410	0.1094
255.6	460	0.1080
283.3	510	0.1053
311.1	560	0.1024
338.9	610	0.0990
366.7	660	0.0960
394.4	710	0.0930

(See Figure IX-11-5)

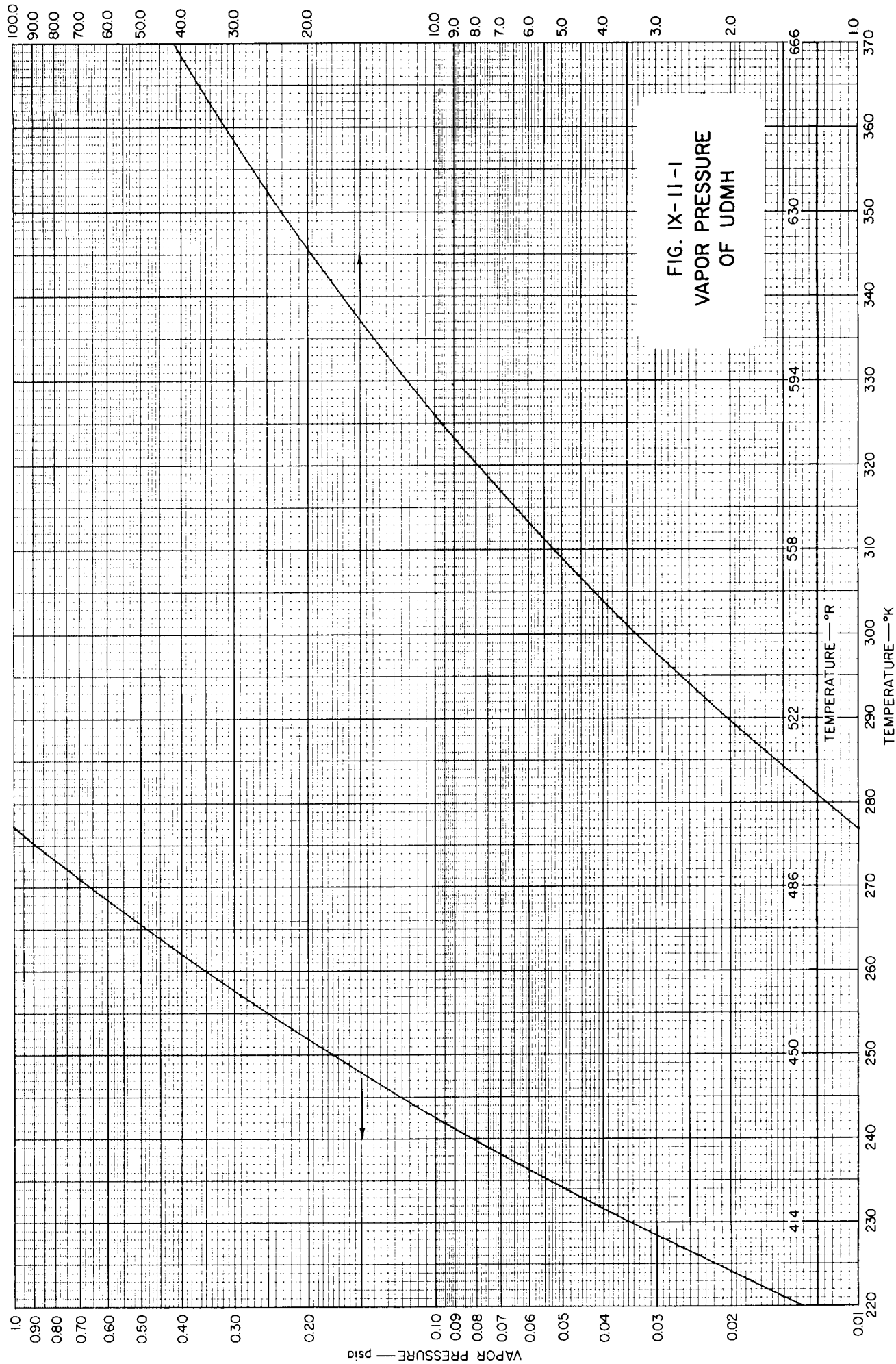
)

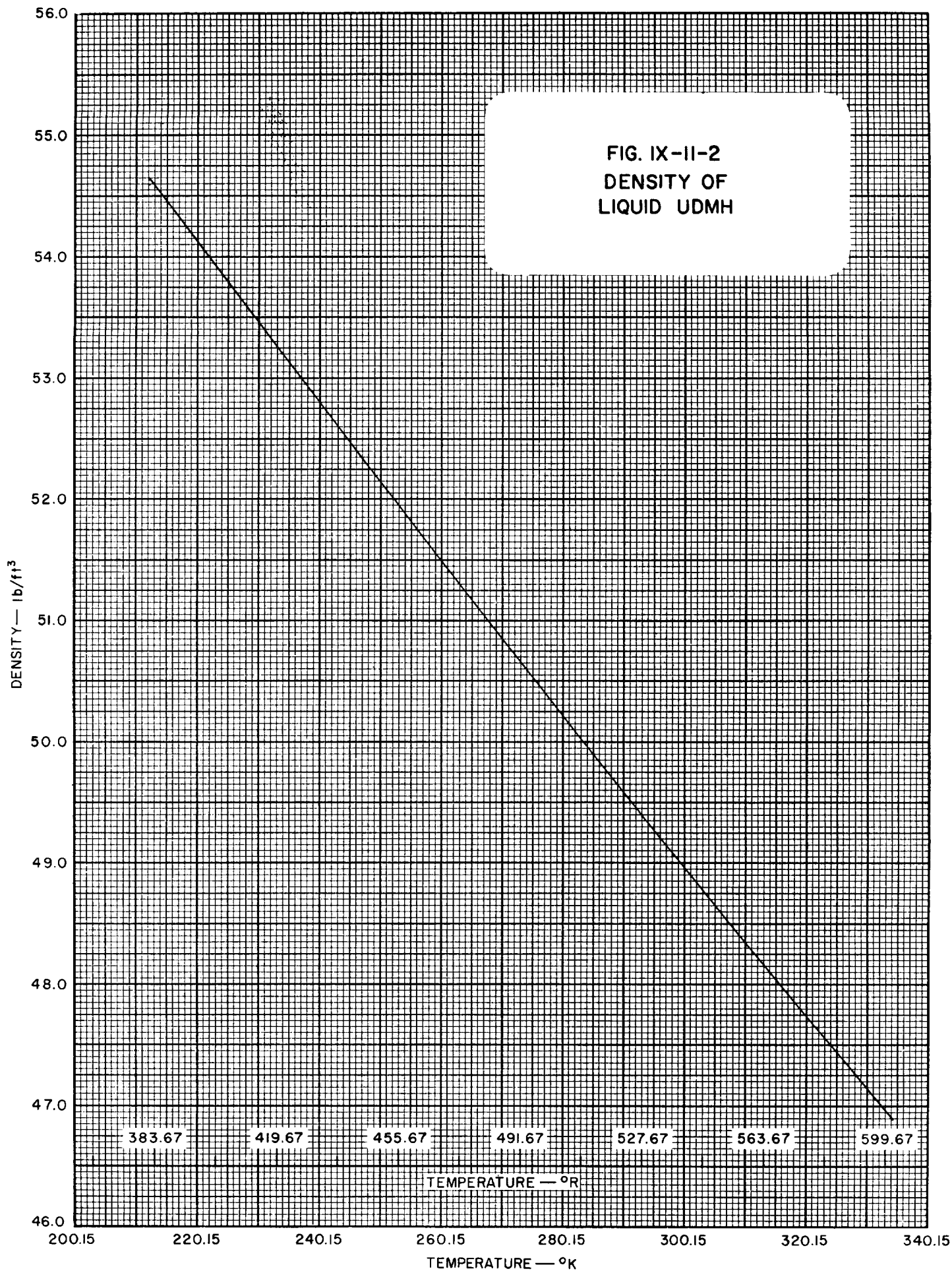
)

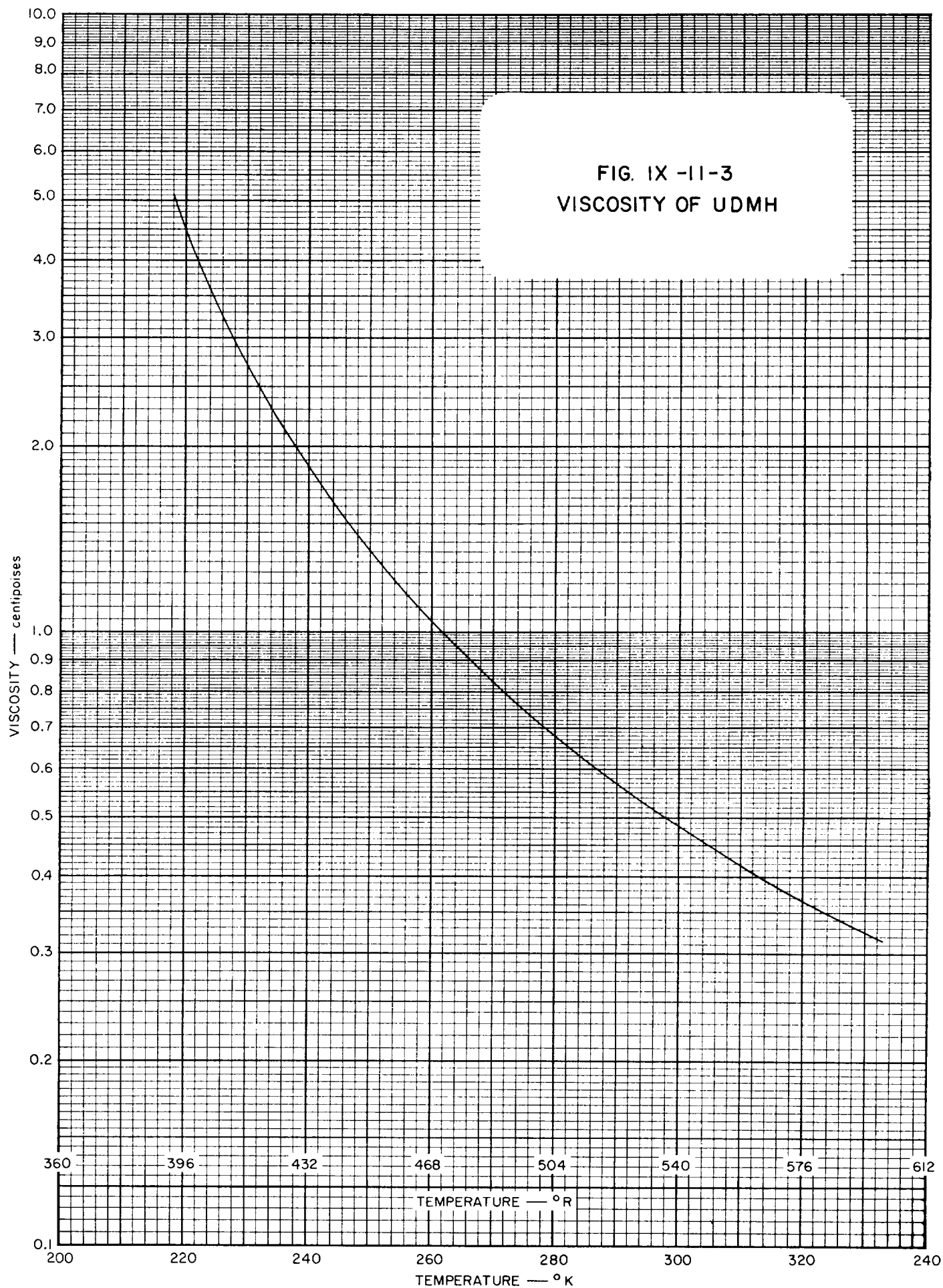
)

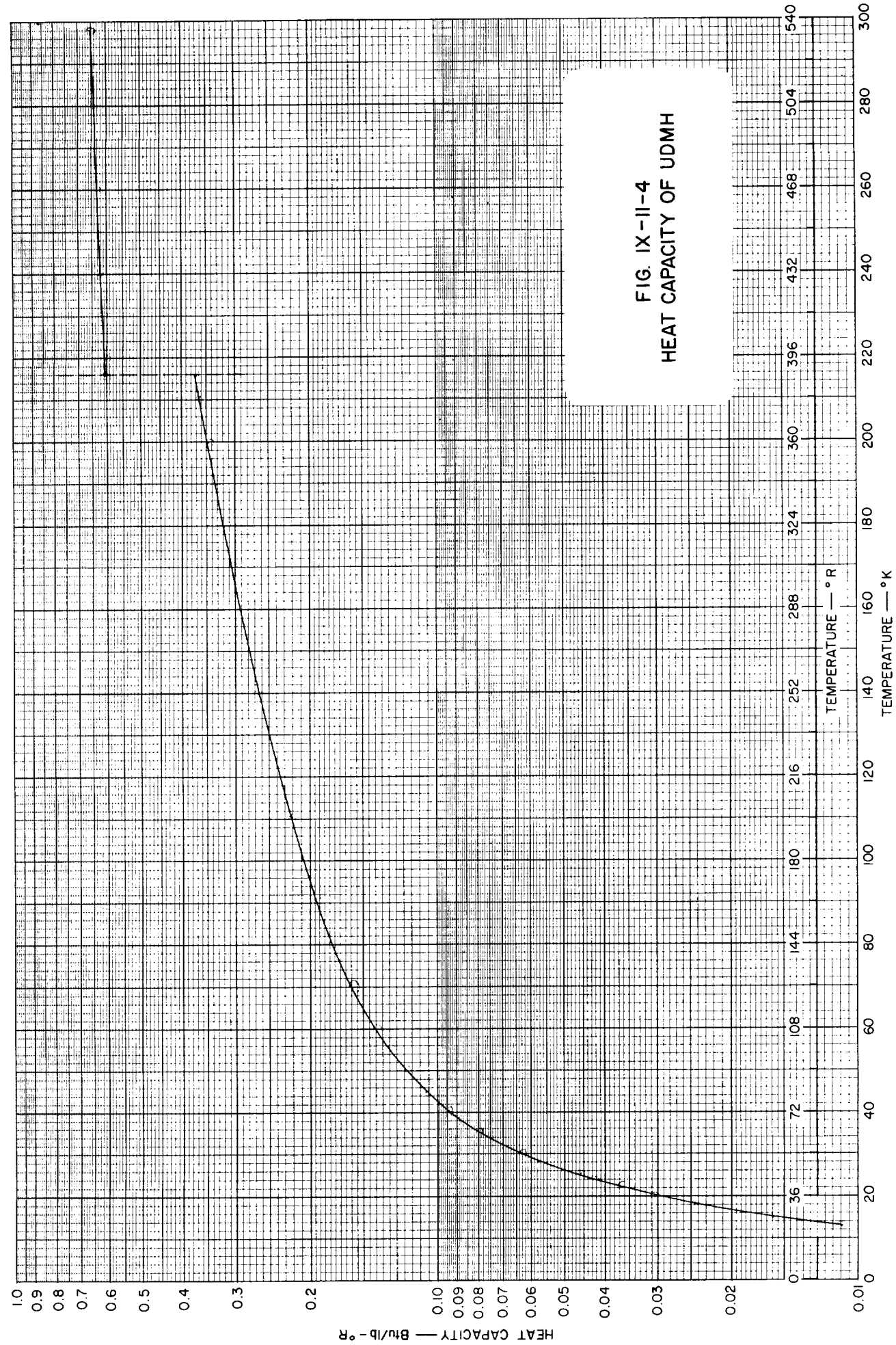
)

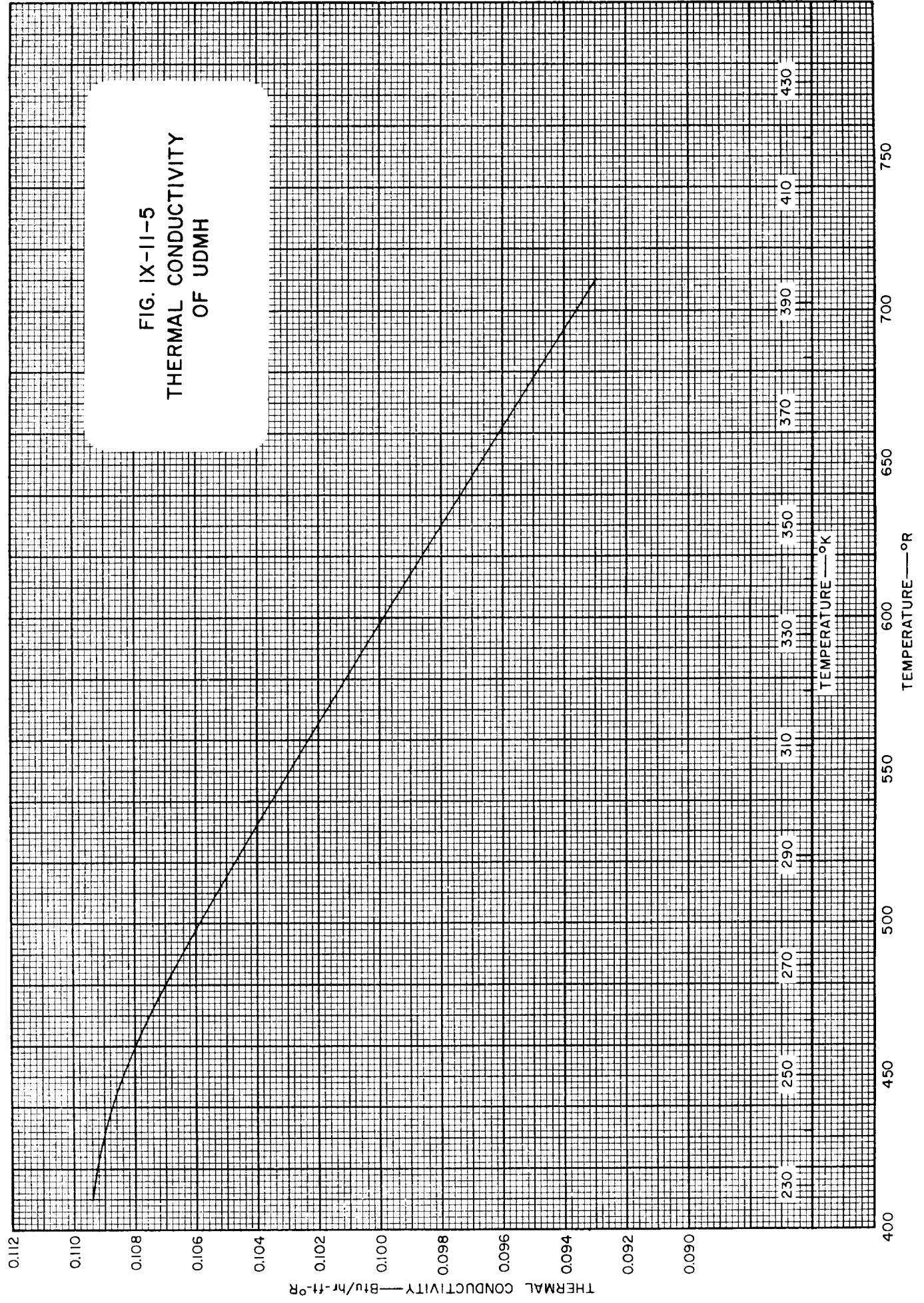
)











)

)

)

)

)

IX-11 UDMH REFERENCES

1. Aston, J. G., Wood, J. L., and Zolki, T. P., *J. Am. Chem. Soc.*, **75**, 6202 (1953).
2. Petrozzi, P. J., and Dean, L. E., Aerojet-General Corp., *Report No. LRP-178*, 13 July 1960.
3. Weber, H. F., *Wiedeman's Ann.*, **10**, 103 (1880).

)

)

)

)

)

Table IX-12-1
GENERAL PROPERTIES OF WATER

PROPERTY	TEMPERATURE				PRESSURE			REF
	°C	°K	°F	°R	psia	atm	mm of Hg	
Melting Point	0.00	273.15	32.0	491.67				6
Boiling Point	100.000	373.15	212.0	671.67				6
Triple Point	0.0099	273.16	32.02	491.69	0.0886	0.00603		6
Critical Temp.	374.15	647.30	705.47	1165.14				6
Critical Press.					3209.46	218.39		6
Mol. Wt.	18.016							
Heat of Vaporization	582.3 cal/g at 25°C or 1048.1 Btu/lb @ 77							6
Heat of Fusion	79.71 cal/g or 143.4 Btu/lb							8

Table IX-12-1.1
SOME VALUES OF THE GAS CONSTANT, *R*, FOR WATER
(See also Conversion Tables, Section I)

TEMPERATURE IN °K				
Pressure Density	atm	kg/cm ²	mm of Hg	lb/in ²
g/cm ³	4.55466	4.70660	3461.54	66.9353
mole/cm ³	82.0567	84.7832	62363.1	1205.91
mole/liter	0.0820544	0.0847809	62.3613	1.20587
lb/ft ³	0.0729579	0.0753821	55.4480	1.07219
lb/mole/ft ³	1.31441	1.35808	998.952	19.3166
TEMPERATURE IN °R				
Pressure Density	atm	kg/cm ²	mm of Hg	lb/in ²
g/cm ³	2.53037	2.61444	1923.08	37.1863
mole/cm ³	45.5871	47.1018	34646.2	669.950
mole/liter	0.0455853	0.0471005	34.6452	0.669928
lb/ft ³	0.0405322	0.0418789	30.8044	0.595661
lb/mole/ft ³	0.730228	0.754489	554.973	10.7314

Table IX-12-2
VAPOR PRESSURE OF ICE
(Ref. 4)

TEMPERATURE		VAPOR PRESSURE
$^{\circ}\text{K}$	$^{\circ}\text{R}$	atm
154	277.2	0.0000000001
155	279.0	0.0000000003
160	288.0	0.0000000008
170	306.0	0.0000000007
180	324.0	0.000000005
190	342.0	0.000000032
200	360.0	0.00000158
210	378.0	0.00000687
220	396.0	0.0000262
230	414.0	0.0000883
240	432.0	0.0002696
250	450.0	0.000751
260	468.0	0.001933
270	486.0	0.004633
273	491.4	0.005946

(See Figure IX-12-1)

Table IX-12-3
VAPOR PRESSURE OF WATER (Ref. 4)

TEMPERATURE		VAPOR PRESSURE	TEMPERATURE		VAPOR PRESSURE
°K	°R	atm	°K	°R	atm
274	493.2	0.006406	420	756	4.3127
275	495	0.006883	440	792	7.2372
280	504	0.009774	460	828	11.554
290	522	0.018917	480	864	17.670
300	540	0.034844	500	900	26.050
320	576	0.10388			
340	612	0.26785			
360	648	0.61290			
380	684	1.2702			
400	720	2.4232			

(See Figure IX-12-2)

Table IX-12-4
ABSOLUTE DENSITY OF WATER (Ref. 3)

TEMPERATURE		ABSOLUTE DENSITY	TEMPERATURE		ABSOLUTE DENSITY
°K	°R	lb/ft ³	°K	°R	lb/ft ³
273.15	491.67	62.420	373.15	671.67	59.830
283.15	509.67	62.411	393.15	707.67	58.89
293.15	527.67	62.318	413.15	743.67	57.83
303.15	545.67	62.158	433.15	779.67	56.65
313.15	563.67	61.944	453.15	815.67	55.35
323.15	581.67	61.684	473.15	851.67	53.86
333.15	599.67	61.382	493.15	887.67	52.3
343.15	617.67	61.043	503.15	905.67	51.4
343.15	635.67	60.670			
363.15	653.67	60.265			

(See Figure IX-12-3)

Table IX-12-5
DENSITY OF STEAM
(Ref. 4)

TEMPERATURE		DENSITY—lb/ft ³	
°K	°R	1 atm	10 atm
380	684	0.0366	
390	702	0.0356	
400	720	0.0346	
420	756	0.0329	
440	792	0.0314	
460	828	0.0300	0.319
480	864	0.0287	0.302
500	900	0.0275	0.287

(See Figure IX-12-4)

Table IX-12-6
SURFACE TENSION OF WATER
IN CONTACT WITH AIR
(Ref. 2)

TEMPERATURE		SURFACE TENSION
°K	°R	dynes/cm
273.15	491.67	75.60
283.15	509.67	74.22
293.15	527.67	72.75
303.15	545.67	71.18
313.15	563.67	69.56
323.15	581.67	67.91
333.15	599.67	66.19
343.15	617.67	64.4
353.15	635.67	62.6
363.15	653.67	60.7
373.15	671.67	58.8
383.15	689.67	56.8*
393.15	707.67	54.8*
403.15	725.67	52.8*

* In contact with steam

(See Figure IX-12-5)

Table IX-12-7
VISCOSITY OF WATER (Ref. 3)

TEMPERATURE		ABSOLUTE VISCOSITY	TEMPERATURE		ABSOLUTE VISCOSITY
°K	°R	centipoises	°K	°R	centipoises
273.15	491.67	1.7291	373.15	671.67	0.2838
283.15	509.67	1.3077	383.15	689.67	0.256
293.15	527.67	1.0050	393.15	707.67	0.232
303.15	545.67	0.8007	403.15	725.67	0.212
313.15	563.67	0.6560	413.15	743.67	0.196
323.15	581.67	0.5494	423.15	761.67	0.184
333.15	599.67	0.4688	433.15	779.67	0.174
343.15	617.67	0.4061			
353.15	635.67	0.3565			
363.15	653.67	0.3165			

(See Figure IX-12-6)

Table IX-12-8
VISCOSITY OF STEAM
AT ONE ATMOSPHERE
(Ref. 4)

TEMPERATURE		ABSOLUTE VISCOSITY
°K	°R	centipoises
280	504	0.00909
300	540	0.00981
320	576	0.01053
340	612	0.01125
360	648	0.01198
380	684	0.01270
400	720	0.01342
420	756	0.01414
440	792	0.01486
460	828	0.01559
480	864	0.01631
500	900	0.01703

(See Figure IX-12-7)

Table IX-12-9
HEAT CAPACITY OF ICE (Ref. 2)

TEMPERATURE		HEAT CAPACITY, C_p	TEMPERATURE		HEAT CAPACITY, C_p
$^{\circ}\text{K}$	$^{\circ}\text{R}$	Btu/lb- $^{\circ}\text{R}$	$^{\circ}\text{K}$	$^{\circ}\text{R}$	Btu/lb- $^{\circ}\text{R}$
20	36	0.0272	160	288	0.3081
30	54	0.0546	170	306	0.3244
40	72	0.0814	180	324	0.3409
50	90	0.1052	190	342	0.3574
60	108	0.1279	200	360	0.3743
70	126	0.1499	210	378	0.3926
80	144	0.1707	220	396	0.4103
90	162	0.1914	230	414	0.4275
100	180	0.2107	240	432	0.4448
110	198	0.2292	250	450	0.4622
120	216	0.2461	260	468	0.4797
130	234	0.2624	270	486	0.4974
140	252	0.2772	273	491	0.504
150	270	0.2922			

(See Figure IX-12-8)

Table IX-12-10
HEAT CAPACITY OF WATER (Ref. 1, 2)

TEMPERATURE		HEAT CAPACITY, C_p Btu/lb- $^{\circ}\text{R}$	
$^{\circ}\text{K}$	$^{\circ}\text{R}$	1 atm	48.4 atm
273.15	491.67	1.0071	1.004
293.15	527.67	0.9985	0.9959
313.15	563.67	0.9975	0.9940
333.15	599.67	0.9989	0.9950
353.15	635.67	1.000	0.9990
373.15	671.67	1.002	1.004
393.15	707.67	1.014	1.011
413.15	743.67	1.0206	1.019
433.15	779.67	1.0275	1.033
453.15	815.67	1.0357	1.050
473.15	851.67	1.0439	1.071

(See Figure IX-12-9)

Table IX-12-11
HEAT CAPACITY OF STEAM
(Ref. 4)

TEMPERATURE		HEAT CAPACITY, C_p Btu/lb-°R	
°K	°R	1 atm	10 atm
380	684	0.492	
390	702	0.485	
400	720	0.480	
420	756	0.475	
440	792	0.473	
460	828	0.472	0.619
480	864	0.472	0.577
500	900	0.473	0.550

(See Figure IX-12-10)

Table IX-12-12
THERMAL CONDUCTIVITY OF WATER
(Ref. 2)

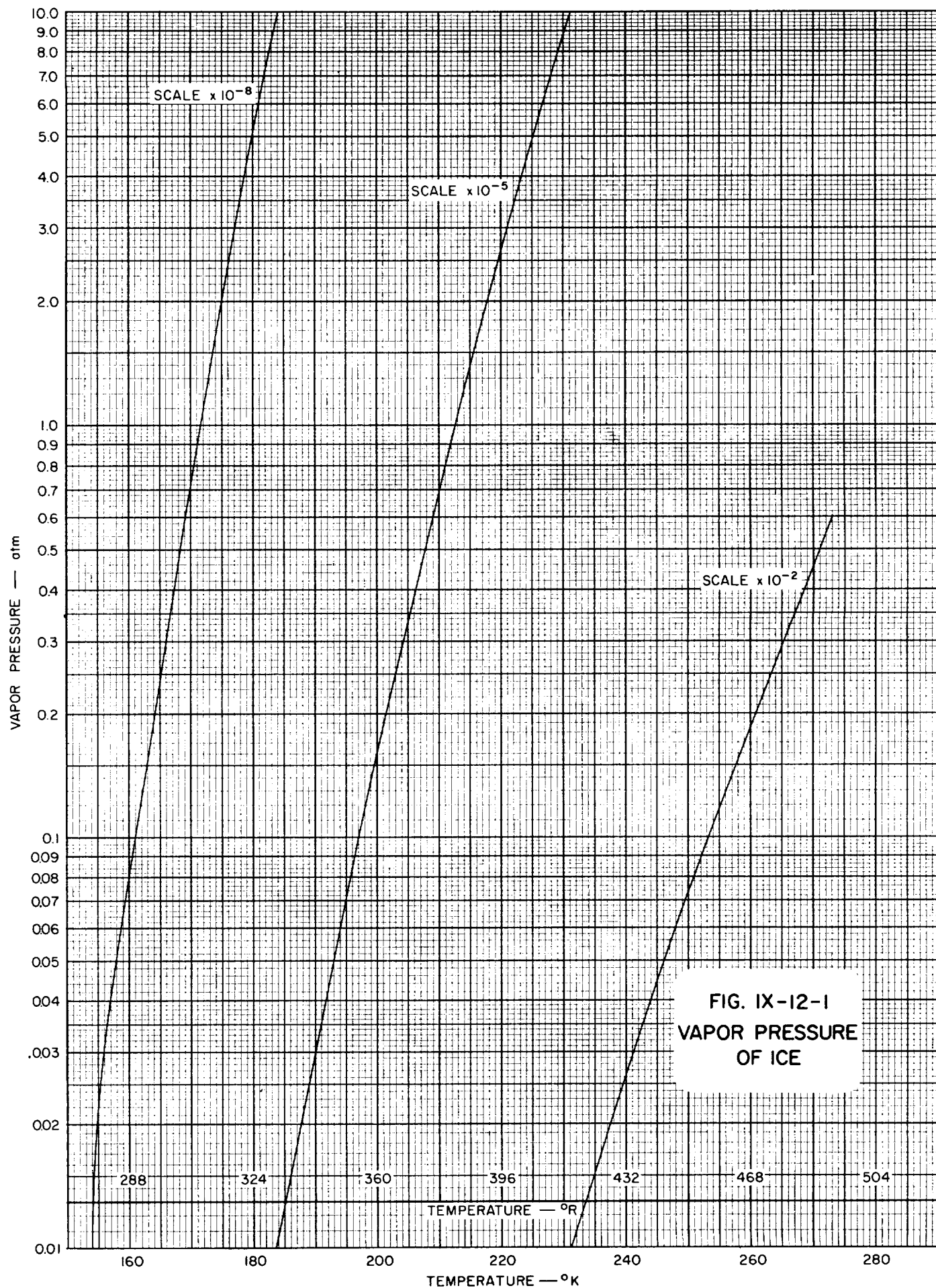
TEMPERATURE		THERMAL CONDUCTIVITY
°K	°R	Btu/hr-ft-°R
273.15	491.67	0.320
283.15	509.67	0.333
293.15	527.67	0.346
303.15	545.67	0.356
313.15	563.67	0.364
323.15	581.67	0.372
333.15	599.67	0.378
343.15	617.67	0.385
353.15	635.67	0.388
363.15	653.67	0.391
373.15	671.67	0.393
393.15	707.67	0.397
413.15	743.67	0.397
433.15	779.67	0.395
453.15	815.67	0.391
473.15	851.67	0.385

(See Figure IX-12-12)

Table IX-12-13
TOTAL ENTHALPY VALUES AND SPECIFIC VOLUMES FOR THE WATER SYSTEM

TEMP.	TOTAL ENTHALPY—Btu/lb			SP. VOL. VAPOR	TEMP.	TOTAL ENTHALPY—Btu/lb			SP. VOL. VAPOR
^o R	Ice	Water	Vapor	ft ³ /lb	^o R	Ice	Water	Vapor	ft ³ /lb
600		381.9	1395.52	122.61	475	121.8	256.8	1340.9	5,498.55
595		375.9	1393.63	138.42	470	119.1	251.8	1338.7	6,996.49
590		371.9	1391.68	156.67	465	116.6	246.7	1336.7	8,950.55
585		366.9	1389.65	177.78	460	114.1	241.7	1334.7	11,258.4
580		361.9	1387.60	202.18	455	111.7	236.7	1332.7	18,616.4
575		356.9	1385.48	230.58	450	109.3	231.7	1330.7	24,271.2
570		351.9	1383.35	263.69	445	107.0	226.7	1328.7	31,623.1
565		346.9	1381.19	302.52	440	104.7	221.8	1326.7	41,473.2
560		341.9	1377.99	347.85	435	102.4	216.7	1324.7	54,908.4
555		336.9	1376.75	401.21	430	100.2	211.7	1322.8	72,816.0
550		331.8	1374.50	464.23	425	98.1	206.6	1320.9	97,481
545		326.8	1372.15	538.62	420	96.0	201.2	1319.0	130,866
540		321.8	1369.98	627.75	415	93.8	194.2	1317.1	171,181
535		316.8	1367.83	733.31	410	91.7	181.1	1315.2	244,227
530		311.8	1365.70	859.69	405	89.6	141.0	1313.4	336,167
525		306.7	1363.51	1012.75	400	87.6		1310.6	466,928
520		301.8	1361.32	1195.41	390	83.5		1305.3	929,255
515		296.7	1359.12	1416.49	380	79.4		1300.	1,915,177
510		291.7	1356.88	1685.27	360	71.4		1290.	9,229,215
505		286.7	1354.67	2017.51	350	67.5		1285.	21,480,455
500		281.6	1352.48	2421.45	330	60.0		1275.	140,705,052
495		276.7	1350.20	2913.04	310	53.0		1267.	12,556,860,000
490	129.2	271.7	1347.90	3591.74					
485	126.7	266.8	1345.55	4433.62					
480	124.2	261.8	1342.9	5498.55					

(See Figure IX-12-14
Figure IX-12-15)



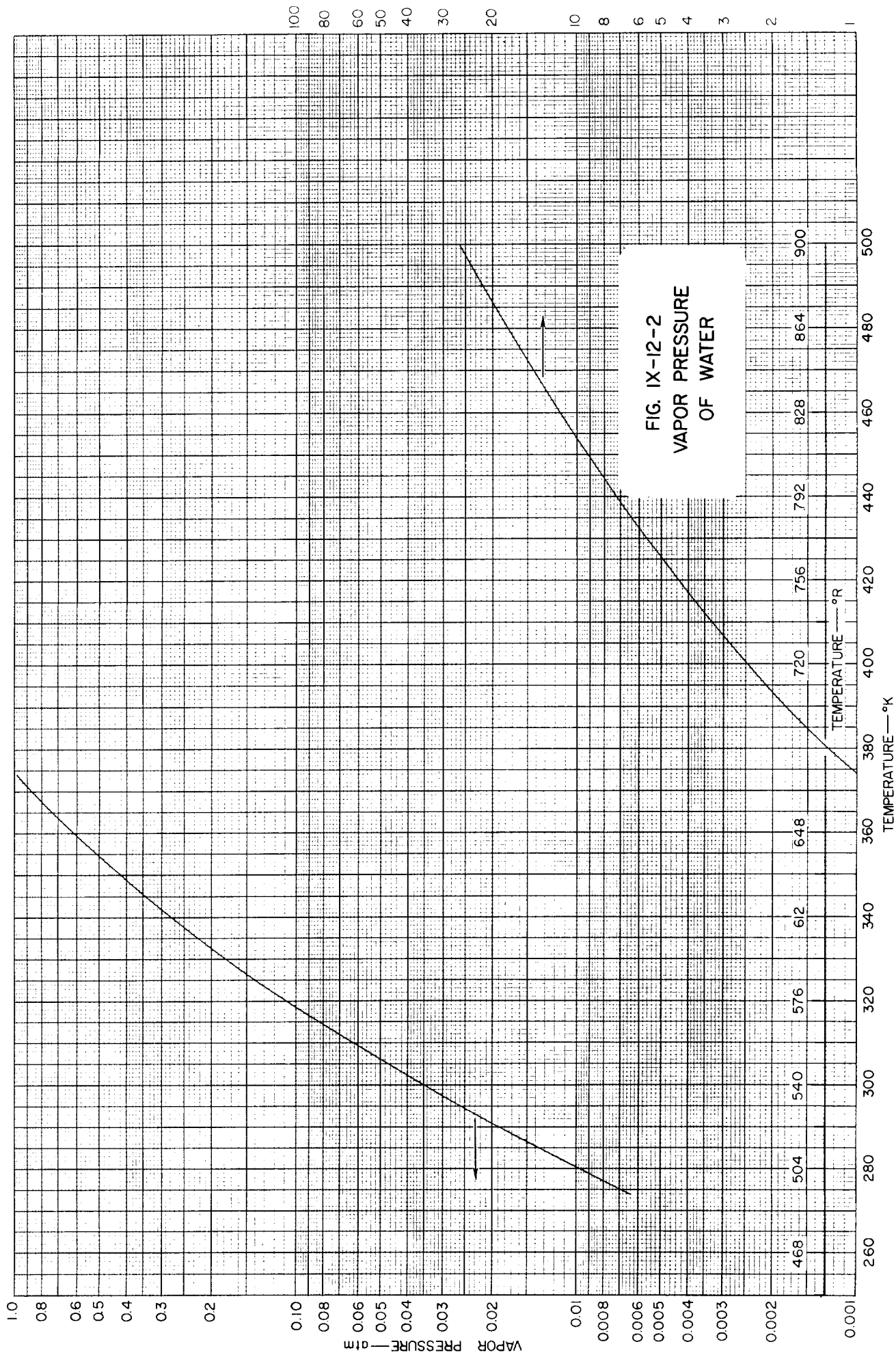


FIG. IX-12-3
ABSOLUTE DENSITY
OF WATER

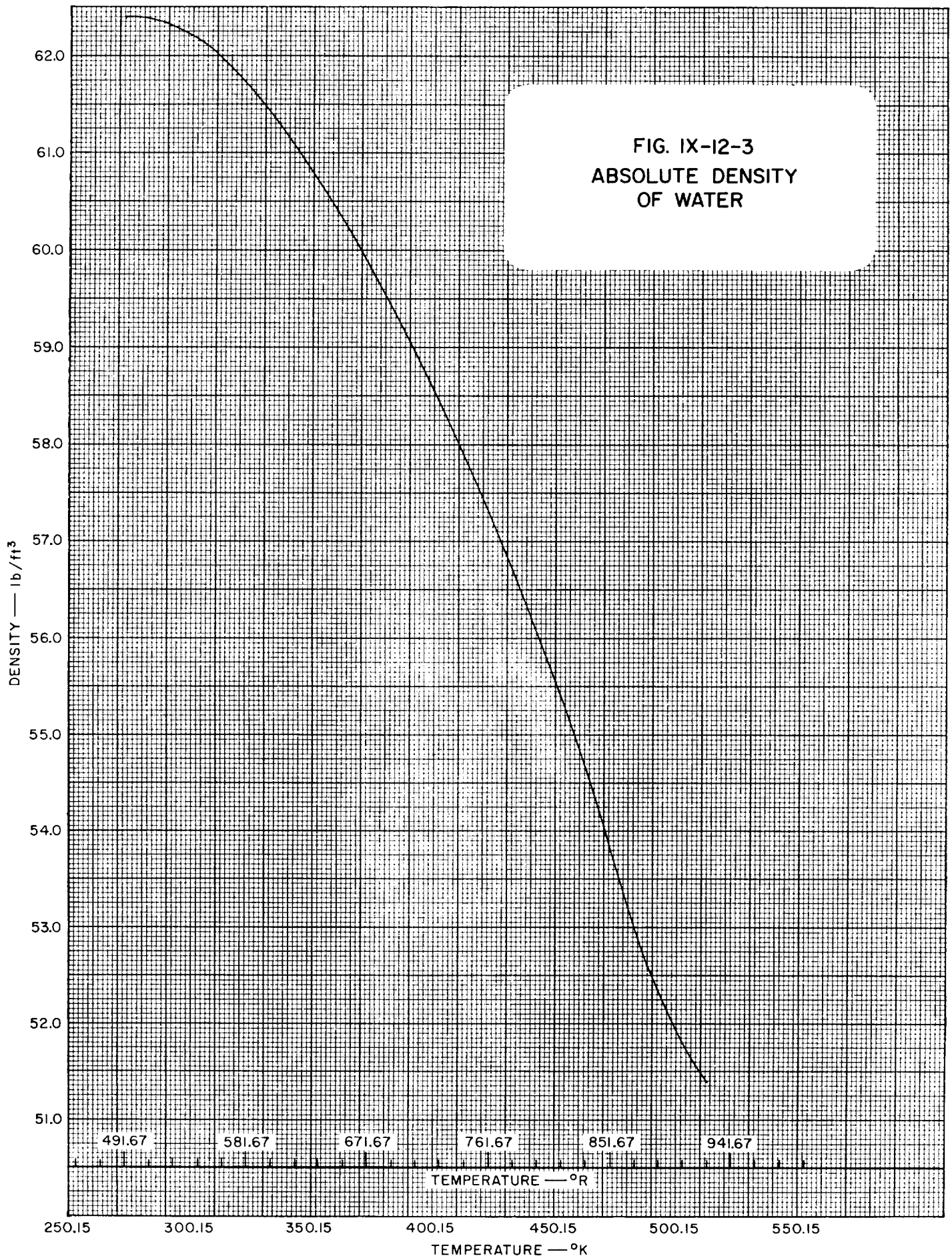
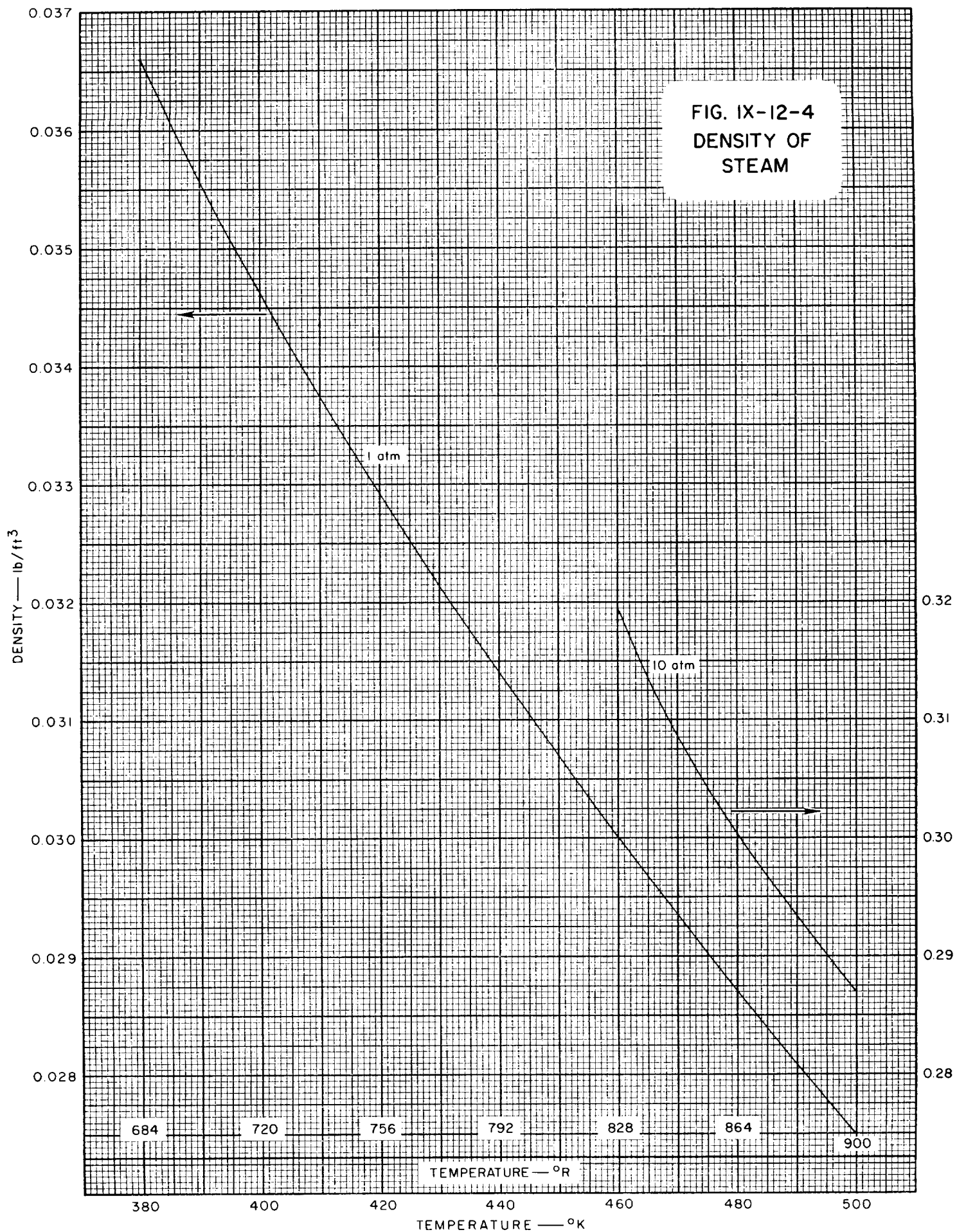
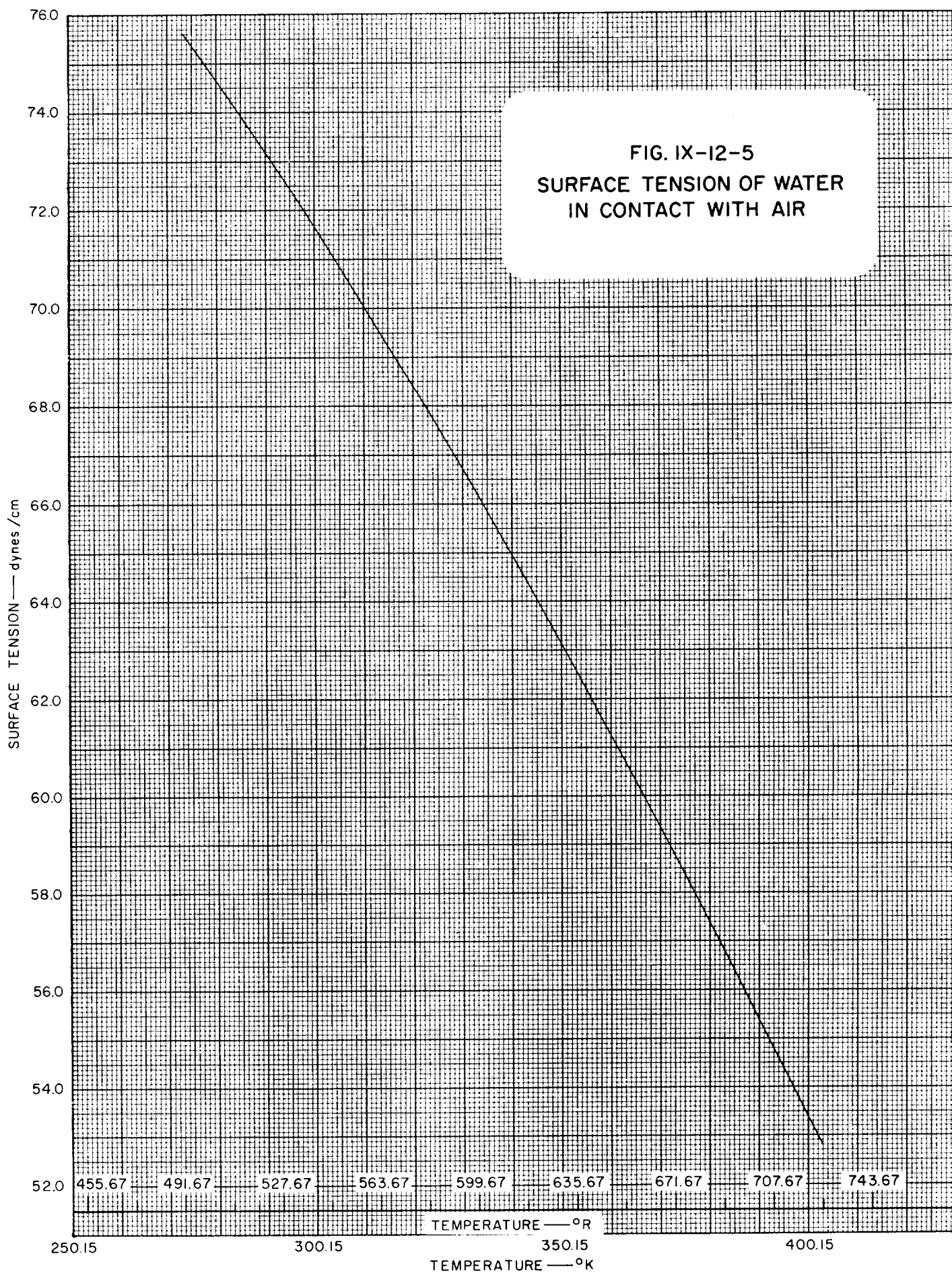
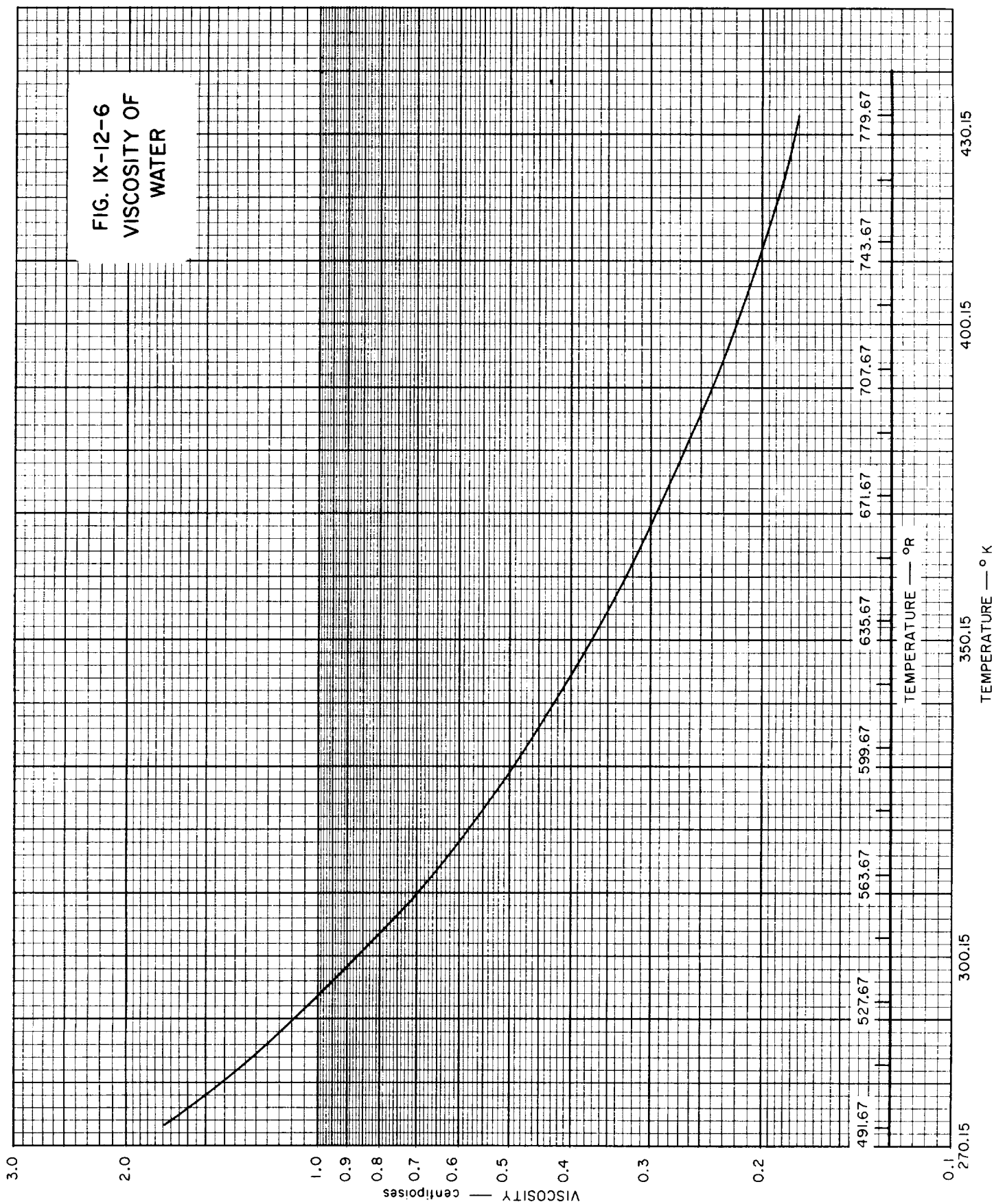
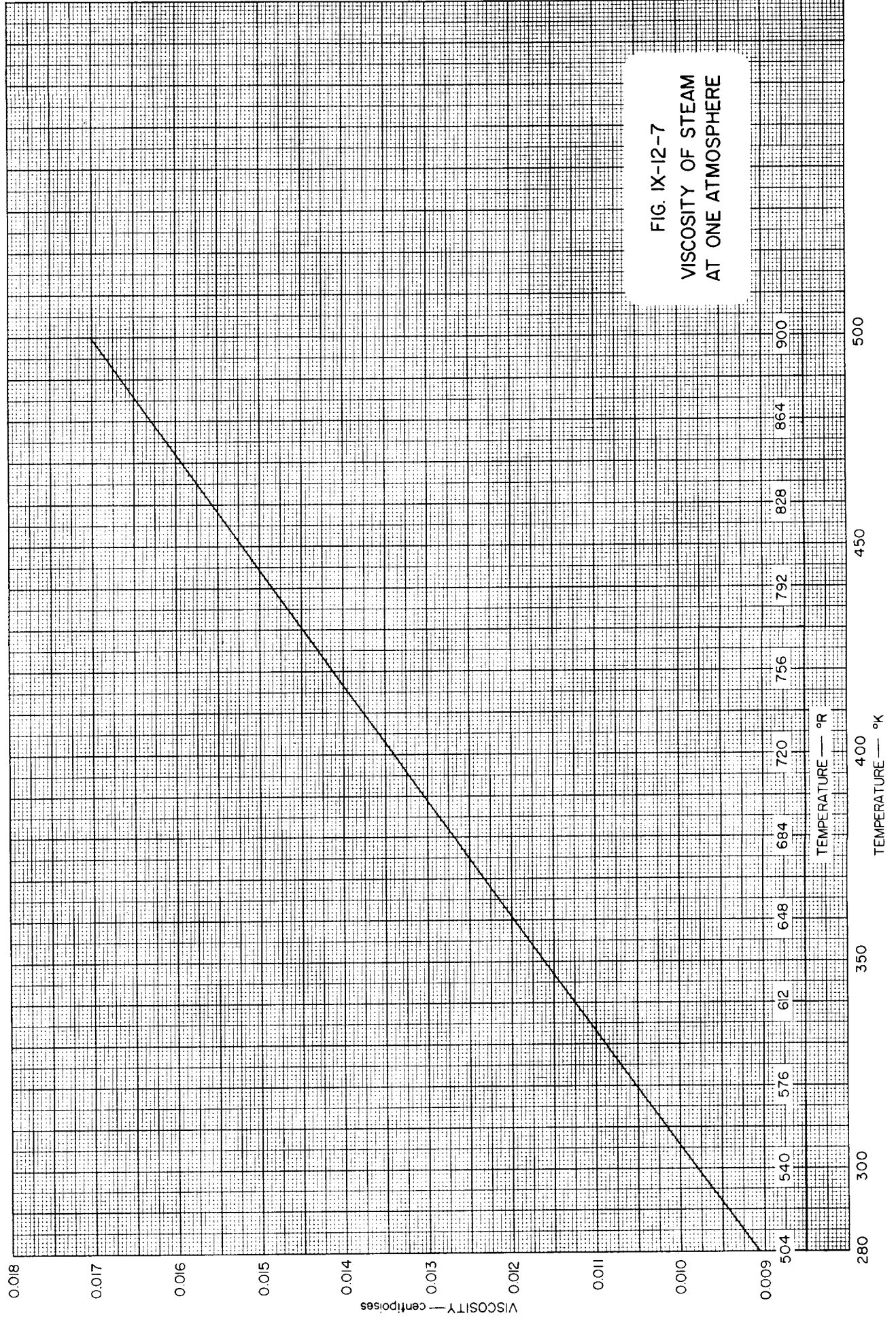


FIG. IX-12-4
DENSITY OF
STEAM









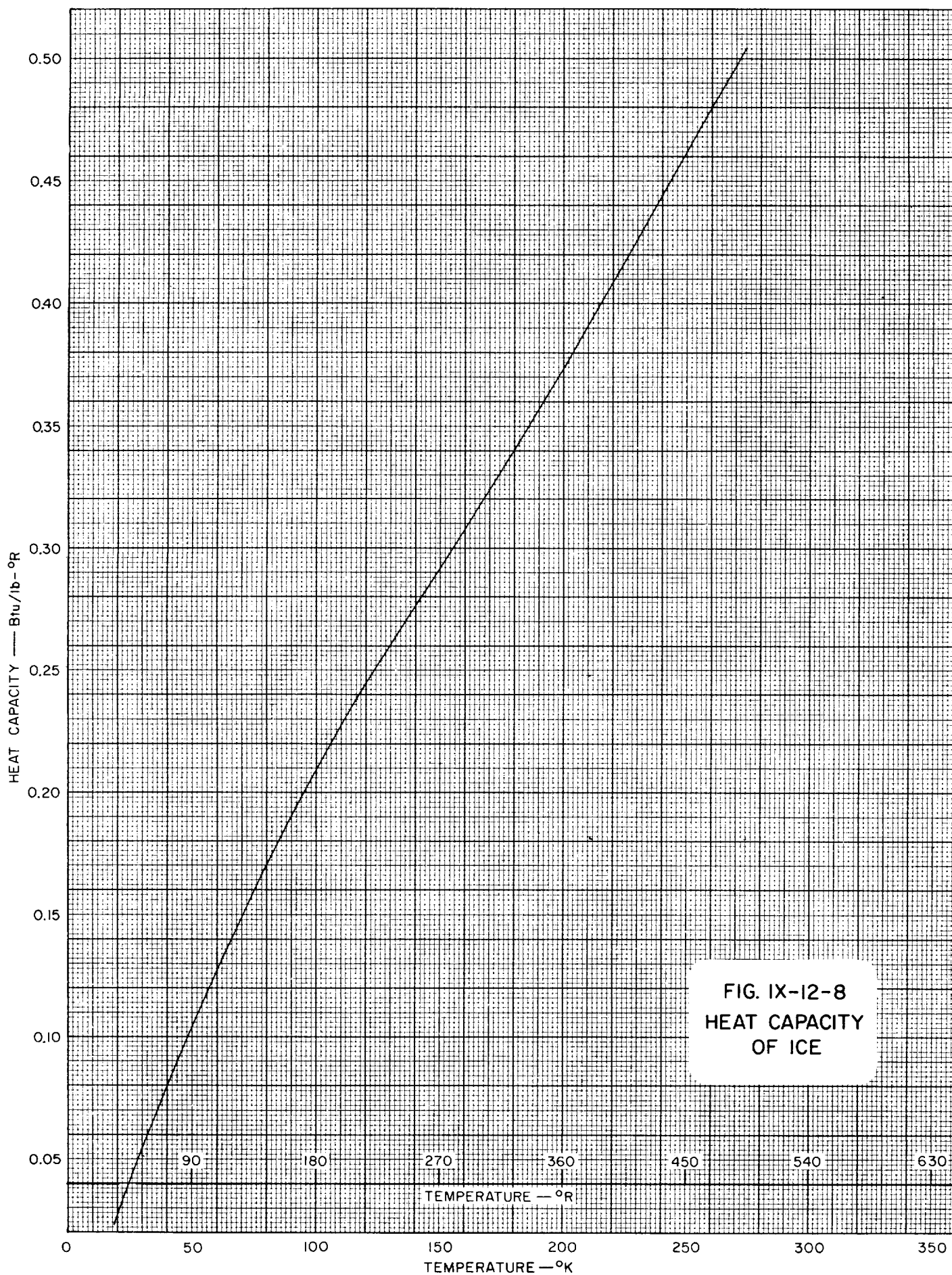
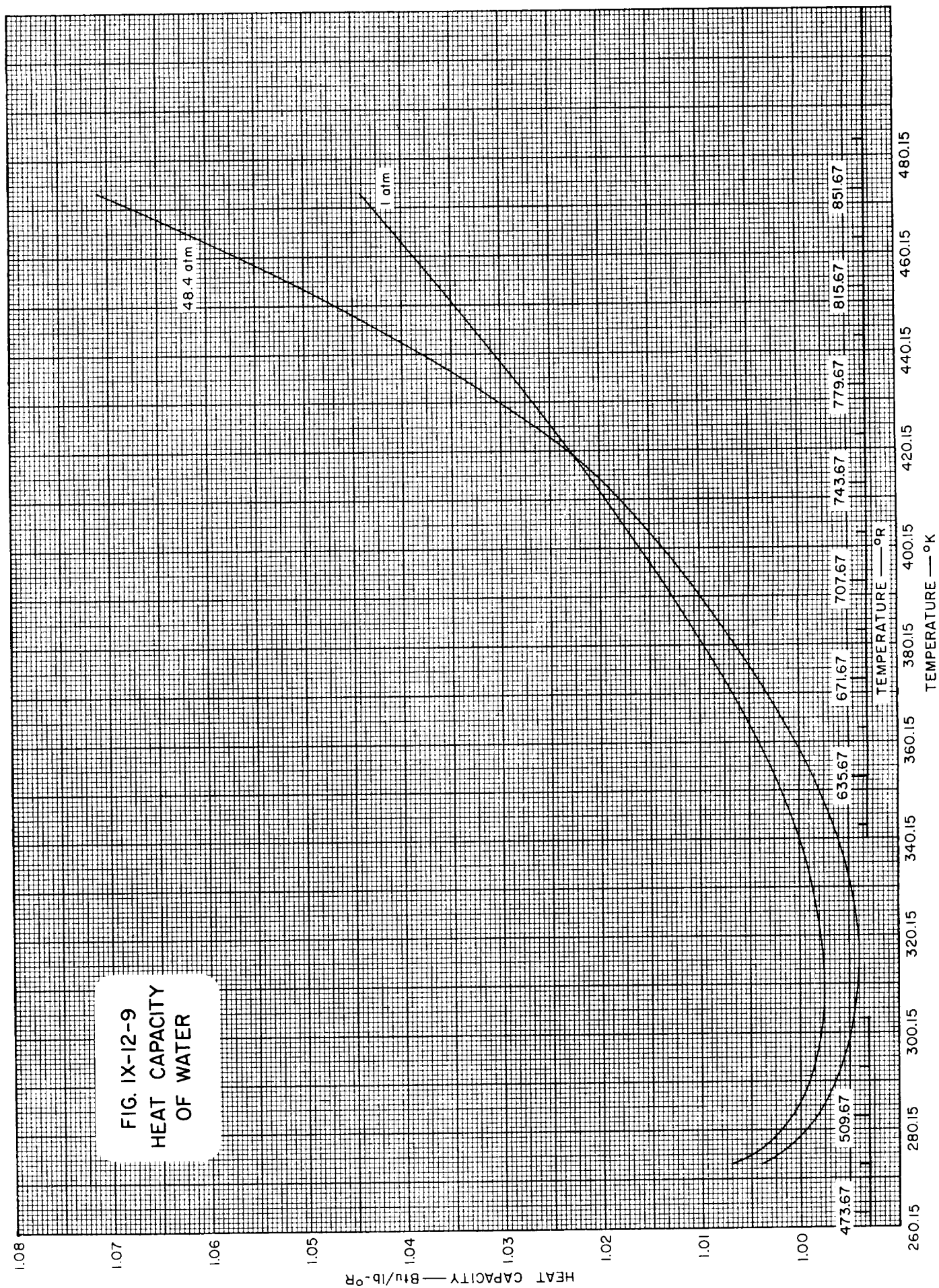
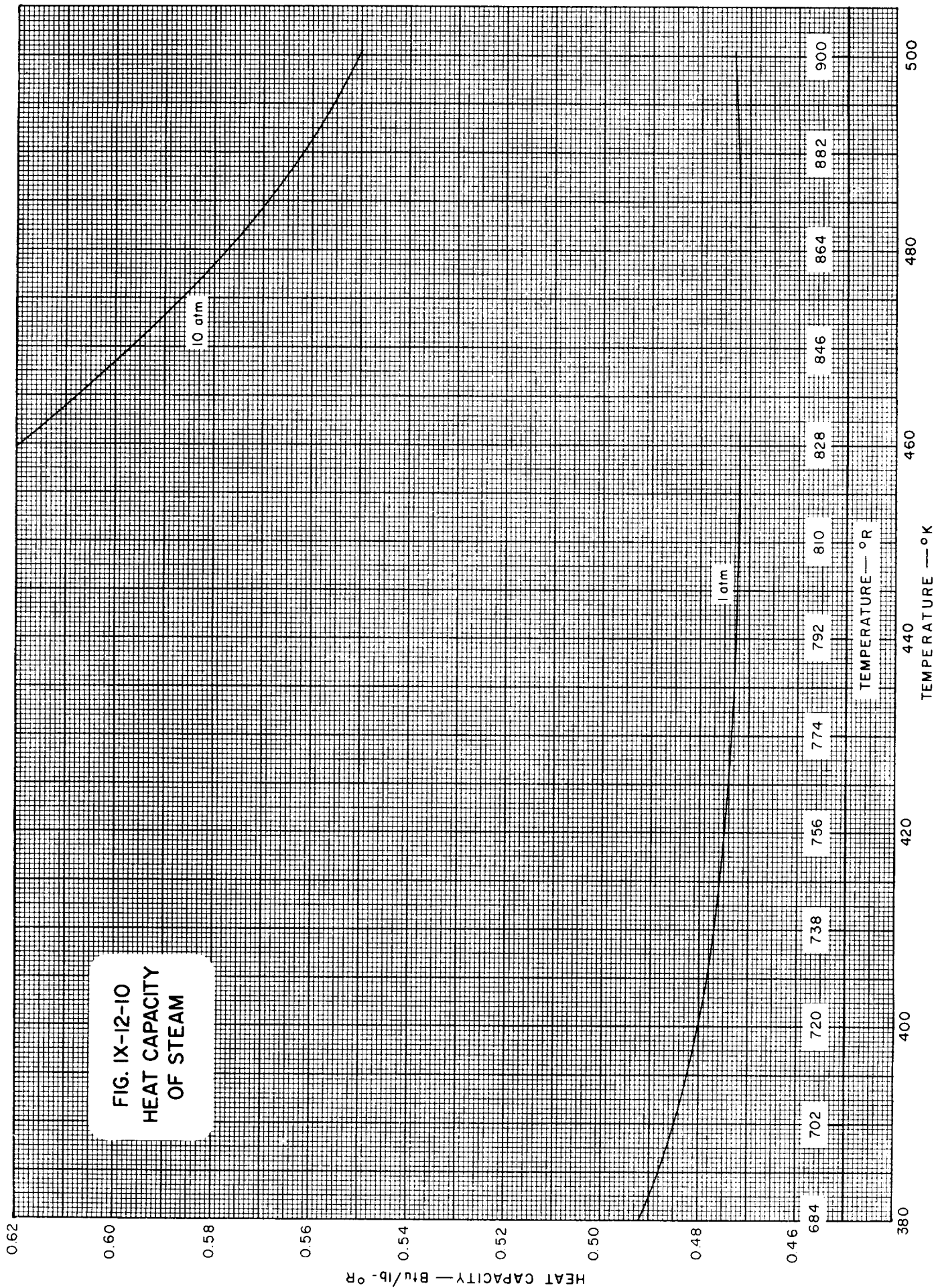
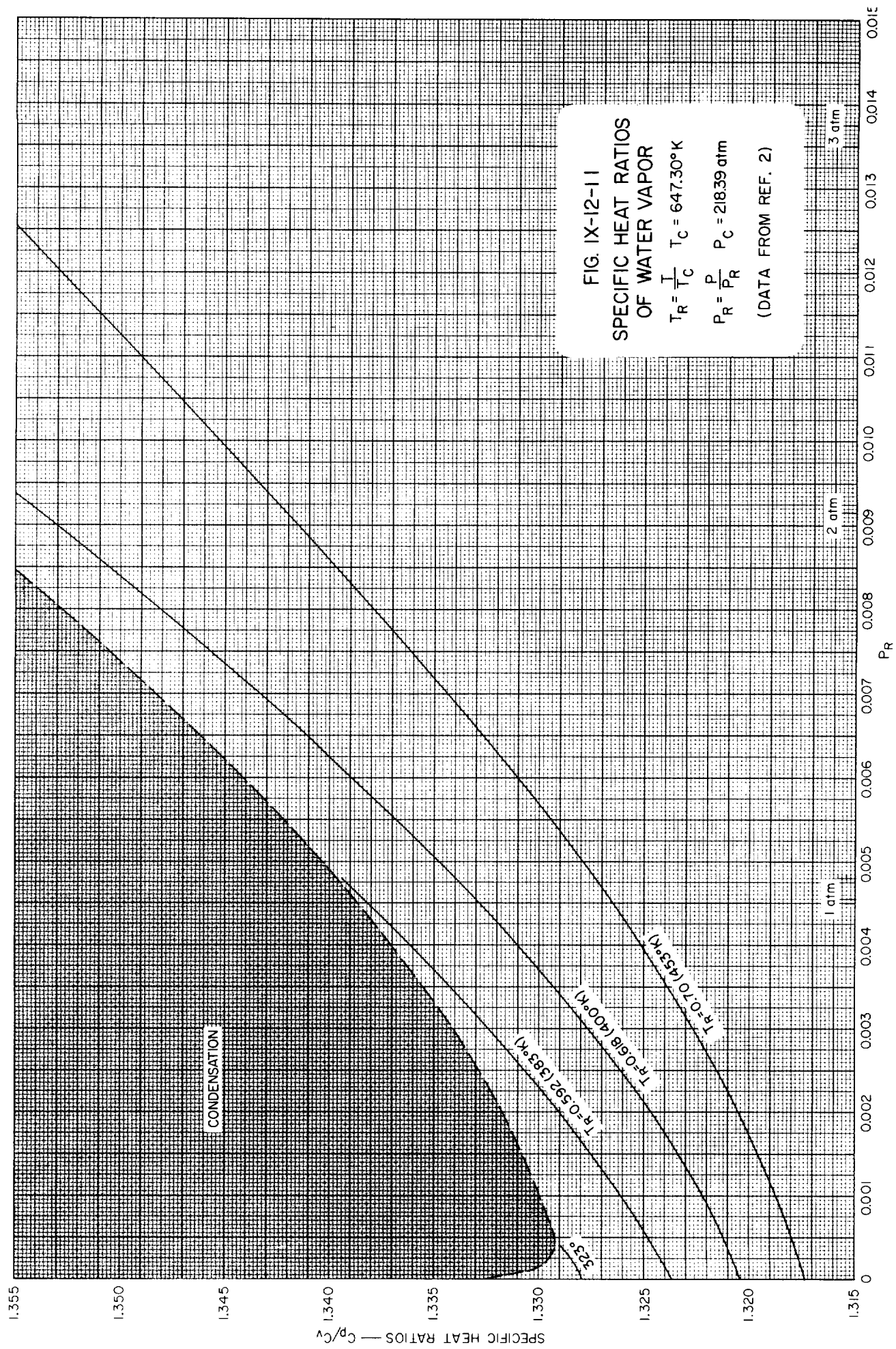
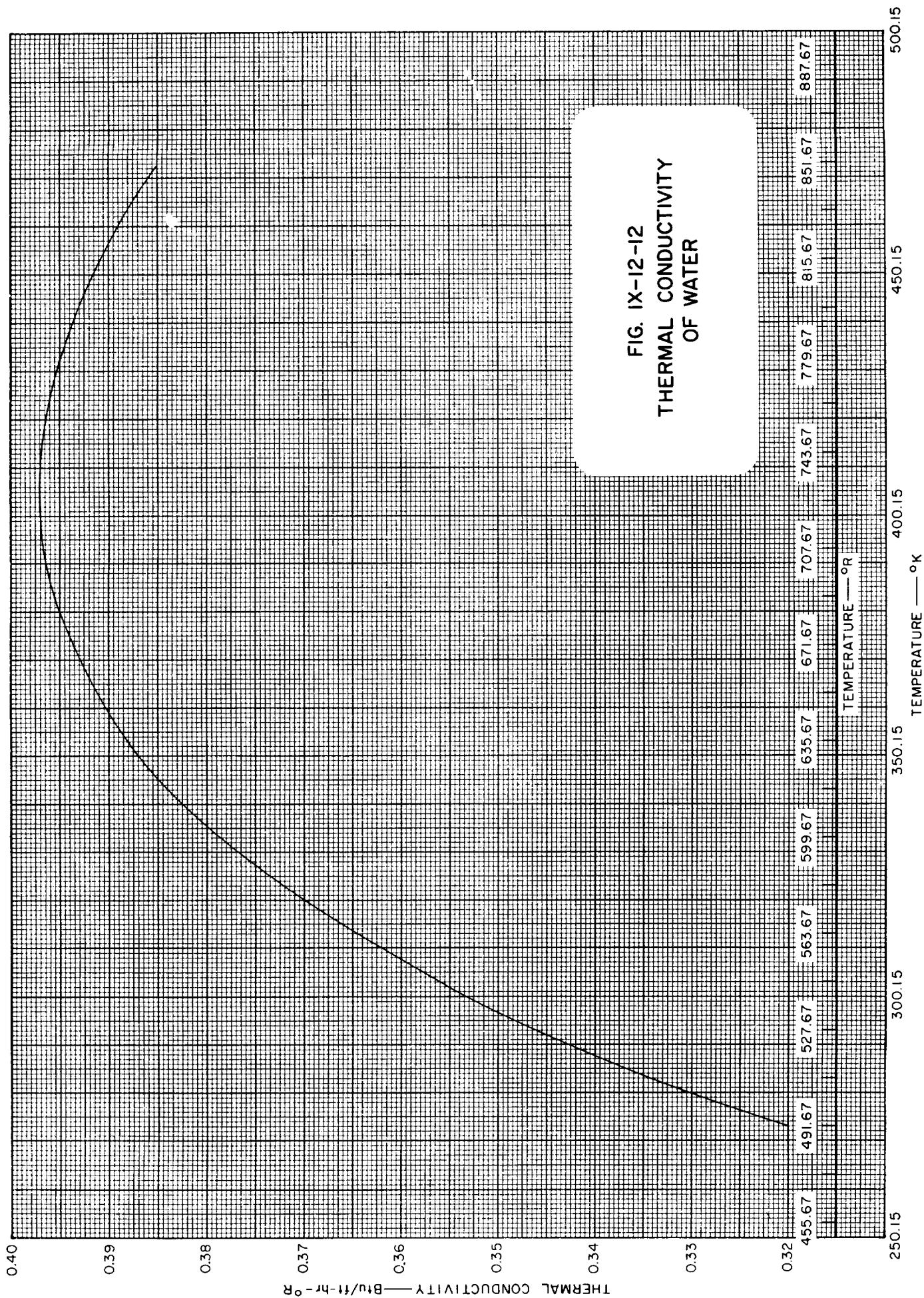


FIG. IX-12-8
HEAT CAPACITY
OF ICE









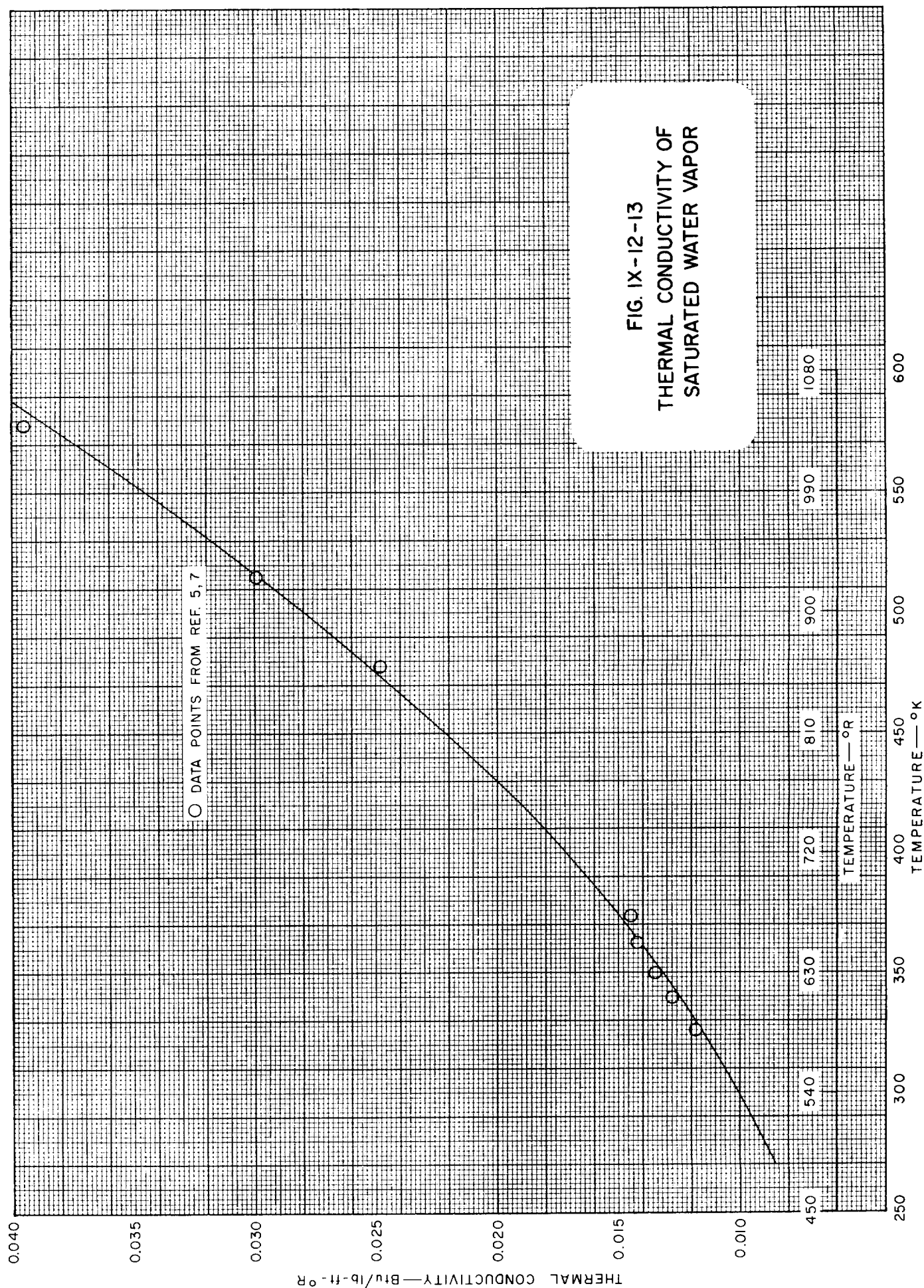
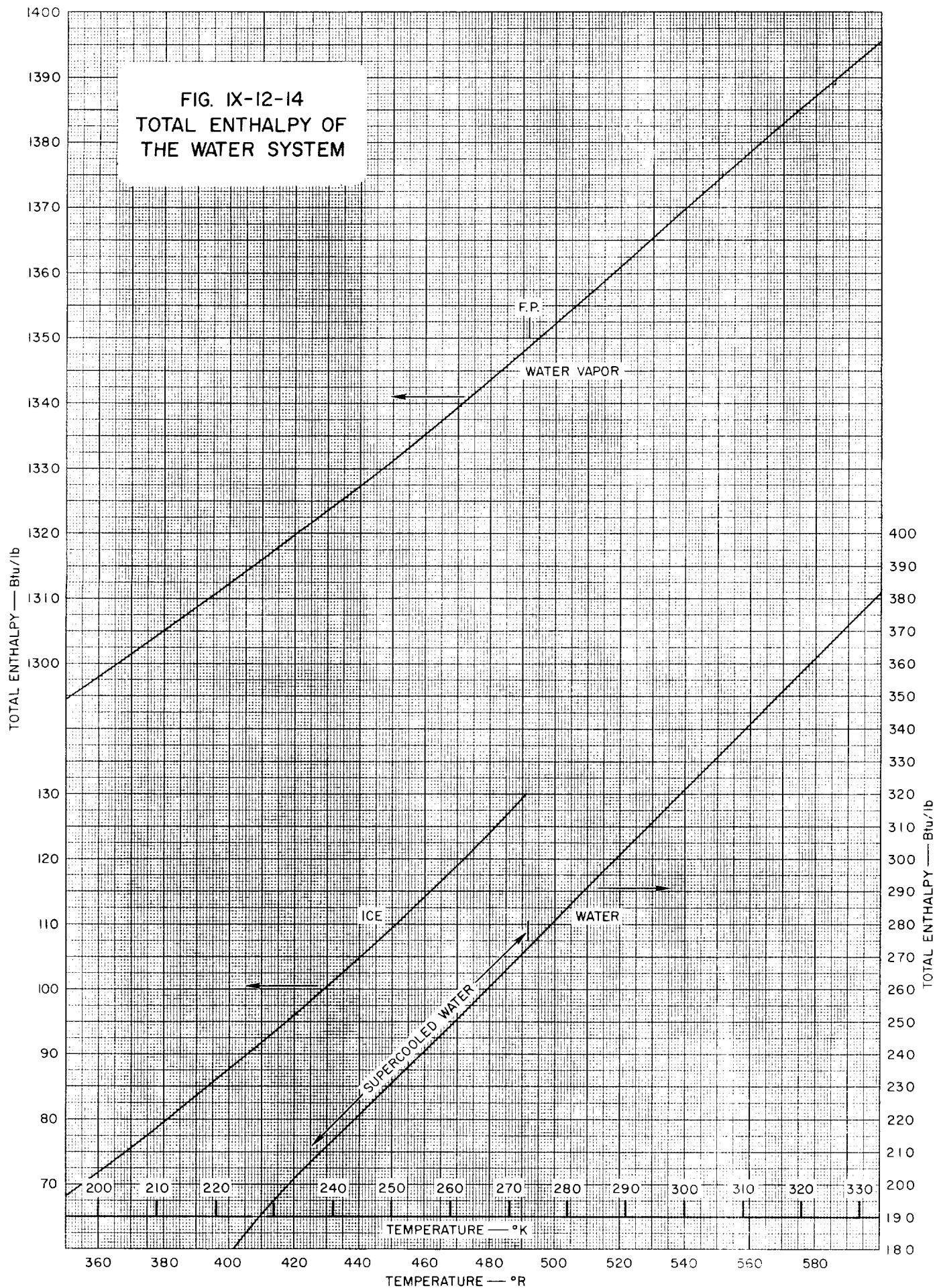
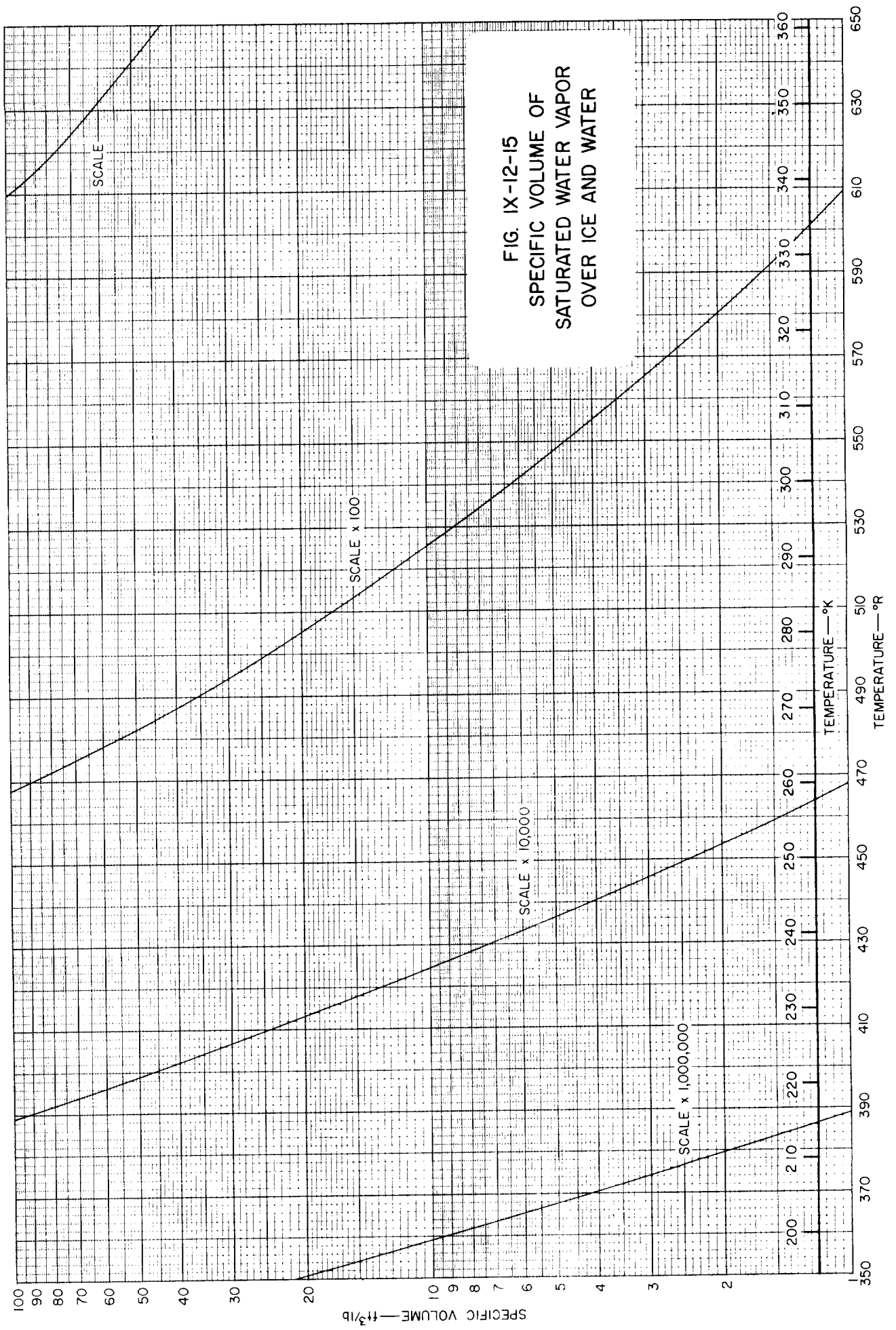
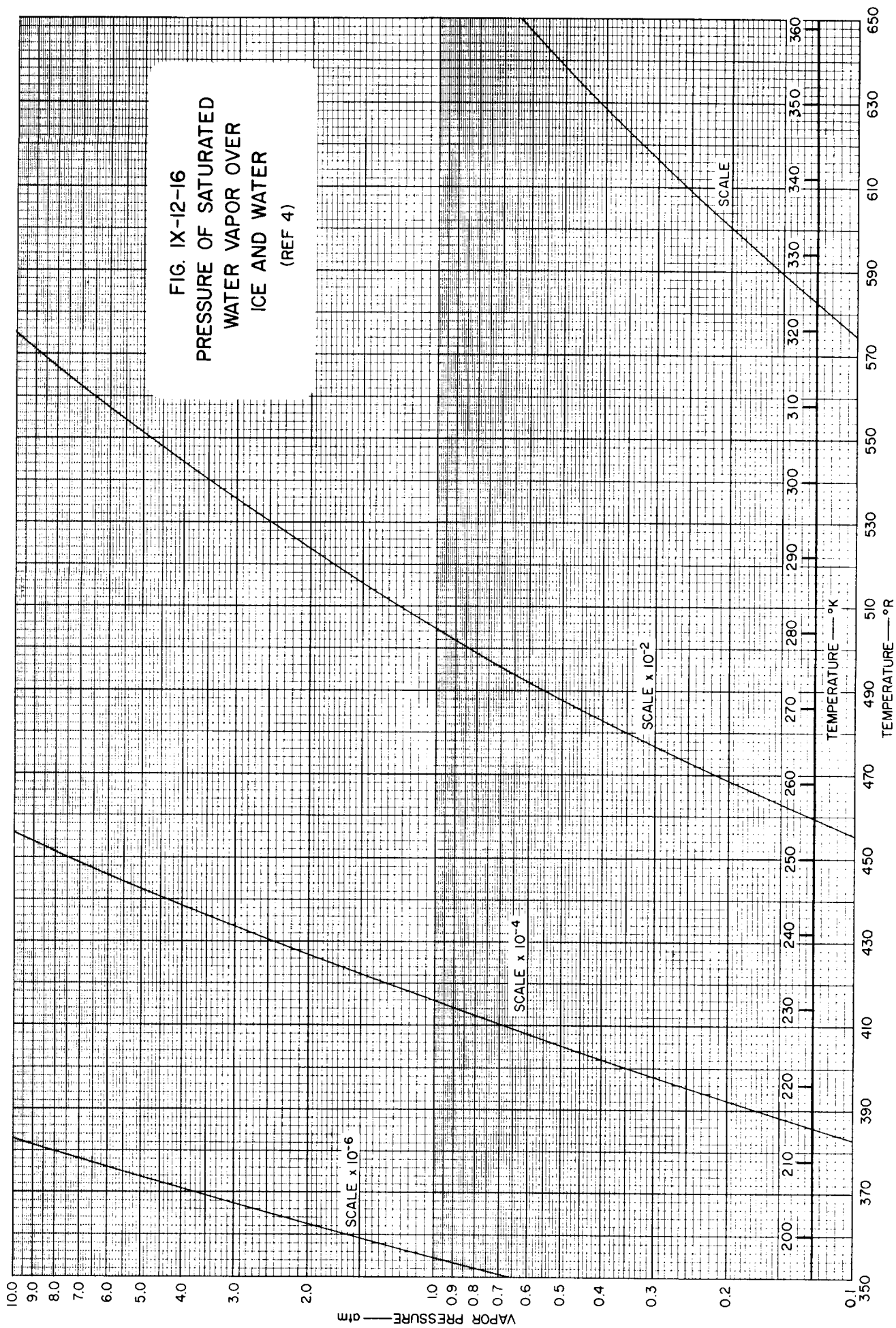


FIG. IX-12-14
TOTAL ENTHALPY OF
THE WATER SYSTEM







IX-12 WATER REFERENCES

1. Awberry, J. H., *Int. Crit. Tables*, **5**, 113 (1929).
2. Dorsey, N. E., *Properties of Ordinary Water Substance*, ACS Monograph No. 81, Reinhold Publishing Co., New York, 1940.
3. *Handbook of Chemistry and Physics*, 42nd Edition, Chemical Rubber Publishing Company, Cleveland, Ohio, 1962-63.
4. Hilsenrath, Joseph, *et al.*, *Tables of Thermodynamic and Transport Properties of Gases*, Pergamon Press, New York, 1960.
5. Keenan, J. H., and Keyes, F. G., *Thermodynamic Properties of Steam*, John Wiley & Sons, Inc., New York, 1936, 10th Impression, 1944.
6. Lange, N. A., *Handbook of Chemistry*, 10th Edition, Handbook Publishers, Inc., Sandusky, Ohio, 1961.
7. Milverton, S. W., *Proc. Roy. Soc. (London)*, **A150**, 287 (1935).

)

)

)

)

)

Table IX-13-1
GENERAL PROPERTIES OF PROPANE

PROPERTY	TEMPERATURE				PRESSURE			REF
	°C	°K	°F	°R	psia	atm	mm of Hg	
Melting Point	-187.69	85.46	-305.84	153.83				6
Boiling Point	- 42.07	231.08	- 43.73	415.94				6
Triple Point	-187.68	85.47	-305.82	153.85				6
Critical Temp.	96.81	369.96	206.26	665.93				6
Critical Press.					617.38	42.01	31,928	6
Mol. Wt. 44.097								6
Heat of Vaporization. See Table IX-13-9								
Heat of Fusion 19.10 cal/g or 34.38 Btu/lb								

Table IX-13-1.1
SOME VALUES OF THE GAS CONSTANT, *R*, FOR PROPANE
(See also Conversion Tables, Section I)

TEMPERATURE IN °K				
Pressure Density	atm	kg/cm ²	mm of Hg	lb/in ²
g/cm ³	1.86083	1.92265	141.4023	27.3468
mole/cm ³	82.0567	84.7832	62363.1	1205.91
mole/liter	0.0820544	0.0847809	62.3613	1.20587
lb/ft ³	0.0298072	0.0307976	22.65351	0.438048
lb/mole/ft ³	1.31441	1.35808	998.952	19.3166
TEMPERATURE IN °R				
Pressure Density	atm	kg/cm ²	mm of Hg	lb/in ²
g/cm ³	1.03379	1.06814	785.681	15.1926
mole/cm ³	45.5871	47.1018	34646.2	669.950
mole/liter	0.0455858	0.0471005	34.6452	0.669928
lb/ft ³	0.0165596	0.0171098	12.5853	0.226773
lb/mole/ft ³	0.730228	0.754489	554.973	10.7314

Table IX-13-2

VAPOR PRESSURE OF LIQUID PROPANE (Ref. 1, 2, 3, 8)

TEMPERATURE		VAPOR PRESSURE	TEMPERATURE		VAPOR PRESSURE
$^{\circ}\text{K}$	$^{\circ}\text{R}$	psia	$^{\circ}\text{K}$	$^{\circ}\text{R}$	psia
105.35	189.63	0.000019	194.26	349.67	2.036
108.25	194.85	0.000039	199.82	359.67	2.896
112.45	202.41	0.000097	205.37	369.67	4.029
			210.93	379.67	5.499
115.75	208.35	0.000193	216.48	389.67	7.365
119.25	214.62	0.000387			
124.35	223.83	0.000967			
128.35	231.03	0.001933	222.04	399.67	9.705
132.85	239.13	0.003867	227.59	409.67	12.592
			233.15	419.67	16.2
139.15	250.47	0.009668	244.26	439.67	25.4
144.35	259.83	0.01933	255.37	459.67	38.2
149.95	269.91	0.03867	266.48	479.67	55.5
158.15	284.67	0.09668	277.59	499.67	78.0
164.75	296.55	0.1933	294.26	529.67	124.0
			305.37	549.67	164.0
166.48	299.67	0.2324	316.48	569.67	212.0
172.04	309.67	0.3825			
177.59	319.67	0.6074	327.59	589.67	272.0
183.15	329.67	0.9348	333.15	599.67	305.0
188.71	339.67	1.398			

(See Figure IX-13-1,
Figure IX-13-1.1)

Table IX-13-3
DENSITY OF LIQUID PROPANE (Ref. 6)

TEMPERATURE		DENSITY	TEMPERATURE		DENSITY
°K	°R	lb/ft ³	°K	°R	lb/ft ³
83.15	149.67	45.70	233.15	419.67	36.11
93.15	167.67	45.14	243.15	437.67	35.36
103.15	185.67	44.57	253.15	455.67	34.59
113.15	203.67	44.01	263.15	473.67	33.80
123.15	221.67	43.45	273.15	491.67	32.98
133.15	239.67	42.83	283.15	509.67	32.13
143.15	257.67	42.20	293.15	527.67	31.25
153.15	275.67	41.58	299.82	539.67	30.70
163.15	293.67	40.95	305.37	549.67	30.15
173.15	311.67	40.33	310.93	559.67	29.58
183.15	329.67	39.64	316.48	569.67	28.96
193.15	347.67	38.96	322.04	579.67	28.30
203.15	365.67	38.27	327.59	589.67	27.64
213.15	383.67	37.56	333.15	599.67	27.00
223.15	401.67	36.83			

(See Figure IX-13-2)

Table IX-13-4
DENSITY OF SATURATED PROPANE VAPOR (Ref. 2)

TEMPERATURE		DENSITY	TEMPERATURE		DENSITY
°K	°R	lb/ft ³	°K	°R	lb/ft ³
213.71	384.67	0.0690	288.71	519.67	0.990
216.48	389.67	0.0775	294.26	529.67	1.13
219.26	394.67	0.0885	299.82	539.67	1.30
222.04	399.67	0.111	305.37	549.67	1.49
227.59	409.67	0.129	310.93	559.67	1.69
233.15	419.67	0.163	316.48	569.67	1.92
238.71	429.67	0.203	322.04	579.67	2.18
244.26	439.67	0.250	327.59	589.67	2.48
249.82	449.67	0.307	333.15	599.67	2.78
255.37	459.67	0.369			
260.93	469.67	0.441			
266.48	479.67	0.526			
272.04	489.67	0.625			
277.59	499.67	0.730			
283.15	509.67	0.847			

(See Figure IX-13-3)

Table IX-13-5

HEAT CAPACITY OF SOLID AND LIQUID PROPANE (Ref. 3)

TEMPERATURE		HEAT CAPACITY	TEMPERATURE		HEAT CAPACITY
$^{\circ}\text{K}$	$^{\circ}\text{R}$	Btu/lb- $^{\circ}\text{R}$	$^{\circ}\text{K}$	$^{\circ}\text{R}$	Btu/lb- $^{\circ}\text{R}$
15	27	0.0150	90	162	0.4581
20	36	0.0361	100	180	0.4606
25	45	0.0598	110	198	0.4631
30	54	0.0854	120	216	0.4661
35	63	0.1125	130	234	0.4697
40	72	0.1360	140	252	0.4733
45	81	0.1570	150	270	0.4774
50	90	0.1761	160	288	0.4819
55	99	0.1944	170	306	0.4869
60	108	0.2119	180	324	0.4928
65	117	0.2286	190	342	0.4996
70	126	0.2443	200	360	0.5069
75	135	0.2590	210	378	0.5148
80	144	0.2731	220	396	0.5232
85	153	0.2867	230	414	0.5327
85.45	153.81	Melting Point	231.04	415.87	Boiling Point

(See Figure IX-13-4)

Table IX-13-6

HEAT CAPACITY OF PROPANE GAS (Ref. 4)

TEMPERATURE		HEAT CAPACITY—Btu/lb- $^{\circ}\text{R}$		
$^{\circ}\text{K}$	$^{\circ}\text{R}$	1 atm	10 atm	20 atm
240	432	0.340		
260	468	0.361		
280	504	0.381		
300	540	0.401		
320	576	0.424		
340	612	0.444	0.483	
360	648	0.465	0.492	
380	684	0.488	0.508	0.542
400	720	0.510	0.526	0.549
420	756	0.533	0.547	0.565
440	792	0.556	0.567	0.581
460	828	0.578	0.587	0.599
480	864	0.599	0.608	0.617
500	900	0.617	0.626	0.635
520	936	0.637	0.646	0.653
540	976	0.653	0.660	0.667
560	1008	0.669	0.676	0.680
580	1044	0.683	0.687	0.692
600	1080	0.696	0.701	0.705

(See Figure IX-13-5)

Table IX-13-7
SURFACE TENSION OF LIQUID
PROPANE (Ref. 6)

TEMPERATURE		SURFACE TENSION
$^{\circ}\text{K}$	$^{\circ}\text{R}$	lb/ft ²
143.15	257.8	0.0581
153.15	275.4	0.0549
163.15	293.4	0.0520
173.15	311.4	0.0489
183.15	329.4	0.0460
193.15	347.4	0.0430
203.15	365.4	0.0401
213.15	383.4	0.0373
223.15	401.4	0.0344
233.15	419.4	0.0316

(See Figure IX-13-8)

Table IX-13-8
VISCOSITY OF LIQUID PROPANE (Ref. 2, 6, 7)

TEMPERATURE		ABSOLUTE VISCOSITY	PRESSURE
$^{\circ}\text{K}$	$^{\circ}\text{R}$	micro- poises	atm
213.15	383.67	2560	1 (total)
223.15	401.67	2228	1 (total)
277.59	499.67	1170	saturated
288.71	519.67	1060	saturated
299.82	539.67	970	saturated
310.93	559.67	860	saturated
322.04	579.67	770	saturated
333.15	599.67	670	saturated
344.26	619.67	573	saturated
360.93	649.67	440	saturated

(See Figure IX-13-9)

Table IX-13-9
HEAT OF VAPORIZATION OF LIQUID PROPANE (Ref. 2)

TEMPERATURE		LATENT HEAT	TEMPERATURE		LATENT HEAT
$^{\circ}\text{K}$	$^{\circ}\text{R}$	Btu/lb	$^{\circ}\text{K}$	$^{\circ}\text{R}$	Btu/lb
216.48	389.67	189.0	272.04	489.67	163.4
222.04	399.67	185.5	277.59	499.67	160.3
227.59	409.67	183.2	283.15	509.67	156.5
233.15	419.67	180.8	288.71	519.67	152.6
238.71	429.67	178.7	294.26	529.67	148.3
244.26	439.67	176.2	299.82	539.67	145.1
249.82	449.67	173.2	305.37	549.67	140.0
255.37	459.67	171.5	310.93	559.67	135.8
260.93	469.67	167.2	322.04	579.67	125.4
266.48	479.67	166.3	333.15	599.67	112.5

(See Figure IX-13-10)

Table IX-13-10
TOTAL ENTHALPY VALUES AND SPECIFIC VOLUMES FOR THE PROPANE SYSTEM
(Computed from References 1, 2, 3, 8, 9)

TEMPERA- TURE	TOTAL ENTHALPY—Btu/lb			SPEC. VOL. VAPOR	TEMPERA- TURE	TOTAL ENTHALPY—Btu/lb			SPEC. VOL. VAPOR
°R	Solid	Liquid	Vapor	ft ³ /lb	°R	Solid	Liquid	Vapor	ft ³ /lb
0	0				370		159.1	352.4	21.4
40	0.50				380		164.3	355.4	15.2
60	2.00				390		169.3	358.3	12.3
80	4.62				400		174.4	360.8	9.55
100	8.14				410		179.5	364.0	7.55
120	12.46				420		184.7	366.9	6.05
140	17.48				430		190.1	369.9	4.93
150		53.90			440		195.6	373.0	4.03
153.83	21.30	55.65			450		201.6	376.3	3.33
160		58.40			460		206.8	378.6	2.75
170		62.90			470		212.4	381.2	2.28
180		67.40			480		218.3	384.0	1.92
190		71.80		2 311 920.	490		223.9	386.6	1.62
200		76.30	311.1	666 740.	500		230.2	389.6	1.37
210		81.00	313.	217 470.	510		235.3	391.3	1.17
220		85.70	315.	82 368.	520		241.3	393.6	0.99
230		90.40	317.	31 623.	530		247.4	395.7	0.86
240		95.10	319.	13 906.	540		253.6	397.8	0.74
250		99.90	322.	6 427.3	550		259.9	399.7	0.64
260		104.8	324.	3 163.7	560		266.3	402.7	0.55
270		109.7	326.	1 663.5	570		272.9	403.6	0.475
280		114.5	329.	896.6	580		279.7	405.3	0.41
290		119.5	331.	526.7	590		286.9	406.9	0.355
300		124.3	334.	313.3	600		294.4	408.4	0.32
310		129.2	336.	203.9					
320		134.2	339.	129.8					
330		139.1	341.	87.8					
340		144.2	344.	57.0					
350		149.1	347.	40.0					
360		154.2	350.	29.2					

(See Figure IX-13-12,
Figure IX-13-13)

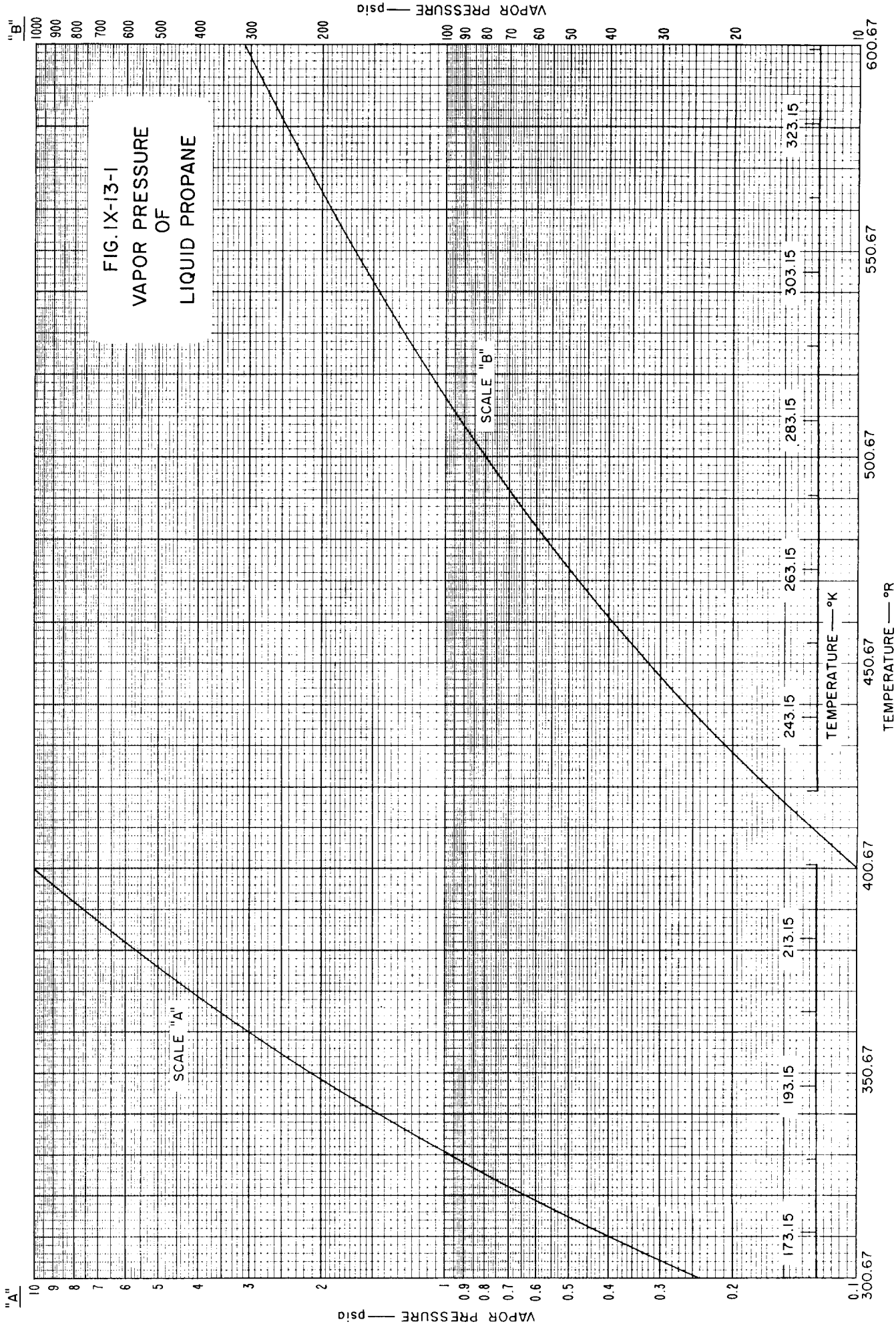
)

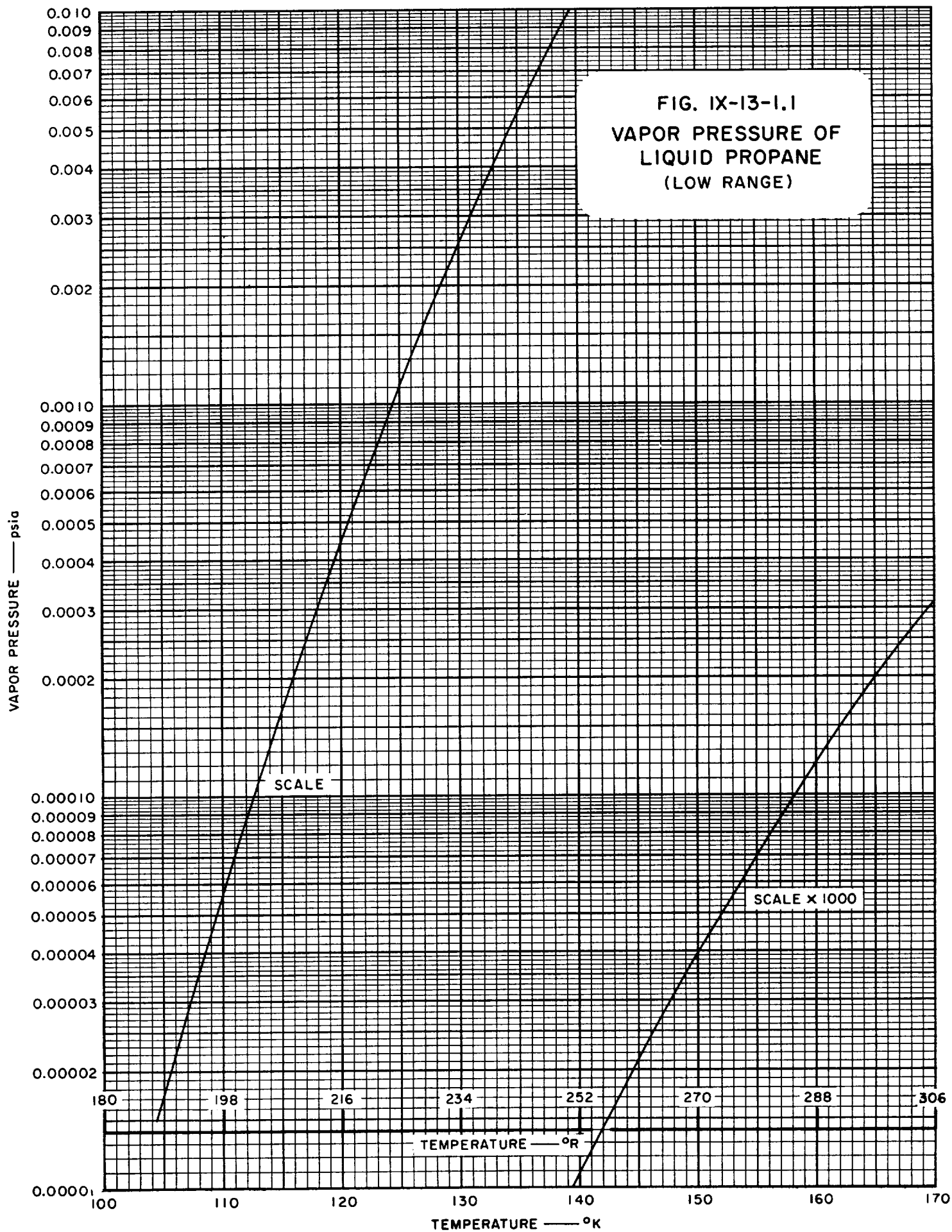
)

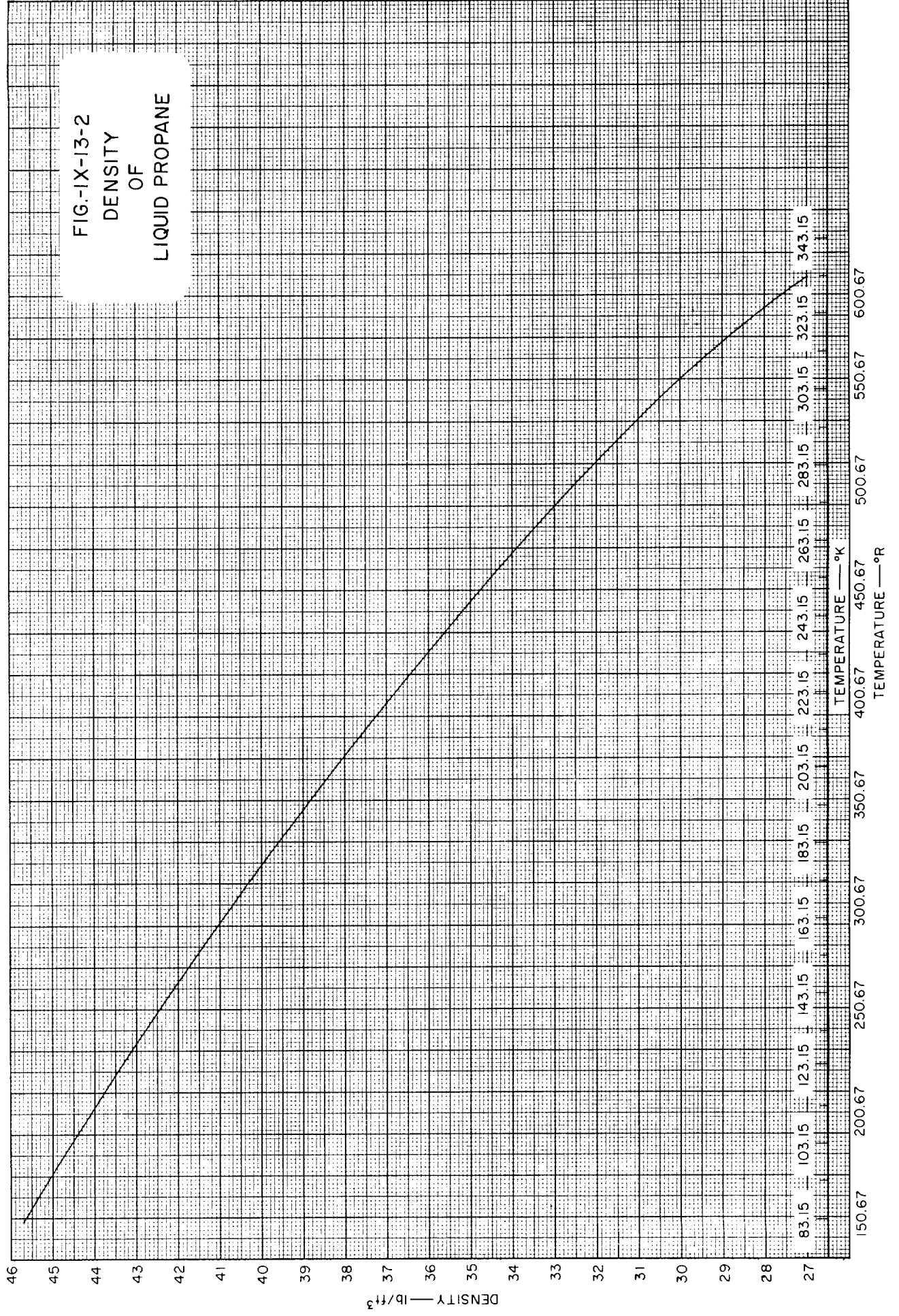
)

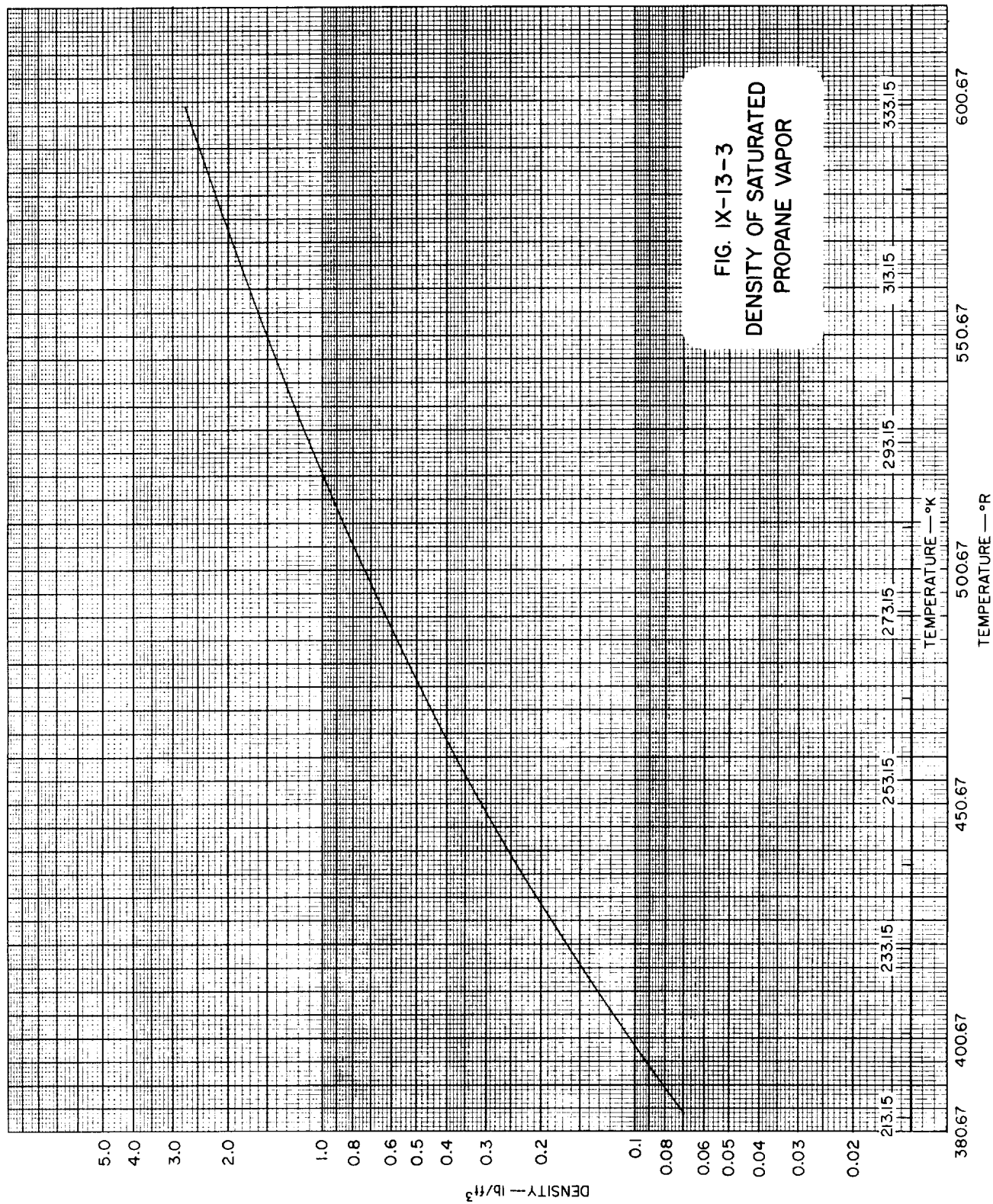
)

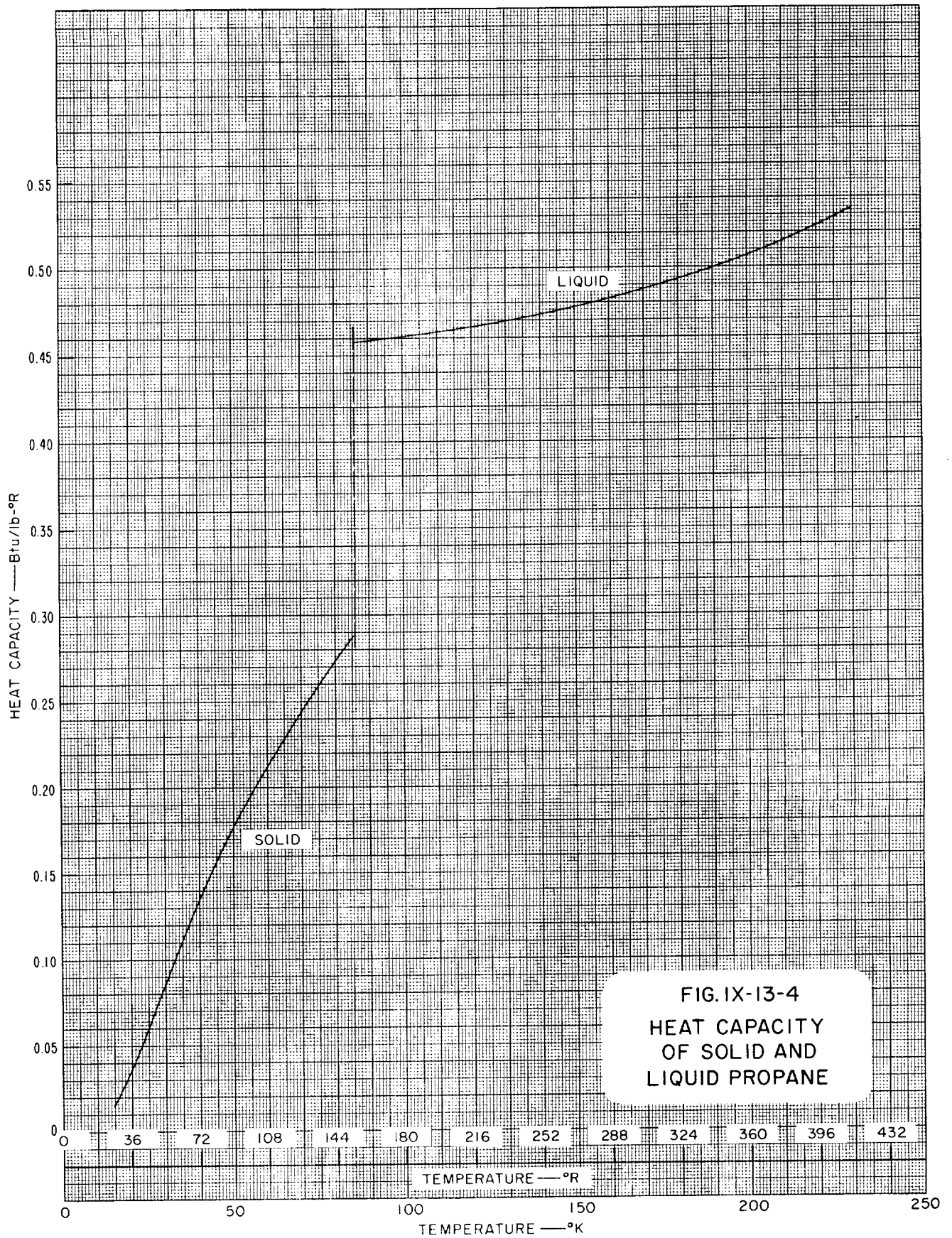
)

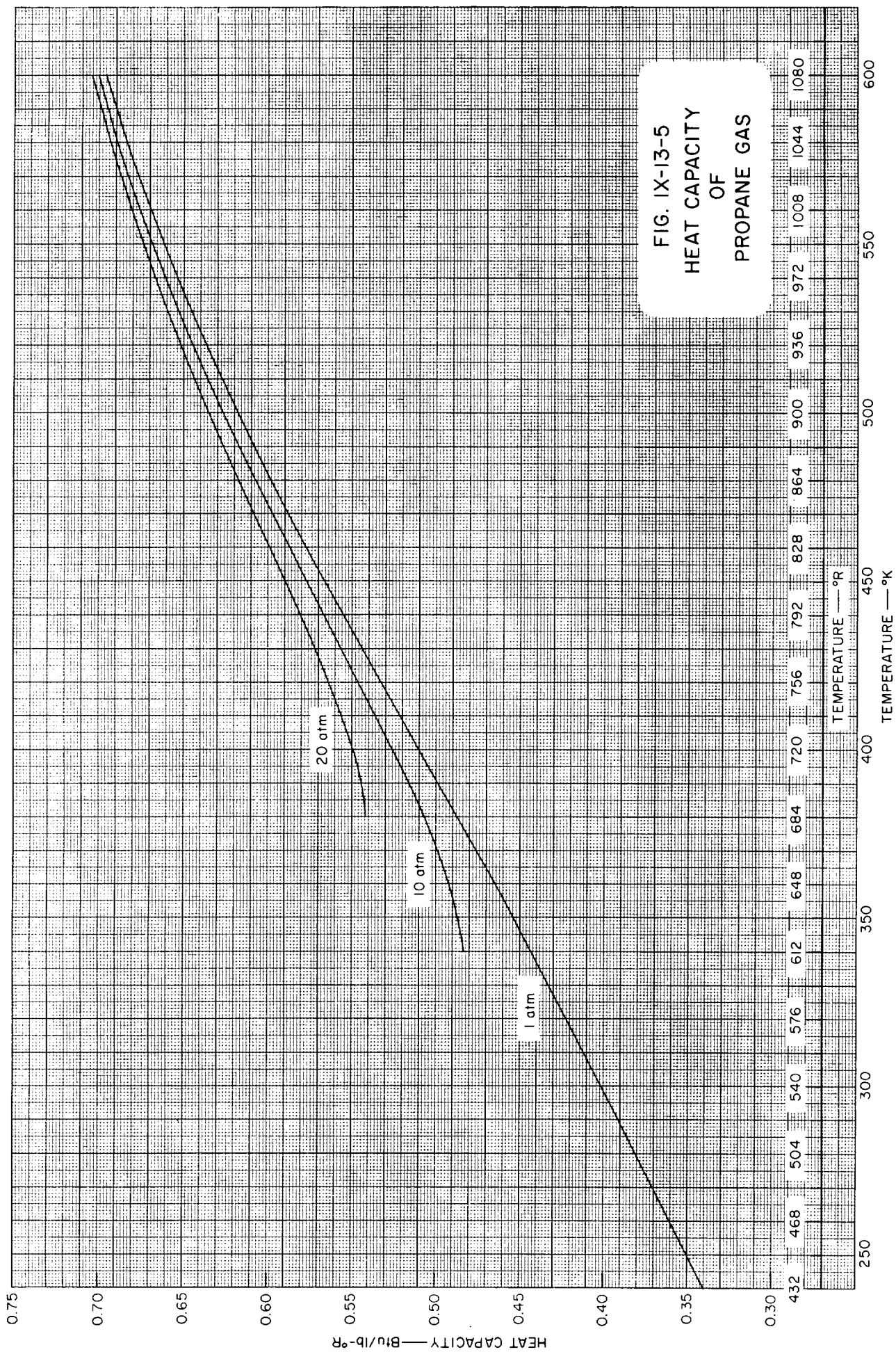












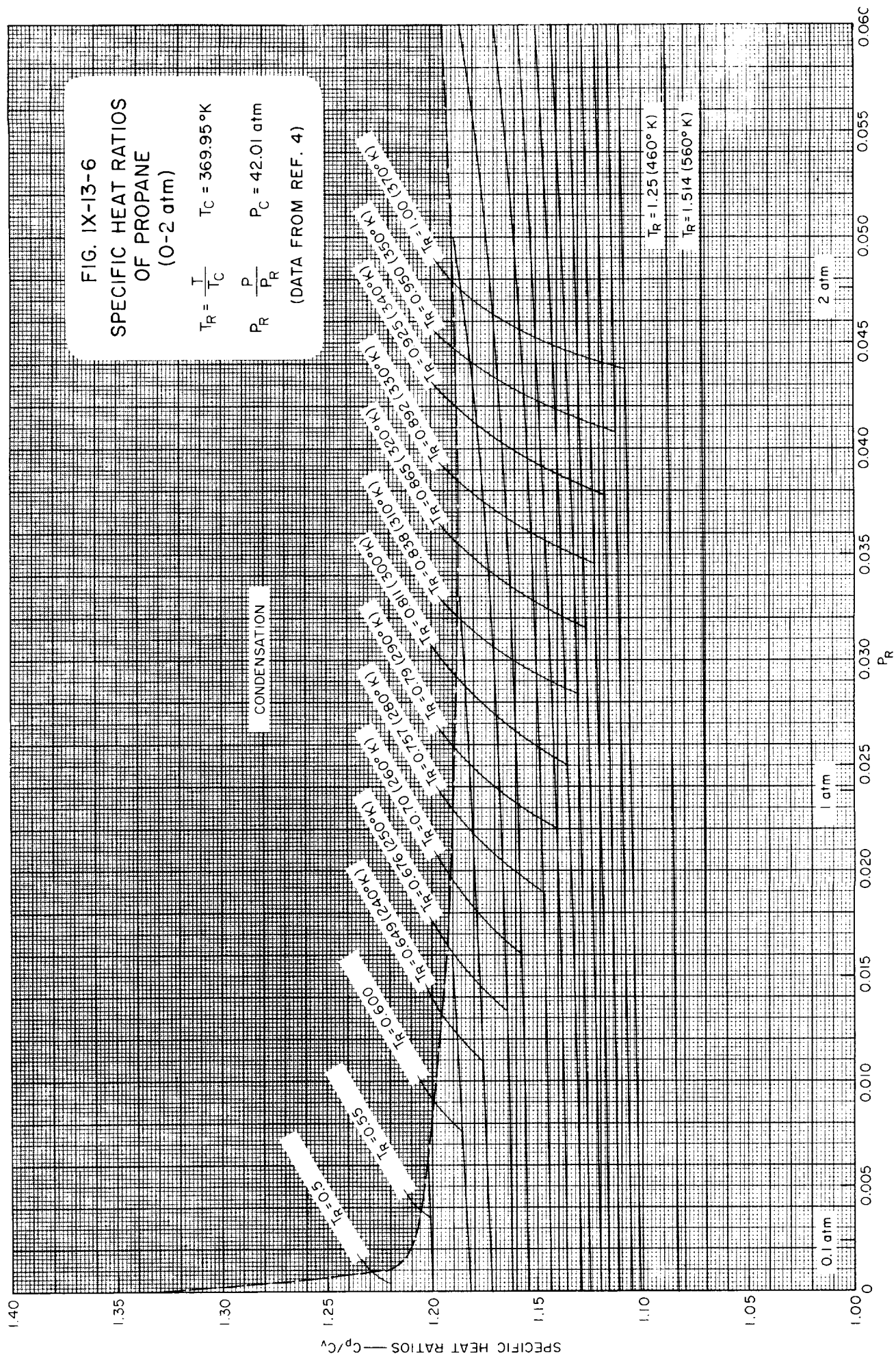


FIG. IX-13-7

SPECIFIC HEAT RATIOS
OF PROPANE
(0-20 atm)

$$T_R = \frac{T}{T_C} \quad T_C = 369.95^\circ\text{K}$$

$$P_R = \frac{P}{P_C} \quad P_C = 42.01 \text{ atm}$$

(DATA FROM REF. 4)

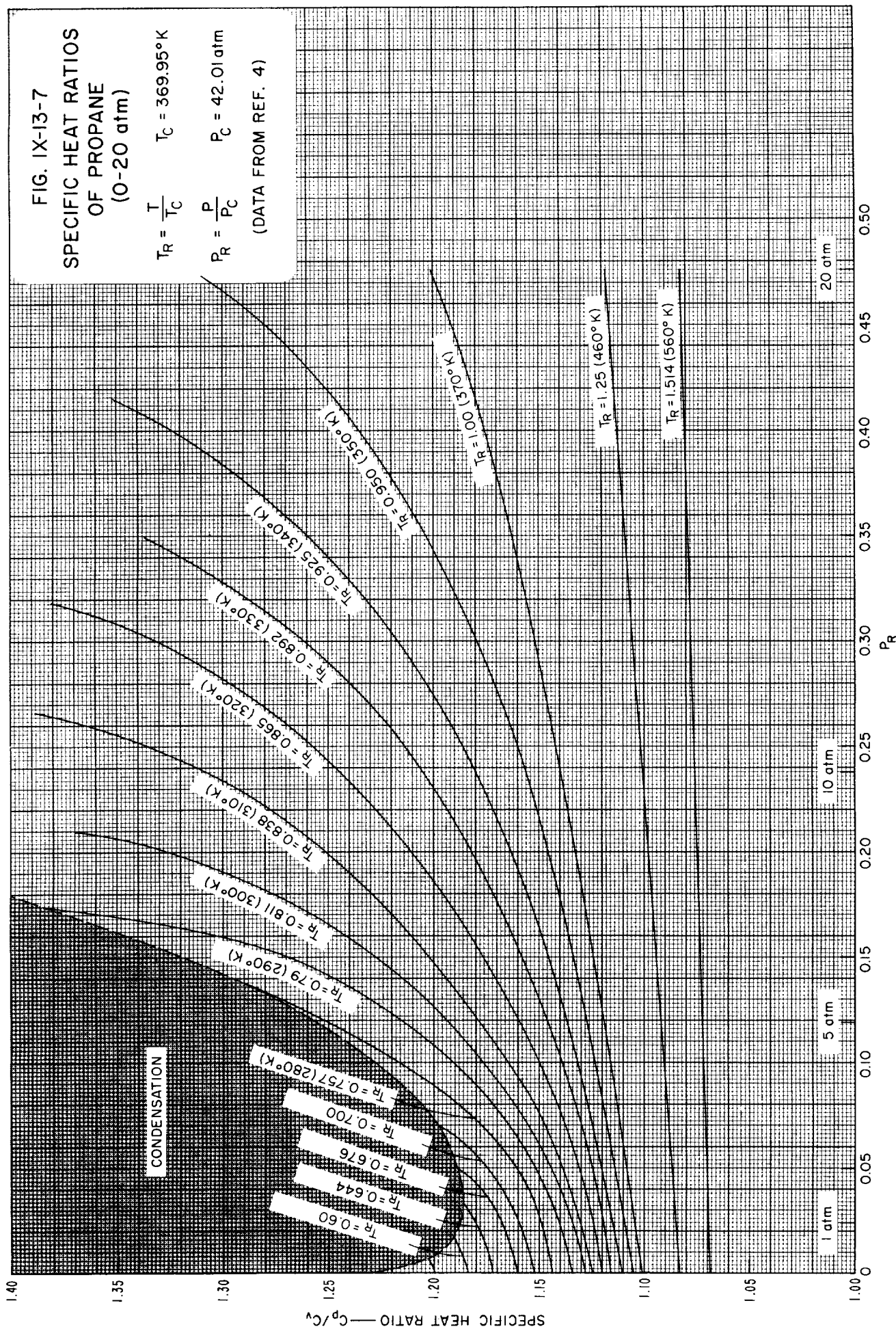
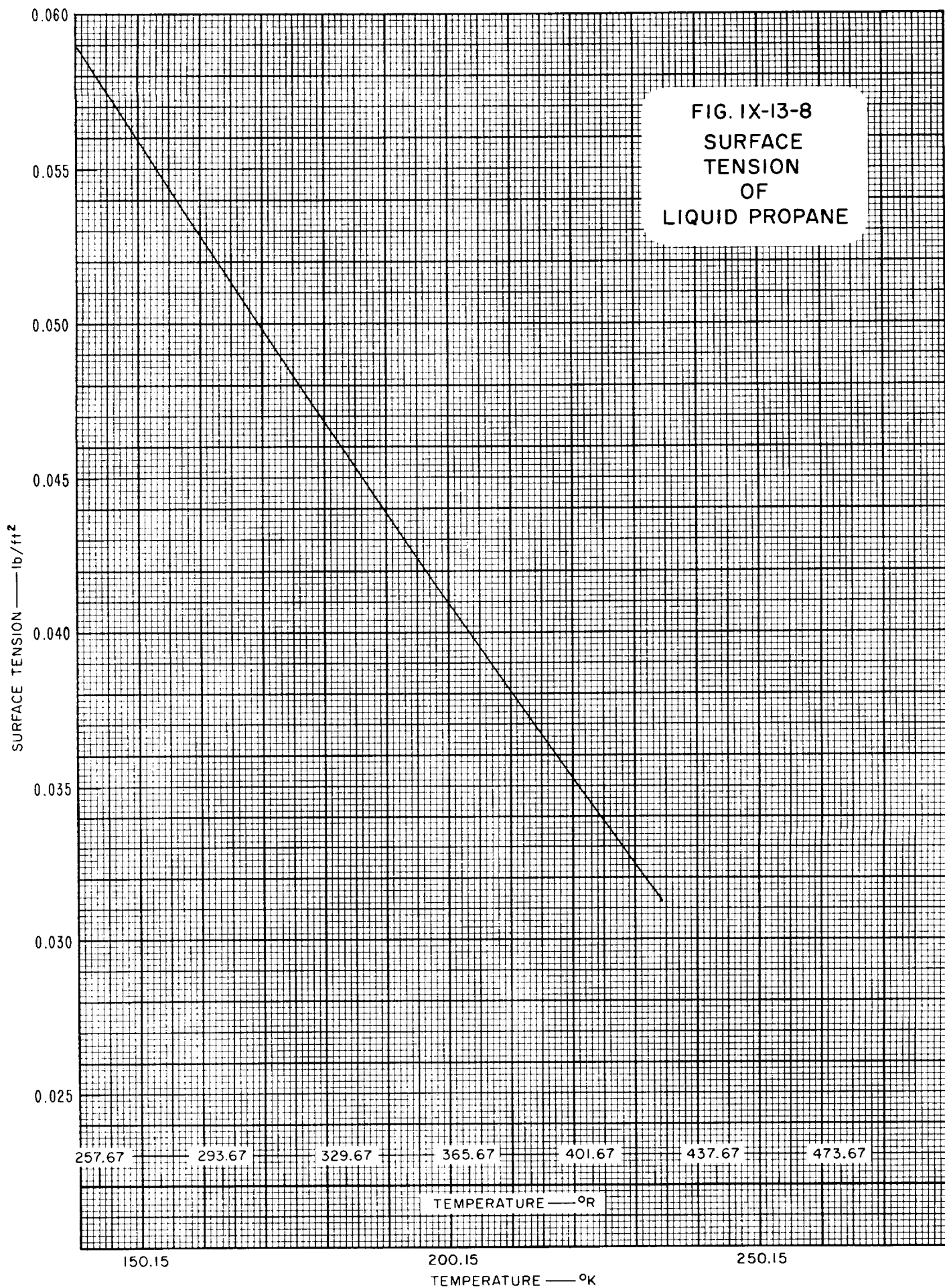
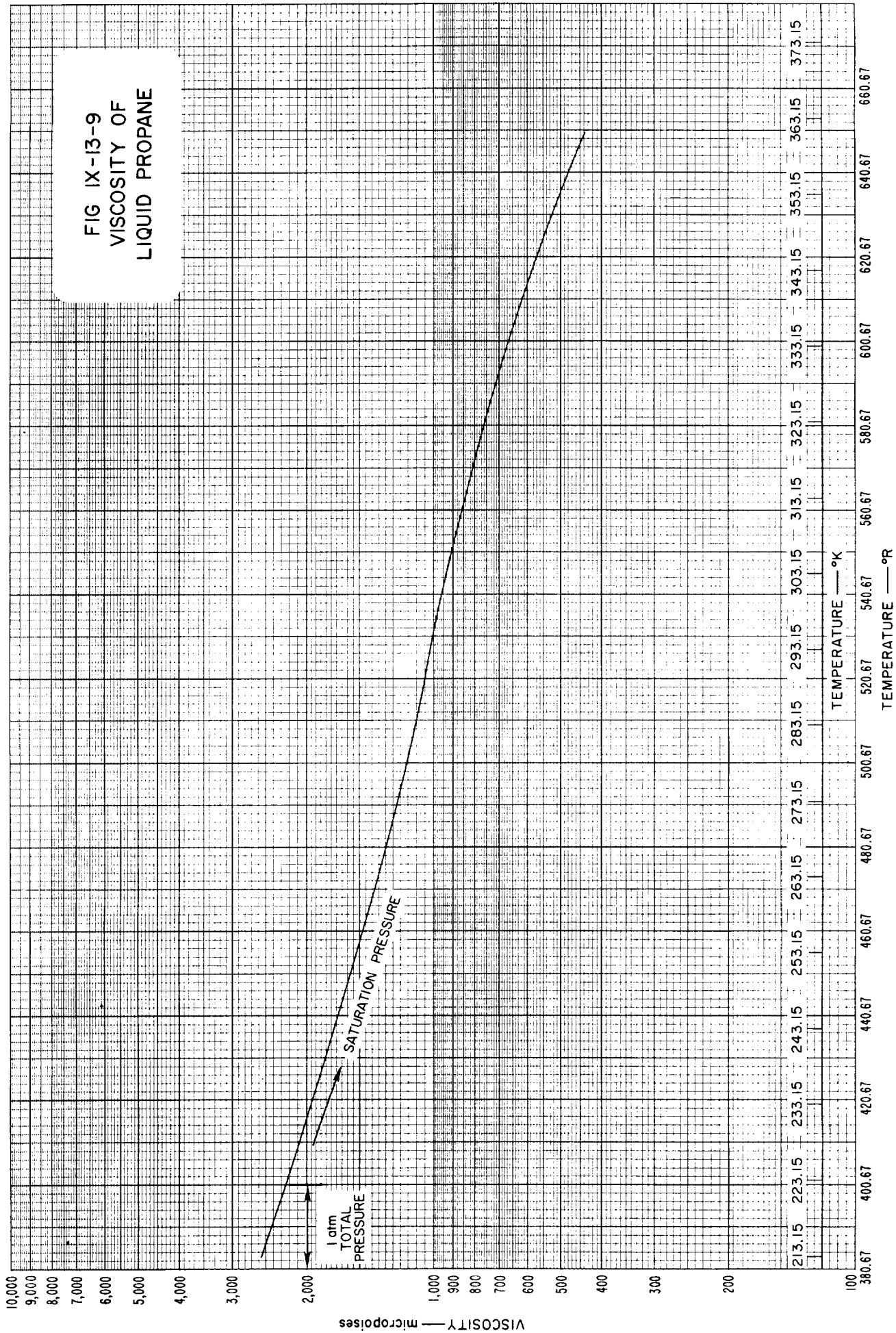


FIG. IX-13-8
SURFACE
TENSION
OF
LIQUID PROPANE





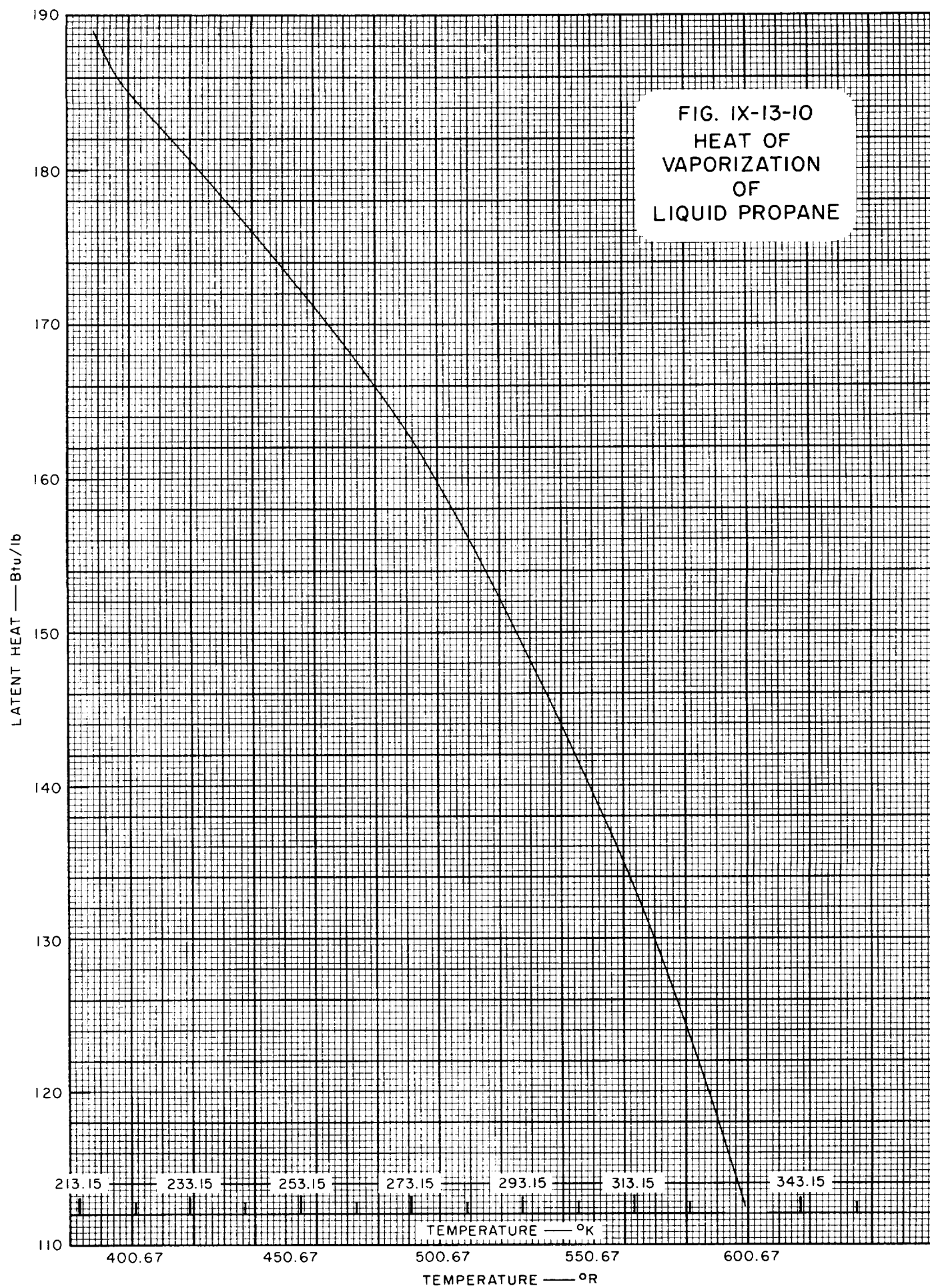
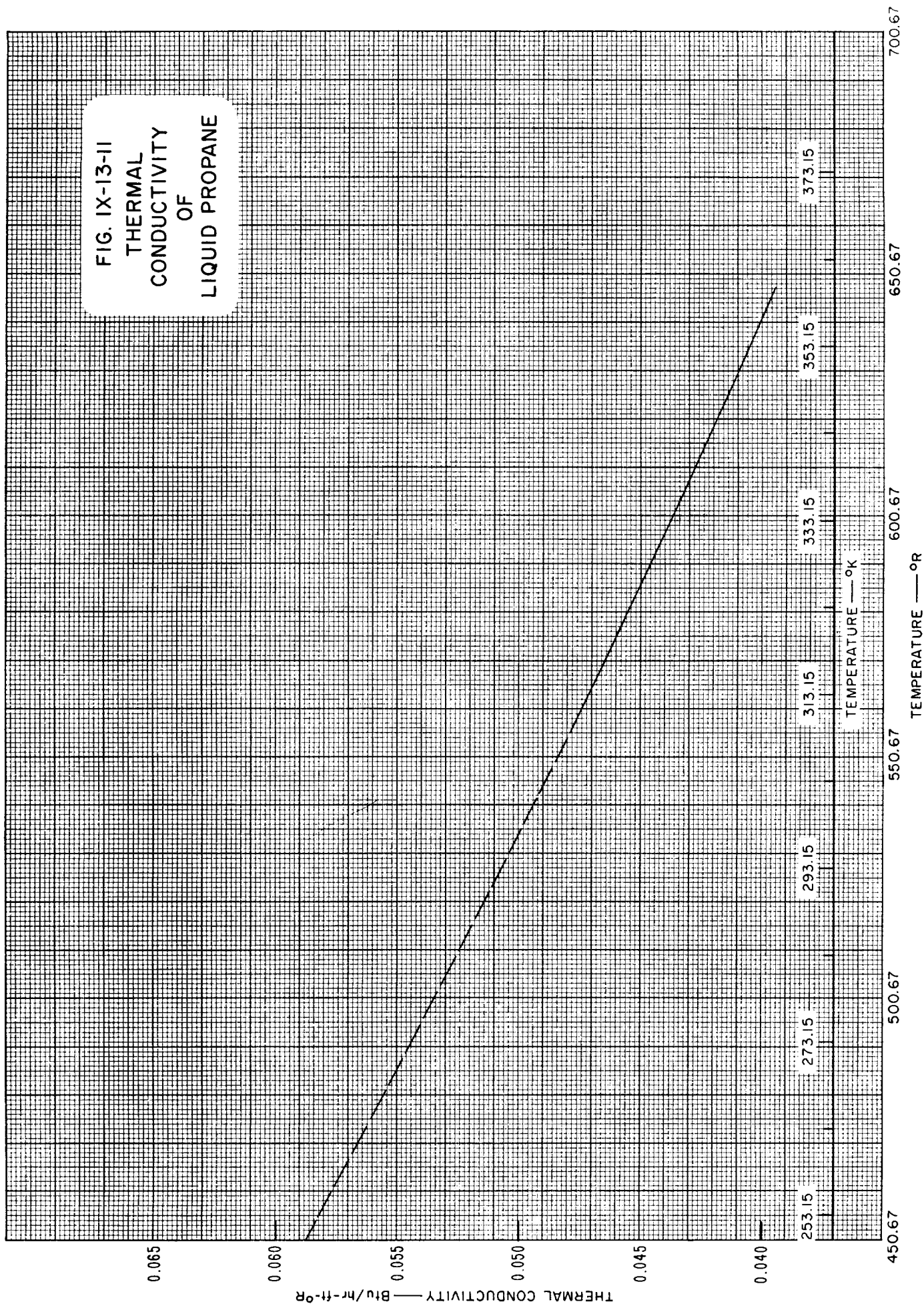
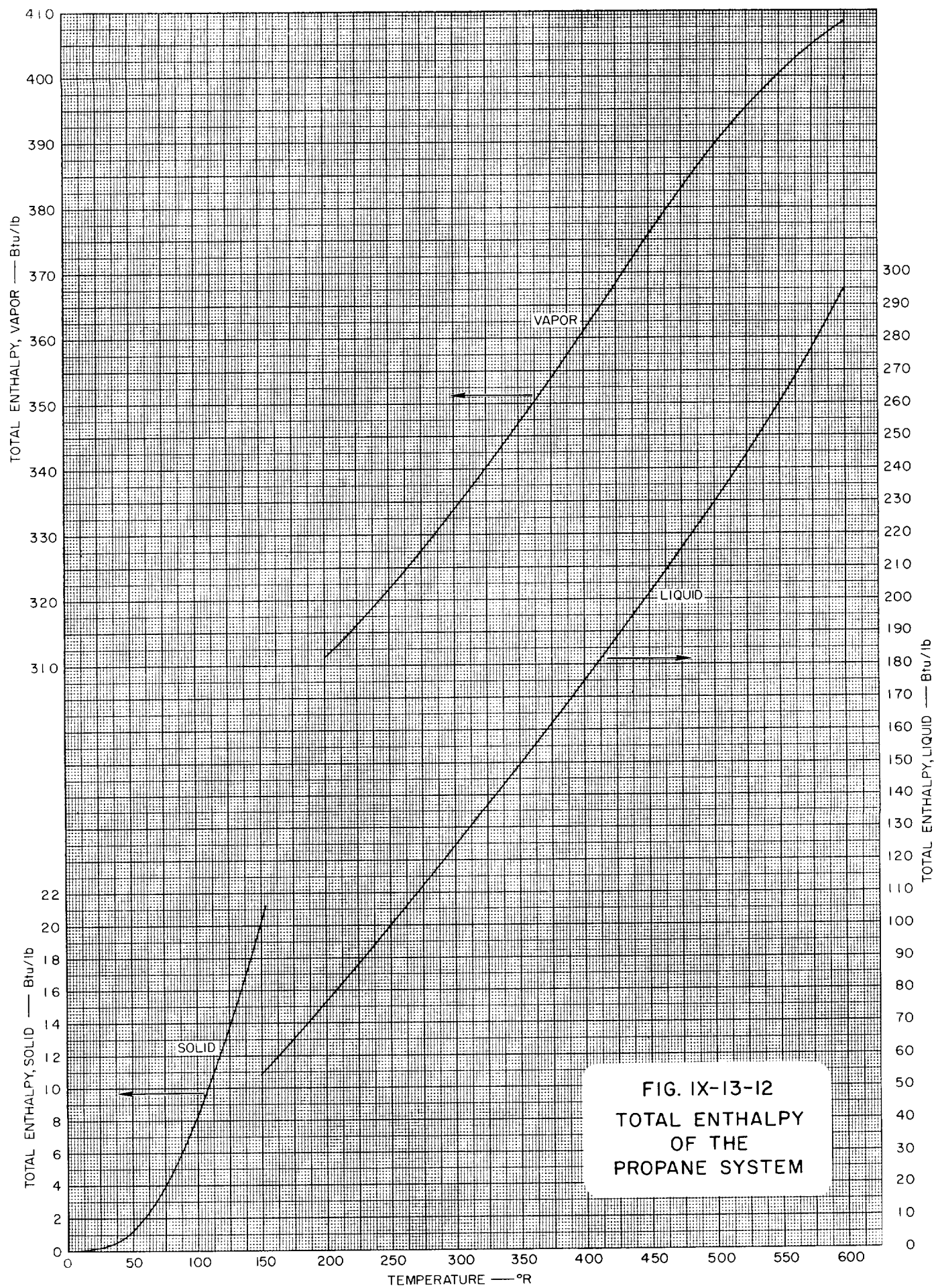
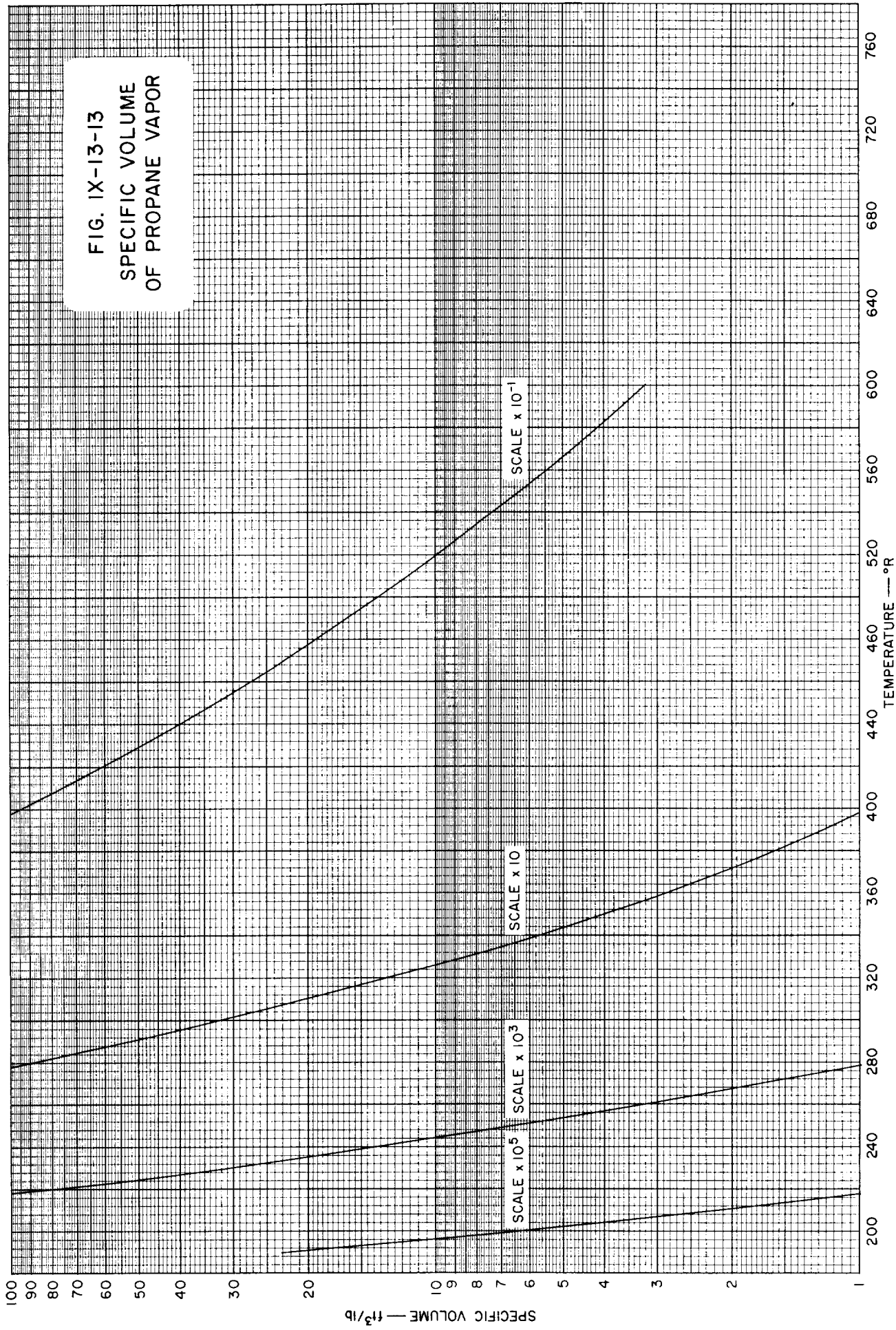


FIG. IX-13-II
THERMAL
CONDUCTIVITY
OF
LIQUID PROPANE



(((((





IX-13 PROPANE REFERENCES

1. Dana, L. I., Jenkins, A. C., Burdick, J. N., and Timm, R. C., *Refrig. Eng.*, **12**, 387 (1926).
2. Denny, L. C., and Luxon, L. L. (eds.), *Handbook Butane-Propane*, 3d Edition, Jenkins Publications, Los Angeles, California, 1951.
3. Kemp, J. D., and Egan, C. J., *J. Am. Chem. Soc.*, **60**, 1521 (1938).
4. Kuloor, N. R., Newitt, D. M., and Bateman, J. S., in Din (ed.), *Thermodynamic Functions of Gases*, Butterworths, London, Vol. 2, 1962.
5. Leng, D. E., and Comings, E. W., *Ind. Eng. Chem.*, **49**, 2042 (1957).
6. Rossini, F. D., *et al.*, *Selected Values of Physical and Thermodynamic Properties of Hydrocarbons and Related Compounds*, API-44, Carnegie Press, Pittsburgh, Pennsylvania, 1953.
7. Sage, B. H., and Lacey, W. N., *Ind. Eng. Chem.*, **30**, 829 (1938).
8. Tickner, A. W., and Lossing, F. P., *J. Phys. and Colloid Chem.*, **55**, 733 (1951).
9. Stearns, W. V., and George, E. J., *Ind. Eng. Chem.*, **35**, 602 (1943).

)

)

)

)

)

Table IX-14-1
GENERAL PROPERTIES OF *n*-BUTANE

PROPERTY	TEMPERATURE				PRESSURE			REF
	°C	°K	°F	°R	psia	atm	mm of Hg	
Melting Point	-138.35	134.80	-217.03	242.64				4
Boiling Point	- 0.50	272.65	31.10	490.8				4
Triple Point	-138.33	134.82	-216.99	242.68				4
Critical Temp.	152.01	425.16	305.62	765.31				4
Critical Press.					550.7	37.47		4
Mol. Wt.	58.12							
Heat of Vaporization.	See Table IX-14-7							
Heat of Fusion	19.17 cal/g or 34.50 Btu/lb							4

Table IX-14-1.1
SOME VALUES OF THE GAS CONSTANT, *R*, FOR *n*-BUTANE
(See also Conversion Tables, Section I)

TEMPERATURE IN °K				
Pressure Density	atm	kg/cm ²	mm of Hg	lb/in ²
g/cm ³	1.41185	1.45876	1073.06	20.7486
mole/cm ³	82.0567	84.7832	62363.1	1205.91
mole/liter	0.0820544	0.0847809	62.3613	1.20587
lb/ft ³	0.0226155	0.0233668	17.1877	0.332357
lb/mole/ft ³	1.31441	1.35808	998.952	19.3166
TEMPERATURE IN °R				
Pressure Density	atm	kg/cm ²	mm of Hg	lb/in ²
g/cm ³	0.784361	0.810423	596.114	11.5270
mole/cm ³	45.5871	47.1018	34646.2	669.950
mole/liter	0.0455858	0.0471005	34.6452	0.669928
lb/ft ³	0.0125641	0.0129816	9.54874	0.184642
lb/mole/ft ³	0.730228	0.754489	554.973	10.7314

Table IX-14-2
VAPOR PRESSURE OF n-BUTANE (Ref. 2, 4)

TEMPERATURE		PRESSURE	TEMPERATURE		PRESSURE
°K	°R	psia	°K	°R	psia
127.65	229.77	0.000019	238.71	429.67	3.273
131.15	236.07	0.000039	244.26	439.67	4.326
135.85	244.53	0.000097	249.82	449.67	5.64
139.95	251.91	0.000193	255.37	459.67	7.25
144.25	259.65	0.000387	260.93	469.67	9.20
149.95	269.91	0.000967	266.48	479.67	11.56
154.75	278.55	0.001933	272.04	489.67	14.36
159.85	287.73	0.003867	277.59	499.67	17.66
166.95	300.51	0.009668	283.14	509.67	21.53
172.85	311.13	0.01933	288.70	519.67	26.3
179.25	322.65	0.03867	294.26	529.67	31.6
188.45	339.21	0.09668	299.82	539.67	37.6
195.85	352.53	0.1933	305.37	549.67	44.5
200.37	360.67	0.2845	310.92	559.67	52.2
205.37	369.67	0.422	316.48	569.67	60.8
210.92	379.69	0.625	322.03	579.67	70.8
216.48	389.67	0.906	327.59	589.67	81.4
222.03	399.67	1.285	333.15	599.67	92.6
227.59	409.67	1.787			
233.15	419.67	2.439			

(See Figure IX-14-1,
Figure IX-14-2)

Table IX-14-3
DENSITY OF LIQUID n-BUTANE (Ref. 4)

TEMPERATURE		DENSITY	TEMPERATURE		DENSITY
°K	°R	lb/ft ³	°K	°R	lb/ft ³
138.71	249.67	45.9	222.03	399.67	40.72
144.26	259.67	45.6	227.59	409.67	40.39
149.82	269.67	45.3	233.15	419.67	40.05
155.37	279.67	44.9	238.71	429.67	39.71
160.93	289.67	44.6	244.26	439.67	39.37
166.48	299.67	44.21	249.82	449.67	39.02
172.04	309.67	43.82	255.37	459.67	38.67
177.59	319.67	43.45	260.93	469.67	38.32
183.15	329.67	43.07	266.48	479.67	37.96
188.70	339.67	42.73	272.04	489.67	37.60
194.26	349.67	42.39	277.59	499.67	37.24
199.81	359.67	42.05	283.14	509.67	36.88
205.37	369.67	41.71	288.70	519.67	34.46
210.92	379.67	41.37	294.26	529.67	36.05
216.48	389.67	41.04			

(See Figure IX-14-3)

Table IX-14-4
DENSITY OF SATURATED n-BUTANE VAPOR (Ref. 2)

TEMPERATURE		DENSITY	TEMPERATURE		DENSITY
°K	°R	lb/ft ³	°K	°R	lb/ft ³
255.37	459.67	0.0901	310.93	559.67	0.552
258.15	464.67	0.100	313.71	564.67	0.588
260.93	469.67	0.112	316.48	569.67	0.633
263.71	474.67	0.124	319.26	574.67	0.676
266.48	479.67	0.138	322.04	579.67	0.730
269.26	484.67	0.153	324.82	584.67	0.783
272.04	489.67	0.169	327.59	589.67	0.840
274.82	494.67	0.186	330.37	594.67	0.900
277.59	499.67	0.205	333.15	599.67	0.965
280.37	504.67	0.224	335.93	604.67	1.035
283.15	509.67	0.246	338.70	609.67	1.115
285.93	514.67	0.268	341.48	614.67	1.190
288.71	519.67	0.294	344.26	619.67	1.275
291.48	524.67	0.321	347.04	624.67	1.365
294.26	529.67	0.347	349.82	629.67	1.455
297.04	534.67	0.377	352.59	634.67	1.557
299.82	539.67	0.407	355.37	639.67	1.660
302.59	544.67	0.439			
305.37	549.67	0.476			
308.15	554.67	0.510			

(See Figure IX-14-4)

Table IX-14-5
SPECIFIC HEAT OF LIQUID n-BUTANE (Ref. 1, 2)

TEMPERATURE		SPECIFIC HEAT	TEMPERATURE		SPECIFIC HEAT
$^{\circ}\text{K}$	$^{\circ}\text{R}$	Btu/lb	$^{\circ}\text{K}$	$^{\circ}\text{R}$	Btu/lb
12	21.6	0.0065	180	324	0.4823
15	27	0.0134	190	342	0.4866
20	36	0.0186	200	360	0.4917
30	54	0.0740	210	378	0.4972
40	72	0.1129	220	396	0.5029
50	90	0.1480	230	414	0.5098
60	108	0.1770	240	432	0.5165
70	126	0.2037	250	450	0.5255
80	144	0.2288	260	468	0.5351
90	162	0.2514	270	486	0.5446
100	180	0.2743	272.66	490.68	Boiling Point
107.53	193.55	Transition	273	492	0.545
110	198	0.3412	278	500	0.554
120	216	0.3465	283	510	0.565
130	234	0.3551	289	520	0.576
134.87	247.77	Melting Point	294	530	0.587
140	252	0.4673	300	540	0.598
150	270	0.4732	305	550	0.609
160	288	0.4773			
170	306	0.4793			

(See Figure IX-14-5)

Table IX-14-6
SPECIFIC HEAT OF n-BUTANE GAS (Ref. 4)

TEMPERATURE		SPECIFIC HEAT
$^{\circ}\text{K}$	$^{\circ}\text{R}$	Btu/lb
255.37	459.67	0.3578
273.15	491.67	0.3751
283.15	509.67	0.3851
288.71	519.67	0.3908
310.93	559.67	0.4142
338.71	609.67	0.4441
366.48	659.67	0.4739
422.04	759.67	0.5316
477.19	859.67	0.5865
533.15	959.67	0.6374

(See Figure IX-14-6)

Table IX-14-7
HEAT OF VAPORIZATION OF n-BUTANE (Ref. 2)

TEMPERATURE		LATENT HEAT	TEMPERATURE		LATENT HEAT
°K	°R	Btu/lb	°K	°R	Btu/lb
255.37	459.67	171.5	310.93	559.67	150.5
260.93	469.67	169.7	316.48	569.67	147.6
266.48	479.67	167.6	322.04	579.67	144.9
272.04	489.67	165.7	327.59	589.67	141.5
277.59	499.67	163.8	333.15	599.67	138.3
283.15	509.67	161.6	338.70	609.67	134.5
288.71	519.67	159.4	344.26	619.67	131.1
294.26	529.67	157.4	349.87	629.67	126.9
299.82	539.67	155.3	355.37	639.67	123.4
305.37	549.67	153.0			

(See Figure IX-14-7)

Table IX-14-8
VISCOSITY OF n-BUTANE (Ref. 2, 4)

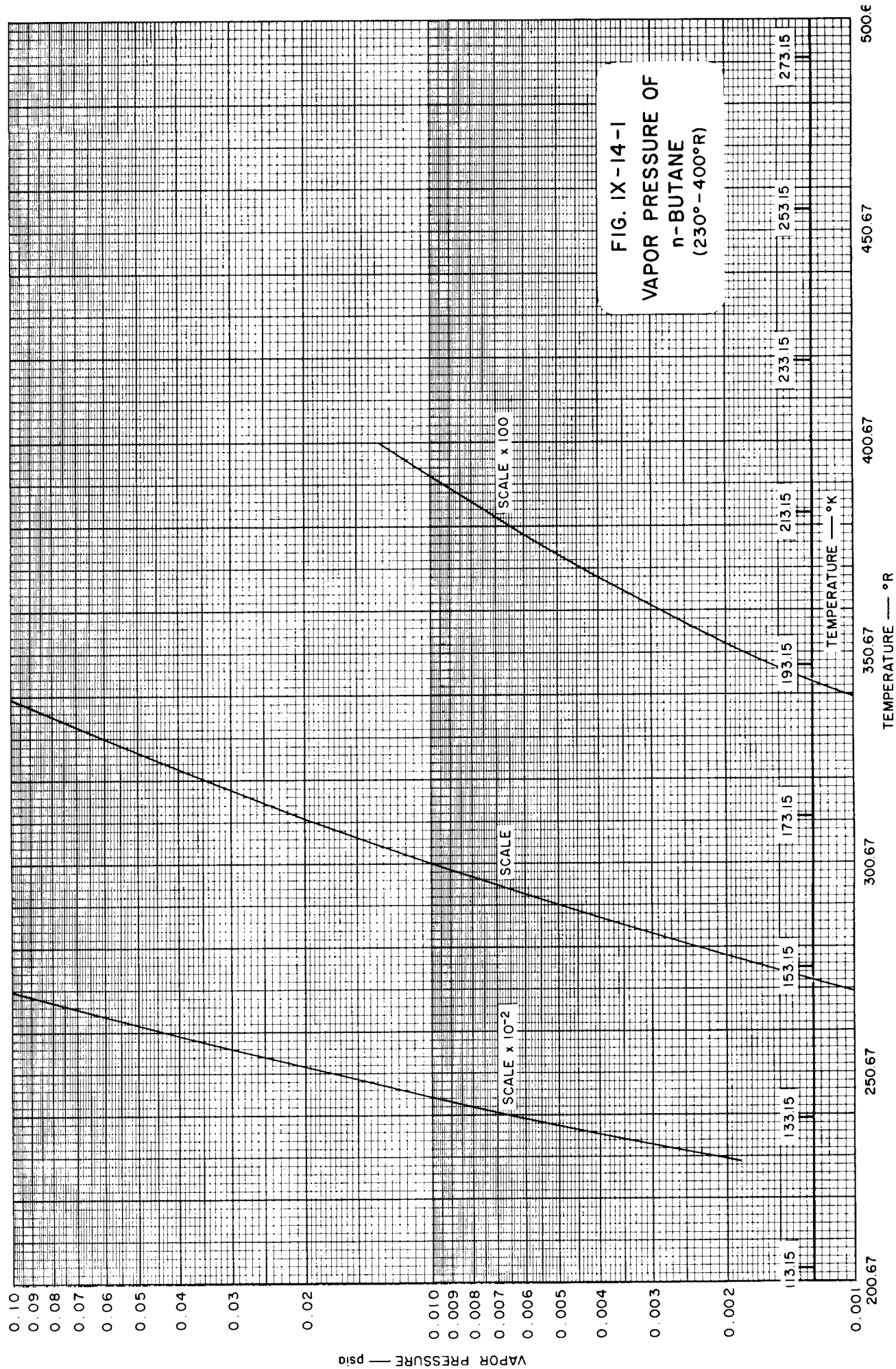
TEMPERATURE		ABSOLUTE VISCOSITY
°K	°R	centi-poise
183.15	329.67	0.63
193.15	347.67	0.536
203.15	365.67	0.462
213.15	383.67	0.403
223.15	401.67	0.355
233.15	419.67	0.315
243.15	437.67	0.282
253.15	455.67	0.253
263.15	473.67	0.229
273.15	491.67	0.210
277.59	499.67	0.200
288.71	519.67	0.180
299.82	539.67	0.162
310.93	559.67	0.147
322.04	579.67	0.131
333.15	599.67	0.116

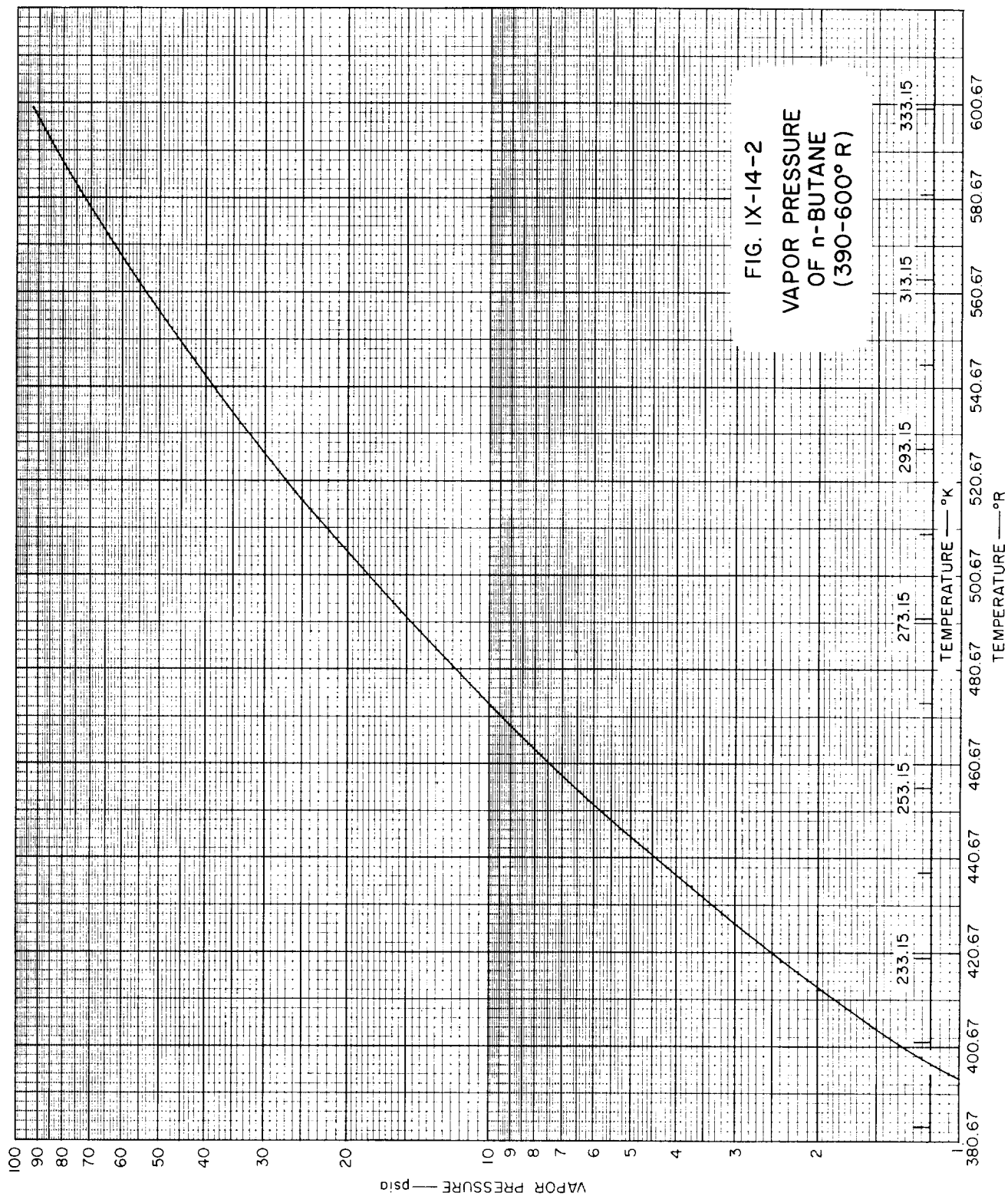
(See Figure IX-14-8)

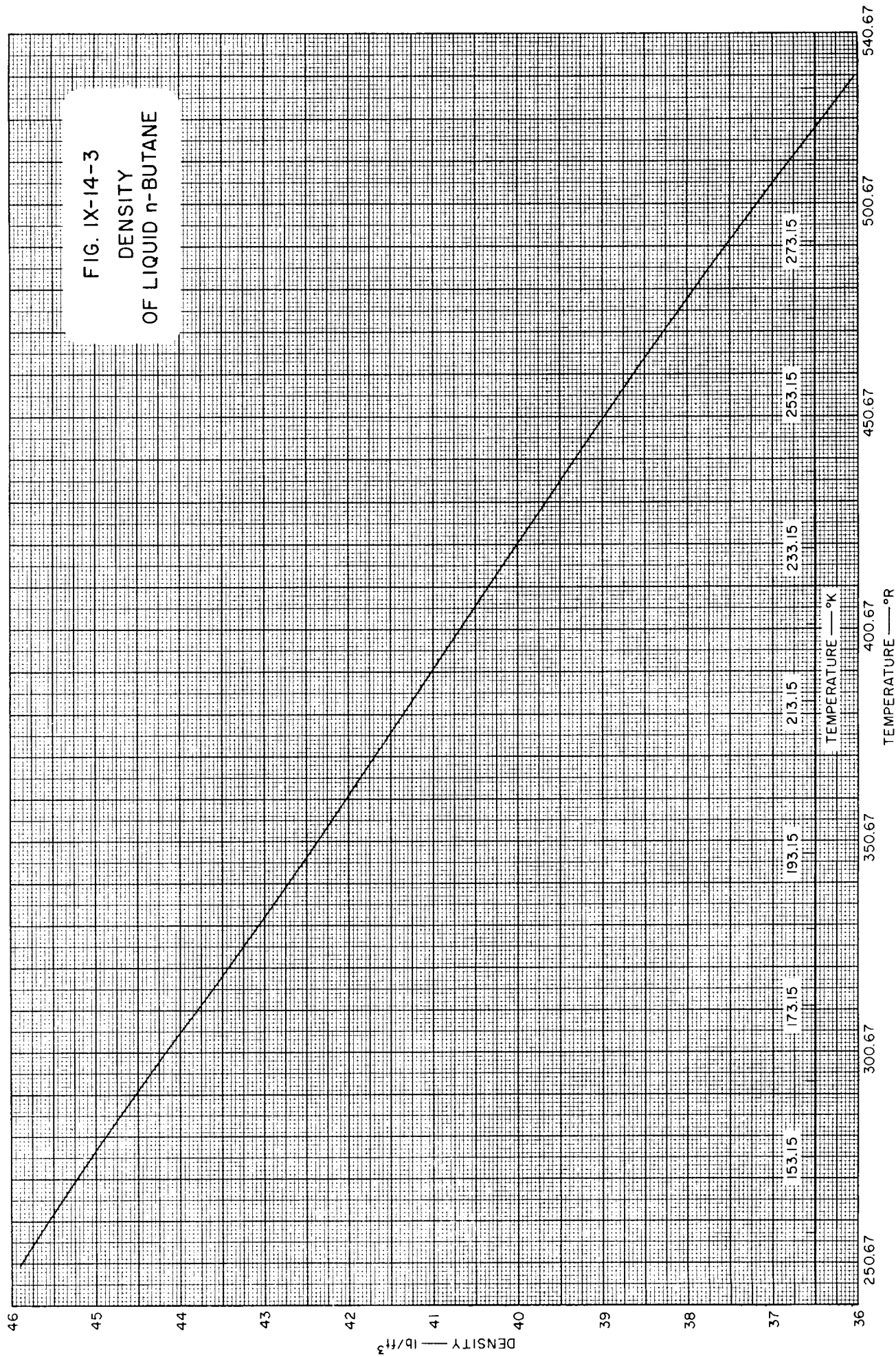
Table IX-14-9
TOTAL ENTHALPY AND SPECIFIC VOLUME OF THE n-BUTANE SYSTEM
(Computed from data in References 1, 2, 4)

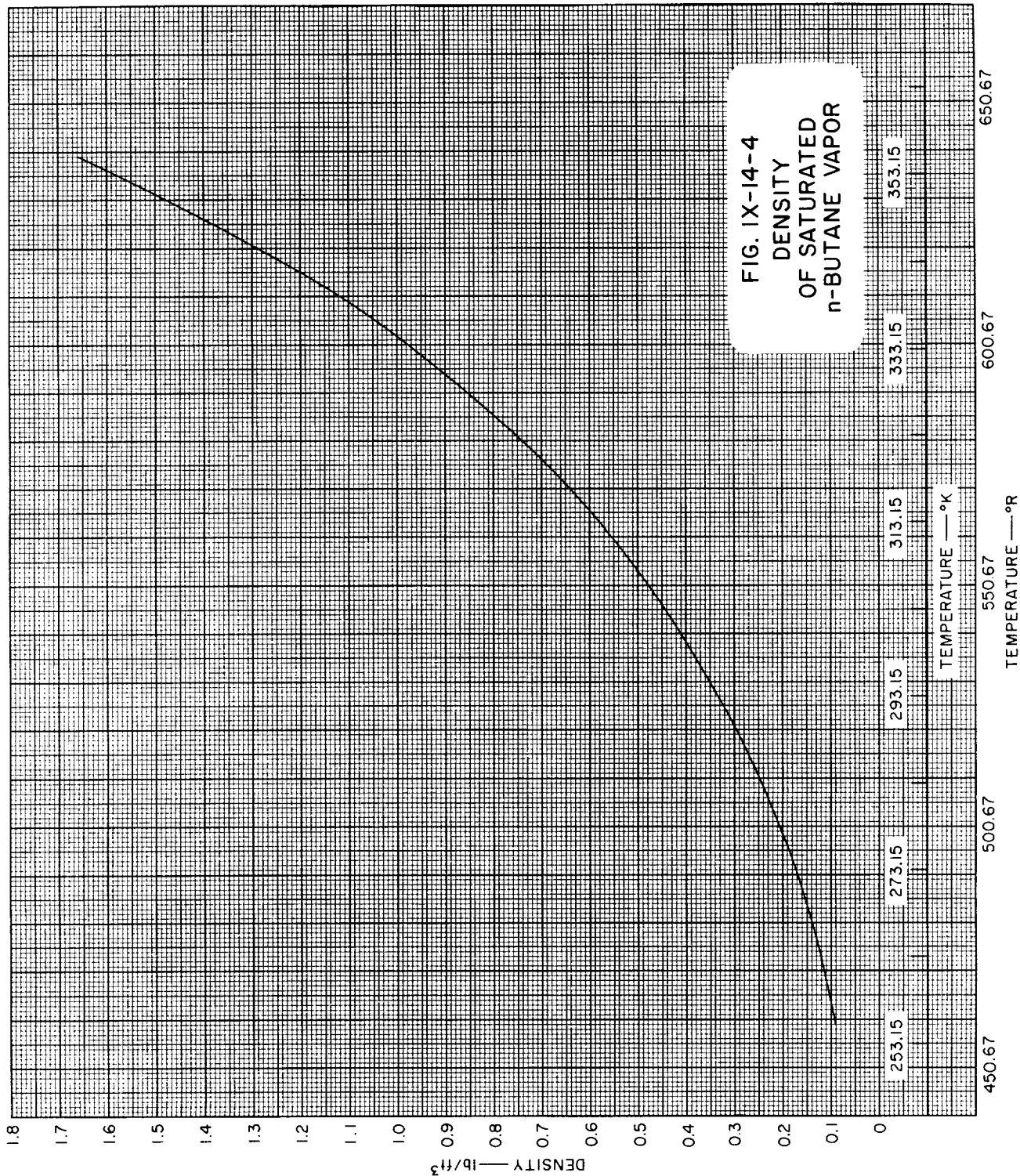
TEMP.	TOTAL ENTHALPY—Btu/lb			SPEC. VOL. VAPOR	TEMP.	TOTAL ENTHALPY—Btu/lb			SPEC. VOL. VAPOR
°R	Solid	Liquid	Vapor	ft ³ /lb	°R	Solid	Liquid	Vapor	ft ³ /lb
0	0				370				159.5
20	0.1				380		163.4	350.4	111.0
40	0.5				390				78.5
60	2.92				400		173.5	356.6	56.6
80	5.70				410				42.1
100	8.82				420		184.6	362.6	31.2
120	12.50				430				23.9
140	16.70				440		193.3	368.6	18.5
160	21.50				450				14.4
180	26.75				460		202.0	374.8	11.0
193.55	30.51				470			377.6	8.91
(transition)					480		210.4	380.6	7.18
193.55	45.81				490.8		217.7	383.5	5.65
200	47.80				500			386.0	4.85
210	51.00				510			389.2	4.05
220	54.5				520			392.3	3.38
230	58.10				530			395.5	2.88
242.77	62.95	97.44			540			398.6	2.44
250		101.7			550			401.7	2.12
260		106.0	(312.2)	1 240 000	560			404.7	1.81
270				278 000					
280		115.0	(318.8)	69 500	570			407.8	1.58
290				17 800	580			410.8	1.36
300		124.5	(325.0)	6 100	590			413.5	1.18
310				3 080	600			416.3	1.04
320		134.2	(331.6)	1 730					
330				1 025					
340		143.8	(338.0)	618					
350				380					
360		153.6	(344.2)	242					

(See Figure IX-14-9,
Figure IX-14-10)









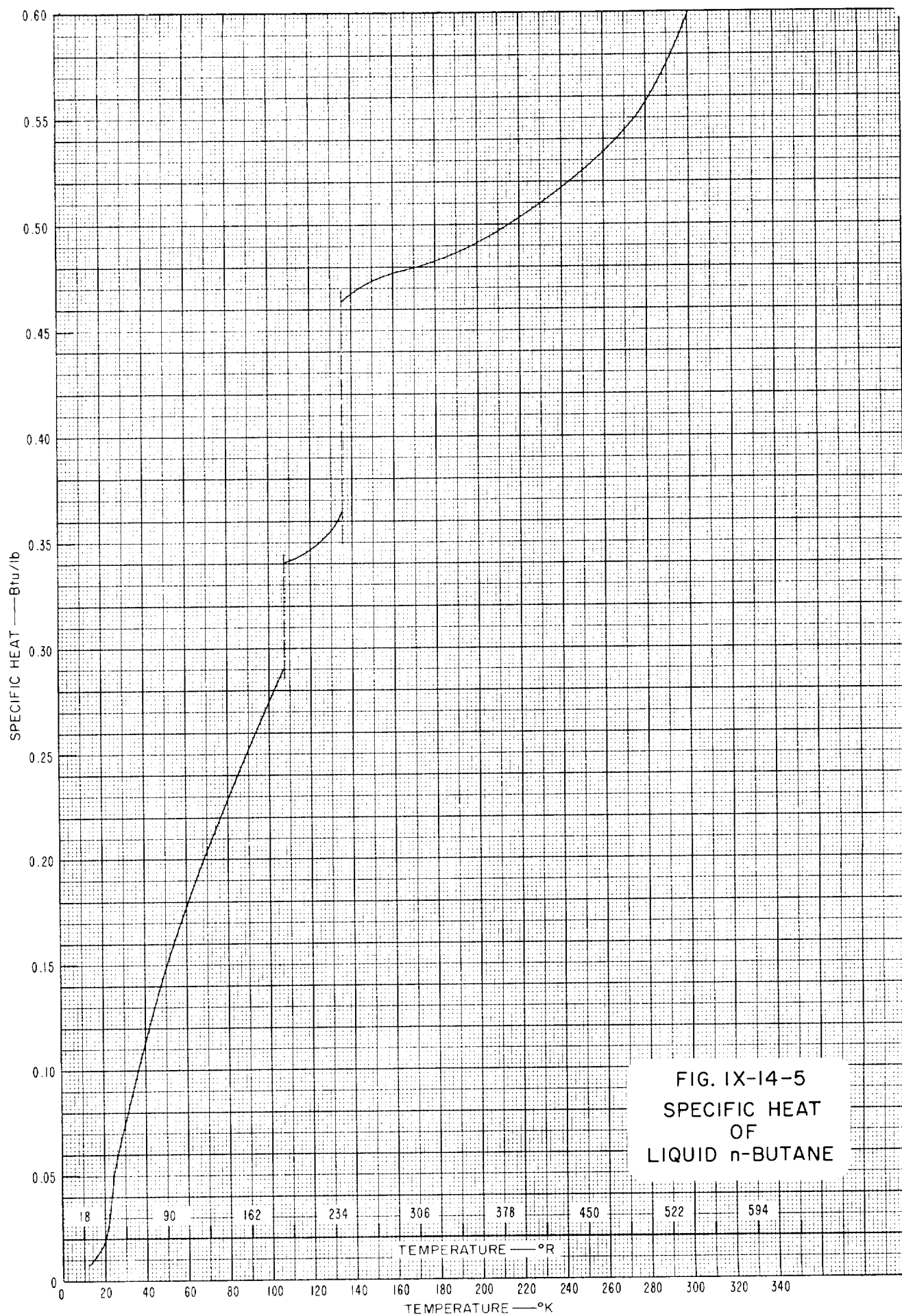
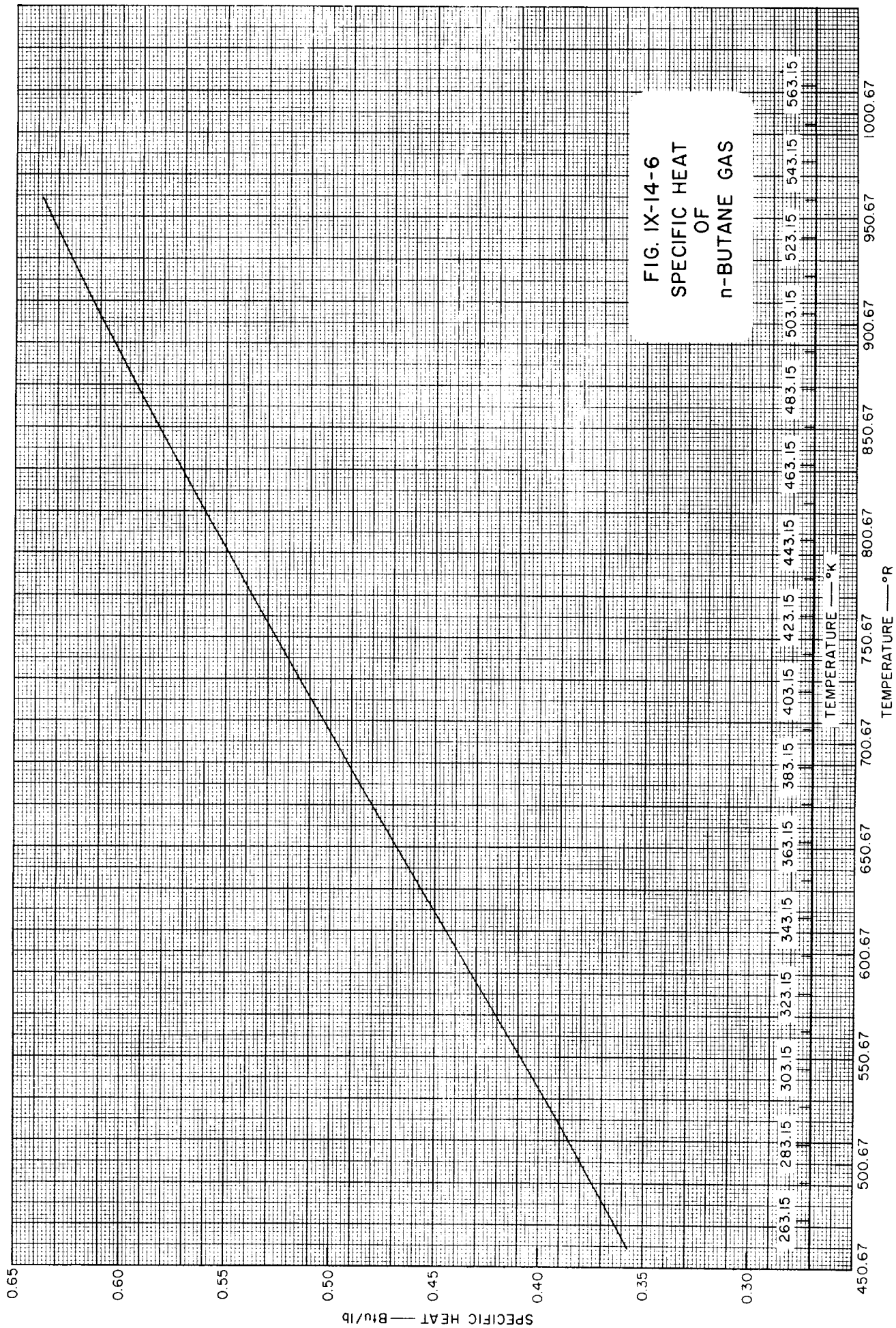


FIG. IX-14-5
SPECIFIC HEAT
OF
LIQUID n-BUTANE



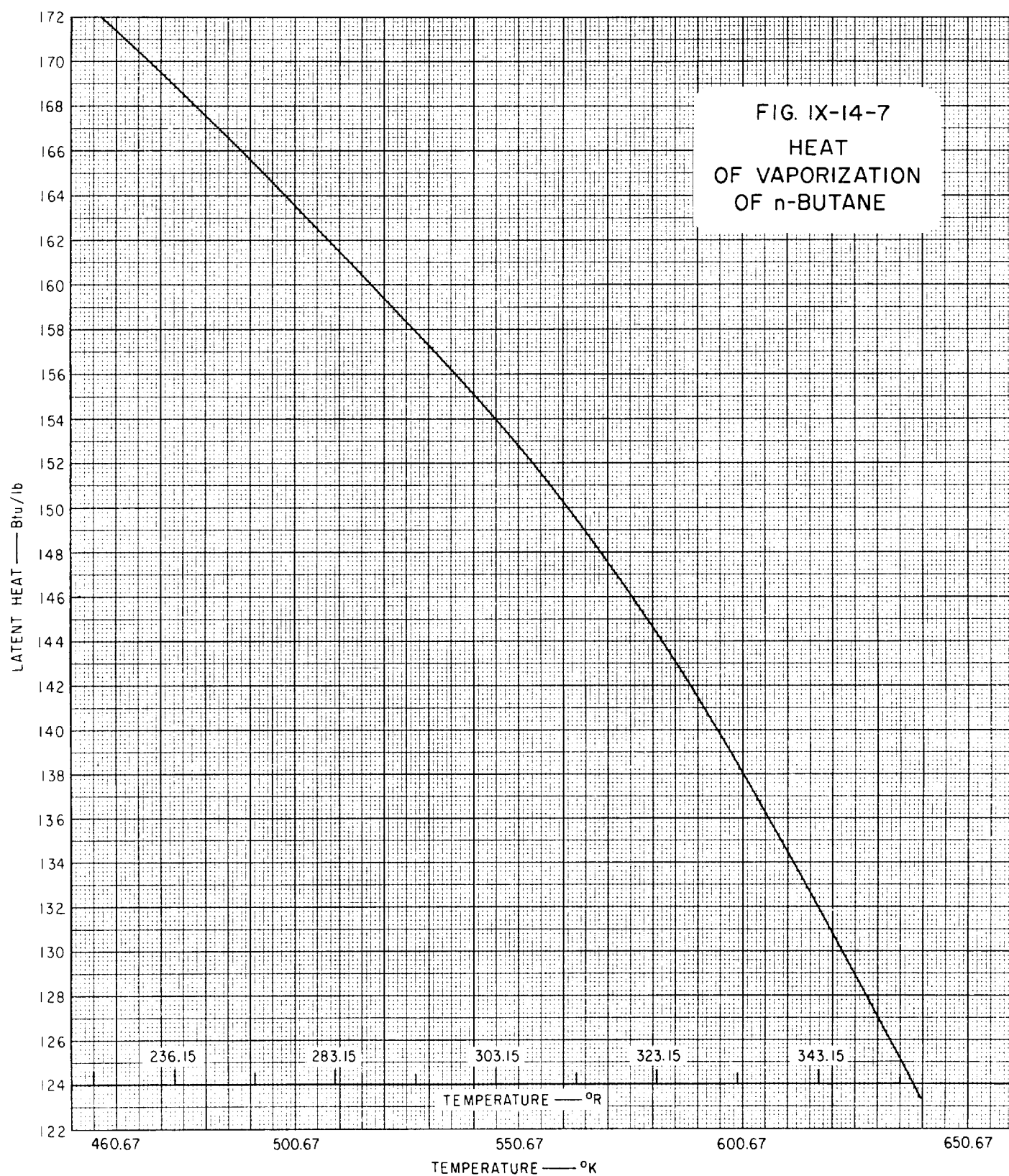
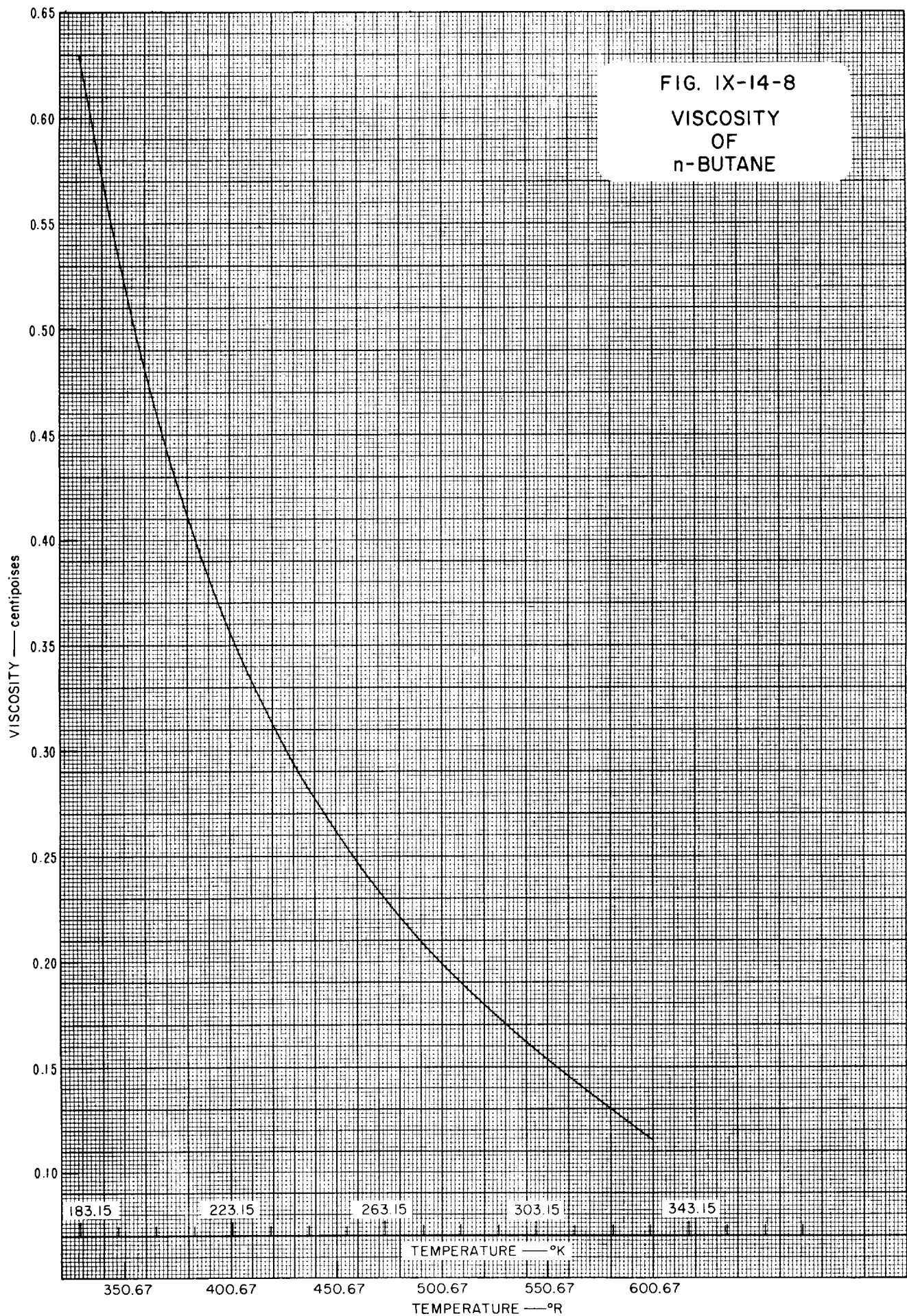
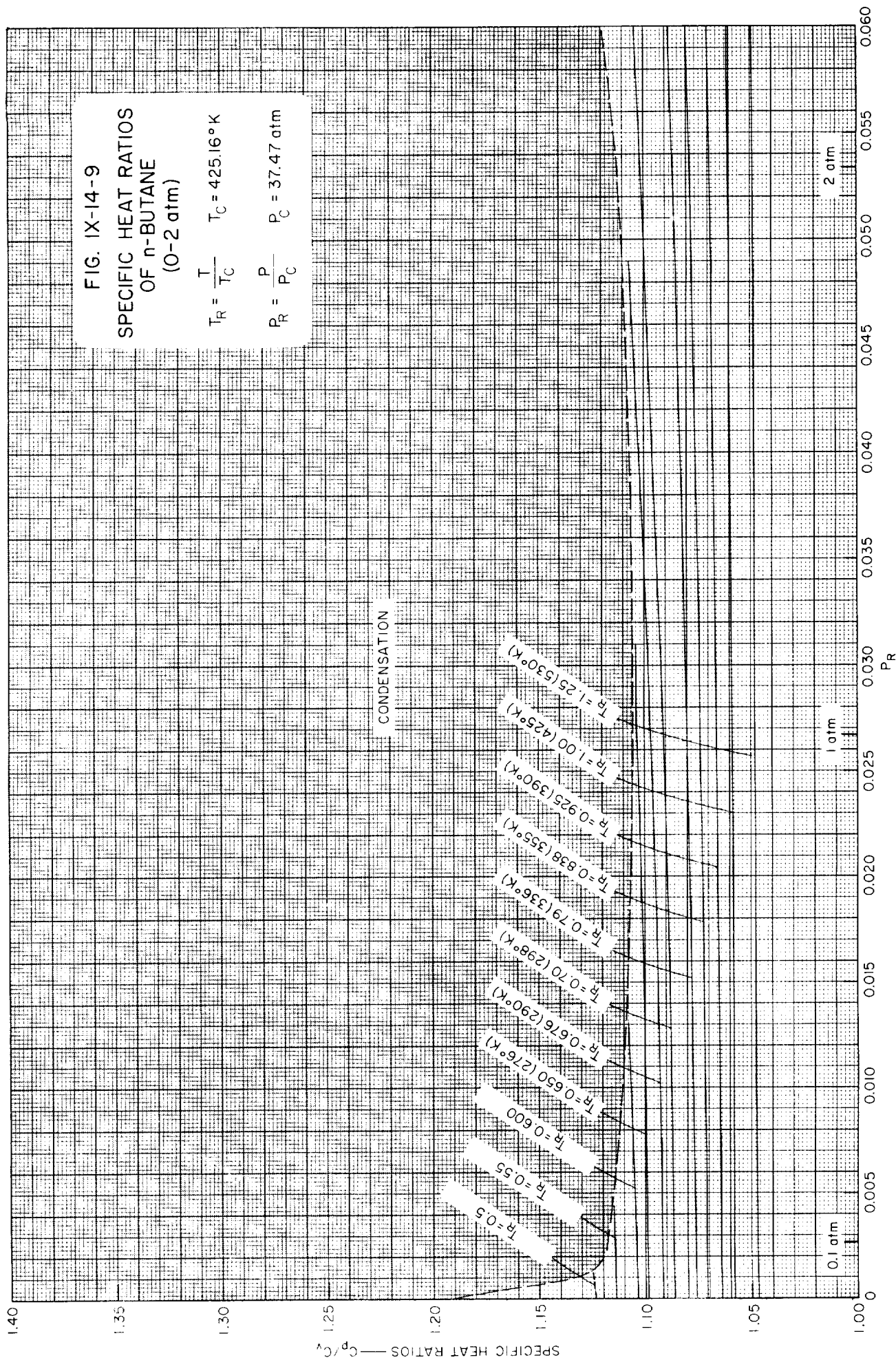
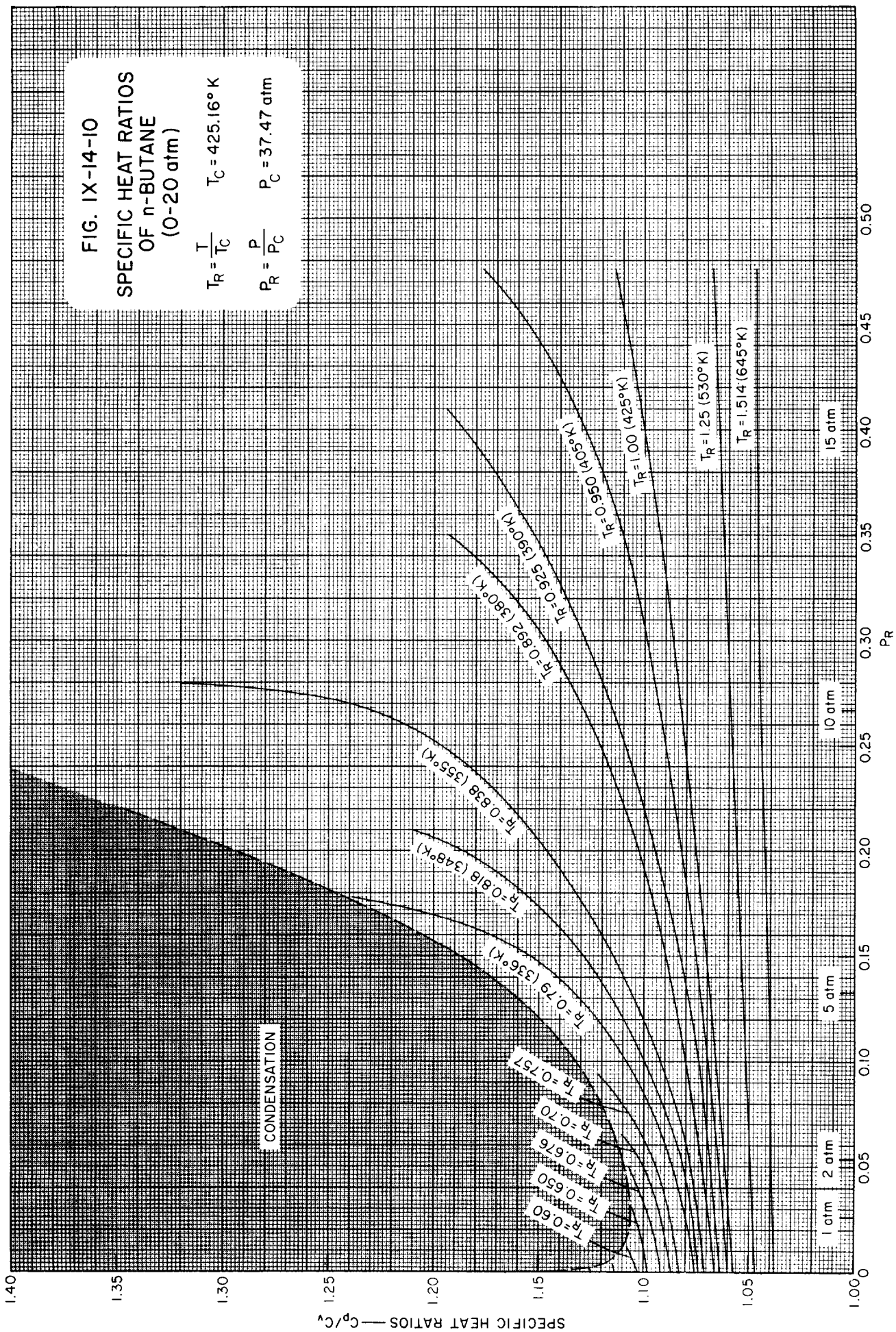


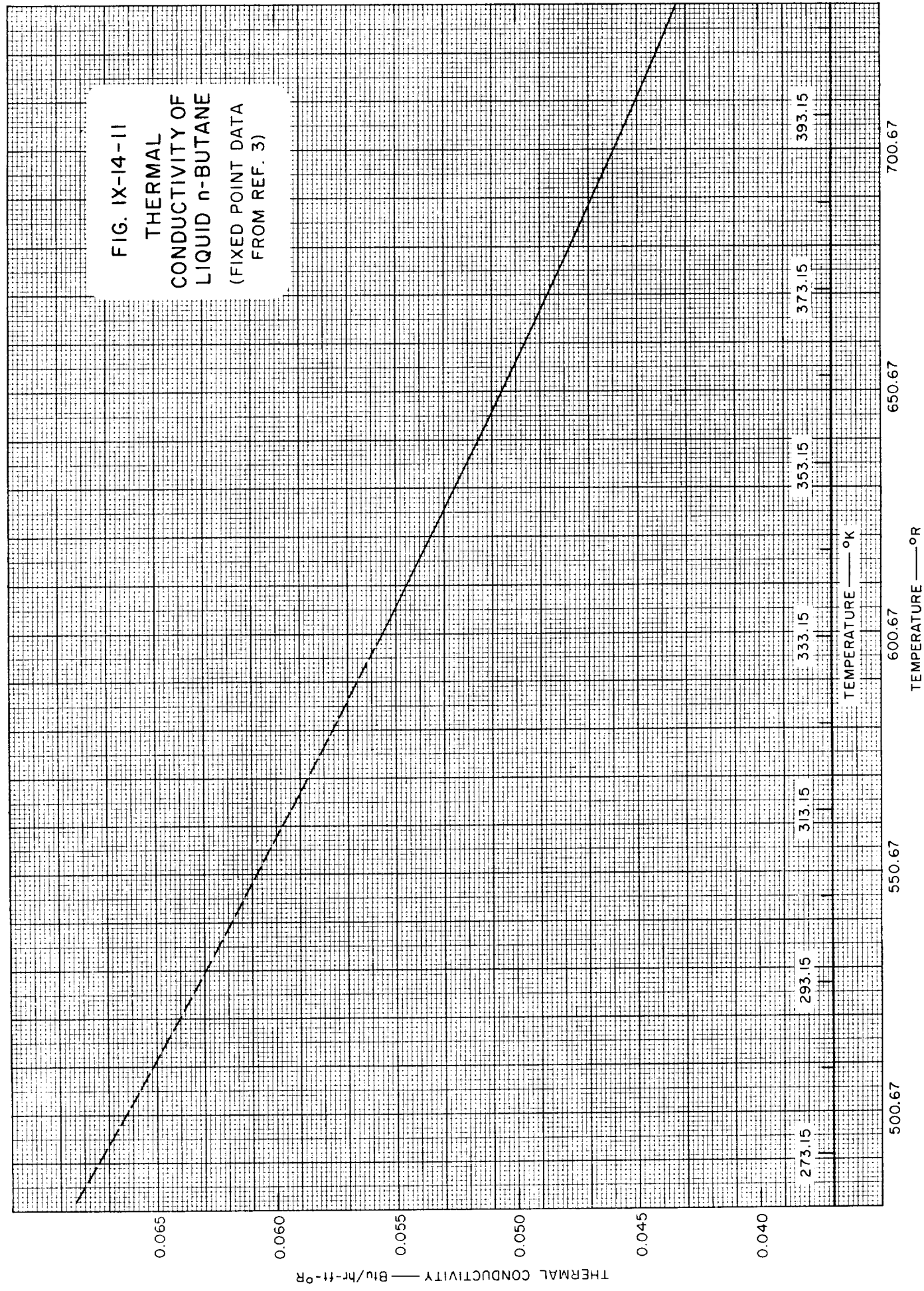
FIG. IX-14-8

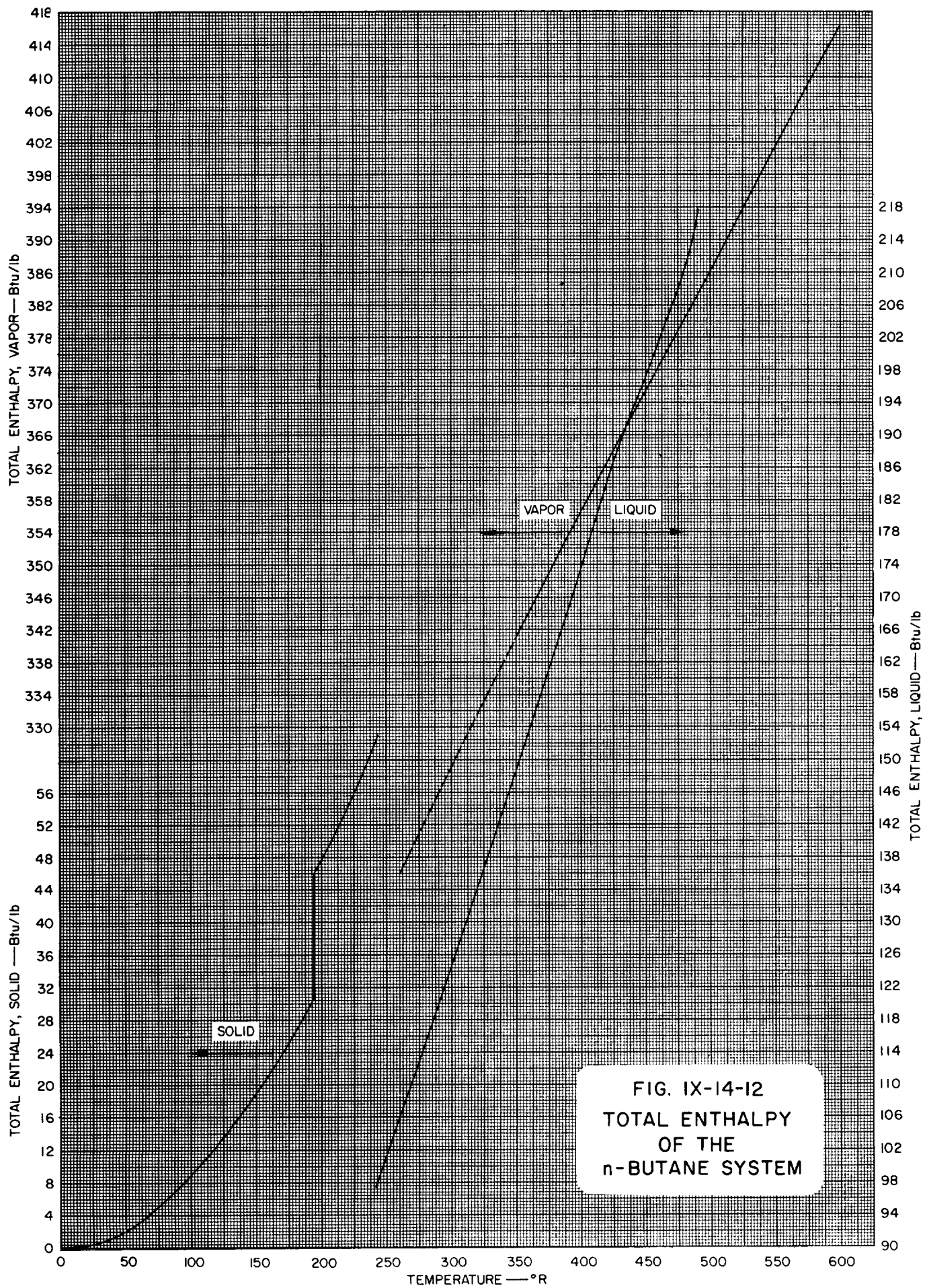
VISCOSITY
OF
n-BUTANE

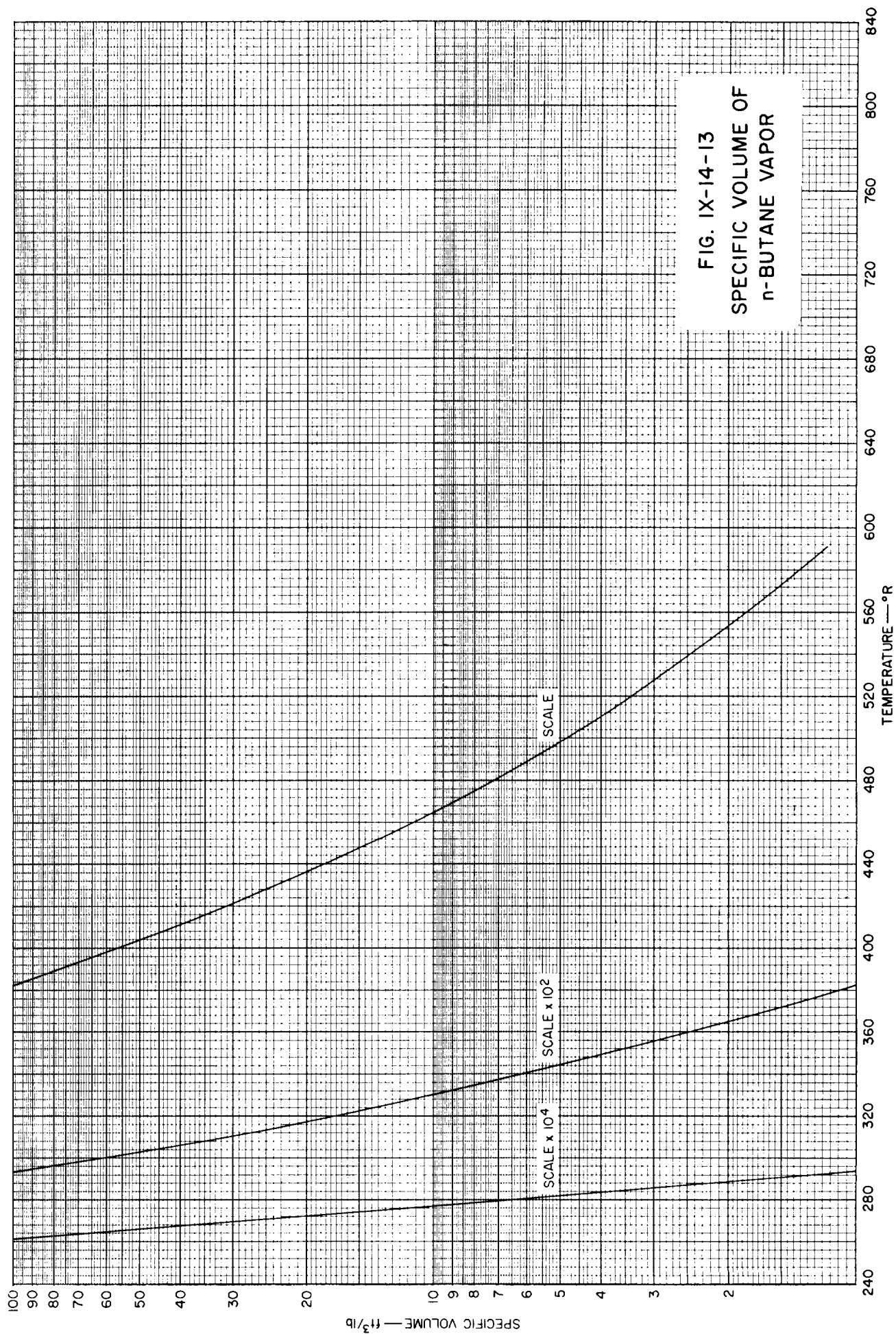












)

)

)

)

)

IX-14 n-BUTANE REFERENCES

1. Aston, J. G., and Messerley, G. H., *J. Am. Chem. Soc.*, **62**, 1917 (1944).
2. Denny, L. C., and Luxon, L. L., (eds.), *Handbook: Butane-Propane*, 3d Edition, Jenkins Publications, Los Angeles, California, 1951.
3. Kramer, F. R., and Comings, F. W., *J. Chem. Eng. Data*, **5**, No. 4, 462 (1960).
4. Rossini, F. D., et al., *Selected Values of Physical and Thermodynamic Properties of Hydrocarbons and Related Compounds*, API-44, Carnegie Press, Pittsburgh, Pennsylvania, 1953.

)

)

)

)

)

Table IX-15-1
GENERAL PROPERTIES OF AMMONIA

PROPERTY	TEMPERATURE				PRESSURE			REF
	$^{\circ}\text{C}$	$^{\circ}\text{K}$	$^{\circ}\text{F}$	$^{\circ}\text{R}$	psia	atm	mm of Hg	
Melting Point	- 77.74	195.41	-107.93	351.74				1
Boiling Point	- 33.42	239.73	- 28.16	431.51				6
Triple Point	- 77.74	195.41	-107.93	351.74				6
Critical Temp.	132.90	406.05	271.22	730.89				6
Critical Press.					1650.36	112.3	85,348	1
Mol. Wt.	17.03							
Heat of Vaporization	5581 cal/mole or 589.9 Btu/lb at B.P.							6
Heat of Fusion	1351.6 cal/mole or 142.85 Btu/lb							6

Table IX-15-1.1
SOME VALUES OF THE GAS CONSTANT, R, FOR AMMONIA
(See also Conversion Tables, Section I)

TEMPERATURE IN $^{\circ}\text{K}$				
Pressure	atm	kg/cm^2	mm of Hg	lb/in^2
Density				
g/cm^3	4.81836	4.97846	3661.96	70.8109
mole/cm^3	82.0567	84.7832	62363.1	1205.91
mole/liter	0.0820544	0.0847809	62.3613	1.20587
lb/ft^3	0.0771820	0.0797463	58.6584	1.13427
$\text{lb}/\text{mole}/\text{ft}^3$	1.31441	1.35808	998.952	19.3166
TEMPERATURE IN $^{\circ}\text{R}$				
Pressure	atm	kg/cm^2	mm of Hg	lb/in^2
Density				
g/cm^3	2.67687	2.76581	2034.42	39.3394
mole/cm^3	45.5871	47.1018	34646.2	669.950
mole/liter	0.0455858	0.0471005	34.6452	0.669928
lb/ft^3	0.0428789	0.0443035	32.5880	0.630147
$\text{lb}/\text{mole}/\text{ft}^3$	0.730228	0.754489	554.973	10.7314

Table IX-15-2
VAPOR PRESSURE OF LIQUID AMMONIA
(Ref. 4)

TEMPERATURE		VAPOR PRESSURE	
$^{\circ}\text{K}$	$^{\circ}\text{R}$	atm	psia
195.15	351.27	0.0582	0.857
205.15	369.27	0.1246	1.831
215.15	387.27	0.2461	3.617
225.15	405.27	0.4536	6.666
235.15	423.27	0.7875	11.573
245.15	441.27	1.2992	19.093
255.15	459.27	2.0499	30.125
265.15	477.27	3.1112	45.722
275.15	495.27	4.5640	67.073
285.15	513.27	6.4985	95.502
295.15	531.27	9.0125	132.448
305.15	549.27	12.212	179.47
315.15	567.27	16.209	238.21
325.15	585.27	21.121	310.39
335.15	603.27	27.079	397.95
345.15	621.27	34.227	503.00
355.15	639.27	42.712	627.70
365.15	657.27	52.677	774.14
375.15	675.27	64.274	944.57
385.15	693.27	77.668	1141.4
395.15	711.27	93.045	1367.4
405.15	729.27	110.613	1625.6
405.9	730.62	112.3 (c.p.)	1650.4

(See Figure IX-15-1)

Table IX-15-3
DENSITY OF SATURATED AMMONIA VAPOR
(Ref. 4, 7)

TEMPERATURE		DENSITY	TEMPERATURE		DENSITY
°K	°R	lb/ft ³	°K	°R	lb/ft ³
198.15	356.67	0.00488	303.15	545.67	0.564
203.15	365.67	0.00696	313.15	563.67	0.750
213.15	383.67	0.0133	323.15	582.67	0.984
223.15	401.67	0.0238	333.15	599.67	1.279
233.15	419.67	0.0403	343.15	617.67	1.656
243.15	437.67	0.0648	353.15	635.67	2.131
253.15	455.67	0.100	363.15	653.67	2.738
263.15	473.67	0.149	373.15	671.67	3.547
273.15	491.67	0.216	406.05	730.9	14.576 (c.p.)
283.15	509.67	0.303			
293.15	527.67	0.417			

(See Figure IX-15-2)

Table IX-15-4
DENSITY OF LIQUID AMMONIA (Ref. 4, 7)

TEMPERATURE		DENSITY	TEMPERATURE		DENSITY
°K	°R	lb/ft ³	°K	°R	lb/ft ³
198.15	356.67	45.63	293.15	527.67	38.10
203.15	365.67	45.28	303.15	545.67	37.16
213.15	383.67	44.56	313.15	563.67	36.18
223.15	401.67	43.83	323.15	582.67	35.14
233.15	419.67	43.08	333.15	599.67	34.04
243.15	437.67	42.31	343.15	617.67	32.86
253.15	455.67	41.52	353.15	635.67	31.57
263.15	473.67	40.70	363.15	653.67	30.15
273.15	491.67	39.87	373.15	671.67	28.53
283.15	509.67	39.00	406.05	730.9	14.58 (c.p.)

(See Figure IX-15-3)

Table IX-15-5
DENSITY OF GASEOUS AMMONIA (Ref. 3)

TEMPERATURE		DENSITY—lb/ft ³		
°K	°R	8.9 atm	89.0 atm	890 atm
324.4	583.92	0.3829		39.89
344.68	620.42	0.3536		38.58
364.95	656.91	0.3300		37.22
385.23	693.41	0.3096		35.81
395.36	711.65	0.3008	5.619	35.11
405.4	729.72	0.2919	4.739	34.42
425.78	766.40	0.2758	3.844	33.05
446.05	802.89	0.2626	3.374	31.65
486.60	875.88	0.2377	2.773	28.87
527.15	948.87	0.2186	2.450	26.16
567.70	1021.86	0.2025	2.186	23.59
608.25	1094.85	0.1878	2.010	21.52

(See Figure IX-15-4)

Table IX-15-6
HEAT CAPACITIES OF SOLID AND LIQUID AMMONIA
(Ref. 6)

TEMPERATURE		C _P	TEMPERATURE		C _P
°K	°R	Btu/lb-°R	°K	°R	Btu/lb-°R
20	36	0.0216	170	306	0.6119
30	54	0.0607	180	324	0.6476
40	72	0.1081	190	342	0.6876
50	90	0.1564	195.41	351.74	M. P.
60	108	0.2040	200	360	1.032
70	126	0.2485	210	378	1.042
80	144	0.2909	220	396	1.051
90	162	0.3295	230	414	1.059
100	180	0.3667	239.73	431.51	B. P.
110	198	0.4038	240	432	1.064
120	216	0.4402			
130	234	0.4757			
140	252	0.5108			
150	270	0.5444			
160	288	0.5782			

(See Figure IX-15-5)

Table IX-15-7
HEAT CAPACITY OF AMMONIA GAS
(Btu/lb-°F) (Ref. 2)

TEMPERATURE		PRESSURE IN ATMOSPHERES		
°K	°R	1	10	20
243.15	437.67	0.5513		
253.15	455.67	0.5344		
263.15	473.67	0.5247		
273.15	491.67	0.5194		
283.15	509.67	0.5168		
293.15	527.67	0.5161		
303.15	545.67	0.5167	0.7289	
312.15	563.67	0.5181	0.6826	
323.15	581.67	0.5201	0.6510	0.9173
333.15	599.67	0.5227	0.6290	0.8244
343.15	617.67	0.5256	0.6136	0.7621
353.15	635.67	0.5288	0.6029	0.7192
363.15	653.67	0.5323	0.5955	0.6890
373.15	671.67	0.5359	0.5905	0.6674
383.15	689.67	0.5397	0.5874	0.6518
393.15	707.67	0.5437	0.5856	0.6404
403.15	725.67	0.5478	0.5850	0.6322
413.15	743.67	0.5520	0.5852	0.6263
423.15	761.67	0.5563	0.5860	0.6223

(See Figure IX-15-6)

Table IX-15-8
HEAT OF VAPORIZATION OF AMMONIA (Ref. 7)

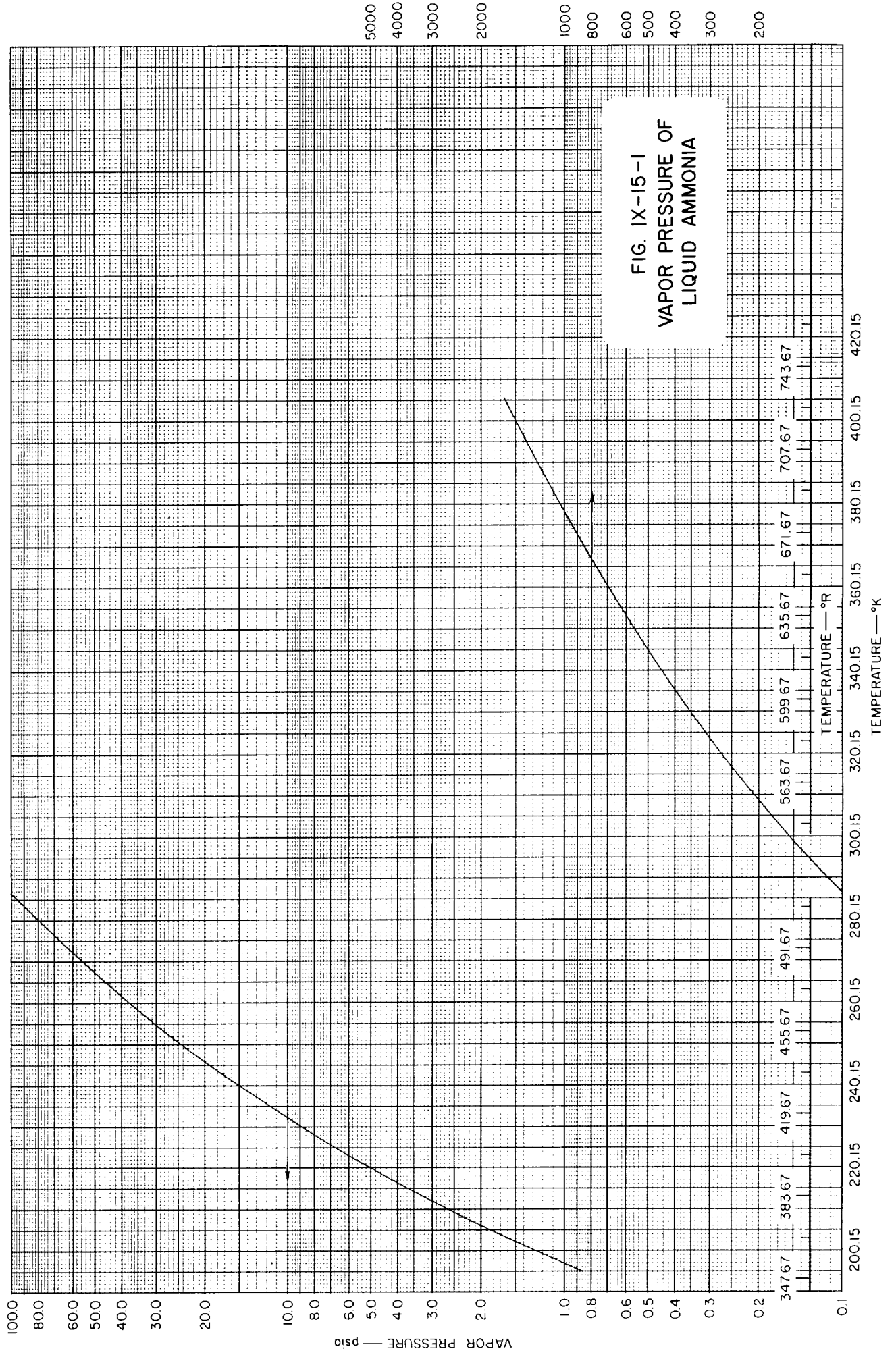
TEMPERATURE		LATENT HEAT	TEMPERATURE		LATENT HEAT
°K	°R	Btu/lb	°K	°R	Btu/lb
238.7	429.7	590.7	294.3	529.7	508.6
244.3	439.7	583.6	299.8	539.7	498.7
249.8	449.7	576.4	305.4	549.7	488.5
255.4	459.7	568.9	310.9	559.7	477.8
260.9	469.7	561.1	316.5	569.7	466.7
266.5	479.7	553.1	322.0	579.7	455.0
272.0	489.7	544.8	324.8	584.7	448.9
277.6	499.7	536.2			
283.2	509.7	527.3			
288.7	519.7	518.1			

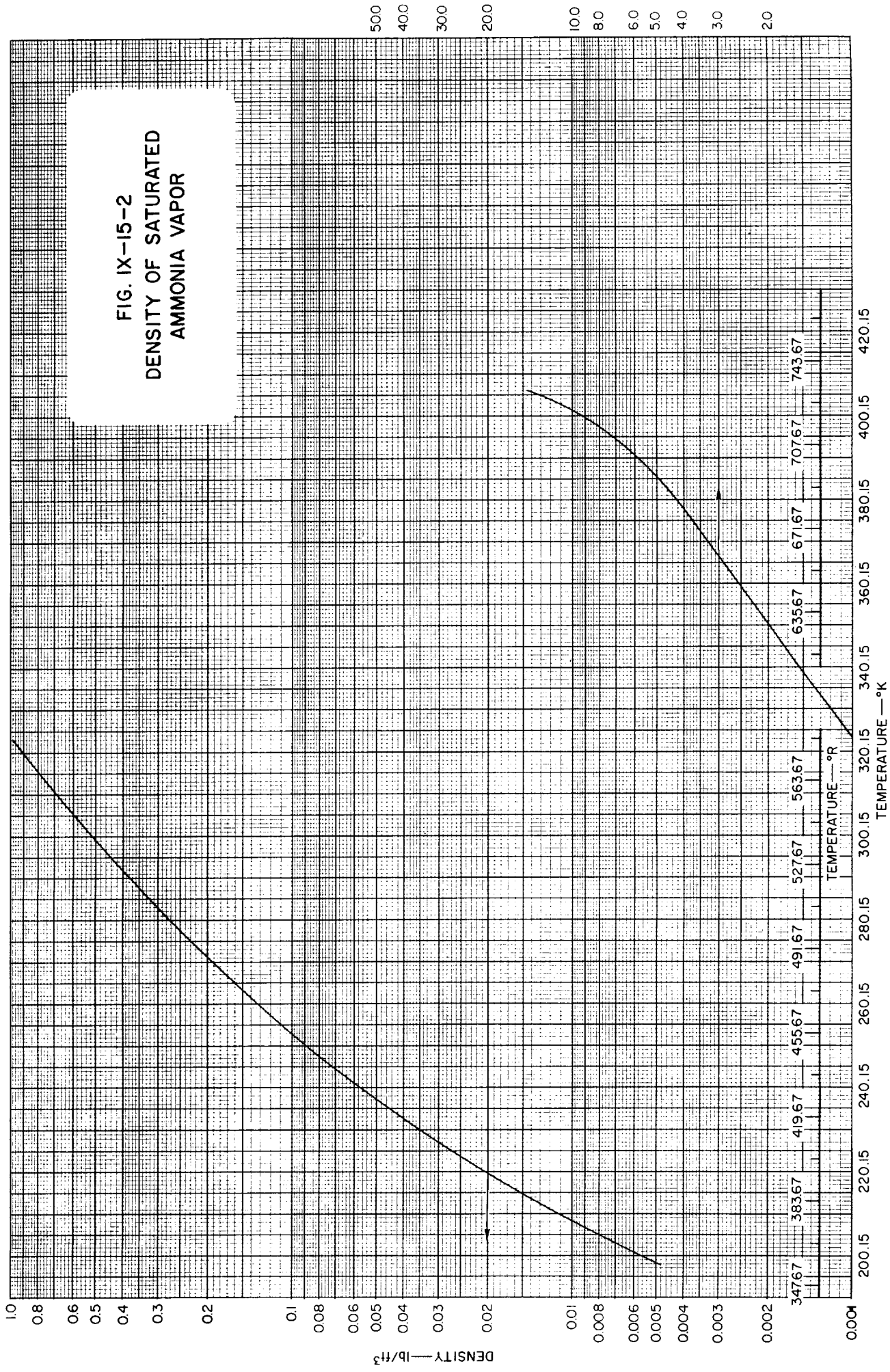
(See Figure IX-15-9)

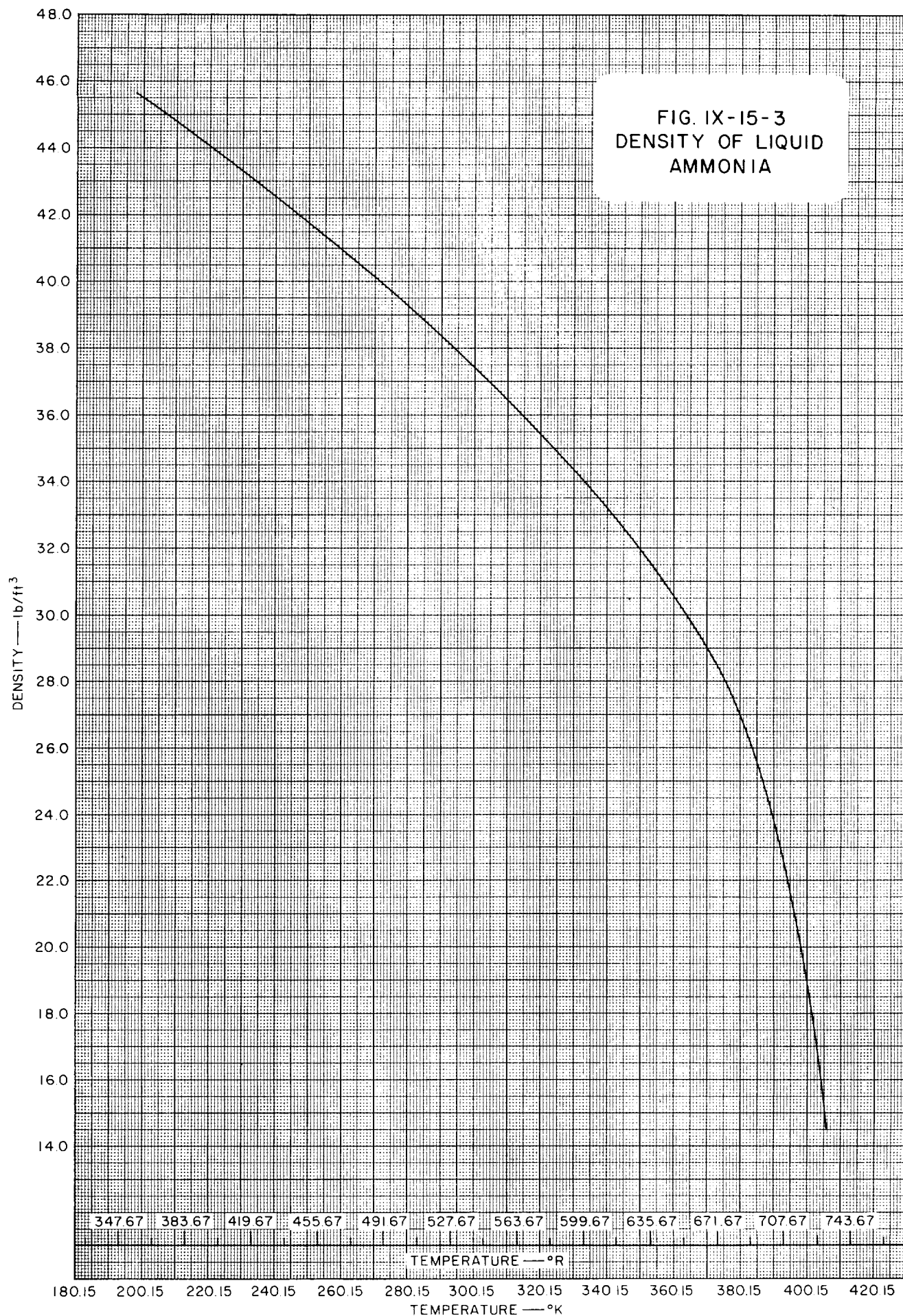
Table IX-15-9
TOTAL ENTHALPY AND SPECIFIC VOLUME
OF THE AMMONIA SYSTEM
(Computed from data in References 4, 6)

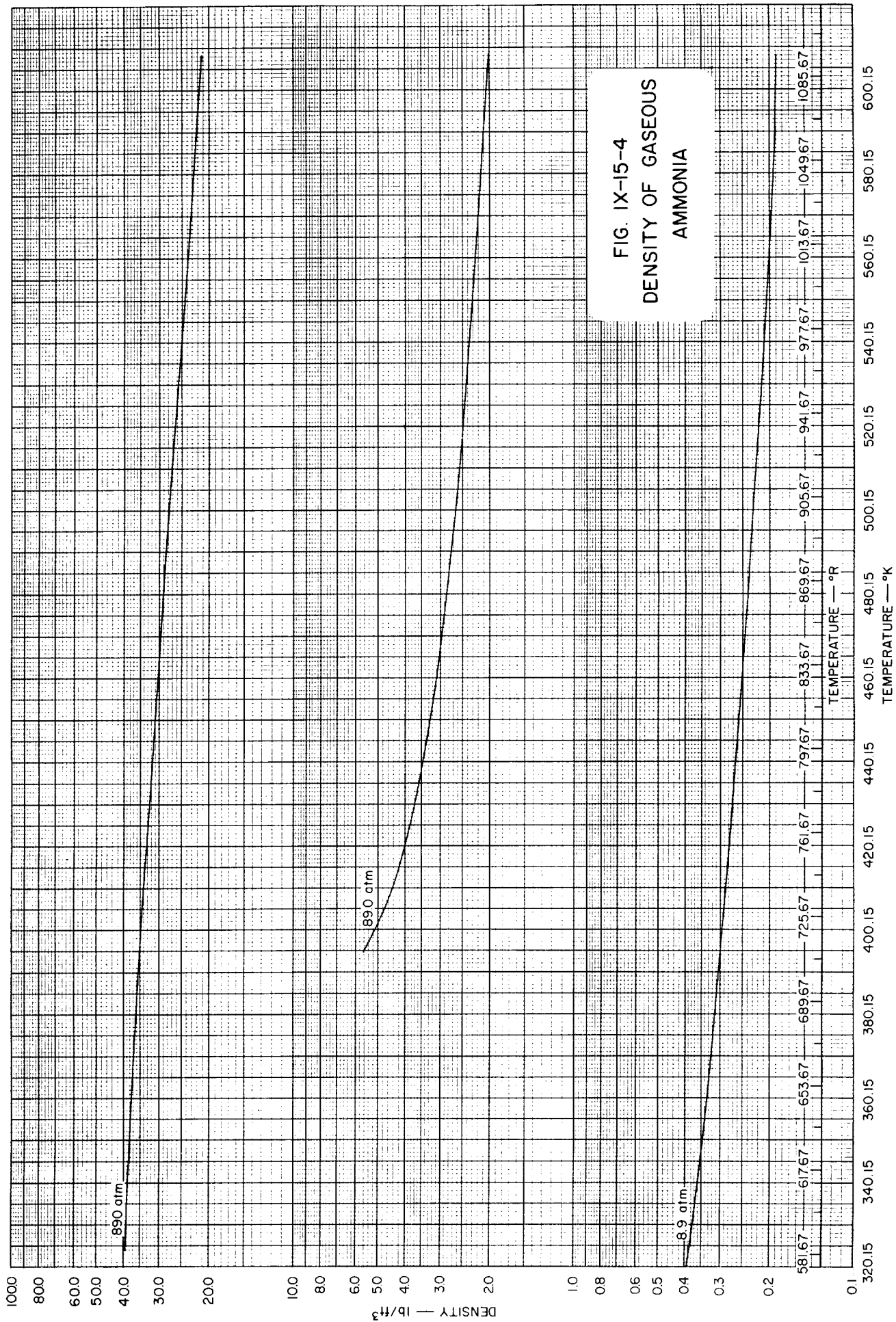
TEMPERATURE	TOTAL ENTHALPY—Btu/lb			SPEC. VOL. VAPOR
^o R	Solid	Liquid	Vapor	ft ³ /lb
0	0			
50	0.723			
100	6.56			
150	18.93			
200	36.78			
250	59.69			
300	87.38			
351.65	120.15	263.0	903.6	251.3
360		271.6	907.2	180.1
380		292.4	915.7	85.32
400		313.3	923.9	44.28
420		334.5	931.9	24.64
431.42		346.6	936.1	18.12
440		355.8	939.2	14.63
460		377.5	946.1	9.048
480		399.1	951.9	5.870
500		421.2	957.1	3.946
520		443.6	961.4	2.735
540		466.6	964.0	1.944
560		489.8	967.2	1.412
580		513.5	968.1	1.042

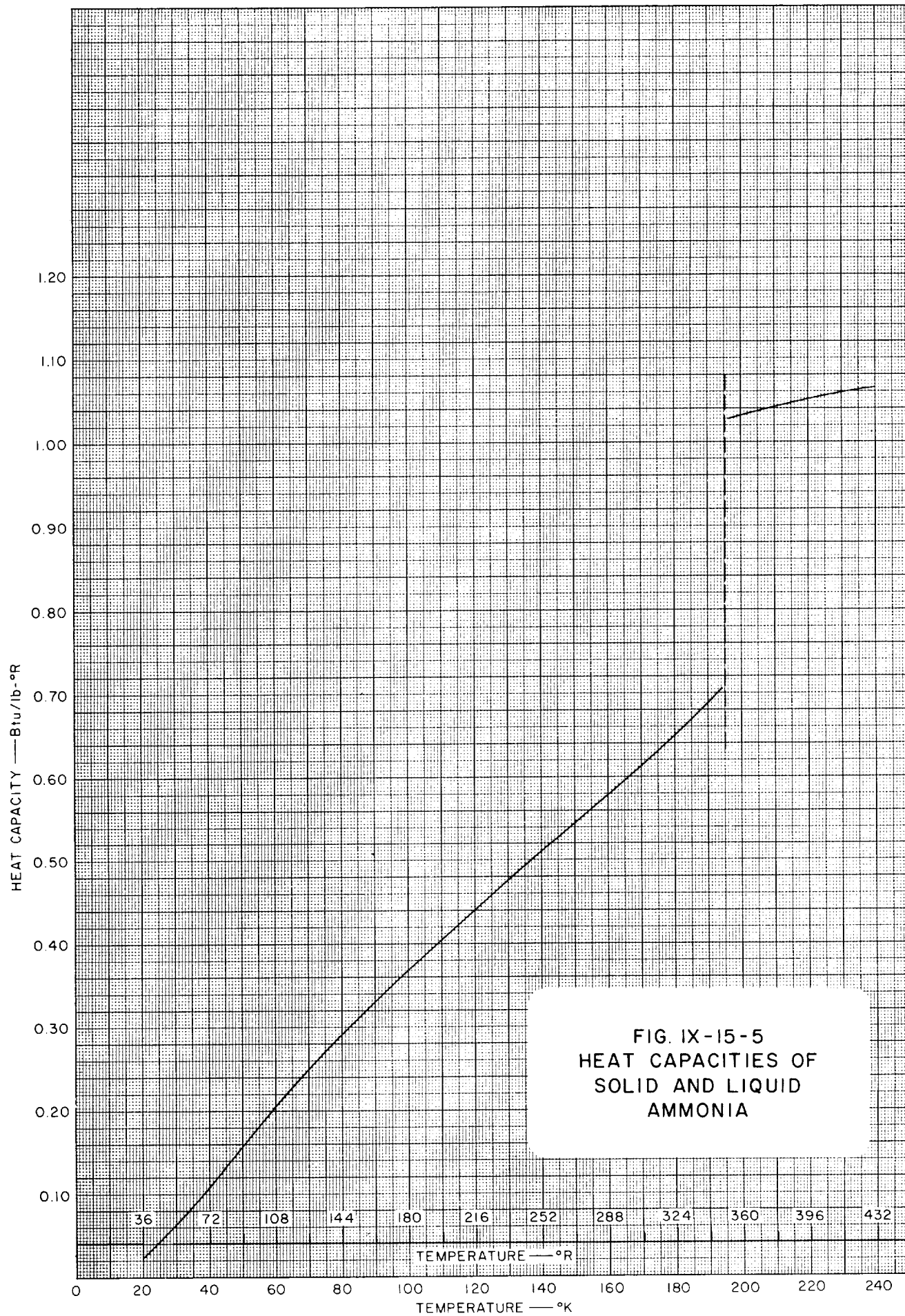
(See Figure IX-15-12
Figure IX-15-13)

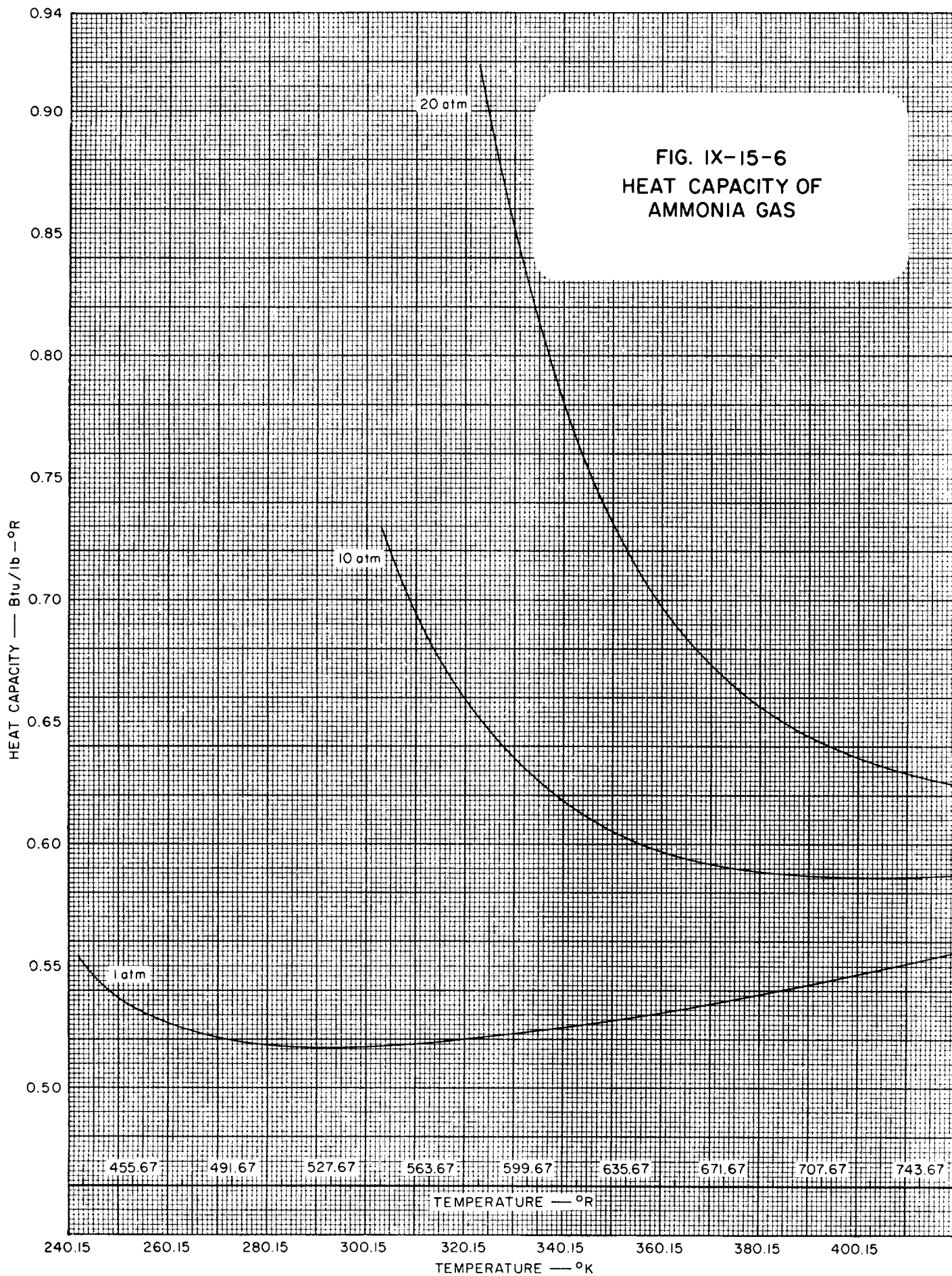


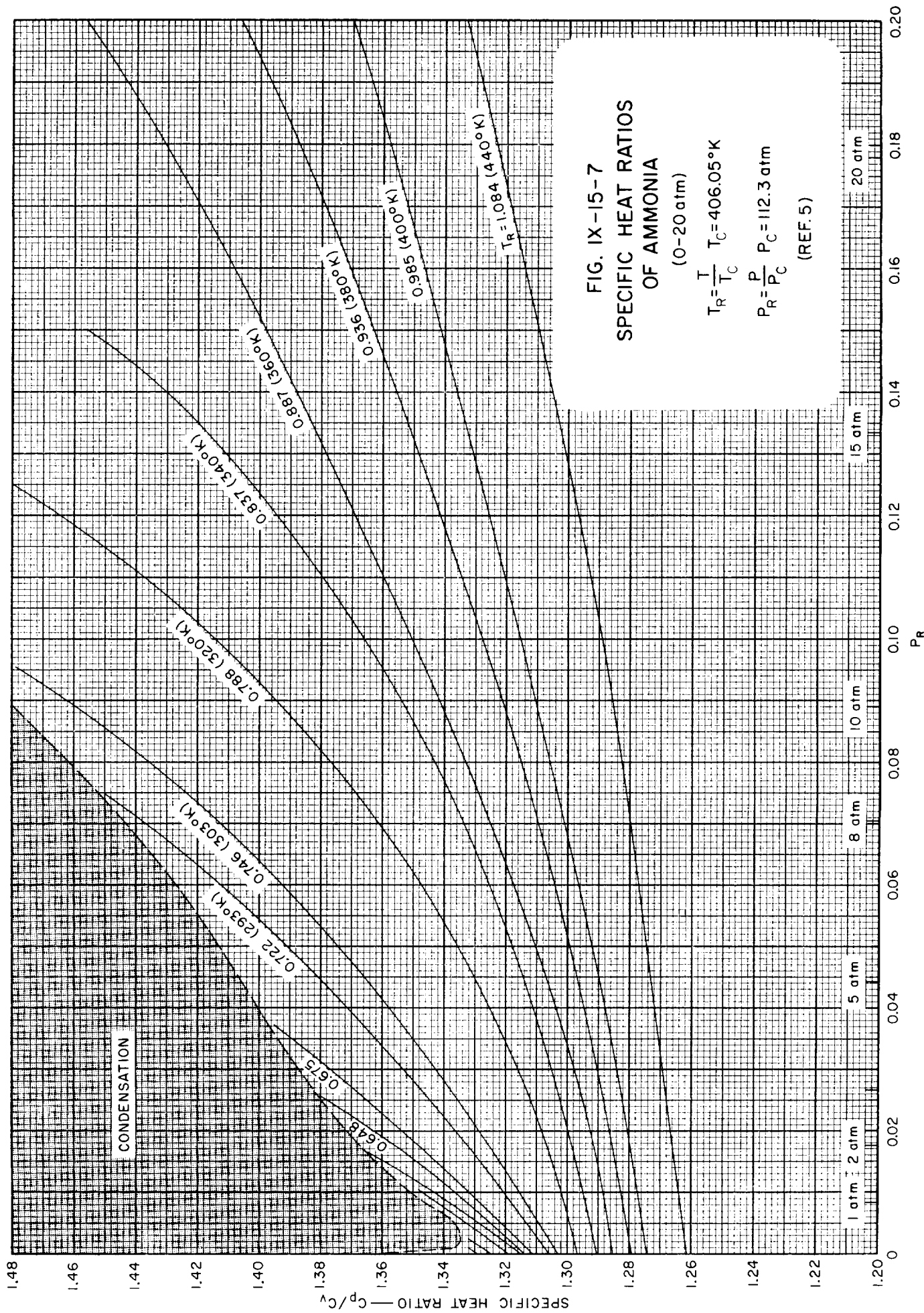


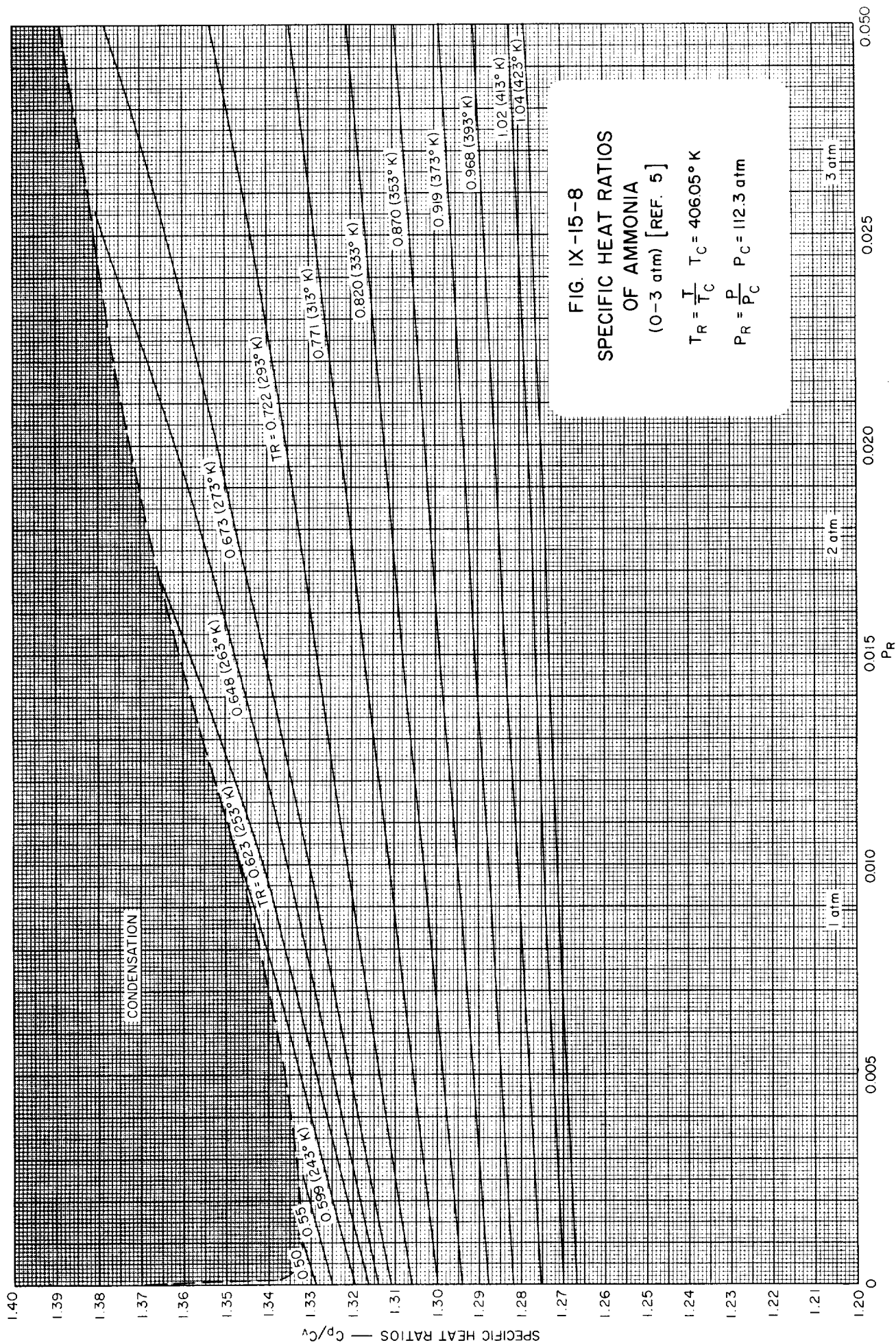


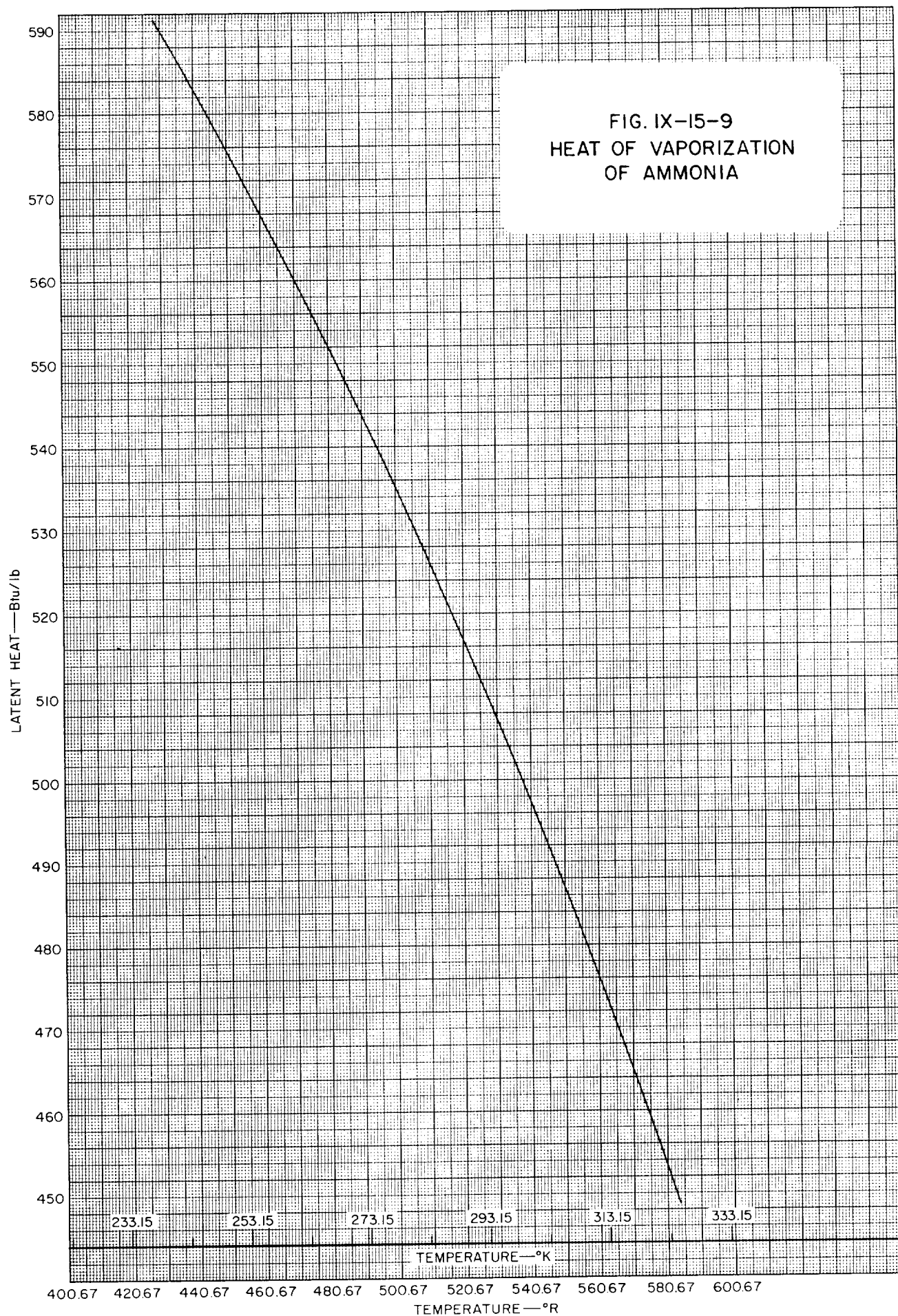












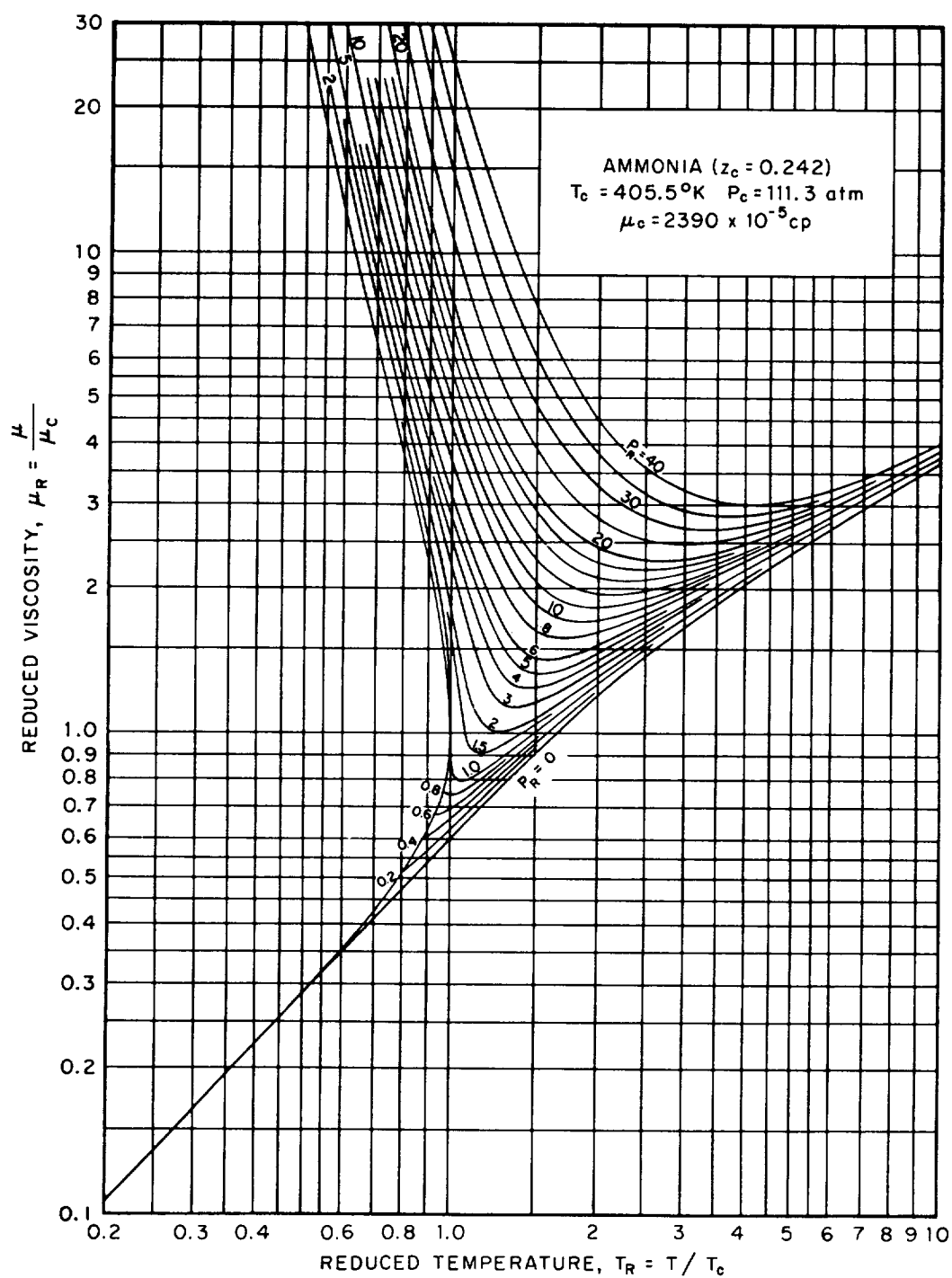


FIG. IX-15-10 VISCOSITY OF GASEOUS AND LIQUID AMMONIA*

*From: Groenier, W. S., and Thodos, G., *J. Chem. Eng. Data*, 6, No. 2, 243 (1961).
 (Ref. 3).

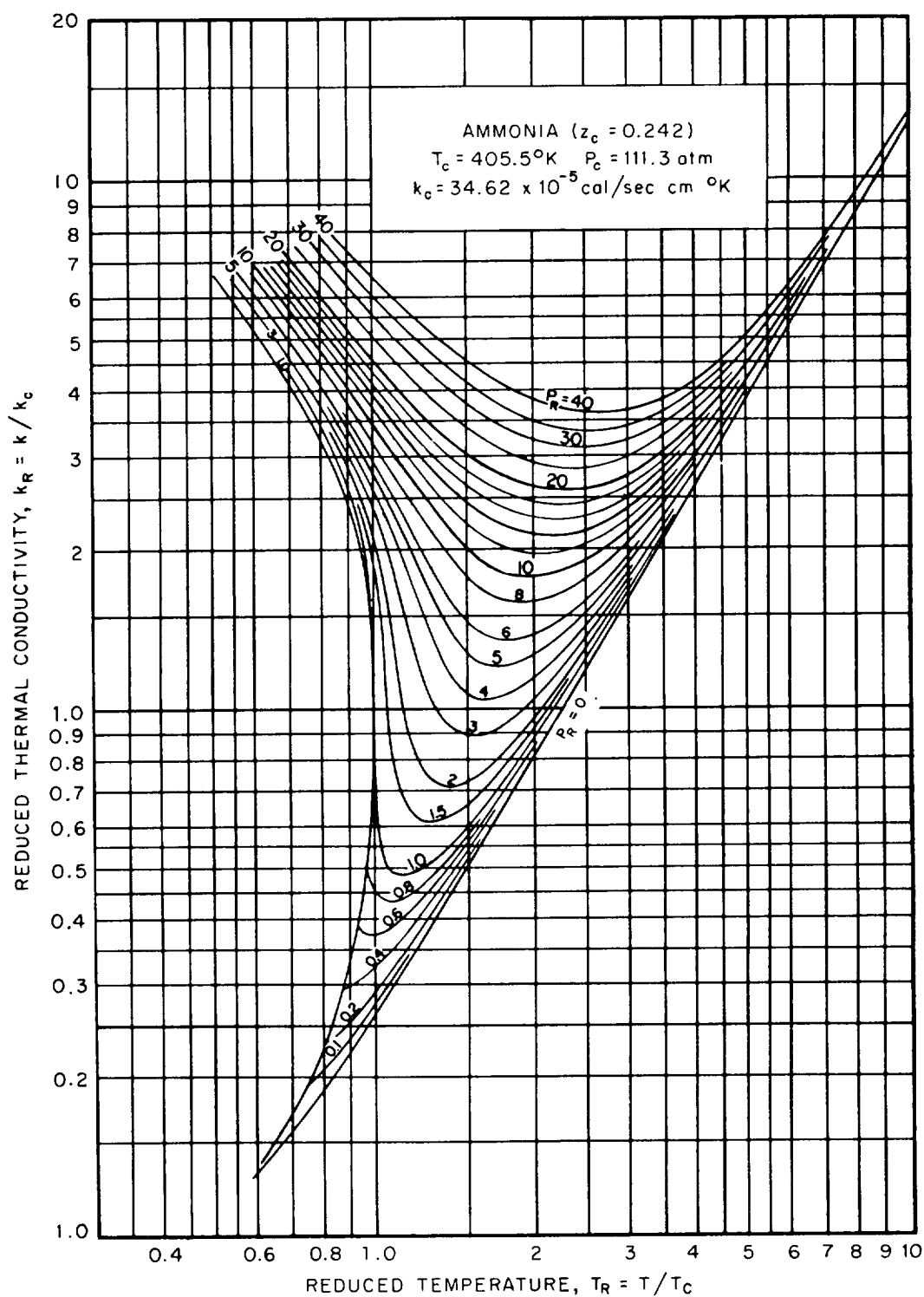


FIG. IX-15-11 THERMAL CONDUCTIVITY OF GASEOUS AND LIQUID AMMONIA*

*From: Groenier, W. S., and Thodos, G., *J. Chem. Eng. Data*, 6, No. 2, 244 (1961).
 (Ref. 3).

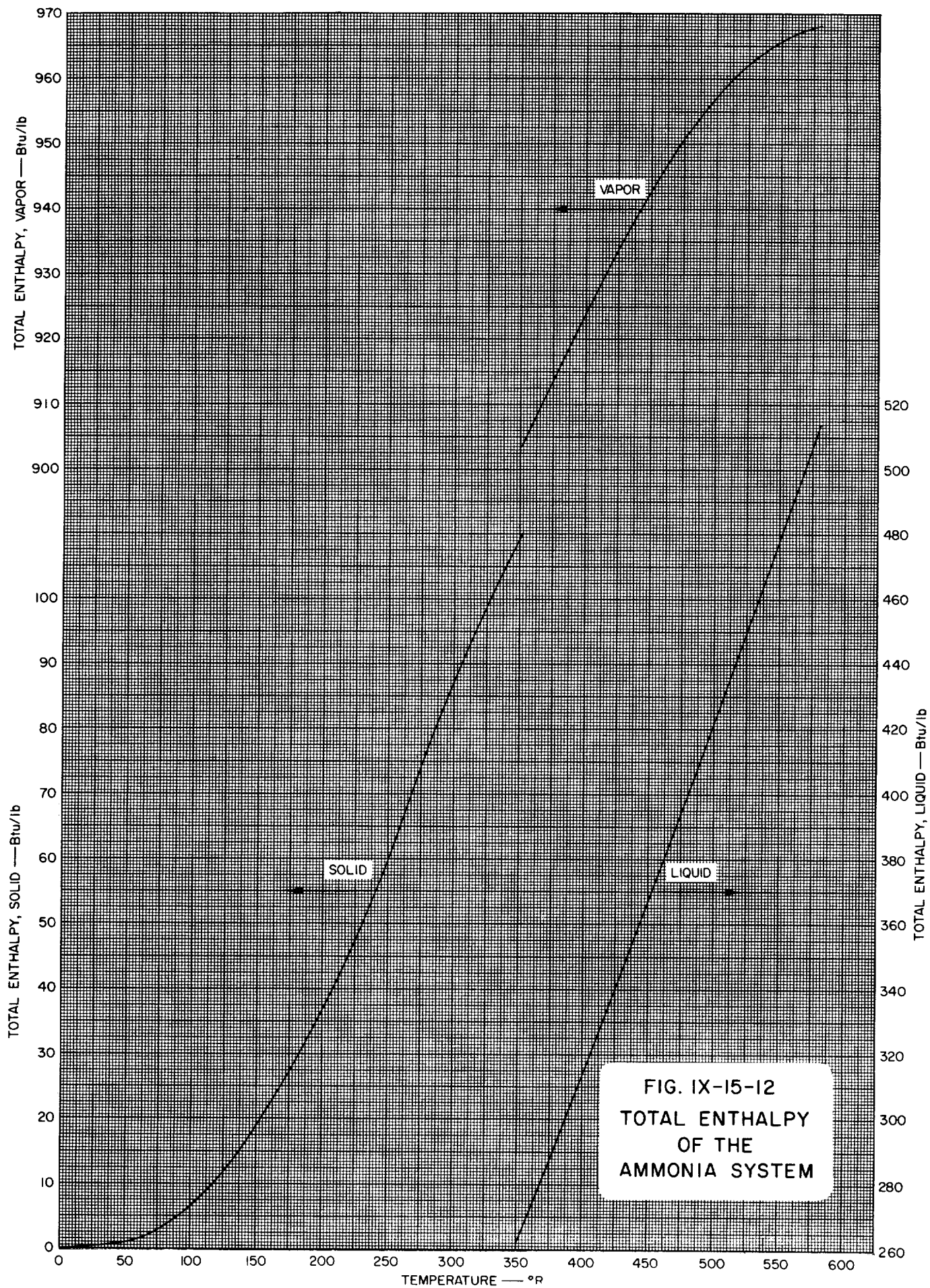
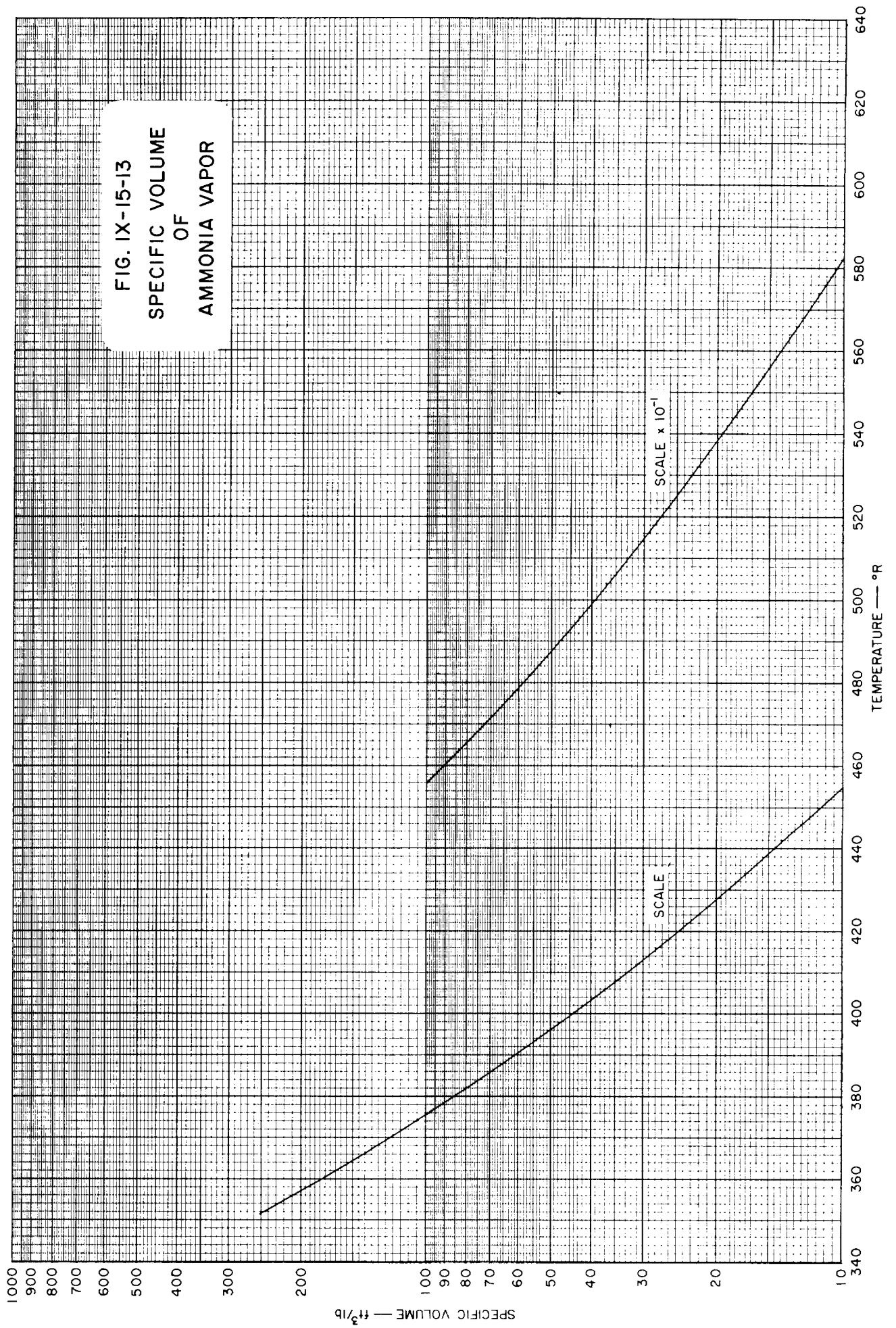


FIG. IX-15-12
TOTAL ENTHALPY
OF THE
AMMONIA SYSTEM



)

)

)

)

)

IX-15 AMMONIA REFERENCES

1. Cardoso, E., and Giltay, A., *Arch. sci. phys. nat. Geneve*, **34**, 20 (1912).
2. Cragoe, C. S., *Refrig. Eng.*, **12**, No. 5, 131 (1925).
3. Groenier, W. S., and Thodos, G., *J. Chem. Eng. Data*, **5**, No. 3, 242 (1960).
4. Lange, N. A., *Handbook of Chemistry*, 10th Edition, Handbook Publishers, Inc., Sandusky, Ohio, 1961.
5. Newitt, D. M., Pai, M. U., Kuloor, N. R., and Huggill, J. A. W., in Din (ed.), *Thermodynamic Functions of Gases*, Butterworths, London, 1962, Vol. I.
6. Overstreet, R., and Giauque, W. F., *J. Am. Chem. Soc.*, **59**, 254 (1937).
7. U.S. Bureau of Standards, *Circular No. 142*, 1st Edition, 1923.

)

)

)

)

)

Table IX-16-1
GENERAL PROPERTIES OF HYDROGEN PEROXIDE

PROPERTY	TEMPERATURE				PRESSURE			REF
	°C	°K	°F	°R	psia	atm	mm of Hg	
Melting Point	0.41	272.74	31.26	490.93				4
Boiling Point	150.2	423.35	302.4	762.0				6
Triple Point	0.42	272.73	31.24	490.91				4
Critical Temp.	457	730	85.5	1315				6
Critical Press.					3145	214	--	6
Mol. Wt.	34.02							
Heat of Vaporization	362.6 cal/g or 652.7 Btu/lb at 25°C							5
Heat of Fusion	87.80 cal/g or 158.0 Btu/lb							4

Table IX-16-1.1
SOME VALUES OF THE GAS CONSTANT, *R*, FOR HYDROGEN PEROXIDE
(See also Conversion Tables, Section I)

TEMPERATURE IN °K				
Pressure Density	atm	kg/cm ²	mm of Hg	lb/in ²
g/cm ³	2.41201	2.49216	1833.13	35.4471
mole/cm ³	82.0567	84.7832	62363.1	1205.91
mole/liter	0.0820544	0.0847809	62.3613	1.20587
lb/ft ³	0.0386364	0.0399200	29.3637	0.567801
lb/mole/ft ³	1.31441	1.35808	998.952	19.3166
TEMPERATURE IN °R				
Pressure Density	atm	kg/cm ²	mm of Hg	lb/in ²
g/cm ³	1.34001	1.38453	1018.41	19.6928
mole/cm ³	45.5871	47.1018	34646.2	669.950
mole/liter	0.0455858	0.0471005	34.6452	0.669928
lb/ft ³	0.0214647	0.0221778	16.3131	0.315444
lb/mole/ft ³	0.730228	0.754489	554.973	10.7314

Table IX-16-2
TOTAL VAPOR PRESSURE OF 98-100%
HYDROGEN PEROXIDE SOLUTIONS
(Ref. 6)

TEMPERATURE		PRESSURE	
$^{\circ}\text{K}$	$^{\circ}\text{R}$	psia	atm
263.2	473.8	0.002	0.00015
273.2	491.8	0.005	0.00036
283.2	509.8	0.012	0.00082
293.2	527.8	0.026	0.0018
303.2	545.8	0.054	0.0037
313.2	563.8	0.104	0.0071
323.2	581.8	0.192	0.0131
333.2	599.8	0.340	0.0231
343.2	617.8	0.578	0.0394
353.2	635.8	0.951	0.065
363.2	653.8	1.51	0.103
373.2	671.8	2.34	0.160
383.2	689.8	3.54	0.241

(See Figure IX-16-1)

Table IX-16-3
DENSITY OF HYDROGEN PEROXIDE
(Ref. 1)

TEMPERATURE		DENSITY	
°K	°R	g/cc	lb/ft ³
273.2	491.7	1.4710	91.83
298.2	536.7	1.4422	90.04
323.2	581.7	1.4134	88.24
369.2	664.5	1.358	84.78

(See Figure IX-16-2)

Table IX-16-4
SURFACE TENSION OF HYDROGEN
PEROXIDE (Ref. 1)

TEMPERATURE		SURFACE TENSION-- dynes/cm	
°K	°R	100%	95.75%
273.15	491.67	83.3	82.93
293.15	527.67	80.4	79.87

Table IX-16-5
VISCOSITY OF HYDROGEN PEROXIDE
(Ref. 1)

TEMPERATURE		ABSOLUTE VISCOSITY-- centipoises	
°K	°R	100%	98%
273.15	491.67	1.798	1.81
298.15	536.67	1.156	1.156
323.15	581.67	0.819	0.815

Table IX-16-6
HEAT CAPACITY OF SOLID HYDROGEN PEROXIDE (Ref. 4)

TEMPERATURE		HEAT CAPACITY	TEMPERATURE		HEAT CAPACITY
°K	°R	Btu/lb-°R	°K	°R	Btu/lb-°R
12	21.6	0.0018	70	126.0	0.1231
13	23.4	0.0023	75	135.0	0.1336
14	25.2	0.0029	80	144.0	0.1439
15	27.0	0.0036	85	153.0	0.1541
16	28.8	0.0044	90	162.0	0.1636
17	30.6	0.0053	95	171.0	0.1724
18	32.4	0.0063	100	180.0	0.1806
19	34.2	0.0074	110	198.0	0.1962
20	36.0	0.0087	120	216.0	0.2106
22	39.6	0.0114	130	234.0	0.2238
24	43.2	0.0145	140	252.0	0.2363
26	46.8	0.0180	150	270.0	0.2480
28	50.4	0.0216	160	288.0	0.2593
30	54.0	0.0256	170	306.0	0.2702
32	57.6	0.0298	180	324.0	0.2809
34	61.2	0.0342	190	342.0	0.2915
36	64.8	0.0389	200	360.0	0.3023
38	68.4	0.0436	210	378.0	0.3132
40	72.0	0.0484	220	396.0	0.3246
42	75.6	0.0533	230	414.0	0.3362
44	79.2	0.0583	240	432.0	0.3485
46	82.8	0.0634	250	450.0	0.361*
48	86.4	0.0684	255	459.0	0.369*
50	90.0	0.0736	260	468.0	0.381*
55	99.0	0.0864	265	477.0	0.406*
60	108.0	0.0991	268	482.4	0.461*
65	117.0	0.1115			

* Marked Premelting

Table IX-16-7
SPECIFIC HEAT OF 98% HYDROGEN
PEROXIDE SOLUTION (Ref. 2)

TEMPERATURE		SPECIFIC HEAT
$^{\circ}\text{K}$	$^{\circ}\text{R}$	Btu/lb- $^{\circ}\text{R}$
283.15	509.67	0.623
310.93	559.67	0.640
533.15	959.67	0.780

(See Figure IX-16-3)

Table IX-16-8
HEAT CAPACITY OF HYDROGEN
PEROXIDE VAPOR (Ref. 4)

TEMPERATURE		HEAT CAPACITY
$^{\circ}\text{K}$	$^{\circ}\text{R}$	Btu/lb- $^{\circ}\text{R}$
285	513.0	0.3202
290	522.0	0.3215
300	540.0	0.3240
310	558.0	0.3266
320	576.0	0.3292
330	594.0	0.3318
340	602.0	0.3344
350	620.0	0.3370

(See Figure IX-16-4)

Table IX-16-9
THERMAL CONDUCTIVITY OF 98%
HYDROGEN PEROXIDE (Ref. 3)

TEMPERATURE		THERMAL CONDUCTIVITY
$^{\circ}\text{K}$	$^{\circ}\text{R}$	Btu/hr-ft- $^{\circ}\text{R}$
273.15	491.67	0.322
297.04	534.67	0.338
338.71	609.67	0.357
380.37	684.67	0.367
422.04	759.67	0.367
463.70	834.67	0.363

(See Figure IX-16-5)

)

)

)

)

)

FIG. IX-16-1
TOTAL VAPOR PRESSURE OF
98-100% HYDROGEN
PEROXIDE SOLUTIONS

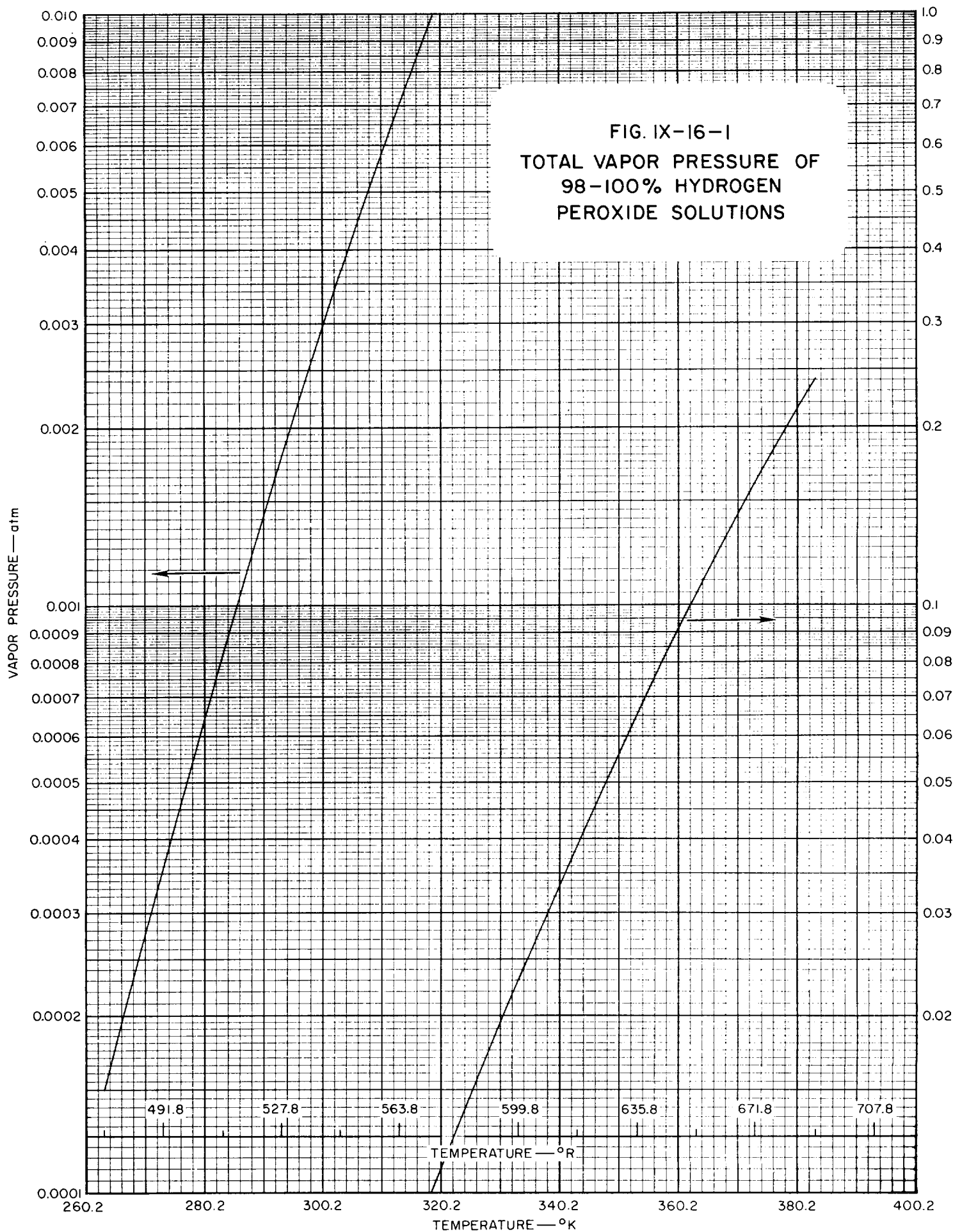
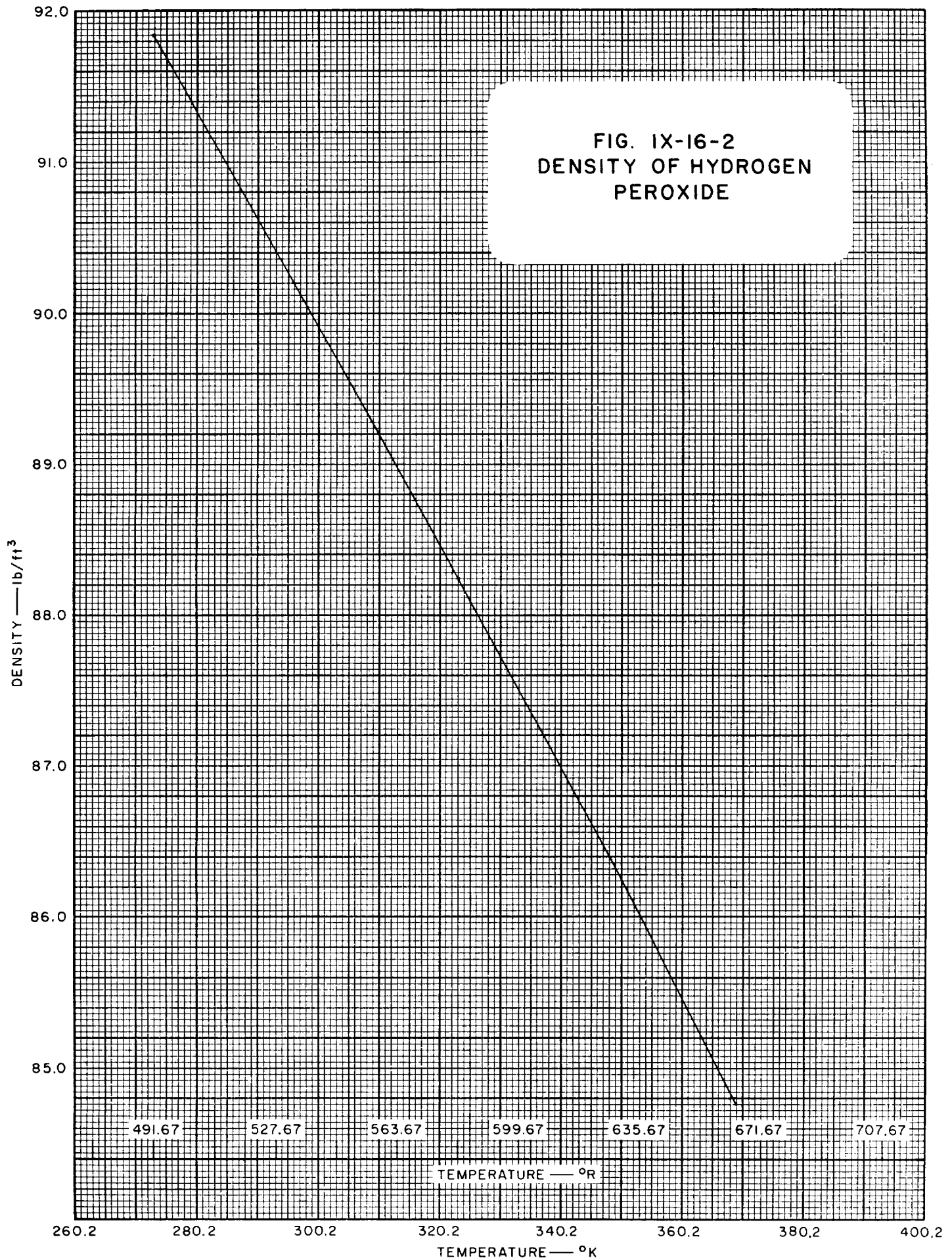
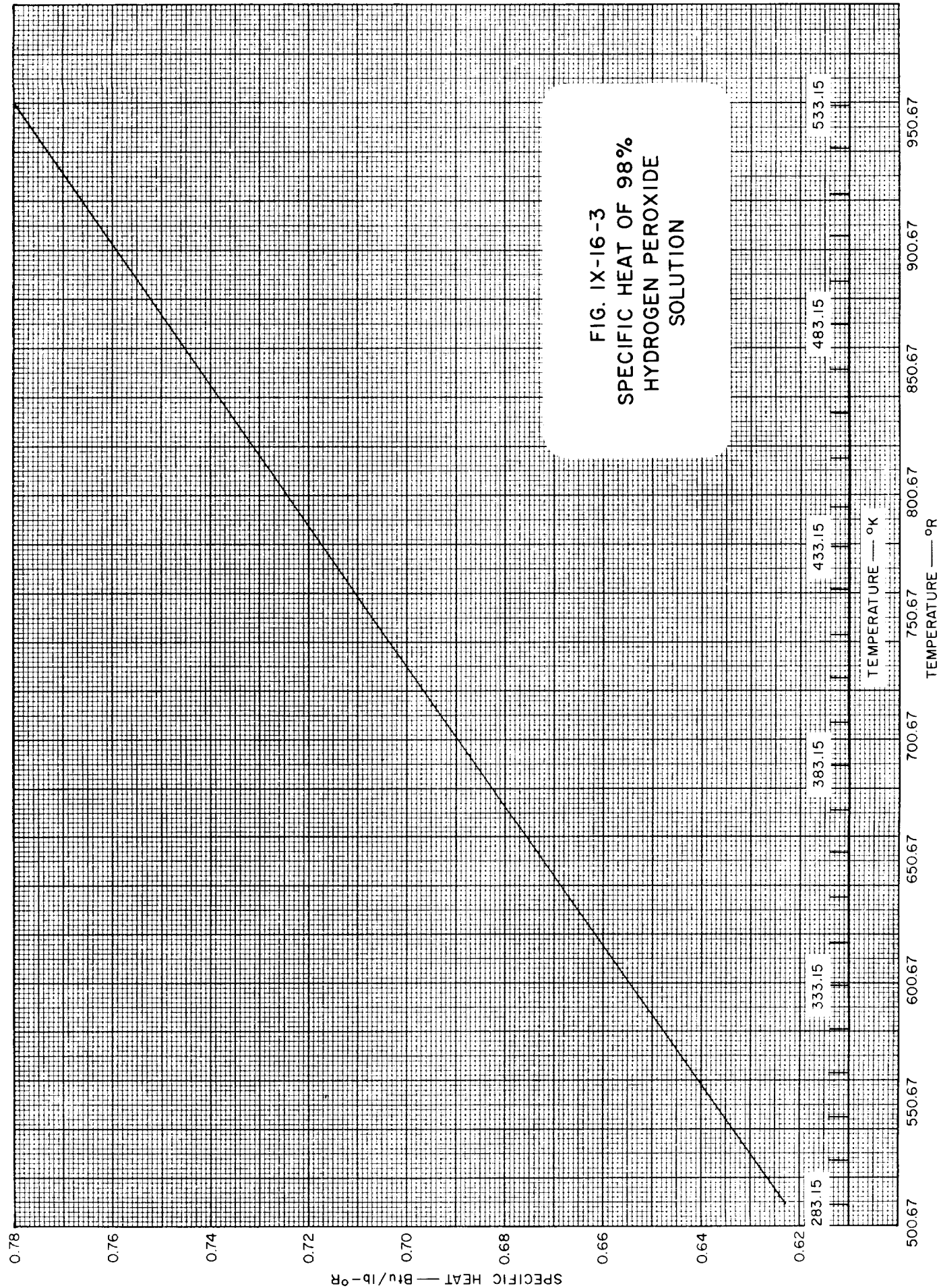
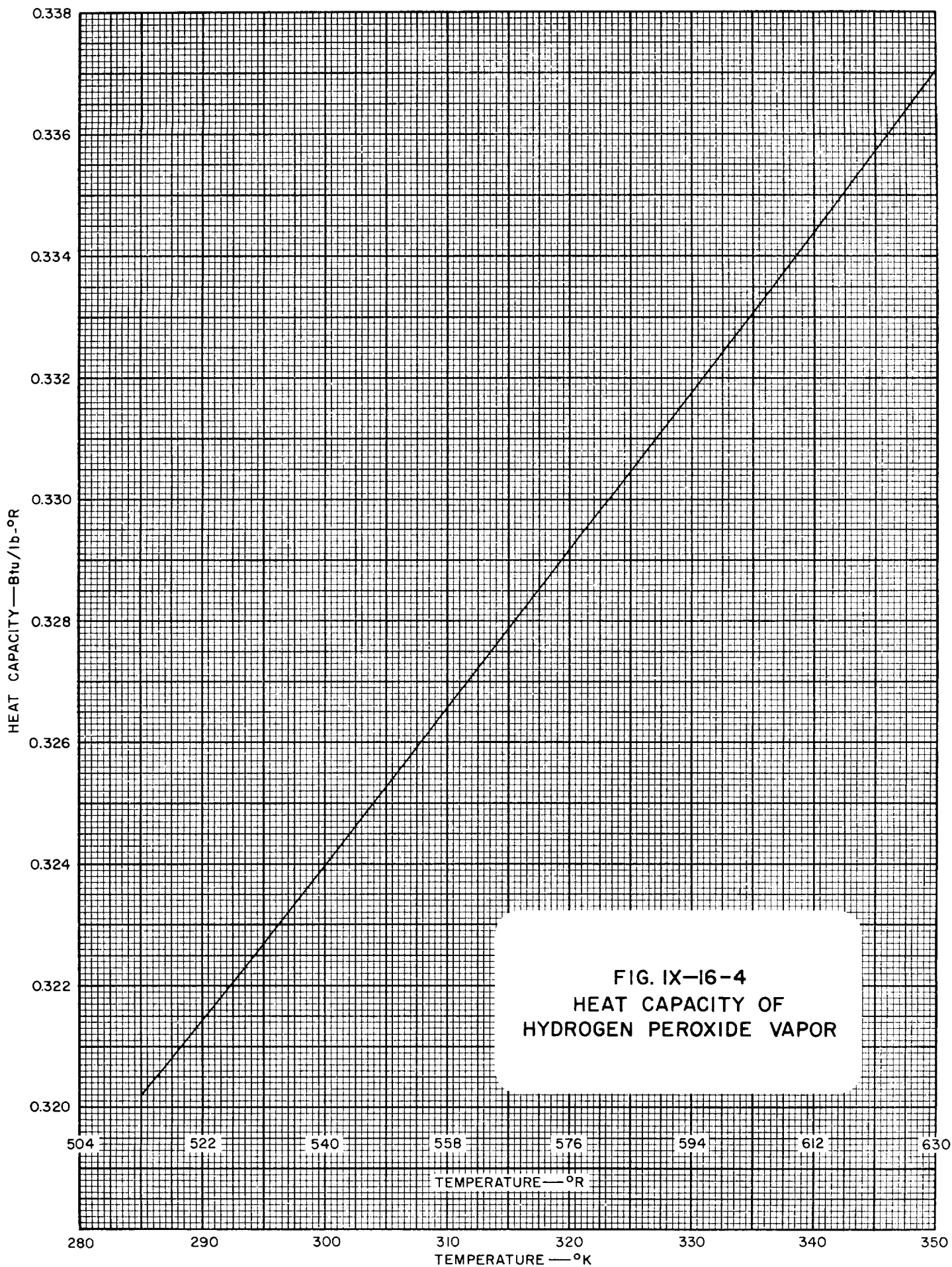


FIG. IX-16-2
DENSITY OF HYDROGEN
PEROXIDE







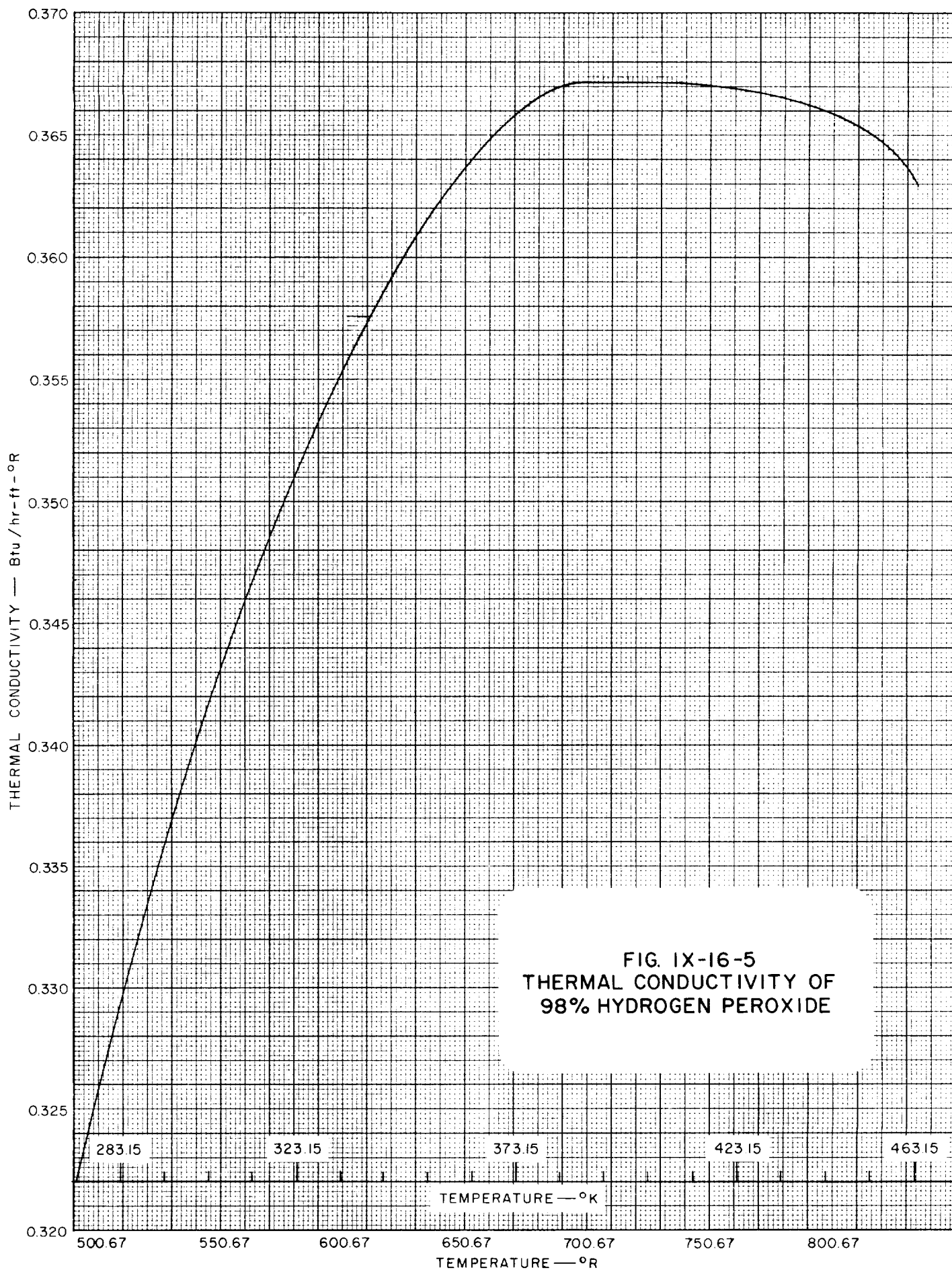


FIG. IX-16-5
THERMAL CONDUCTIVITY OF
98% HYDROGEN PEROXIDE

)

)

)

)

)

IX-16 HYDROGEN PEROXIDE REFERENCES

1. FMC Corporation, Becco Chemical Division, *Bulletin No. 67*, 2nd Edition, 1955.
2. FMC Corporation, Becco Chemical Division, *Bulletin No. 93*, 1958.
3. FMC Corporation, Becco Chemical Division, *Special Project Report SP-2002*, 1958.
4. Giguere, P. A., Liu, I. D., Dugdale, J. S., and Morrison, J., *Can. J. Chem.*, **32**, 117 (1951).
5. Giguere, P. A., Morisette, B. G., Olmos, A. W., and Knop, O., *Can. J. Chem.*, **33**, 804 (1955).
6. Schatchard, G., Kavanagh, G. M., and Ticknor, L. B., *J. Am. Chem. Soc.*, **74**, 3715 (1952).

)

)

)

)

)

Table IX-17-1
GENERAL PROPERTIES OF FREON-11 (CCl_3F)

PROPERTY	TEMPERATURE				PRESSURE			REF
	°C	°K	°F	°R	psia	atm	mm of Hg	
Melting Point	-111.0	162.12	-168.0	291.67				1
Boiling Point	23.77	296.92	74.78	534.45				1
Triple Point								
Critical Temp.	198.0	471.2	388.4	848.1				1
Critical Press.					635	43.2		1
Mol. Wt. 137.38								1
Heat of Vaporization 43.51 cal/g or 78.31 Btu/lb at B.P.								
Heat of Fusion								

Table IX-17-1.1
SOME VALUES OF THE GAS CONSTANT, R , FOR FREON-11
(See also Conversion Tables, Section I)

TEMPERATURE IN $^{\circ}\text{K}$				
Pressure	atm	kg/cm^2	mm of Hg	lb/in^2
Density				
g/cm^3	0.597297	0.617144	453.946	8.77202
mole/cm^3	82.0567	84.7832	62363.1	1205.91
mole/liter	0.0820544	0.0847809	62.3613	1.20587
lb/ft^3	0.00956770	0.00988557	7.27145	0.140607
$\text{lb}/\text{mole}/\text{ft}^3$	1.31441	1.35808	998.952	19.3166
TEMPERATURE IN $^{\circ}\text{R}$				
Pressure	atm	kg/cm^2	mm of Hg	lb/in^2
Density				
g/cm^3	0.331832	0.342858	252.192	4.87662
mole/cm^3	45.5871	47.1018	34646.2	669.950
mole/liter	0.0455858	0.0471005	34.6452	0.669928
lb/ft^3	0.00531539	0.00549199	4.03969	0.0781147
$\text{lb}/\text{mole}/\text{ft}^3$	0.730228	0.754489	554.973	10.7314

Table IX-17-2
VAPOR PRESSURE OF FREON-11 (Ref. 1)

TEMPERATURE		VAPOR PRESSURE	TEMPERATURE		VAPOR PRESSURE
°K	°R	psia	°K	°R	psia
205.37	369.67	0.100	322.04	579.67	33.0
210.93	379.67	0.156	333.15	599.67	45.3
222.04	399.67	0.356	344.26	619.67	61.0
233.15	419.67	0.738	355.37	639.67	79.5
244.26	439.67	1.425	366.48	659.67	104.
255.37	459.67	2.55	377.59	679.67	130.
266.48	479.67	4.30	388.71	699.67	164.
277.59	499.67	7.00	399.82	719.67	204.
288.71	519.67	10.08	410.93	739.67	248.
299.82	539.67	16.25	422.04	759.67	300.
310.93	559.67	23.50			

(See Figure IX-17-1)

Table IX-17-3
VISCOSITY OF SATURATED LIQUID FREON-11 (Ref. 2)

TEMPERATURE		ABSOLUTE VISCOSITY	TEMPERATURE		ABSOLUTE VISCOSITY
$^{\circ}\text{K}$	$^{\circ}\text{R}$	centipoises	$^{\circ}\text{K}$	$^{\circ}\text{R}$	centipoises
233.15	419.67	0.980	322.04	579.67	0.349
244.26	439.67	0.801	333.15	599.67	0.323
255.37	459.67	0.677	344.26	619.67	0.300
266.48	479.67	0.586	355.37	639.67	0.281
277.59	499.67	0.517	366.48	659.67	0.263
288.71	519.67	0.461	377.59	679.67	0.248
299.82	539.67	0.417	388.71	699.67	0.232
310.93	559.67	0.380			

(See Figure IX-17-2)

Table IX-17-4
VISCOSITY OF FREON-11 VAPOR AT ONE ATMOSPHERE (Ref. 2)

TEMPERATURE		ABSOLUTE VISCOSITY	TEMPERATURE		ABSOLUTE VISCOSITY
$^{\circ}\text{K}$	$^{\circ}\text{R}$	centipoises	$^{\circ}\text{K}$	$^{\circ}\text{R}$	centipoises
233.15	419.67	0.0088	322.04	579.67	0.0116
244.26	439.67	0.0092	333.15	599.67	0.0120
255.37	459.67	0.0096	344.26	619.67	0.0123
266.48	479.67	0.0099	355.37	639.67	0.0126
277.59	499.67	0.0103	366.48	659.67	0.0129
288.71	519.67	0.0106	377.59	679.67	0.0132
299.82	539.67	0.0110	388.71	699.67	0.0135
310.93	559.67	0.0113			

(See Figure IX-17-3)

Table IX-17-5
HEAT CAPACITY OF FREON-11
(Ref. 4)

TEMPERATURE		HEAT CAPACITY
$^{\circ}\text{K}$	$^{\circ}\text{R}$	Btu/lb- $^{\circ}\text{R}$
100	180	0.07476
150	270	0.09485
200	360	0.1116
250	450	0.1251
298.16	336.70	0.1355
300	540	0.1359
400	720	0.1515
500	900	0.1616
600	1080	0.1682

(See Figure IX-16-4)

Table IX-17-6
THERMAL CONDUCTIVITY OF SATURATED FREON-11
(Ref. 2)

TEMPERATURE		THERMAL CONDUCTIVITY— Btu/hr-ft- $^{\circ}\text{R}$	
$^{\circ}\text{K}$	$^{\circ}\text{R}$	Liquid	Vapor (at 1 atm)
253.15	455.67	0.060	
293.15	527.67	0.055	
303.15	545.67		0.00505
363.15	653.67		0.00621

(See Figure IX-16-5)

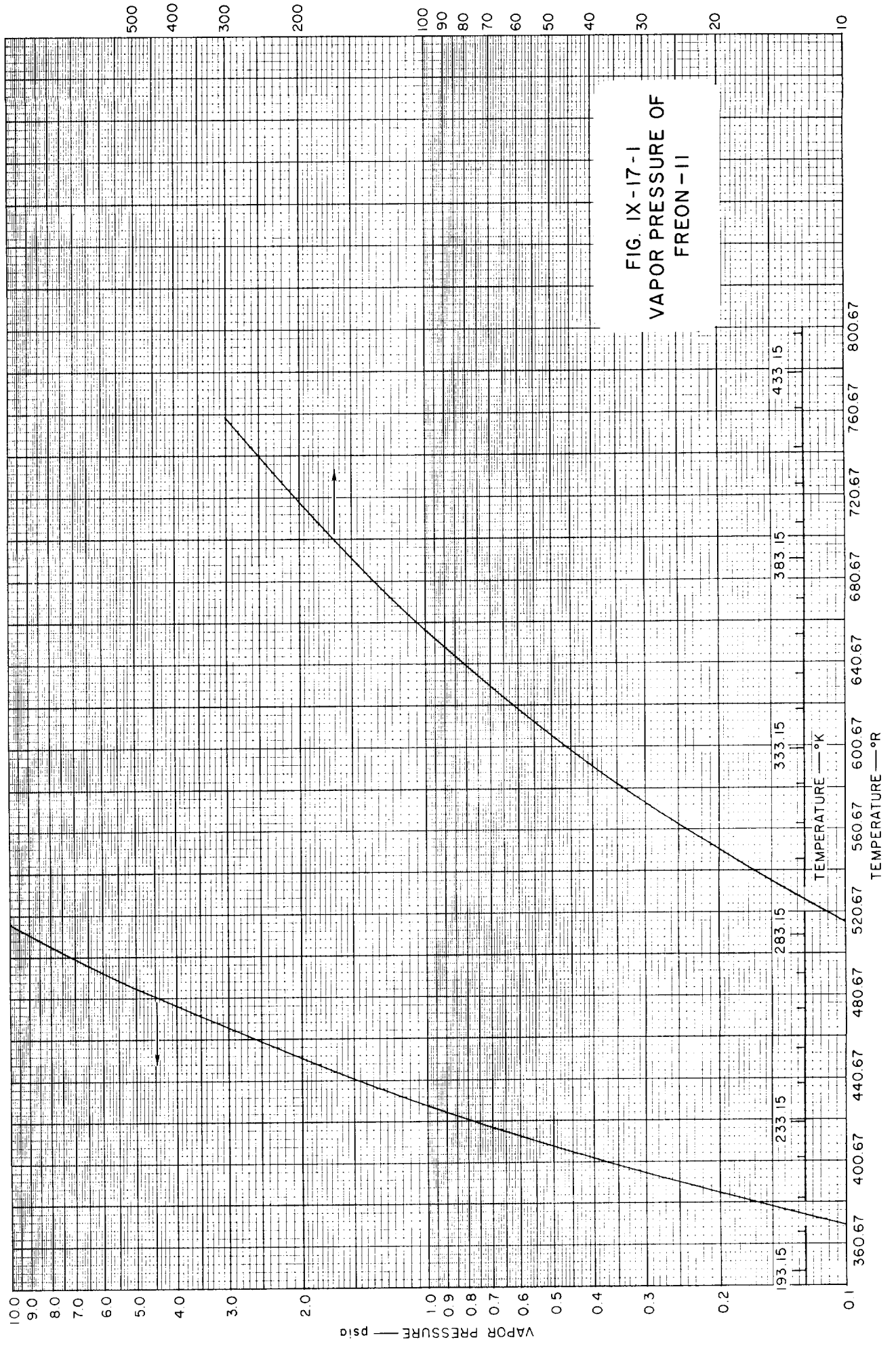
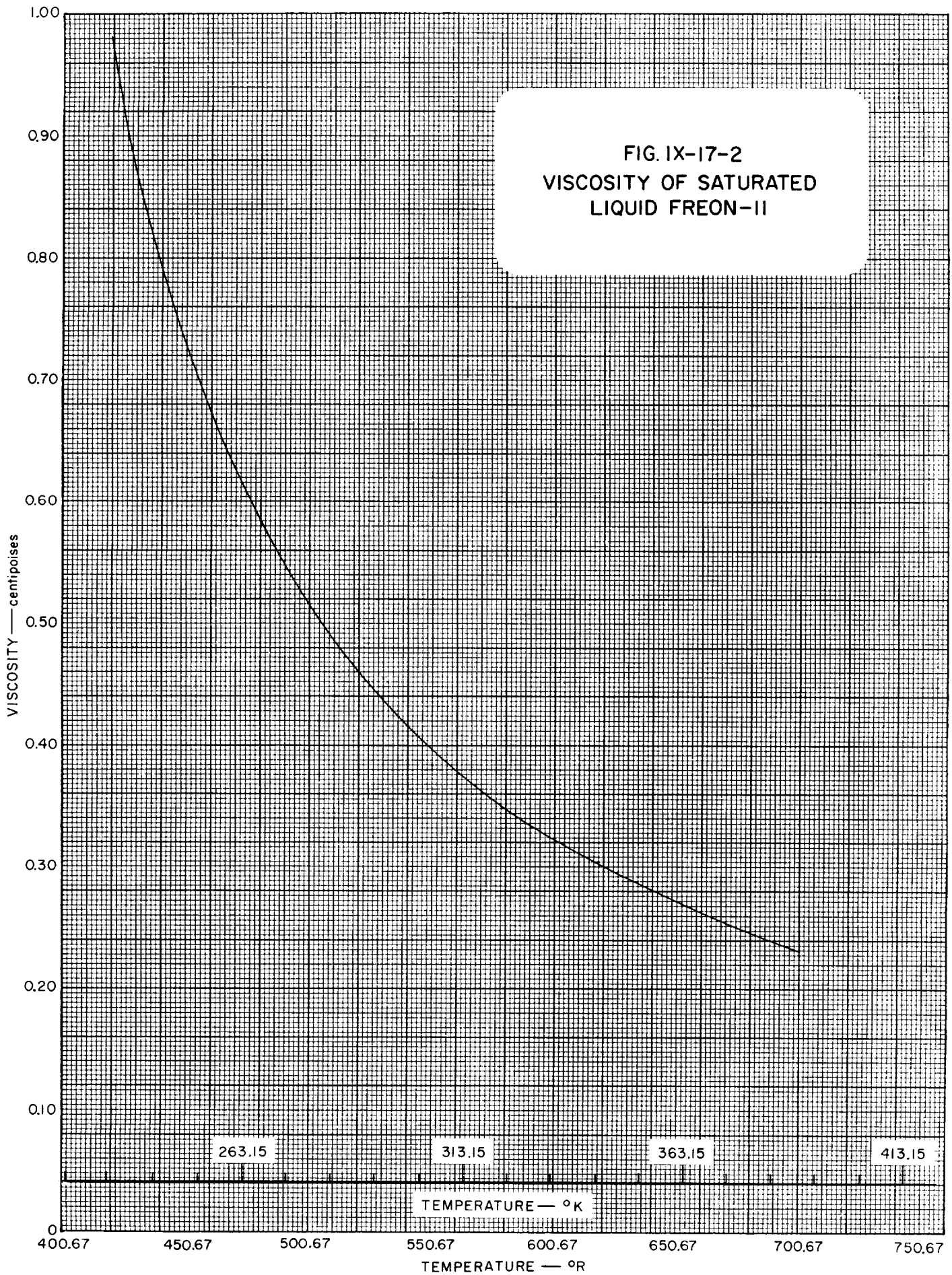
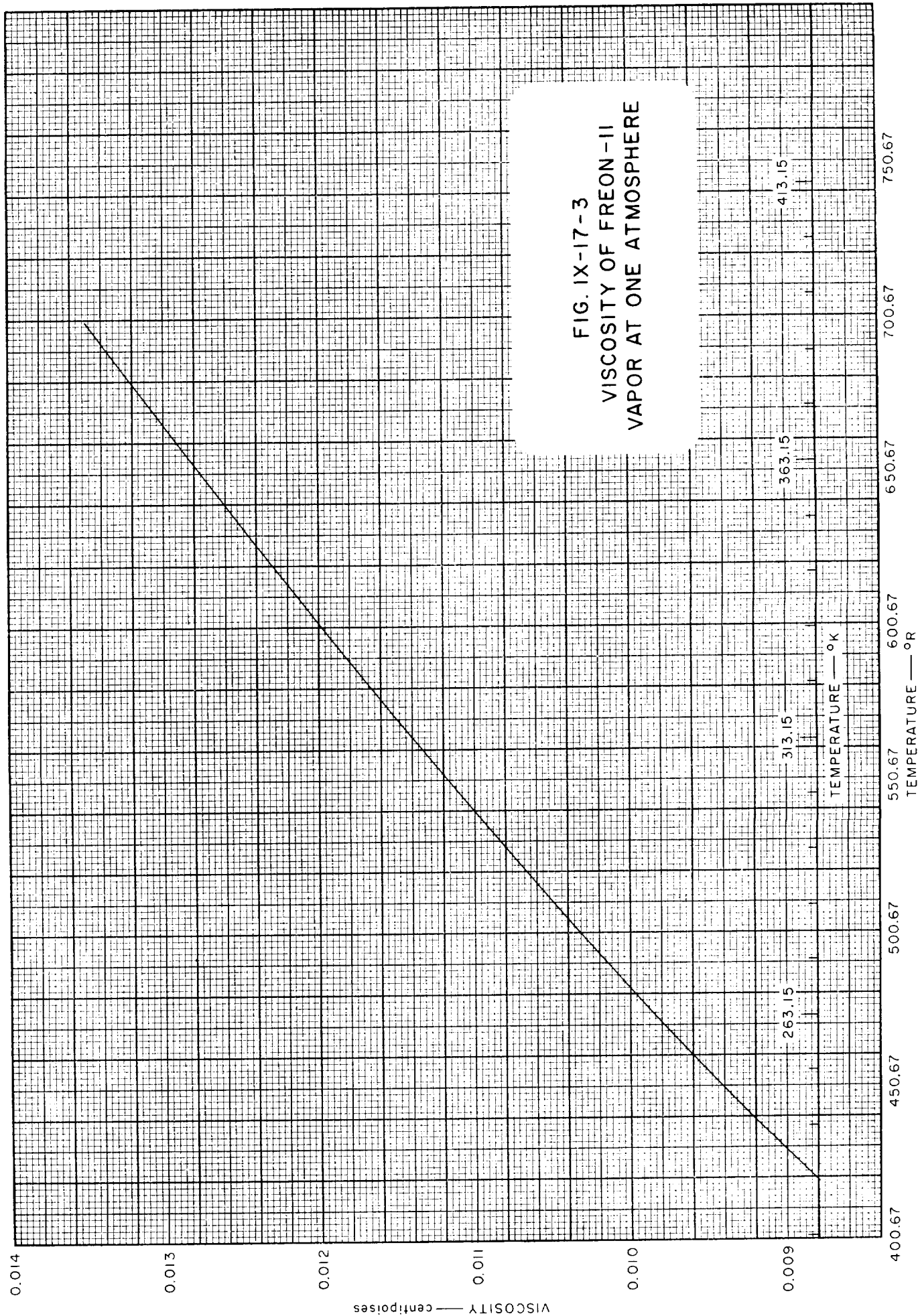
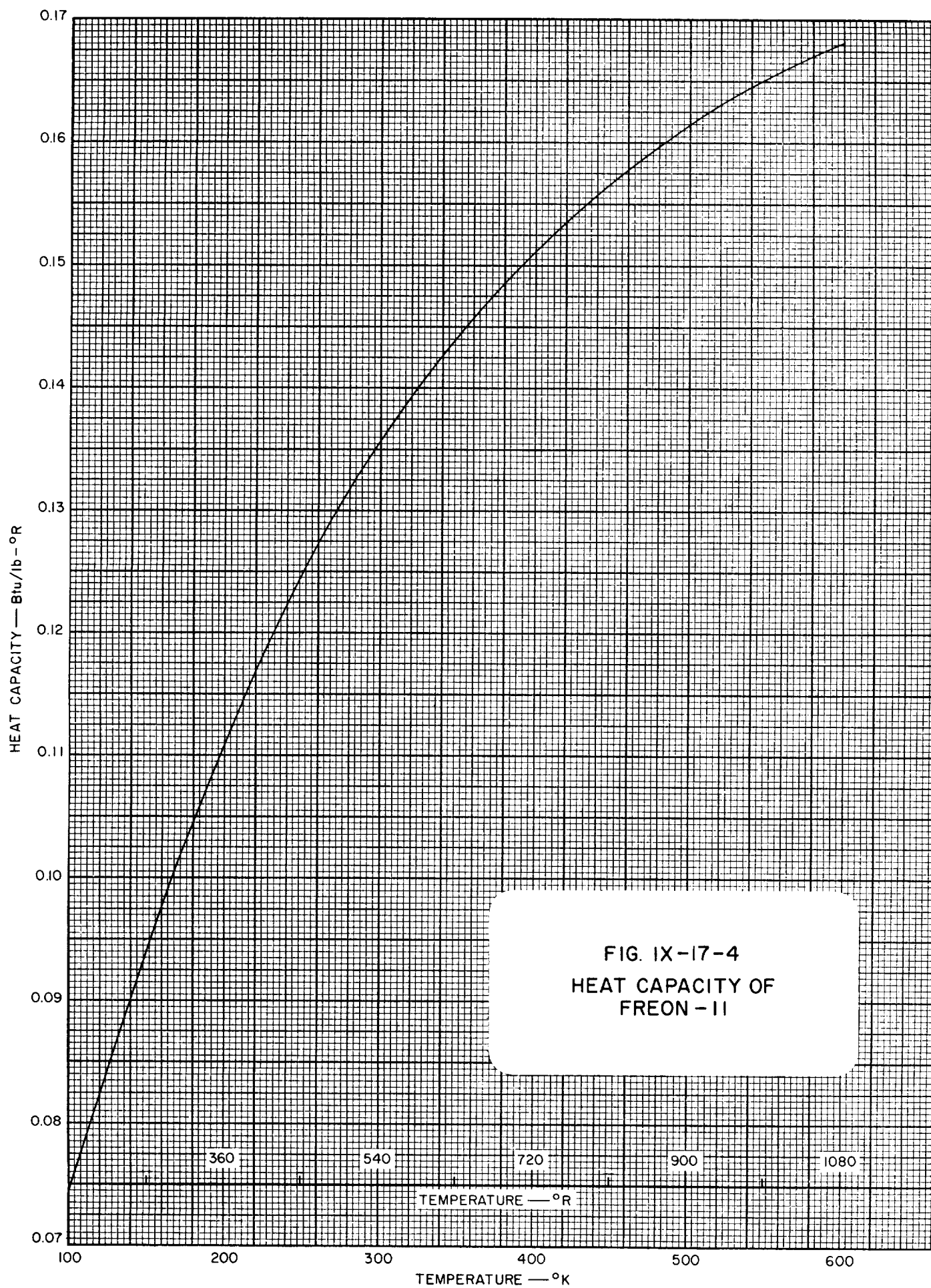


FIG. IX-17-2
VISCOSITY OF SATURATED
LIQUID FREON-11







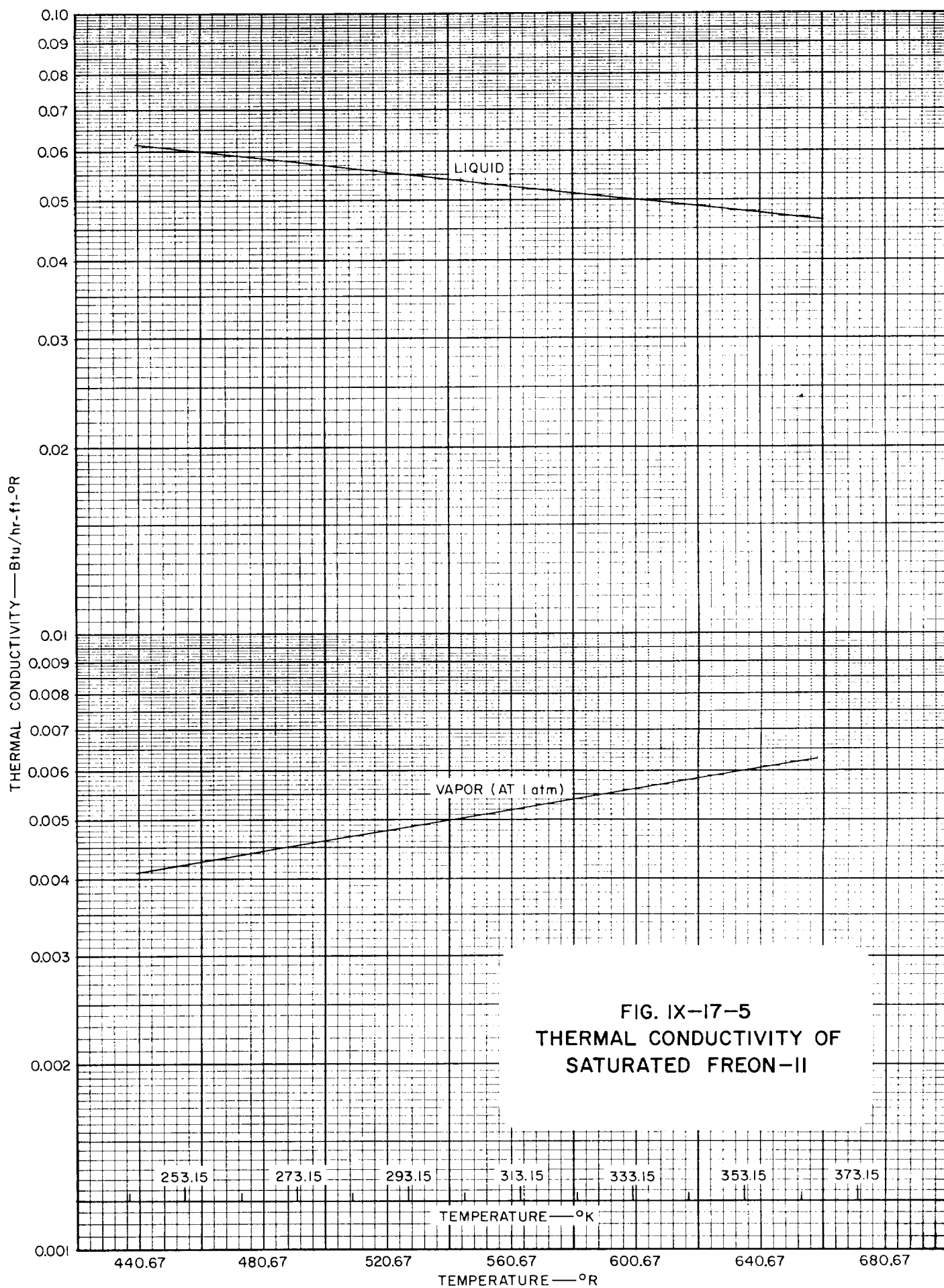


FIG. IX-17-5
THERMAL CONDUCTIVITY OF
SATURATED FREON-II

)

)

)

)

)

IX-17 FREON-11 REFERENCES

1. Du Pont de Nemours, E. I., & Co., *Technical Bulletin B-2*.
2. Du Pont de Nemours, E. I., & Co., *Bulletin B-9A*.
3. Du Pont de Nemours, E. I., & Co., *Bulletin B-10A*.
4. Gelles, E., and Pitzer, K. S., *J. Am. Chem. Soc.*, **75**, 5259 (1953).

)

)

)

)

)

(

Table IX-18-1
GENERAL PROPERTIES OF FREON-12 (CCl_2F_2)

PROPERTY	TEMPERATURE				PRESSURE			REF
	°C	°K	°F	°R	psia	atm	mm of Hg	
Melting Point	-158.0	115.0	-252.0	207.7				9
Boiling Point	- 29.79	243.36	- 21.62	438.05				9
Triple Point								
Critical Temp.	112.0	385.2	233.6	693.3				9
Critical Press.					596.9	40.6		9
Mol. Wt.	120.93							9
Heat of Vaporization	39.47 cal/g or 71.04 Btu/lb at B.P.							
Heat of Fusion								

Table IX-18-1.1
SOME VALUES OF THE GAS CONSTANT, R , FOR FREON-12
(See also Conversion Tables, Section I)

TEMPERATURE IN $^{\circ}\text{K}$				
Pressure Density	atm	kg/cm^2	mm of Hg	lb/in^2
g/cm^3	0.678547	0.701093	515.696	9.97197
mole/cm^3	82.0567	84.7832	62363.1	1205.91
mole/liter	0.0820544	0.0847809	62.3613	1.20587
lb/ft^3	0.0108691	0.0112303	8.26058	0.159734
$\text{lb}/\text{mole}/\text{ft}^3$	1.31441	1.35808	998.952	19.3166
TEMPERATURE IN $^{\circ}\text{R}$				
Pressure Density	atm	kg/cm^2	mm of Hg	lb/in^2
g/cm^3	0.376971	0.389496	286.498	5.53998
mole/cm^3	45.5871	47.1018	34646.2	669.950
mole/liter	0.0455858	0.0471005	34.6452	0.669928
lb/ft^3	0.00603844	0.00623906	4.58921	0.0887406
$\text{lb}/\text{mole}/\text{ft}^3$	0.730228	0.754489	554.973	10.7314

Table IX-18-2
VAPOR PRESSURE OF FREON-12 (Ref. 2)

TEMPERATURE		VAPOR PRESSURE	TEMPERATURE		VAPOR PRESSURE
°K	°R	psia	°K	°R	psia
170.93	307.67	0.1380	249.82	449.67	19.19
172.04	309.67	0.1536	255.37	459.67	23.85
177.59	319.67	0.2562	260.93	469.67	29.34
183.15	329.67	0.4122	266.48	479.67	35.74
188.70	339.67	0.6419	272.04	489.67	43.15
194.26	349.67	0.9703	283.15	509.67	61.40
199.82	359.67	1.428	294.26	529.67	84.89
205.37	369.67	2.051	305.37	549.67	114.5
210.93	379.67	2.881	316.48	569.67	151.1
216.48	389.67	3.965	327.67	589.67	195.7
222.04	399.67	5.358	344.26	619.67	279.8
227.59	409.67	7.117	360.93	649.67	388.0
233.15	419.67	9.308	372.04	669.67	475.5
238.70	429.67	12.00	383.15	689.67	577.0
244.26	439.67	15.27			

(See Figure IX-18-1)

Table IX-18-3
DENSITY OF SATURATED LIQUID FREON-12 (Ref. 2)

TEMPERATURE		DENSITY	TEMPERATURE		DENSITY
°K	°R	lb/ft ³	°K	°R	lb/ft ³
170.93	307.67	104.52	249.82	449.67	91.69
172.04	309.67	104.36	255.37	459.67	90.66
177.59	319.67	103.54	260.93	469.67	89.61
183.15	329.67	102.71	266.48	479.67	88.53
188.70	339.67	101.87	272.04	489.67	87.43
194.26	349.67	101.00	283.15	509.67	85.14
199.82	359.67	100.15	294.26	529.67	82.72
205.37	369.67	99.27	305.37	549.67	80.14
210.93	379.67	98.38	316.48	569.67	77.38
216.48	389.67	97.48	327.59	589.67	74.37
222.04	399.67	96.55	344.26	619.67	69.21
227.59	409.67	95.62	360.93	649.67	62.73
233.15	419.67	94.66	372.04	669.67	56.82
238.70	429.67	93.69	383.15	689.67	45.76
244.26	439.67	92.70			

(See Figure IX-18-2)

Table IX-18-4
DENSITY OF SATURATED VAPOR OF FREON-12 (Ref. 2)

TEMPERATURE		DENSITY	TEMPERATURE		DENSITY
°K	°R	lb/ft ³	°K	°R	lb/ft ³
170.93	307.67	0.00506	249.82	449.67	0.507
172.04	309.67	0.00560	255.37	459.67	0.622
177.59	319.67	0.00905	260.93	469.67	0.755
183.15	329.67	0.0141	266.48	479.67	0.910
188.70	339.67	0.0214	272.04	489.67	1.088
194.26	349.67	0.0315	283.15	509.67	1.526
199.82	359.67	0.0451	294.26	529.67	2.091
205.37	369.67	0.0632	305.37	549.67	2.815
210.93	379.67	0.0867	316.48	569.67	3.736
216.48	389.67	0.117	327.59	589.67	4.911
222.04	399.67	0.154	344.26	619.67	7.351
227.59	409.67	0.201	360.93	649.67	11.18
233.15	419.67	0.258	372.04	669.67	15.42
238.70	429.67	0.327	383.15	689.67	25.36
244.20	439.67	0.409			

(See Figure IX-18-3)

Table IX-18-5
 VISCOSITY OF SATURATED LIQUID FREON-12 (Ref. 4)

TEMPERATURE		ABSOLUTE VISCOSITY	TEMPERATURE		ABSOLUTE VISCOSITY
°K	°R	centi- poises	°K	°R	centi- poises
233.15	419.67	0.423	344.26	619.67	0.214
244.26	439.67	0.371	355.37	639.67	0.207
255.37	459.67	0.335	366.48	659.67	0.200
266.48	479.67	0.308			
277.59	499.67	0.286			
288.71	519.67	0.269			
299.82	539.67	0.255			
310.93	559.67	0.242			
322.04	579.67	0.232			
333.15	599.67	0.222			

(See Figure IX-18-4)

Table IX-18-6
 VISCOSITY OF FREON-12 VAPOR AT ONE ATMOSPHERE (Ref. 4)

TEMPERATURE		ABSOLUTE VISCOSITY	TEMPERATURE		ABSOLUTE VISCOSITY
°K	°R	centi- poises	°K	°R	centi- poises
233.15	419.67	0.0106	344.26	619.67	0.0138
244.26	439.67	0.0109	355.37	639.67	0.0140
255.37	459.67	0.0113	366.48	659.67	0.0143
266.48	479.67	0.0116	377.59	679.67	0.0146
277.59	499.67	0.0119	388.71	699.67	0.0149
288.71	519.67	0.0123			
299.82	539.67	0.0126			
310.93	559.67	0.0129			
322.04	579.67	0.0132			
333.15	599.67	0.0135			

(See Figure IX-18-5)

Table IX-18-7
HEAT CAPACITY OF FREON-12 (Ref. 5)

TEMPERATURE		HEAT CAPACITY
$^{\circ}\text{K}$	$^{\circ}\text{R}$	Btu/lb- $^{\circ}\text{R}$
100	180	0.0782
150	270	0.0974
200	360	0.1154
250	450	0.1306
298.16	336.7	0.1429
300	540	0.1433
400	720	0.1627
500	900	0.1760
600	1080	0.1850

(See Figure IX-18-6)

Table IX-18-8
THERMAL CONDUCTIVITY OF SATURATED FREON-12 (Ref. 3)

TEMPERATURE		THERMAL CONDUCTIVITY- Btu/hr-ft- $^{\circ}\text{R}$	
$^{\circ}\text{K}$	$^{\circ}\text{R}$	Liquid	Vapor (at 1 atm)
253.15	455.67	0.051	
293.15	527.67	0.042	
303.15	545.67		0.00591
363.15	653.67		0.00738

(See Figure IX-18-9)

)

)

)

)

)

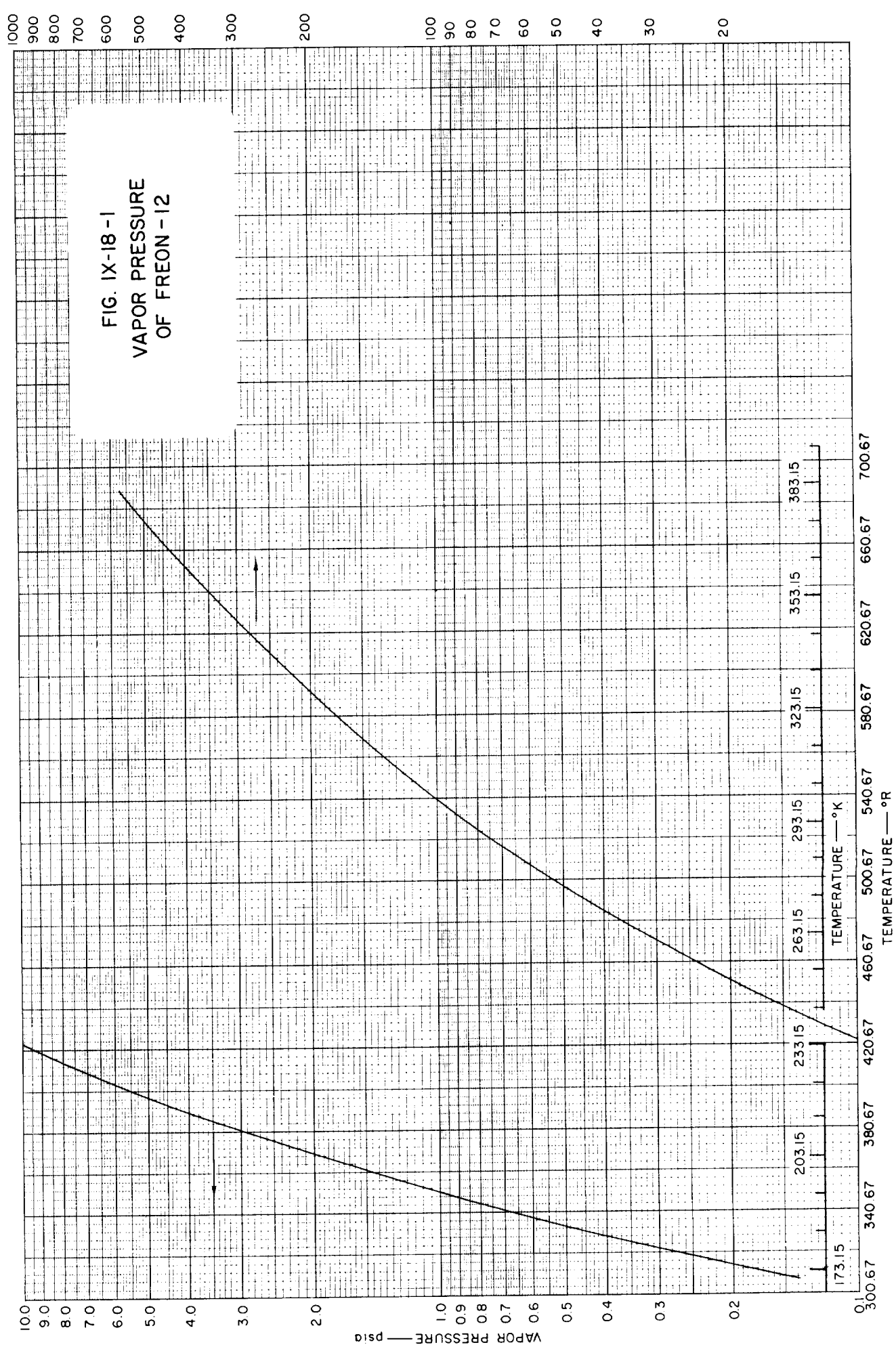
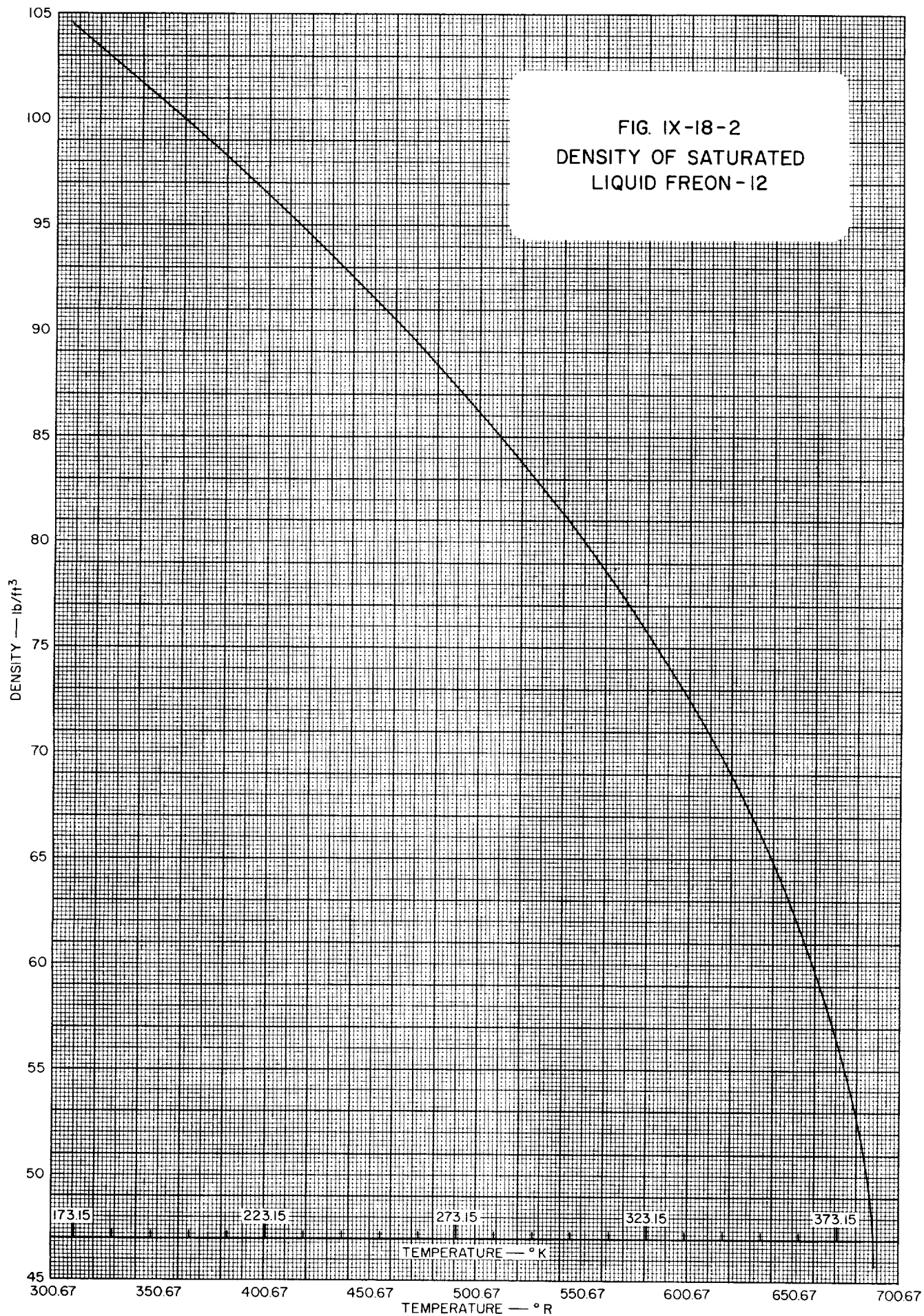


FIG. IX-18-2
DENSITY OF SATURATED
LIQUID FREON-12



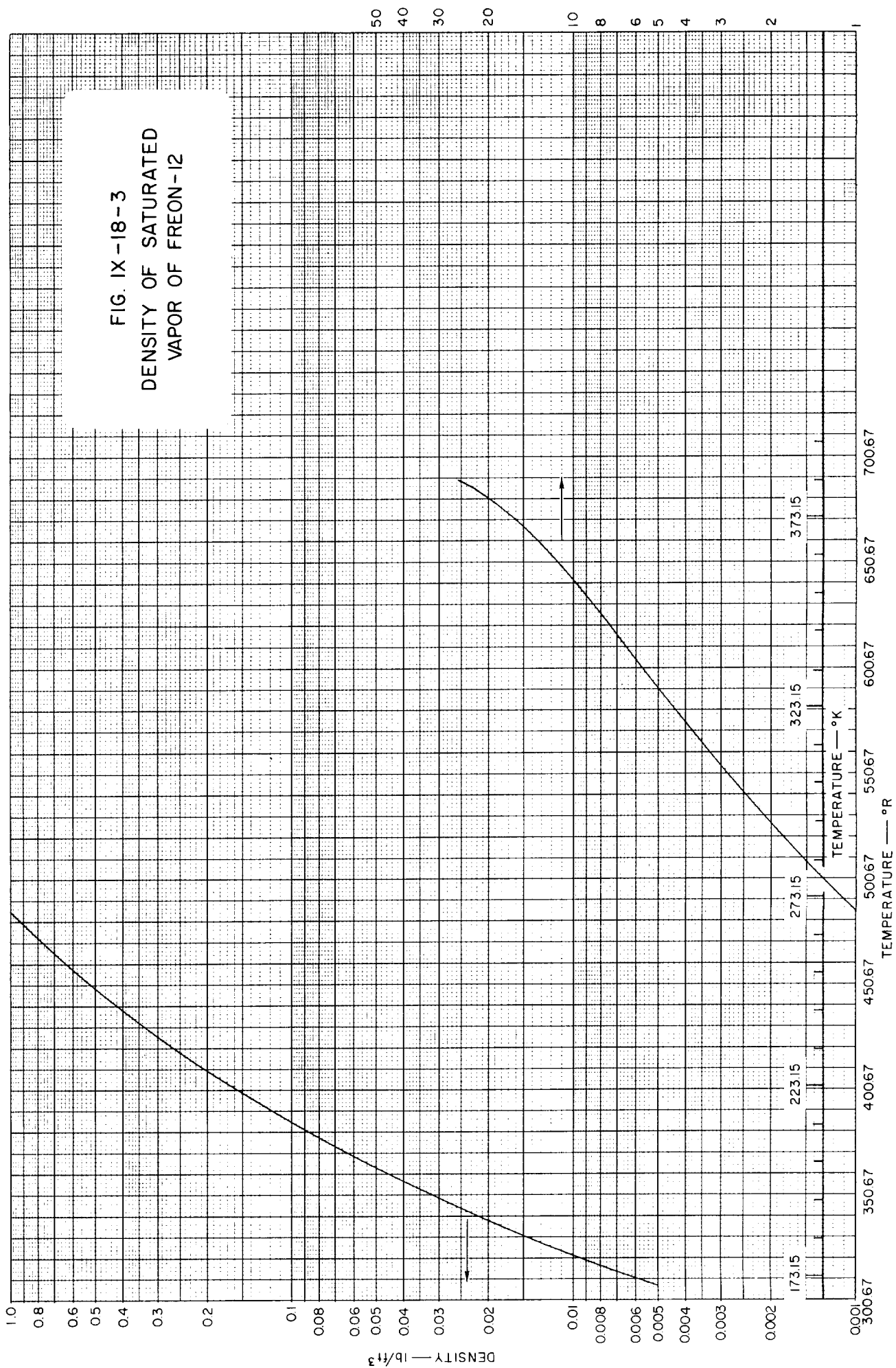
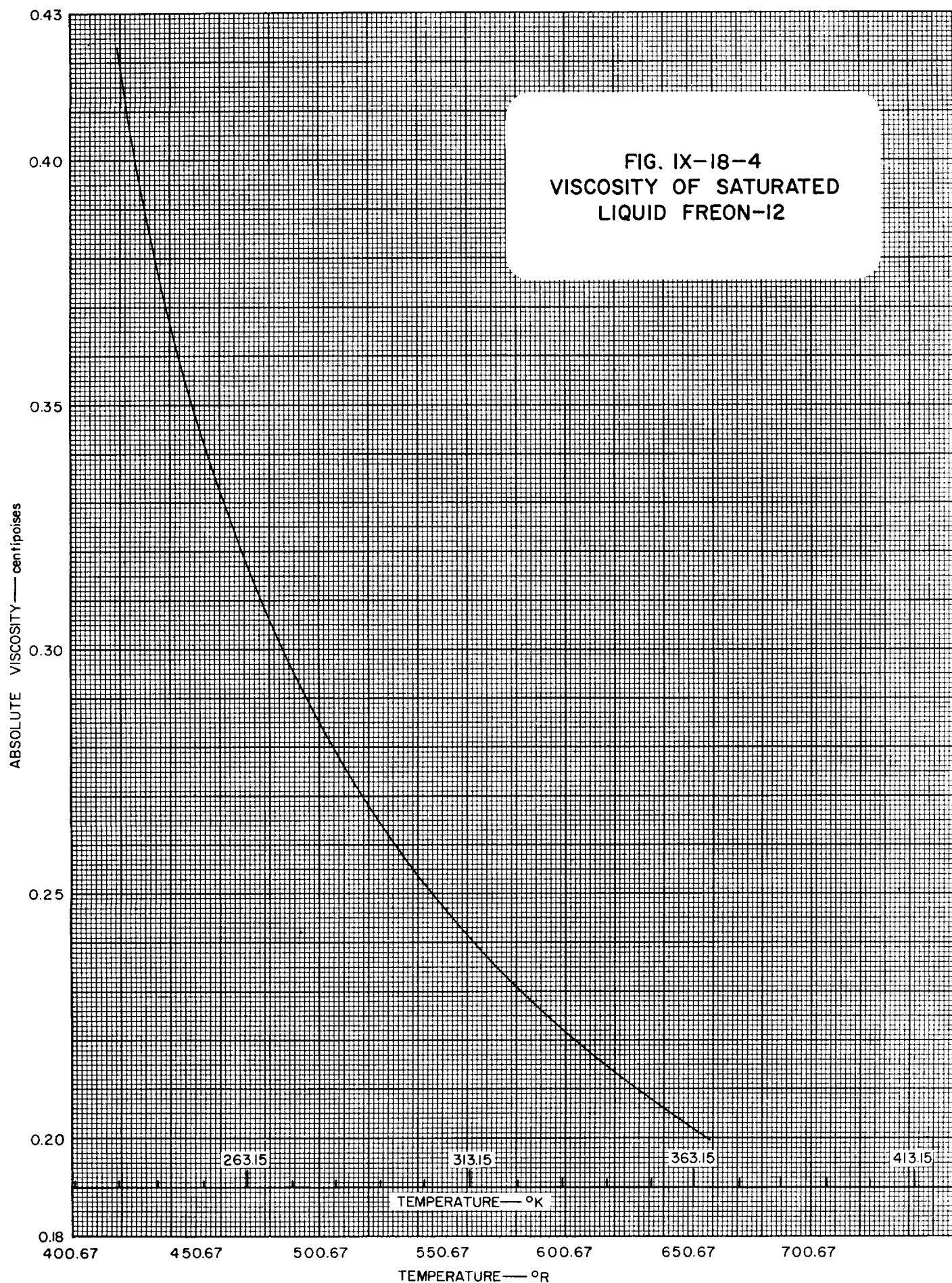
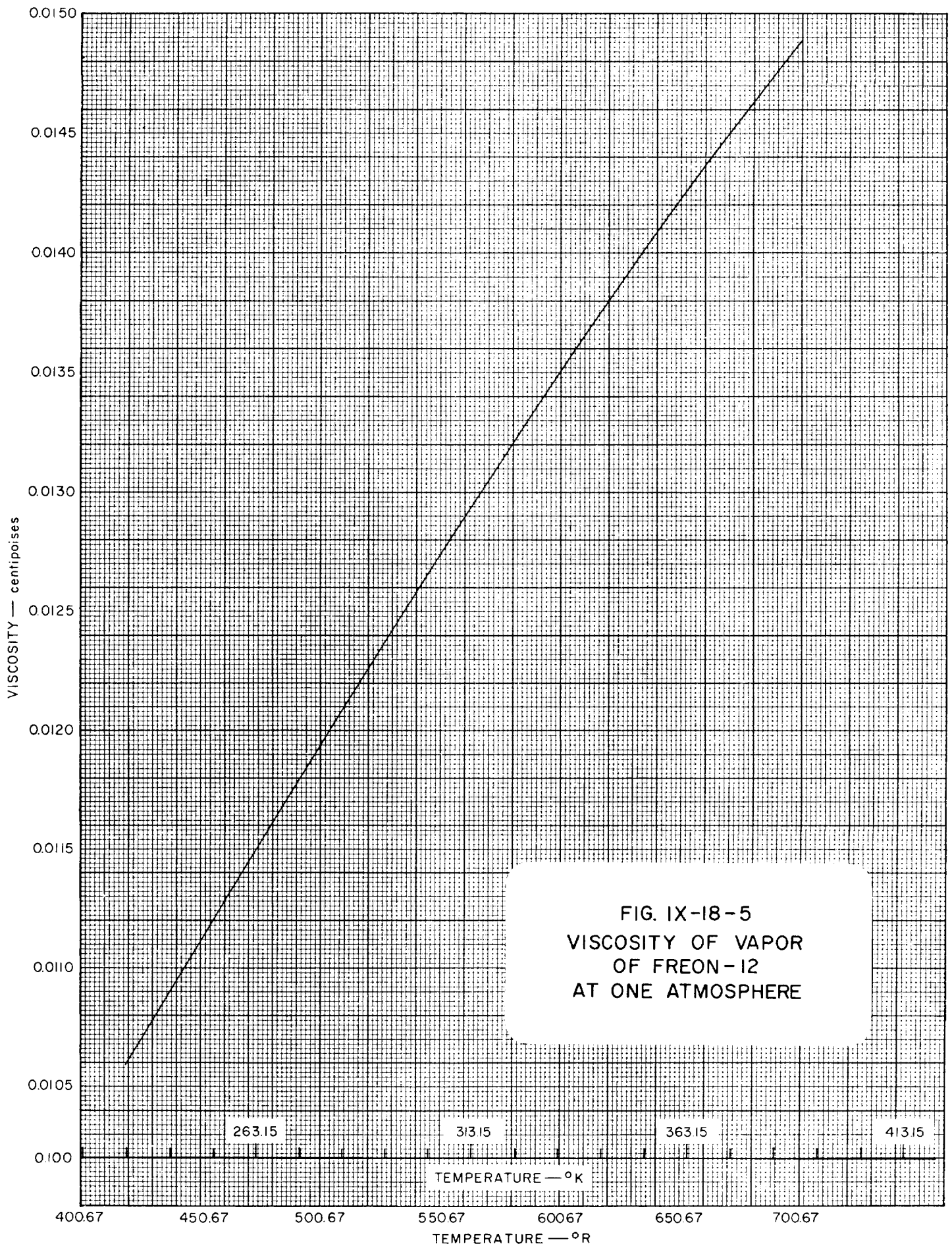
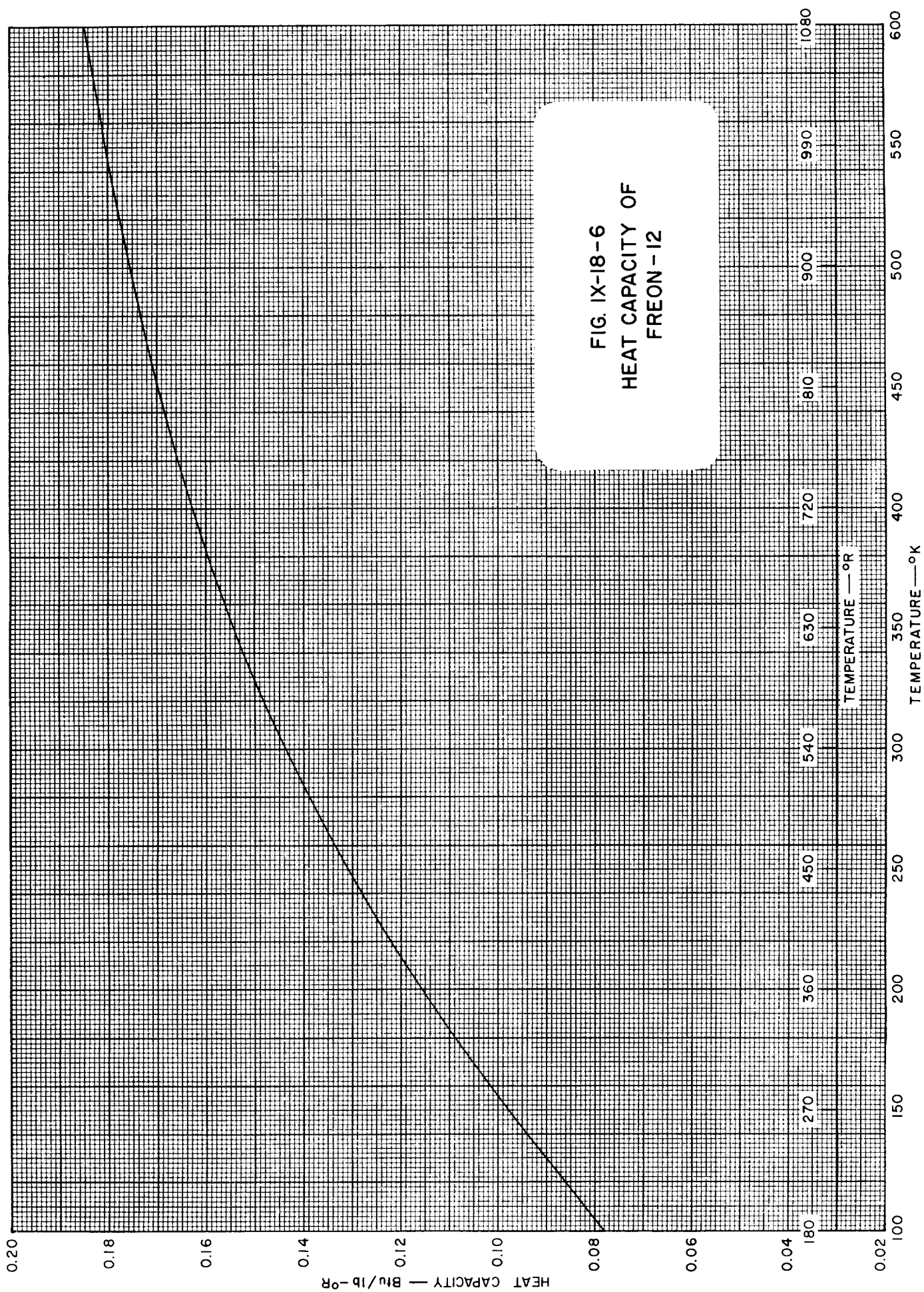
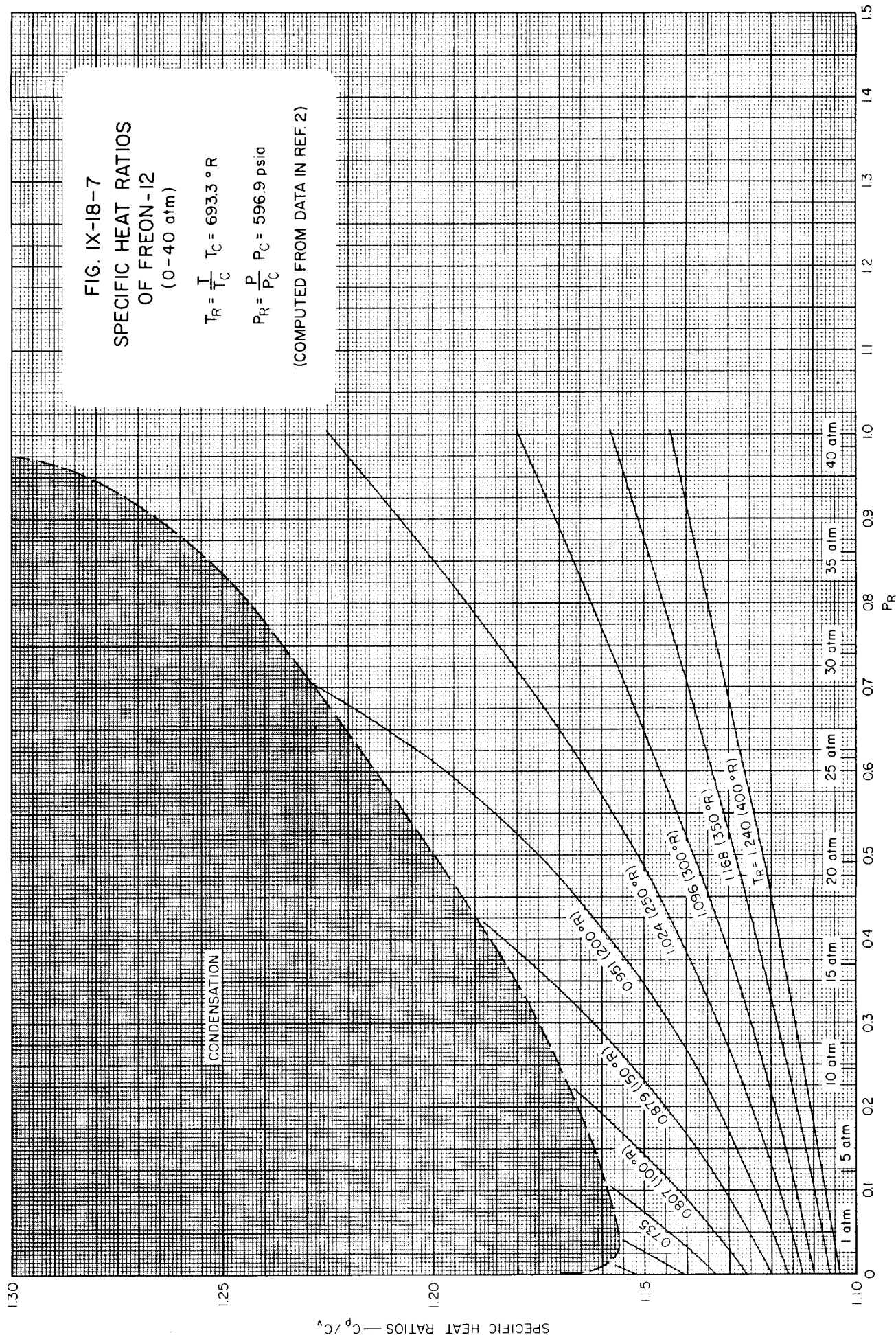


FIG. IX-18-4
VISCOSITY OF SATURATED
LIQUID FREON-12









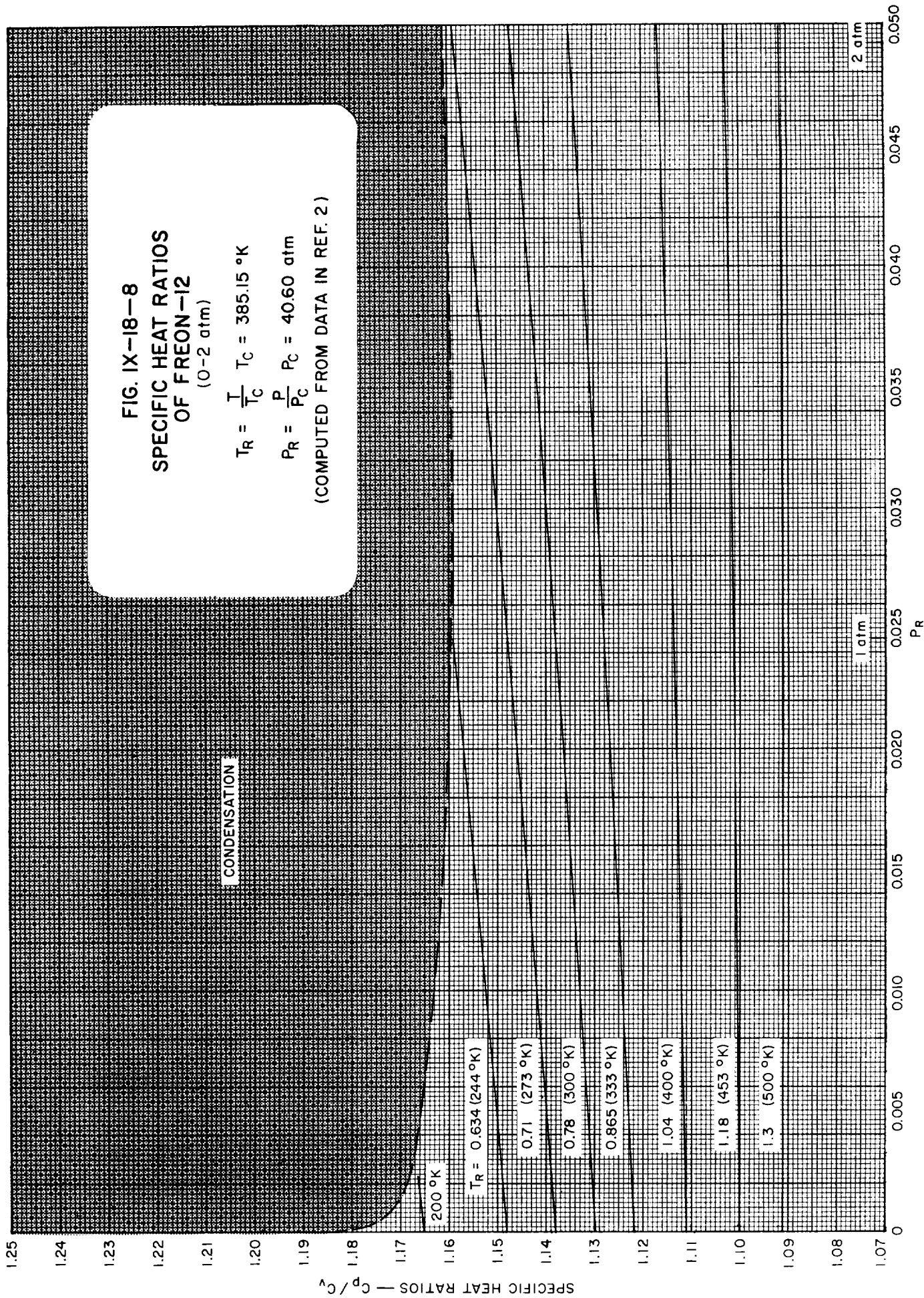


FIG. IX-18-8
SPECIFIC HEAT RATIOS
OF FREON-12
(0-2 atm)

$$T_R = \frac{T}{T_C} \quad T_C = 385.15 \text{ }^\circ\text{K}$$

$$P_R = \frac{P}{P_C} \quad P_C = 40.60 \text{ atm}$$

(COMPUTED FROM DATA IN REF. 2)

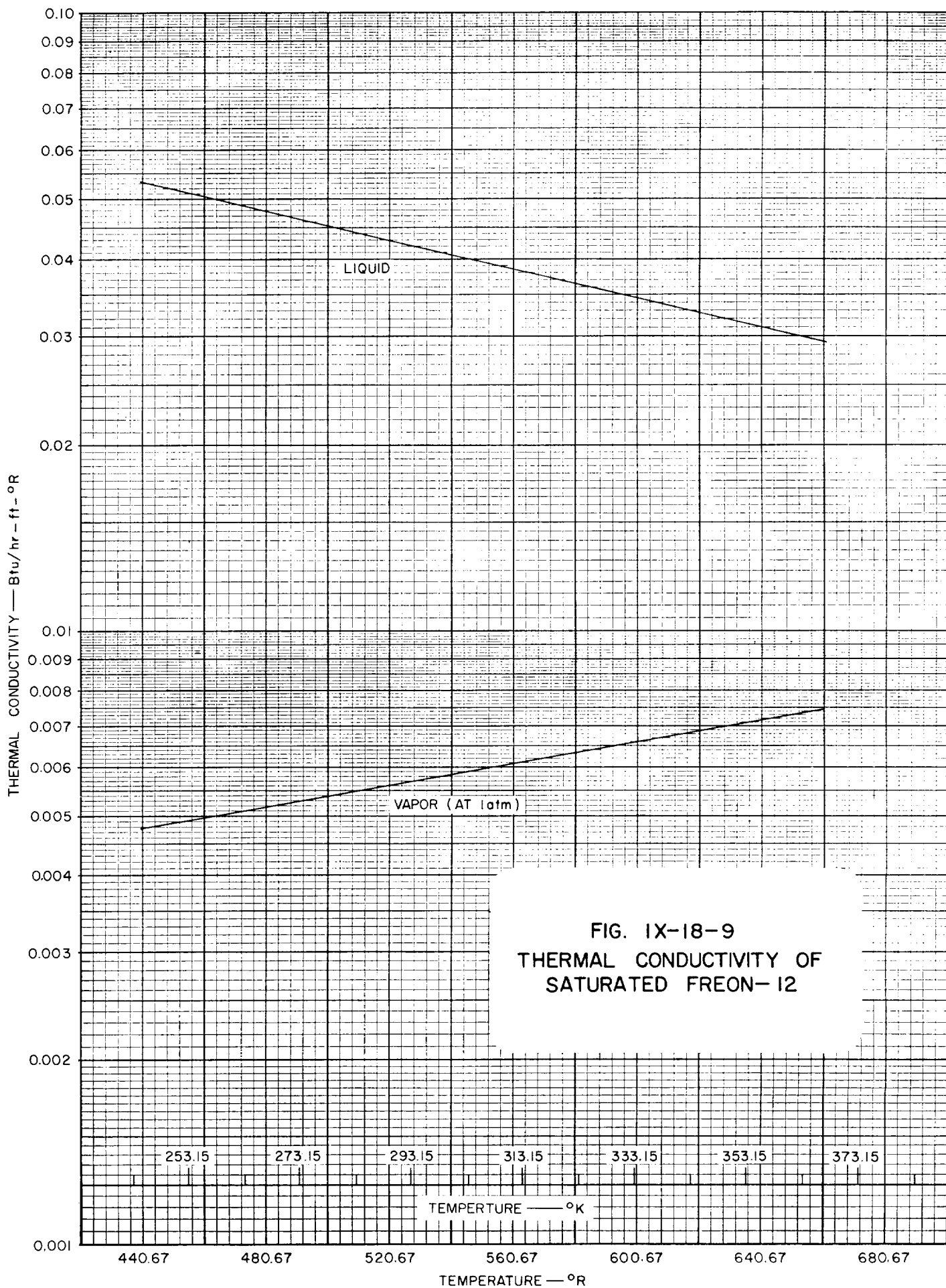


FIG. IX-18-9
THERMAL CONDUCTIVITY OF
SATURATED FREON-12

)

)

)

)

)

IX-18 FREON-12 REFERENCES

1. Du Pont de Nemours, E. I., & Co., *Technical Bulletin B-2*.
2. Du Pont de Nemours, E. I., & Co., *Technical Bulletin T-12*.
3. Du Pont de Nemours, E. I., & Co., *Bulletin B-9A*.
4. Du Pont de Nemours, E. I., & Co., *Bulletin B-10A*.
5. Gelles, E., and Pitzer, K. S., *J. Am. Chem. Soc.*, **75**, 5259 (1953).

)

)

)

)

)

Table IX-19-1
GENERAL PROPERTIES OF FREON-13 (CClF₃)

PROPERTY	TEMPERATURE				PRESSURE			REF
	°C	°K	°F	°R	psia	atm	mm of Hg	
Melting Point	-181.0	92.2	-294.0	165.7				1
Boiling Point	- 81.4	191.8	-114.6	345.1				1
Triple Point								
Critical Temp.	28.9	302.1	83.9	543.6				1
Critical Press.					561	38.2		1
Mol. Wt. 104.47								1
Heat of Vaporization 35.47 cal/g or 63.85 Btu/lb at B.P.								
Heat of Fusion								

Table IX-19-1.1
SOME VALUES OF THE GAS CONSTANT, *R*, FOR FREON-13
(See also Conversion Tables, Section I)

TEMPERATURE IN °K				
Pressure	atm	kg/cm ²	mm of Hg	lb/in ²
Density				
g/cm ³	0.785457	0.811555	596.947	11.5431
mole/cm ³	82.0567	84.7832	62363.1	1205.91
mole/liter	0.0820544	0.0847809	62.3613	1.20587
lb/ft ³	0.0125817	0.0129997	9.56209	0.184901
lb/mole/ft ³	1.31441	1.35808	998.952	19.3166
TEMPERATURE IN °R				
Pressure	atm	kg/cm ²	mm of Hg	lb/in ²
Density				
g/cm ³	0.436365	0.450864	331.637	6.41285
mole/cm ³	45.5871	47.1018	34646.2	669.950
mole/liter	0.0455858	0.0471005	34.6452	0.669928
lb/ft ³	0.00698983	0.00722206	5.31227	0.102722
lb/mole/ft ³	0.730228	0.754489	554.973	10.7314

Table IX-19-2
VAPOR PRESSURE OF FREON-13 (Ref. 2)

TEMPERATURE		VAPOR PRESSURE	TEMPERATURE		VAPOR PRESSURE
$^{\circ}\text{K}$	$^{\circ}\text{R}$	psia	$^{\circ}\text{K}$	$^{\circ}\text{R}$	psia
144.26	259.67	0.4329	233.15	419.67	87.43
155.37	279.67	1.238	244.26	439.67	126.4
166.48	299.67	3.104	255.37	459.67	176.8
177.59	319.67	6.455	266.48	479.67	240.4
188.70	339.67	12.48	277.59	499.67	319.60
199.82	359.67	22.23	288.71	519.67	417.0
210.93	379.67	36.98	299.82	539.67	535.5
222.04	399.67	58.19			

(See Figure IX-19-1)

Table IX-19-3
DENSITY OF SATURATED LIQUID FREON-13 (Ref. 2)

TEMPERATURE		DENSITY	TEMPERATURE		DENSITY
°K	°R	lb/ft ³	°K	°R	lb/ft ³
144.26	259.67	105.6	233.15	419.67	84.10
155.37	279.67	103.2	244.26	439.67	80.71
166.48	299.67	100.8	255.37	459.67	76.98
177.59	319.67	98.33	266.48	479.67	72.73
188.70	339.67	95.69	277.59	479.67	67.70
199.82	359.67	93.02	288.71	519.67	61.09
210.93	379.67	90.17	299.82	539.67	48.85
222.04	399.67	87.26			

(See Figure IX-19-2)

Table IX-19-4
DENSITY OF SATURATED VAPOR OF FREON-13 (Ref. 2)

TEMPERATURE		DENSITY	TEMPERATURE		DENSITY
°K	°R	lb/ft ³	°K	°R	lb/ft ³
144.26	259.67	0.0163	233.15	419.67	2.362
155.37	279.67	0.0435	244.26	439.67	3.413
166.48	299.67	0.1026	255.37	459.67	4.840
177.59	319.67	0.2020	266.48	479.67	6.788
188.70	339.67	0.3730	277.59	499.67	9.565
199.82	359.67	0.6393	288.71	519.67	13.91
210.93	379.67	1.032	299.82	539.67	24.21
222.04	399.67	1.590			

(See Figure IX-19-3)

Table IX-19-5
VISCOSITY OF FREON-13 (Ref. 4)

TEMPERATURE		ABSOLUTE VISCOSITY
$^{\circ}\text{K}$	$^{\circ}\text{R}$	micro- poises
100	180	50.6
200	360	101.9
300	540	150.2
400	720	193.1
500	900	231.5
600	1080	266.6

(See Figure IX-19-4)

Table IX-19-6
HEAT CAPACITY OF FREON-13 (Ref. 3)

TEMPERATURE		HEAT CAPACITY
$^{\circ}\text{K}$	$^{\circ}\text{R}$	Btu/lb- $^{\circ}\text{R}$
100	180	0.0839
150	270	0.1017
200	360	0.1210
250	450	0.1383
298.16	336.7	0.1529
300	540	0.1553
400	720	0.1774
500	900	0.1945
600	1080	0.2068

(See Figure IX-19-5)

Table IX-19-7
THERMAL CONDUCTIVITY OF GASEOUS
FREON-13 (Ref. 4)

TEMPERATURE		THERMAL CON- DUCTIVITY
$^{\circ}\text{K}$	$^{\circ}\text{R}$	Btu/hr-ft $^{\circ}\text{R}$
100	180	0.00148
200	360	0.00416
300	540	0.00767
400	720	0.0113
500	900	0.0149
600	1080	0.0182

)

)

)

)

)

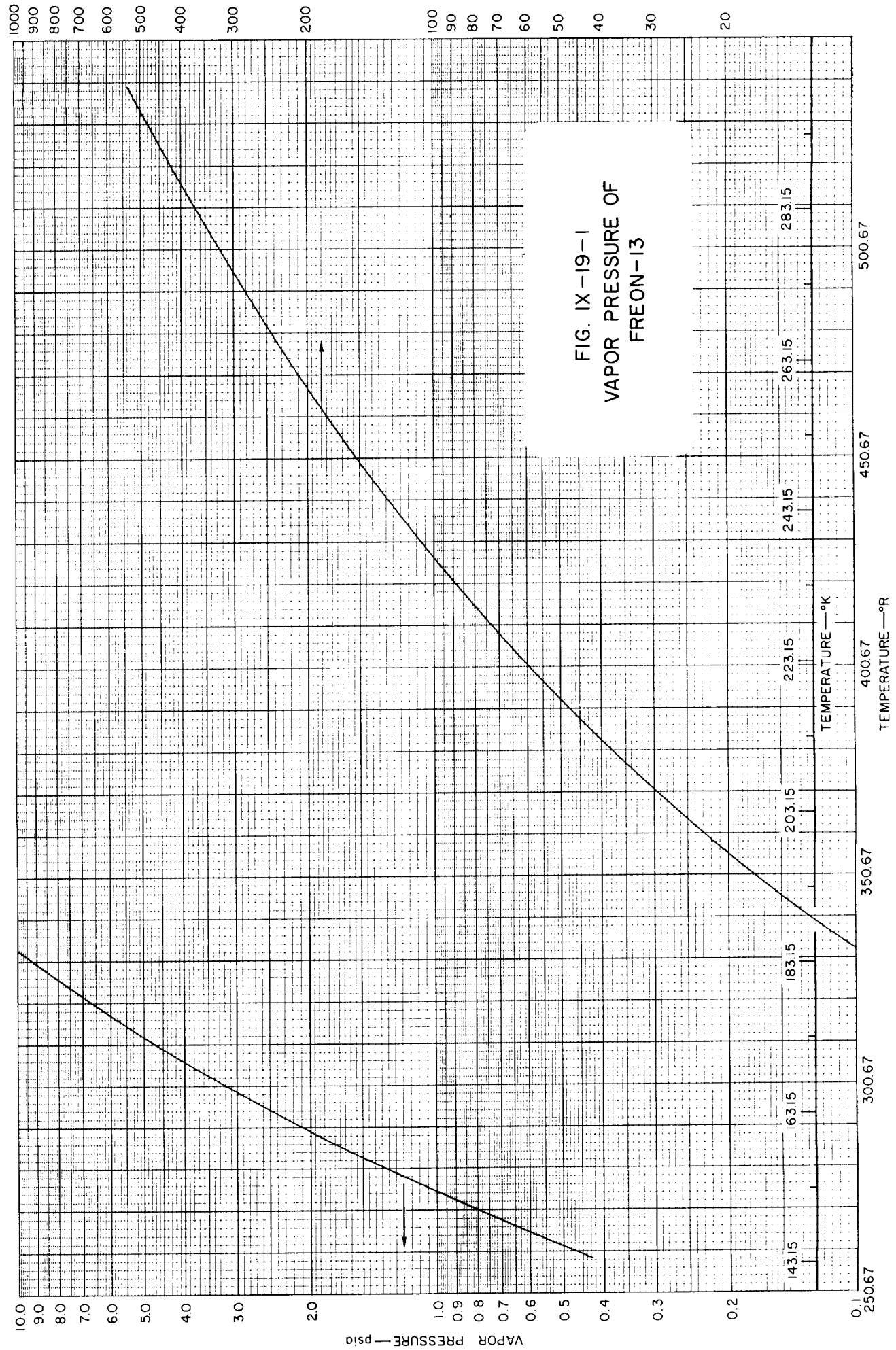
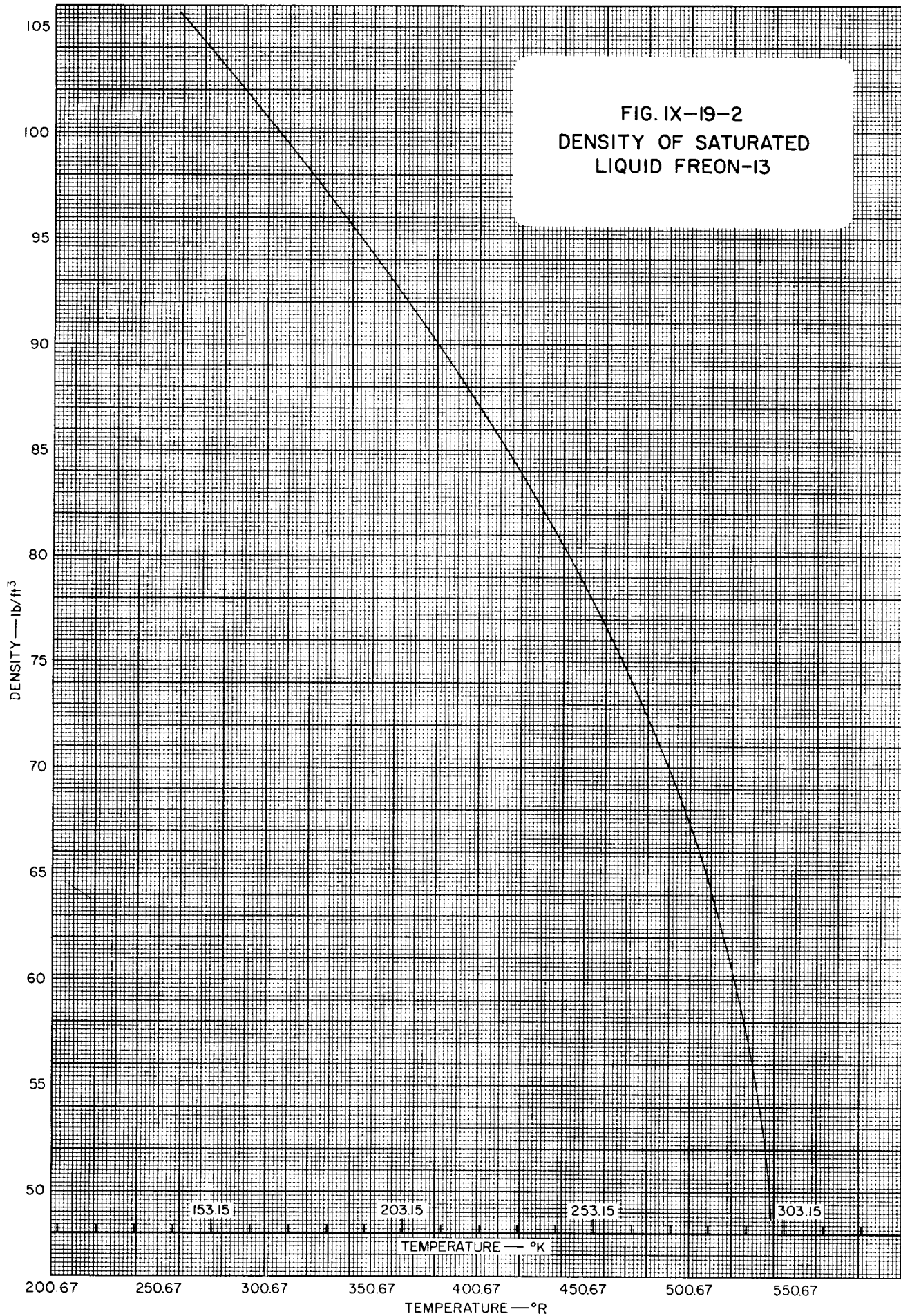
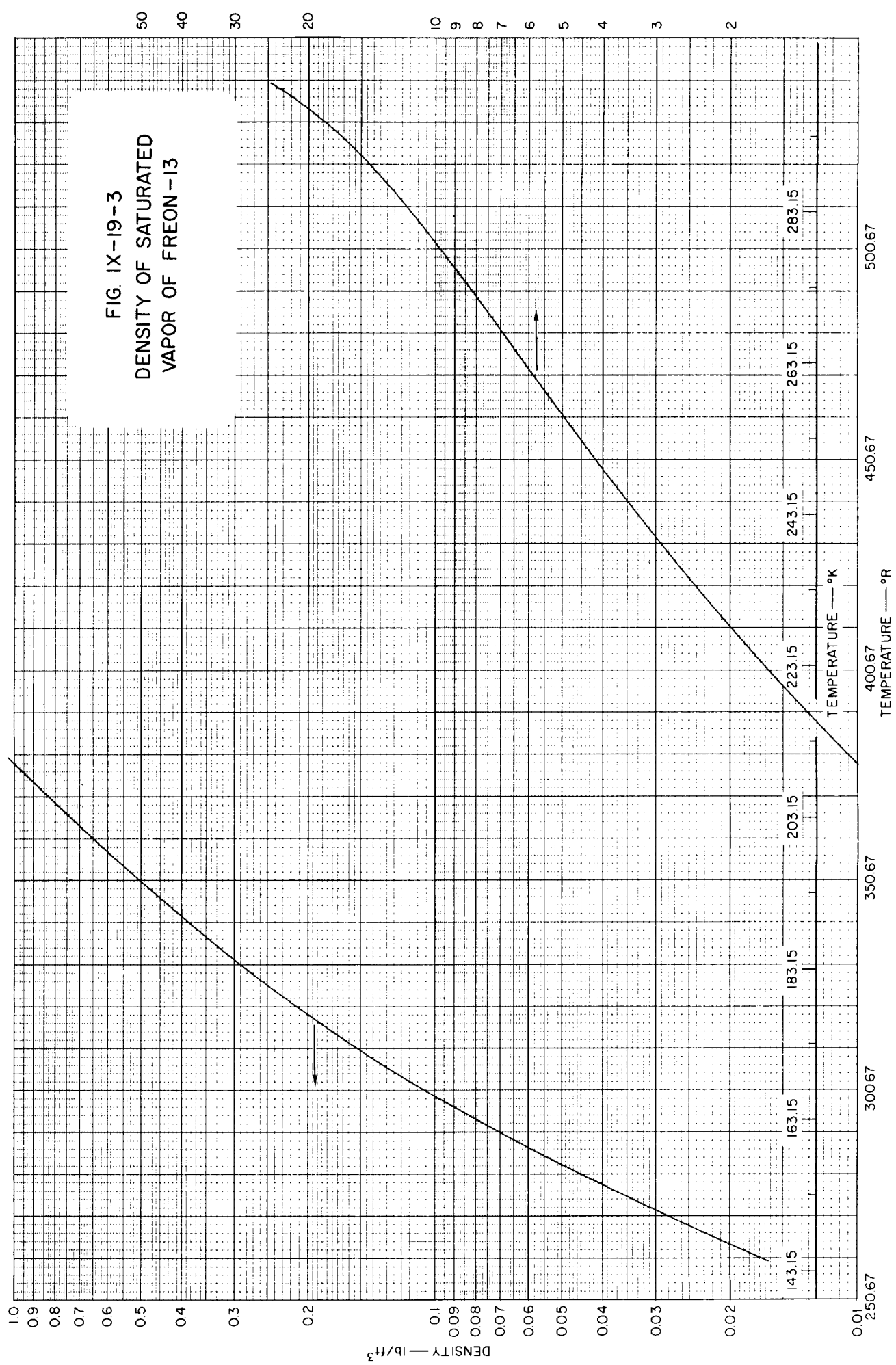


FIG. IX-19-2
DENSITY OF SATURATED
LIQUID FREON-13





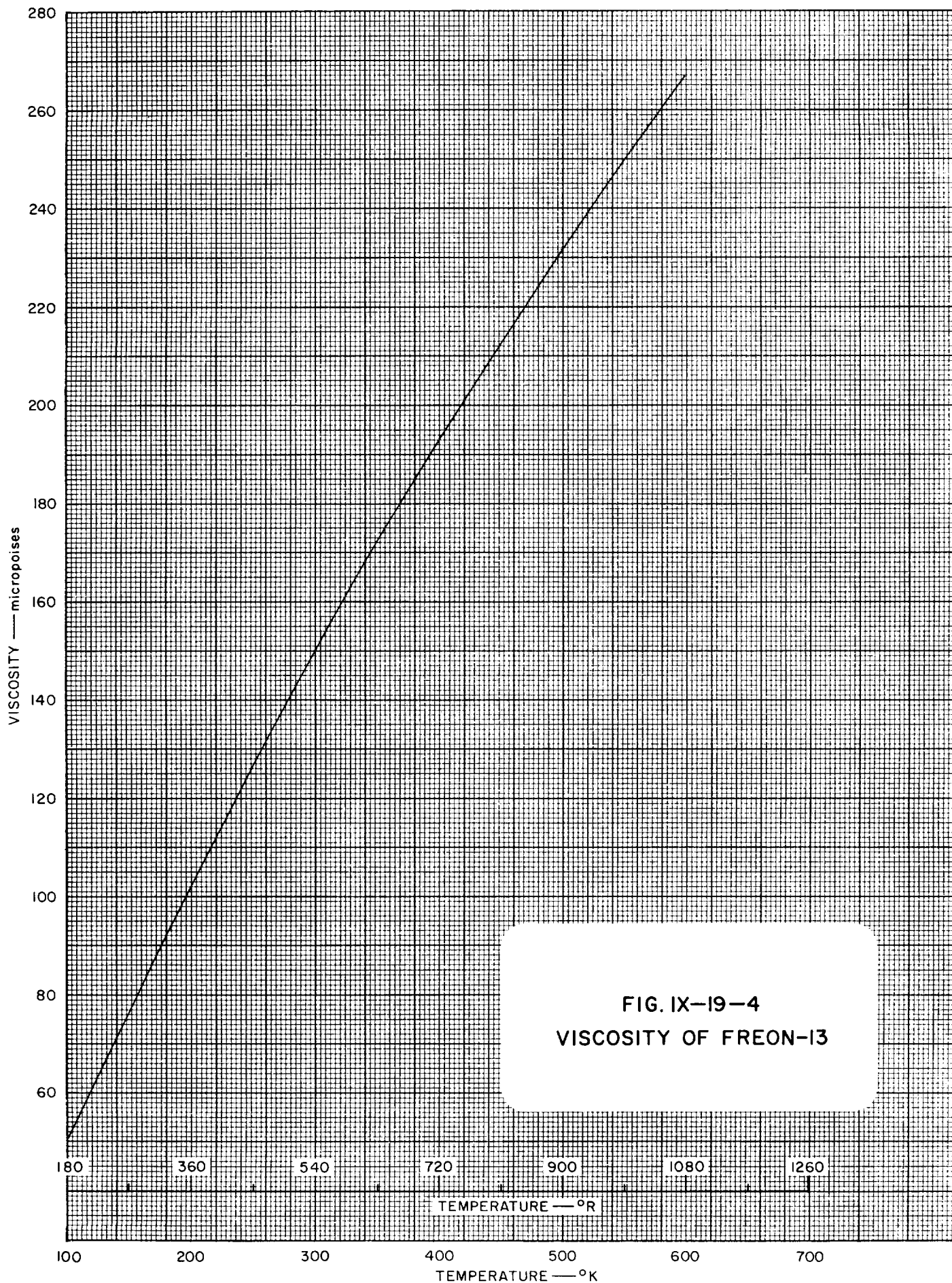
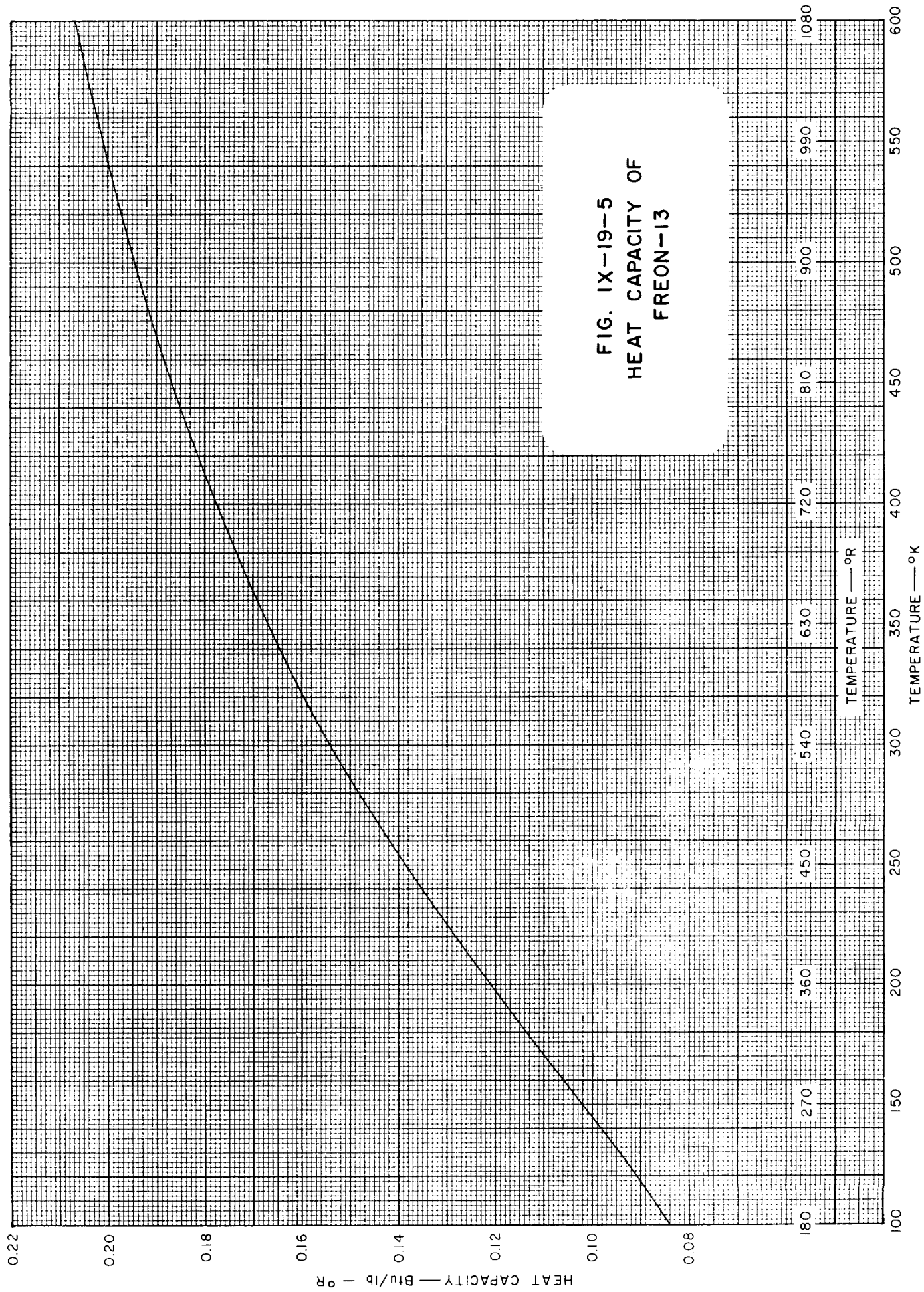


FIG. IX-19-4
VISCOSITY OF FREON-13



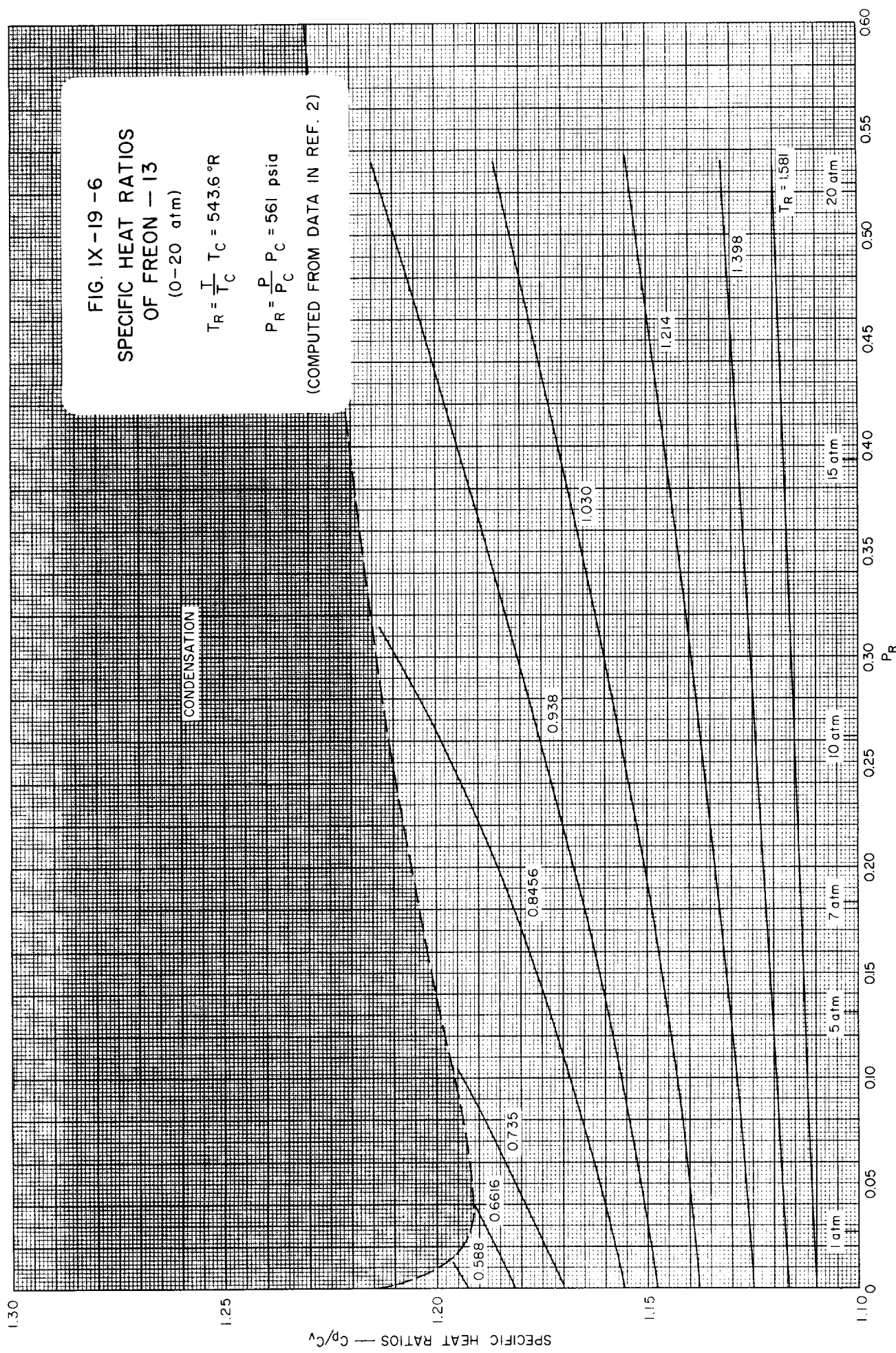
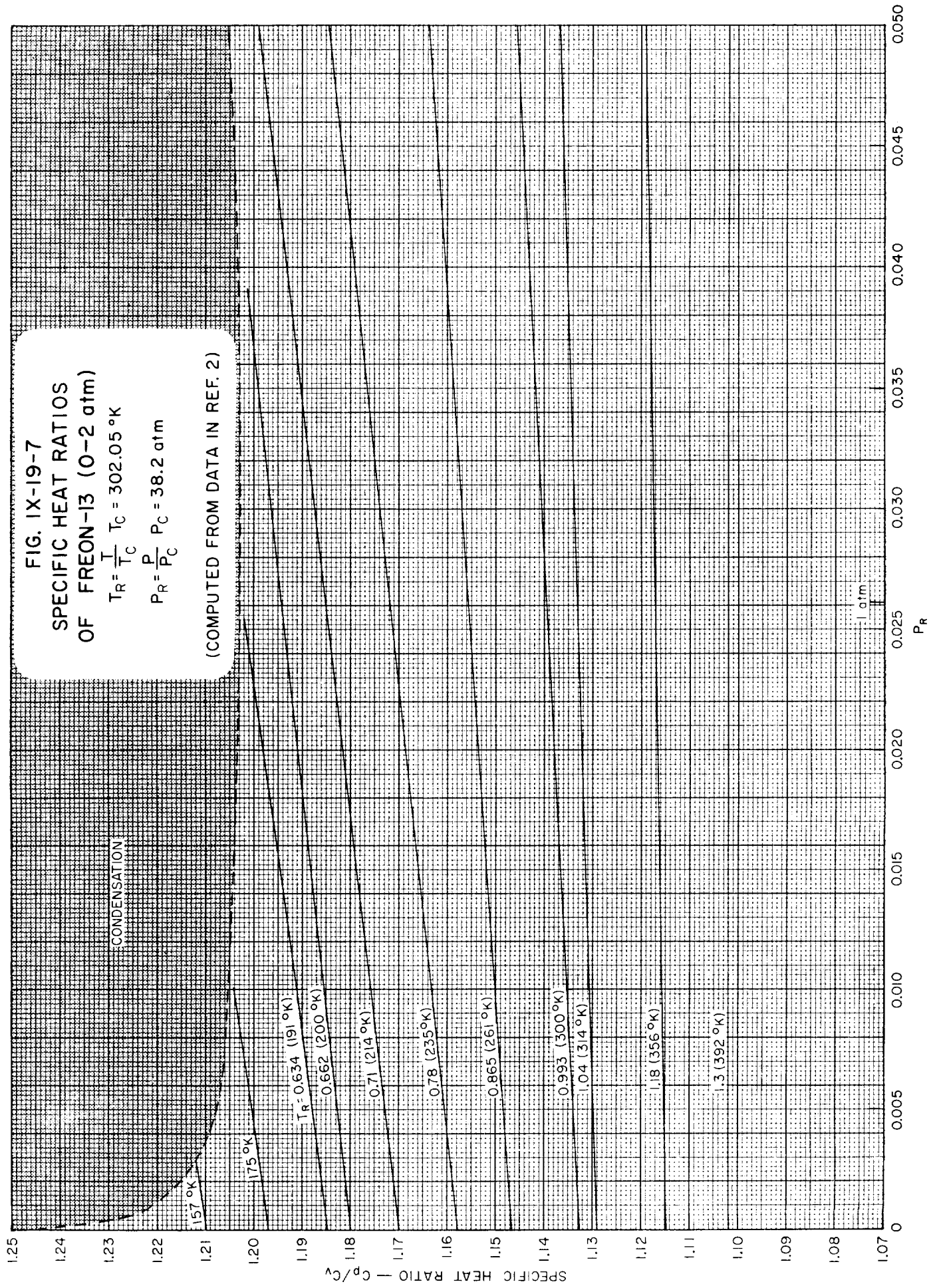


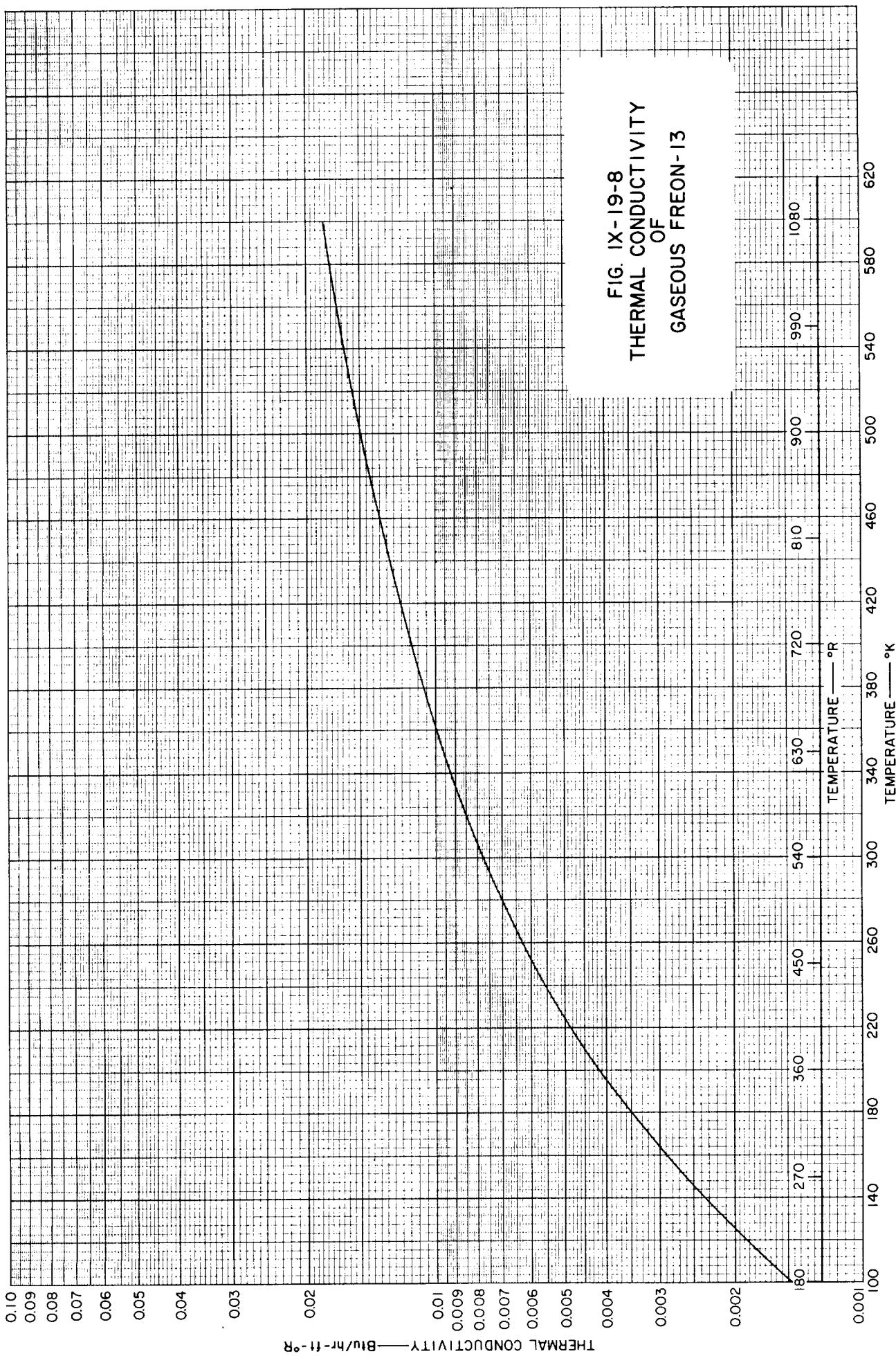
FIG. 1X-19-7
SPECIFIC HEAT RATIOS
OF FREON-13 (0-2 atm)

$$T_R = \frac{T}{T_C} \quad T_C = 302.05^\circ\text{K}$$

$$P_R = \frac{P}{P_C} \quad P_C = 38.2 \text{ atm}$$

(COMPUTED FROM DATA IN REF. 2)





IX-19 FREON-13 REFERENCES

1. Du Pont de Nemours, E. I., & Co., *Technical Bulletin B-2*.
2. Du Pont de Nemours, E. I., & Co., *Technical Bulletin T-13*.
3. Gelles, E., and Pitzer, *J. Am. Chem. Soc.*, **75**, 5259 (1953).
4. Svehla, P. A., *NASA TR R-132*, 1962.

)

)

)

)

)

Table IX-20-1
GENERAL PROPERTIES OF FREON-14 (CF₄)

PROPERTY	TEMPERATURE				PRESSURE			REF
	°C	°K	°F	°R	psia	atm	mm of Hg	
Melting Point	-184.0	89.2	-299.0	160.7				1
Boiling Point	-128.0	145.2	-198.4	261.3				1
Triple Point								
Critical Temp.	- 45.5	227.7	- 49.9	409.8				1
Critical Press.					542	36.9		1
Mol. Wt.	88.01							1
Heat of Vaporization	32.58 cal/g or 58.64 Btu/lb at B.P.							
Heat of Fusion								

Table IX-20-1.1
SOME VALUES OF THE GAS CONSTANT, R, FOR FREON-14
(See also Conversion Tables, Section I)

TEMPERATURE IN °K				
Pressure	atm	kg/cm ²	mm of Hg	lb/in ²
Density				
g/cm ³	0.932357	0.963336	708.591	13.7020
mole/cm ³	82.0567	84.7832	62363.1	1205.91
mole/liter	0.0820544	0.0847809	62.3613	1.20587
lb/ft ³	0.0149348	0.0154310	11.3504	0.219482
lb/mole/ft ³	1.31441	1.35808	998.952	19.3166
TEMPERATURE IN °R				
Pressure	atm	kg/cm ²	mm of Hg	lb/in ²
Density				
g/cm ³	0.517976	0.535187	393.662	7.61220
mole/cm ³	45.5871	47.1018	34646. 2	669.950
mole/liter	0.0455858	0.0471005	34.6452	0.669928
lb/ft ³	0.00829710	0.00857276	6.30579	0.121934
lb/mole/ft ³	0.730228	0.754489	554.973	10.7314

Table IX-20-2
VAPOR PRESSURE OF FREON-14 (Ref. 2)

TEMPERATURE		VAPOR PRESSURE	TEMPERATURE		VAPOR PRESSURE
^o K	^o R	psia	^o K	^o R	psia
127.59	229.67	3.463	183.15	329.67	117.4
133.15	239.67	5.726	188.70	339.67	147.49
138.70	249.67	9.050	194.26	349.67	182.8
144.26	259.67	13.75	199.82	359.67	223.8
147.82	269.67	20.17	205.37	369.67	271.2
155.37	279.67	28.69	210.93	379.67	325.7
160.93	289.67	39.72	216.48	389.67	388.4
166.48	299.67	53.67	222.04	399.67	460.6
172.04	309.67	70.97	227.04	408.67	535.8
177.59	319.67	92.07			

(See Figure IX-20-1)

Table IX-20-3
DENSITY OF SATURATED LIQUID FREON-14
(Ref. 2)

TEMPERATURE		DENSITY	TEMPERATURE		DENSITY
°K	°R	lb/ft ³	°K	°R	lb/ft ³
127.59	229.67	107.78	183.15	329.67	87.08
133.15	239.67	106.0	188.70	339.67	84.45
138.70	249.67	104.17	194.26	349.67	81.63
144.26	259.67	102.29	199.82	359.67	78.57
149.82	269.67	100.35	205.39	369.67	75.17
155.37	279.67	98.35	210.93	379.67	71.30
160.93	289.67	96.28	216.48	389.67	66.63
166.48	299.67	94.14	222.04	399.67	60.31
172.04	309.67	91.90	227.04	408.67	47.94
177.59	319.67	89.55			

(See Figure IX-20-2)

Table IX-20-4
DENSITY OF SATURATED VAPOR OF FREON-14 (Ref. 2)

TEMPERATURE		DENSITY	TEMPERATURE		DENSITY
°K	°R	lb/ft ³	°K	°R	lb/ft ³
127.59	229.67	0.1250	183.15	329.67	3.471
133.15	239.67	0.1991	188.70	339.67	4.387
138.70	249.67	0.3042	194.26	349.67	5.507
144.26	259.67	0.4482	199.82	359.67	6.890
149.82	269.67	0.6402	205.37	369.67	8.623
155.37	279.67	0.8903	210.93	379.67	10.86
160.93	289.67	1.210	216.48	389.67	13.93
166.48	299.67	1.611	222.04	399.67	18.73
172.04	309.67	2.109	227.04	408.67	30.32
177.59	319.67	2.722			

(See Figure IX-20-3)

Table IX-20-5
 VISCOSITY OF FREON-14
 (Ref. 4)

TEMPERATURE		ABSOLUTE VISCOSITY
$^{\circ}\text{K}$	$^{\circ}\text{R}$	micropoises
100	180	62.4
200	360	123.9
300	540	176.7
400	720	222.2
500	900	262.7
600	1080	299.6

(See Figure IX-20-4)

Table IX-20-6
 HEAT CAPACITY OF FREON-14
 (Ref. 3)

TEMPERATURE		HEAT CAPACITY
$^{\circ}\text{K}$	$^{\circ}\text{R}$	Btu/lb- $^{\circ}\text{R}$
100	180	0.09431
150	270	0.1092
200	360	0.1286
250	450	0.1485
298.16	336.7	0.1660
300	540	0.1667
400	720	0.1969
500	900	0.2195
600	1080	0.2360

(See Figure IX-20-5)

Table IX-20-7
THERMAL CONDUCTIVITY
OF GASEOUS FREON-14
(Ref. 4)

TEMPERATURE		THERMAL CONDUCTIVITY
$^{\circ}\text{K}$	$^{\circ}\text{R}$	Btu/hr-ft- $^{\circ}\text{R}$
100	180	0.00203
200	360	0.00540
300	540	0.00990
400	720	0.0147
500	900	0.0193
600	1080	0.0237

(See Figure IX-20-6)

)

)

)

)

)

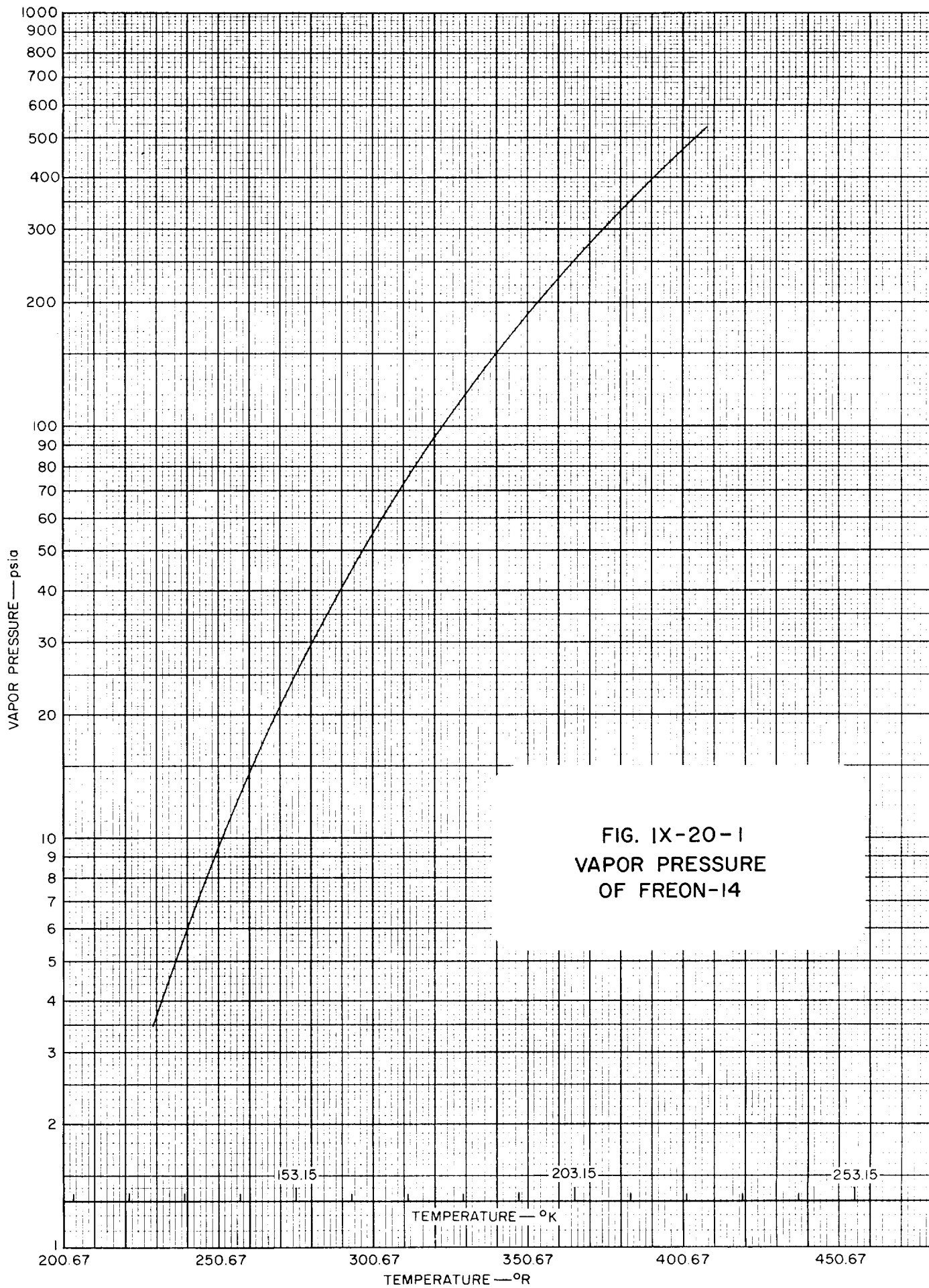
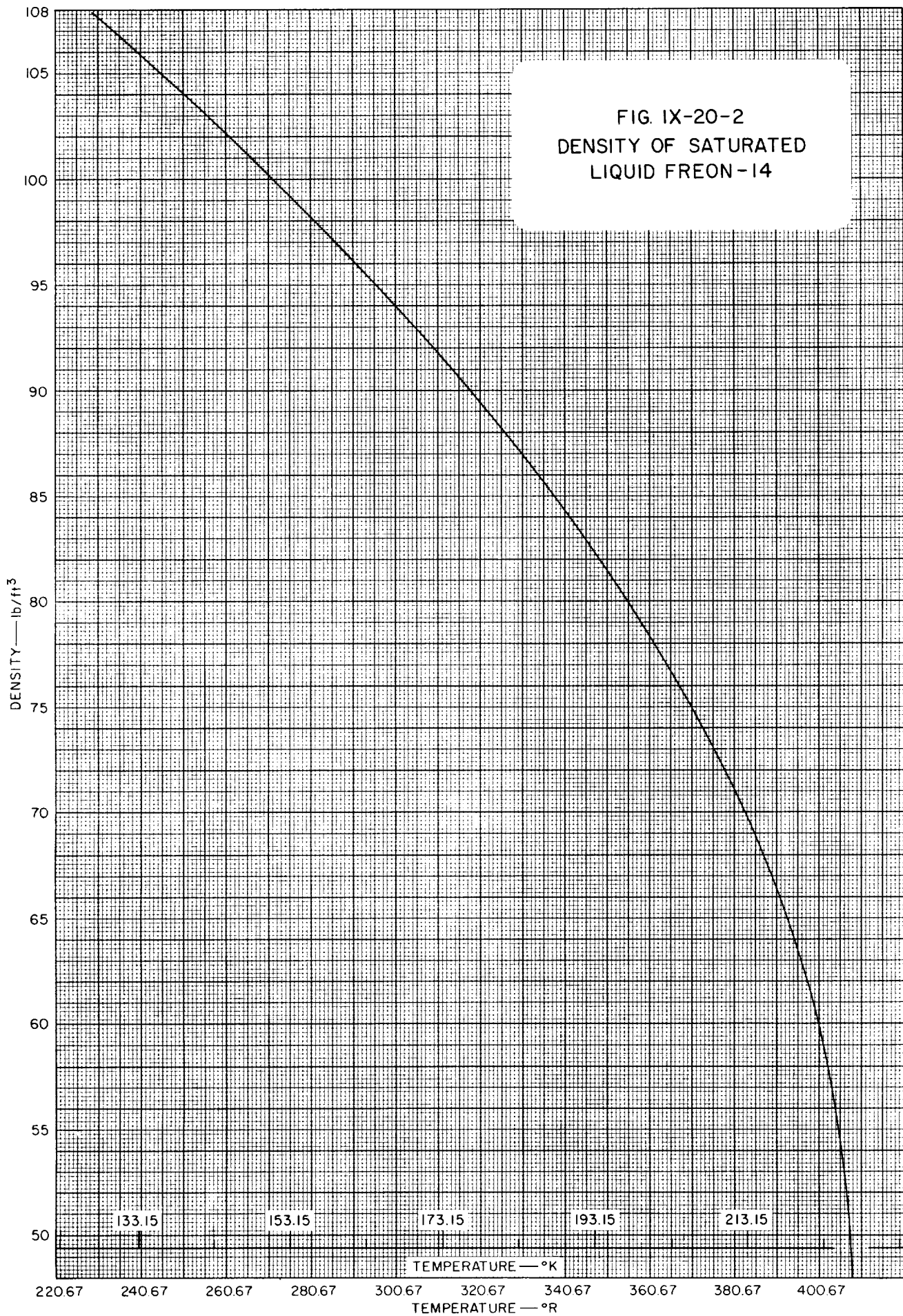
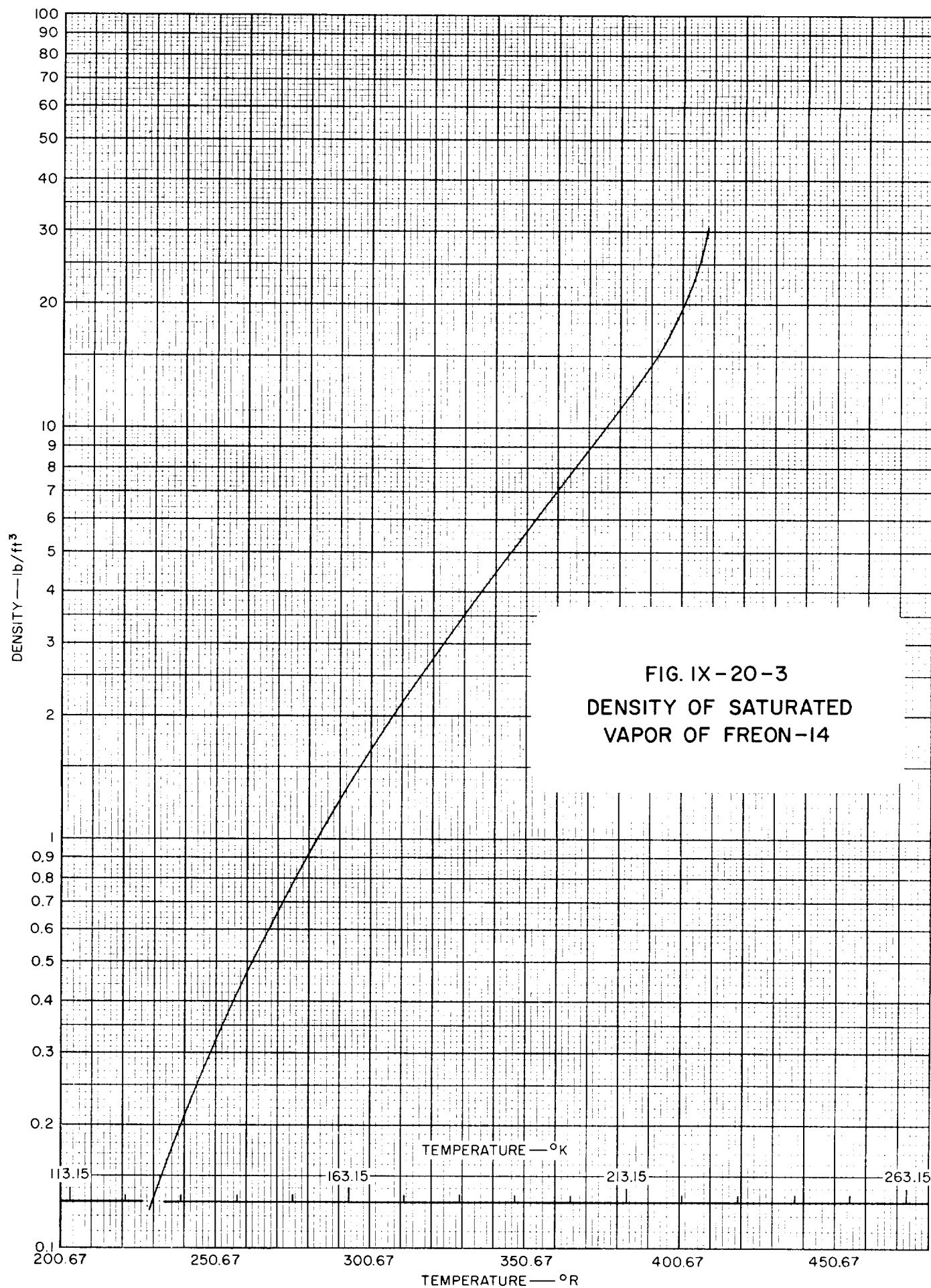
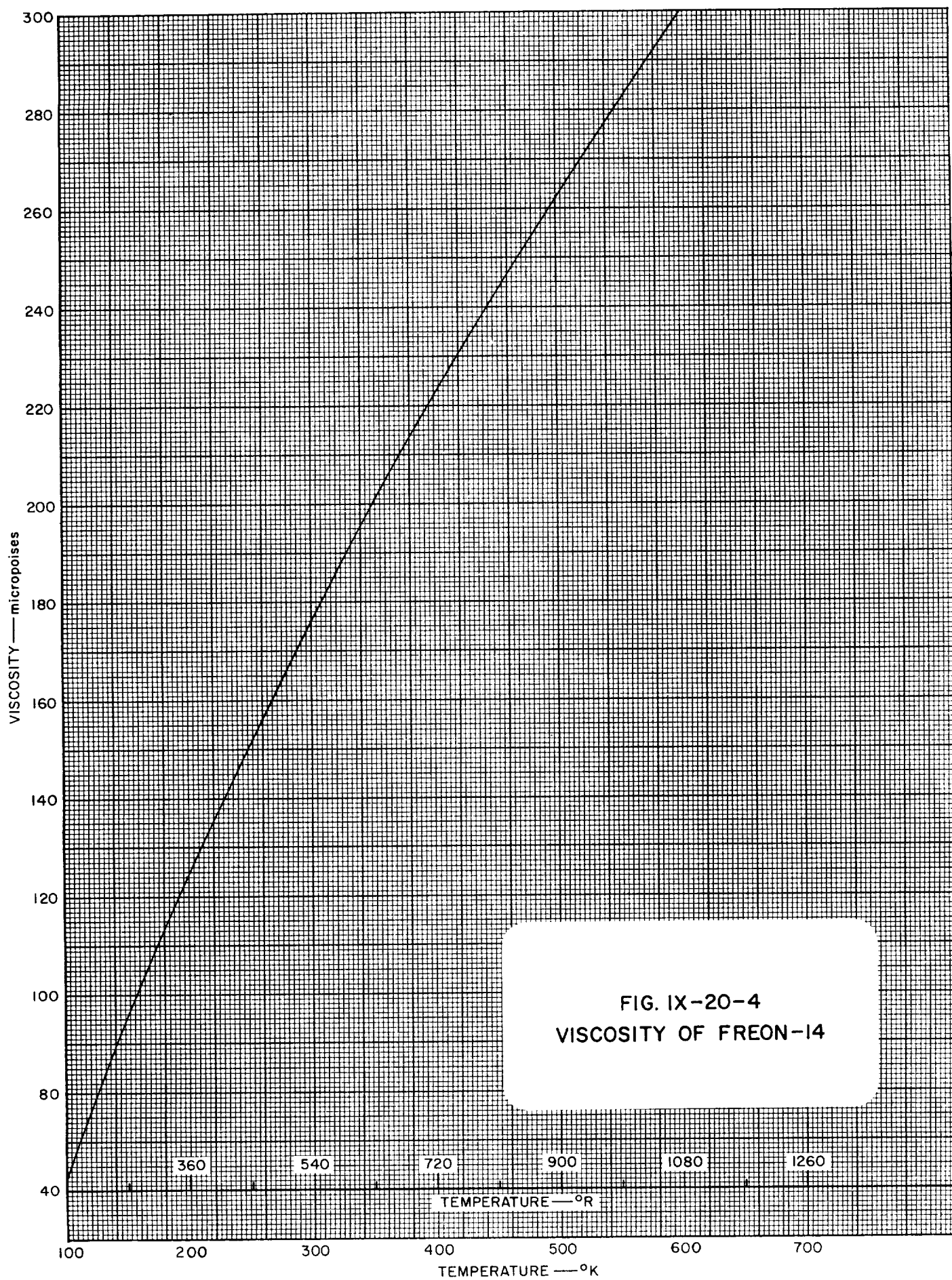


FIG. IX-20-2
DENSITY OF SATURATED
LIQUID FREON-14







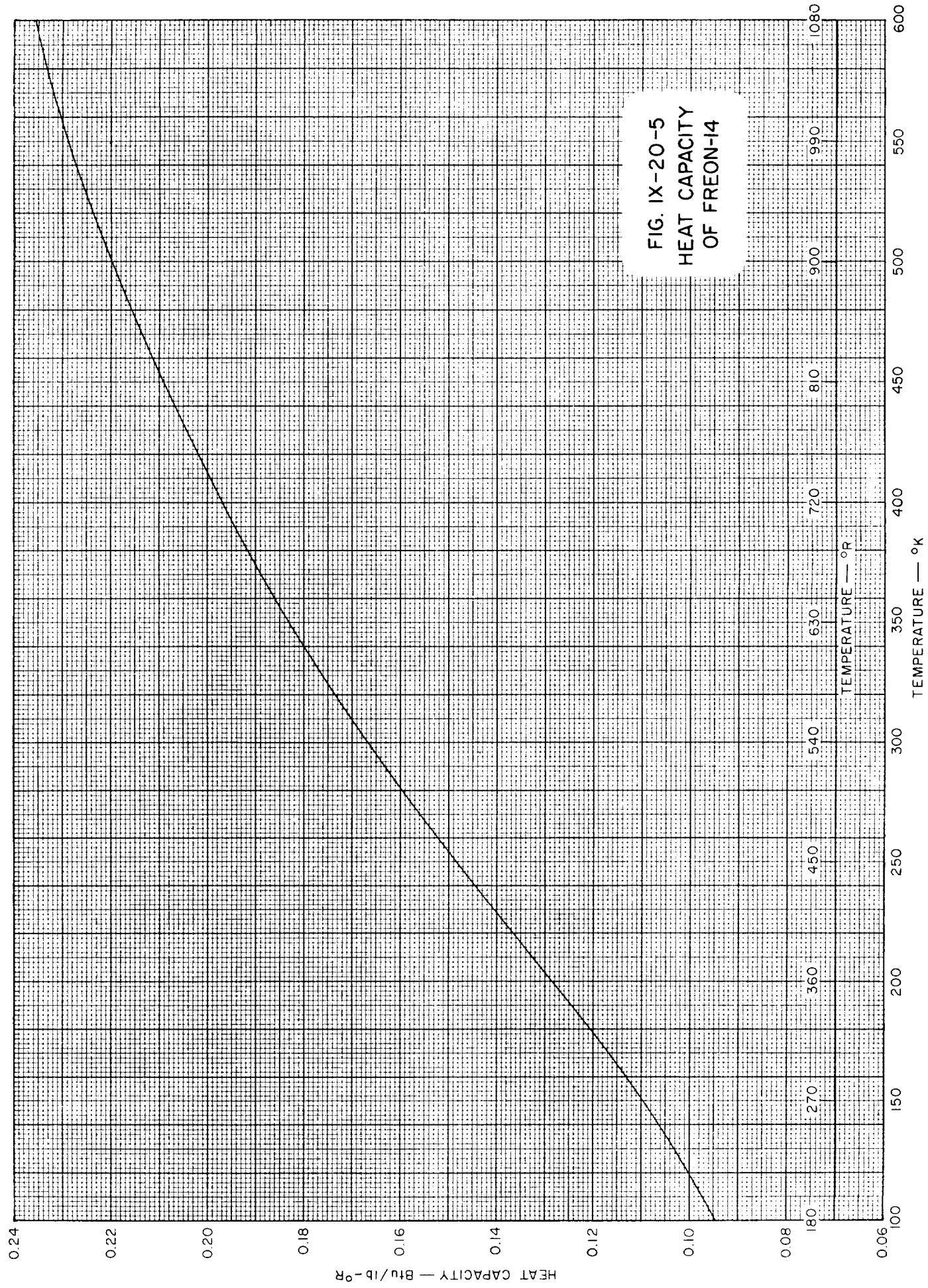
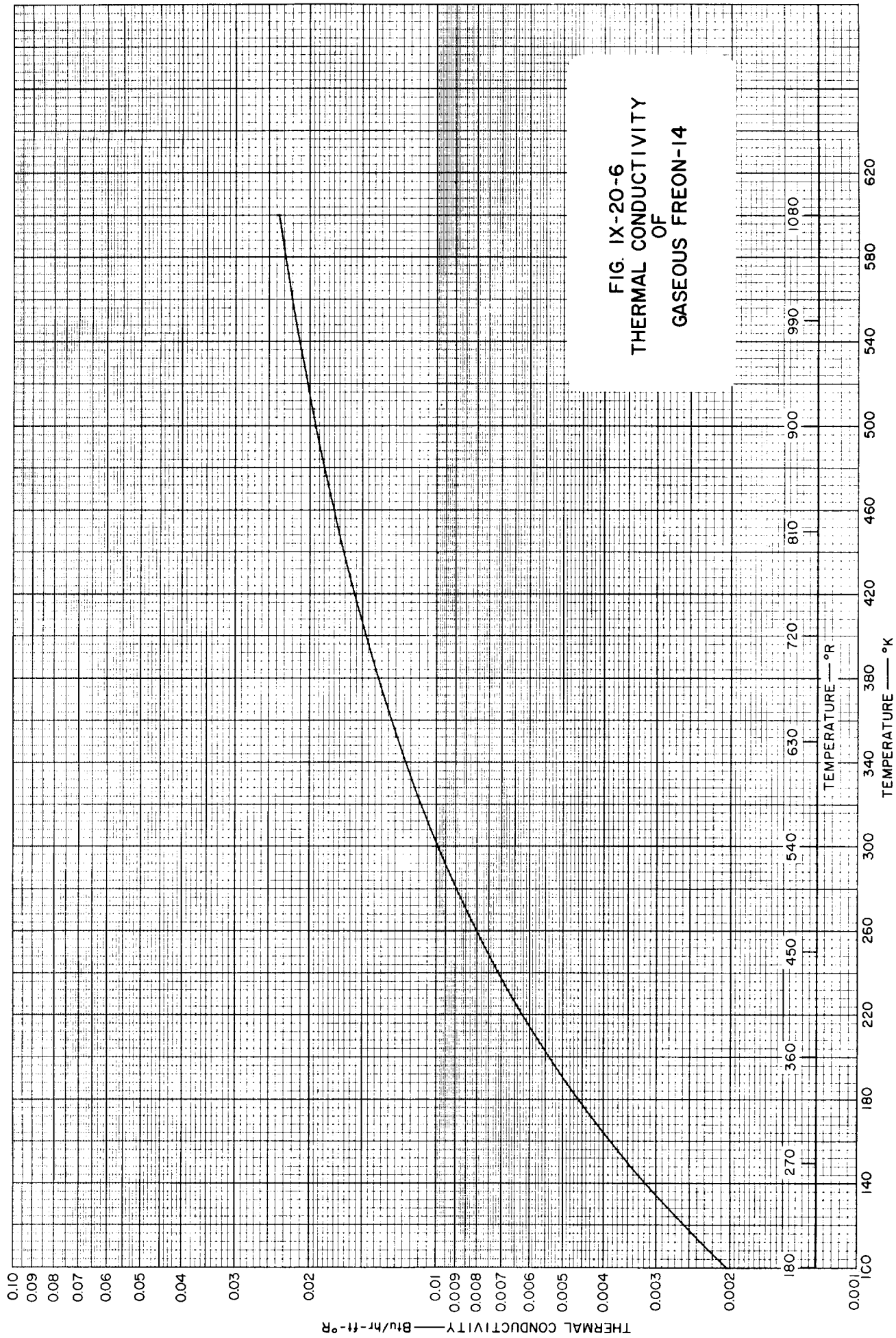


FIG. IX-20-5
HEAT CAPACITY
OF FREON-14



IX-20 FREON-14 REFERENCES

1. Du Pont de Nemours, E. I., & Co., *Technical Bulletin B-2*.
2. Du Pont de Nemours, E. I., & Co., *Technical Bulletin T-14*.
3. Gelles, E., and Pitzer, K. S., *J. Am. Chem. Soc.*, **75**, 5259 (1953).
4. Svehla, R. A., *NASA TR R-132*, 1962.

)

)

)

)

)

X PRESSURE VESSELS

Table of Contents

<u>Section-Part</u>	<u>Title</u>	<u>Section-Part-Page</u>
X-0	List of Figures	X-0.1
X-1	Introduction	X-1.1
X-2	Spherical Vessels	X-2.1
X-3	Cylindrical Vessels	X-3.1
X-4	Design Weights of Pressure Vessels	X-4.1
X-5	Pressure Vessel References	X-5.1

X-0 LIST OF FIGURES

<u>Section-Part.Figure</u>	<u>Title</u>	<u>Section-Part.Page</u>
X-4-1	Surface Area of Spherical Tanks	X-4.5
X-4-2	Surface Area of Oblate Spheroidal Tanks	X-4.6
X-4-3	Volume of Spherical Tanks	X-4.7
X-4-4	Volume of Oblate Spheroidal Tanks	X-4.8
X-4-5	Spherical Tank Weights for Various Pressures	X-4.9

X-1 INTRODUCTION

Pressure vessels for use in spacecraft must be as light as possible; consequently, the membrane stresses at working pressures are designed to be as high as possible and usually approach the material's yield stress. Static fatigue may occur under these conditions because of inherent stress concentrations and because localized points may be subjected to high stresses for extended periods of time. Fatigue may also occur because some materials show a marked reduction in strength under low-cycle, high-stress loading.

The yield point of biaxially stressed material rises, but the strain at which fracture occurs is lowered. Thus, since this is the type of loading common to high-pressure vessels, the materials used for their construction exhibit lowered ductility, especially at very low temperatures. Care must be exercised in the selection of material for constructing low temperature tanks because some metals exhibit a transition temperature below which their energy absorption is sharply reduced.

Fusion welding appears to be the most practical method of fabricating pressure vessels. Uniform, high quality welds must be produced because they will be under considerable tension. Unfortunately, the strengths of welds must be obtained by a statistical series of tests or approximated by nondestructive techniques.

Stress concentrations are common in any type of fabricated construction subject to loadings. Regions of highly localized stresses exist in pressure vessels where line fittings join the shell, at knuckle regions where the head joins the shell, and at all welds or joints. In general, stress concentrations cannot be computed accurately.

The strength of pressure vessels is severely influenced by thermal stresses; aerodynamic heating, cryogenic fuel boil-off, and sloshing of cold liquids on warm walls are examples of the kind of thermal stresses to which pressure vessels may be subjected. It is not uncommon to encounter conditions in which a small amount of a liquid may splash on the

X-1.1

middle of a large hot plate and produce circumferential and radial tensile stresses of magnitude

$$S = \frac{rE \Delta T}{1 - Z}$$

where r = tank radius, E = Young's modulus, ΔT = temperature difference, and Z = Poisson's ratio. When these stresses are combined with pressure stresses, the yield stress of the material of construction may be exceeded.

Materials of Construction

The optimum material for construction of a pressure vessel for a particular application is determined largely by factors such as the pressure vessel shape, design details, supports, weld efficiencies, operating temperature, weight limitations, maximum pressure loading, etc. Although accurate material evaluation tests to permit selection of the best material of construction have not been devised, it is generally agreed that the most important properties are: (a) yield-to-ultimate ratio and ductility (uniaxial); (b) high stress-low cycle fatigue strength; (c) fusion weld strength; (d) energy absorption.

Fatigue strength is extremely important for pressure vessels which must have a high degree of reliability for long periods of time (such as for pressurized-gas storage in spacecrafts). Further, materials for use in highly reliable pressure vessels should have Charpy keyhole notch energy absorptions of more than 10 ft-lb over the temperature region expected to be encountered.

Material which can be welded efficiently should always be used. In general, welding reduces the mechanical properties of the tank material adjacent to the welds, especially if the material has initially been heat-treated or cold-worked. An increase in the thickness of material in the vicinity of welds may compensate for loss of strength and avoid weak regions; welds in some newer type materials strengthen on aging, and small tanks of most materials may be treated after welding.

Design Considerations

The design of vessels for storing pressurized gases takes into consideration the usual details applicable to any highly stressed structure. Of course, the exact details of design are governed by each individual

application, and the greater attention must be given to static factors and material selection because the design details are not ideal. In an early stage of design, efforts should be made to reduce the possibility of occurrence of regions of high stress, for example, avoiding sudden changes of geometry, and spot welds or fillet welds. Since the maximum stresses in the head of a pressure vessel occur in the knuckle region close to the junction of the head and shell, a smooth transition should be provided and welding in this region should be avoided. Uniform thickness of material at welds should be required and, whenever possible, the number of welds or bosses for threaded fittings should be kept at a minimum. Spherical tanks with continuous welds at the equator are best.

The fatigue strength of the material must be sufficient to permit several operational pressure cycles for test and a few to spare; the maximum number of cycles should be taken into consideration at the time of design, and provision should be made to insure discarding of overworked vessels.

Stresses Due to Steady-State Temperature and Internal Pressure

Vessels to withstand high pressures are usually designed on the basis that the internal pressure leads to elastic failure at the inside surface. However, thermal gradients cause stresses which may easily achieve levels comparable to or greater than the pressurization stresses. Thus, it is important to take into account thermal and pressurization stresses simultaneously in the design of pressure vessels.

The behavior of spherical and cylindrical vessels stressed by pressure and temperature when the stresses are everywhere below the elastic limit is well known,¹ but it is not always possible to maintain stresses below the elastic limit. The behavior of vessels subjected to both pressure and temperature stresses when the elastic limit has been exceeded was studied by Whalley.²

The equations given below are based on the following assumptions:²

- (1) A brittle material is perfectly elastic up to its ultimate strength. When it fractures, according to the maximum principal stress theory, it does so without appreciable yielding.
- (2) A ductile material is perfectly elastic up to the yield point; thereafter it yields at constant maximum shear stress (Tresca theory); no strain hardening occurs.

- (3) The temperature is low enough so that creep is negligible.
- (4) Temperature and stress have no effect on elastic moduli and the yield point; the coefficient of thermal expansion is negligible.
- (5) The Bauschinger effect does not occur (reduction in yield point due to previous plastic flow in the reverse direction).
- (6) The strains are small compared with the dimensions of the vessel.
- (7) Important stress raisers are absent.

X-2 SPHERICAL VESSELS

Failure of Brittle Material in Spherical Vessels

In a symmetrical vessel, the maximum principal stress is the tangential stress, and failure of a vessel made of brittle material will occur when the tangential stress equals the fracture stress, σ_μ . Thus, by equating the right-hand side of Equation (2) to the fracture stress, it becomes obvious that the pressure at which failure occurs is dependent on the thermal stresses; however, the thermal stresses may oppose the pressure stresses (increasing failure pressure) or reinforce and decrease the failure pressure. Two values of σ_μ exist: one positive, indicating tensile failure, and one negative, indicating compressive failure; the tensile failure is the only one of concern in spacecraft design.

Failure of Ductile Material in Spherical Vessels

Yielding can occur at any position within the walls of a pressure vessel, and this is determined by pressure stresses and thermal gradients. In the absence of temperature gradients,

$$\frac{\Delta P_y}{\pm \sigma_y} = \frac{k^3 - 1}{(3/2)k^3} \quad (1)$$

where ΔP_y is the yield pressure difference and σ_μ is the yield stress.

Completely Elastic Vessels

If the entire vessel is in the elastic region, the principal stresses are given by:

$$\begin{aligned} \text{radial stress} = & - \frac{P_i}{k^3 - 1} \left(\frac{b^3}{r^3} - 1 \right) - \frac{P_0 k^3}{k^3 - 1} \left(1 - \frac{a^3}{r^3} \right) \\ & + \frac{2\alpha E}{1 - \nu} \left[\frac{1 - a^3/r^3}{b^3 - a^3} \int_a^b T r^2 dr - \frac{1}{r^3} \int_a^r T r^2 dr \right] \end{aligned} \quad (2)$$

$$\begin{aligned} \text{tangential stress} = \sigma_t = & \frac{P_i}{k^3 - 1} \left(\frac{b^3}{2r^3} + 1 \right) - \frac{P_o k^3}{k^3 - 1} \left(1 + \frac{a^3}{2r^3} \right) \\ & + \frac{2\alpha E}{1 - Z} \left[\frac{1 + a^3/2r^3}{b^3 - a^3} \int_a^b T r^2 dr + \frac{1}{2r^3} \int_a^r T r^2 dr - \frac{1}{2} T \right] \end{aligned} \quad (3)$$

where

- a = inside radius, in.
- b = outside radius, in.
- E = Young's modulus, lb/in.²
- k = b/a
- P_i = inside pressure, lb/in.²
- P_o = outside pressure, lb/in.²
- α = coefficient of thermal expansion
- T = temperature at radius r
- Z = Poisson's ratio

When temperature gradients are present, three separate treatments are required to compute the yield pressure, ΔP_y : (a) The value of ΔP_y for yielding at $r = a$ is numerically less than its value at all other radii, i.e., if for all values of r

$$\pm \frac{3\alpha E}{(1 - Z)\sigma_y} \left[\frac{1}{r^3 - a^3} \int_a^r T r^2 dr - \frac{1}{3} \frac{r^3 T - a^3 T_i}{r^3 - a^3} \right] < 1 \quad (4)$$

Then yielding will begin at the inside surface of the pressure vessel and the yield pressure is given by:

$$\pm \frac{\Delta P_y}{\sigma_y} = \frac{k^3 - 1}{(3/2)k^3} \left[1 \mp \frac{3\alpha E}{(1 - Z)\sigma_y} \left(\frac{1}{b^3 - a^3} \int_a^b T r^2 dr - \frac{1}{3} T_i \right) \right] \quad (5)$$

(b) The value of Δp_y for yielding at $r = b$ is numerically less than all other values of r ; i.e., if for all values of r

$$\pm \frac{3\alpha E}{(1 - \nu)\sigma_y} \left[\frac{1}{b^3 - r^3} \int_r^b T r^2 dr - \frac{1}{3} \frac{b^3 T_0 - r^3 T}{b^3 - r^3} \right] > 1 \quad (6)$$

then yielding will begin at the outer surface of the pressure vessel, and the yield pressure is given by

$$\pm \frac{\Delta p_y}{\sigma_y} = \frac{k^3 - 1}{3/2} \left[1 \mp \frac{3\alpha E}{(1 - \nu)\sigma_y} \left(\frac{1}{b^3 - a^3} \int_a^b T r^2 dr - \frac{1}{3} T_0 \right) \right] \quad (7)$$

(c) If neither of the two conditions are met, yielding will occur between the inside and outside walls of the vessel at radius r , and a yield pressure given by:

$$\pm \frac{\Delta p_y}{\sigma_y} = \frac{k^3 - 1}{(3/2)b^3/r_y^3} \left[1 \mp \frac{3\alpha E}{(1 - \nu)\sigma_y} \left(\frac{a^3/r_y^3}{b^3 - a^3} \int_a^b T r^2 dr + \frac{1}{r_y^3} \int_a^{r_y} T r^2 dr - \frac{1}{3} T_y \right) \right] \quad (8)$$

where T_y is the temperature at r_y . The value of r_y obtained by Equation (8) is that at which the difference between tangential and radial stresses is at a maximum.

Partially Plastic Spherical Vessels

Plastic flow occurs when the stresses in a vessel made of ductile material exceed the yield point, and the stresses will tend to be relieved or readjusted. Under these conditions, the pressure required to cause the walls to become plastic is independent of thermal stress. The original reference should be consulted for additional details (Ref. 2).

)

)

)

)

)

X-3 CYLINDRICAL VESSELS

Completely Elastic Vessels

In the elastic region, the principal stresses are given by:

$$\begin{aligned} \sigma_r = & -\frac{P_i}{k^2 - 1} \left(\frac{b^2}{r^2} - 1 \right) - \frac{P_0 k^2}{k^2 - 1} \left(1 - \frac{a^2}{r^2} \right) \\ & + \frac{\alpha E}{1 - Z} \left[\frac{1 - a^2/r^2}{b^2 - a^2} \int_a^b T r dr - \frac{1}{r^2} \int_a^r T r dr \right] \end{aligned} \quad (9)$$

$$\begin{aligned} \sigma_t = & \frac{P_i}{k^2 - 1} \left(\frac{b^2}{r^2} + 1 \right) - \frac{P_0 k^2}{k^2 - 1} \left(1 + \frac{a^2}{r^2} \right) \\ & + \frac{\alpha E}{1 - Z} \left[\frac{1 + a^2/r^2}{b^2 - a^2} \int_a^b T r dr + \frac{1}{r^2} \int_a^r T r dr - T \right] \end{aligned} \quad (10)$$

Failure of Brittle Material in Cylindrical Vessels

There is no difference in the mechanism of failure for brittle materials in cylindrical vessels in comparison with spherical vessels.

Failure of Ductile Material in Cylindrical Vessels

Failure occurs, in general, when the tensile yield stress is reached:

$$\pm \sigma_y = \frac{2\Delta P}{k^2 - 1} \frac{b^2}{r^2} + \frac{2\alpha E}{1 - Z} \left[\frac{a^2/r^2}{b^2 - a^2} \int_a^b T r dr + \frac{1}{r^2} \int_a^r T r dr - \frac{1}{2} T \right] \quad (11)$$

When temperature and pressure stresses are present, the yield pressure can be found by the following:

(a) The value of ΔP_y for yielding at $r = a$ is numerically less than its value at all other radii, i.e., if for all values of r

$$\pm \frac{2\alpha E}{(1-Z)\sigma_y} \left[\frac{1}{r^2 - a^2} \int_a^r T r dr - \frac{1}{2} \frac{r^2 T - a^2 T_i}{r^2 - a^2} \right] < 1 \quad (12)$$

then yielding will begin at the inside surface of the pressure vessel and the yield pressure is given by:

$$\frac{\Delta P_y}{\pm \sigma_y} = \frac{k^2 - 1}{2k^2} \left[1 \mp \frac{2\alpha E}{(1-Z)\sigma_y} \left(\frac{1}{b^2 - a^2} \int_a^b T r dr - \frac{1}{2} T_i \right) \right] \quad (13)$$

(b) The value of ΔP_y for yielding at $r = b$ is numerically less than at all other values of r ; i.e., if for all values of r

$$\pm \frac{2\alpha E}{(1-Z)\sigma_y} \left[\frac{1}{b^2 - r^2} \int_r^b T r dr - \frac{1}{2} \frac{b^2 T_0 - r^2 T}{b^2 - r^2} \right] > 1 \quad (14)$$

then yielding will begin at the outer surface of the pressure vessel, and the yield pressure is given by:

$$\frac{\Delta P_y}{\pm \sigma_y} = \frac{(k^2 - 1)}{2} \left[1 \mp \frac{2\alpha E}{(1-Z)\sigma_y} \left(\frac{1}{b^2 - a^2} \int_a^b T r dr - \frac{1}{2} T_0 \right) \right] \quad (15)$$

(c) If neither of the two conditions are met, yielding will occur inside the wall at radius r_y and at a yield pressure given by:

$$\frac{\Delta P_y}{\pm \sigma_y} = \frac{k^2 - 1}{2b^2/r_y^2} \left[1 \mp \frac{2\alpha E}{(1-Z)\sigma_y} \left(\frac{a^2/r_y^2}{b^2 - a^2} \int_a^b T r dr - \frac{1}{r_y^2} \int_a^{r_y} T r dr - \frac{1}{2} T_y \right) \right] \quad (16)$$

where T_y is the temperature at r_y ; at this value of r_y , the difference between the tangential and radial stresses is at a maximum in Equation (16).

Stress in the Head of a Pressure Vessel

Most theoretical treatments of stresses in the walls of pressure vessels consider the walls as uniform membranes. However, studies of the stresses occurring in and near the head of pressure vessels indicate that the bending couples predominate and, thus, it is improper to apply equations developed by treatment of walls as membranes. The local effects of the reactions set up at the junction of the head and cylinder appear to be the result of stresses being reflected as uniformly distributed shearing forces and bending couples. The effect at any point may thus be computed as a resultant by the superposition method (see Ref. 3).

)

)

)

)

)

X-4 DESIGN WEIGHTS OF PRESSURE VESSELS

The minimum weight of a pressure vessel depends upon the permissible level of stress in which the material of construction is to operate. In general, the stress level at proof pressure is used for development of equations and formulae for computing minimum weight. The actual weight of a vessel is determined by the number and thickness of bosses, the required thickness at butt-welded joints to maintain strength, and, among other such considerations, safety factors and available techniques for fabrication.

Spherical Vessels

The thickness of the vessel walls is given by:

$$t = \frac{Pd}{4\sigma - P}$$

where d = inside diameter and σ is the maximum stress level for the material; the weight-to-volume ratio is:

$$\frac{W}{V} = \frac{96\rho P\sigma^2}{(4\sigma - P)^3}$$

where ρ is the density of the material.

Cylindrical Shells

The wall thickness of the shell of a cylindrical pressure vessel at some distance away from the ends must be:

$$t = \frac{Pd}{2\sigma - P}$$

and the weight-to-volume ratio is

$$\frac{W}{V} = 4(d + t)Pt/d^2$$

X-4.1

Elliptical Ends

The maximum stresses in the knuckle region and the dome region are given by:

(1) Knuckle region

The maximum stress is

$$\sigma = KPa/t_1$$

where K is a stress factor for an elliptical ratio e , P = differential pressure, and a = inside radius.

(2) Dome region

The maximum stress in this region is

$$\sigma = \frac{PR}{2t} = \frac{ePa}{2t_2}$$

Solving for $t_1 + t_2$ and taking an average value, there is found an effective end thickness:

$$t_e = \frac{Pa}{2\sigma} \left(K + \frac{e}{2} \right)$$

and the weight to volume ratio is:

$$\frac{W}{V} = \frac{3}{8} \frac{\rho P}{\sigma} \left(K + \frac{e}{2} \right) L$$

where

$$L = 2e + \frac{1}{\sqrt{e^2 - 1}} \ln \left(\frac{e + \sqrt{e^2 - 1}}{e - \sqrt{e^2 - 1}} \right)$$

Fiberglass Pressure Vessels

Reinforced plastic pressure vessels have several advantages over those of metal:

- (1) They are lighter than metal vessels of the same size
- (2) They can be made in a greater variety of shapes than metal tanks
- (3) They are, generally, noncorrodable.

On the other hand, they have certain limitations and disadvantages:

- (1) They tend to be permeable to gasses at high pressures
- (2) Without close control, the heterogeneous nature of the material of construction may lead to difficulties
- (3) Leakage may occur at points where metal bosses must be inserted
- (4) Pressure cycling leads to creep, volumetric expansion, distortion, and lowering of burst strength.
- (5) The material is subject to fatigue.

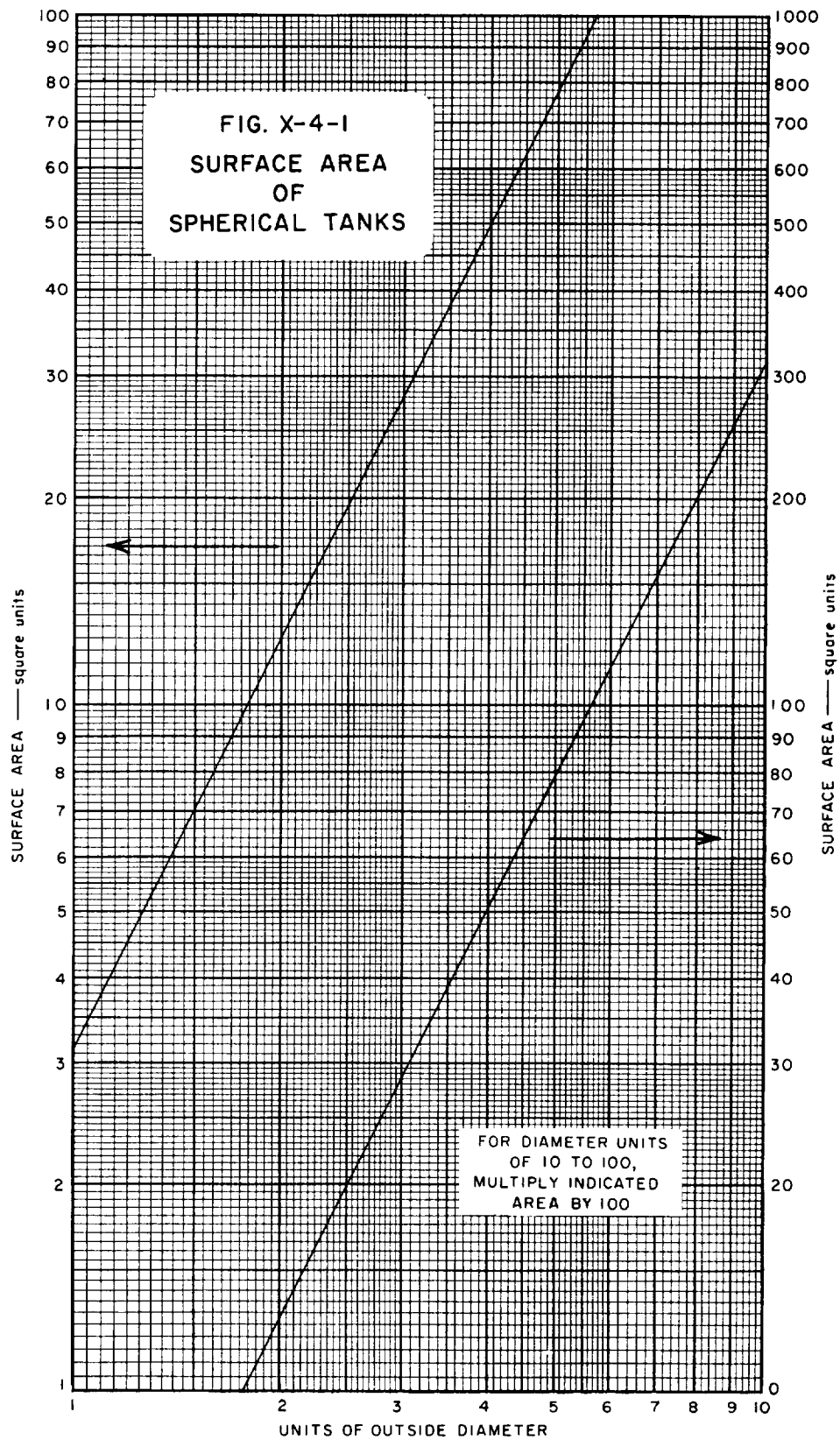
)

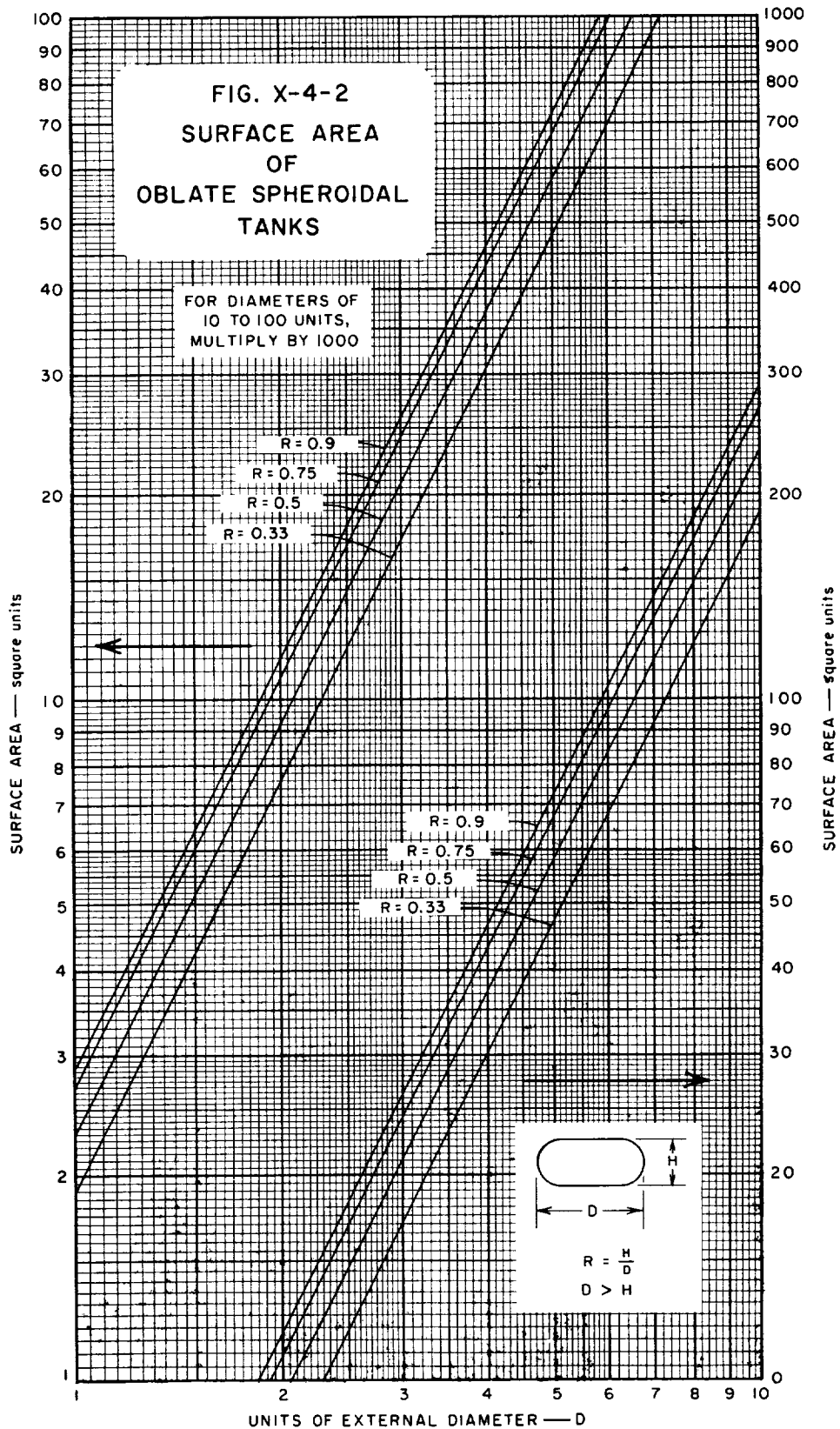
)

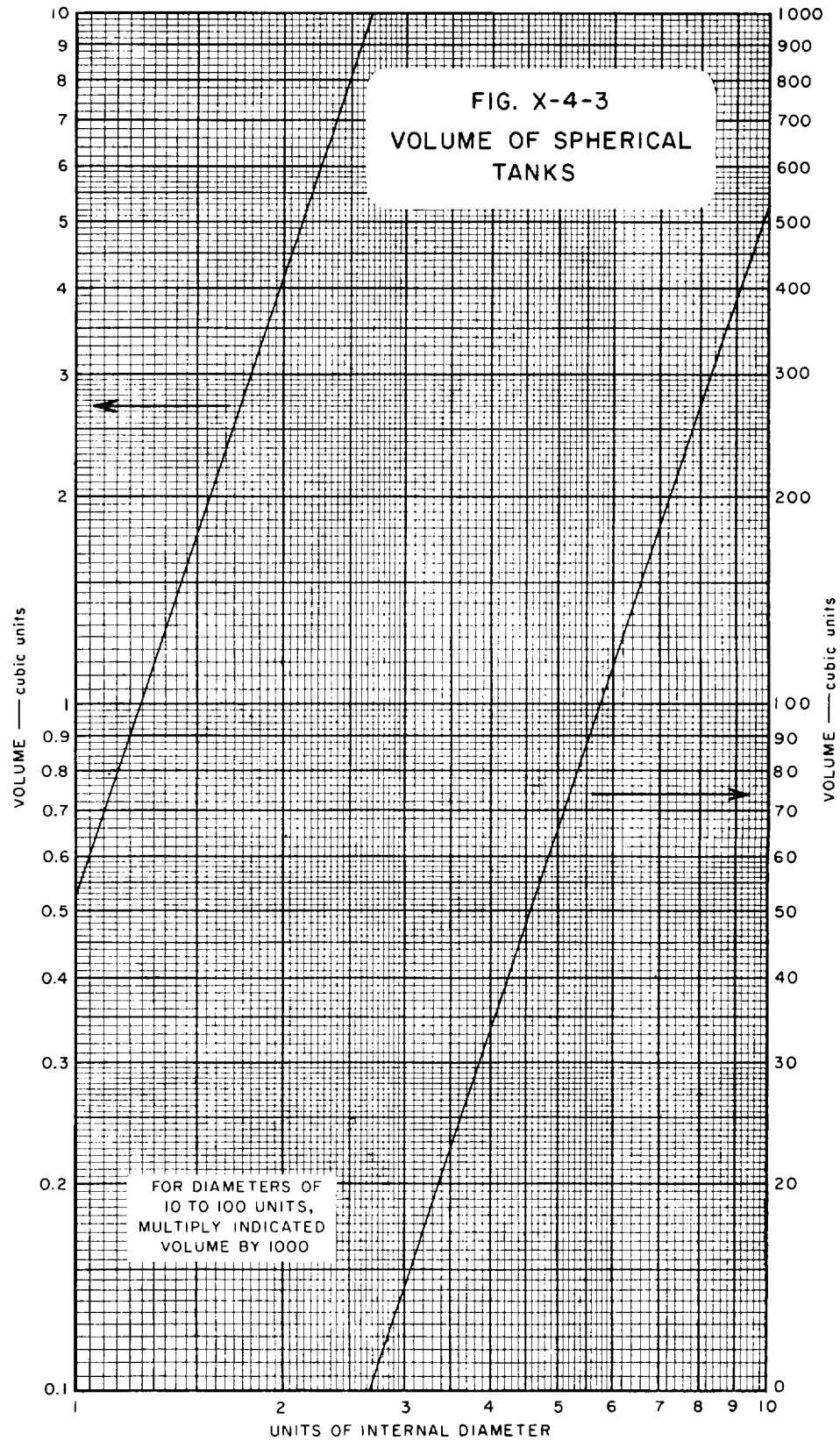
)

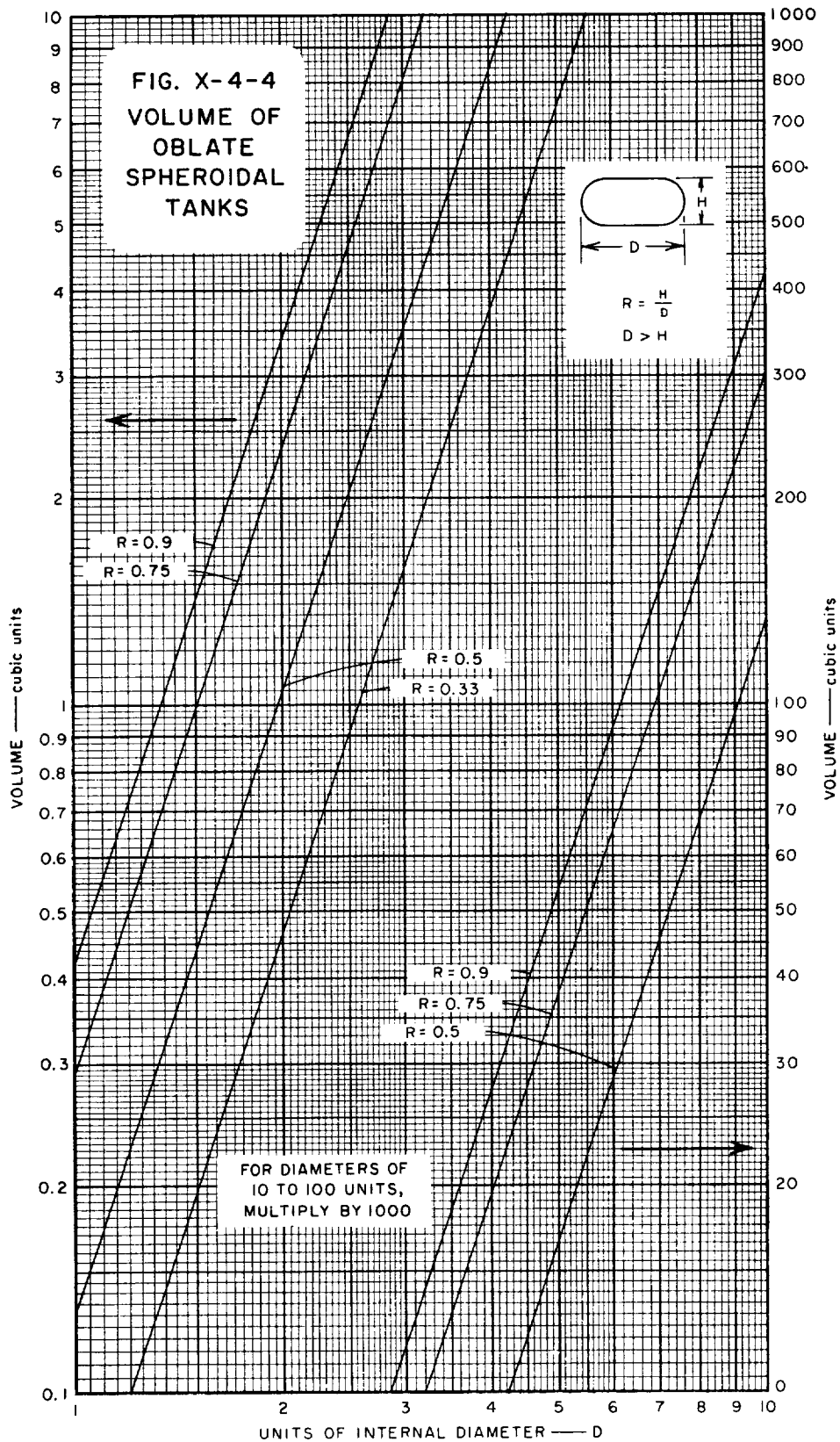
)

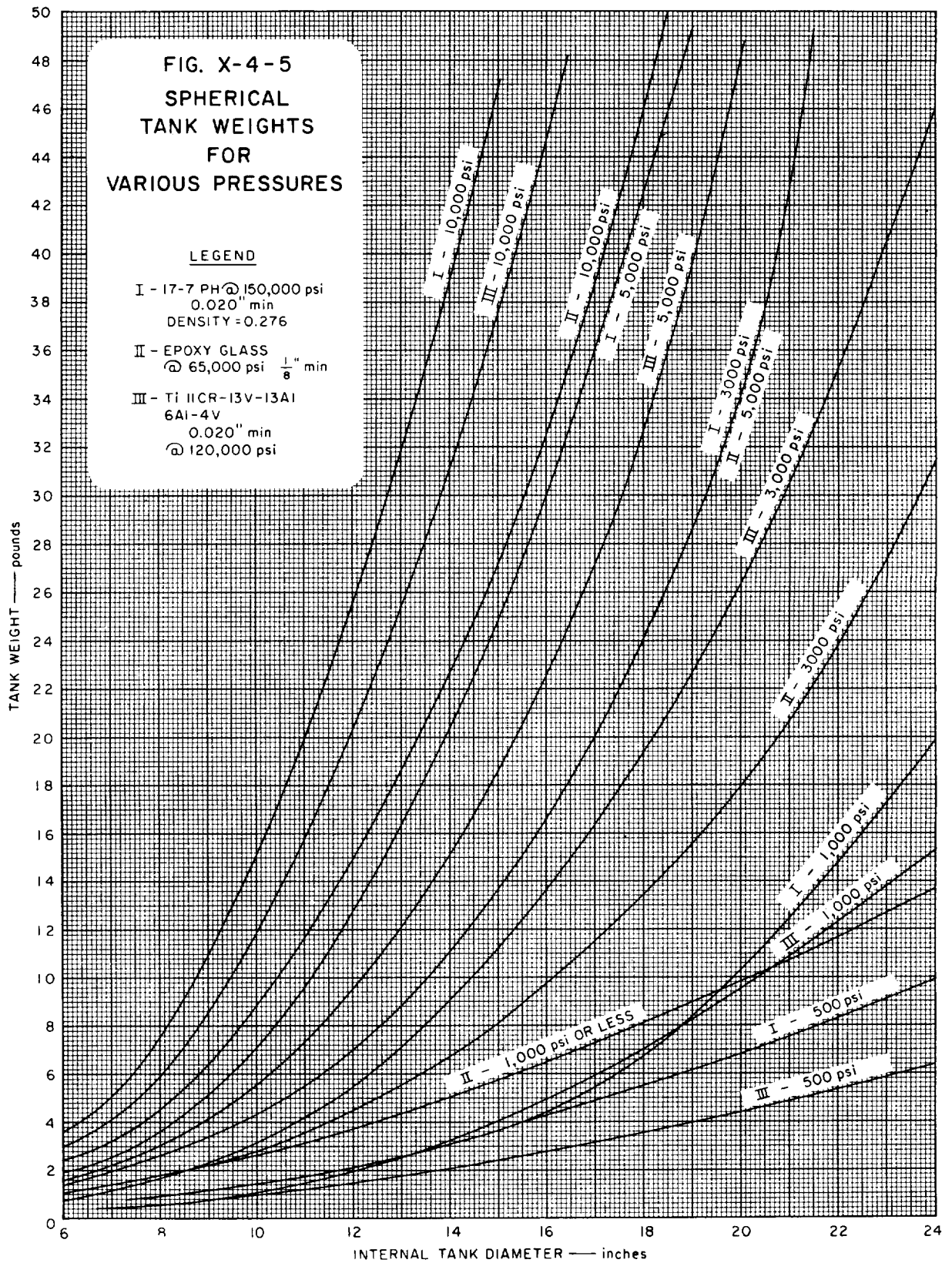
)











)

)

)

)

)

X-5 PRESSURE VESSEL REFERENCES

1. Timoshenko, S., and Goodier, J. N., *Theory of Elasticity*, 2nd Ed., McGraw-Hill Book Co., Inc., New York, 1951.
2. Whalley, E., *Canadian Journal of Technology*, **34**, 268, 291 (1956).
3. Coates, W. M., *ASME Trans.*, **52**, No. 12 (1930).

)

)

)

)

)

XII MATERIALS

Table of Contents

<u>Section-Part</u>	<u>Title</u>	<u>Section-Part, Page</u>
XII-0	List of Tables	XII-0.2
XII-0	List of Figures	XII-0.3
XII-1	Introduction	XII-1.1
XII-2	Compatibility of Selected Materials with Pressurizing Gases and Propellants	XII-2.1
	References	XII-2.3
XII-3	Properties of Materials Used for Pressure Tanks Aluminum Alloys Stainless Steel Alloys Titanium Alloys Epoxy-Glass Fiber Filament	XII-3.1
	References	XII-3.5
XII-4	Permeability of Materials to Gases Polymeric Materials Glasses Metals	XII-4.1
	References	XII-4.7

XII-0 LIST OF TABLES

<u>Section-Part-Table</u>	<u>Title</u>	<u>Section-Part-Page</u>
XII-2-1	Compatibility of Selected Metals with Gases and Liquid Propellants	XII-2.1
XII-2-2	Compatibility of Selected Non-Metals with Gases and Liquid Propellants	XII-2.2
XII-3-1	General Data on Aluminum Alloys	XII-3.1
XII-3-2	General Data on Stainless Steel Alloys	XII-3.2
XII-3-3	General Data on Titanium Alloys	XII-3.3
XII-3-4	General Data on Epoxy-Fiber Glass Filament	XII-3.4
XII-4-1	Permeability of Polymeric Materials to H ₂ , He, N ₂ , O ₂ , and CO ₂	XII-4.3
XII-4-2	Permeability of Polymeric Materials to Propane and to Water	XII-4.4
XII-4-3	Permeability of Glasses	XII-4.5
XII-4-4	Permeability of Metals	XII-4.6

XII-0 LIST OF FIGURES

<u>Section-Part-Figure</u>	<u>Title</u>
XII-3-1	Strength of Aluminum Alloys
XII-3-2	Thermal Conductivity and Modulus of Elasticity of Aluminum Alloys
XII-3-3	Specific Heat of Aluminum Alloys
XII-3-4	Strength of 17-7PH Stainless Steel
XII-3-5	Strength of AISI-302 Stainless Steel
XII-3-6	Thermal Conductivity and Modulus of Elasticity of 17-7PH Stainless Steel
XII-3-7	Thermal Conductivity and Modulus of Elasticity of AISI-302 Stainless Steel (Annealed)
XII-3-8	Specific Heat of Stainless Steels
XII-3-9	Strength of B-120-VCA Titanium
XII-3-10	Strength of C-120-AV Titanium
XII-3-11	Thermal Conductivity and Modulus of Elasticity of Titanium Alloys
XII-3-12	Specific Heat of Titanium and Alloys

)

)

)

)

)

XII-1 INTRODUCTION

This section contains information pertinent to materials of construction for pressurized gas systems.

Ratings of the compatibility of construction materials with pressurizing gases and/or propellants are given in tabular form for selected metallic and nonmetallic materials.

Because there is a wealth of data on the properties of metals and alloys, only selected properties are given for the alloys most typically used in pressure vessel construction, *i.e.*, aluminum, stainless steel, and titanium, as well as some general properties for epoxy-fiber glass composite.

Data are tabulated for the permeability of polymeric materials, glasses, and metals to various pressurizing gases.

)

)

)

)

)

Table XII-2-1

COMPATIBILITY OF SELECTED METALS WITH GASES AND LIQUID PROPELLANTS*

	Al	Ti 6Al-4V	Ti A110AT	Ti C110M	S.S. 302	S.S. 304	S.S. AM350	S.S. 17-4PH	S.S. 17-7PH
O ₂	1	3	3	3	1	1	1	1	1
N ₂	1	1	1	1	1	1	1	1	1
H ₂	1	1	1	1	1	1	1	1	1
He	1	1	1	1	1	1	1	1	1
H ₂ O ₂	1	4	4	4	4	2	2	2	2
N ₂ O ₄	1	4	4	4	1	1	1	1	1
UDMH	1	4	4	4	1	1	1	1	1
Freon-11	1	1	1	1	1	1	1	1	1
Freon-12	1	1	1	1	1	1	1	1	1
Freon-13	1	1	1	1	1	1	1	1	1
Freon-14	1	1	1	1	1	1	1	1	1
Freon-21	1	1	1	1	1	1	1	1	1
C ₃ H ₈	1	1	1	1	1	1	1	1	1
C ₄ H ₁₀	1	1	1	1	1	1	1	1	1
N ₂ H ₄	1	4	4	4	1	1	2	1	1
CO ₂	1	1	1	1	1	1	1	1	1
NH ₃	2	1	1	1	1	1	2	1	1
ClF ₃	2	4	4	4	2	2	2	2	2
ClO ₃ F	1	3	3	3	2	2	2	2	2

Ratings

- 1 Acceptable
- 2 Acceptable (limited service)
- 3 Unacceptable
- 4 Check manufacturer's recommendations

* References on p. XII-2.3.

Table XII-2-2

COMPATIBILITY OF SELECTED NON-METALS WITH CASES AND LIQUID PROPELLANTS*

	TEFLON	KEL-F	MYLAR	VITON A	VITON B	POLY- ETHYLENE	EPOXY/ GLASS	NEO- PRENE	RUBBER
O ₂	2	2	2	3	3	3	3	3	3
N ₂	1	1	1	1	1	1	1	1	1
H ₂	1	1	1	1	1	1	1	1	1
He	1	1	1	1	1	1	1	1	1
H ₂ O ₂	1	1	1	3	3	1	4	3	3
N ₂ O ₄	2	2	2	3	3	3	3	3	3
UDMH	2	2	2	3	3	3	3	3	3
Freon-11	4	4	4	4	4	4	4	4	4
Freon-12	4	4	4	4	4	4	4	4	4
Freon-13	4	4	4	4	4	4	4	4	4
Freon-14	4	4	4	4	4	4	4	4	4
Freon-21	4	4	4	4	4	4	4	4	4
C ₃ H ₈	1	1	1	2	2	1	1	1	2
C ₄ H ₁₀	1	1	1	2	2	1	1	1	2
N ₂ H ₄	1	1	3	3	3	3	4	3	3
CO ₂	1	1	1	2	2	1	4	2	2
NH ₃	2	2	2	3	3	2	2	4	2
ClF ₃	2	2	2	3	3	3	3	2	3
ClO ₃ F	1	1	1	4	4	1	1	2	3

Ratings

- 1 Acceptable
- 2 Acceptable (limited service)
- 3 Unacceptable
- 4 Check manufacturer's recommendations

* References on p. XII-2.3.

XII-2 REFERENCES

1. Bell Aerosystem Company "Storable Propellant Data for the Titan II Program," *AFBMD TR-61-65*, March 1962.
2. Coplan, H. I., "Screening Tests on Twenty Elastomers for Compatibility in Nitrogen Tetroxide," Aerojet-General Corp., *MN-146*.
3. Eldridge, E. A., and Deem, H. W., "Report on Physical Properties of Metals and Alloys from Cryogenic to Elevated Temperatures," American Society for Testing Materials, Philadelphia, Pennsylvania.
4. Du Pont de Nemours, E. I., and Co. (Inc.) "Effect of 'Freon' Fluorocarbons on Elastomers," Booklet B-12A (preliminary).
5. Eiseman Jr., B. J. "Effect on Elastomers of 'Freon' Compounds and other Halohydrocarbons," *Refrig. Eng.*, December, 1949.
6. Liberto, R. R., "Research and Development on the Basic Design of Storable High-Energy Propellants Systems and Components," Bell Aerosystems Company, *AFFTC TR-60-61*, May 19, 1961.
7. Liberto, R. R., "Titan II Storable Propellant Handbook" Bell Aerosystem Company, *AFBMD TR-62-2*, 1962.
8. Liquid Propellant Information Agency, "Liquid Propellant Manual," *LPIA/LPM-1*, 1961.
9. Lockheed-Georgia "Main Propellant Tank Pressurization System Study and Test Program, Vol. III, Design Handbook," *AFFTC TR-61-21*, 1961.
10. Lyons, R. H., "Materials for Nitrogen Tetroxide Service," Aerojet-General Corp., F-02668(101216-2).
11. Pennsalt Chemicals Corporation, "Perchloryl Fluoride," Booklet DC-1819.
12. York, H. J., "Compatibility of Various Materials of Construction with Nitrogen Tetroxide," Aerojet-General Corp., *RM-13*.

)

)

)

)

)

Table XII-3-1
GENERAL DATA ON ALUMINUM ALLOYS (Ref. 4)

GENERAL DATA	ALUMINUM 2024 (T86)	ALUMINUM 7075 (T6)
Nominal Composition	Cu, 3.8-4.9% Mg, 1.2-1.8% Si, 0.5% max. Cr, 0.1% max. Zn, 0.25% max. Fe, 0.5% max.	Zn, 5.1-6.1% Mg, 2.1-2.9% Cr, 0.18-0.40% Fe, 0.7% max. Mn, 0.3% max. Si, 0.5% max. Ti, 0.2% max.
Rockwell Hardness	B - 77-83	B - 85-95
Density	0.100 lb/in ³	0.101 lb/in ³
Mean Coefficient of Thermal Expansion	12.2 microinches/in/°F	12.2 microinches/in/°F
Heat Treatment		
Annealing	775 °F for 2-3 hr, cool to 500°F	775 °F for 2-3 hr, A.C.
Solution Treating	910-930 °F, 10-60 min in salt bath, W.Q. T86, 370-380 °F, 7-9 hr	860-930 °F, 10-60 min in salt bath, W. Q. T6 precipitation, 245-255 °F, 24-28 hr
Forging	500-900 °F	500-850 °F

Table XII-3-2
GENERAL DATA ON STAINLESS STEEL ALLOYS (Ref. 4)

GENERAL DATA	STAINLESS STEEL 17-7PH	STAINLESS STEEL 302
Nominal Composition	C, 0.07% Mn, 0.70% Si, 0.40% Cr, 17% Ni, 7% Al, 1.15%	C, 0.15% max. Mn, 2.00% max. Si, 1.0% max. Cr, 17-19% Ni, 8-10%
Rockwell Hardness	C - 43-(TH1050) C - 48-(RH950)	B - 80
Density	0.29 lb/in ³	0.29 lb/in ³
Mean Coefficient of Thermal Expansion	9.6 microinches/in/°F	9.6 microinches/in/°F
Heat Treatment		
Annealing	TH1050, heat annealed material to 1400 °F, 1-1/2 hr; age at 1050 °F for 1-1/2 hr	Rapid cool from 1900 °F
Solution Treating	RH950, solution annealed; re-heat 1750 °F for 10 min, A.C.; -100 °F for 8 hr, re-heat 950 °F for 1 hr.	
Forging		220-1725 °F
Stress Relieving		Not over 750 °F

Table XII-3-3
GENERAL DATA ON TITANIUM ALLOYS (Ref. 4)

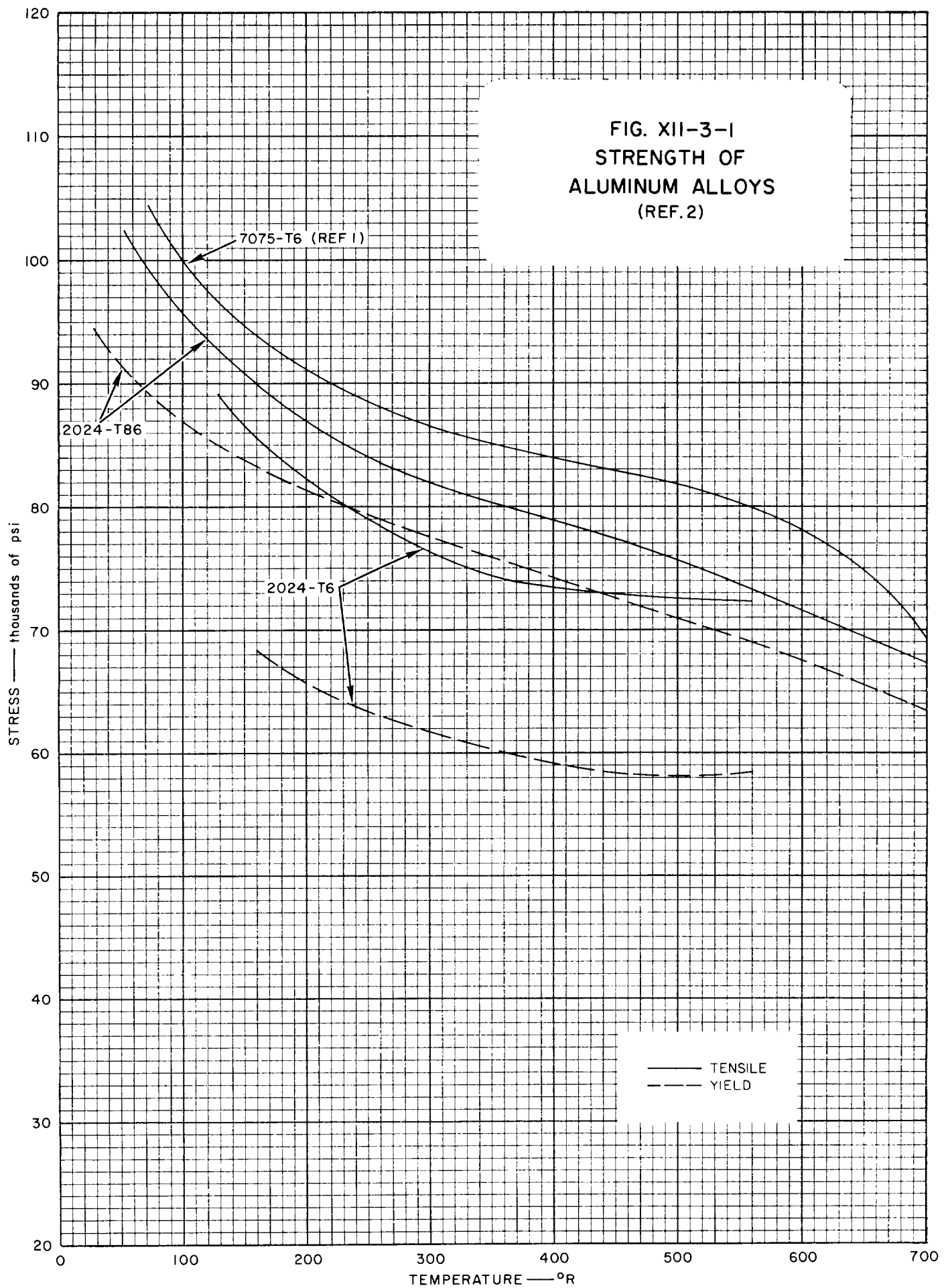
GENERAL DATA	TITANIUM B-120-VCA (Ti-13V-11Cr-3Al)	TITANIUM C-120-AV (Ti-6Al-4V)
Nominal Composition	C, 0.05% max. N, 0.08% max. H, 0.025% max. Al, 2.5-3.5% V, 12.5-14.5% Cr, 10-11%	C, 0.08% max. N, 0.05% max. H, 0.015% max. Al, 5.75-6.75% V, 3.5-4.5%
Type Structure	Beta	Alpha-Beta
Rockwell Hardness	C - 32-36	C - 36
Density	0.176 lb/in ³	0.160 lb/in ³
Mean Coefficient of Thermal Expansion	5.4 microinches/in/°F	4.9 microinches/in/°F
Heat Treatment		
Beta Transus	1325 °F	1820 °F
Forging	2000-1400 °F	1900-1750 °F
Annealing	1450 °F, 15-60 min, A.C.	1300-1550 °F, 1-8 hr, slow cooled at 1050 °F, A.C.
Solution Treating		1660-1725 °F, 5-20 min, W.Q.
Aging	900 °F, 2-60 hr	1000 °F, 4 hr, A.C.
Stress Relieving		900-1200 °F, 1-4 hr, A.C.

Table XII-3-4
GENERAL DATA ON EPOXY-FIBER GLASS FILAMENT*
(Ref. 7)

PHYSICAL PROPERTIES	
Density	0.061-0.079 lb/in ³
Specific Heat	0.24 Btu/lb-°F
Thermal Conductivity	1.92-2.28 Btu/hr-ft ² -°F-in
Thermal Coefficient of Expansion	2-6 microinches/in/°F
MECHANICAL PROPERTIES	
Rockwell Hardness	M - 98-120
Flexural Strength	100,000-270,000 psi
Flexural Modulus	$5 \times 10^6 - 7 \times 10^6$ psi
Tensile Strength	80,000-250,000 psi
Tensile Modulus	$4 \times 10^6 - 9 \times 10^6$ psi

* 60-90% fiber glass content; high and low ranges reflect range of glass content

FIG. XII-3-1
STRENGTH OF
ALUMINUM ALLOYS
(REF. 2)



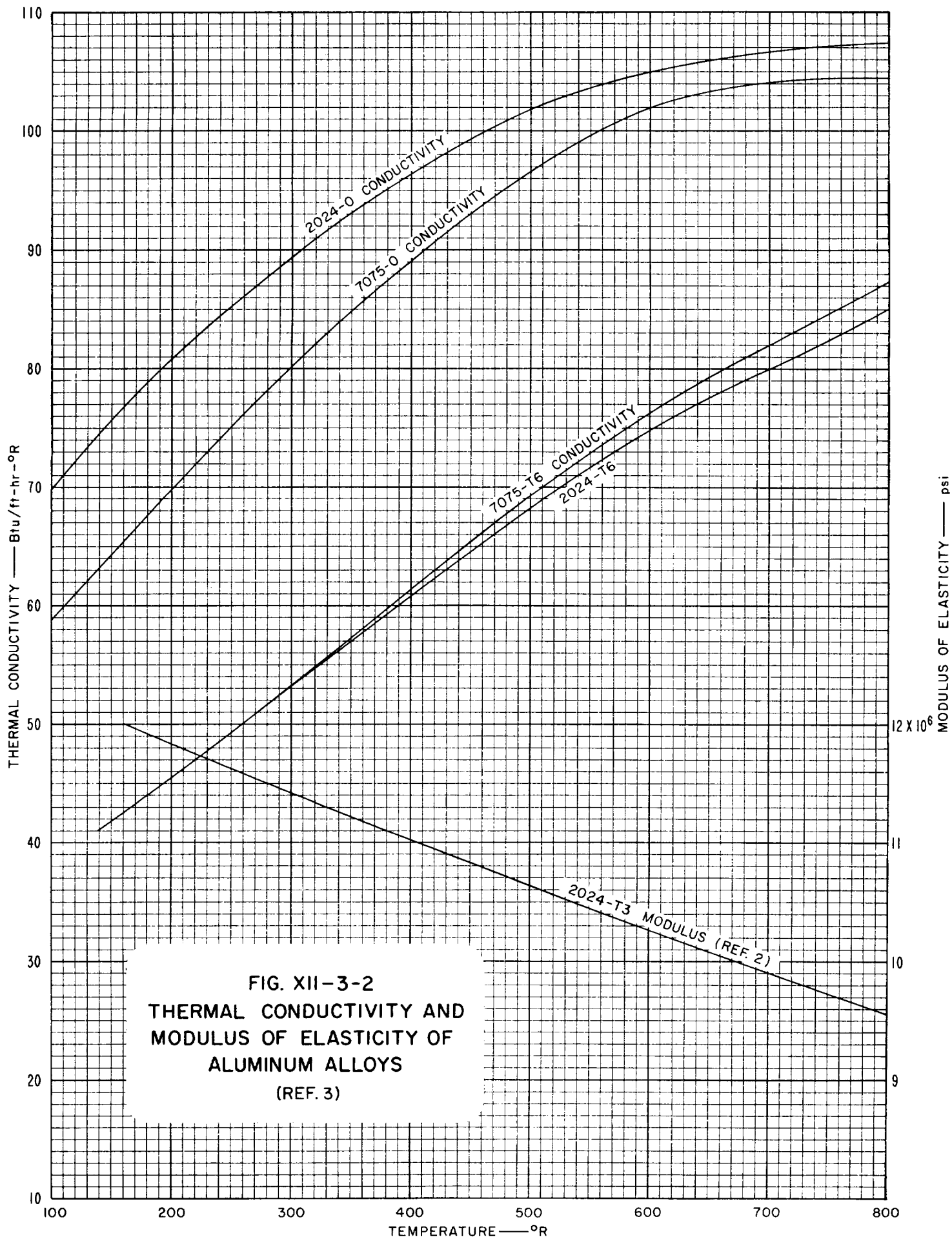
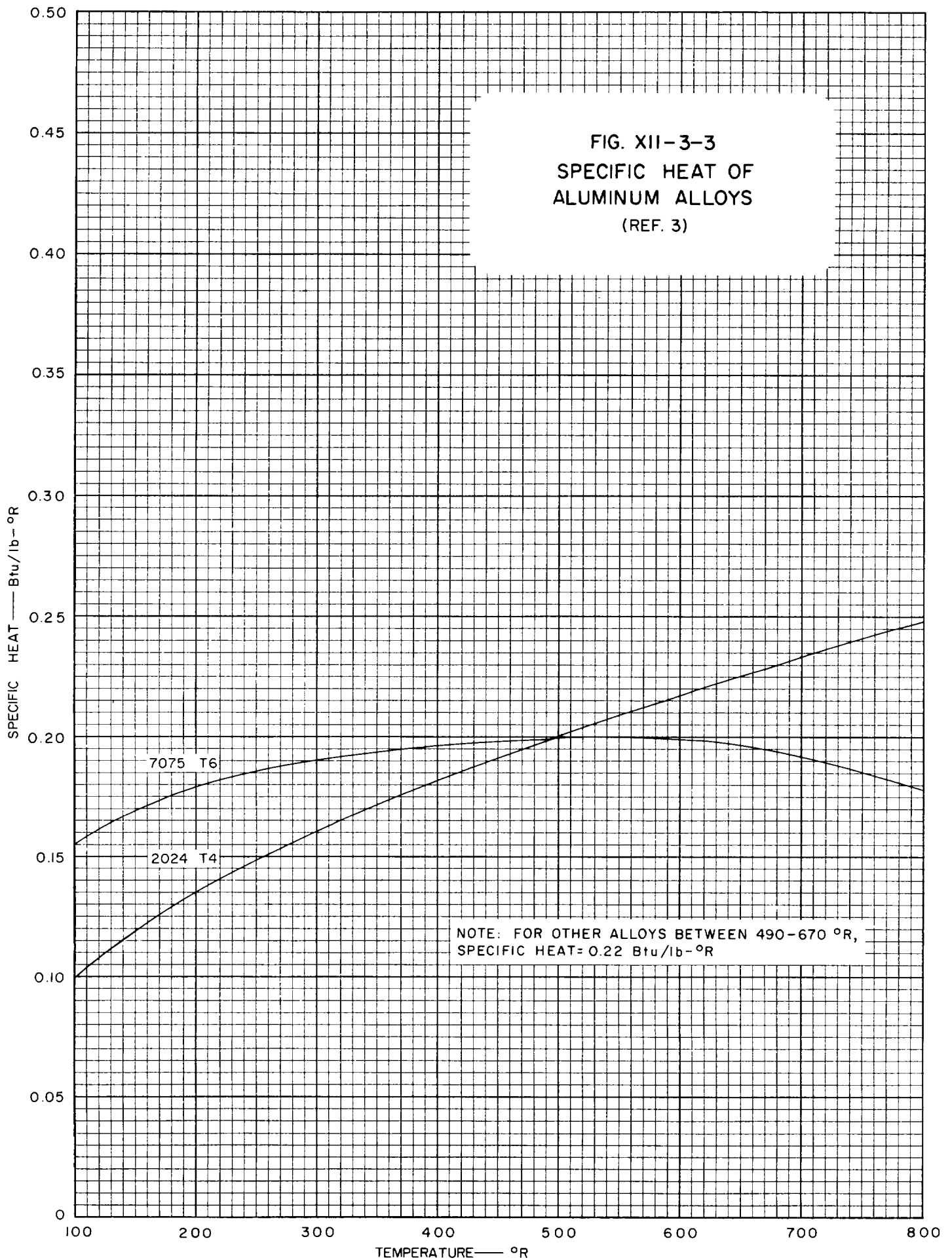


FIG. XII-3-2
THERMAL CONDUCTIVITY AND
MODULUS OF ELASTICITY OF
ALUMINUM ALLOYS
(REF. 3)

FIG. XII-3-3
SPECIFIC HEAT OF
ALUMINUM ALLOYS
(REF. 3)



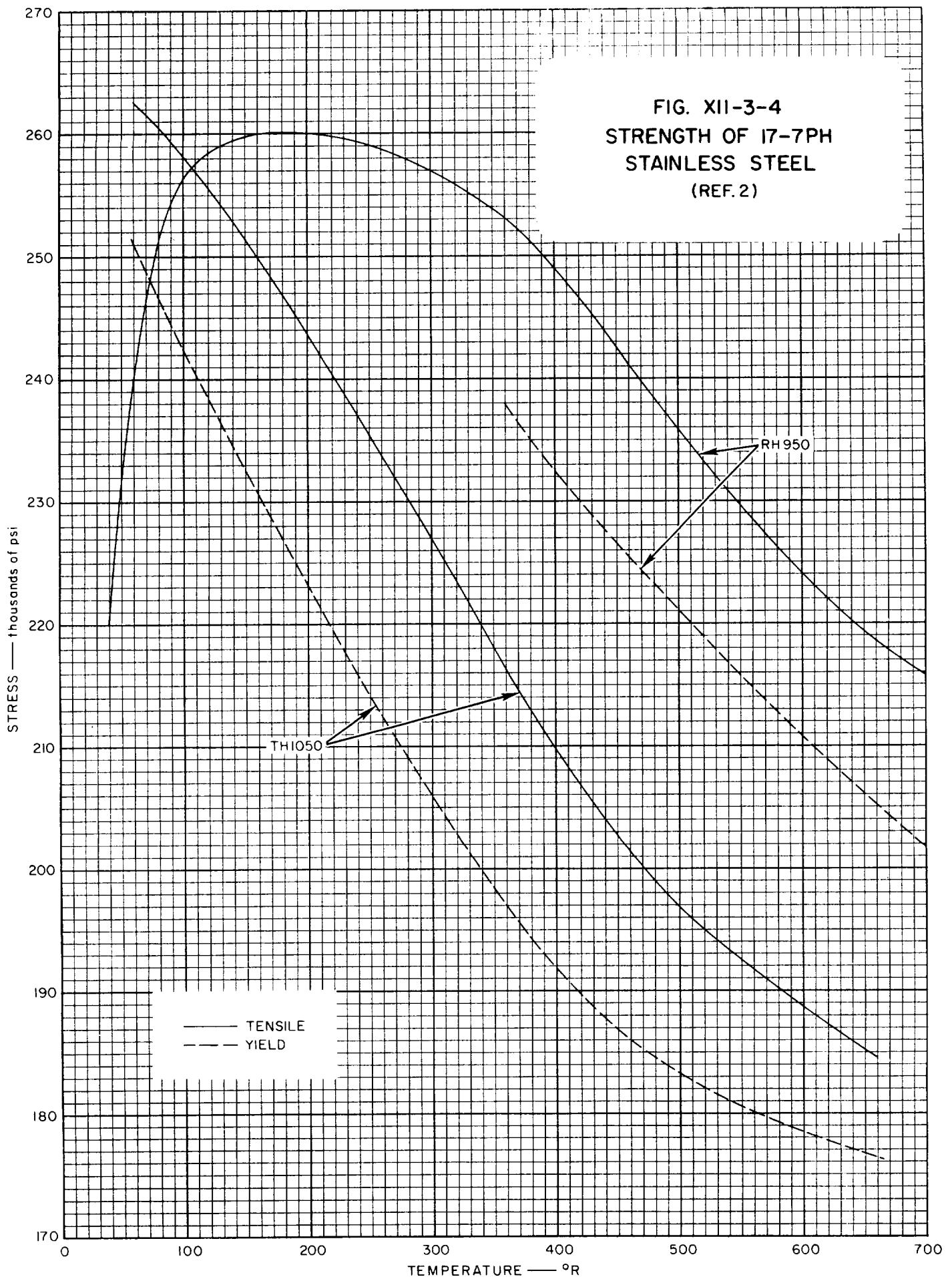


FIG. XII-3-5
STRENGTH OF AISI 302
STAINLESS STEEL
(REF. 2)

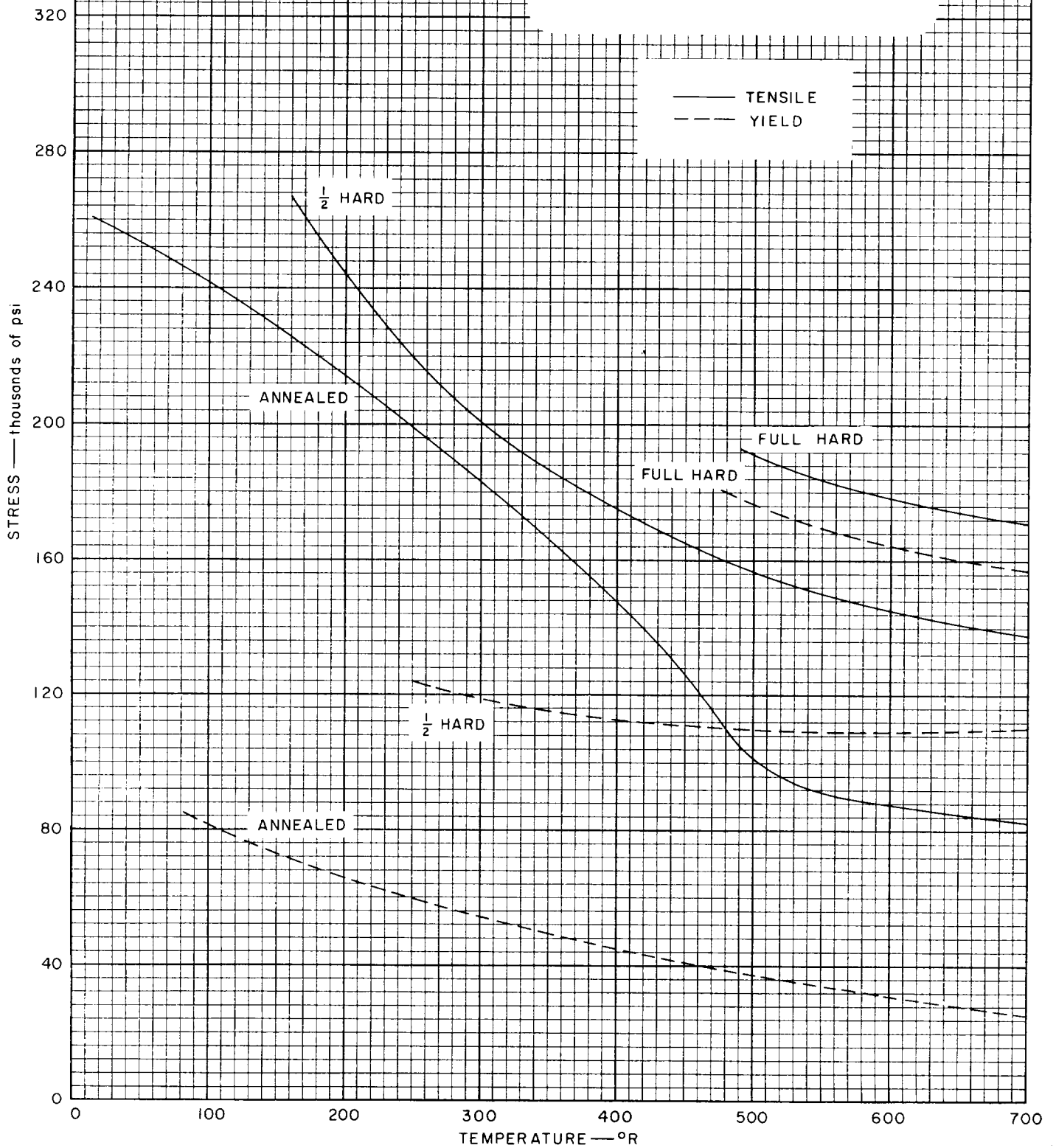


FIG. XII-3-6
THERMAL CONDUCTIVITY AND
MODULUS OF ELASTICITY OF
17-7 PH STAINLESS STEEL

THERMAL CONDUCTIVITY — Btu/ft-hr-°R

MODULUS OF ELASTICITY — psi

31×10^6

30

29

28

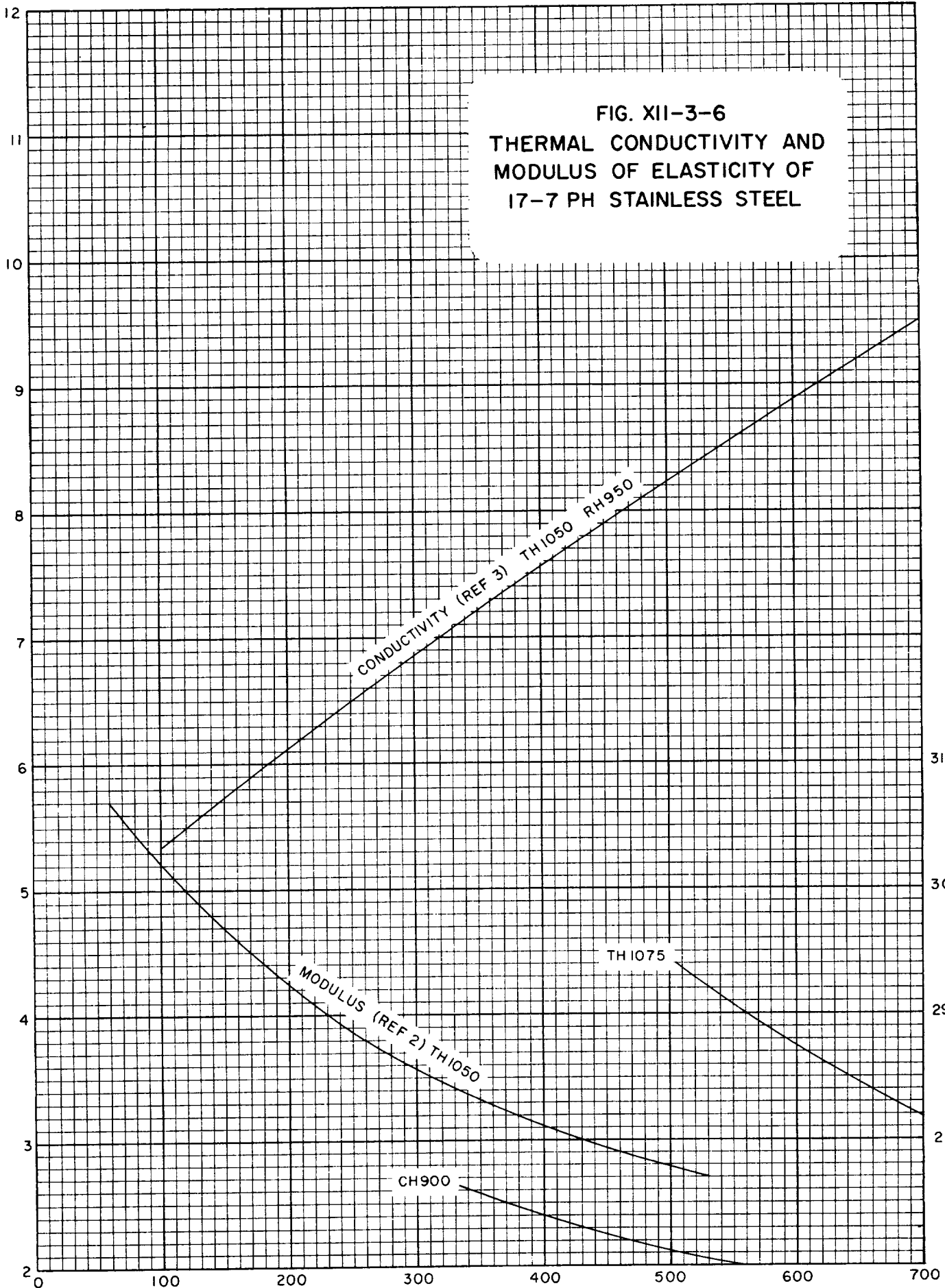
CONDUCTIVITY (REF 3) TH1050 RH950

MODULUS (REF 2) TH1050

TH1075

CH900

TEMPERATURE — °R



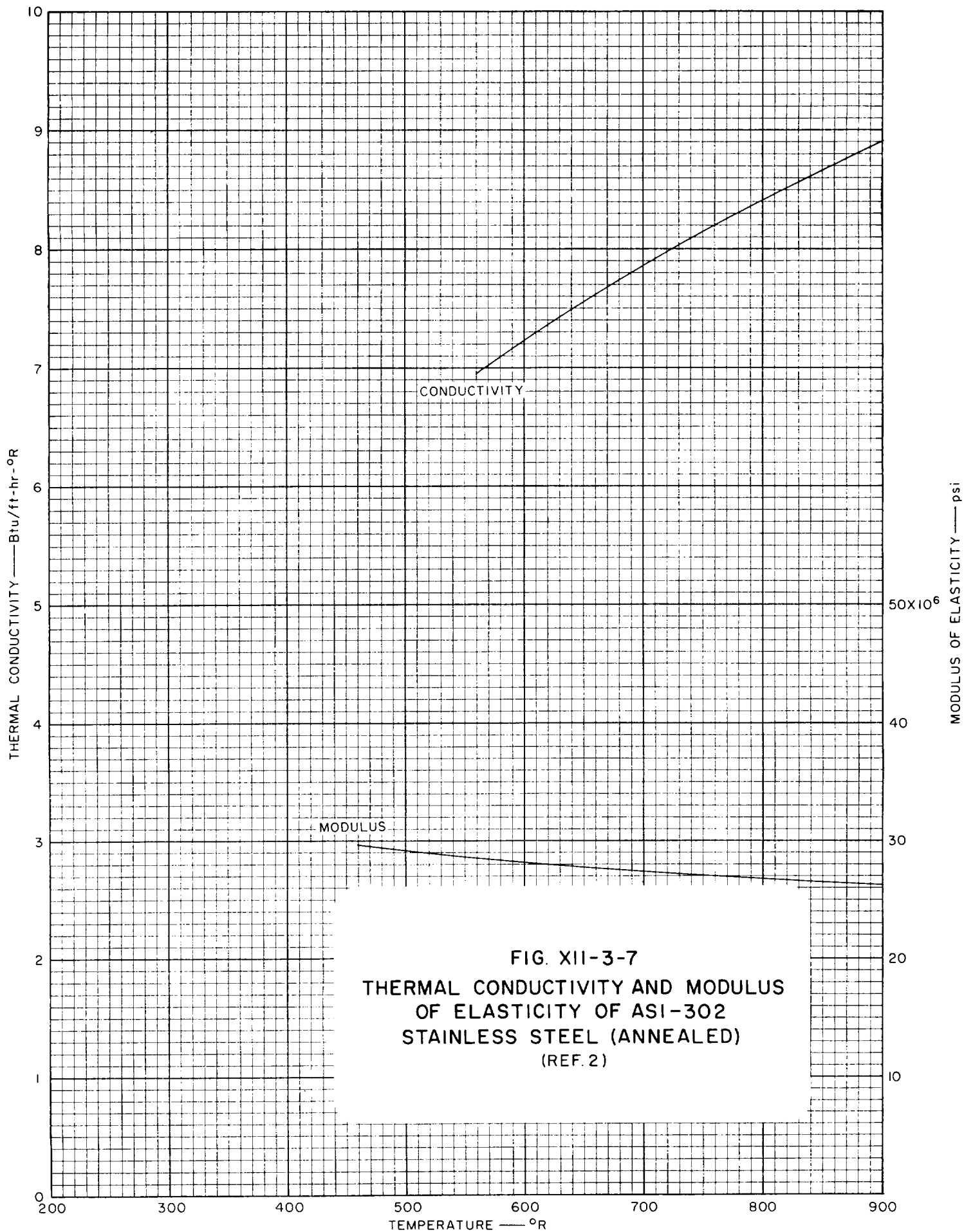


FIG. XII-3-7
THERMAL CONDUCTIVITY AND MODULUS
OF ELASTICITY OF AISI-302
STAINLESS STEEL (ANNEALED)
(REF. 2)

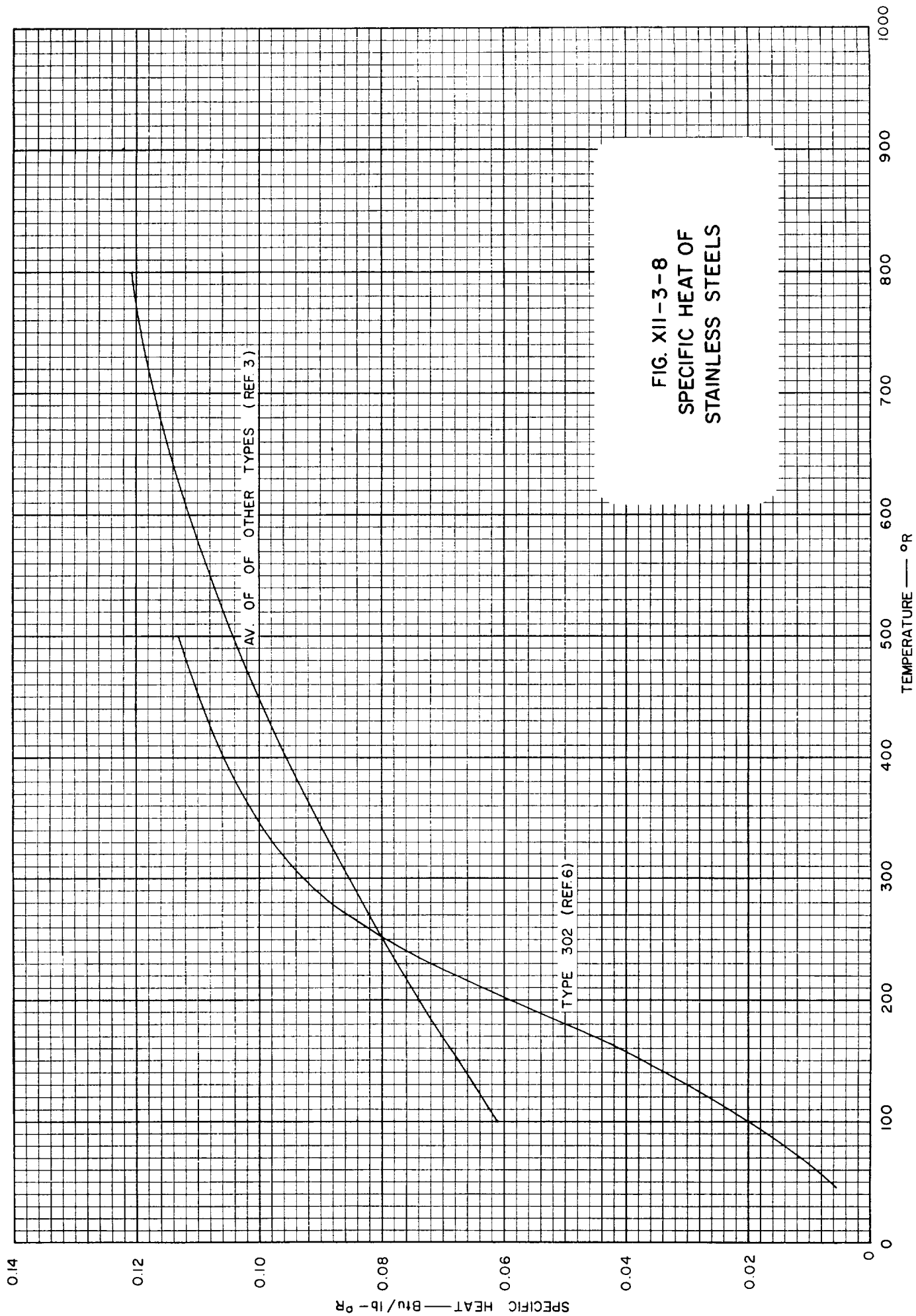


FIG. XII-3-9
STRENGTH OF B-120-VCA
TITANIUM
(REF. 2)

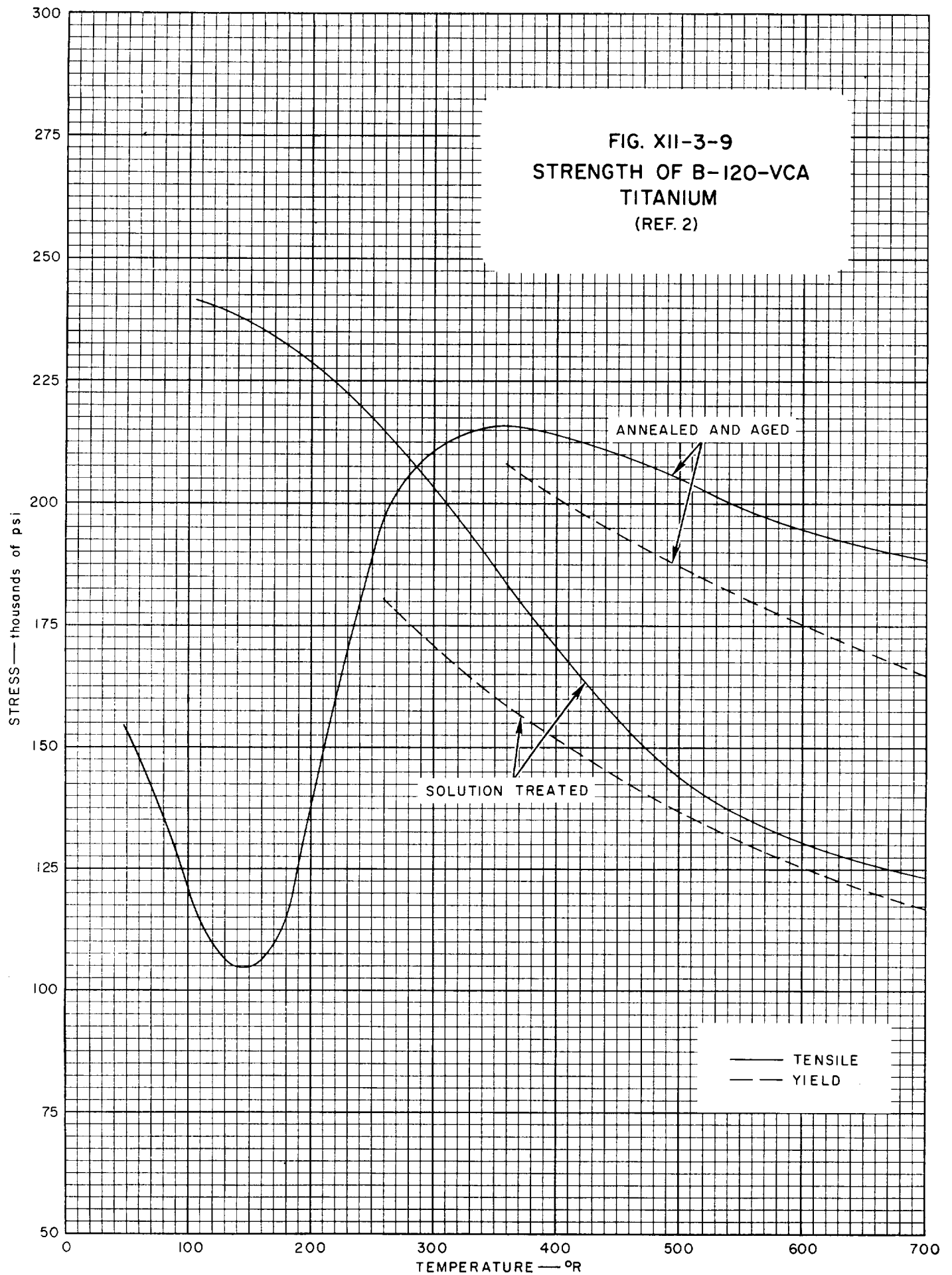


FIG. XII-3-10
STRENGTH OF C-120-AV
TITANIUM
(REF. 2)

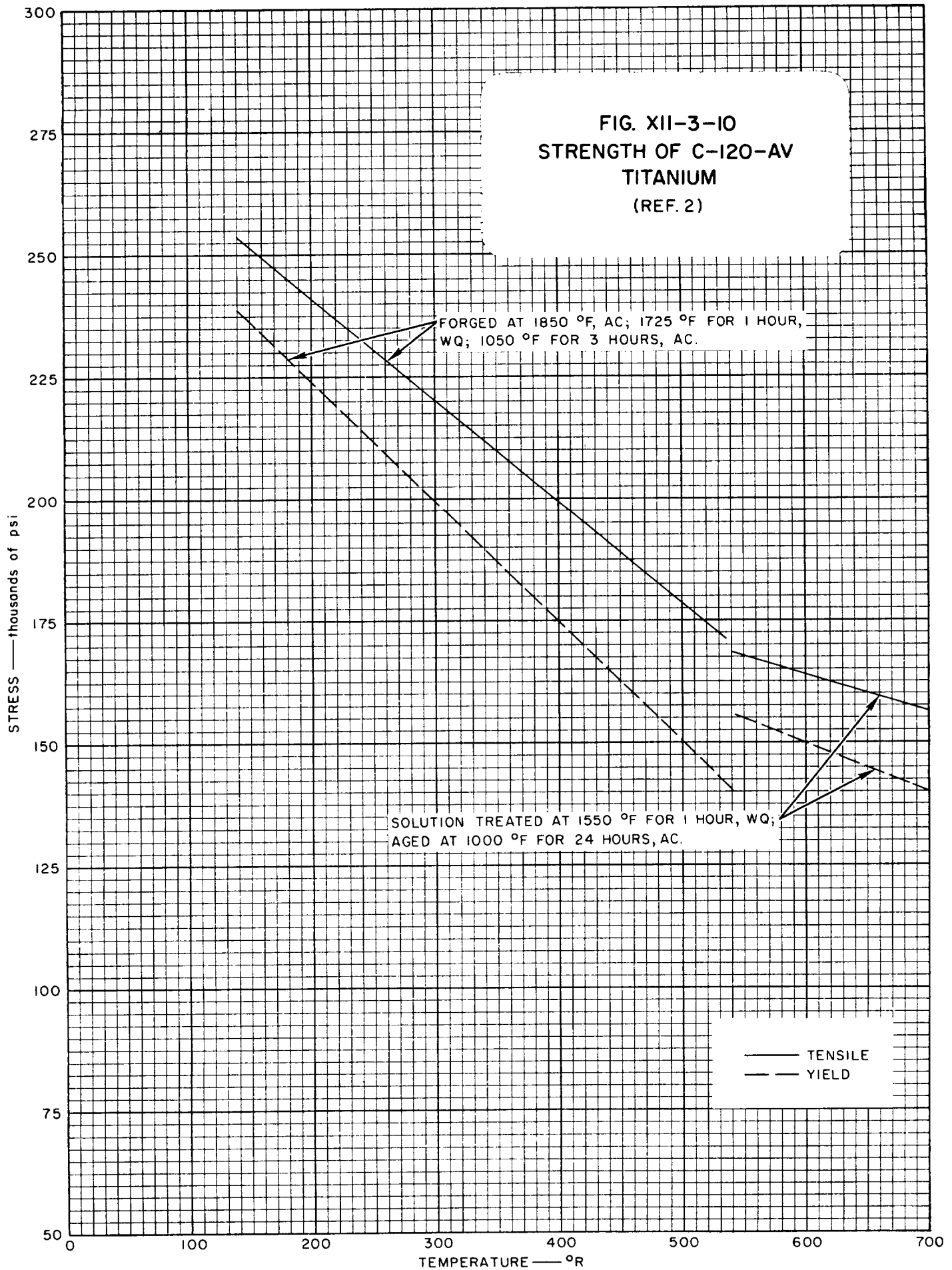
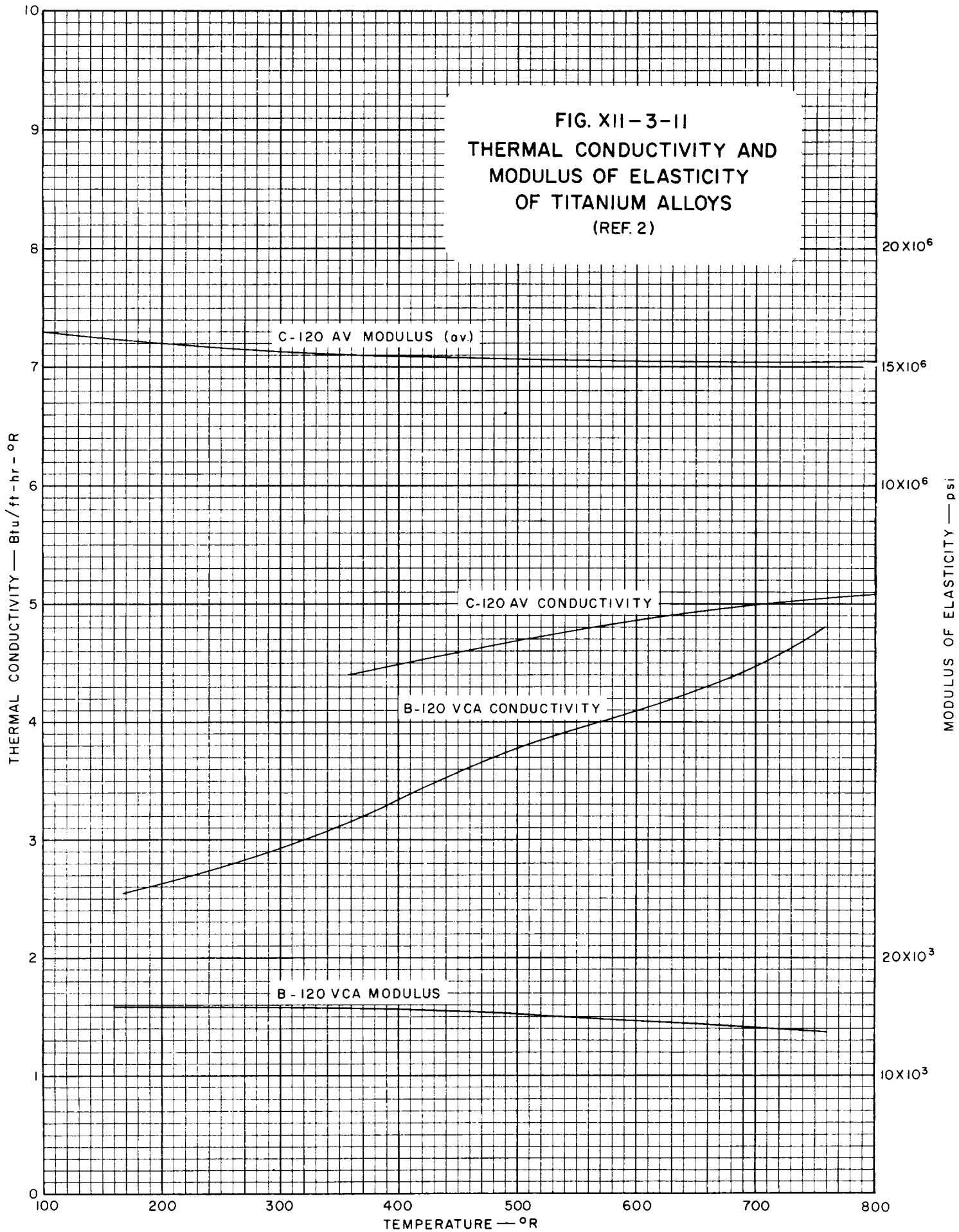
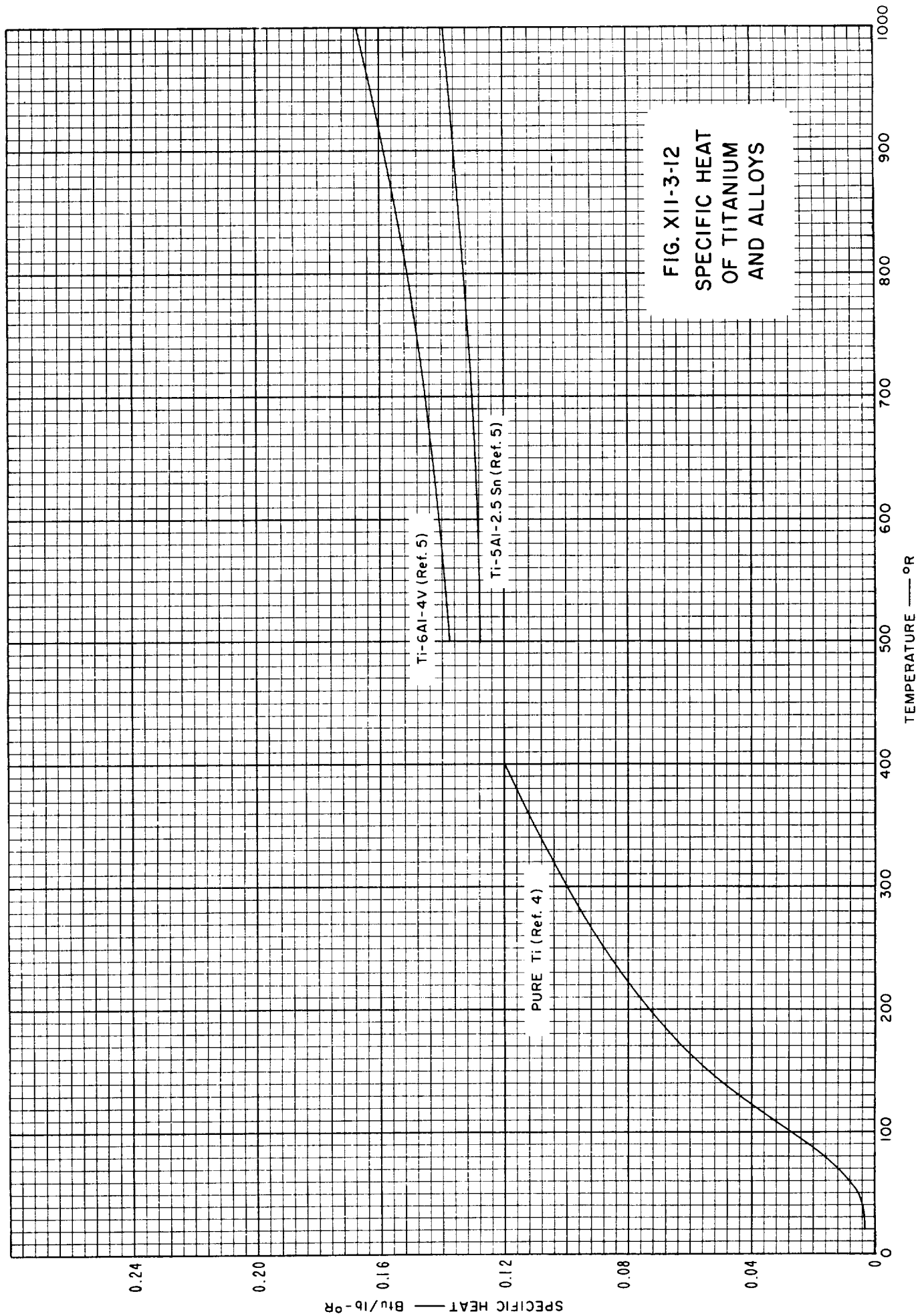


FIG. XII-3-II
THERMAL CONDUCTIVITY AND
MODULUS OF ELASTICITY
OF TITANIUM ALLOYS
(REF. 2)





XII-3 REFERENCES FOR PROPERTIES OF MATERIALS

1. Durham, T. F., McClintock, R. M., and Reed, R. P., *Cryogenic Materials Data Handbook*, Cryogenic Engineering Laboratory, Boulder Colorado.
2. Eldridge, E. A., and Deem, H. W., *Report on Physical Properties of Metals and Alloys from Cryogenic to Elevated Temperatures*, ASTM, Philadelphia, Pennsylvania.
3. Goldsmith, A., Waterman, T. E., and Herschhorn, H. J., *Handbook of Thermophysical Properties of Solid Materials, Vol. II*, Rev. Ed., Armour Research Foundation, MacMillan Co., New York, 1961.
4. Johnson, V. J., Ed., *Properties of Materials at Low Temperatures, Phase I*, Pergamon Press, New York, 1961.
5. *Metals Handbook*, Eighth Edition, American Society for Metals, Novelty, Ohio, 1961.
6. Scott, R. B., *Cryogenic Engineering*, D. Van Nostrand Co., New Jersey, 1959.
7. Anon., *Metal Progress*, **81**, No. 6, 106 (1962).

)

)

)

)

)

XII-4 PERMEABILITY OF MATERIALS TO GASES

Tables XII-4-1 and XII-4-2 give selected permeabilities of various polymeric materials to H_2 , He, N_2 , O_2 , CO_2 , H_2O , and C_3H_8 . Values for H_2 and He (plus one value for N_2) and typical glasses are given in Table XII-4-3. It will be recalled from Section VIII that the permeability of glasses drops off sharply at a molecular diameter of the permeant over about 2.5 Å and that it is also decreased as the content of glass formers, SiO_2 , B_2O_3 , and P_2O_5 , is decreased. In Table XII-4-4, permeability data for various gases through metals are collected.

In all the tables, where there are sufficient data to allow calculation, the permeability is given in parametric form:

$$\log_{10} P = A - B/T$$

where the units of P are in cc (STP)-mm/cm²-sec-atm in the case of polymers and glasses and cc (STP)-mm/cm²-sec-(atm)^{1/2} in the case of metals; B is in °K in all cases. This assumes the Arrhenius type exponential law is followed in temperature and that the permeation rate is proportional to the pressure difference across the membrane in the case of polymers and glasses and to the difference in the square root of the pressure in the case of metals. Although these assumptions are often safe, there are many exceptions, as discussed in Section VIII. For convenience in quick comparisons the permeability at 25°C (77°F), P_{25} , is also given in the tables.

XII-4.1

)

)

)

)

)

Table XII-4-1

PERMEABILITY OF POLYMERIC MATERIALS TO H₂, He, N₂, O₂ AND CO₂P in cc(STP)-mm/cm²-sec-atm, B in °K

MATERIAL	TRADE NAME OR CODE	H ₂			He			N ₂			O ₂			CO ₂			REF.
		A	B	P ₂₅ × 10 ⁷	A	B	P ₂₅ × 10 ⁷	A	B	P ₂₅ × 10 ⁷	A	B	P ₂₅ × 10 ⁷	A	B	P ₂₅ × 10 ⁷	
Natural Rubber	Pliofilm 140-N ₂	0.663-1	1508	39	0.146-1	1420	23	0.672-0	2032	6.6	0.903-1	1442	18	0.556-1	1355	102	29
Rubber Hydrochloride	Pliofilm FM-1	0.206-3	1228	1.21				0.386-1	2185	0.11	0.767-2	1836	0.40	0.134-0	2227	0.49	31
Poly(butadiene)	Hydrolol	0.342-1	1442	32	0.241-0	1836	12.0	0.724-1	1792	4.9	0.362-1	1551	14.5	0.160-1	1879	0.71	29
Poly(butadiene), hydrogenated								0.695-1	2447	3.0	0.214-0	2141	8.6	0.839-2	1136	105	16
Poly(dimethyl butadiene)	Methyl rubber	0.000-0	1748	13	0.892-2	1442	11	0.342+2	2906	0.36	0.518+1	2469	1.6	0.946-0	1901	36.8	29
Poly(isobutylene)	Oppanol B-200 (butyl rubber)	0.672-0	2076	4.9	0.544-1	1726	5.6	0.740+1	2797	0.22	0.820-0	2333	0.90	0.892-2	1442	11	29
Poly(butadiene-acrylonitrile)	Perbunan (German)	0.996-1	1770	11.5	0.079-1	1530	8.7	0.041+1	2404	0.89	0.398-0	2054	3.2	0.991-0	2207	3.8	29
	Perbunan 18	0.830-2	1355	19.2	0.098-1	1486	12.9	0.542-0	2163	1.92	0.100-0	1879	6.2	0.462-0	1814	23	29
	Hycar CR 15	0.187-0	1923	5.4	0.364-1	1683	5.2	0.375+2	3016	0.18	0.662+1	2622	0.73	0.818-1	1530	48	30
	Hycar CR 25	0.967-1	1792	9.0	0.302-1	1617	7.5	0.684+1	2688	0.46	0.949-0	2294	1.78	0.453+1	2294	5.7	30
Poly(butadiene-styrene)	Buna S, CR-S	0.491-1	1486	30.5	0.114-0	1442	17.5	0.079-0	1901	4.8	0.477-1	1595	13	0.750-0	1967	14.1	30
Poly(chloroprene)	Neoprene G	0.954-1	1770	10.3				0.079-0	1901	4.8	0.732-0	2163	3.0	0.146-0	1246	94	29
Poly(vinyl chloride-methylacrylate)	Mipolam MP	0.176-0	1945	4.4				0.748-0	2316	0.89	0.505-0	2568	0.70	0.518-0	1857	19.5	29
Poly(alkyl polysulfide)	Thiokol B	0.869-0	2316	1.2						0.2	0.505-0	2568	0.70	0.832-0	2141	4.0	29
Poly(esteramide-diisocyanate)	Valcaprene A	0.280-0	1967	4.8				0.519+1	2666	0.37	0.255+2	2950	0.22	0.839+1	2513	2.4	29
Polyethylene (density 0.914)	DE2400	0.220-0	1921	5.96	0.662-1	1814	3.75	0.524+1	2579	0.74	0.822-0	2229	2.20	0.042+1	2054	14.1	30
Polyethylene (density 0.964)	Alathon 14	--	--	--	0.144-2	1551	0.87	0.004-1	2076	0.11	0.651-2	1836	0.31	0.801-0	2032	9.6	8, 16
Poly(ethylene glycol terephthalate)	Grex	0.678-4	1201	0.445	0.390-4	1198	0.74	0.995-5	1639	0.0031	0.960-5	1398	0.019	0.718-3	1573	0.28	16
Polystyrene	Mylar A													0.509-4	1356	0.90	8, 31
	Dow 0641	0.077-5	72	68.5				0.713-7	-18	5.92	0.235-6	-10	18.5	0.178-5	219	277	7
Polyvinyl chloride + 20% DCP	Geon 101	0.818-6	418	2.6										0.611-7	217	0.762	7
Polyvinyl chloride + 25% DCP	Bakelite VB1930	0.549-5	216	66.7										0.896-6	-332	1025	7
Polyvinylidene chloride	Saran 517	0.133-5	478	3.4										0.472-5	799	0.49	7
Poly(caprolactam)	Nylon 6	0.074-1	1621	4.3	0.942-2	1570	4.8	0.023-2	2820	0.37	0.933-0	2320	1.4	0.150-0	1931	4.1	7
Poly(tetrafluoroethylene)	Teflon			0.050				0.960+1	3671	0.00044	0.922+1	3474	0.0018	0.399-0	2688	0.024	26, 31
Poly(chlorotrifluoroethylene)	Trithene, Kel-F	0.008-2	1535	18				0.386-1	2447	0.0064	0.995-2	2273	0.023	0.085-1	2120	0.093	31
plasticized Ethyl cellulose (plasticized)	Ethocel 610	0.160-0	2018	2.4	0.015-1	1485	10.7	0.971+1	3021	0.054	0.390-0	2353	0.31	0.017+1	2346	1.4	19, 31
Cellulose acetate (plasticized)	Celanese P-912	0.877-4	751	22.7				0.787-4	905	5.6	0.022-3	324	18.1	0.524-5	305	32	7, 31
Cellulose acetate-butylate	Kodapak II	0.220-0	1149	6.7	0.533-3	1038	10.9	0.995-4	1420	0.17	0.580-4	1093	0.82	0.075-1	1556	7.0	8, 31
Polypropylene (d = 0.907)		0.231-3	393	16				0.765-2	1710	1.1	0.041-2	1370	2.8	0.484-3	921	24	8
Cellulose nitrate								0.111+2	2906	0.23	0.449+1	2491	1.2	0.386-0	1988	5.2	18
										0.38			1.5			1.6	14

Table XII-4-2
PERMEABILITY OF POLYMERIC MATERIALS TO PROPANE AND TO WATER
P in cc (STP)-mm/cm²-sec-atm, B in °K

MATERIAL	TRADE NAME OR CODE	H ₂ O			PROPANE			REF.
		A	B	P ₂₅ x 10 ⁷	A	B	P ₂₅ x 10 ⁷	
Natural Rubber								
Rubber Hydrochloride								
Poly(butadiene), hydrogenated	Pliofilm NO	0.0707-0	1726	2600	0.141-1	1202	128	13, 16
Poly(isobutylene)	Hydropol			19				17
Poly(chloroprene)	Butyl rubber				0.241+2	2273	41	16
Poly(alkyl polysulfide)	Neoprene GN				0.951-0	2338	1.3	4
Polyethylene (density 0.922)	Thiokol 3000 ST						5.5	28
(density 0.914)							1.1	28
(density 0.960)								17
(density 0.964)								16
Polyethylene (d = 0.907)	Alathon 14	0.869-0	1748	68.4	0.662-1	2447	7.2	17
Poly(ethylene glycol terephthalate)	Grex			9.1				16
Polystyrene								17
Poly(vinyl chloride)								16
Poly(vinyl chloride-acetate)	Mylar A	0.960+1	2207	35.7	0.459-0	2338	0.41	18
Poly(vinylidene chloride)		0.508-5	153	98.8				17
Polyamide		0.80-5	0	630				4
Poly(chlorotrifluoroethylene)	Geon 101	0.78-4	514	110				4
Ethyl cellulose (plasticized)	Vynlite VYNWO	0.37-2	874	275				4
Cellulose acetate	Saran 517	0.941-7	2404	7.5				17, 26
(plus 15% DCP)	Nylon 6-6			53-516*			0.00027	17
Cellulose nitrate	Kel F 300	0.222-1	2050	0.22				19, 31
Poly(methylmethacrylate)	Ethocell 610	0.995-4	0	9880				17
		0.621-4	0	4180				17
		0.750-4	0	5620			2.8	14, 17
				4800			0.0058	13, 17
	Lucite			2200				13

* Humidity dependent.

Table XII-4-3

PERMEABILITY OF GLASSES

P in cc (STP)-mm/cm²-sec-atm, B in °K

SYSTEM	A	B	P ₂₅	REFERENCE
H ₂ -Fused silica	0.398-5	1873	1.12 x 10 ⁻¹²	1
-Vycor (Corning 7900)	0.520-5	1826	3.9 x 10 ⁻¹²	1
He-Fused silica (GE)	0.401-4	1049	0.76 x 10 ⁻⁷	1
-Vycor (Corning 7900)	0.579-4	1049	1.14 x 10 ⁻⁷	1
-Pyrex (Corning 7740)	0.654-4	1398	0.91 x 10 ⁻⁸	20
-Soda lime (Corning 0080)	0.822-4	2403	5.7 x 10 ⁻¹²	20
-X-ray shield (Pittsburgh Plate Glass)	0.662-5	2731	3.1 x 10 ⁻¹⁴	20
N ₂ -Fused silica	0.967-4	4820	6.2 x 10 ⁻²⁰	2

Table XII-4-4
PERMEABILITY OF METALS
P in cc (STP)-mm/cm²-sec (atm)^{1/2}, B in °K

SYSTEM	A	B	P ₂₅	REFERENCE
H ₂ -Aluminum	0.589-1	3017	7.5 x 10 ⁻¹¹	27
Copper	0.621-1	3933	2.6 x 10 ⁻¹⁴	6
Hastalloy B	0.701-1	3657	2.7 x 10 ⁻¹³	23
Inconel	0.847-1	3649	4.0 x 10 ⁻¹³	6
Iron	0.554-2	1836	2.6 x 10 ⁻⁸	6
Kovar	0.352-1	3497	4.1 x 10 ⁻¹³	6
Monel	0.161-1	2797	5.9 x 10 ⁻¹¹	6
Nickel	0.520-1	2885	6.9 x 10 ⁻¹¹	6
Niobium	0.749-1	1137	8.7 x 10 ⁻⁵	24
Palladium	0.929-1	2296	1.7 x 10 ⁻⁸	3
Platinum	0.512-1	3936	2.1 x 10 ⁻¹⁴	12
Steel				
Cold drawn	0.554-2	1879	1.8 x 10 ⁻⁸	6
low carbon	0.312-2	2288	4.2 x 10 ⁻¹⁰	22
Stainless 303	0.435-1	3540	4.6 x 10 ⁻¹³	6
304	0.586-1	3715	1.3 x 10 ⁻¹³	6
316, 321	0.273-1	3252	2.3 x 10 ⁻¹²	11
347	0.634-2	3180	9.2 x 10 ⁻¹³	11
410	0.188-1	3260	5.7 x 10 ⁻¹²	11
N ₂ -Iron	0.093-1	5204	4.3 x 10 ⁻¹⁹	25
Molybdenum	0.359-0	9837	4.4 x 10 ⁻³³	27
CO-Iron	0.554-2	4066	8.1 x 10 ⁻¹⁶	25
O ₂ -Silver	0.754-1	4941	1.5 x 10 ⁻¹⁷	15

XII-4. REFERENCES

1. Altomose, V. O., *J. Appl. Phys.*, **32**, 1309 (1961).
2. Barrer, R. M., *J. Chem. Soc.*, **1934**, 378.
3. Barrer, R. M., *Trans. Faraday Soc.*, **36**, 1235 (1940).
4. Barrer, R. M., and Skirrow, G., *J. Polymer Sci.*, **3**, 549 (1948).
5. Barton, R. S., *AERE-M599* (1960).
6. Borman, J. K., and Nardella, W. R., *Vacuum*, **12**, 19 (June, 1962).
7. Brubaker, D. W., and Kammermeyer, K., *Ind. Eng. Chem.*, **44**, 1465 (1952).
8. Brubaker, D. W., and Kammermeyer, K., *ibid.*, **45**, 1148 (1953).
9. Brubaker, D. W., and Kammermeyer, K., *ibid.*, **46**, 733 (1954).
10. Doty, P. M., Aiken, W. H., and Mark, H., *ibid.*, **38**, 788 (1946).
11. Flint, P. S., *KAPL-659* (1951).
12. Hamm, W. R., *J. Chem. Phys.*, **1**, 476 (1933).
13. Hare, E. F., Contract No. NONr 2848(00), *Interim Report No. 1* (July, 1960).
14. Hsieh, P. Y., Contract No. NONr 2848(00), *Interim Report No. 2* (January, 1961).
15. Johnson, F. M. G., and Larose, P., *J. Am. Chem. Soc.*, **46**, 1377 (1924); **49**, 312 (1927).
16. Michaels, A. S., and Bixler, H. J., *J. Polymer Sci.*, **50**, 413 (1961).
17. Myers, A. W., Meyer, J. A., Rogers, C. E., Stannett, V., and Szwarc, M., *TAPPI*, **44**, 58 (1961).
18. Myers, A. W., Stannett, V., and Szwarc, M., *J. Polymer Sci.*, **35**, 285 (1959).
19. Myers, A. W., Tammela, V., Stannett, V., and Szwarc, M., *Modern Plastics*, **37**, 139 (June, 1960).
20. Norton, F. J., *J. Am. Ceramic Soc.*, **36**, 90 (March, 1953).
21. Norton, F. J., *J. Chem. Phys.*, **22**, 1145 (1954).
22. Norton, F. J., quoted in Ref. 11.
23. Rudd, R. W., and Vetrano, J. B., *NAA-SR-4898 Rev.*, (1961).
24. Rudd, R. W., Vose, D. W., and Johnson, S., *J. Phys. Chem.*, **65**, 1018 (1961).
25. Ryder, H. M., *Elect. J.*, **17**, 161 (1920).
26. Sarge, T. W., *Anal. Chem.*, **19**, 396 (1947).
27. Smithells, C. J., and Ransley, C. E., *Proc. Royal Soc. (London)*, **A150**, 172 (1935).
28. Stout, L. E., Geisman, R., and Mozley, J. M., Jr., *Chem. Eng. Progress*, **44**, 219 (1948).
29. Van Amerongen, G. J., *J. Appl. Phys.*, **17**, 972 (1946).
30. Van Amerongen, G. J., *J. Polymer Sci.*, **5**, 307 (1950).
31. Waak, R., Alex, N. H., Frisch, H. L., Stannett, V., and Szwarc, M., *Ind. Eng. Chem.*, **47**, 2524 (1955).

)

)

)

)

)

XIII RELIABILITY

Table of Contents

Section-Part	Title	Section-Part	Page
XIII-0	List of Tables	XIII-0.2	
XIII-1	Introduction	XIII-1.1	
XIII-2	Reliability Models	XIII-2.1	
XIII-3	Probability Distribution	XIII-3.1	
XIII-4	Reliability Sampling	XIII-4.1	
XIII-5	Design of Experiments	XIII-5.1	
XIII-6	Tolerance Limits	XIII-6.1	
XIII-7	References	XIII-7.1	

XIII-0 LIST OF TABLES

<u>Section-Part-Table</u>	<u>Title</u>	<u>Section-Part,Page</u>
XIII-2-1	Reliability Each Component Must Have To Bring Out Over-all Reliability of a Serially Constructed System of Individual Components	XIII-2.5
XIII-3-1	Operational Probabilities	XIII-3.5
XIII-6-1	Tolerance Factors for Normal Distritution	XIII-6.3

XIII-1 INTRODUCTION

The objective of this section is briefly to mention and illustrate a few techniques of statistical reliability theory in order to make the reader aware of their existence and applicability to the determination of the reliability of pressurized gas systems and components. The fundamental theories of reliability mathematics are discussed in some detail in the Interim Report, issued in August 1963, and several texts are cited at the end of this section as references for the reliability engineer.

Reliability may be defined as the probability that a device will perform a specific function without failure under given environmental conditions for a given period of time. Probability is a mathematical term referring to the chance of occurrence. Failure means any variation in performance beyond allowable limits, not necessarily total failure. Conditioning environmental factors under which the device must operate are such factors as temperature, vibration, shock, pressure, moisture, etc. Time refers to the life span designed for the device under consideration; it might be fifteen years for a household appliance and thirty minutes for a missile.

This section considers some of the pertinent factors and computations involved in the various aspects of reliability which are defined in the above paragraph.

Although the causes of unreliability are many, with reference to space vehicles the primary cause is due to the complexity of the equipment involved. In general, a space vehicle requires that all of its subsystems, components, and parts must operate correctly in order for the flight to be successful. Probability theory determines a vehicle's reliability. The probability of a successful mission is equal to the product of the probabilities that each lesser device within the vehicle will operate successfully. In effect, reliability tends to decrease as the complexity of a device increases.

A reliability program to be successful must be based upon a well-organized and carefully planned system for collecting, analyzing, and following up reliability data. Lloyd and Lipow⁶ present an example of an on-line reliability data reporting system which effectively illustrates the dependence of the reliability program upon the adequacy of the reporting system.

XIII-2 RELIABILITY MODELS

Reliability models are concerned first with the relationship between the components of a system and second with the aggregate component effect upon the systems performance. The performance of an individual component must be considered separately, and then the relationship between the components which form the structure of the system are analyzed. The objective in specifying the reliability model is to determine the reliability (R) of a system composed of components with either known or estimated reliabilities.

Consider an attitude control system that is comprised of n components, and let S equal the event that the system is successful, and S_j , $j = 1 \dots, n$ the events that each of the components are successful. If S can occur only when all the S_j occur, the system is called *serial*, and:

$$R = P(S) = P(S_1 S_2 S_3 \dots S_n) \quad .$$

If the S_j are mutually independent (the probability of success for each subsystem is independent of the success or failure of all other subsystems) then:

$$R = P(S) = \prod_{j=1}^n P(S_j)$$

or

$$R = \prod_{j=1}^n \frac{(n_j - f_j)}{n_j}$$

where

n_j = number of tests of component j

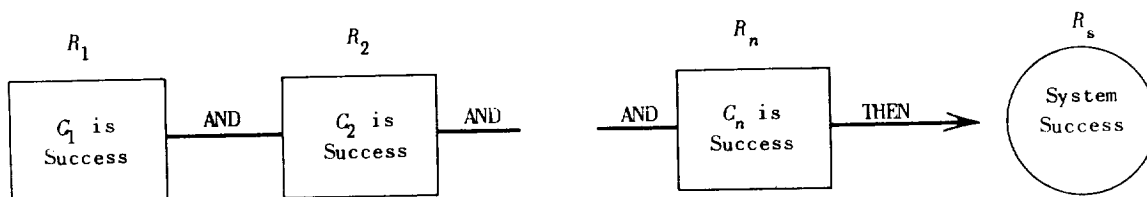
f_j = number of failures in n_j test.

If $n = 2$ and $n_1 = 50$; $n_2 = 100$; $f_1 = 2$; and $f_2 = 3$ then

$$R = \left[\frac{50 - 2}{50} \right] \cdot \left[\frac{100 - 3}{100} \right] = 0.9312$$

A parallel system is one consisting of n subsystems such that the system fails only if all subsystems fail. Or conversely, the system is successful if at least one subsystem operates. This property of parallel systems is commonly called redundancy and a frequently used measure of the amount of redundancy in a system is the ratio of the total number of components available for a particular task to the number of components actually necessary. The term stand-by redundancy refers to systems composed of two or more subsystems where the system is first made operational by turning on system one. If system one fails before the required operating time, system two becomes operative and the system fails only if system two fails before the required time of operation has elapsed.

Consider a simple serial system, that is, one with no redundancy, made up of n independent components.



and

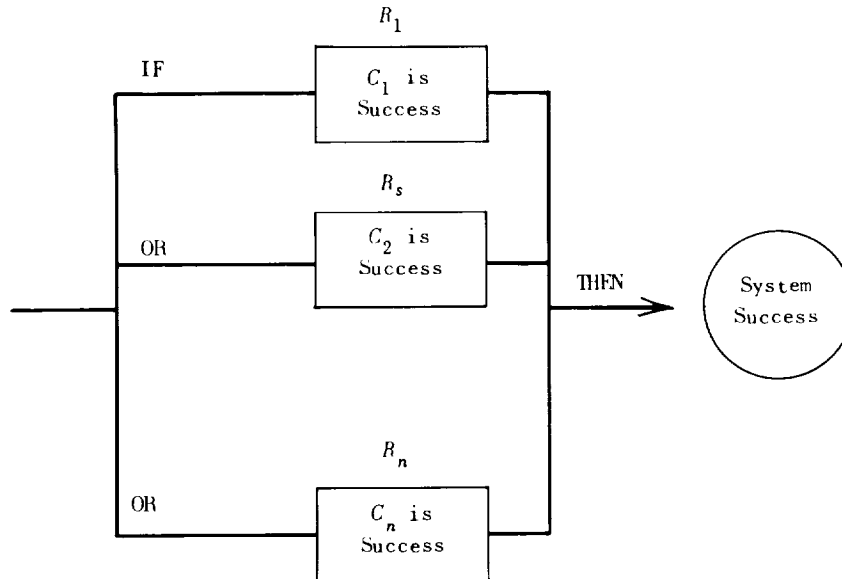
$$R_s = P[(C_1 \text{ success}) \cap (C_2 \text{ success}) \cap \dots \cap (C_n \text{ success})]$$

or

$$R_s = R_1 \cdot R_2 \dots R_n$$

Table XIII-2-1 illustrates this relationship between component and system reliability.

For a simple parallel system with $n - 1$ components redundant:

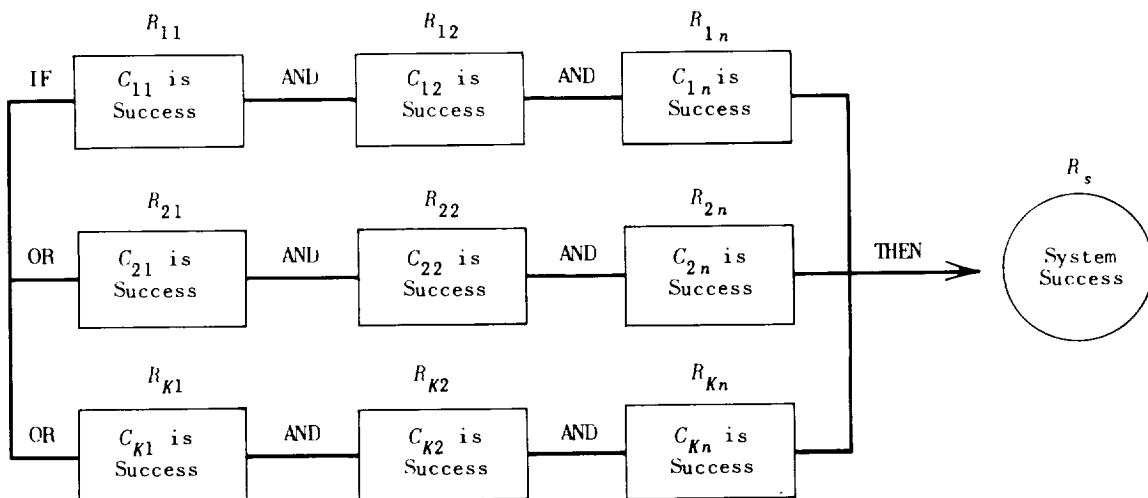


The probability that C_n will fail is $F_n = 1 - R_n$, and $R_s = 1 - (1 - R_1)(1 - R_2) \dots (1 - R_n)$. Or $R_s = 1 - (1 - R_n)^n$ if $R_1 = R_2 = \dots R_n$.

For example if a system is composed of three redundant components with $R_1 = 0.5$, $R_2 = 0.6$ and $R_3 = 0.4$ the reliability of the system would be

$$R_s = 1 - (1 - 0.5)(1 - 0.6)(1 - 0.4) = 0.88$$

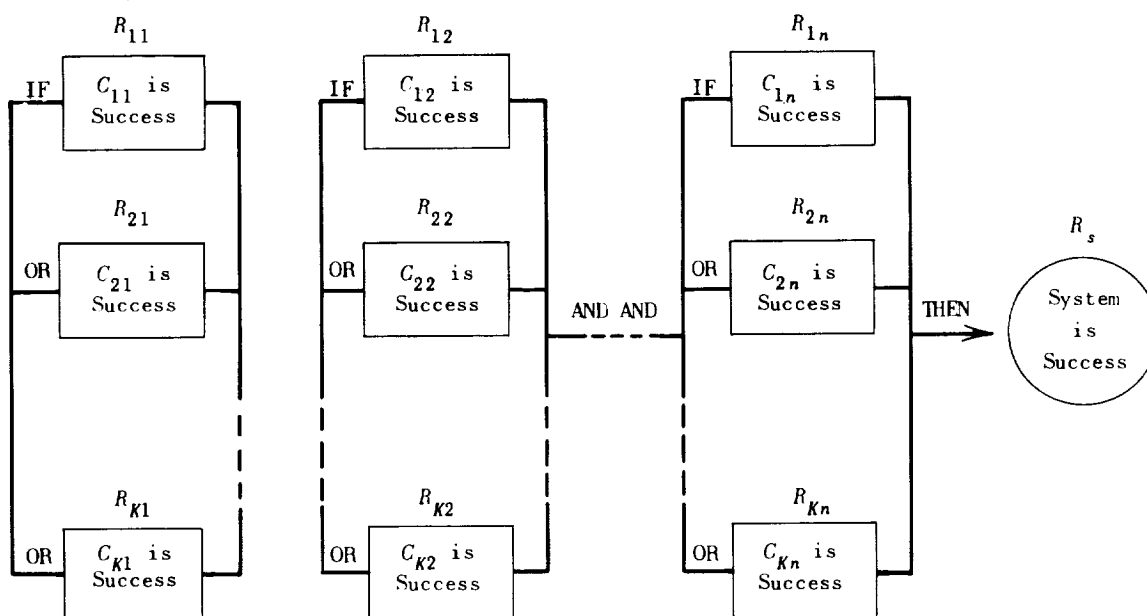
If each component of the parallel system was replaced with a serial system of components, the reliability structure would be:



and the system's reliability is:

$$R_s = [1 - (1 - R_{11} \cdot R_{12} \dots R_{1n})(1 - R_{21} \cdot R_{22} \dots R_{2n}) \dots (1 - R_{K1} \cdot R_{K2} \dots R_{Kn})]$$

Parallel-serial systems involve replacing each component of a serial system with a parallel system of components and the reliability structure is:



and

$$R_s = [1 - (1 - R_{11})(1 - R_{21}) \dots (1 - R_{K1})] \cdot [1 - (1 - R_{12})(1 - R_{22}) \dots (1 - R_{K2})] \dots [1 - (1 - R_{1n})(1 - R_{2n}) \dots (1 - R_{Kn})]$$

From the four basic reliability structures it is obvious that the magnitude of R_s can be changed by the number of components and the way in which they are arranged. Additional redundant components of course, add to the physical complexity of the circuitry and to the weight and space requirements.

Table XIII-2-1

RELIABILITY EACH COMPONENT MUST HAVE TO BRING
OUT OVER-ALL RELIABILITY OF A SERIALLY
CONSTRUCTED SYSTEM OF INDEPENDENT COMPONENTS

NUMBER OF SERIAL COMPONENTS	REQUIRED OVER-ALL RELIABILITY			
	0.95	0.9	0.7	0.5
1	0.95	0.9	0.7	0.5
2	0.9745	0.9486	0.8368	0.7071
3	0.9831	0.9654	0.8880	0.7938
4	0.9872	0.9738	0.9147	0.8409
5	0.9897	0.9790	0.9311	0.8706
6	0.9915	0.9826	0.9423	0.8908
7	0.9926	0.9851	0.9504	0.9057
8	0.9913	0.9870	0.9563	0.9170
9	0.9942	0.9883	0.9612	0.9260
10	0.9949	0.9897	0.9649	0.9330
15	0.9965	0.9928	0.9766	0.9548
20	0.9974	0.9947	0.9824	0.9661
50	0.9991	0.9979	0.9928	0.9863
100	0.9995	0.9988	0.9965	0.9931

Example: It is required to bring out success with 90 per-
cent probability, using 10 serial components.
Each must have a reliability of at least 9897.

)

)

)

)

)

XIII-3 PROBABILITY DISTRIBUTION

Statements such as "the attitude control system performed as intended," "the time to failure of a pressure valve exceeds 7," "the output of this power supply system is between 112 and 117 volts," etc., could all be expressed as the simple event success. The probability of success occurring is called reliability. Quite frequently the event failure, the ratio of the number of failures to the number of trials, is actually observed while what is really desired is a measure of success. The measure (probability) of success is, of course, simply defined as one minus the measure of failure.

For experiments which can be characterized by the discrete events success or failure, and one wishes to determine the probability of exactly x successes in n trials, the binomial probability distribution applies.

The binomial distribution states that if an experiment consists of N independent trials, each with a probability of success of p and a probability of failure of q ($q = 1 - p$), then the probability of exactly X successes and $N - X$ failures is:

$$P(X) = \binom{N}{X} p^X q^{N-X}$$

in which the expression

$$\binom{N}{X} = N! / X! (N - X)! \quad .$$

As an example, given that the reliability of an attitude control system is 0.90, i.e., the probability of successful operation on a mission is 0.90. What is the probability that it will work successfully in each of ten consecutive missions?

$$P(X) = \binom{10}{10} (0.90)^{10} (0.10)^0 = (1)(0.349) = 0.349 \quad .$$

If the question had been, "what is the probability of at least nine successes in ten missions?," then the event X is the union of two events, exactly 9 successes and 10 successes. Since these two events are mutually exclusive, the probability of their union is the sum of their individual probabilities and:

$$\begin{aligned} P(X) &= \binom{10}{9}(0.90)^9(0.10)^1 + \binom{10}{10}(0.90)^{10}(0.10)^0 \\ &= 10(0.387)(0.10) + 0.349 = 0.736 \end{aligned}$$

Another distribution that arises whenever a discrete event may occur randomly over a time period, and one considers as a random variable the number of times this event will occur over the given period of time, is the Poisson distribution:

$$P(X) = \frac{\lambda^X \cdot e^{-\lambda}}{X!}$$

where X is the number of occurrences of the event; λ is the expected number of occurrences; i.e., λ = average of X .

Given that a control system pressure valve-failure rate over a long period of time has been 3.41 per 10,000 cycles, and that a particular mission will require the valve to cycle 1,000 times, what is the probability of no valve failure during the mission?

The expected number of failures per 1,000 cycles is $\lambda = 0.341$, and

$$\begin{aligned} P(X = 0) &= \frac{\lambda^X \cdot e^{-\lambda}}{X!} \quad \text{note } 0! = 1 \\ &= (0.341)^0 \cdot e^{-0.341} \\ &\approx 0.71 \end{aligned}$$

Continuous probability distributions are used to measure the probability of events having a time characteristic such as the event "the time-to-failure exceeds T " or events like "the output of this rectifier is within certain limits."

A continuous probability distribution of particular importance in reliability calculations is the exponential distribution of time-to-failure. If reliability R is defined as the probability that a device will operate for a period of time equal to or greater than T , then by the exponential distribution

$$R = \int_T^{\infty} \frac{1}{\theta} \cdot e^{-T/\theta} = e^{-T/\theta}$$

and since T is known, R is a function of θ .

If θ , the mean time-to-failure of a device, is equal to 10 hours then the probability that a device will operate for 3 hours or more would be

$$P = e^{-T/\theta} = 2.718^{-3/10} = 0.74$$

Table XIII-3-1 lists R for several values of T and θ .

Many output characteristics exhibit a normal (Gaussian) probability distribution. In fact when non-normality is observed, it often indicates that something is wrong. In order to compute the reliability of an item R when the value of the performance factor has a continuous probability distribution, it is necessary to integrate over a range of values constituting successful performance. The normal distribution is defined as

$$R = \int_{X_1}^{X_2} \frac{1}{S\sqrt{2\pi}} \cdot \exp \left[-\frac{(X - M)^2}{2S^2} \right] dx$$

R is a function of X_1 , X_2 , M and S . Since X_1 and X_2 are usually given but M and S (the populations mean and standard deviation) are usually not known, it is first necessary to estimate these parameters and then solve for R .

To obtain estimates of the means and standard deviations of probability distributions, the method of maximum likelihood is usually used. It is easy to apply, yields the best estimates according to widely used criteria, and has the property that as the size of the sample grows larger, the distribution of the estimates approaches the normal distribution regardless of the probability distribution originally considered. This

fact makes it possible to state confidence limits for the estimated probability distribution parameters. Although widely used in reliability work, a discussion of confidence limits is beyond the scope of this discussion and the reader is referred to any of the several referenced statistical texts.

Table XIII-3-1
OPERATIONAL PROBABILITIES

Mean time to failure	Probability of Operational Time														
	1/2 sec	1 sec	2 sec	3 sec	10 sec	1 min	2 min	3 min	10 min	1 hr	2 hr	3 hr	10 hr	1 day	etc.
1 sec	0.61	0.37	0.14	0.05	0	0									
2 sec	0.78	0.61	0.37	0.22	0.01	0									
3 sec	0.85	0.72	0.51	0.37	0.04	0									
10 sec	0.95	0.90	0.82	0.74	0.37	0	0	0	0						
1 min	0.99	0.99	0.97	0.95	0.85	0.37	0.14	0.05	0						
2 min	1.	1.	0.99	0.98	0.92	0.61	0.37	0.22	0.01	0					
3 min	1.	1.	1.	0.99	0.95	0.72	0.51	0.37	0.04	0					
10 min	1.	1.	1.	1.	0.99	0.90	0.82	0.74	0.37	0	0	0	0		
1 hr	1.	1.	1.	1.	1.	0.99	0.97	0.95	0.85	0.37	0.14	0.05	0		
2 hr	1.	1.	1.	1.	1.	1.	1.	1.	1.	0.61	0.37	0.22	0.01	0	
3 hr	1.	1.	1.	1.	1.	1.	1.	1.	1.	0.72	0.51	0.37	0.04	0	
10 hr	1.	1.	1.	1.	1.	1.	1.	1.	1.	0.90	0.82	0.74	0.37	0	
1 day	1.	1.	1.	1.	1.	1.	1.	1.	1.	0.99	0.97	0.95	0.85	0.37	
etc.															

Examples (1) If the mean time to failure is 10 min, the probability of remaining operational for at least 2 min is 0.82
(2) If the mean time to failure is θ , the probability of remaining operational for at least T is $e^{-T/\theta}$

)

)

)

)

)

XIII-4 RELIABILITY SAMPLING

Reliability sampling refers to sampling plan techniques used in order to determine if reliability requirements are met. In general, these techniques involve random sampling from populations with only success or failure attributes or from continuous populations such as time-to-failure distributions. In either case the problem is to estimate a function of the parameters of the population which can be defined as the reliability R of the system.

A binomial sampling plan consists of testing a group of items one by one and recording either a success or a failure on each trial. The result of each trial is independent of the result of any other trial and the objective of the testing is to determine if the item is sufficiently reliable for its intended purpose.

It is, of course, first necessary to specify the maximum value of unreliability P that will be tolerated. Then if the devices unreliability P' is less than this value, it is accepted as meeting the reliability standard, and conversely, if greater, the device is rejected as not meeting the reliability standard. Since no sampling plan is 100 percent efficient, any plan can at times result in rejecting a device because the estimated value of P' exceeds the value of P when in actuality the true value of the populations unreliability P' is less than P . Alternately a sampling plan due to these sampling errors in estimating P' can lead to the acceptance of the item when it would be rejected if the true value of P' were known.

Instead of estimating a single value of P' , the usual procedure is to determine two values A and B such that there is given probability α that the true value of P' lies outside the interval A and B . The probability that the interval A and B contains the true value of P' is then, of course, $1 - \alpha$. The values A and B are called the 100 $(1 - \alpha)$ percent confidence limits for the parameter P' and the interval between them a 100 $(1 - \alpha)$ confidence interval.

The specification of P and α enables one to determine the maximum number of failures permissible (F) in N trials in order to reach an

acceptance decision. For any explanation of the theory of and the techniques used for determining these values, see Ref. 3, Ch. 10 and Ref. 5, p. 140ff. For use in reliability work, extensive tables and graphs have been constructed relating the reliability specifications P , α , N , and F .

Wald sequential sampling plans¹² are based on the fact that the acceptance and rejection boundaries in a failures versus life (time) plane can be approximated by two parallel straight lines. The lines are functions of the reliability specifications only and are plotted in a failure-life graph before testing starts. Testing then continues until a plot of the observed life versus failures first crosses or touches one of the boundaries at which time the appropriate decision is made.

XIII-5 DESIGN OF EXPERIMENTS

In testing components or systems, the objective is to subject them to conditions such that the real characteristics of the items tested can be observed.

Time or life testing is important for considerations other than estimating and demonstrating numerical reliability. Which part in a component or which component in the system failed and the types of and the reasons for the failures must be specified and analyzed. Time-to-failure testing by generating failures helps to answer these questions when time is the critical parameter of the item.

In event testing, samples are cycled repeatedly until failure; it is used when starting and stopping operations are more destructive than the accumulation of time. In this type of testing, the mean cycles to failure becomes the principal parameter.

Environmental testing is undertaken to determine the reactions of the item tested to ambient conditions resembling as closely as possible the environment in which the item is expected to operate.

The design and analysis of experiments, statistical experimentation, differs from the traditional method in that more than one factor at a time is allowed to vary. Varying only one factor at a time is not only inefficient but can produce wrong results as well as obscuring factor interaction. The fundamental basis of statistical experimentation is to apply the factors in such a manner that their effects can be factored out and the variations caused by the factors on performance can be measured and compared. This type of test is called a factorial experiment.

Assume a rocket engine is to be tested to determine the chamber pressure under three environmental conditions (factors) and at two levels for each condition. This represents a factorial design involving a total of 8 treatment combinations (an experiment involving K factors at X levels and XK combinations). The data from such a test could be shown in the following way.

Environment

Environment	level							
	a_1				a_2			
	b_1		b_2		b_1		b_2	
	c_1	c_2	c_1	c_2	c_1	c_2	c_1	c_2
Pressure	11.8	20.9	8.5	16.2	9.9	18.3	8.1	16.0

An estimate of the total effect of factor A upon the pressure is given by the sum of all pressures observed at level a_2 minus the sum of those at level a_1 .

$$A = (9.9 + 18.3 + 8.1 + 16.0) - (11.8 + 20.9 + 8.5 + 16.2) = -5.1$$

and
$$B = (8.5 + 16.2 + 8.1 + 16.0) - (11.8 + 20.9 + 9.9 + 18.3) = -12.1$$

$$C = (20.9 + 16.2 + 18.3 + 16.0) - (11.8 + 8.5 + 9.9 + 8.1) = 33.1$$

The interaction effect of A and B is the difference between the effect of A at the upper level of B and the effect of A at the lower level of B .

$$\begin{aligned} AB &= [(16.0 - 16.2) + (8.1 - 8.5)] \\ &\quad - [(18.3 - 20.9) + (9.9 - 11.8)] = 3.9 \end{aligned}$$

and
$$\begin{aligned} AC &= [(16.0 - 16.2) + (18.3 - 20.9)] \\ &\quad - [(8.1 - 8.5) + (9.9 - 11.8)] = -0.5 \end{aligned}$$

$$\begin{aligned} BC &= [(16.0 - 18.3) + (16.2 - 20.9)] \\ &\quad - [(8.1 - 9.9) + (8.5 - 11.8)] = -1.9 \end{aligned}$$

The AB interaction for the two levels of C are

$$[(16.0 - 16.2) - (18.3 - 20.9)] \quad \text{and} \quad [(8.1 - 8.5) - (9.9 - 11.8)]$$

and the difference between these two expressions represents the effects of *C* upon the *AB* interaction; i.e.,

$$ABC = (2.4) - (1.5) = 0.9 \quad .$$

These factor effects are summarized in the table below:

FACTOR	EFFECT	(Effect) ² /8*
A	-5.1	3.251
B	-21.1	18.301
C	33.1	136.951
AB	3.9	1.901
AC	-0.5	0.031
BC	-1.9	0.451
ABC	0.9	0.101

* This column represents the contribution to the sum of the squares of each chamber pressure observation that is made by each factor. To obtain this, the effect is squared and then divided by 8 (the total number of combinations; i.e., 2³).

In order to determine the significance of the factors upon performance a formal analysis of variance shows that factors *B* and *C* are significant at the 99 percent level. That is, the odds are 99 to 1 that the improved performance due to a decrease in vibration and an increase in humidity is not due to chance alone. For an explanation of analysis of variance theory and techniques, see Bennett and Franklin (Ref. 2, Ch. 7, pp. 319-477).

)

)

)

)

)

XIII-6 TOLERANCE LIMITS

Whenever parameters, such as permeability rates, are experimentally determined, it is preferable for design and reliability evaluation to specify tolerance limits such that a certain percentage of future measurements may be expected to fall between the limits. Experience has shown that the majority of experimental data are approximately normally distributed; moreover, moderate departures from normality do not seriously affect the tolerance limits computed on the basis of normal distribution. Assuming normality, if the true mean and standard deviation of the population were known, tolerance limits would be formed by adding to and subtracting from the mean a certain multiple K of the standard deviation. For example, if the mean μ and standard deviation of the population σ are known, then the limits $\mu \pm 1.645\sigma$ will include 90 percent of the distribution of the mean. However, the same assertion cannot be made about the limits $\bar{X} \pm 1.645 \cdot S$ where \bar{X} is the mean and S is the standard deviation of a sample of N observations. In fact, if K is fixed, no two samples from a given population will yield identical tolerance limits as both the sample means and standard deviations will vary from sample to sample. Therefore, the proportion of the population that is included between the limits $\bar{X} \pm K \cdot S$ is a random variable and it is impossible to determine so that the limits will always contain a specific proportion of the population. It is, however, possible to determine K so that a certain proportion γ (called the confidence coefficient) of the tolerance limits $\bar{X} \pm K \cdot S$ will contain a fixed percentage of the population P .

Table XIII-6-1 presents values of K associated with a specified coefficient γ , sample size N , and population proportion P assuming a normal distribution. Confidence limits $\gamma = 0.95$ or 0.99 are most frequently used in practice.

It is occasionally appropriate to specify a single tolerance limit $\bar{X} - K \cdot S$ such that a fixed proportion of the population lies above this limit, or a limit $\bar{X} + K \cdot S$ such that a fixed proportion lies below the limit. These single limits are called one-sided tolerance limits. [See Bowker and Lieberman (Ref. 3, p. 230-1) for a table of K values to use in computing one-sided tolerance limits.]

XIII-6.1

)

)

)

)

)

Table XIII-6-1

TOLERANCE FACTORS FOR NORMAL DISTRIBUTIONS*

Factors K such that the probability is that at least the proportion P of the distribution lies between the interval $\bar{X} \pm Ks$, where \bar{X} and s are the mean and standard deviation computed from a sample of size N

N \ P	$\gamma = 0.90$				$\gamma = 0.95$				$\gamma = 0.99$			
	0.75	0.90	0.95	0.99	0.75	0.90	0.95	0.99	0.75	0.90	0.95	0.99
2	11.407	15.978	18.800	21.167	22.858	32.019	37.674	48.430	114.363	160.193	188.191	242.300
3	4.132	5.847	6.919	8.971	5.922	8.380	9.916	12.861	13.378	18.930	22.401	29.055
4	2.932	4.166	4.943	6.410	3.779	5.369	6.370	8.299	6.614	9.398	11.150	14.527
5	2.454	3.494	4.152	5.423	3.002	4.275	5.079	6.634	4.613	6.612	7.855	10.260
6	2.196	3.131	3.723	4.870	2.604	3.712	4.414	5.775	3.743	5.337	6.345	8.301
7	2.034	2.902	3.452	4.521	2.361	3.369	4.007	5.248	3.233	4.613	5.488	7.187
8	1.921	2.743	3.264	4.278	2.197	3.136	3.732	4.891	2.905	4.147	4.936	6.168
9	1.839	2.626	3.125	4.098	2.078	2.967	3.532	4.631	2.677	3.822	4.550	5.966
10	1.775	2.535	3.018	3.959	1.987	2.839	3.379	4.433	2.508	3.582	4.265	5.594
11	1.724	2.463	2.933	3.849	1.916	2.737	3.259	4.277	2.378	3.397	4.045	5.308
12	1.683	2.404	2.863	3.758	1.858	2.655	3.162	4.150	2.274	3.250	3.870	5.079
13	1.648	2.355	2.805	3.682	1.810	2.587	3.081	4.044	2.190	3.130	3.727	4.893
14	1.619	2.314	2.756	3.618	1.770	2.529	3.012	3.955	2.120	3.029	3.608	4.737
15	1.594	2.278	2.713	3.562	1.735	2.480	2.954	3.878	2.060	2.945	3.507	4.605
16	1.572	2.246	2.676	3.514	1.705	2.437	2.903	3.812	2.009	2.872	3.421	4.492
17	1.552	2.219	2.643	3.471	1.679	2.400	2.858	3.754	1.965	2.808	3.345	4.393
18	1.535	2.194	2.614	3.433	1.655	2.366	2.819	3.702	1.926	2.753	3.279	4.307
19	1.520	2.172	2.588	3.399	1.635	2.337	2.784	3.656	1.891	2.703	3.221	4.230
20	1.506	2.152	2.564	3.368	1.616	2.310	2.752	3.615	1.860	2.659	3.168	4.161
21	1.493	2.135	2.543	3.340	1.599	2.286	2.723	3.577	1.833	2.620	3.121	4.100
22	1.482	2.118	2.524	3.315	1.584	2.264	2.697	3.543	1.808	2.584	3.078	4.044
23	1.471	2.103	2.506	3.292	1.570	2.244	2.673	3.512	1.785	2.551	3.040	3.993
24	1.462	2.089	2.489	3.270	1.557	2.225	2.651	3.483	1.764	2.522	3.004	3.947
25	1.453	2.077	2.474	3.251	1.545	2.208	2.631	3.457	1.745	2.494	2.972	3.904
28	1.430	2.044	2.435	3.199	1.514	2.164	2.579	3.388	1.695	2.424	2.888	3.794
30	1.417	2.025	2.413	3.170	1.497	2.140	2.549	3.350	1.668	2.385	2.841	3.733
32	1.405	2.009	2.393	3.145	1.481	2.118	2.524	3.318	1.644	2.351	2.801	3.680
34	1.395	1.994	2.376	3.122	1.468	2.099	2.501	3.286	1.623	2.320	2.764	3.632
36	1.386	1.981	2.361	3.102	1.455	2.081	2.479	3.258	1.604	2.293	2.732	3.590
38	1.377	1.969	2.346	3.083	1.446	2.068	2.464	3.237	1.587	2.269	2.703	3.552
40	1.370	1.959	2.334	3.066	1.435	2.052	2.445	3.213	1.571	2.247	2.677	3.518
45	1.354	1.935	2.306	3.030	1.414	2.021	2.408	3.165	1.539	2.200	2.621	3.444
50	1.340	1.916	2.284	3.001	1.396	1.996	2.379	3.126	1.512	2.162	2.576	3.385

* K values taken from Eisenhart, Hastay, and Wallis, "Techniques of Statistical Analysis," McGraw-Hill Book Co., Inc. 1947.

)

)

)

)

)

XIII-7 RELIABILITY REFERENCES

1. Anon., "A Manual of Reliability," *Product Eng.*, May 1960.
2. Bennett, Carl A., and Franklin, N. L., "Statistical Analysis in Chemistry and the Chemical Industry," John Wiley and Sons, Inc., 1954.
3. Bowker, A. H., and Lieberman, G. J., "Engineering Statistics," Prentice-Hall, Inc., 1959.
4. Dull, Raymond W., and Dull, Richard, "Mathematics for Engineers," McGraw-Hill, 1951.
5. Feller, W., "An Introduction to Probability Theory and Its Applications," John Wiley and Sons, Inc., 1957.
6. Lloyd, David K., and Lipow, M., "Reliability: Management, Methods, and Mathematics," Prentice-Hall, Inc., 1962.
7. Lusser, Robert, "Reliability of Guided Missiles, AD-44 456, 1954.
8. Mood, A. M., "Introduction to the Theory of Statistics," McGraw-Hill, 1950.
9. Morrison, S. C., "Maximizing Reliability," *Aerospace Eng.*, March 1962.
10. Mosteller, Bourke, and Thomas, "Probability and Statistics," Addison-Wesley Publishing Co., Inc., 1961.
11. Mood, A. M., "Introduction to the Theory of Statistics," McGraw-Hill, 1950.
12. Wald, Abraham, "Sequential Analysis," John Wiley and Sons, Inc., 1947.

1

2

3

4

5

XV RINGS AND SEALS

Table of Contents

	<u>Title</u>	<u>Section-Page</u>
Section XV	Rings and Seals	XV-1
Table XV-1	Effects of High Vacuum and Temperature on Mechanical Properties of Seal Materials	XV- 5
Table XV-2	Service Temperature and Radiation Stability of some Seal Materials	XV- 6
	References	XV-7

)

)

)

)

)

XV RINGS AND SEALS

Rings and seals are used to provide leakless junctures between component parts of pressurized-gas systems. Five methods for joining components are widely employed:

- (1) Metal-to-metal by fusion, intermediary metal, or solder.
- (2) Metal-to-metal by accurately tapered threads with no intermediary material (cold-welding).
- (3) Surface-to-surface by threads rendered tight with the assistance of intermediary material such as dopes, soft metals, etc.
- (4) Surface-to-surface entirely by intermediary material such as elastomers (gaskets).
- (5) Surface-to-surface by confining intermediary materials such as elastomers or metals between grooves or wedges and flats.

Metal-to-metal junctures effected by welding can be made as leakless as the bulk of the metal used to construct the gas system, and are recommended for use whenever feasible since they are the only reliable, leakless joints which can be made. Soldered joints have little place in space vehicles largely because they are easily embrittled, but also because they are inherently weak. Solder may be weakened by preferential distillation of components in the vacuum of space.

It is extremely difficult to machine accurately-tapered threads which can be screwed together to form cold-welded surfaces; moreover, it is perhaps impossible to ensure (with very high reliability) that the welding has taken place so uniformly that no pin-holes or porosity results. As a consequence, this type of juncture must be avoided in spacecraft systems.

Threaded connections made leak-tight by intermediary materials such as dopes, soft metals, or externally-applied varnishes or putties are commonplace, but they are not recommended for spacecraft without reservation. Intermediaries such as dopes or varnishes generally make a seal at the outer edges of a threaded connection and seldom penetrate the annular space of more than one or two threads. When the intermediary is applied before the threads are meshed, there is a tendency for it

to lubricate the threads and also occupy voids where metal-to-metal contact can not take place because of irregularities. A thin coat of solder applied to threads before meshing acts similarly; however, it is to be recommended over dopes because no shrinkage can occur from evaporation of solvents, etc. Solder is sometimes applied to the exterior of a threaded joint; such joints are strong and leakless, but cannot be recommended for use over extended periods of time in a space environment.

Junctures made between flat or rugose surfaces with intermediary elastomeric or polymeric material (gaskets) are to be avoided in pressurized gas systems. These types of joints slowly develop leaks because of the cold-flow or volume changes suffered by elastomeric materials, especially in a space environment. Gaskets with restrictors to prevent flow or distortion tend to be superior to unsupported kinds, but the seal depends on the physical properties of the elastomer and any change of properties may lead to leakage or porosity. Gaskets made of soft metals maintain their physical properties for very long periods of time, but the continual "working" at junctions because of temperature changes will eventually loosen them. If the metal gasket in such a joint is made of material with essentially the same thermal coefficient of expansion as the bulk of the joint and its tighteners, "working" normally does not occur and a tight seal can be maintained. Cone-and-seat type of fittings of the type commonly used to connect metal tubing depend on intimate metal-to-metal contact for sealing action; however, the gross irregularities which often are present on the relatively hard metal surfaces prevent sealing action. The interposition of a relatively soft metal-cone (such as copper) generally leads to a "zero-leak" joint. These joints seldom can be re-seated once the soft metal has been distorted; however, they are recommended for one-time use for spacecraft pressure systems provided the joint is compressed very tightly so as to prevent loosening by temperature cycling.

Surface-to-surface seals made by confining soft metals are recommended for space use so long as compressive force can be maintained reliably. The form of the seal is not critical and several commercially-available products can be found. When the intermediary material is an elastomer, compression is provided by the material itself. In these instances, it is necessary to utilize materials which maintain physical properties for long periods of time in a space environment and, for added reliability, the seal design should provide the elastomer

with maximum protection from the space environment. Thus, notch-and-groove seats should be used preferentially over groove-and-flats because in the former the elastomer is well-protected from radiation and only a minimum surface area is exposed to the vacuum of space. Further, the notch-and-groove seat minimizes the area exposed to the pressurized gas and permeability is kept to insignificant proportions.

A common surface-to-surface seal affected by a confined intermediary is the O-ring. Rings of elastomeric materials can be utilized in properly machined and rounded groove-and-flats which grossly distort (cold-flow) the rings and leave exposed areas approximating the notch-and-groove seats; the cross-sectional area of such a groove-and-flat must be 10-15% *less* than the area of the undistorted ring. The usual designs for V-shaped O-ring grooves which permit movement and flow of the elastomer ring under pressure gradients are useless for reliable, leakless pressurized-gas systems.

Seals utilizing the physical properties of elastomers depend heavily upon maintenance of these properties in a space environment. Tables XV-1 and XV-2 provide data on the effect of space environment on seal materials.

Recently there have been made available hollow, metallic O-rings that furnish a natural resiliency which permits their replacing the elastomeric counterparts. These rings are made by forming metal tubes in a hoop, welding the ends together, and then grinding the weld flush. Other types are made in which the gas confined within the tube is at about 600 psi pressure. Fully-confined hollow-metal, pressurized O-rings should be able to function as their elastomeric counterparts in round-bottom V-notches which distort the rings to round-cornered squares; such seals depend upon the resiliency of the enclosed gas and the surrounding metal, and should not be affected by the space environment.

)

)

)

)

)

Table XV-1
EFFECTS OF HIGH VACUUM AND TEMPERATURE ON
MECHANICAL PROPERTIES OF SEAL MATERIALS
(Ref. 1, 2, 3, 4)

MATERIAL.	EXPOSURE			CHANGES IN PROPERTIES (%)			
	<i>t</i> , hr	<i>T</i> , °C	<i>P</i> , mm Hg	Elastic Modulus	Tensile Strength	Elongation	Hardness
Polyethylene (low density)	24	21	1×10^{-6}	0	0		
Polyethylene (low density)	24	70	1×10^{-6}	+20	0		
Polyethylene (high density)	24	21	9×10^{-7}	0	+75		
Polyethylene (high density)	24	88	2×10^{-6}	0	+75		
Teflon	3	21	5×10^{-6}		<±7		
Teflon	3	185	7×10^{-6}		<±3		
Polyvinyl Chloride	3	21	4×10^{-6}		<±10		<±2
Neoprene	1344	21	1×10^{-5}	+7	+3	-1	+4
Neoprene	120	100	8×10^{-6}	+55	+6	-14	+15
Nitrile Rubber	1344	21	1×10^{-5}	-2	+8	+5	-12
Nitrile Rubber	120	100	8×10^{-6}	+120	+57	-19	+19
Butyl Rubber	24	27	1×10^{-5}		+13	-7	
Butyl Rubber	312	27	1×10^{-5}		+5.4	-8.5	
Silicone Rubber	4.5	333	1×10^{-4}		0	-10.2	0
Viton Fluororubber	6.5	204	6×10^{-4}		-12.3	-5.5	+1.4

Table XV-2
SERVICE TEMPERATURE AND RADIATION STABILITY OF SOME SEAL MATERIALS
(Ref. 5, 6, 7)

MATERIAL	SERVICE TEMPERATURE °F	EFFECT OF PENETRATING RADIATION (rad*)	
		Threshold Damage	25% Damage
Elastomers			
Natural Rubber	-60 to 225	2×10^6	2.5×10^7
Styrene-Butadiene Rubber	to 250	2×10^6	1×10^7
Butyl Rubber	-60 to 275	2×10^6	4×10^6
Nitrile Rubber (Buna N)	-65 to 250	2×10^6	7×10^6
Polysulfide Rubber	to 150	5×10^5	1.5×10^6
Neoprene	-65 to 250	2×10^6	5.5×10^6
Silicone Rubber	-100 to 400	1.3×10^6	4.2×10^6
Acrylic Rubber	to 450	1×10^6	3.3×10^6
Plastics			
Polyethylene	0 to 165	1.9×10^7	9.3×10^7
Teflon	-65 to 400	1.7×10^4	3.7×10^4
Kel-F	-100 to 300		1×10^8
Polyvinyl Chloride	to 212	1.9×10^7	1.1×10^8
Metals			
Aluminum	-300 to 700		10^{12}
Stainless Steels	-300 to 1500		10^{12}

* 1 rad = 100 ergs/gram

XV REFERENCES

1. Lehr, S. N., Tronolone, V. J., and Horton, P. V., Space Technology Laboratories, Inc., *Report No. STL/TR-60-0000-09224*, September 1960, p. 15. (AD-269 301).
2. Mauri, R. E., "Space Materials Handbook," Lockheed Missiles and Space Company, January 1962, p. 344. (AD-284 547).
3. Ossefort, Z. T., and Ruby, J. D., Rock Island Arsenal, *Laboratory Report No. 61-1999*, 15 May 1961, p. 657. (AD-259 557).
4. Synder, Carl E., and Cross, William B., "Coatings for the Aerospace Environment," *WADD TR 60-773*, July 1961, p. 79. (AD-267 310).
5. Berg, Robert J., Jet Propulsion Laboratory, *Prog. Rept. No. 20-340*, March 7, 1958.
6. Lehr, S. N., Tronolone, V. J., and Horton, P. V., Space Technology Laboratories, Inc., *Rept. No. STL/TR-60-0000-09224*, p. 29.
7. Mauri, R. E., "Space Materials Handbook," Lockheed Missiles & Space Company, January 1962, p. 339.

)

)

)

)

)

DISTRIBUTION LIST

ORGANIZATION	NO. OF COPIES	ORGANIZATION	NO. OF COPIES
NASA Western Operations Office 150 Pico Boulevard Santa Monica, California		Marshall Space Flight Center Huntsville, Alabama	2
Office of Technical Information	1	Manned Spacecraft Center	2
Contracting Officer	1	Houston, Texas	
Patent Office	1	Advanced Research Projects Agency	1
NASA Lewis Research Center		Pentagon, Room 3D154	
21000 Brookpark Road		Washington 25, D.C.	
Cleveland 35, Ohio		Aeronautical Systems Division	1
Office of Technical Information	1	Air Force Systems Command	
Contracting Officer	1	Wright-Patterson Air Force Base, Ohio	
Patent Office	1	Air Force Missile Development Center	1
NASA Marshall Space Flight Center		Holloman Air Force Base, New Mexico	
Huntsville, Alabama		Air Force Missile Test Center	1
Office of Technical Information, M-MS-IPC	1	Patrick Air Force Base, Florida	
Contracting Officer, M-P&C-C	1	Air Force Systems Command, Dyna-Soar	1
Patent Office, M-PAT	1	Air Force Unit Post Office	
NASA HEADQUARTERS		Los Angeles 45, California	
Washington 25, D.C.		Army Ordnance Missile Command	1
Contracting Officer, BRA	1	Redstone Arsenal, Alabama	
Patent Office, AGP	1	Arnold Engineering Development Center	1
Mr. Henry Burlage, Jr.	4	A.E.O.R.	
Chief, Liquid Propulsion Systems, RPL		Tullahoma, Tennessee	
Mr. A. O. Tischler	1	Bureau of Naval Weapons	1
Assistant Director for Propulsion, MLP		Department of the Navy	
TECHNICAL MANAGER		Washington 25, D.C.	
Mr. Richard N. Porter	1	Central Intelligence Agency	1
Liquid Propulsion Section		2430 E Street, N.W.	
Propulsion Division		Washington 25, D.C.	
Jet Propulsion Laboratory		Defense Documentation Center Headquarters	1
4800 Oak Grove Drive		Cameron Station, Building 5	
Pasadena, California		Alexandria, Virginia 22314	
Scientific and Technical Information Facility	25	Attn: TISIA	
NASA Representative, Code CRT		Headquarters, United States Air Force	1
P.O. Box 5700		Washington 25, D.C.	
Bethesda, Maryland 20014		Picatinny Arsenal	1
Ames Research Center	2	Dover, New Jersey	
Moffett Field, California		Rocket Research Laboratories	1
Goddard Space Flight Center	2	Edwards Air Force Base, California	
Greenbelt, Maryland		U.S. Naval Ordnance Test Station	1
Jet Propulsion Laboratory	2	China Lake, California	
California Institute of Technology		U.S. Atomic Energy Commission	1
4800 Oak Grove Drive		Technical Information Services	
Pasadena, California		Box 62	
Langley Research Center	2	Oak Ridge, Tennessee	
Langley Field, Virginia			
Lewis Research Center	2		
21000 Brookpark Road			
Cleveland 35, Ohio			

DISTRIBUTION LIST

ORGANIZATION	NO. OF COPIES	ORGANIZATION	NO. OF COPIES
CPIA Chemical Propellant Information Agency Johns Hopkins University Applied Physics Laboratory 8621 Georgia Avenue Silver Spring, Maryland	1	Fairchild Stratos Corporation Aircraft Missiles Division Hagerstown, Maryland	1
Aerojet-General Corporation P.O. Box 296 Azusa, California	1	General Electric Company Missile and Space Vehicle Department Box 8555 Philadelphia, Pennsylvania	1
Aerojet-General Corporation P.O. Box 1947 Sacramento 9, California	1	General Electric Company Rocket Propulsion Units Building 300 Cincinnati 15, Ohio	1
Aeronutronic A Division of Ford Motor Company Ford Road Newport Beach, California	1	Grumman Aircraft Engineering Corporation Bethpage, Long Island, New York	1
Aerospace Corporation 2400 East El Segundo Boulevard El Segundo, California	1	Kidde Aero-Space Division Walter Kidde and Company, Inc. 675 Main Street Belleville 9, New Jersey	1
Arthur D. Little, Inc. Acorn Park Cambridge 40, Massachusetts	1	Lockheed Aircraft Corporation Missile and Space Division Sunnyvale, California	1
Astropower, Inc., Subsidiary of Douglas Aircraft Company, Inc. 2968 Randolph Avenue Costa Mesa, California	1	Lockheed California Company 10445 Glen Oaks Boulevard Pacoima, California	1
Astrosystems, Inc. 82 Naylor Avenue Livingston, New Jersey	1	Lockheed Propulsion Company P.O. Box 111 Redlands, California	1
Atlantic Research Corporation Edsall Road and Shirley Highway Alexandria, Virginia	1	Marquardt Corporation 16555 Saticoy Street Box 2013 - South Annex Van Nuys, California	1
Beech Aircraft Corporation Boulder Facility Box 631 Boulder, Colorado	1	Martin Division Martin Marietta Corporation Baltimore 3, Maryland	1
Bell Aerosystems Company P.O. Box 1 Buffalo 5, New York	1	Martin Denver Division Martin Marietta Corporation Denver, Colorado	1
Bendix Systems Division Bendix Corporation Ann Arbor, Michigan	1	McDonnell Aircraft Corporation P.O. Box 6101 Lambert Field, Missouri	1
Boeing Company P.O. Box 3707 Seattle 24, Washington	1	North American Aviation, Inc. Space and Information Systems Division Downey, California	1
Convair (Astronautics) Division of General Dynamics Corporation P.O. Box 2672 San Diego 12, California	1	Northrop Corporation 1001 East Broadway Hawthorne, California	1
Curtiss-Wright Corporation Wright Aeronautical Division Wood-ridge, New Jersey	1	Pratt & Whitney Aircraft Corporation Florida Research & Development Center West Palm Beach, Florida	1
Douglas Aircraft Company, Inc. Missile and Space Systems Division 3000 Ocean Park Boulevard Santa Monica, California	1	Philco Corporation Western Development Laboratories 3825 Fabian Way Palo Alto, California	1

DISTRIBUTION LIST

ORGANIZATION	NO. OF COPIES	ORGANIZATION	NO. OF COPIES
Radio Corporation of America Astro-Electronics Division Defense Electronic Products Princeton, New Jersey	1		
Reaction Motors Division Thiokol Chemical Corporation Denville, New Jersey	1		
Republic Aviation Corporation Farmingdale Long Island, New York	1		
Rocketdyne (Library Dept. 586-306) Division of North American Aviation, Inc. 6633 Canoga Avenue Canoga Park, California	1		
Space General Corporation 9200 Flair Avenue El Monte, California	1		
Space Technology Laboratories P.O. Box 95001 Airport Station Los Angeles 45, California	1		
Stanford Research Institute 333 Ravenswood Avenue Menlo Park, California	1		
TAPCO Division Thompson-Ramo-Wooldridge, Inc. 23555 Euclid Avenue Cleveland 17, Ohio	1		
Thiokol Chemical Corporation Redstone Division Huntsville, Alabama	1		
United Aircraft Corporation East Hartford Plant 400 Main Street Hartford, Connecticut	1		
United Technology Corporation 587 Mathilda Avenue Sunnyvale, California	1		
Vought Astronautics Box 5907 Dallas 22, Texas	1		
Vickers Incorporated Aerospace Division 3201 Lomita Boulevard Torrance, California	1		

